frontiers

RESEARCH TOPICS

THE REGULATED SECRETORY PATHWAY IN NEUROENDOCRINE CELLS

Topic Editors
Rafael Vazquez-Martinez
and Stéphane Gasman

frontiers in
ENDOCRINOLOGY

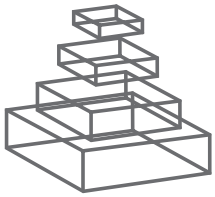

frontiers

ISSN 1664-8714
ISBN 978-2-88919-246-5
DOI 10.3389/978-2-88919-246-5

ABOUT FRONTIERS

Frontiers is more than just an open-access publisher of scholarly articles: it is a pioneering approach to the world of academia, radically improving the way scholarly research is managed. The grand vision of Frontiers is a world where all people have an equal opportunity to seek, share and generate knowledge. Frontiers provides immediate and permanent online open access to all its publications, but this alone is not enough to realize our grand goals.

FRONTIERS JOURNAL SERIES

The Frontiers Journal Series is a multi-tier and interdisciplinary set of open-access, online journals, promising a paradigm shift from the current review, selection and dissemination processes in academic publishing.
All Frontiers journals are driven by researchers for researchers; therefore, they constitute a service to the scholarly community. At the same time, the Frontiers Journal Series operates on a revolutionary invention, the tiered publishing system, initially addressing specific communities of scholars, and gradually climbing up to broader public understanding, thus serving the interests of the lay society, too.

DEDICATION TO QUALITY

Each Frontiers article is a landmark of the highest quality, thanks to genuinely collaborative interactions between authors and review editors, who include some of the world's best academicians. Research must be certified by peers before entering a stream of knowledge that may eventually reach the public - and shape society; therefore, Frontiers only applies the most rigorous and unbiased reviews.
Frontiers revolutionizes research publishing by freely delivering the most outstanding research, evaluated with no bias from both the academic and social point of view.
By applying the most advanced information technologies, Frontiers is catapulting scholarly publishing into a new generation.

WHAT ARE FRONTIERS RESEARCH TOPICS?

Frontiers Research Topics are very popular trademarks of the Frontiers Journals Series: they are collections of at least ten articles, all centered on a particular subject. With their unique mix of varied contributions from Original Research to Review Articles, Frontiers Research Topics unify the most influential researchers, the latest key findings and historical advances in a hot research area!
Find out more on how to host your own Frontiers Research Topic or contribute to one as an author by contacting the Frontiers Editorial Office: researchtopics@frontiersin.org

THE REGULATED SECRETORY PATHWAY IN NEUROENDOCRINE CELLS

Topic Editors:
Rafael Vazquez-Martinez, University of Cordoba, Cordoba, Spain
Stéphane Gasman, Institut des Neurosciences Cellulaires et Intégratives, CNRS UPR 3212, Strasbourg, France

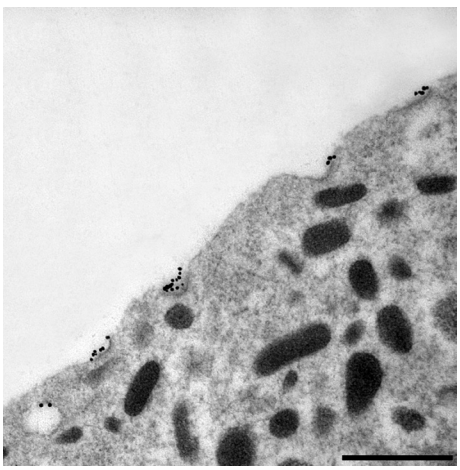

The image is the property of: Haeberlé A.M., Bailly Y. and Gasman S : Institut des Neurosciences Cellulaires et Intégratives (INCI), CNRS UPR3212; Plateforme Imagerie In Vitro, Neuropôle, Strasbourg.

The regulated secretory pathway is a hallmark of neuroendocrine cells. This process comprises many sequential steps, which include ER-associated protein synthesis, post-translational modification of proteins in the Golgi complex, sorting and packing of secretory proteins into carrier granules, cytoskeleton-based granule transport towards the plasma membrane and tethering, docking and fusion of granules with specialized releasing zones. Each stage is subjected to a rigorous regulation by a plethora of factors that function in a spatially and temporarily coordinated fashion. Much effort has been devoted to characterize the precise role of the regulatory proteins participating in the different steps of this process and to identify new factors in order to obtain a unifying picture of the secretory pathway. In spite of this and given the enormous complexity of the process, certain stages are not fully understood yet and many players remain to be identified. The aim of this Research Topic is to gather review articles and original research papers on the molecular mechanisms that govern and ensure the correct release of neuropeptides.

Table of Contents

frontiers in
ENDOCRINOLOGY

EDITORIAL
published: 08 April 2014
doi: 10.3389/fendo.2014.00048

The regulated secretory pathway in neuroendocrine cells

Rafael Vazquez-Martinez [1,2]* ***and Stéphane Gasman*** [3]*

[1] *Department of Cell Biology, Physiology and Immunology, Instituto Maimónides de Investigaciones Biomédicas de Córdoba (IMIBIC), Reina Sofia University Hospital, University of Córdoba, Córdoba, Spain*

[2] *CIBER Fisiopatología de la Obesidad y Nutrición (CIBERobn), Córdoba, Spain*

[3] *Centre National de la Recherche Scientifique (CNRS UPR 3212), Institut des Neurosciences Cellulaires et Intégratives (INCI), Université de Strasbourg, Strasbourg, France*

**Correspondence: bc2vamar@uco.es; gasman@inci-cnrs.unistra.fr*

Edited and reviewed by:
Hubert Vaudry, University of Rouen, France

Keywords: secretion, neuroendocrine cells, membrane trafficking, large dense core vesicles, regulated exocytosis, endocytosis, super-resolution microscopy

The regulated secretory pathway shared by excitable cells, including neurons and neuroendocrine cells is an intricate process that comprises multiple, tightly regulated steps. After their synthesis in the endoplasmic reticulum, hormones and neuropeptides have to be sorted and packed into large dense core vesicles (also named secretory granules) in the Golgi apparatus. Granules are transported toward the plasma membrane in a cytoskeleton-dependent manner and mature into competent organelles for secretagogue-induced exocytosis. Granules are then tethered to the plasma membrane, docked, and primed, before finally releasing their contents after fusing with the plasma membrane. To ensure that neurotransmission and neuroendocrine secretion operate correctly, all these steps must be tightly regulated and coordinated both spatially and temporally. Currently, when the field of intracellular trafficking has been honored by the 2013 Nobel Prize in Physiology or Medicine (awarded to James Rothman, Randy Schekman, and Thomas Südhof for their pioneering works on vesicular transport), this issue of Frontiers in Neuroendocrine Science is aimed to providing an up-to-date overview of the cellular and molecular mechanisms governing the regulated secretory pathway in neuroendocrine cells. Reviews presented here are widely covering this topic, from the architecture of the organelle involved in secretory cargo processing and sorting, the biogenesis of secretory granules, their specific transport toward the plasma membrane to the late steps of exocytosis, and the secretory granule membrane recapture.

Early stages of the secretory pathway have been discussed by two groups. Emma Martinez-Alonso and colleagues discuss the Golgi complex architecture, as well as the regulatory proteins that govern extra- and intra-Golgi transport, and the still controversial, but not mutually exclusive, theoretical models proposed to explain cargo progression through the Golgi stack (1). The group of Richard Mains discusses the specific roles of cytosolic adaptor proteins such as AP-1A, PACS-1, and GGAs in the assembly and maturation of secretory granules (2).

Closer to the cell surface, several groups discuss the molecular mechanisms regulating the late stage of exocytosis. The group of Frédéric Meunier reviews recent insights of the role of the cortical acto-myosin network (3), whereas the role of different tethering and priming factors such as CAPS, Munc13, and Doc2 proteins is described by the groups of Ury Ashery and Tom Martin (4, 5). Paanteha Moghadam and Meyer Jackson review how various synaptotagmins regulate fusion pore kinetics and control the mode of release (6). Lipids have emerged as key players of the regulated exocytosis and the group of Nicolas Vitale presents an overview on the diverse roles that lipids play in defining exocytotic sites, both by affecting membrane topology and by regulating secretory vesicle priming and fusion (7).

Finally, exocytosis cannot exist without a compensatory membrane intake process (i.e., endocytosis), which allows recycling of granule components and maintains organelle integrity. The groups of Stéphane Gasman and Alla Rynditch discuss the mechanisms that coordinate clathrin-mediated compensatory endocytosis with exocytosis, highlighting the specific role of the intersectin family of scaffold proteins in exocytosis and endocytosis (8, 9). The group of Ana-Maria Cardenas reviews the pleiotropic role of the mechano-GTPase dynamin-2, on intracellular membrane fission and fusion events, vesicle traffic, and cytoskeleton dynamics, as well as the impact of dynamin-2 mutations on the correct functioning of the secretory pathway (10).

On a more physiological point of view, Maria-Luisa Durán-Pasten and Tatiana Fiordelisio present an example of how pituitary gonadotrophs receive and transduce extracellular signals to promote luteinizing (LH) and follicle-stimulating (FSH) secretion, highlighting the tremendous plasticity of the system for adapting to different physiological demands (11). Wei-Jye Lin and Stephen Salton report that single nucleotide polymorphisms in genes encoding secreted proteins are associated with neuropsychiatric or endocrine/metabolic disorders (12). Finally, Jennifer Fitch-Tewfik and Robert Flaumenhaft demonstrate how the regulated secretory pathway is similar in mast cells compared to neuroendocrine cells from the adrenal gland (13), and Burton Dickey's group describes the regulatory mechanism of mucin secretion in a non-neuroendocrine cell model (14).

On a more technical point of view, recent improvements in detection technologies, especially in optical microscopy, continually push the limits of sensitivity and resolution. The groups of Colin Rickman and Ute Becherer discuss how advances over the last decade in fluorescence microscopy provided spatial and temporal details on the subcellular organization of the molecular machinery governing the regulated secretory pathway (15, 16), whereas the group of Rory Duncan describes how the combination of new imaging approaches with super-resolution microscopy and novel calcium indicators is appropriate for accurate study of

voltage-gated calcium channel locations, interactions, dynamics, and composition in living cells (17).

Collectively, this compilation of reviews intends to illustrate the recent progress made to understand the complex regulation of the granule secretory pathways in neuroendocrine cells. We are grateful to all the authors who have contributed to this Research Topic and to the dedicated reviewers who helped us reaching the highest quality standards.

REFERENCES

1. Martinez-Alonso E, Tomas M, Martinez-Menarguez JA. Morpho-functional architecture of the Golgi complex of neuroendocrine cells. *Front Endocrinol* (2013) **4**:41. doi:10.3389/fendo.2013.00041
2. Bonnemaison ML, Eipper BA, Mains RE. Role of adaptor proteins in secretory granule biogenesis and maturation. *Front Endocrinol* (2013) **4**:101. doi:10.3389/fendo.2013.00101
3. Papadopulos A, Tomatis VM, Kasula R, Meunier FA. The cortical actomyosin network: from diffusion barrier to functional gateway in the transport of neurosecretory vesicles to the plasma membrane. *Front Endocrinol* (2013) **4**:153. doi:10.3389/fendo.2013.00153
4. Friedrich R, Gottfried I, Ashery U. Munc13-1 translocates to the plasma membrane in a Doc2B- and calcium-dependent manner. *Front Endocrinol* (2013) **4**:119. doi:10.3389/fendo.2013.00119
5. James DJ, Martin TF. CAPS and Munc13: CATCHRs that SNARE vesicles. *Front Endocrinol* (2013) **4**:187. doi:10.3389/fendo.2013.00187
6. Moghadam PK, Jackson MB. The functional significance of synaptotagmin diversity in neuroendocrine secretion. *Front Endocrinol* (2013) **4**:124. doi:10.3389/fendo.2013.00124
7. Ammar MR, Kassas N, Chasserot-Golaz S, Bader MF, Vitale N. Lipids in regulated exocytosis: what are they doing? *Front Endocrinol* (2013) **4**:125. doi:10.3389/fendo.2013.00125
8. Gubar O, Morderer D, Tsyba L, Croise P, Houy S, Ory S, et al. Intersectin: the crossroad between vesicle exocytosis and endocytosis. *Front Endocrinol* (2013) **4**:109. doi:10.3389/fendo.2013.00109
9. Houy S, Croise P, Gubar O, Chasserot-Golaz S, Tryoen-Toth P, Bailly Y, et al. Exocytosis and endocytosis in neuroendocrine cells: inseparable membranes! *Front Endocrinol* (2013) **4**:135. doi:10.3389/fendo.2013.00135
10. Gonzalez-Jamett AM, Momboisse F, Haro-Acuna V, Bevilacqua JA, Caviedes P, Cardenas AM. Dynamin-2 Function and dysfunction along the secretory pathway. *Front Endocrinol* (2013) **4**:126. doi:10.3389/fendo.2013.00126
11. Duran-Pasten ML, Fiordelisio T. GnRH-induced Ca signaling patterns and gonadotropin secretion in pituitary gonadotrophs. Functional adaptations to both ordinary and extraordinary physiological demands. *Front Endocrinol* (2013) **4**:127. doi:10.3389/fendo.2013.00127
12. Lin WJ, Salton SR. The regulated secretory pathway and human disease: insights from gene variants and single nucleotide polymorphisms. *Front Endocrinol* (2013) **4**:96. doi:10.3389/fendo.2013.00096
13. Fitch-Tewfik JL, Flaumenhaft R. Platelet granule exocytosis: a comparison with chromaffin cells. *Front Endocrinol* (2013) **4**:77. doi:10.3389/fendo.2013.00077
14. Adler KB, Tuvim MJ, Dickey BF. Regulated mucin secretion from airway epithelial cells. *Front Endocrinol* (2013) **4**:129. doi:10.3389/fendo.2013.00129
15. Bost A, Pasche M, Schirra C, Becherer U. Super-resolution microscopy in studying neuroendocrine cell function. *Front Neurosci* (2013) **7**:222. doi:10.3389/fnins.2013.00222
16. Graczyk A, Rickman C. Exocytosis through the lens. *Front Endocrinol* (2013) **4**:147. doi:10.3389/fendo.2013.00147
17. Hiersemenzel K, Brown ER, Duncan RR. Imaging large cohorts of single ion channels and their activity. *Front Endocrinol* (2013) **4**:114. doi:10.3389/fendo.2013.00114

Conflict of Interest Statement: The authors declare that the research was conducted in the absence of any commercial or financial relationships that could be construed as a potential conflict of interest.

Received: 10 March 2014; accepted: 24 March 2014; published online: 08 April 2014.
*Citation: Vazquez-Martinez R and Gasman S (2014) The regulated secretory pathway in neuroendocrine cells. Front. Endocrinol. **5**:48. doi: 10.3389/fendo.2014.00048*
This article was submitted to Neuroendocrine Science, a section of the journal Frontiers in Endocrinology.

frontiers in
ENDOCRINOLOGY

REVIEW ARTICLE
published: 28 March 2013
doi: 10.3389/fendo.2013.00041

Morpho-functional architecture of the Golgi complex of neuroendocrine cells

Emma Martínez-Alonso[1], Mónica Tomás[2] and José A. Martínez-Menárguez[1]*

[1] *Department of Cell Biology and Histology, Medical School, University of Murcia, Murcia, Spain*
[2] *Department of Human Anatomy and Embryology, Medical School, Valencia University, Valencia, Spain*

Edited by:
Rafael Vazquez-Martinez, University of Cordoba, Spain

Reviewed by:
Maite Montero-Hadjadje, INSERM U982, France
David Cruz-Garcia, Centre for Genomic Regulation, Spain
Gustavo Egea, University of Barcelona, Spain

***Correspondence:**
José A. Martínez-Menárguez, Department of Cell Biology and Histology, Medical School, University of Murcia, 30100 Murcia, Spain.
e-mail: jamartin@um.es

In neuroendocrine cells, prohormones move from the endoplasmic reticulum to the Golgi complex (GC), where they are sorted and packed into secretory granules. The GC is considered the central station of the secretory pathway of proteins and lipids en route to their final destination. In most mammalian cells, it is formed by several stacks of cisternae connected by tubules, forming a continuous ribbon. This organelle shows an extraordinary structural and functional complexity, which is exacerbated by the fact that its architecture is cell type specific and also tuned by the functional status of the cell. It is, indeed, one the most beautiful cellular organelles and, for that reason, perhaps the most extensively photographed by electron microscopists. In recent decades, an exhaustive dissection of the molecular machinery involved in membrane traffic and other Golgi functions has been carried out. Concomitantly, detailed morphological studies have been performed, including 3D analysis by electron tomography, and the precise location of key proteins has been identified by immunoelectron microscopy. Despite all this effort, some basic aspects of Golgi functioning remain unsolved. For instance, the mode of intra-Golgi transport is not known, and two opposing theories (vesicular transport and cisternal maturation models) have polarized the field for many years. Neither of these theories explains all the experimental data so that new theories and combinations thereof have recently been proposed. Moreover, the specific role of the small vesicles and tubules which surround the stacks needs to be clarified. In this review, we summarize our current knowledge of the Golgi architecture in relation with its function and the mechanisms of intra-Golgi transport. Within the same framework, the characteristics of the GC of neuroendocrine cells are analyzed.

Keywords: golgi complex, neuroendocrine cells, morphology, transport vesicles, tubules, intra-golgi transport

INTRODUCTION

A century ago the Italian anatomist Camillo Golgi described a new organelle that nowadays bears his name, the Golgi apparatus or Golgi complex (GC) (Golgi, 1898). Using a silver impregnation method, the "black reaction," he found a reticular structure in neurons that he called "apparato reticolare interno." Due to the difficulties and variability inherent to the technique, it was not clear for decades whether this structure was anything more than an artifact. The electron microscope clearly demonstrated that, the GC is indeed a real organelle, which is composed of flattened cisternae surrounded by tubules and vesicles (Dalton and Felix, 1956). These first ultrastructural images obtained from ultrathin sections showed the exceptional complexity of the organelle and, consequently, high voltage electron microscopy and stereology were used to obtained 3D information (Rambourg et al., 1974). Ultrastructural immunocytochemical methods provide great impetus to the morpho-functional analysis of the GC through the precise location of key molecular components (Rabouille and Klumperman, 2005). Electron tomography has increased our knowledge of the 3D architecture of the GC (Ladinsky et al., 1999). Another advance has been the use of correlative light-electron microscopy, whereby cell organelles are visualized first by light microscopy in living cells transfected with fluorescent proteins, and then the same structures are identified under the electron microscope (Polishchuk et al., 2000; Mironov et al., 2008; van Rijnsoever et al., 2008). The combination of immunoelectron microscopy and electron tomography is a powerful approach for scrutinizing the secrets of this organelle (Zeuschner et al., 2006). In parallel to morphological approaches, biochemical and genetic analyses have described in detail the molecular machineries operating in the secretory/endocytic pathways.

The GC has two main functions. The first is the post-translational modification of proteins and lipids arriving from the endoplasmic reticulum (ER), mainly their glycosylation. The second function is the concentration, packing, and export of these modified products to the final destination in or outside of the cell. Thus, the GC is at the same time an efficient glycan factory and a post office. Helping to carry these functions is a surprisingly complex array of membranes equipped with an accurate machinery. Despite the large volume of incoming and outgoing traffic, it is able to maintain its architecture, although it is also flexible enough to disassemble and reassemble under certain conditions, such as mitosis. In neuroendocrine cells, prohormones are frequently glycosylated and proteolytically processed before being sorted into secretory granules (reviewed in Vázquez-Martínez et al., 2012). A summary of the current knowledge on the morphology of this

organelle and early steps of the secretory pathway (i.e., ER-Golgi and intra-Golgi transport) is given below. Post-Golgi events, such as secretory granule formation, and other aspects of the Golgi functions are omitted in this description and can be found in excellent reviews elsewhere.

MORPHOLOGY OF THE GOLGI RIBBON

In mammalian cells, this organelle consists of a pile of flat, disk-like membranes, the cisternae (**Figures 1–3**). This pile of cisternae is called the Golgi stack. The number of cisternae per stacks varies between different organisms but is characteristic of each species, usually numbering between 3 and 11 (Rambourg and Clermont, 1997). The diameter of the cisternae is also cell type-dependent, and is usually 0.5–1 μm (Weidman et al., 1993). The lumen of the cisternae is usually quite narrow (10–20 nm), allowing the interaction of the glycosylation enzymes present in its membranes and the cargo. Typically, cisternae are of uniform thickness in the central part but dilated near the lateral rims. In secretory cells, cisternae may show distensions filled with a material of low electron density, known as pro-secretory granules. These elements can be observed in the trans side alone (prolactin cells) or in all the cisternae, although, in the latter case, their size increases in the trans direction (Rambourg and Clermont, 1997). Cisternae may show small (fenestrae) and large holes, which are sometimes aligned to form wells (Ladinsky et al., 1999). Usually, such wells are filled with vesicles and exposed to both the cis and lateral sides of the stacks (Ladinsky et al., 1999). Fenestrations are less abundant in the medial cisternae of the stack and increase in both cis and trans directions.

Early histochemical and immunoelectron microscopical analysis demonstrated that the Golgi stack is polarized. Thus, based on the distribution of resident proteins, the Golgi stack can be divided into three regions: cis, medial, and trans. Glycosyltransferases, sugar nucleotide transporters, and many other Golgi proteins are preferentially found in one of these sub compartments. However, the resident proteins are not restricted to a few cisternae, but exhibit a gradient of concentration through out the cisternae of the stack, suggesting a state of dynamic equilibrium (Rabouille et al., 1995).

The GC of most mammalian cells is formed of several stacks that are laterally interconnected by tubules forming the Golgi ribbon (Rambourg et al., 1979; Rambourg and Clermont, 1997; Marsh et al., 2001) (**Figures 1** and **2A**). Thus, although it is not always apparent, the stacks observed in typical electron microscopic images of the Golgi area, belong to the same ribbon. Due to their appearance, the pile of cisternae and the lateral tubular network are called the compact and non-compact zones, respectively. Usually, the tubules connect cisternae located in the same positions in the respective stacks. However, heterotypic connections, even between the cis-most and trans-most cisternae of adjacent stacks,

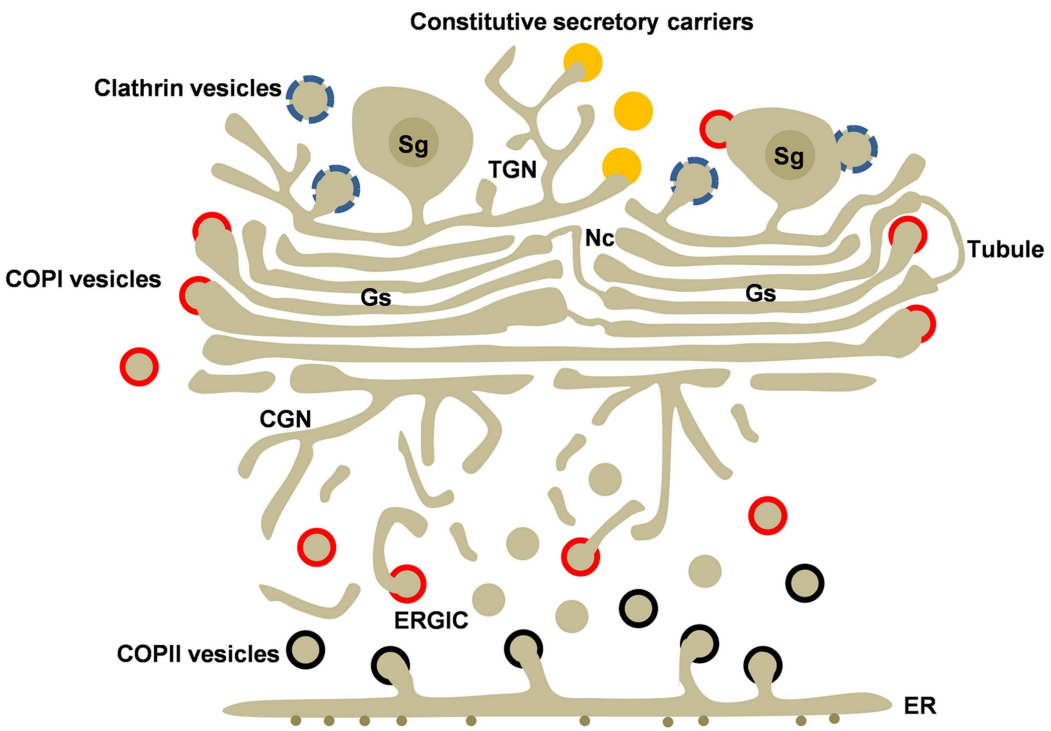

FIGURE 1 | Golgi structure and transport carriers in secretory cells. The Golgi ribbon is formed by adjacent Golgi stacks (Gs) separated by non-compact regions (Nc) containing tubules and vesicles. Golgi stacks are connected to the cis and trans Golgi networks (CGN and TGN). Newly synthesized cargo leaves the endoplasmic reticulum (ER) by COPII-coated vesicles (black). COPI-coated (red) vesicles mediate recycling from the Golgi and the ERGIC. Transport carriers at the TGN include clathrin-coated vesicles (blue), regulated secretory granules (Sg), and the poorly understood constitutive secretory carriers (orange) Clathrin and COPI coats are also associated to secretory granules. Heterotypic and homotypic tubular connections between cisternae may be involved in anterograde and/or retrograde intra-Golgi transport.

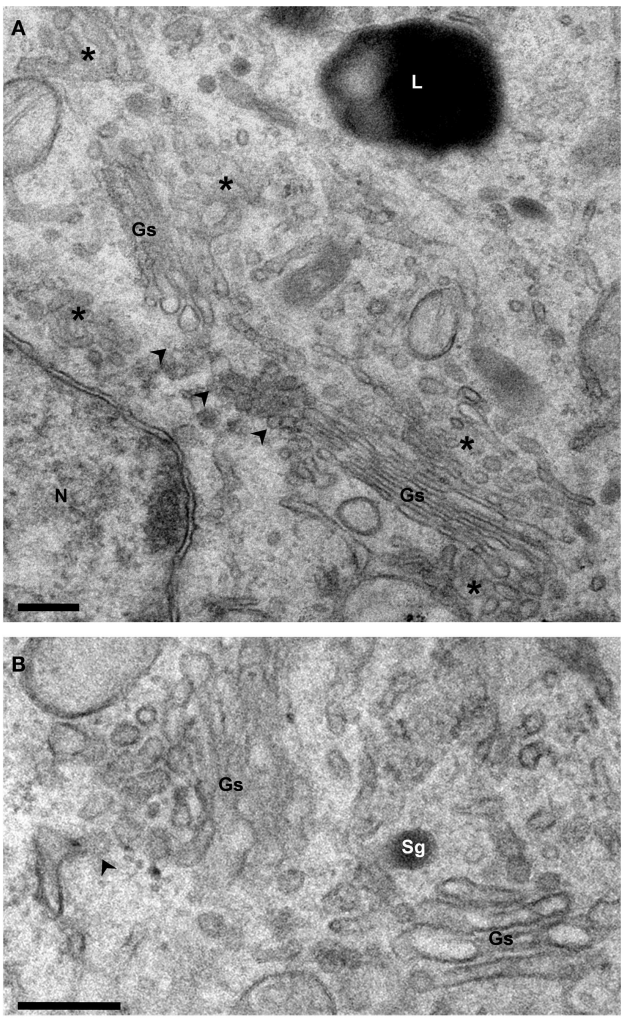

FIGURE 2 | Structure of the Golgi ribbon. Electron micrographs of Epon-embedded PC12 cells. **(A)** The Golgi stacks (Gs) are surrounded by tubule-vesicular elements (asterisks). Arrowheads point to the non-compact area of the ribbon which connects the stacks laterally. **(B)** The cis and trans sides of the stacks are identified by the presence of ER exit sites (arrowhead) and secretory granules (Sg), respectively. Gs, Golgi stack; L, Lysosome; N, Nucleus. Bars, 200 nm.

are abundant in some cell types (Rambourg and Clermont, 1997; Vivero-Salmerón et al., 2008). Frontal views of cisternae point to lateral networks of tubules emerging from the fenestrated rims (Weidman et al., 1993). Some of these tubular membranes fuse with the same cisterna, whereas others grow toward the cytoplasm. A single cisterna may have tubules oriented toward the cis and trans sides (Ladinsky et al., 1999). Many tubules, however, extend laterally and fuse with tubules from adjacent Golgi stacks, forming the tubular network that bridges adjacent stacks.

Usually, the ribbon is located close to the nucleus, around the microtubule organizing centers (MTOC), and the spatial configuration of the GC is closely related to the arrangement and orientation of the microtubules. The maintenance of the Golgi ribbon strongly depends on the microtubules and the action of motor proteins (Egea and Rios, 2008). Microtubule de-polymerizing agents such as nocodazole induce fragmentation of the ribbon into mini stacks (Storrie et al., 1998). In fact, the GC acts as a secondary MOTC. Golgi organization also depends on the actin cytoskeleton (Egea et al., 2006).

The structure of the ribbon is also supported by the so-called Golgi matrix, a ribosome-free area surrounding the cisternae (Xiang and Wang, 2011). This matrix can be visualized as small fibers connecting the cisternae (Mollenhauer and Morre, 1998) and also connecting the Golgi membranes and transport vesicles (Orci et al., 1998). The matrix is formed by structural proteins, some of them identified as auto-antigens and others isolated from detergent-insoluble salt-resistant Golgi fractions (Slusarewicz et al., 1994). These components include Golgi reassembly stacking proteins (GRASPs) and golgins (Xiang and Wang, 2011). These proteins are very dynamic and cycle between membrane-associated and a cytoplasmic forms.

The morphology of the GC (the number of cisternae per stack, the number of fenestrations, the complexity of associated tubule-vesicular elements, etc.) is cell type specific and depends on the activity of the cell. The level of cargo reaching the GC is an important factor in Golgi appearance. In general, when the input of cargo is low, the GC decreases in size and becomes larger when the synthetic activity is stimulated (Clermont et al., 1993; Taylor et al., 1997; Aridor et al., 1999; Glick, 2000). The relationship between cell activity and Golgi organization was clearly shown in prolactin cells. When the activity of these cells is reduced by removing the litters from lactating rats, the number of cisternal fenestrations and peri-Golgi vesicles increases concomitantly with a reduction in the number of Golgi tubules and mature secretory granules (Rambourg et al., 1993).

CIS AND TRANS GOLGI NETWORK

The Golgi stack is flanked by two tubule-vesicular networks located at the cis and trans sides, which represent the entry and exit sides of the stack, respectively (**Figure 1**). At the cis-side, the cis-Golgi network (CGN) is involved in ER-Golgi transport. At the trans side, the trans Golgi network (TGN) receives and packs proteins and lipids that have traversed the stack and deliver them to their final destinations.

The CGN is formed of tubules connected to the first Golgi cisterna (Sesso et al., 1994; Rambourg and Clermont, 1997). This element is well developed in some cell types such as spermatids (Vivero-Salmerón et al., 2008) but less so in others, such as prolactin cells (Rambourg and Clermont, 1997). In early electron microscopical studies, these tubules were selectively identified by using reducing osmic for prolonged times. The functional relationship of this tubular network connected to the stack (the CGN) and ER-derived pre-Golgi elements [intermediate compartment (IC), see below] remains to be established.

Trans Golgi network is involved in the final steps of protein glycosylation and maturation and in the sorting of products to the apical and basolateral plasma membranes, early and late endosomes, and secretory granules (Griffiths and Simons, 1986; Keller and Simons, 1997; De Matteis and Luini, 2008). In neuroendocrine cells, the secretory proteins are concentrated in secretory granules that can be rapidly released after stimulation (Kelly, 1985). This

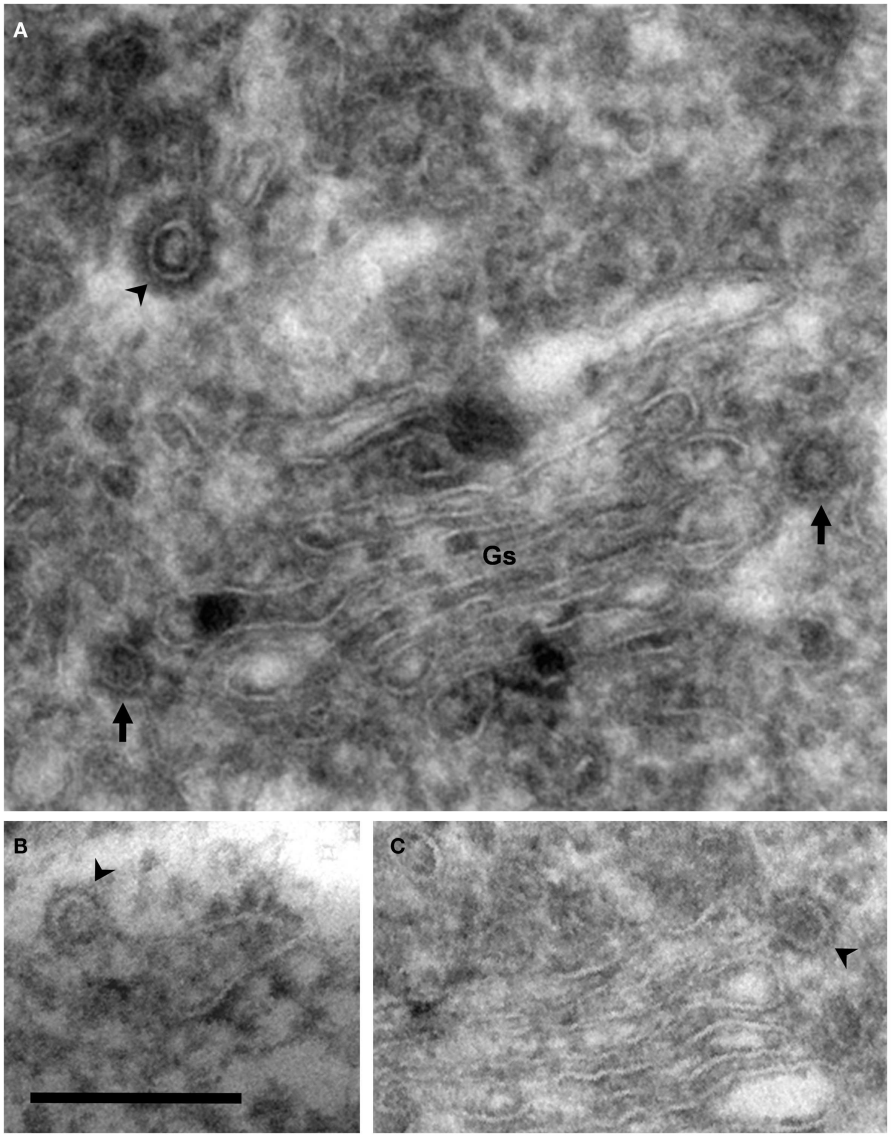

FIGURE 3 | Coated vesicles and buds. Electron micrographs of cryosections of PC12 cells. Using this methodology, membranes appear negatively stained, whereas coats are identified as electron dense areas around vesicles and buds. **(A)** COP- (arrows) and clathrin-coated (arrowhead) vesicles are observed in the lateral and trans Golgi sides, respectively. Note the different thickness of these coats. **(B)** COPII-coated bud associated to the endoplasmic reticulum (arrowhead). **(C)** COPI-coated bud in the lateral rim of cisterna (arrowhead). COPII- and COPI-coated buds are identified by their locations because the thickness of these coats is identical. Bar, 200 nm.

regulated secretory pathway co-exists with the constitutive secretory pathway that is common to all cell types (Arvan and Castle, 1998). The sorting process can take place in the TGN (sorting-for-entry) or in immature secretory granules (sorting-by-retention) (Borgonovo et al., 2006). Different carriers and associated molecular machineries may be used for different routes (Traub and Kornfeld, 1997). Structurally, the TGN is formed of a large tubular network in continuity with the trans-most cisterna of the Golgi stack (Griffiths et al., 1985; Clermont et al., 1995). This is not always evident and, in some cell types, TGN can be found some distance from the stack (Clermont et al., 1995). The TGN can vary significantly in both size and composition, depending on the amount and type of cargo, and is reduced or absent in cells producing secretory granules in contrast with cells with an extensive lysosomal system (Clermont et al., 1995).

VESICLES

The Golgi stack is surrounded by a high number of 50–100 nm vesicles, the smallest ones at the cis-side and lateral rims, and the largest ones at the trans side (Marsh et al., 2001). Many of these vesicles have a coat, an electron dense proteinaceous layer on the cytoplasmic leaflets of their membranes (**Figure 3**). These coats are also found in certain areas of the secretory/endocytic compartments, which represent forming vesicles. Three types of

coat complex (COPI, COPII, and clathrin) have been identified and characterized. COPI- and COPII-coated vesicles are almost identical under the electron microscope. The overall size and coat thickness are 50–60 and 10 nm, respectively. COPII-coated buds are restricted to the ER, while COPI-coated buds are found in pre-Golgi and Golgi membranes (Griffiths et al., 1985; Oprins et al., 1993; Orci et al., 1997; Martinez-Menárguez et al., 2001; Rabouille and Klumperman, 2005). The trans-most cisternae of the Golgi and the TGN contains another type of coat, the clathrin coat (Pearse and Robinson, 1990) which is also found in the plasma membrane and endosomes. Clathrin-coated vesicles are unambiguously identified by their size (100 nm) and the thickness of the coat (18 nm) (Orci et al., 1984; Heuser and Kirchhausen, 1985; Kirchhausen et al., 1986; Oprins et al., 1993; Ladinsky et al., 2002). Interestingly, clathrin and COPI coats are also observed in forming secretory granules (Martínez-Menárguez et al., 1999).

Vesicles represent the best known type of transport intermediate. A huge amount of information has been accumulated on the molecular machinery involved in regulation of intercompartmental transport in the secretory pathway. Most data refer to vesicles as transport carriers but it can be assumed that the same or similar mechanisms operate in other carriers. While the formation of vesicles and the selection of cargo depend on the coat machinery, the specific targeting and fusion of the carriers with the target membranes depend on tethering factors, Rab and SNARE (soluble *N*-ethylmaleimide-sensitive factor attachment protein receptors) proteins, and other accessory proteins (Bonifacino and Glick, 2004).

SNARE proteins are involved in docking and the specific fusion of transport intermediates with the target membranes (Bonifacino and Glick, 2004; Hong, 2005; Jahn and Scheller, 2006). The SNAREs associated with vesicles (or other transport intermediates) and target membranes have been named v- and t-SNARE, respectively. SNAREs have also been divided into R- and Q-SNAREs, according to the central residue (R/Gln or Q/Arg, respectively) of the SNARE domain, a conserved region of 60–70 residues found in all members of this family. Commonly, v-SNARE and t-SNARE are R-SNARE and Q-SNARE, respectively. Interaction between one v-SNARE and two/three t-SNAREs induces the formation of the trans-SNARE complex, which catalyzes the fusion of the membranes. After fusion, a cis-SNARE complex is formed in the target membrane, which is later disassembled by the action of the cytosolic proteins α-SNAP (soluble *N*-ethylmaleimide-sensitive factor attachment protein) and the ATPase NSF (*N*-ethylmaleimide-sensitive factor). Now, v-SNARE can be transported back to the donor compartment to be reused. SNARE proteins are sufficient to drive membrane fusion so that they are considered the minimal membrane fusion machinery. Two SNARE complexes have been implicated in intra-Golgi transport (Malsam and Söllner, 2011). One complex is formed of v-SNARE GS15 and the t-SNAREs syntaxin5, GOS28, and Ykt6, and is involved in COPI-dependent intra-Golgi transport. The second complex is formed of v-SNARE rBet1 and the t-SNAREs syntaxin 5, membrin (GS27), ERS24/Sec22. This second complex has also been implicated in ER-to-Golgi and intra-Golgi transport (Volchuk et al., 2000). SNARE complex assembly is regulated by SM (Sec1/Munc18) proteins, a family of cytosolic proteins. Sly1 I is the only member of this family operating in the ER-Golgi area (Laufman et al., 2009), whereas Munc18-1 is involved in the exocytosis of dense-core granules in neuroendocrine cells (Burgoyne et al., 2009).

Rab proteins are a family of small GTPases that regulate membrane transport by recruiting effectors, including sorting adaptors, tethering factors, kinases, phosphatases, and motor proteins (Jahn and Scheller, 2006; Stenmark, 2009). Rab proteins switch between an active form (GTP-bound) and a cytosolic inactive form (GDP-bound). They have been implicated in vesicle budding, uncoating, mobility, and transport. Rab proteins in the GTP-bound form are reversibly associated with membranes by geranylgeranyl groups. The replacement of GDP by GTP is facilitated by guanine nucleotide exchange factors (GEFs), and their low intrinsic GTPase activity is enhanced by GTPase-activating proteins (GAP). Rab protein is a large family, including more than 60 members in humans, which are specifically associated with distinct compartments and transport events (Stenmark, 2009). Interestingly, the specific membrane recruitment of Rabs has recently been demonstrated to depend on the activity of GEFs (Blümer et al., 2013). The Golgi-associated Rab family playing a key role in Golgi maintenance and functioning includes Rab1, Rab2, Rab6, Rab33B, Rab18, and Rab43 (Liu and Storrie, 2012). Rab3 (A–D), Rab11, Rab18, Rab26, Rab27 (A,B), and Rab37 are involved in regulated secretion (Fukuda, 2008; Stenmark, 2009). Rab3A, Rab11, Rab18, and Rab27A regulate exocytosis in neuroendocrine cells by interacting directly with secretory vesicles (Vázquez-Martínez and Malagón, 2011). A few GEFs and GAPs for secretory Rabs have been identified. The specific role of secretory Rabs in the formation and maturation of the secretory vesicles, and their docking and fusion with the plasma membrane, remains controversial.

Tethering factors are a group of membrane-associated proteins or multi-subunit complexes that link transport vesicles with the target membranes to ensure correct docking and fusion. In addition to tethering, they play a role in Golgi stacking and form the Golgi matrix. They have been classified into three classes: oligomeric complexes that work as Rab effectors and bind SNARE, oligomeric complexes that function as GEFs for Rab proteins and, finally, coiled-coil tethers (Sztul and Lupashin, 2009). Golgi-associated members of the last group are called golgins. The golgin family includes p115, a protein believed to be involved in tethering COPII vesicles to pre-Golgi membranes, transport from these elements to the cis-Golgi and intra-Golgi transport. GM130 is another coiled-coil protein associated with the cis-Golgi. GM130 and p115 are also components of the Golgi matrix. Apart from their role as tethers, they are involved, together with other members of the golgin and GRASP families such as giantin and GRASP65, in maintaining the stacked morphology of the cisterna and the Golgi ribbon (De Matteis et al., 2008). NECC1 (neuroendocrine long coiled-coil protein 1) is a new component of this family, which is mainly present in neuroendocrine tissues (Cruz-Garcia et al., 2007). NECC1 is the first long coiled-coil protein described that has a role as a negative modulator of the regulated secretion in neuroendocrine cells (Cruz-García et al., 2012). Dsl1, conserved oligomeric Golgi (COG), and transport protein particle (TRAPP) are multi-subunit complexes associated with the GC (Sztul and Lupashin, 2009). Dsl1 is a three unit complex involved

in Golgi-to-ER transport, where it acts to tether COPI vesicles. The COG complex formed of eight subunits (Cog1–8) found at the cis and medial Golgi cisternae is believed to be involved in transport to the Golgi and the intra-Golgi recycling of Golgi resident proteins (Miller and Ungar, 2012). TRAPP is another multi-subunit complex that works as tethering factor (Sacher et al., 2008). At least two TRAPP complexes exist in mammals. TRAPPI tethers COPII-coated vesicles and mediates ER-to-Golgi transport (Barrowman et al., 2010). TRAPII has been involved in intra-Golgi transport, post-Golgi traffic, endosome-to-Golgi, and autophagy (Yu and Liang, 2012). They work as GEF for Rab1 and the activation of this GTPase might recruit other tethers (Sztul and Lupashin, 2009).

Some lipidic species, such as diacylglycerol, phosphatidic acid and lysophosphatidic acid, and enzymes associated with their metabolism play a key role in carrier formation by regulating the curvature of membranes. Diacylglycerol has been implicated in the formation of post-Golgi carriers and is necessary to recruit protein kinase D, a regulator of the fission of transport carriers (Bard and Malhotra, 2006). Diacylglycerol has also seen to be involved in Golgi-to-ER retrograde transport mediated by tubules (Fernández-Ulibarri et al., 2007). Phosphatidic acid, which is generated by phospholipase D2, is involved in COPI vesicle formation (Yang et al., 2008). This phospholipid is necessary to maintain the structure of the GC and secretion in neuroendocrine cells (Siddhanta et al., 2000). Lysophosphatidic acid generated by the enzyme phospholipase A2 has been involved in the retrograde transport mediated by tubules (de Figueiredo et al., 2000; Brown et al., 2003). This enzyme is involved in the formation of tubular continuities between cisternae (San Pietro et al., 2009) and tubular transport intermediates at the TGN (Schmidt et al., 2010). Interestingly, two lipid-modifying enzymes, lysophosphatidic acid acyltransferase γ and phospholipase A2-α, which promote or inhibit COPI fission, respectively, work together, regulating the morphology of Golgi carriers (vesicles vs. tubules) (Yang et al., 2011).

THE GOLGI COMPLEX OF NEUROENDOCRINE CELLS

The hypothalamus-hypophysis system is the most important and well-known neuroendocrine system. Important clues on Golgi functioning have been obtained by studying the GC of the pituitary gland. In addition, neuroendocrine cell lines, such as corticotropic tumor AtT20, pheochromocytoma PC12, and frog melanotrope cells, provide important clues as regards secretory granule formation and regulation (Morvan and Tooze, 2008). Thus, the discovery that immature secretory granules originated from Golgi cisternae was made in mammotroph cells (Farquhar, 1961). In the same cell type it was also found that that there is a step during which secretory material is condensed in the GC (Smith and Farquhar, 1966). AtT20 cells have been used to show that there are different routes from the GC to the plasma membrane (Gumbiner and Kelly, 1982). However, detailed morphological studies of the Golgi ribbon of neuroendocrine cells, with some exceptions, are scarce. The morphology of the GC and the formation of secretory granules in prolactin cells were described in early microscopic studies. In these cells, the Golgi ribbon forms a hollow sphere in the perinuclear area. The stacks of prolactin cells have four to five (mostly flattened) cisternae and show a reduced CGN and TGN (Rambourg and Clermont, 1997). The trans cisternae show distensions that are gradually transformed into tubular progranules at the trans face and are finally condensed into compact polymorphous granules (Clermont et al., 1993). As indicated above, the morphology of this compartment is strongly dependent on cell activity (Rambourg et al., 1993). Many other cells of the anterior pituitary gland have not been extensively studied, although some of these cell types have a spherical GC, with cis and trans side representing the outer and inner part of this sphere, respectively (Watanabe et al., 2012).

ER-TO-GOLGI TRANSPORT

Newly synthesized proteins and lipids in general, and prohormones in neuroendocrine cells, exit the ER in specific places of this compartment, called ER exit sites (ERES). These places are formed by tubular buds of different length containing a COPII coat (Sesso et al., 1994; Bannykh et al., 1996; Zeuschner et al., 2006), which assists in the deformation of ER membranes into vesicles containing membrane and soluble cargo *en route* to the GC (Barlowe et al., 1994). The COPII coat complex is formed of five soluble proteins: Sec23, Sec24, Sec13, Sec31, and Sar1 (Barlowe et al., 1994; Bickford et al., 2004). Formation of the COPII coat begins with the recruitment of the GTPase Sar1 in ER membranes. This binding depends on the activation of this GTPase by Sec12, a GEF present in ER membranes (Jensen and Schekman, 2011). During this process some proteins are selectively recruited into COPII vesicles (Barlowe, 1998, 2003), whereas others enter unspecifically, a process known as bulk flow (Martínez-Menárguez et al., 1999). Sorting of the transmembrane cargo depends on Sec24 (Mancias and Goldberg, 2008). The soluble cargo present in the lumen of the ER binds to cargo receptors, such as ER-Golgi IC (ERGIC)-53, p24, and the Erv families (Szul and Sztul, 2011). These cargo receptors cycle between the ER and Golgi and also are included in recycling COPI vesicles. The p24 family comprises 8–10 isoforms and a subset of these proteins is up-regulated, together with proopiomelanocortin, after the activation of neuroendocrine frog melanotrope cells (Strating et al., 2011). The size of COPII vesicles is regulated by ubiquitination of Sec31, allowing the formation of large COPII vesicles (Jin et al., 2012). After formation, COPII vesicles are quickly uncoated and fuse to each other to form the so-called ERGIC, IC, or vesicular-tubular clusters (VTCs), the first of these being the most used (Hauri and Schweizer, 1992; Farquhar and Hauri, 1997). This compartment was initially identified as tubule-vesicular membranes in which the cargo accumulates when cells are cultured at low temperatures (15°C) (Saraste and Kuismanen, 1984; Schweizer et al., 1990). This compartment is located close to the GC and is also distributed throughout the cell (Lotti et al., 1992; Klumperman et al., 1998), and is associated to ERES (Bannykh et al., 1996). ERGIC is formed by vesicles and tubules, sometimes branched (Bannykh et al., 1996). Although adjacent to the ERES, ERGIC is an independent compartment and there is no continuity between them (Bannykh et al., 1998). ERGIC membranes do not have COPII coats but another type of coat complex, the COPI coat, which is involved in retrograde transport (see below). Thus, the presence of these coats can be used to discriminate between these closely related compartments. Whether the ERGIC is a stable compartment or a transitory element moving toward the GC is still a matter of debate (Ben-Tekaya et al.,

2005). The fact that all the proteins associated with this compartment cycle between the ER and Golgi argues against the idea that it is a stable compartment. ERGIC-53, a type I transmembrane protein of the lectin family, is the prototypical marker of this compartment (Zhang et al., 2009). However, *in vivo* experiments showed that ERGIC-53 is located in long-lived stationary elements connected by highly mobile elements (Ben-Tekaya et al., 2005), supporting the view that ERGIC is a stable compartment. ERGIC elements or ERGIC-derived carriers move to the Golgi area along the microtubule track guided by dynein motors, where they may fuse to each other to form the CGN or, conversely, fuse with a pre-existing cisterna (Presley et al., 1997).

GOLGI-TO-ER TRANSPORT

Organelle identity is determined by its composition, and its functional integrity is due to its ability to maintain this composition despite the continuous traffic between compartments. An important mechanism involved in this process is retrograde transport. In the early secretory pathway, ERGIC is the first place where this process occurs. Here, the presence of COPI coats ensure the recycling of proteins to the ER while anterograde cargo is separated and concentrated (Scales et al., 1997; Klumperman et al., 1998; Martínez-Menárguez et al., 1999; Shima et al., 1999; Stephens et al., 2000). The function of the COPI coats in the Golgi-to-ER retrograde transport of soluble and membrane proteins has been convincingly demonstrated (Letourneur et al., 1994). However, there are retrograde routes to the ER independent of COPI (Girod et al., 1999). It is also possible that a population of COPI vesicles is involved in anterograde transport across the Golgi stack (Orci et al., 1997).

COPI-coated vesicles are found in peripheral and central ERGIC elements, at cis and lateral Golgi sides (Oprins et al., 1993) and, occasionally, at the trans Golgi side/TGN (Martínez-Menárguez et al., 1996). COPI-coated buds are observed at the lateral rims of cisternae, decreasing in number in a cis to trans direction (Ladinsky et al., 1999). COPI coats are formed of seven subunits (α, β, β', γ, δ, ε, ζ-COP) assembled in the cytosol, the coatomer, and small GTPase ADP-ribosylation factors (Arf1). Arf1 belong to the Arf family, which is made up of six members in mammals (D'Souza-Schorey and Chavrier, 2006). Arfs 1–5 have been described at the ER-Golgi interface, where they may have redundant functions. Besides, it has been suggested that different pairs of Arfs may be necessary for each transport step (Volpicelli-Daley et al., 2005). Arf1 and 4 and Arfs 3–5 are associated to the cis and trans Golgi sides, respectively (Donaldson and Jackson, 2011). Arf 4 and 5 interact with calcium-dependent activator for secretion (CASP), regulating the formation of neuroendocrine secretory granules (Sadakata et al., 2010). Arf1-GDP is recruited to membranes by p23, a member of the p24 family (Gommel et al., 2001), and, once there, it is activated by a GEF. GTP-bound Arf1 is able to recruit coatomer *en bloc* to membranes. At the ERGIC and Golgi membranes, GBF1 (Golgi-associated BFA-resistant protein) is the major GEF for ARF1 during COPI vesicle formation and is the target of the drug brefeldin A (Kawamoto et al., 2002; Garcia-Mata et al., 2003), while Big1 and Big2 (BFA-inhibited GEF) are described as GEFs for Arf1 in the TGN and endosomes (Ishizaki et al., 2008). ArfGAPs stimulate the GTP hydrolysis of Arf, which has low intrinsic GTPase activity (Inoue and Randazzo, 2007). It has been postulated that this reaction triggers uncoating (Tanigawa et al., 1993); however, ArfGAP1 has also been described as a coatomer component and also as a sensor of membrane curvature, so the role of this protein is under discussion (Shiba and Randazzo, 2012). ArfGAP1, phosphatidic acid generated by phospholipase D and BARS (brefeldin A-ribosylated substrate) have been implicated in COPI vesicle fission (Yang et al., 2008).

Many transmembrane proteins transported into COPI vesicles bear di-lysine motifs at their C-terminus (Letourneur et al., 1994), including ERGIC-53 (Schindler et al., 1993). The coatomer subunits, α- and β'-COP, directly bind this signal (Jackson et al., 2012). The p24 family of proteins is recruited by direct interaction of their cytoplasmic tail, which contains phenylalanine- and di-lysine-based signals, with γ-COP (Nickel et al., 1997; Béthune et al., 2006). Not all cargo incorporated in COPI vesicles has this sorting signal so that the cargo may require adaptors. This is the case with glycosylation enzymes (Popoff et al., 2011). One example of an adaptor for soluble proteins is the KDEL receptor, a transmembrane protein mostly present in the cis-Golgi and ERGIC, which interacts with the coatomer through a di-lysine motif in the cytosolic tail, whereas the luminal part interacts with soluble proteins bearing a K-D-E-L sequence found in many ER-resident proteins (Semenza et al., 1990; Majoul et al., 2001). In this way, soluble proteins that have escaped from the ER are retrieved.

As indicated above, it is possible that there are several subpopulations of COPI vesicles with different compositions and locations, each carrying out its specific functions (Moelleken et al., 2007). Indeed, γ and ζ-COP present two isoforms localized differently along the GC, enabling the existence of four types of coatomer, which may act in different routes and types of cargo (Popoff et al., 2011). Thus, this coat conforms versatile vesicles that may play different roles at the ER-Golgi interface (Orci et al., 1997; Shima et al., 1999; Malsam et al., 2005).

INTRA-GOLGI TRANSPORT

Once cargo has reached the GC, the manner in which it moves through the stack remains controversial, and two classical models have been proposed: vesicular transport and cisternal maturation. The first proposes that Golgi cisternae are static so that the cargo must use vesicles to move. The second model proposes that cisternae are dynamic structures that move from the cis to trans Golgi sides. Thus, according to this model, the entire cisterna is the carrier. The postulated roles of COPI vesicles in vesicular and cisternal maturation models are completely different, since they are regarded as being responsible for anterograde and retrograde transport, respectively.

Launched by Palade (1975), the vesicular transport model postulates that cisternae are stable compartments. Thus, cargo must leave one cisterna and move to an adjacent one in order to advance through the stack. This process is mediated by COPI vesicles. For decades this model was widely accepted since it was based on new experimental data, especially the analysis of cell-free systems and immunomicroscopical studies (Rothman and Fine, 1980; Orci et al., 1986; Barlowe et al., 1994). It provided a good explanation for the well-known compartmentalization of the Golgi resident enzymes (Roth and Berger, 1982; Dunphy et al., 1985). Besides,

it was strongly supported by the discovery of COPI and COPII vesicles which, it was postulated, act sequentially in the early secretory pathway (Rothman and Wieland, 1996). It was clearly demonstrated that COPII vesicles are involved in ER exit (Barlowe et al., 1994), while COPI were identified in *in vitro* assays as being responsible for anterograde transport between cisternae (Orci et al., 1986). However, this model was questioned when a clear role for COPI vesicles in retrograde transport was demonstrated (Cosson and Letourneur, 1994; Letourneur et al., 1994). Even so, the model remained in force even when two types of COPI vesicle were seen to be involved in anterograde and retrograde transport in the Golgi stack (Orci et al., 1997). The weakest point of this model is that it does not explain how large cargo is transported.

A cisternal maturation model was postulated by Grasse (1957) based on early electron microscopy observations, but it was not until the early 1990s that it was re-considered (Bonfanti et al., 1998; Glick and Malhotra, 1998). According to this model, cisternae are formed at the cis-side of the GC by fusion of ER-derived membranes and then these newly formed cisternae move from the cis to the trans side. This model fits very well with the observation that the Golgi resident enzymes are not strictly compartmentalized through the Golgi stack (Nilsson et al., 1993; Rabouille et al., 1995). Furthermore, this model is able to explain the transport of large cargo, such as procollagen (300 nm rigid rod) (Bonfanti et al., 1998) or algal scales (up to 1.5–2 μm) (Melkonian et al., 1991), which do not fit within 50–60 nm vesicles. During cisternal progression, Golgi resident enzymes must be packed into COPI vesicles and transported backwards. Thus, Golgi enzymes are not lost but recycled in a trans to cis direction, maintaining the polarity of the organelle (Glick et al., 1997). Immunocytochemical (Martinez-Menárguez et al., 2001; Mironov et al., 2001) and proteomic (Gilchrist et al., 2006) analyses of these vesicles showed that they are mostly devoid of anterograde transport markers but enriched in glycosylation enzymes. However, other studies on COPI vesicle composition provided conflicting results. Thus, the role of COPI vesicles remains controversial (Cosson et al., 2002). Life cell imaging studies in yeast involving direct real time visualization of cisternal maturation strongly support this model (Losev et al., 2006; Matsuura-Tokita et al., 2006).

Since neither of these models explains all the experimental data, a combination of the same models (dual model) as well as new models (rapid partitioning, kiss-and-run) have been proposed (reviewed in Glick and Luini, 2011). The cisternal maturation model seems to be more efficient, given that it seems easier to transport anterograde cargo using a large carrier (the cisterna) than to use many small vesicles between adjacent cisternae and repeat this process several times until reaching the TGN. However, these models are not mutually exclusive and a combination of both might serve (Pelham and Rothman, 2000). Cisternae may move slowly, whereas vesicles transport anterograde and retrograde cargo more rapidly. Large molecules may use the cisternal maturation mechanism, while small molecules can be transported using vesicular transport (Orci et al., 2000; Pelham and Rothman, 2000). In addition, other mechanisms might operate in this transport step as several new models postulate. According to the rapid partitioning model, the GC operates as a single compartment but contains processing and export domains of differing lipid composition, which allow the specific retention of resident enzymes and cargo proteins (Patterson et al., 2008). The cargo associates with these domains and then leaves the compartment from every level. However, this model has difficulty in explaining many previous observations including the well-known polarized distribution of glycosylation processing enzymes, the progression of procollagen and other cargo across the stack or the role of COPI vesicles. The kiss-and-run model, meanwhile, proposes that two cisternae may fuse to each other through narrow tubules, connecting their lumens transiently, and allowing the transit of anterograde and retrograde cargo before disconnection (Mironov and Beznoussenko, 2012). Given that specific retrograde transport is not necessary in this model, COPI might be involved in the fission process. It is also not clear how all the experimental data available concerning the role of COPI coats in retrograde transport fit this model.

Despite the abundance and development of Golgi-associated tubules, as described above, most models of intra-Golgi transport do not include a role for these elements. Tubules may act as intermediate transport carriers, alone or with vesicles, and in anterograde and retrograde transport (Griffiths, 2000; Mironov et al., 2003; Marsh et al., 2004; Trucco et al., 2004; Martínez-Alonso et al., 2005, 2007; Vivero-Salmerón et al., 2008). In fact, it has recently been found that a similar mechanism involving COPI and lipid-modifying enzymes may regulate the formation of both types of carrier in the GC (Yang et al., 2011). With some exceptions, intercisternal tubular connections are scarce in control cells but increase when secretory activity is stimulated (Marsh et al., 2004; Trucco et al., 2004), supporting the view that tubules may be involved in anterograde transport when there is an excess of cargo. In fact, it has been postulated that all secretory compartments are connected by tubules and the cargo moves along this pathway like food through the gut (Griffiths, 2000). Supporting this idea, although unusual, a Golgi stack formed by a single cisterna arranged helically and direct connections between the Golgi cisternae and the ER have been described (Tanaka et al., 1986). In order to clarify the role of tubules, it is first necessary to determine their composition, which is a difficult task. The number of tubules can be increased by the use of the fungal drug brefeldin A. Nowadays it is well accepted that brefeldin A-induced tubules are involved in Golgi-to-ER transport. Although this system is artificial, it is believed that brefeldin A intensifies a process that occurs naturally (Lippincott-Schwartz et al., 1990). Tubules can also be enhanced by lowering the temperature (Martínez-Alonso et al., 2005, 2007). These tubules exclude anterograde and retrograde cargo but recruit Golgi resident enzymes and a specific set of Rab and SNARE proteins involved in intra-Golgi transport (Martínez-Alonso et al., 2005, 2007). Thus, these induced tubules may be indicative of the recycling mechanisms of Golgi enzymes postulated by the cisternal maturation model.

CONCLUDING REMARKS

The GC has fascinated scientists for more than a century. Although it is without doubt the most photographed cell structure, it still retains most of its mystery. What is the reason for its beautiful architecture? Why does it form a ribbon in most cells? What are that the functions of the tubular networks? Do vesicles and tubules

have specific functions? Is there a single mode of intra-Golgi transport? Do COPI vesicles take part in anterograde transport? Is the ERGIC a real compartment? These and many other questions remain unanswered, which, in itself, is surprising, given the intense research and the large number of research groups working in the field. It is to be hoped that new approaches and research models will help fill the gaps in our knowledge of this beautiful organelle.

ACKNOWLEDGMENTS

The work in this review was supported by grants from the Ministerio de Ciencia e Innovación (Spain) Consolider COAT CSD2009-00016) and Fundación Séneca de la Comunidad Autónoma de la Región de Murcia (04542/GERM/06) to José A. Martínez-Menárguez and a grant from the University of Valencia (UV-INV-AE11-41831) to Mónica Tomás.

REFERENCES

Aridor, M., Bannykh, S. I., Rowe, T., and Balch, W. E. (1999). Cargo can modulate COPII vesicle formation from the endoplasmic reticulum. *J. Biol. Chem.* 274, 4389–4399.

Arvan, P., and Castle, D. (1998). Sorting and storage during secretory granule biogenesis: looking backward and looking forward. *Biochem. J.* 332(Pt 3), 593–610.

Bannykh, S. I., Nishimura, N., and Balch, W. E. (1998). Getting into the Golgi. *Trends Cell Biol.* 8, 21–25.

Bannykh, S. I., Rowe, T., and Balch, W. E. (1996). The organization of endoplasmic reticulum export complexes. *J. Cell Biol.* 135, 19–35.

Bard, F., and Malhotra, V. (2006). The formation of TGN-to-plasma-membrane transport carriers. *Annu. Rev. Cell Dev. Biol.* 22, 439–455.

Barlowe, C. (1998). COPII and selective export from the endoplasmic reticulum. *Biochim. Biophys. Acta* 1404, 67–76.

Barlowe, C. (2003). Signals for COPII-dependent export from the ER: what's the ticket out? *Trends Cell Biol.* 13, 295–300.

Barlowe, C., Orci, L., Yeung, T., Hosobuchi, M., Hamamoto, S., Salama, N., et al. (1994). COPII: a membrane coat formed by Sec proteins that drive vesicle budding from the endoplasmic reticulum. *Cell* 77, 895–907.

Barrowman, J., Bhandari, D., Reinisch, K., and Ferro-Novick, S. (2010). TRAPP complexes in membrane traffic: convergence through a common Rab. *Nat. Rev. Mol. Cell Biol.* 11, 759–763.

Ben-Tekaya, H., Miura, K., Pepperkok, R., and Hauri, H. P. (2005). Live imaging of bidirectional traffic from the ERGIC. *J. Cell Sci.* 118, 357–367.

Béthune, J., Kol, M., Hoffmann, J., Reckmann, I., Brugger, B., and Wieland, F. (2006). Coatomer, the coat protein of COPI transport vesicles, discriminates endoplasmic reticulum residents from p24 proteins. *Mol. Cell. Biol.* 26, 8011–8021.

Bickford, L. C., Mossessova, E., and Goldberg, J. (2004). A structural view of the COPII vesicle coat. *Curr. Opin. Struct. Biol.* 14, 147–153.

Blümer, J., Rey, J., Dehmelt, L., Mazel, T., Wu, Y. W., Bastiaens, P., et al. (2013). RabGEFs are a major determinant for specific Rab membrane targeting. *J. Cell Biol.* 200, 287–300.

Bonfanti, L., Mironov, A. A. Jr., Martinez-Menarguez, J. A., Martella, O., Fusella, A., Baldassarre, M., et al. (1998). Procollagen traverses the Golgi stack without leaving the lumen of cisternae: evidence for cisternal maturation. *Cell* 95, 993–1003.

Bonifacino, J. S., and Glick, B. S. (2004). The mechanisms of vesicle budding and fusion. *Cell* 116, 153–166.

Borgonovo, B., Ouwendijk, J., and Solimena, M. (2006). Biogenesis of secretory granules. *Curr. Opin. Cell Biol.* 18, 365–370.

Brown, W. J., Chambers, K., and Doody, A. (2003). Phospholipase A2 (PLA2) enzymes in membrane trafficking: mediators of membrane shape and function. *Traffic* 4, 214–221.

Burgoyne, R. D., Barclay, J. W., Ciufo, L. F., Graham, M. E., Handley, M. T., and Morgan, A. (2009). The functions of Munc18-1 in regulated exocytosis. *Ann. N. Y. Acad. Sci.* 1152, 76–86.

Clermont, Y., Rambourg, A., and Hermo, L. (1995). Trans-Golgi network (TGN) of different cell types: three-dimensional structural characteristics and variability. *Anat. Rec.* 242, 289–301.

Clermont, Y., Xia, L., Rambourg, A., Turner, J. D., and Hermo, L. (1993). Structure of the Golgi apparatus in stimulated and nonstimulated acinar cells of mammary glands of the rat. *Anat. Rec.* 237, 308–317.

Cosson, P., Amherdt, M., Rothman, J. E., and Orci, L. (2002). A resident Golgi protein is excluded from peri-Golgi vesicles in NRK cells. *Proc. Natl. Acad. Sci. U.S.A.* 99, 12831–12834.

Cosson, P., and Letourneur, F. (1994). Coatomer interaction with di-lysine endoplasmic reticulum retention motifs. *Science* 263, 1629–1631.

Cruz-García, D., Díaz-Ruiz, A., Rabanal-Ruiz, Y., Peinado, J. R., Gracia-Navarro, F., Castaño, J. P., et al. (2012). The Golgi-associated long coiled-coil protein NECC1 participates in the control of the regulated secretory pathway in PC12 cells. *Biochem. J.* 443, 387–396.

Cruz-Garcia, D., Vazquez-Martinez, R., Peinado, J. R., Anouar, Y., Tonon, M. C., Vaudry, H., et al. (2007). Identification and characterization of two novel (neuro)endocrine long coiled-coil proteins. *FEBS Lett.* 581, 3149–3156.

Dalton, A. J., and Felix, M. D. (1956). A comparative study of the Golgi complex. *J. Biophys. Biochem. Cytol.* 2, 79–84.

de Figueiredo, P., Drecktrah, D., Polizotto, R. S., Cole, N. B., Lippincott-Schwartz, J., and Brown, W. J. (2000). Phospholipase A2 antagonists inhibit constitutive retrograde membrane traffic to the endoplasmic reticulum. *Traffic* 1, 504–511.

De Matteis, M. A., and Luini, A. (2008). Exiting the Golgi complex. *Nat. Rev. Mol. Cell Biol.* 9, 273–284.

De Matteis, M. A., Mironov, A., and Beznoussenko, V. (2008). "The Golgi ribbon and the function of the golgins," in *The Golgi Apparatus*, eds A. A. Mironov and M. Pavelka (Wien: Springer-Verlag), 223–246.

Donaldson, J. G., and Jackson, C. L. (2011). ARF family G proteins and their regulators: roles in membrane transport, development and disease. *Nat. Rev. Mol. Cell Biol.* 12, 362–375.

D'Souza-Schorey, C., and Chavrier, P. (2006). ARF proteins: roles in membrane traffic and beyond. *Nat. Rev. Mol. Cell Biol.* 7, 347–358.

Dunphy, W. G., Brands, R., and Rothman, J. E. (1985). Attachment of terminal N-acetylglucosamine to asparagine-linked oligosaccharides occurs in central cisternae of the Golgi stack. *Cell* 40, 463–472.

Egea, G., Lazaro-Dieguez, F., and Vilella, M. (2006). Actin dynamics at the Golgi complex in mammalian cells. *Curr. Opin. Cell Biol.* 18, 168–178.

Egea, G., and Rios, R. M. (2008). "The role of the cytoskeleton in the structure and function of the Golgi apparatus," in *The Golgi Apparatus*, eds A. A. Mironov and M. Pavelka (Wien: Springer-Verlag), 270–300.

Farquhar, M. G. (1961). Origin and fate of secretory granules in cells of the anterior pituitary gland. *Trans. N. Y. Acad. Sci.* 23, 346–351.

Farquhar, M. G., and Hauri, H. P. (1997). "Protein sorting and vesicular traffic in the Golgi apparatus," in *The Golgi Apparatus*, eds E. G. Berger and J. Roth (Basel: Birkhauser Verlag), 63–129.

Fernández-Ulibarri, I., Vilella, M., Lazaro-Dieguez, F., Sarri, E., Martinez, S. E., Jimenez, N., et al. (2007). Diacylglycerol is required for the formation of COPI vesicles in the Golgi-to-ER transport pathway. *Mol. Biol. Cell* 18, 3250–3263.

Fukuda, M. (2008). Regulation of secretory vesicle traffic by Rab small GTPases. *Cell. Mol. Life Sci.* 65, 2801–2813.

Garcia-Mata, R., Szul, T., Alvarez, C., and Sztul, E. (2003). ADP-ribosylation factor/COPI-dependent events at the endoplasmic reticulum-Golgi interface are regulated by the guanine nucleotide exchange factor GBF1. *Mol. Biol. Cell* 14, 2250–2261.

Gilchrist, A., Au, C. E., Hiding, J., Bell, A. W., Fernandez-Rodriguez, J., Lesimple, S., et al. (2006). Quantitative proteomics analysis of the secretory pathway. *Cell* 127, 1265–1281.

Girod, A., Storrie, B., Simpson, J. C., Johannes, L., Goud, B., Roberts, L. M., et al. (1999). Evidence for a COP-I-independent transport route from the Golgi complex to the endoplasmic reticulum. *Nat. Cell Biol.* 1, 423–430.

Glick, B. S. (2000). Organization of the Golgi apparatus. *Curr. Opin. Cell Biol.* 12, 450–456.

Glick, B. S., Elston, T., and Oster, G. (1997). A cisternal maturation mechanism can explain the asymmetry of the Golgi stack. *FEBS Lett.* 414, 177–181.

Glick, B. S., and Luini, A. (2011). Models for Golgi traffic: a critical assessment. *Cold Spring Harb. Perspect. Biol.* 3, a005215.

Glick, B. S., and Malhotra, V. (1998). The curious status of the Golgi apparatus. *Cell* 95, 883–889.

Golgi, C. (1898). Sur la structure des cellules nerveuses. *Arch. Ital. Biol.* 30, 60–71.

Gommel, D. U., Memon, A. R., Heiss, A., Lottspeich, F., Pfannstiel, J., Lechner, J., et al. (2001). Recruitment to Golgi membranes of ADP-ribosylation factor 1 is mediated by the cytoplasmic domain of p23. *EMBO J.* 20, 6751–6760.

Grasse, P. P. (1957). Ultrastructure, polarity and reproduction of Golgi apparatus. *C. R. Hebd. Seances Acad. Sci.* 245, 1278–1281.

Griffiths, G. (2000). Gut thoughts on the Golgi complex. *Traffic* 1, 738–745.

Griffiths, G., Pfeiffer, S., Simons, K., and Matlin, K. (1985). Exit of newly synthesized membrane proteins from the trans cisterna of the Golgi complex to the plasma membrane. *J. Cell Biol.* 101, 949–964.

Griffiths, G., and Simons, K. (1986). The trans Golgi network: sorting at the exit site of the Golgi complex. *Science* 234, 438–443.

Gumbiner, B., and Kelly, R. B. (1982). Two distinct intracellular pathways transport secretory and membrane glycoproteins to the surface of pituitary tumor cells. *Cell* 28, 51–59.

Hauri, H. P., and Schweizer, A. (1992). The endoplasmic reticulum-Golgi intermediate compartment. *Curr. Opin. Cell Biol.* 4, 600–608.

Heuser, J., and Kirchhausen, T. (1985). Deep-etch views of clathrin assemblies. *J. Ultrastruct. Res.* 92, 1–27.

Hong, W. (2005). SNAREs and traffic. *Biochim. Biophys. Acta* 1744, 120–144.

Inoue, H., and Randazzo, P. A. (2007). Arf GAPs and their interacting proteins. *Traffic* 8, 1465–1475.

Ishizaki, R., Shin, H. W., Mitsuhashi, H., and Nakayama, K. (2008). Redundant roles of BIG2 and BIG1, guanine-nucleotide exchange factors for ADP-ribosylation factors in membrane traffic between the trans-Golgi network and endosomes. *Mol. Biol. Cell* 19, 2650–2660.

Jackson, L. P., Lewis, M., Kent, H. M., Edeling, M. A., Evans, P. R., Duden, R., et al. (2012). Molecular basis for recognition of dilysine trafficking motifs by COPI. *Dev. Cell* 23, 1255–1262.

Jahn, R., and Scheller, R. H. (2006). SNAREs – engines for membrane fusion. *Nat. Rev. Mol. Cell Biol.* 7, 631–643.

Jensen, D., and Schekman, R. (2011). COPII-mediated vesicle formation at a glance. *J. Cell Sci.* 124, 1–4.

Jin, L., Pahuja, K. B., Wickliffe, K. E., Gorur, A., Baumgartel, C., Schekman, R., et al. (2012). Ubiquitin-dependent regulation of COPII coat size and function. *Nature* 482, 495–500.

Kawamoto, K., Yoshida, Y., Tamaki, H., Torii, S., Shinotsuka, C., Yamashina, S., et al. (2002). GBF1, a guanine nucleotide exchange factor for ADP-ribosylation factors, is localized to the cis-Golgi and involved in membrane association of the COPI coat. *Traffic* 3, 483–495.

Keller, P., and Simons, K. (1997). Post-Golgi biosynthetic trafficking. *J. Cell Sci.* 110(Pt 24), 3001–3009.

Kelly, R. B. (1985). Pathways of protein secretion in eukaryotes. *Science* 230, 25–32.

Kirchhausen, T., Harrison, S. C., and Heuser, J. (1986). Configuration of clathrin trimers: evidence from electron microscopy. *J. Ultrastruct. Mol. Struct. Res.* 94, 199–208.

Klumperman, J., Schweizer, A., Clausen, H., Tang, B. L., Hong, W., Oorschot, V., et al. (1998). The recycling pathway of protein ERGIC-53 and dynamics of the ER-Golgi intermediate compartment. *J. Cell Sci.* 111(Pt 22), 3411–3425.

Ladinsky, M. S., Mastronarde, D. N., McIntosh, J. R., Howell, K. E., and Staehelin, L. A. (1999). Golgi structure in three dimensions: functional insights from the normal rat kidney cell. *J. Cell Biol.* 144, 1135–1149.

Ladinsky, M. S., Wu, C. C., McIntosh, S., McIntosh, J. R., and Howell, K. E. (2002). Structure of the Golgi and distribution of reporter molecules at 20 degrees C reveals the complexity of the exit compartments. *Mol. Biol. Cell* 13, 2810–2825.

Laufman, O., Kedan, A., Hong, W., and Lev, S. (2009). Direct interaction between the COG complex and the SM protein, Sly1, is required for Golgi SNARE pairing. *EMBO J.* 28, 2006–2017.

Letourneur, F., Gaynor, E. C., Hennecke, S., Demolliere, C., Duden, R., Emr, S. D., et al. (1994). Coatomer is essential for retrieval of dilysine-tagged proteins to the endoplasmic reticulum. *Cell* 79, 1199–1207.

Lippincott-Schwartz, J., Donaldson, J. G., Schweizer, A., Berger, E. G., Hauri, H. P., Yuan, L. C., et al. (1990). Microtubule-dependent retrograde transport of proteins into the ER in the presence of brefeldin A suggests an ER recycling pathway. *Cell* 60, 821–836.

Liu, S., and Storrie, B. (2012). Are Rab proteins the link between Golgi organization and membrane trafficking? *Cell. Mol. Life Sci.* 69, 4093–4106.

Losev, E., Reinke, C. A., Jellen, J., Strongin, D. E., Bevis, B. J., and Glick, B. S. (2006). Golgi maturation visualized in living yeast. *Nature* 441, 1002–1006.

Lotti, L. V., Torrisi, M. R., Pascale, M. C., and Bonatti, S. (1992). Immunocytochemical analysis of the transfer of vesicular stomatitis virus G glycoprotein from the intermediate compartment to the Golgi complex. *J. Cell Biol.* 118, 43–50.

Majoul, I., Straub, M., Hell, S. W., Duden, R., and Soling, H. D. (2001). KDEL-cargo regulates interactions between proteins involved in COPI vesicle traffic: measurements in living cells using FRET. *Dev. Cell* 1, 139–153.

Malsam, J., Satoh, A., Pelletier, L., and Warren, G. (2005). Golgin tethers define subpopulations of COPI vesicles. *Science* 307, 1095–1098.

Malsam, J., and Söllner, T. H. (2011). Organization of SNAREs within the Golgi stack. *Cold Spring Harb. Perspect. Biol.* 3, a005249.

Mancias, J. D., and Goldberg, J. (2008). Structural basis of cargo membrane protein discrimination by the human COPII coat machinery. *EMBO J.* 27, 2918–2928.

Marsh, B. J., Mastronarde, D. N., Buttle, K. F., Howell, K. E., and McIntosh, J. R. (2001). Organellar relationships in the Golgi region of the pancreatic beta cell line, HIT-T15, visualized by high resolution electron tomography. *Proc. Natl. Acad. Sci. U.S.A.* 98, 2399–2406.

Marsh, B. J., Volkmann, N., McIntosh, J. R., and Howell, K. E. (2004). Direct continuities between cisternae at different levels of the Golgi complex in glucose-stimulated mouse islet beta cells. *Proc. Natl. Acad. Sci. U.S.A.* 101, 5565–5570.

Martínez-Alonso, E., Ballesta, J., and Martinez-Menarguez, J. A. (2007). Low-temperature-induced Golgi tubules are transient membranes enriched in molecules regulating intra-Golgi transport. *Traffic* 8, 359–368.

Martínez-Alonso, E., Egea, G., Ballesta, J., and Martinez-Menarguez, J. A. (2005). Structure and dynamics of the Golgi complex at 15 degrees C: low temperature induces the formation of Golgi-derived tubules. *Traffic* 6, 32–44.

Martínez-Menárguez, J. A., Geuze, H. J., and Ballesta, J. (1996). Identification of two types of beta-COP vesicles in the Golgi complex of rat spermatids. *Eur. J. Cell Biol.* 71, 137–143.

Martínez-Menárguez, J. A., Geuze, H. J., Slot, J. W., and Klumperman, J. (1999). Vesicular tubular clusters between the ER and Golgi mediate concentration of soluble secretory proteins by exclusion from COPI-coated vesicles. *Cell* 98, 81–90.

Martinez-Menárguez, J. A., Prekeris, R., Oorschot, V. M., Scheller, R., Slot, J. W., Geuze, H. J., et al. (2001). Peri-Golgi vesicles contain retrograde but not anterograde proteins consistent with the cisternal progression model of intra-Golgi transport. *J. Cell Biol.* 155, 1213–1224.

Matsuura-Tokita, K., Takeuchi, M., Ichihara, A., Mikuriya, K., and Nakano, A. (2006). Live imaging of yeast Golgi cisternal maturation. *Nature* 441, 1007–1010.

Melkonian, M., Becker, B., and Becker, D. (1991). Scale formation in algae. *J. Electron Microsc. Tech.* 17, 165–178.

Miller, V. J., and Ungar, D. (2012). Re'COG'nition at the Golgi. *Traffic* 13, 891–897.

Mironov, A. A., and Beznoussenko, G. V. (2012). The kiss-and-run Model of intra-Golgi transport. *Int. J. Mol. Sci.* 13, 6800–6819.

Mironov, A. A., Beznoussenko, G. V., Nicoziani, P., Martella, O., Trucco, A., Kweon, H. S., et al. (2001). Small cargo proteins and large aggregates can traverse the Golgi by a common mechanism without leaving the lumen of cisternae. *J. Cell Biol.* 155, 1225–1238.

Mironov, A. A., Mironov, A. A. Jr., Beznoussenko, G. V., Trucco, A., Lupetti, P., Smith, J. D., et al. (2003). ER-to-Golgi carriers arise through direct en bloc protrusion and multistage maturation of specialized ER exit domains. *Dev. Cell* 5, 583–594.

Mironov, A. A., Polishchuk, R. S., and Beznoussenko, G. V. (2008). Combined video fluorescence and 3D electron microscopy. *Methods Cell Biol.* 88, 83–95.

Moelleken, J., Malsam, J., Betts, M. J., Movafeghi, A., Reckmann, I., Meissner, I., et al. (2007). Differential localization of coatomer complex isoforms within the Golgi apparatus. *Proc. Natl. Acad. Sci. U.S.A.* 104, 4425–4430.

Mollenhauer, H. H., and Morre, D. J. (1998). The tubular network of the Golgi apparatus. *Histochem. Cell Biol.* 109, 533–543.

Morvan, J., and Tooze, S. A. (2008). Discovery and progress in our understanding of the regulated secretory pathway in neuroendocrine cells. *Histochem. Cell Biol.* 129, 243–252.

Nickel, W., Sohn, K., Bunning, C., and Wieland, F. T. (1997). p23, a major COPI-vesicle membrane protein, constitutively cycles through the early secretory pathway. *Proc. Natl. Acad. Sci. U.S.A.* 94, 11393–11398.

Nilsson, T., Pypaert, M., Hoe, M. H., Slusarewicz, P., Berger, E. G., and Warren, G. (1993). Overlapping distribution of two glycosyltransferases in the Golgi apparatus of HeLa cells. *J. Cell Biol.* 120, 5–13.

Oprins, A., Duden, R., Kreis, T. E., Geuze, H. J., and Slot, J. W. (1993). Beta-COP localizes mainly to the cis-Golgi side in exocrine pancreas. *J. Cell Biol.* 121, 49–59.

Orci, L., Glick, B. S., and Rothman, J. E. (1986). A new type of coated vesicular carrier that appears not to contain clathrin: its possible role in protein transport within the Golgi stack. *Cell* 46, 171–184.

Orci, L., Halban, P., Amherdt, M., Ravazzola, M., Vassalli, J. D., and Perrelet, A. (1984). A clathrin-coated, Golgi-related compartment of the insulin secreting cell accumulates proinsulin in the presence of monensin. *Cell* 39, 39–47.

Orci, L., Perrelet, A., and Rothman, J. E. (1998). Vesicles on strings: morphological evidence for processive transport within the Golgi stack. *Proc. Natl. Acad. Sci. U.S.A.* 95, 2279–2283.

Orci, L., Ravazzola, M., Volchuk, A., Engel, T., Gmachl, M., Amherdt, M., et al. (2000). Anterograde flow of cargo across the golgi stack potentially mediated via bidirectional "percolating" COPI vesicles. *Proc. Natl. Acad. Sci. U.S.A.* 97, 10400–10405.

Orci, L., Stamnes, M., Ravazzola, M., Amherdt, M., Perrelet, A., Sollner, T. H., et al. (1997). Bidirectional transport by distinct populations of COPI-coated vesicles. *Cell* 90, 335–349.

Palade, G. (1975). Intracellular aspects of the process of protein synthesis. *Science* 189, 347–358.

Patterson, G. H., Hirschberg, K., Polishchuk, S., Gerlich, D., Phair, R. D., and Lippincott-Schwartz, J. (2008). Transport through the Golgi apparatus by rapid partitioning within a two-phase membrane system. *Cell* 133, 1055–1067.

Pearse, B. M., and Robinson, M. S. (1990). Clathrin, adaptors, and sorting. *Annu. Rev. Cell Biol.* 6, 151–171.

Pelham, H. R., and Rothman, J. E. (2000). The debate about transport in the Golgi – two sides of the same coin? *Cell* 102, 713–719.

Polishchuk, R. S., Polishchuk, E. V., Marra, P., Alberti, S., Buccione, R., Luini, A., et al. (2000). Correlative light-electron microscopy reveals the tubular-saccular ultrastructure of carriers operating between Golgi apparatus and plasma membrane. *J. Cell Biol.* 148, 45–58.

Popoff, V., Adolf, F., Brugger, B., and Wieland, F. (2011). COPI budding within the Golgi stack. *Cold Spring Harb. Perspect. Biol.* 3, a005231.

Presley, J. F., Cole, N. B., Schroer, T. A., Hirschberg, K., Zaal, K. J., and Lippincott-Schwartz, J. (1997). ER-to-Golgi transport visualized in living cells. *Nature* 389, 81–85.

Rabouille, C., Hui, N., Hunte, F., Kieckbusch, R., Berger, E. G., Warren, G., et al. (1995). Mapping the distribution of Golgi enzymes involved in the construction of complex oligosaccharides. *J. Cell Sci.* 108(Pt 4), 1617–1627.

Rabouille, C., and Klumperman, J. (2005). Opinion: the maturing role of COPI vesicles in intra-Golgi transport. *Nat. Rev. Mol. Cell Biol.* 6, 812–817.

Rambourg, A., and Clermont, Y. (1997). "Three-dimensional structure of the Golgi apparatus in mammalian cells," in *The Golgi Apparatus*, eds E. G. Berger and J. Roth (Basel: Birkhauser Verlag), 37–61.

Rambourg, A., Clermont, Y., Chretien, M., and Olivier, L. (1993). Modulation of the Golgi apparatus in stimulated and nonstimulated prolactin cells of female rats. *Anat. Rec.* 235, 353–362.

Rambourg, A., Clermont, Y., and Hermo, L. (1979). Three-dimensional architecture of the golgi apparatus in Sertoli cells of the rat. *Am. J. Anat.* 154, 455–476.

Rambourg, A., Clermont, Y., and Marraud, A. (1974). Three-dimensional structure of the osmium-impregnated Golgi apparatus as seen in the high voltage electron microscope. *Am. J. Anat.* 140, 27–45.

Roth, J., and Berger, E. G. (1982). Immunocytochemical localization of galactosyltransferase in HeLa cells: codistribution with thiamine pyrophosphatase in trans-Golgi cisternae. *J. Cell Biol.* 93, 223–229.

Rothman, J. E., and Fine, R. E. (1980). Coated vesicles transport newly synthesized membrane glycoproteins from endoplasmic reticulum to plasma membrane in two successive stages. *Proc. Natl. Acad. Sci. U.S.A.* 77, 780–784.

Rothman, J. E., and Wieland, F. T. (1996). Protein sorting by transport vesicles. *Science* 272, 227–234.

Sacher, M., Kim, Y. G., Lavie, A., Oh, B. H., and Segev, N. (2008). The TRAPP complex: insights into its architecture and function. *Traffic* 9, 2032–2042.

Sadakata, T., Shinoda, Y., Sekine, Y., Saruta, C., Itakura, M., Takahashi, M., et al. (2010). Interaction of calcium-dependent activator protein for secretion 1 (CAPS1) with the class II ADP-ribosylation factor small GTPases is required for dense-core vesicle trafficking in the trans-Golgi network. *J. Biol. Chem.* 285, 38709–38710.

San Pietro, E., Capestrano, M., Polishchuk, E. V., DiPentima, A., Trucco, A., Zizza, P., et al. (2009). Group IV phospholipase A(2)alpha controls the formation of inter-cisternal continuities involved in intra-Golgi transport. *PLoS Biol.* 7:e1000194. doi:10.1371/journal.pbio.1000194

Saraste, J., and Kuismanen, E. (1984). Pre- and post-Golgi vacuoles operate in the transport of Semliki Forest virus membrane glycoproteins to the cell surface. *Cell* 38, 535–549.

Scales, S. J., Pepperkok, R., and Kreis, T. E. (1997). Visualization of ER-to-Golgi transport in living cells reveals a sequential mode of action for COPII and COPI. *Cell* 90, 1137–1148.

Schindler, R., Itin, C., Zerial, M., Lottspeich, F., and Hauri, H. P. (1993). ERGIC-53, a membrane protein of the ER-Golgi intermediate compartment, carries an ER retention motif. *Eur. J. Cell Biol.* 61, 1–9.

Schmidt, J. A., Kalkofen, D. N., Donovan, K. W., and Brown, W. J. (2010). A role for phospholipase A2 activity in membrane tubule formation and TGN trafficking. *Traffic* 11, 1530–1536.

Schweizer, A., Fransen, J. A., Matter, K., Kreis, T. E., Ginsel, L., and Hauri, H. P. (1990). Identification of an intermediate compartment involved in protein transport from endoplasmic reticulum to Golgi apparatus. *Eur. J. Cell Biol.* 53, 185–196.

Semenza, J. C., Hardwick, K. G., Dean, N., and Pelham, H. R. (1990). ERD2, a yeast gene required for the receptor-mediated retrieval of luminal ER proteins from the secretory pathway. *Cell* 61, 1349–1357.

Sesso, A., de Faria, F. P., Iwamura, E. S., and Correa, H. (1994). A three-dimensional reconstruction study of the rough ER-Golgi interface in serial thin sections of the pancreatic acinar cell of the rat. *J. Cell Sci.* 107(Pt 3), 517–528.

Shiba, Y., and Randazzo, P. A. (2012). ArfGAP1 function in COPI mediated membrane traffic: currently debated models and comparison to other coat-binding ArfGAPs. *Histol. Histopathol.* 27, 1143–1153.

Shima, D. T., Scales, S. J., Kreis, T. E., and Pepperkok, R. (1999). Segregation of COPI-rich and anterograde-cargo-rich domains in endoplasmic-reticulum-to-Golgi transport complexes. *Curr. Biol.* 9, 821–824.

Siddhanta, A., Backer, J. M., and Shields, D. (2000). Inhibition of phosphatidic acid synthesis alters the structure of the Golgi apparatus and inhibits secretion in endocrine cells. *J. Biol. Chem.* 275, 12023–12031.

Slusarewicz, P., Nilsson, T., Hui, N., Watson, R., and Warren, G. (1994). Isolation of a matrix that binds medial Golgi enzymes. *J. Cell Biol.* 124, 405–413.

Smith, R. E., and Farquhar, M. G. (1966). Lysosome function in the regulation of the secretory process in cells of the anterior pituitary gland. *J. Cell Biol.* 31, 319–347.

Stenmark, H. (2009). Rab GTPases as coordinators of vesicle traffic. *Nat. Rev. Mol. Cell Biol.* 10, 513–525.

Stephens, D. J., Lin-Marq, N., Pagano, A., Pepperkok, R., and Paccaud, J. P. (2000). COPI-coated ER-to-Golgi transport complexes segregate from COPII in close proximity to ER exit sites. *J. Cell Sci.* 113(Pt 12), 2177–2185.

Storrie, B., White, J., Rottger, S., Stelzer, E. H., Suganuma, T., and Nilsson, T. (1998). Recycling of golgi-resident glycosyltransferases through the ER reveals a novel pathway and provides an explanation for nocodazole-induced Golgi scattering. *J. Cell Biol.* 143, 1505–1521.

Strating, J. R., Bouw, G., Hafmans, T. G., and Martens, G. J. (2011). p24 Proteins from the same subfamily are functionally nonredundant. *Biochimie* 93, 528–532.

Sztul, E., and Lupashin, V. (2009). Role of vesicle tethering factors in the ER-Golgi membrane traffic. *FEBS Lett.* 583, 3770–3783.

Szul, T., and Sztul, E. (2011). COPII and COPI traffic at the ER-Golgi interface. *Physiology (Bethesda)* 26, 348–364.

Tanaka, K., Mitsushima, A., Fukudome, H., and Kashima, Y. (1986). Three-dimensional architecture of the Golgi complex observed by high resolution scanning electron microscopy. *J. Submicrosc. Cytol.* 18, 1–9.

Tanigawa, G., Orci, L., Amherdt, M., Ravazzola, M., Helms, J. B., and Rothman, J. E. (1993). Hydrolysis of bound GTP by ARF protein triggers uncoating of Golgi-derived COP-coated vesicles. *J. Cell Biol.* 123, 1365–1371.

Taylor, R. S., Jones, S. M., Dahl, R. H., Nordeen, M. H., and Howell, K. E. (1997). Characterization of the Golgi complex cleared of proteins in transit and examination of calcium uptake activities. *Mol. Biol. Cell* 8, 1911–1931.

Traub, L. M., and Kornfeld, S. (1997). The trans-Golgi network: a late secretory sorting station. *Curr. Opin. Cell Biol.* 9, 527–533.

Trucco, A., Polishchuk, R. S., Martella, O., Di Pentima, A., Fusella, A., Di Giandomenico, D., et al. (2004). Secretory traffic triggers the formation of tubular continuities across Golgi sub-compartments. *Nat. Cell Biol.* 6, 1071–1081.

van Rijnsoever, C., Oorschot, V., and Klumperman, J. (2008). Correlative light-electron microscopy (CLEM) combining live-cell imaging and immunolabeling of ultrathin cryosections. *Nat. Methods* 5, 973–980.

Vázquez-Martínez, R., Díaz-Ruiz, A., Almabouada, F., Rabanal-Ruiz, Y., Gracia-Navarro, F., and Malagon, M. M. (2012). Revisiting the regulated secretory pathway: from frogs to human. *Gen. Comp. Endocrinol.* 175, 1–9.

Vázquez-Martínez, R., and Malagón, M. M. (2011). Rab proteins and the secretory pathway: the case of rab18 in neuroendocrine cells. *Front. Endocrinol.* 2:1. doi:10.3389/fendo.2011.00001

Vivero-Salmerón, G., Ballesta, J., and Martínez-Menárguez, J. A. (2008). Heterotypic tubular connections at the endoplasmic reticulum-Golgi complex interface. *Histochem. Cell Biol.* 130, 709–717.

Volchuk, A., Amherdt, M., Ravazzola, M., Brügger, B., Rivera, V. M., Clackson, T., et al. (2000). Megavesicles implicated in the rapid transport of intracisternal aggregates across the Golgi stack. *Cell* 102, 335–348.

Volpicelli-Daley, L. A., Li, Y., Zhang, C. J., and Kahn, R. A. (2005). Isoform-selective effects of the depletion of ADP-ribosylation factors 1-5 on membrane traffic. *Mol. Biol. Cell* 16, 4495–4508.

Watanabe, T., Sakai, Y., Koga, D., Bochimoto, H., Hira, Y., Hosaka, M., et al. (2012). A unique ball-shaped Golgi apparatus in the rat pituitary gonadotrope: its functional implications in relation to the arrangement of the microtubule network. *J. Histochem. Cytochem.* 60, 588–602.

Weidman, P., Roth, R., and Heuser, J. (1993). Golgi membrane dynamics imaged by freeze-etch electron microscopy: views of different membrane coatings involved in tubulation versus vesiculation. *Cell* 75, 123–133.

Xiang, Y., and Wang, Y. (2011). New components of the Golgi matrix. *Cell Tissue Res.* 344, 365–379.

Yang, J. S., Gad, H., Lee, S. Y., Mironov, A., Zhang, L., Beznoussenko, G. V., et al. (2008). A role for phosphatidic acid in COPI vesicle fission yields insights into Golgi maintenance. *Nat. Cell Biol.* 10, 1146–1153.

Yang, J. S., Valente, C., Polishchuk, R. S., Turacchio, G., Layre, E., Moody, D. B., et al. (2011). COPI acts in both vesicular and tubular transport. *Nat. Cell Biol.* 13, 996–1003.

Yu, S., and Liang, Y. (2012). A trapper keeper for TRAPP, its structures and functions. *Cell. Mol. Life Sci.* 69, 3933–3944.

Zeuschner, D., Geerts, W. J., van Donselaar, E., Humbel, B. M., Slot, J. W., Koster, A. J., et al. (2006). Immuno-electron tomography of ER exit sites reveals the existence of free COPII-coated transport carriers. *Nat. Cell Biol.* 8, 377–383.

Zhang, Y. C., Zhou, Y., Yang, C. Z., and Xiong, D. S. (2009). A review of ERGIC-53: its structure, functions, regulation and relations with diseases. *Histol. Histopathol.* 24, 1193–1204.

Conflict of Interest Statement: The authors declare that the research was conducted in the absence of any commercial or financial relationships that could be construed as a potential conflict of interest.

Received: 17 January 2013; accepted: 14 March 2013; published online: 28 March 2013.

*Citation: Martínez-Alonso E, Tomás M and Martínez-Menárguez JA (2013) Morpho-functional architecture of the Golgi complex of neuroendocrine cells. Front. Endocrinol. **4**:41. doi: 10.3389/fendo.2013.00041*

This article was submitted to Frontiers in Neuroendocrine Science, a specialty of Frontiers in Endocrinology.

frontiers in
ENDOCRINOLOGY

REVIEW ARTICLE
published: 14 August 2013
doi: 10.3389/fendo.2013.00101

Role of adaptor proteins in secretory granule biogenesis and maturation

Mathilde L. Bonnemaison[1], Betty A. Eipper[1,2] and Richard E. Mains[2]*

[1] *Department of Molecular, Microbial and Structural Biology, University of Connecticut Health Center, Farmington, CT, USA*
[2] *Department of Neuroscience, University of Connecticut Health Center, Farmington, CT, USA*

Edited by:
Rafael Vazquez-Martinez, University of Cordoba, Spain

Reviewed by:
Juan Ramon Peinado, University of Castilla la Mancha, Spain
J. David Castle, University of Virginia Health System, USA

***Correspondence:**
Richard E. Mains, Department of Neuroscience, University of Connecticut Health Center, 263 Farmington Avenue, Farmington, CT 06030-3401, USA
e-mail: mains@nso.uchc.edu

In the regulated secretory pathway, secretory granules (SGs) store peptide hormones that are released on demand. SGs are formed at the *trans*-Golgi network and must undergo a maturation process to become responsive to secretagogues. The production of mature SGs requires concentrating newly synthesized soluble content proteins in granules whose membranes contain the appropriate integral membrane proteins. The mechanisms underlying the sorting of soluble and integral membrane proteins destined for SGs from other proteins are not yet well understood. For soluble proteins, luminal pH and divalent metals can affect aggregation and interaction with surrounding membranes. The trafficking of granule membrane proteins can be controlled by both luminal and cytosolic factors. Cytosolic adaptor proteins (APs), which recognize the cytosolic domains of proteins that span the SG membrane, have been shown to play essential roles in the assembly of functional SGs. Adaptor protein 1A (AP-1A) is known to interact with specific motifs in its cargo proteins and with the clathrin heavy chain, contributing to the formation of a clathrin coat. AP-1A is present in patches on immature SG membranes, where it removes cargo and facilitates SG maturation. AP-1A recruitment to membranes can be modulated by Phosphofurin Acidic Cluster Sorting protein 1 (PACS-1), a cytosolic protein which interacts with both AP-1A and cargo that has been phosphorylated by casein kinase II. A cargo/PACS-1/AP-1A complex is necessary to drive the appropriate transport of several cargo proteins within the regulated secretory pathway. The Golgi-localized, γ-ear containing, ADP-ribosylation factor binding (GGA) family of APs serve a similar role. We review the functions of AP-1A, PACS-1, and GGAs in facilitating the retrieval of proteins from immature SGs and review examples of cargo proteins whose trafficking within the regulated secretory pathway is governed by APs.

Keywords: regulated secretory pathway, maturation, cargo, AP-1, GGA, PACS-1, prohormone

THE REGULATED SECRETORY PATHWAY

Neuroendocrine cells synthesize, process, and store peptide hormones so that they are available for secretion upon demand (1). These professional secretory cells devote as much as half of their total protein synthesis to the production of a single hormone (2). The regulated secretory pathway allows intracellular storage of peptide hormones until an external stimulus triggers exocytosis of the secretory granules (SGs) that contain the peptides. Neuroendocrine tumors and metabolic disease are linked to defects in hormone secretion, observed via an increase in circulating hormone levels due to impaired intracellular storage or cellular response. The alterations which result in loss of storage and secretagogue responsiveness are poorly understood.

Peptide hormones are first synthesized as inactive precursors. The signal peptide found at the N-terminus of the preprohormone is recognized by signal recognition particle, which stops translation and directs entry of the nascent preprohormone into the lumen of the endoplasmic reticulum (3); removal of the signal peptide by signal peptidase yields the prohormone. Most proteins which are going to be secreted undergo this step. The endoplasmic reticulum is also the site at which disulfide-bond formation and N-linked glycosylation occur (**Figure 1**) (3, 4, 5). Professional secretory cells have developed specialized sensing mechanisms to avoid triggering the endoplasmic reticulum stress pathway, which can lead to cell death; for example, increased expression of Stress-associated Endoplasmic Reticulum Protein 1 (SERP1) prevents endoplasmic reticulum stress in the anterior pituitary and pancreas (6).

After exiting the endoplasmic reticulum, prohormones are transported to the Golgi apparatus, where additional post-translational modifications such as oligosaccharide maturation and phosphorylation can occur (**Figure 1**) (5, 7). When they reach the *trans*-Golgi network (TGN), prohormones, and their processing enzymes are concentrated into granules budding from the TGN; these structures presumably represent newly forming SGs (1). These new SGs are immature and must undergo a maturation process before they are capable of secreting peptide hormone in response to secretagogue. Maturation involves remodeling of the immature SG membrane by removal of non-regulated secretory proteins and excess membrane; this process involves clathrin-coated vesicles mediated by adaptor proteins (APs) (**Figure 1**)

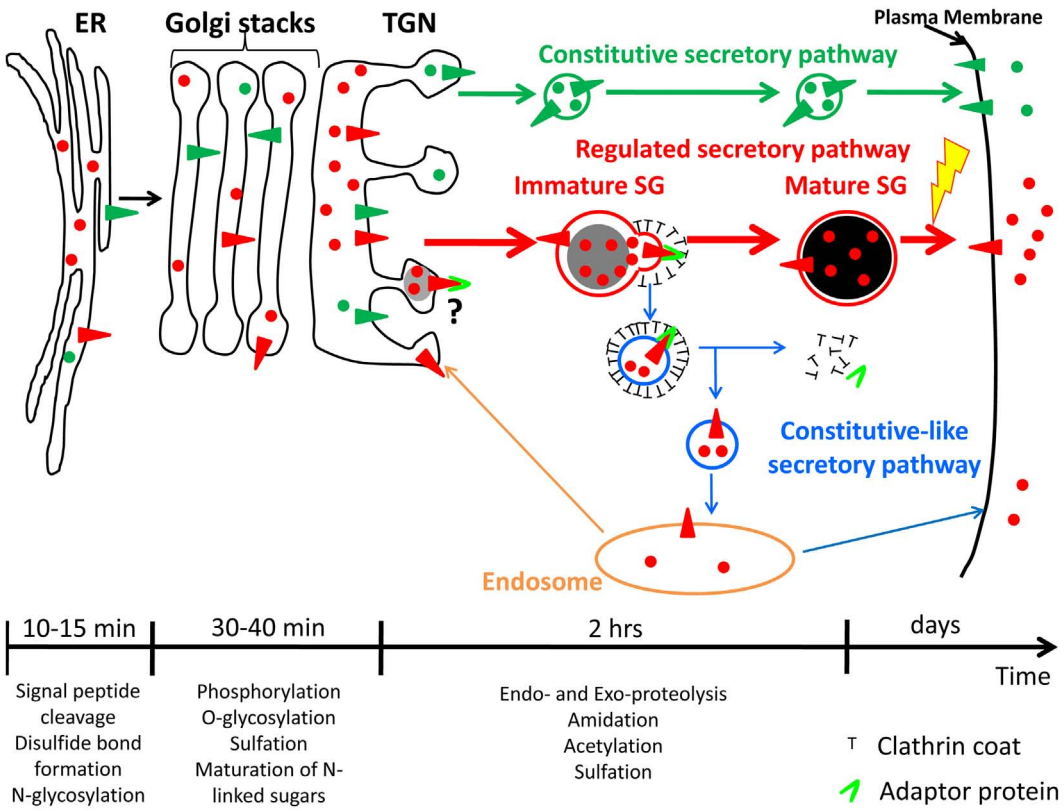

FIGURE 1 | Constitutive and regulated secretory pathways. Soluble and membrane proteins are represented with circles and triangles, respectively. Constitutive secretory pathway proteins are green; regulated secretory pathway proteins are red. Examples of post-translational modifications that occur in each organelle are shown. The time-scale is representative of the time spent by hormones and hormone processing enzymes in each organelle of the regulated secretory pathway. Until newly synthesized proteins reach the *trans*-Golgi network (TGN), proteins from both secretory pathways share the same compartments. Secretory proteins are sorted into constitutive secretory vesicles or immature secretory granule (SGs) in the TGN. Immature SGs undergo a maturation process to become mature SGs. The yellow lightning bolt represents the external stimulus triggering secretion of mature SG content. The maturation process involves remodeling of immature SG membranes, generating the constitutive-like secretory pathway (blue); the fate of the vesicles leaving immature SGs is not clear; return to an endosomal compartment from which proteins can be secreted in a constitutive-like fashion or recycled to the TGN is shown. ER, endoplasmic reticulum.

(8, 9), acidification of the lumen, aggregation of content proteins and, at least in some cell systems, fusion of immature SGs (10, 11). The final post-translational modifications needed to generate bioactive peptide hormones occur in immature and mature SGs (12, 13). Mature SGs, which appear dense in the electron microscope and during sucrose density gradient centrifugation, can contain more than 300 mg/ml protein, largely peptide hormones (14). Unlike constitutively secreted proteins, which are found in the extracellular compartment within minutes after exit from the TGN, it takes about 90 min for peptide hormones to go from the TGN to mature SGs (**Figure 1**) (15, 16). In addition, mature SG content can be stored for many days before being secreted into the extracellular compartment in response to a stimulus (**Figure 1**) (17, 18); proteins and peptides stored in the regulated secretory pathway are released at a low rate (basal secretion) even in the absence of secretagogue (19, 20).

The study of immature SGs remains a challenge due to their transient role as intermediates between the TGN and mature SGs. Morphologists describe immature SGs as vacuoles found in close proximity to the TGN which contain dense material surrounded by a loose membrane with a partial clathrin coat, while biochemists distinguish immature SGs from mature SGs by their inability to respond to secretagogue or by their release of incompletely processed newly synthesized products (14, 21). Early studies using $^{35}SO_4$ to label sugars and Tyr residues demonstrated high K^+/Ca^{2+}-stimulated release of $^{35}SO_4$-labeled SG components as soon as 15 min after synthesis (16); it is not clear how to relate $^{35}SO_4$ labeling to biosynthetic or endocytic trafficking. In the end, what controls and triggers the formation and maturation of immature SGs remains unclear. Both soluble and membrane proteins destined for the regulated secretory pathway must enter immature SGs when they exit the TGN, but how the trafficking of soluble and membrane proteins is coordinated is still under debate.

FORMATION OF IMMATURE SGs

Proteins destined for the regulated secretory pathway are sorted in the TGN and in immature SGs. Although the sorting mechanisms are not completely understood, the diverse biophysical and biochemical properties of soluble and membrane proteins suggest that they are targeted to the regulated secretory pathway through

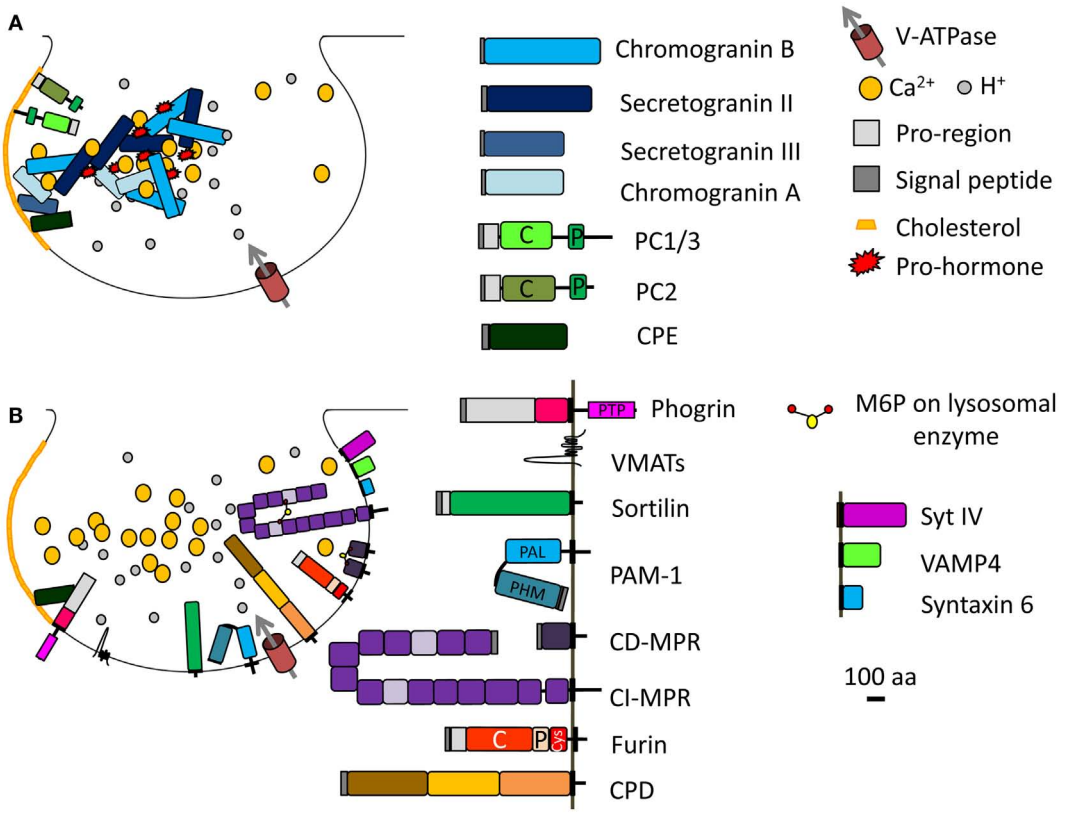

FIGURE 2 | Immature SG formation at the TGN. **(A)** Granins and prohormones aggregate in response to the high calcium, mildly acidic conditions in the TGN. Several soluble proteins interact with cholesterol or cholesterol-rich membranes; their sorting into immature SGs depends on this interaction. **(B)** Membrane proteins identified in immature SGs and discussed in the main text are shown; their cytosolic tails can interact with adaptor proteins. The SNARE and synaptotagmin proteins that enter immature SGs (synaptotagmin IV, VAMP4, syntaxin 6) are replaced during the maturation process. Proteins known to enter immature SGs are drawn approximately to scale (except for the vacuolar proton pump, V-ATPase, and VMATs). PC, prohormone convertase; C, catalytic domain; P, P domain; PTP, protein-tyrosine phosphatase; PHM, peptidylglycine α-hydroxylating monooxygenase; PAL, peptidylglycine α-amidating lyase; CI-MPR contains 15 domains; CPD contains three similar domains; Cys, cysteine-rich domain.

different mechanisms. The TGN is a cellular crossroad; departing proteins can enter vesicles targeted to endosomes, lysosomes, endoplasmic reticulum, or the plasma membrane (1, 22). One of the first studies demonstrating sorting of regulated secretory proteins at the TGN was performed using a cell-free system from PC12 cells, a neuroendocrine tumor cell line: vesicles budding from the TGN contained either heparin sulfate proteoglycan, a soluble protein of the constitutive secretory pathway, or secretogranin II, a soluble protein of the regulated secretory pathway (23).

VIEW FROM THE LUMINAL SIDE

The mildly acidic pH (pH 6.4) and high calcium (1–10 mM) environment of the TGN can induce aggregation of selected proteins (e.g., secretogranin II, chromogranin B, and prolactin) destined for the regulated secretory pathway, resulting in their segregation from the constitutive secretory pathway (**Figure 2A**) (24–26). Other regulated SG proteins bind specific lipids in the TGN, resulting in their sorting and entry into immature SGs; prohormone convertase 1/3 and prohormone convertase 2 interact with lipid rafts and secretogranin III binds to cholesterol (**Figure 2A**) (27–29). Indeed, chromogranin A, which enhances prohormone aggregation, interacts at the TGN with secretogranin III, and thus with cholesterol-rich membranes (**Figure 2A**) (28, 30). If the interaction of chromogranin A with secretogranin III is blocked, chromogranin A is not sorted correctly (31). Finally, a role for receptor-mediated sorting of regulated secretory proteins exiting the TGN has been considered. Carboxypeptidase E was proposed as a prohormone sorting receptor because it interacts with the N-terminal region of proopiomelanocortin (POMC), which was previously reported to serve as a sorting domain (15, 32). This conclusion is controversial because the sorting of proinsulin, luteinizing hormone, and follicle stimulating hormone does not depend on carboxypeptidase E (33, 34). Although the sorting of cargo upon binding to a receptor is an attractive concept, SG protein sorting appears to involve multiple processes. Carboxypeptidase E was recently shown to interact with phogrin, a SG membrane protein of the Insulinoma Associated protein 2 (IA-2) family; this interaction involves the pro-region of the luminal domain of phogrin and mature carboxypeptidase E (**Figure 2B**). When one binding partner is missing, the other does not accumulate in SGs, instead localizes to the perinuclear region; the sorting of carboxypeptidase E and phogrin at the TGN is inter-dependent (35).

VIEW FROM THE CYTOSOLIC SIDE

Sorting signals contributed by SG membrane protein trafficking

Membrane proteins cannot aggregate as extensively as soluble proteins. The identification of trafficking signals in the cytosolic domains of endocytic cargo led to the postulate that the cytosolic domains of SG membrane proteins would carry signals to ensure their entry into immature SGs (**Figure 2B**). Indeed, deletion or mutation of the cytosolic domain of phogrin results in a decrease in its entry into SGs (36, 37). Similar observations were made for peptidylglycine α-amidating monooxygenase 1 (PAM-1) (**Figure 2B**). PAM-1 is a bifunctional enzyme catalyzing the amidation of glycine-extended peptides, rendering them bioactive. Exogenous expression of a truncated PAM-1 protein lacking its cytosolic domain resulted in its inefficient storage in SGs. Metabolic labeling revealed that 20–40% of the newly synthesized truncated PAM protein entered the regulated secretory pathway, but endocytic trafficking and SG re-entry of the truncated PAM-1 protein were eliminated (38). The cytosolic domain of PAM-1, which is highly phosphorylated, interacts with several cytosolic proteins (39). Two sites in the cytosolic domain of PAM-1 are phosphorylated by casein kinase II (CKII) (**Table 1**); both sites were mutated to Asp (PAM-1/TS/DD), to try to mimic phosphorylation, or to Ala (PAM-1/TS/AA) to prevent phosphorylation. When expressed in AtT-20 corticotrope tumor cells, exogenous PAM-1/TS/DD entered immature SGs more efficiently than PAM-1, while PAM-1/TS/AA did not enter immature SGs efficiently and was degraded (40). This study suggests that phosphorylation of the cytosolic tail of PAM-1 enhances its entry into immature SGs.

Similar conclusions were reached in studies of two different neurotransmitter transporters, Vesicular Monoamine Transporter 2 (VMAT2) and Vesicular Acetylcholine Transporter (VAChT). Using the pH gradient established by the vacuolar proton pump, VMAT2, and VAChT translocate monoamines and acetylcholine, respectively, from the cytosol into the lumen. VMAT2 and VAChT enter two different types of vesicles in PC12 cells: VMAT2 is preferentially targeted to SGs while VAChT is found in synaptic-like microvesicles (**Figure 2B**) (41). The cytoplasmic domain of the VAChT contains a di-leucine motif with adjacent conserved Glu and Ser residues. Phosphorylation of this Ser by protein kinase C or mutation to a phosphomimetic residue results in a preference for VAChT entry into SGs, rather than into synaptic-like microvesicles (41). Additionally, VMAT2 contains two conserved Glu residues upstream of its di-leucine-like motif (**Table 1**, in blue); mutation of these Glu residues into Ala results in accumulation of VMAT2 in synaptic-like microvesicles (41).

These studies suggest that the sorting of membrane proteins into the regulated secretory pathway requires cytosolic signals and/or luminal/transmembrane signals. The negatively charged region within the cytosolic domain of membrane proteins is probably required for efficient sorting and entry into SGs. Since the cytosolic domain is involved in their sorting, cytosolic proteins must come into play in the formation of immature SGs and protein sorting in the regulated secretory pathway.

ADP-ribosylation factor 1 is required for SG biogenesis

In the 1990s, the cytosolic protein ADP-ribosylation factor 1 (Arf1), a member of the ADP-ribosylation family (Arf), was shown to promote the formation of immature SGs using cell-free systems from PC12 and GH_3 cells, two neuroendocrine cell lines (42, 43). Arf proteins, which belong to the Ras superfamily of small GTPases, were originally identified as necessary for the ADP-ribosylation reaction catalyzed by cholera toxin (44). Despite their names, the cellular function of Arfs does not involve ADP ribosylation, but rather membrane trafficking (45). Arf proteins are divided into three classes: class I (Arf1, Arf2, and Arf3), class II (Arf4 and Arf5), and class III (Arf6). Class I and class II Arfs are present at the Golgi and their main function is to regulate Golgi trafficking, while Arf6 functions at the plasma membrane and in the endocytic pathway. Arfs exist in two states: GDP-bound Arf is cytosolic and inactive while GTP-bound Arf is membrane-associated and active (**Figure 3**) (45, 46). All Arfs contain an N-terminal myristoylated amphipathic helix, which

Table 1 | Summary of known motifs for membrane proteins in SGs.

Protein	Host	ID	Amino acid sequence of the cytosolic tail
Furin	Rat	P23377.1	*TMD* H^{736}RCSGFSFRGVKVYTMDRGLISYKGLPPEAWQEECP**S**D**S**EEDEGRGERTAFIKDQSAL^{793} *COOH*
PAM	Rat	P14925.1	*TMD* R^{891}WKKSRAFGD^{900} [...]Y^{936}SRKGFDRVS**T**EG**S**DQEKDEDDGTESEEEYSAPLPKPAPSS^{976} *COOH*
Phogrin	Rat	NP_113788.1	*TMD* A^{625}YCLRHN^{631} [...] A^{645}DPSADATEAYQELCRQRMAVRPQ^{668} [...] E^{993}EVNAILKALPQ^{1004} *COOH*
CPD	Rat	NP_036968.1	*TMD* C^{1319}ICSIKSNRHKDGFHRL^{1335} [...] S^{1356}LLSHEFQDE**T**D**T**EEETLYSSKH^{1378} *COOH*
Sortilin	Rat	O54861.3	*TMD* V^{776}KKYVCGGRFLVHRYSVLQQHAEADGVEALDTASHAKSGYHDD**S**DEDLLE^{825} *COOH*
VAMP4	Mouse	O70480	NH_2 M^{1}PPKFKRHLNDDDVTGSVKSERRNLLEDD**S**DEEEDFFLRGPSGPRF^{46} [...] R^{112}GCKIKAI^{119} *TMD*
VMAT2	Rat	Q01827.2	*TMD* F^{464}APLCFFLRSPPAKEEKMAILMDHNCPIKRKMYTQNNVQSYPIGDDEE**S**E**S**D^{515} *COOH*
CI-MPR	Mouse	Q07113.1	*TMD* H^{2317} [...] C^{2333}RRSSGVSYKYSKVSKEEETDENETE^{2358} [...] V^{2470}SFHDD**S**DEDLLHI^{2483} *COOH*
CD-MPR	Mouse	Q6AY20	*TMD* L^{210}YQRLVVGAKG^{220} [...] R^{250}SVPAAYRGVGDDQLGEE**S**EERDDHLLPM^{278} *COOH*

Protein, host, and ID are shown. Acidic clusters are in red. CKII sites are in bold. AP-1 and AP-1-like sites are in blue and GGA sites are underlined in green. TMD, transmembrane domain; COOH, C-terminus of the protein; NH_2, N-terminus of the protein. The gray shade and italic font was to help the reader distinguish COOH or TMD or NH_2 from the amino acid sequence.

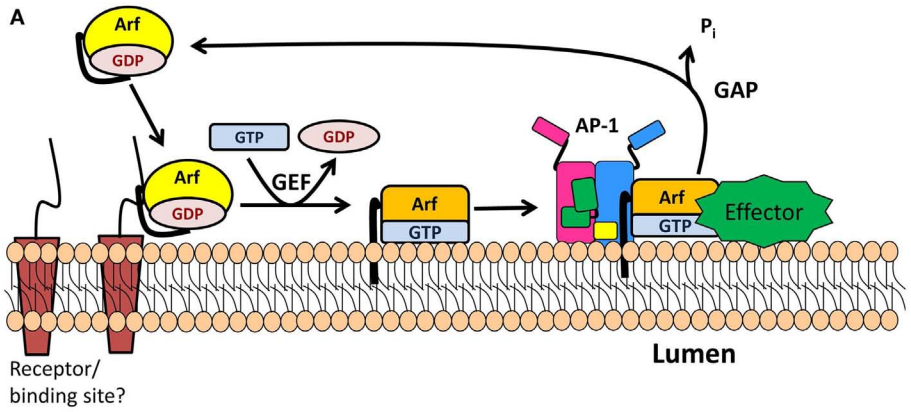

B

Effector types	Examples
Adaptor proteins	AP-1, AP-3, AP-4, GGA1-3, COPI
Lipid modifying enzymes	PI4KIIIβ, phospholipase D, PI(4)P(5) kinase α
Other	ArfGAP, Arfaptin, FAPP1-2

FIGURE 3 | The Arf/GEF/GAP cycle. **(A)** GDP-Arf is cytosolic and is thought to be recruited to its target membrane by interaction with a receptor. The exchange of Arf-bound GDP for GTP is catalyzed by an Arf-GEF, which induces a conformational change in Arf and release of GDP. GTP-bound Arf binds to the membrane through its N-terminal myristoylated amphipathic helix and recruits cytosolic proteins which function in membrane trafficking (effectors). One of these effectors is an Arf-GAP, which promotes the GTPase activity of Arf, resulting in its detachment from the membrane. **(B)** Table identifying type of effectors.

allows their association with membranes. This region is buried in a hydrophobic pocket when GDP is bound, but becomes accessible to membranes when GTP replaces GDP, triggering conformational changes in the switch 1 and switch 2 regions which surround the nucleotide binding site (45–47). A resident TGN protein, cargo, or lipid may interact with GDP-bound Arf1, bringing it near the TGN (**Figure 3**). In the context of COPI vesicles, which are involved in retrograde transport from the Golgi to the endoplasmic reticulum, p23, a transmembrane resident Golgi protein, is thought to recruit GDP-bound Arf (48).

The removal of GDP and binding of GTP is catalyzed by a guanine nucleotide exchange factor (GEF) (**Figure 3**) (45, 46). The two Arf GEFs identified at the TGN are BIG1 and BIG2 (brefeldin A inhibited GEFs). Interestingly, GBF1, a GEF known to be involved in the GDP/GTP exchange of Arf4 and Arf5 in the *cis*-Golgi compartment, has recently been identified on the TGN membrane (49). BIG1 and BIG2 are recruited to the TGN membrane upon binding to GTP-bound Arf4 and Arf5, whose nucleotide exchange was mediated by GBF1 (49). Both BIGs contain a Sec7 domain, which is the active site for the nucleotide switch and the target of brefeldin A, a fungal product. Treatment of neuroendocrine and exocrine cells with brefeldin A blocks the formation and maturation of immature SGs but does not alter mature SG exocytosis (50, 51).

Once nucleotide exchange has occurred, GTP-bound Arf recruits APs, enzyme modifying lipids, and effectors to the membrane before reacting with a GTPase activating protein (GAP) that promotes hydrolysis of GTP to GDP and release of Arf from the membrane (**Figure 3**). The Arf-GAP family is composed of 24 members, each with a GAP domain essential for its activity on Arf (45). GAP activity is modulated by the presence of coat proteins previously recruited by the GTP-bound Arf. When COPI is bound to Arf1, GAP activity is increased (52). Golgi-localized, γ-adaptin ear containing, Arf-binding (GGA) 3 is a coat protein involved in TGN-to-endosome transport. In contrast, when Arf1 recruits GGA3, it blocks the hydrolysis of GTP-bound to Arf1 (53).

Using the cell-free PC12 system, Arf1 was shown to enhance the formation of SGs and constitutive vesicles (42). Moreover, when Arf1 is bound to membranes isolated from PC12 cells, it recruits a set of different proteins, including the adaptor protein 1A (AP-1A) (54, 55). In non-endocrine secretory systems, such as rhoptries in *Toxoplasma gondii* (56), glue granules in *Drosophila* (57), and Weibel–Palade bodies in endothelial cells (58), AP-1A is required for the formation of SGs. Although it is not clear if AP-1A is required for SG formation in neuroendocrine cells, there is evidence that AP-1A is required for SG maturation (**Figure 4A**).

Membranes and SG formation: phosphatidylinositol-4-phosphate and cholesterol

The appropriate lipid composition is essential for normal TGN function and SG biogenesis. The TGN membrane is enriched in phosphatidylinositol-4-phosphate (PI4P). In mammalian cells, three enzymes that synthesize PI4P from phosphatidylinositol (PI) have been found at the Golgi, PI4KIIα, PI4KIIIα, and PI4KIIIβ; PI4KIIα (59) and PI4KIIIβ (60) have been implicated in export of material from the Golgi to the plasma membrane. PI4KIIα resides primarily in the TGN, endosomes, and SGs (61–64). Indeed, PI4KIIα was found on adrenal chromaffin granule membranes (65–67), cellugyrin-positive Glucose Transporter four vesicles (68), *Drosophila* salivary gland glue granules (69), synaptic

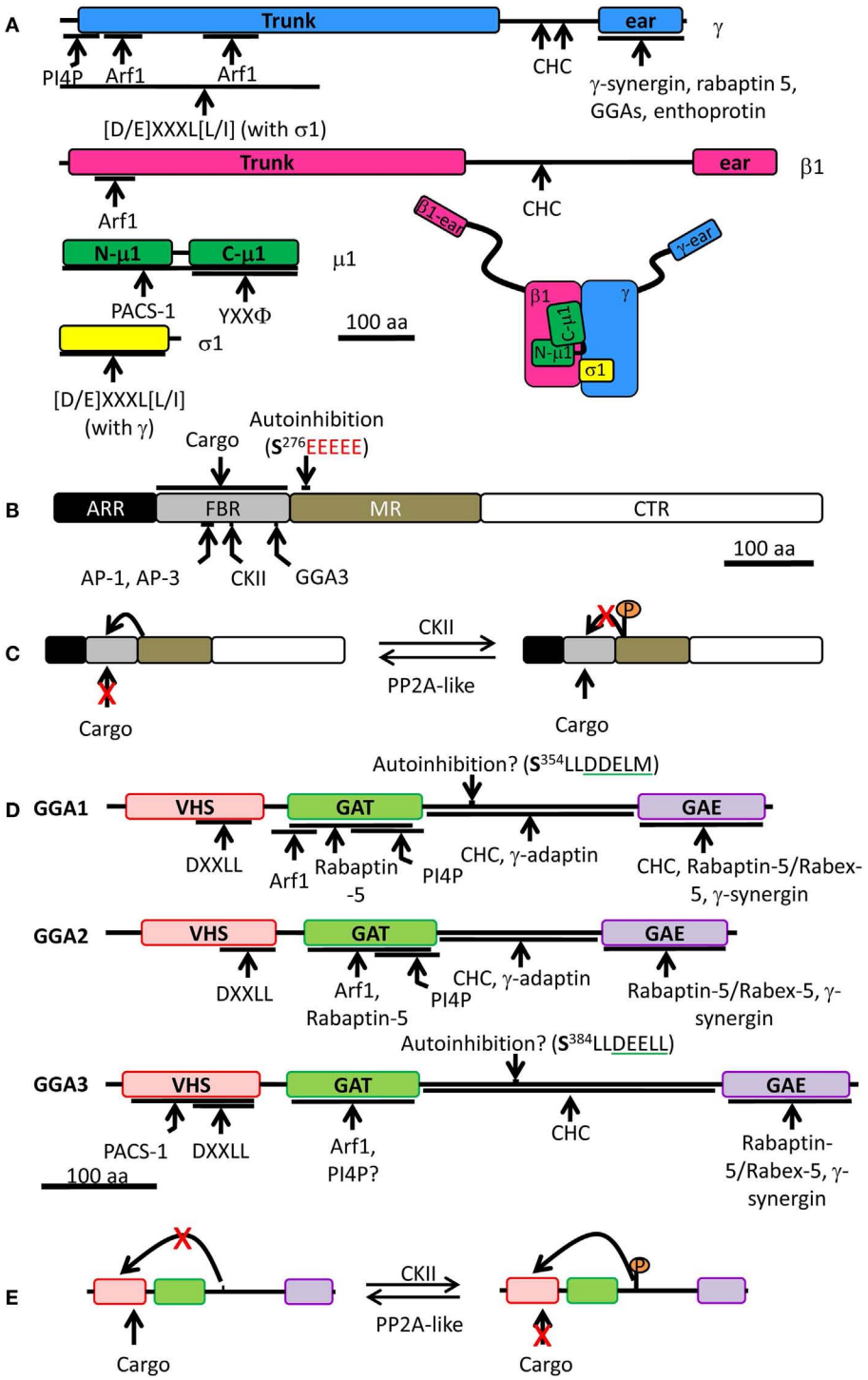

FIGURE 4 | Schematic of the AP-1 complex, PACS-1, and mammalian GGAs. **(A)** AP-1 is made of four different subunits: γ (blue), β1 (pink), μ1 (green), and σ1 (yellow). For each subunit, binding partners or binding motifs that are recognized are indicated; Φ indicates a hydrophobic residue; X can be any amino acid. The overall organization of the complex is shown at the bottom right. **(B)** PACS-1 is composed of four domains: ARR (atrophin-1-related region, black), FBR (furin binding region, gray), MR (middle region, tan), and CTR (C-terminus region, white). The autoinhibition sequence in the MR is shown (CKII phosphorylation site is in bold and the acidic cluster in red), along with the CKII binding site in the FBR. AP-1 and AP-3 interact with the same site in the FBR while GGA3 interacts with a different site. The FBR is also responsible for interactions with cargo. **(C)** Autoinhibition mechanism: the autoinhibition domain binds FBR, preventing PACS-1 interaction with cargo. When CKII phosphorylates Ser^{276} of the autoinhibition domain, it inhibits the internal binding and promotes cargo interaction with PACS-1. PP2A, protein phosphatase 2A. **(D)** Each GGA is composed of four domains: VHS (pink), GAT (green), hinge (bar), and GAE (purple). Regulatory domain

(Continued)

FIGURE 4 | Continued
and sites of protein-protein interaction are shown. Autoinhibition sequence is shown (CKII phosphorylation site is in bold and the DXLL motif is underlined in green). VHS, Vps27p, Hrs, Stam; GAT, GGA, and TOM; GAE, γ-adaptin ear. **(E)** Autoinhibition mechanism: when phosphorylated by CKII, the autoinhibition domain binds VHS preventing cargo interaction. When the autoinhibition is dephosphorylated, no internal binding occurs allowing cargo interaction with GGA. The single letter code for amino acids was used; CHC, clathrin heavy chain; CKII, casein kinase II.

vesicles (70), and immature SG membranes from PC12 cells (71). PI4KIIα is recruited to membranes upon palmitoylation of a central CCPCC motif (62). Deletion of the CCPCC motif or prevention of its palmitoylation resulted in loss of PI4KIIα perinuclear localization and loss of PI4KIIα activity (62). PI4KIIα palmitoylation is required for kinase activity and for localization to lipid rafts at the TGN but its targeting motif to Golgi membranes remains to be determined (63, 72). Lipid rafts are enriched in cholesterol and reduction of endogenous cholesterol levels resulted in loss of PI4P synthesis by PI4KIIα (63, 73). The membranes of neuroendocrine SGs contain high levels of cholesterol (74, 75). A decrease in the cholesterol level in AtT-20 cells inhibited the formation of constitutive secretory vesicles and SGs (76). Since PI4KIIα requires cholesterol for activity and membrane localization (63) and cholesterol is required for SG formation, this suggests that PI4KIIα is required for SG biogenesis.

MATURATION OF SGs

Once immature SGs are formed, they are not responsive to secretagogues and must undergo a maturation process to gain this ability. SG maturation involves a decrease in lumenal pH, SG fusion, and membrane remodeling.

pH DECREASE

The lumen of the TGN and the lumen of immature SGs are comparable in pH (pH 6.3), while mature SGs are more acidic (luminal pH 5.5). Secretogranin II processing in PC12 cells exogenously expressing prohormone convertase 2 occurs in immature SGs but not in the TGN (77). Although similar in lumenal pH, the TGN and immature SGs are two distinctly different compartments; the proteolytic processing of some prohormones and granins starts in immature SGs, not in the TGN. The decrease in pH during SG maturation is necessary for full processing of prohormones and granins because some hormone processing enzymes, such as PAM-1, exhibit maximal catalytic activity at pH 4.5–5 (78).

SG FUSION

Maturation of SGs can be characterized by a decrease or an increase in size. Analysis of immature and mature SGs in PC12 cells and mammotrophs revealed an increase in SG size during maturation (16, 79). An elegant biochemical assay revealed that the increase of SG size in PC12 cells was due to homotypic fusion of immature SGs (10). SG fusion involves syntaxin 6, a target (t)-SNARE [Soluble NSF (*N*-ethylmaleimide-Sensitive Factor) Associated Protein (SNAP) Receptor] protein, and synaptotagmin IV (80, 81). The SNARE complex is involved in membrane fusion and is composed of two t-SNAREs, located on the target membrane, and one vesicle (v)-SNARE on the vesicle membrane. Members of the synaptotagmin family are associated with the vesicular membrane and regulate membrane fusion with the SNARE complex. Syntaxin 6 localizes to the TGN, endosomes, and immature SGs (82, 83), while synaptotagmin IV is largely present at the Golgi and in immature SGs (84, 85). Blocking the fusion event decreases prohormone convertase 2 processing and activity, resulting in impaired SG maturation (80). Although this concept is attractive, there is no evidence of SG fusion in other types of neuroendocrine cells. SG fusion of a different type is clearly observed during compound exocytosis; mature SGs fuse together to promote rapid release of SG content (86).

MEMBRANE REMODELING

The reduction of SG size during maturation may be explained by membrane remodeling. The presence of a clathrin coat on patches of immature SG membrane revealed egress of material in clathrin-coated vesicles, mediated by the AP, AP-1A (8, 9, 54). As a result, proteins like vesicle associated membrane protein 4 (VAMP4) (87, 88), furin (89), and both mannose 6-phosphate receptors (MPRs) (83, 90–92), each of which is known to have a canonical AP-1A binding site in its cytosolic domain, are found in immature SGs but not in mature SGs. Although the fate of the material retrieved from immature SGs is not entirely clear, there are lines of evidence suggesting that it can be recycled to the TGN or secreted in a process called constitutive-like secretion (**Figure 1**). The study of constitutive-like secretion is difficult to monitor since it refers only to the non-stimulated secretion of regulated SG proteins as they traverse immature SGs; without a means of assessing the time since synthesis, it is impossible to distinguish basal from constitutive-like secretion. Nevertheless, constitutive-like secretion has held many scientists' attention due to its potential link to cancer and metabolic disease. Much of our knowledge of constitutive-like secretion comes from studying retrieval of material from immature SGs. The cytosolic machinery involved in this process contains the APs, AP-1A, and GGAs, and their partner phosphofurin acidic cluster sorting protein 1 (PACS-1). The discovery of an interaction between the cytosolic tail of membrane SG proteins retrieved during SG maturation with these cytosolic proteins has expanded our understanding of membrane remodeling during SG maturation. Each cytosolic component essential for maturation is presented below, followed by the description of SG membrane proteins trafficking involving AP-1A, GGAs, or PACS-1.

CYTOSOLIC MACHINERY

ADAPTOR PROTEIN 1A

The adaptor protein family

The adaptor protein family includes five cytosolic heterotetrameric complexes: AP-1 (γ/β1/μ1/σ1), AP-2 (α/β2/μ2/σ2), AP-3 (δ/β3/μ3/σ3), AP-4 (ε/β4/μ4/σ4), and AP-5 (ζ/β5/μ5/σ5) (93–96). In mammals, several isoforms have been reported for subunits of AP-1, AP-2, and AP-3: AP-1 has two γ subunits (γ1 and γ2), two

μ subunits (μ1A and μ1B), and three σ subunits (σ1A, σ1B, and σ1C); AP-2 has two α subunits (α1 and α2); AP-3 has two β subunits (β3A and β3B), two μ subunits (μ3A and μ3B); and two σ subunits (σ3A and σ3B) (93, 97–101). Every subunit is ubiquitously expressed except for μ1B, which is found exclusively in polarized epithelial cells, and β3B and μ3B, which are only found in neurons and neuroendocrine cells (99–101). Each adaptor protein carries transmembrane proteins on a defined intracellular route: AP-1 brings cargo between the TGN and endosomes and removes material from immature SGs; AP-2 is an important player in clathrin-mediated endocytosis; AP-3 carries cargo to lysosomes and lysosome-related organelles; AP-4 transports cargo from the TGN to the plasma membrane or endosomes; AP-5 is found on late endosomal membranes.

The cytosolic domains of cargo proteins present motifs which are recognized by adaptor protein complexes. For example, the Tyr sorting motif (YXXΦ, where X is any residue and ϕ is a hydrophobic residue) is recognized by the μ subunit of all adaptor protein complexes, with the possible exception of AP-5, which has not yet been studied (**Figure 4A**) (102–105). The di-leucine sorting motif [(D/E)XXXL(L/I)] interacts at the interface of two subunits: γ/σ1 in AP-1, α/σ2 in AP-2, and ε/σ3 in AP-3 (**Figure 4A**) (106, 107); AP-4 and AP-5 have not been shown to interact with the di-leucine motif. The γ/α/δ/ε/ζ and β1-5 subunits contain a large N-terminal trunk domain that associates with the other three subunits of the complex, followed by a hinge region and a C-terminal ear domain, which can interact with cytosolic proteins (**Figure 4A**) (108–111). The hinge region of the β subunits of AP-1, AP-2, and AP-3 is capable of binding the terminal domain of the clathrin heavy chain *in vitro*, while the β subunits of AP-4 and AP-5 lack such a motif (**Figure 4A**) (112–114). Although the β3 subunit of AP-3 can bind clathrin, purified clathrin-coated vesicles lack AP-3, suggesting that AP-3 works independently of clathrin (115). In addition, there is also evidence that the γ and α hinge domains of AP-1 and AP-2 interact with clathrin (**Figure 4A**) (116, 117).

AP-1A recruitment to membranes depends on Arf1 and PI4P

Adaptor protein 1A (γ/β1/μ1A/σ1) accumulates at the TGN, which is enriched in PI4P. *In vitro* binding assays revealed that purified AP-1A interacts preferentially with PI4P (**Figure 4A**) (59). Indeed, structural studies on the AP-1A core confirmed the presence of a PI4P binding site within the γ subunit (118). Reduction of PI4KIIα levels in a monkey kidney cell line decreased the TGN content of PI4P and disrupted the TGN localization of AP-1A (59). However, a recent study on development of the *Drosophila* salivary gland revealed no change in the localization of AP-1 in PI4KIIα null flies, suggesting that PI4P synthesis in flies can be carried out by another PI4K (69). Although the presence of PI4KIIα on the membranes of immature SGs suggests that PI4P can be formed there, there is no evidence that AP-1A recruitment to immature SGs requires PI4P in neuroendocrine cells.

Brefeldin A treatment of intact cells produces a diffuse cytoplasmic localization of AP-1A instead of the normal perinuclear, membrane-associated localization. However, pretreatment with GTPγS, a non-hydrolyzable analog of GTP, prevented the membrane dissociation of AP-1A upon addition of brefeldin A in permeabilized normal rat kidney cells (119). Indeed, AP-1A is recruited to membranes upon the binding of GTP-bound Arf1 to the trunk region of its β1 and γ subunits (**Figure 4A**) (55, 120–122). Studies on PC12 cells also show that AP-1A recruitment to immature SG membranes requires Arf1 (54, 55). Interestingly, AP-1A cannot be recruited to mature SG membranes in PC12 cells, in agreement with morphological studies indicating that AP-1A/clathrin coats are not found on mature SGs (55). A recent structural study of AP-1A in complex with GTP-bound Arf1 revealed that Arf1 can change the conformation of μ1A without the presence of PI4P or cargo; the addition of cargo promotes this conformational change (120). This shift in μ1A conformation is thought to promote the association of μ1A with cargo.

In addition to Arf1 and PI4P, AP-1A phosphorylation affects its localization; cytosolic AP-1A is phosphorylated on its β1 subunit, while membrane-associated AP-1A is phosphorylated on its μ1A subunit (123). Phosphorylation of the β1 subunit prevents clathrin binding, while phosphorylation of μ1A may promote conformational changes in the subunit that enable it to interact with cargo (118, 124). The phosphorylation status of AP-1A is thus essential for protein trafficking.

PHOSPHOFURIN ACIDIC CLUSTER SORTING PROTEIN 1 – AN ENHANCER OF AP-1A FUNCTION

Adaptor protein 1A is not the only AP involved in the retrieval of material from immature SGs. Furin, a type I transmembrane endoprotease, cleaves peptides after the last Arg of an R-X-[K/R]-R motif; its discovery was a key advance contributing to the identification of the prohormone convertases that are essential to SG function. Furin is concentrated in the TGN and travels between the TGN, endosomes, and plasma membrane (125). In cells containing a regulated secretory pathway, furin was identified in immature SGs but not in mature SGs (89). The removal of furin from immature SGs involves AP-1A and clathrin-coated vesicles (89). Its cytoplasmic domain contains a Tyr-based sorting motif and an acidic cluster, which includes two Ser residues, both of which are substrates for CKII (**Table 1**) (126, 127). The Tyr motif found in the cytosolic domain of furin mediates TGN exit and plasma membrane internalization; the acidic cluster is important for retrieval of furin from endosomes and immature SGs (89, 127, 128). Mutation of the two CKII phosphorylation sites in furin to Ala (to prevent phosphorylation) resulted in the accumulation in mature SGs in a corticotrope tumor cell line (89, 129). Since AP-1A does not bind to acidic cluster, another interactor was sought. A search for proteins with high affinity for the phosphorylated acidic cluster through yeast two-hybrid screens led to the discovery of PACS-1 (127).

Phosphofurin acidic cluster sorting protein 1 is a ubiquitously expressed cytosolic protein comprised of four domains: at its N-terminus is an atrophin-1-related region (ARR), with limited homology to atrophin-1; this region is followed by a furin binding region (FBR), the middle region (MR), and the C-terminal region (CTR) (**Figure 4B**) (127). The functions of the ARR and the CTR are unknown. The FBR of PACS-1 interacts with acidic clusters in cargo proteins, with APs (AP-1A, AP-3, and GGA), and with CKII (**Figure 4B**) (127, 129, 130). The MR contains an autoinhibition domain, which is composed of an acidic cluster with a CKII phosphorylation site (**Figure 4C**); when this region is not phosphorylated, the MR binds the FBR, resulting in inhibition of

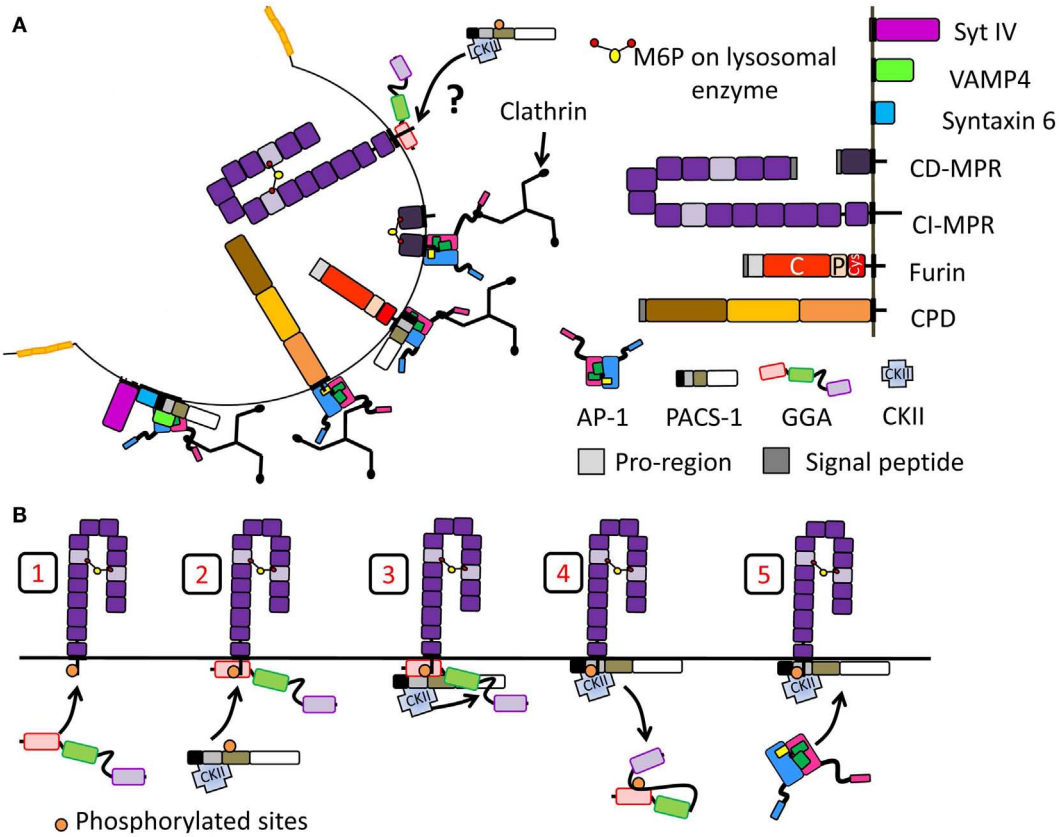

FIGURE 5 | Segregation of proteins at the immature SG during membrane remodeling. Schematic of proteins introduced in **Figure 2** are reused. **(A)** Proteins removed during SG maturation involving the recruitment of clathrin and clathrin adaptor protein. Proteins shown to interact with AP-1 and/or PACS-1 or GGAs are shown. In the case of CI-MPR, it is not clear whether GGAs help the recruitment of PACS-1 and AP-1 thus promoting its retrieval. **(B)** Model of adaptor protein recruitment for CI-MPR transport: GGA3 binds CI-MPR cytosolic tail (step 1). Then, PACS-1, presumably already interacting with CKII, is recruited to the GGA3/cargo complex (step 2). CKII phosphorylates the GGA3 hinge autoinhibitory region (step 3) resulting in GGA3 dissociation from membranes (step 4). PACS-1 then recruits AP-1 for the CI-MPR transport (step 5). Model adapted from (174).

PACS-1 binding to its cargo (131). When the MR is phosphorylated by CKII, it reduces MR affinity for FBR, allowing the FBR to bind to acidic clusters in cargo proteins (130, 131). Furin has been identified in a heterotrimeric complex with AP-1A and PACS-1 (129). Expression of a PACS-1 mutant capable of binding the furin acidic cluster, but not AP-1A, does not alter the distribution of AP-1A, instead resulting in the accumulation of furin in mature SGs (129). This demonstrates that removal of furin from immature SGs is a cooperative process involving both AP-1A and PACS-1 (**Figure 5A**).

GGAs – ANOTHER FAMILY OF ADAPTOR PROTEINS ESSENTIAL FOR SG MATURATION

Golgi-localizing, γ-adaptin ear homology domain, ARF-binding proteins (GGAs) were discovered by several groups interested in different aspects of the proteins. Boman et al. screened for Arf3 binding partners using a yeast two-hybrid system, while Hirst et al. used a bioinformatic approach to look for proteins with homology to the ear region of the γ subunit of AP-1 (109, 132). These studies, combined with the fact that the proteins discovered concentrated in the TGN area, explain the origin of the name GGA (109, 133).

The GGA family contains three members in humans (GGA1, GGA2, and GGA3), two in *Saccharomyces cerevisiae* (Gga1p and Gga2p), and one in *Drosophila melanogaster* and *Caenorhabditis elegans* (109, 132, 134). Each member is ubiquitously expressed and acts as a monomeric clathrin adaptor (132, 135). From their N-terminus to their C-terminus, they are composed of a VHS [vacuolar protein sorting 27 (Vps27), hepatocyte-growth factor-receptor substrate (Hrs), signal-transducing adaptor molecule (Stam)] domain, a GAT [GGA and TOM (Target of Myb)] domain, a hinge, and a GAE (γ-adaptin ear) domain (134) (**Figure 4D**).

The VHS domain was identified based on its role in the trafficking of yeast Vps27p and for its homology to two other monomeric endosome-localized clathrin APs, Hrs, and Stam (109, 132, 136). A yeast two-hybrid screen revealed that the cytosolic domains of proteins containing either a tyrosine sorting motif (YXXΦ) or a di-leucine sorting motif [(D/E)XXXL(L/I)] were not recognized by any GGA proteins, but were specific to adaptor protein complexes (126, 137). The VHS domain of GGAs recognize a motif called acidic cluster-di-leucine motif (DXXLL), which is different from the adaptor protein di-leucine sorting motif [(D/E]XXXL(L/I)] (**Figure 4D**) (134, 137).

Target of Myb1 (TOM1), a protein involved in the trafficking of ubiquitinated proteins, contains a GAT domain similar to the GAT domain in GGAs. Indeed, both yeast Gga1p and mammalian GGAs bind monoubiquitin via their GAT domain (134, 138–141). This interaction is required for the sorting of some ubiquitinated cargo proteins in *S. cerevisiae*, such as Gap1 and Arn1 (134, 138, 142, 143). The GAT domain interacts with GTP-bound Arf1 and Arf3 and the C-terminus of GAT binds PI4P; as for AP-1A, both binding sites are required for proper membrane localization of GGA in cells (**Figure 4D**) (132, 133, 141). Indeed, brefeldin A treatment results in the dissociation of GGAs from TGN membranes and in their accumulation in the cytosol, as seen for AP-1A (109, 132, 133, 135). Interestingly, association of the GAT domain of GGA3 to Arf1 blocks GAP proteins from acting on GTP-bound Arf1, thus stabilizing it on TGN membranes (53).

The hinge region between the GAT and the GAE domains is predicted to lack secondary structure (134) and contains a clathrin binding motif which is necessary for the recruitment of clathrin *in vitro* and in cells (**Figure 4D**) (53, 109). While the GAE domain of GGA1 also interacts with clathrin heavy chain *in vitro*, the GAE domains of GGA2 and GGA3 are unable to do so (53). GGAs are important for the recruitment of clathrin to membranes; overexpression of GGAs increases the TGN localization of clathrin while overexpression of truncated GGA1 lacking the hinge and GAE domains reduces the TGN level of clathrin (53). Moreover, *in vitro* studies revealed that the GGA1-hinge region and the γ subunit of AP-1 interact (**Figures 4A,D**) (108, 144). In addition, the hinge region of both GGA1 and GGA3 contains a DXXL[L/M] motif, which can bind the VHS domain when the surrounding Ser residue has been phosphorylated by CKII (**Figures 4D,E**) (108, 145); this internal binding results in autoinhibition of the AP by loss of cargo binding (108, 145, 146). The autoinhibition is removed when the Ser residue is dephosphorylated by a protein phosphatase 2A-like enzyme (146). *In vitro* phosphorylation by CKII was not observed for GGA2, suggesting that GGA2 is controlled differently (108, 126). Although the autoinhibition concept is attractive, a recent structural report refutes the existence of such a motif within GGA1 and possibly within GGA3 as well (147). These conflicting results are currently unclear, but emphasize the fact that our knowledge of GGAs is incomplete.

The GAE domain has homology to the ear domain of γ-adaptin of AP-1 (109, 132, 133, 135, 148). It interacts with several cytosolic proteins including rabaptin-5, a Rab4/Rab5 effector involved in membrane fusion at the endosomes (109, 149, 150) and γ-synergin (148).

In neuroendocrine cells, reducing the levels of GGA3 or overexpressing a dominant negative form of GGA1 resulted in impaired egress of syntaxin 6, cation-independent MPR (CI-MPR), and VAMP4 from immature SGs and in decreased proteolytic processing of prohormone convertase 2 and secretogranin II (151). Thus GGAs, AP-1A, and PACS-1 are all key components in the maturation of SGs in neuroendocrine cells.

DO GGAs AND AP-1A WORK TOGETHER?

Despite differences in their cargo recognition motifs, GGAs and AP-1A are both recruited to TGN membranes in an Arf1 and PI4P dependent manner, interact with clathrin and share common cargoes, such as CI-MPR (**Table 1**). Using transmission electron microscopy, vesicles budding from the TGN were seen to contain one AP or both GGA2 and AP-1A (108). A novel technique developed in mammalian cells to rapidly inactivate AP-1A or GGA2 revealed that AP-1A is the main AP required for trafficking between the TGN and endosomes; when AP-1A is inactivated, GGA2 is no longer present in clathrin-coated vesicles (152). In addition, GGA2 is thought to be required for proper localization of rabaptin-5, a group of lysosomal hydrolases, both types of MPRs and sortilin in clathrin-coated vesicles. Other substrates, such as Arf1, carboxypeptidase D (CPD), furin, the copper transporters (ATP7A and ATP7B), or the SNARE proteins require AP-1A for localization in clathrin-coated vesicles (152). In agreement with these data, mutation of the GGA binding site in the cytosolic tail of the CI-MPR decreases its amount in clathrin coats at the TGN, suggesting that GGAs help recruit specific cargo with APs and clathrin (108). However, a recent study in yeast using fluorescently tagged proteins suggested that the Gga proteins come into play first, and then recruit other proteins along with AP-1A after being released from the membrane (153). The yeast study also suggested that AP-1 and Gga proteins work mainly in separate vesicles. This divergence between yeast and mammals is unclear and may be linked to changes during evolution. Nevertheless, these studies do not provide information on the mechanism which governs the egress of material at the immature SG. In addition, yeast do not have a regulated secretory pathway, limiting their use in understanding SG maturation.

REAL LIFE EXAMPLES

Most of the integral membrane proteins found in post-TGN membranes contain multiple signaling motifs in their cytosolic tails. The study of protein retrieval from immature SGs was facilitated by our growing knowledge of APs and the motifs they recognize. While our understanding of the rules governing retention vs. retrieval of membrane proteins from immature SGs is not yet complete, detailed studies of the interactions of several immature SG cargo protein cytosolic tails with multiple APs reveals many of the key features (**Figure 5A**; **Table 1**).

SNARE PROTEINS

Similar observations to furin were made with the v-SNARE component, VAMP4 which contains an AP-1A binding motif (dileucine sorting motif) and an acidic cluster surrounding a CKII phosphorylation site (**Table 1**) (87). VAMP4 accumulates at the TGN, on endosomes and on immature SG of PC12 and AtT-20 cell lines (87, 154). As for furin, overexpression of PACS-1 mutant unable to interact with AP-1A but capable of interacting with VAMP4 resulted in accumulation of VAMP4 in mature SG (87). Interestingly, VAMP4 accumulates in mature SGs only if both its AP-1A and its PACS-1 binding motifs are mutated; if either binding motif is remaining, VAMP4 is efficiently removed from immature SGs (87). This is different from furin which accumulated in mature SGs when the CKII sites were mutated. The AP-1A/PACS-1/clathrin sorting system seems to work differently with VAMP4 and furin.

In addition, VAMP4 interacts with syntaxin 6, which binds synaptotagmin IV (80, 154). All three proteins are retrieved from

immature SGs (83, 84, 154). Although *in vitro* studies failed to show binding between syntaxin 6 and AP-1A (87), observation of immature SGs using electron microscopy showed that syntaxin 6 is retrieved in AP-1A and clathrin containing vesicles (83). It remains unclear whether synaptotagmin IV interacts with AP-1A, but since the removal of VAMP4 and syntaxin 6 has been linked with AP-1A, it seems likely that synaptotagmin IV removal is also dependent on the AP-1A/PACS-1/clathrin sorting system due to its indirect binding with VAMP4. Interestingly synaptotagmin IV is known to inhibit calcium triggered exocytosis (84), suggesting that its removal is necessary to make mature SG responsive to secretagogues. Since synaptotagmin IV plays a critical role in SG fusion which is an essential step in SG maturation, these studies would suggest that SG fusion occurs before membrane remodeling.

THE MANNOSE 6-PHOSPHATE RECEPTORS

Mannose 6-phosphate receptors transport soluble lysosomal hydrolases from the TGN to endosomes (137, 155). MPRs are found in immature SGs and are removed during maturation in clathrin-coated vesicles that contain AP-1A (83). Two MPRs have been described: MPR300, the CI-MPR, and MPR46, the cation-dependent MPR (CD-MPR). Much has been learned by studying the multiple trafficking signals in both MPRs. Both MPRs contain Tyr sorting motifs (YXXΦ) and an acidic cluster-di-leucine motif (DXXLL) next to a CKII phosphorylation site (**Table 1**). Early studies revealed that the Tyr motif of CI-MPR is recognized by AP-2 but not by AP-1A (156). CD-MPR contains two tyrosine motifs: the first tyrosine motif is located next to the transmembrane domain, and may not be a signaling motif because of the hindrance caused by the membrane (**Table 1**, Y^{211}QRL). The second tyrosine motif is found away from the membrane (**Table 1**, Y^{256}RGV) and is implicated in the protein internalization (157).

The DXXLL motif is recognized by the VHS domain of GGAs (137, 150). Interestingly, the DXXLL motif found on the cytosolic tail of the CI-MPR binds the VHS domain of all GGAs while the DXXLL motif of the CD-MPR interacts with the VHS domain of GGA1, interacts weakly with GGA3 and does not interact with GGA2 (137, 150). Mutational analyses revealed that the residues surrounding the motif are important for establishing GGA specificity (137). Down-regulation of GGA3 or inhibition of GGA1 results in the accumulation of CI-MPR in mature SGs, suggesting that retrieval of CI-MPR from immature SGs requires GGAs (151).

Independent *in vitro* studies focusing on either CD-MPR or CI-MPR showed that removal of the di-leucine motif from either receptor had little effect on its ability to recruit AP-1A. In CI-MPR, elimination of the CKII phosphorylation site abolished recruitment of AP-1A (90, 127). Indeed, binding of AP-1A to CI-MPR requires prior phosphorylation of its cytosolic domain by CKII (91, 158). These features suggested that PACS-1 might be involved in the trafficking of CI-MPR. In non-neuroendocrine cells, reducing the cellular level of PACS-1 or overexpressing a PACS-1 mutant unable to interact with acidic clusters resulted in accumulation of CI-MPR in endocytic compartments, suggesting that PACS-1 recruitment is necessary for MPR retrieval from the endosomes to the TGN (127, 129). AP-1A binding to CD-MPR requires the acidic cluster; experiments aimed at understanding the role of phosphorylation at the Ser CKII site in CD-MPR in its binding of AP-1A have yielded conflicting results (**Table 1**, Ser^{268}) (91, 159). It is not yet known whether MPRs are retrieved from immature SGs in a PACS-1 dependent manner.

GGA3 and PACS-1 interact with the CI-MPR at sites that are overlapping, but not identical (**Table 1**) (130). The FBR region of PACS-1 binds CKII, enhancing its kinase activity (130). This results in phosphorylation of the MR of PACS-1, releasing the FBR for cargo interaction (**Figure 4C**). In addition, CKII phosphorylates GGA3, decreasing its affinity for cargo and thus making space for PACS-1 to bind (**Figures 4E** and **5B**) (130). Although this study did not focus on immature SGs, it provides a mechanism of why GGA and AP-1A/PACS-1 are necessary for SG maturation.

CARBOXYPEPTIDASE D DOES NOT CONTAIN AN AP-1A BINDING MOTIF

The exopeptidase CPD, a type I transmembrane protein, accumulates in the TGN and cycles between the TGN and plasma membrane via endosomes (160). In AtT-20 cells, CPD is found in immature, but not in mature SGs suggesting that it is removed during SG maturation (161). The isolated luminal domain of CPD primarily enters the constitutive secretory pathway, suggesting that signals in its cytosolic tail play an essential role in CPD entry into immature SGs and in the TGN retention of CPD (161). The CPD cytosolic tail contains an acidic cluster with two CKII phosphorylation sites (TDT), but lacks classical AP and GGA binding motifs (**Table 1**). *In vitro* binding assays revealed that the CPD cytosolic tail binds to AP-1A and AP-2 only when its two CKII phosphorylation sites are phosphorylated or have been mutated to phosphomimetic residues (EDE) (**Table 2**) (162). Deletion of the C-terminus of the CPD tail, which contains the CKII phosphorylation sites does not abolish AP-1A or AP-2 binding (**Table 2**) (162), suggesting a role for additional CPD/AP-1A/2 interaction motifs. A tyrosine-like motif (**Table 2**, F^{1332}HRL) located upstream of the acidic cluster is thought to be important for TGN export and endocytosis and is necessary for AP-1A and AP-2 binding (162). In addition, the C-terminus of CPD may bind another cytosolic protein which would prevent APs to interact. This unidentified protein probably loses its affinity for the C-terminus of CPD when the CKII sites are phosphorylated or removed, allowing APs to interact. Phosphorylation of CPD by CKII promotes AP-1A binding, suggesting that PACS-1 plays a role in its trafficking. The trafficking of CPD at immature SGs probably results from the coordinated work of multiple cytosolic proteins including AP-1A and PACS-1.

VMAT2 SUGGESTS THE EXISTENCE OF ADDITIONAL ADAPTOR PROTEINS

The monoamine transporter, VMAT2, accumulates in mature SGs in neuroendocrine cells. Its cytosolic domain contains an acidic cluster with two CKII sites at the C-terminus; upon CKII phosphorylation, this site interacts with PACS-1 (163). As for furin, expression of VMAT2 in which the CKII sites have been replaced with phosphomimetic mutations promotes its retrieval from immature SGs. Mutation of these same two residues into Ala to prevent phosphorylation promotes VMAT2 accumulation in mature SGs (163); interestingly, expression of VMAT2 lacking the acidic cluster/CKII

Table 2 | Summary of mutational analysis of CPD tail.

Protein	Sequence	AP-1A binding
CPD-tail full, not phosphorylated	*TMD* C^{1319}ICSIKSNRHKDGFHRL^{1335} [. . .] S^{1356}LLSHEFQDETDTEEETLYSSKH^{1378} *COOH*	–
CPD-tail full, phosphomimetic	*TMD* C^{1319}ICSIKSNRHKDGFHRL^{1335} [. . .] S^{1356}LLSHEFQDEEDEEEETLYSSKH^{1378} *COOH*	++
CPD-tail missing the last 18 residues	*TMD* C^{1319}ICSIKSNRHKDGFHRL^{1335} [. . .] S^{1356}LLSH^{1360} *COOH*	+

Results adapted from (162). TMD, transmembrane domain; COOH, C-terminus of the protein. CKII phosphorylation site is in bold, the acidic cluster in red and the AP-1A-like site in blue. Gray marks TMD and COOH

domain resulted in its egress from immature SGs (163). Unlike furin, which accumulates in the TGN at steady state, VMAT2 concentrates in mature SG raising the question of VMAT2 retention mechanism. These findings suggest that additional cytosolic proteins are involved in the sorting of SG proteins at the immature SG and may explain the retention of other membrane proteins in SGs during maturation. Indeed the amidating enzyme, PAM, remains in SGs during maturation, and presents an acidic cluster with two CKII phosphorylation sites (39). Although direct binding between PAM cytosolic domain and PACS-1 has not been shown, it is possible that PAM interacts with the same cytosolic proteins which bind VMAT2 for its retention in SG.

PHOGRIN

Phogrin is a transmembrane protein that spans the membrane of immature and mature SGs. The cytosolic domain of phogrin contains a protein-tyrosine phosphatase (PTP) domain preceded by a 105 residue-long domain and followed by 10 residues at its C-terminus (**Figure 2B**; **Table 1**). The PTP domain of phogrin is an active phosphatidylinositol (PI) phosphatase; its enzymatic activity is thought to play an essential role in its ability to regulate peptide hormone secretion (164). Both domains surrounding the PTP domain are involved in the correct sorting of phogrin in the regulated secretory pathway (36, 37). The 105 residue stretch close to the transmembrane domain contains a tyrosine-extended motif (**Table 1**, Y^{655}QEL) and the 10 residues at the C-terminus present a di-leucine-like motif (**Table 1**, E^{993}EVNAIL). Both motifs are required for entry of phogrin into SGs and internalization at the plasma membrane (36, 37). Interestingly, both motifs are involved in the binding of phogrin to AP-1A and AP-2. Mutation of one of these motifs decreases the binding strength of APs for phogrin but does not abolish the interaction (36, 37). Although phogrin binds AP-1A via unconventional motifs, it still remains to be determined what prevents this transmembrane protein from being removed during SG maturation.

SORTILIN AND PRO-BDNF

Sortilin, a type I transmembrane protein, binds the pro-region of brain-derived neurotrophic factor (pro-BDNF) and transports it to SGs for processing (165). As for CPD, expression of the luminal domain of sortilin results in its entry into the constitutive secretory pathway, suggesting that entry into SGs is mediated by the cytosolic tail (166). A recent study revealed that interaction of sortilin with Huntingtin associated protein 1 (HAP-1) and pro-BDNF must occur for pro-BDNF entry into SGs and subsequent proteolytic processing (167). In the absence of HAP-1, sortilin, and pro-BDNF are targeted to lysosomes. Interestingly, the cytosolic tail of sortilin contains both a tyrosine motif and an acidic cluster-di-leucine motif, classical AP, and GGA binding sites, respectively (**Table 1**). Both motifs are implicated in sortilin internalization (168). As expected, the VHS domain of GGA2 interacts with the acidic cluster-di-leucine motif of sortilin (168). However, the tyrosine motif is recognized by the retromer complex, not by AP-1A (169). The AP-1A binding motif on sortilin remains to be elucidated. Both GGA2 and AP-1A were shown to be important for the TGN-to-endosome transport of sortilin. It is possible that HAP-1 interacts with sortilin to prevent GGA and AP-1A binding and mediates the entry of sortilin and pro-BDNF into SGs. Although sortilin contains AP binding motifs, it is not clear if sortilin is retrieved from immature SGs. One could assume that once in immature SGs, sortilin can release pro-BDNF and be retrieved during SG maturation.

CONCLUSION AND FUTURE DIRECTIONS

Little is known about the cytosolic machinery involved in sorting membrane proteins at the TGN for their entry into immature SGs. A recent study in *Drosophila* suggested that AP-3, the AP transporting proteins to lysosomes, was involved in sorting proteins into the regulated secretory pathway at the TGN level (170). Unfortunately, it is not known whether this is also true in the mammalian neuroendocrine system. In addition, studies on the trafficking of individual proteins raises many questions regarding the cytosolic machinery necessary for their retrieval or retention during SG maturation. It remains to be explained how a membrane protein which contains an AP (AP-1A, PACS-1, or GGAs) binding motif can remain in SGs during maturation. One possibility is that other cytosolic proteins bind the tails of membrane proteins, preventing their interaction with APs. Recent proteomic studies on purified SGs are an excellent source of information and may help identify additional proteins involved in the egress of membrane proteins (171, 172). Another possibility is a binding site within the cytosolic tail of membrane proteins which could prevent AP interaction; a post-translational modification, such as phosphorylation, can abolish this internal interaction while promoting the interaction with APs. Lastly, the membrane of the immature SG may play an important role in concentrating membrane proteins to be removed during maturation. Katsumata et al. addressed this question using the rat parotid gland as a source of SGs. The immature SG membrane revealed spatial segregation of membrane proteins: VAMP2 and Rab3D were in GM1a rich microdomains, while syntaxin 6 and

VAMP4 were not. Since VAMP2 and Rab3D remain in mature SGs while syntaxin 6 and VAMP4 are removed from immature SGs, membrane rearrangement could explain how the right proteins are sorted for retrieval of material at the immature SG (173). The trafficking of individual proteins found in immature SGs can differ based on the cell type or animal model. It is evident that professional secretory cells share a common mechanism, and that the differences they present are probably required for their physiological function.

ACKNOWLEDGMENTS

This work was supported by National Institutes of Health Grants DK32948 and DK32949. We thank Dr. Vishwanatha Kurutihalli and Dr. Yan Yan for thoughtful comments on the manuscript.

REFERENCES

1. Palade G. Intracellular aspects of the process of protein synthesis. *Science* (1975) **189**:867. doi:10.1126/science.1096303
2. Schuit FC, In't Veld PA, Pipeleers DG. Glucose stimulates proinsulin biosynthesis by a dose-dependent recruitment of pancreatic beta cells. *Proc Natl Acad Sci U S A* (1988) **85**:3865–9. doi:10.1073/pnas.85.11.3865
3. Alberts B, Johnson A, Lewis J, Raff M, Roberts K, Walter P. Intracellular compartments and protein sorting. In: Anderson M, Granum S, editors. *Molecular Biology of the Cell.* New York: Garland Science (2008). p. 695–748.
4. Colgan SM, Hashimi AA, Austin RC. Endoplasmic reticulum stress and lipid dysregulation. *Expert Rev Mol Med* (2011) **13**:e4. doi:10.1017/S1462399410001742
5. Mains RE, Cullen EI, May V, Eipper BA. The role of secretory granules in peptide biosynthesis. *Ann N Y Acad Sci* (1987) **493**:278–91. doi:10.1111/j.1749-6632.1987.tb27213.x
6. Hori O, Miyazaki M, Tamatani T, Ozawa K, Takano K, Okabe M, et al. Deletion of SERP1/RAMP4, a component of the endoplasmic reticulum (ER) translocation sites, leads to ER stress. *Mol Cell Biol* (2006) **26**:4257–67. doi:10.1128/MCB.02055-05
7. Alberts B, Johnson A, Lewis J, Raff M, Roberts K, Walter P. Intracellular Vesicular Traffic. In: Anderson M, Granum S, editors. *Molecular Biology of the Cell.* New York: Garland Science (2008). p. 749–812.
8. Tooze J, Tooze SA. Clathrin-coated vesicular transport of secretory proteins during the formation of ACTH-containing secretory granules in AtT-20 cells. *J Cell Biol* (1986) **103**:839–950. doi:10.1083/jcb.103.3.839
9. Orci L, Ravazzola M, Amherdt M, Louvard D, Perrelet A. Clathrin-immunoreactive sites in the Golgi apparatus are concentrated at the trans pole in polypeptide hormone-secreting cells. *Proc Natl Acad Sci U S A* (1985) **82**:5385–9. doi:10.1073/pnas.82.16.5385
10. Urbe S, Page LJ, Tooze SA. Homotypic fusion of immature secretory granules during maturation in a cell-free assay. *J Cell Biol* (1998) **143**:1831–44. doi:10.1083/jcb.143.7.1831
11. Morvan J, Tooze SA. Discovery and progress in our understanding of the regulated secretory pathway in neuroendocrine cells. *Histochem Cell Biol* (2008) **129**:243–52. doi:10.1007/s00418-008-0377-z
12. Milgram SL, Mains RE. Differential effects of temperature blockade on the proteolytic processing of three secretory granule-associated proteins. *J Cell Sci* (1994) **107**(Pt 3):737–45.
13. Orci L, Ravazzola M, Amherdt M, Madsen O, Vassalli JD, Perrelet A. Direct identification of prohormone conversion site in insulin-secreting cells. *Cell* (1985) **42**:671–81. doi:10.1016/0092-8674(85)90124-2
14. Arvan P, Castle D. Protein sorting and secretion granule formation in regulated secretory cells. *Trends Cell Biol* (1992) **2**:327–31. doi:10.1016/0962-8924(92)90181-L
15. Burgess TL, Kelly RB. Constitutive and regulated secretion of proteins. *Annu Rev Cell Biol* (1987) **3**:243–93. doi:10.1146/annurev.cellbio.3.1.243
16. Tooze SA, Flatmark T, Tooze J, Huttner WB. Characterization of the immature secretory granule, an intermediate in granule biogenesis. *J Cell Biol* (1991) **115**:1491–503. doi:10.1083/jcb.115.6.1491
17. Noel G, Mains RE. The ordered secretion of bioactive peptides: oldest or newest first? *Mol Endocrinol* (1991) **5**:787–94. doi:10.1210/mend-5-6-787
18. Suckale J, Solimena M. The insulin secretory granule as a signaling hub. *Trends Endocrinol Metab* (2010) **21**:599–609. doi:10.1016/j.tem.2010.06.003
19. Alvarez de TG, Fernandez-Chacon R, Fernandez JM. Release of secretory products during transient vesicle fusion. *Nature* (1993) **363**:554–8. doi:10.1038/363554a0
20. Surprenant A. Correlation between electrical activity and ACTH/beta-endorphin secretion in mouse pituitary tumor cells. *J Cell Biol* (1982) **95**:559–66. doi:10.1083/jcb.95.2.559
21. Farquhar MG, Palade GE. The Golgi apparatus (complex)-(1954-1981)-from artifact to center stage. *J Cell Biol* (1981) **91**:77s–103. doi:10.1083/jcb.91.3.77s
22. Arvan P, Castle D. Sorting and storage during secretory granule biogenesis: looking backward and looking forward. *Biochem J* (1998) **332**(Pt 3):593–610.
23. Tooze SA, Huttner WB. Cell-free protein sorting to the regulated and constitutive secretory pathways. *Cell* (1990) **60**:837–47. doi:10.1016/0092-8674(90)90097-X
24. Gerdes HH, Rosa P, Phillips E, Baeuerle PA, Frank R, Argos P, et al. The primary structure of human secretogranin II, a widespread tyrosine-sulfated secretory granule protein that exhibits low pH- and calcium-induced aggregation. *J Biol Chem* (1989) **264**:12009–15.
25. Chanat E, Huttner WB. Milieu-induced, selective aggregation of regulated secretory proteins in the trans-Golgi network. *J Cell Biol* (1991) **115**:1505–19. doi:10.1083/jcb.115.6.1505
26. Colomer V, Kicska GA, Rindler MJ. Secretory granule content proteins and the luminal domains of granule membrane proteins aggregate in vitro at mildly acidic pH. *J Biol Chem* (1996) **271**:48–55. doi:10.1074/jbc.271.1.48
27. Blazquez M, Thiele C, Huttner WB, Docherty K, Shennan KI. Involvement of the membrane lipid bilayer in sorting prohormone convertase 2 into the regulated secretory pathway. *Biochem J* (2000) **349**(Pt 3):843–52.
28. Hosaka M, Suda M, Sakai Y, Izumi T, Watanabe T, Takeuchi T. Secretogranin III binds to cholesterol in the secretory granule membrane as an adapter for chromogranin A. *J Biol Chem* (2004) **279**:3627–34. doi:10.1074/jbc.M310104200
29. Dikeakos JD, Di LP, Lacombe MJ, Ghirlando R, Legault P, Reudelhuber TL, et al. Functional and structural characterization of a dense core secretory granule sorting domain from the PC1/3 protease. *Proc Natl Acad Sci U S A* (2009) **106**:7408–13. doi:10.1073/pnas.0809576106
30. Hosaka M, Watanabe T. Secretogranin III: a bridge between core hormone aggregates and the secretory granule membrane. *Endocr J* (2010) **57**:275–86. doi:10.1507/endocrj.K10E-038
31. Hosaka M, Watanabe T, Sakai Y, Uchiyama Y, Takeuchi T. Identification of a chromogranin A domain that mediates binding to secretogranin III and targeting to secretory granules in pituitary cells and pancreatic beta-cells. *Mol Biol Cell* (2002) **13**:3388–99. doi:10.1091/mbc.02-03-0040
32. Cool DR, Normant E, Shen F, Chen HC, Pannell L, Zhang Y, et al. Carboxypeptidase E is a regulated secretory pathway sorting receptor: genetic obliteration leads to endocrine disorders in Cpe(fat) mice. *Cell* (1997) **88**:73–83. doi:10.1016/S0092-8674(00)81860-7
33. Irminger JC, Verchere CB, Meyer K, Halban PA. Proinsulin targeting to the regulated pathway is not impaired in carboxypeptidase E-deficient Cpefat/Cpefat mice. *J Biol Chem* (1997) **272**:27532–4. doi:10.1074/jbc.272.44.27532
34. Srinivasan S, Bunch DO, Feng Y, Rodriguiz RM, Li M, Ravenell RL, et al. Deficits in reproduction and pro-gonadotropin-releasing hormone processing in male Cpefat mice. *Endocrinology* (2004) **145**:2023–34. doi:10.1210/en.2003-1442
35. Saito N, Takeuchi T, Kawano A, Hosaka M, Hou N, Torii S. Luminal interaction of phogrin with carboxypeptidase E for effective targeting to secretory granules. *Traffic* (2011) **12**:499–506. doi:10.1111/j.1600-0854.2011.01159.x
36. Torii S, Saito N, Kawano A, Zhao S, Izumi T, Takeuchi T. Cytoplasmic transport signal is involved in phogrin targeting and localization to secretory granules. *Traffic* (2005) **6**:1213–24. doi:10.1111/j.1600-0854.2005.00353.x

37. Wasmeier C, Burgos PV, Trudeau T, Davidson HW, Hutton JC. An extended tyrosine-targeting motif for endocytosis and recycling of the dense-core vesicle membrane protein phogrin. *Traffic* (2005) **6**:474–87. doi:10.1111/j.1600-0854.2005.00292.x
38. Milgram SL, Mains RE, Eipper BA. COOH-terminal signals mediate the trafficking of a peptide processing enzyme in endocrine cells. *J Cell Biol* (1993) **121**:23–36. doi:10.1083/jcb.121.1.23
39. Rajagopal C, Stone KL, Francone VP, Mains RE, Eipper BA. Secretory granule to the nucleus: role of a multiply phosphorylated intrinsically unstructured domain. *J Biol Chem* (2009) **284**:25723–34. doi:10.1074/jbc.M109.035782
40. Steveson TC, Zhao GC, Keutmann HT, Mains RE, Eipper BA. Access of a membrane protein to secretory granules is facilitated by phosphorylation. *J Biol Chem* (2001) **276**:40326–37.
41. Krantz DE, Waites C, Oorschot V, Liu Y, Wilson RI, Tan PK, et al. A phosphorylation site regulates sorting of the vesicular acetylcholine transporter to dense core vesicles. *J Cell Biol* (2000) **149**:379–96. doi:10.1083/jcb.149.2.379
42. Barr FA, Huttner WB. A role for ADP-ribosylation factor 1, but not COP I, in secretory vesicle biogenesis from the trans-Golgi network. *FEBS Lett* (1996) **384**:65–70. doi:10.1016/0014-5793(96)00285-2
43. Chen YG, Shields D. ADP-ribosylation factor-1 stimulates formation of nascent secretory vesicles from the trans-Golgi network of endocrine cells. *J Biol Chem* (1996) **271**:5297–300. doi:10.1074/jbc.271.10.5297
44. Kahn RA, Gilman AG. The protein cofactor necessary for ADP-ribosylation of Gs by cholera toxin is itself a GTP binding protein. *J Biol Chem* (1986) **261**:7906–11.
45. Gillingham AK, Munro S. The small G proteins of the Arf family and their regulators. *Annu Rev Cell Dev Biol* (2007) **23**:579–611. doi:10.1146/annurev.cellbio.23.090506.123209
46. Kahn RA. Toward a model for Arf GTPases as regulators of traffic at the Golgi. *FEBS Lett* (2009) **583**:3872–9. doi:10.1016/j.febslet.2009.10.066
47. Goldberg J. Structural basis for activation of ARF GTPase: mechanisms of guanine nucleotide exchange and GTP-myristoyl switching. *Cell* (1998) **95**:237–48. doi:10.1016/S0092-8674(00)81754-7
48. Gommel DU, Memon AR, Heiss A, Lottspeich F, Pfannstiel J, Lechner J, et al. Recruitment to Golgi membranes of ADP-ribosylation factor 1 is mediated by the cytoplasmic domain of p23. *EMBO J* (2001) **20**:6751–60. doi:10.1093/emboj/20.23.6751
49. Lowery J, Szul T, Styers M, Holloway Z, Oorschot V, Klumperman J, et al. The Sec7 guanine nucleotide exchange factor GBF1 regulates membrane recruitment of BIG1 and BIG2 guanine nucleotide exchange factors to the trans-Golgi network (TGN). *J Biol Chem* (2013) **288**:11532–45. doi:10.1074/jbc.M112.438481
50. Fernandez CJ, Haugwitz M, Eaton B, Moore HP. Distinct molecular events during secretory granule biogenesis revealed by sensitivities to brefeldin A. *Mol Biol Cell* (1997) **8**:2171–85. doi:10.1091/mbc.8.11.2171
51. Hendricks LC, McClanahan SL, Palade GE, Farquhar MG. Brefeldin A affects early events but does not affect late events along the exocytic pathway in pancreatic acinar cells. *Proc Natl Acad Sci U S A* (1992) **89**:7242–6. doi:10.1073/pnas.89.15.7242
52. Goldberg J. Structural and functional analysis of the ARF1-ARFGAP complex reveals a role for coatomer in GTP hydrolysis. *Cell* (1999) **96**:893–902. doi:10.1016/S0092-8674(00)80598-X
53. Puertollano R, Randazzo PA, Presley JF, Hartnell LM, Bonifacino JS. The GGAs promote ARF-dependent recruitment of clathrin to the TGN. *Cell* (2001) **105**:93–102. doi:10.1016/S0092-8674(01)00299-9
54. Dittie AS, Hajibagheri N, Tooze SA. The AP-1 adaptor complex binds to immature secretory granules from PC12 cells, and is regulated by ADP-ribosylation factor. *J Cell Biol* (1996) **132**:523–36. doi:10.1083/jcb.132.4.523
55. Austin C, Hinners I, Tooze SA. Direct and GTP-dependent interaction of ADP-ribosylation factor 1 with clathrin adaptor protein AP-1 on immature secretory granules. *J Biol Chem* (2000) **275**:21862–9. doi:10.1074/jbc.M908875199
56. Ngo HM, Yang M, Paprotka K, Pypaert M, Hoppe H, Joiner KA. AP-1 in *Toxoplasma gondii* mediates biogenesis of the rhoptry secretory organelle from a post-Golgi compartment. *J Biol Chem* (2003) **278**:5343–52. doi:10.1074/jbc.M208291200
57. Burgess J, Jauregui M, Tan J, Rollins J, Lallet S, Leventis PA, et al. AP-1 and clathrin are essential for secretory granule biogenesis in *Drosophila*. *Mol Biol Cell* (2011) **22**:2094–105. doi:10.1091/mbc.E11-01-0054
58. Lui-Roberts WW, Collinson LM, Hewlett LJ, Michaux G, Cutler DF. An AP-1/clathrin coat plays a novel and essential role in forming the Weibel-Palade bodies of endothelial cells. *J Cell Biol* (2005) **170**:627–36. doi:10.1083/jcb.200503054
59. Wang YJ, Wang J, Sun HQ, Martinez M, Sun YX, Macia E, et al. Phosphatidylinositol 4 phosphate regulates targeting of clathrin adaptor AP-1 complexes to the Golgi. *Cell* (2003) **114**:299–310. doi:10.1016/S0092-8674(03)00603-2
60. Godi A, Di CA, Konstantakopoulos A, Di TG, Alessi DR, Kular GS, et al. FAPPs control Golgi-to-cell-surface membrane traffic by binding to ARF and PtdIns(4)P. *Nat Cell Biol* (2004) **6**:393–404. doi:10.1038/ncb1119
61. Balla A, Tuymetova G, Barshishat M, Geiszt M, Balla T. Characterization of type II phosphatidylinositol 4-kinase isoforms reveals association of the enzymes with endosomal vesicular compartments. *J Biol Chem* (2002) **277**:20041–50. doi:10.1074/jbc.M111807200
62. Barylko B, Mao YS, Wlodarski P, Jung G, Binns DD, Sun HQ, et al. Palmitoylation controls the catalytic activity and subcellular distribution of phosphatidylinositol 4-kinase II{alpha}. *J Biol Chem* (2009) **284**:9994–10003. doi:10.1074/jbc.M900724200
63. Minogue S, Chu KM, Westover EJ, Covey DF, Hsuan JJ, Waugh MG. Relationship between phosphatidylinositol 4-phosphate synthesis, membrane organization, and lateral diffusion of PI4KIIalpha at the trans-Golgi network. *J Lipid Res* (2010) **51**:2314–24. doi:10.1194/jlr.M005751
64. Waugh MG, Minogue S, Blumenkrantz D, Anderson JS, Hsuan JJ. Identification and characterization of differentially active pools of type IIalpha phosphatidylinositol 4-kinase activity in unstimulated A431 cells. *Biochem J* (2003) **376**:497–503. doi:10.1042/BJ20031212
65. Gasman S, Chasserot-Golaz S, Hubert P, Aunis D, Bader MF. Identification of a potential effector pathway for the trimeric Go protein associated with secretory granules. Go stimulates a granule-bound phosphatidylinositol 4-kinase by activating RhoA in chromaffin cells. *J Biol Chem* (1998) **273**:16913–20. doi:10.1074/jbc.273.27.16913
66. Wiedemann C, Schafer T, Burger MM. Chromaffin granule-associated phosphatidylinositol 4-kinase activity is required for stimulated secretion. *EMBO J* (1996) **15**:2094–101.
67. Barylko B, Gerber SH, Binns DD, Grichine N, Khvotchev M, Sudhof TC, et al. A novel family of phosphatidylinositol 4-kinases conserved from yeast to humans. *J Biol Chem* (2001) **276**:7705–8. doi:10.1074/jbc.C000861200
68. Xu Z, Huang G, Kandror KV. Phosphatidylinositol 4-kinase type IIalpha is targeted specifically to cellugyrin-positive glucose transporter 4 vesicles. *Mol Endocrinol* (2006) **20**:2890–7. doi:10.1210/me.2006-0193
69. Burgess J, Del Bel LM, Ma CI, Barylko B, Polevoy G, Rollins J, et al. Type II phosphatidylinositol 4-kinase regulates trafficking of secretory granule proteins in *Drosophila*. *Development* (2012) **139**:3040–50. doi:10.1242/dev.077644
70. Guo J, Wenk MR, Pellegrini L, Onofri F, Benfenati F, De Camilli P. Phosphatidylinositol 4-kinase type IIalpha is responsible for the phosphatidylinositol 4-kinase activity associated with synaptic vesicles. *Proc Natl Acad Sci U S A* (2003) **100**:3995–4000. doi:10.1073/pnas.0230488100
71. Panaretou C, Tooze SA. Regulation and recruitment of phosphatidylinositol 4-kinase on immature secretory granules is independent of ADP-ribosylation factor 1. *Biochem J* (2002) **363**:289–95. doi:10.1042/0264-6021:3630289
72. Graham TR, Burd CG. Coordination of Golgi functions by phosphatidylinositol 4-kinases. *Trends Cell Biol* (2011) **21**:113–21. doi:10.1016/j.tcb.2010.10.002
73. Waugh MG, Minogue S, Chotai D, Berditchevski F, Hsuan JJ. Lipid and peptide control of phosphatidylinositol 4-kinase IIalpha activity on Golgi-endosomal rafts. *J Biol Chem* (2006) **281**:3757–63. doi:10.1074/jbc.M506527200

74. Dhanvantari S, Loh YP. Lipid raft association of carboxypeptidase E is necessary for its function as a regulated secretory pathway sorting receptor. *J Biol Chem* (2000) **275**:29887–93. doi:10.1074/jbc.M005364200
75. Wang R, Hosaka M, Han L, Yokota-Hashimoto H, Suda M, Mitsushima D, et al. Molecular probes for sensing the cholesterol composition of subcellular organelle membranes. *Biochim Biophys Acta* (2006) **1761**:1169–81. doi:10.1016/j.bbalip.2006.06.016
76. Wang Y, Thiele C, Huttner WB. Cholesterol is required for the formation of regulated and constitutive secretory vesicles from the trans-Golgi network. *Traffic* (2000) **1**:952–62. doi:10.1034/j.1600-0854.2000.011205.x
77. Urbe S, Dittie AS, Tooze SA. pH-dependent processing of secretogranin II by the endopeptidase PC2 in isolated immature secretory granules. *Biochem J* (1997) **321**(Pt 1):65–74.
78. Husten EJ, Eipper BA. Purification and characterization of PAM-1, an integral membrane protein involved in peptide processing. *Arch Biochem Biophys* (1994) **312**:487–92. doi:10.1006/abbi.1994.1336
79. Farquhar MG, Reid JJ, Daniell LW. Intracellular transport and packaging of prolactin: a quantitative electron microscope autoradiographic study of mammotrophs dissociated from rat pituitaries. *Endocrinology* (1978) **102**:296–311. doi:10.1210/endo-102-1-296
80. Ahras M, Otto GP, Tooze SA. Synaptotagmin IV is necessary for the maturation of secretory granules in PC12 cells. *J Cell Biol* (2006) **173**:241–51. doi:10.1083/jcb.200506163
81. Wendler F, Page L, Urbe S, Tooze SA. Homotypic fusion of immature secretory granules during maturation requires syntaxin 6. *Mol Biol Cell* (2001) **12**:1699–709. doi:10.1091/mbc.12.6.1699
82. Bock JB, Klumperman J, Davanger S, Scheller RH. Syntaxin 6 functions in trans-Golgi network vesicle trafficking. *Mol Biol Cell* (1997) **8**:1261–71.
83. Klumperman J, Kuliawat R, Griffith JM, Geuze HJ, Arvan P. Mannose 6-phosphate receptors are sorted from immature secretory granules via adaptor protein AP-1, clathrin, and syntaxin 6-positive vesicles. *J Cell Biol* (1998) **141**:359–71. doi:10.1083/jcb.141.2.359
84. Eaton BA, Haugwitz M, Lau D, Moore H-PH. Biogenesis of regulated exocytotic carriers in neuroendocrine cells. *J Neurosci* (2000) **20**:7334–44.
85. Ibata K, Fukuda M, Hamada T, Kabayama H, Mikoshiba K. Synaptotagmin IV is present at the Golgi and distal parts of neurites. *J Neurochem* (2000) **74**:518–26. doi:10.1046/j.1471-4159.2000.740518.x
86. Pickett JA, Edwardson JM. Compound exocytosis: mechanisms and functional significance. *Traffic* (2006) **7**:109–16. doi:10.1111/j.1600-0854.2005.00372.x
87. Hinners I, Wendler F, Fei H, Thomas L, Thomas G, Tooze SA. AP-1 recruitment to VAMP4 is modulated by phosphorylation-dependent binding of PACS-1. *EMBO Rep* (2003) **4**:1182–9. doi:10.1038/sj.embor.7400018
88. Peden AA, Park GY, Scheller RH. The di-leucine motif of vesicle-associated membrane protein 4 is required for its localization and AP-1 binding. *J Biol Chem* (2001) **276**:49183–7. doi:10.1074/jbc.M106646200
89. Dittie AS, Thomas L, Thomas G, Tooze SA. Interaction of furin in immature secretory granules from neuroendocrine cells with the AP-1 adaptor complex is modulated by casein kinase II phosphorylation. *EMBO J* (1997) **16**:4859–70. doi:10.1093/emboj/16.16.4859
90. Dittie AS, Klumperman J, Tooze SA. Differential distribution of mannose-6-phosphate receptors and furin in immature secretory granules. *J Cell Sci* (1999) **112**(Pt 22):3955–66.
91. Mauxion F, Le BR, Munier-Lehmann H, Hoflack B. A casein kinase II phosphorylation site in the cytoplasmic domain of the cation-dependent mannose 6-phosphate receptor determines the high affinity interaction of the AP-1 Golgi assembly proteins with membranes. *J Biol Chem* (1996) **271**:2171–8. doi:10.1074/jbc.271.4.2171
92. Tortorella LL, Schapiro FB, Maxfield FR. Role of an acidic cluster/dileucine motif in cation-independent mannose 6-phosphate receptor traffic. *Traffic* (2007) **8**:402–13. doi:10.1111/j.1600-0854.2007.00541.x
93. Boehm M, Bonifacino JS. Genetic analyses of adaptin function from yeast to mammals. *Gene* (2002) **286**:175–86. doi:10.1016/S0378-1119(02)00422-5
94. Hirst J, Barlow LD, Francisco GC, Sahlender DA, Seaman MN, Dacks JB, et al. The fifth adaptor protein complex. *PLoS Biol* (2011) **9**:e1001170. doi:10.1371/journal.pbio.1001170
95. Robinson MS, Bonifacino JS. Adaptor-related proteins. *Curr Opin Cell Biol* (2001) **13**:444–53. doi:10.1016/S0955-0674(00)00235-0
96. Robinson MS. Adaptable adaptors for coated vesicles. *Trends Cell Biol* (2004) **14**:167–74. doi:10.1016/j.tcb.2004.02.002
97. Dell'Angelica EC, Ohno H, Ooi CE, Rabinovich E, Roche KW, Bonifacino JS. AP-3: an adaptor-like protein complex with ubiquitous expression. *EMBO J* (1997) **16**:917–28. doi:10.1093/emboj/16.5.917
98. Simpson F, Peden AA, Christopoulou L, Robinson MS. Characterization of the adaptor-related protein complex, AP-3. *J Cell Biol* (1997) **137**:835–45. doi:10.1083/jcb.137.4.835
99. Ohno H, Tomemori T, Nakatsu F, Okazaki Y, Aguilar RC, Foelsch H, et al. Mu1B, a novel adaptor medium chain expressed in polarized epithelial cells. *FEBS Lett* (1999) **449**:215–20. doi:10.1016/S0014-5793(99)00432-9
100. Pevsner J, Volknandt W, Wong BR, Scheller RH. Two rat homologs of clathrin-associated adaptor proteins. *Gene* (1994) **146**:279–83. doi:10.1016/0378-1119(94)90306-9
101. Newman LS, McKeever MO, Okano HJ, Darnell RB. Beta-NAP, a cerebellar degeneration antigen, is a neuron-specific vesicle coat protein. *Cell* (1995) **82**:773–83. doi:10.1016/0092-8674(95)90474-3
102. Aguilar RC, Boehm M, Gorshkova I, Crouch RJ, Tomita K, Saito T, et al. Signal-binding specificity of the mu4 subunit of the adaptor protein complex AP-4. *J Biol Chem* (2001) **276**:13145–52. doi:10.1074/jbc.M010591200
103. Hirst J, Bright NA, Rous B, Robinson MS. Characterization of a fourth adaptor-related protein complex. *Mol Biol Cell* (1999) **10**:2787–802. doi:10.1091/mbc.10.8.2787
104. Ohno H, Stewart J, Fournier MC, Bosshart H, Rhee I, Miyatake S, et al. Interaction of tyrosine-based sorting signals with clathrin-associated proteins. *Science* (1995) **269**:1872–5. doi:10.1126/science.7569928
105. Ohno H, Aguilar RC, Yeh D, Taura D, Saito T, Bonifacino JS. The medium subunits of adaptor complexes recognize distinct but overlapping sets of tyrosine-based sorting signals. *J Biol Chem* (1998) **273**:25915–21. doi:10.1074/jbc.273.40.25915
106. Doray B, Lee I, Knisely J, Bu G, Kornfeld S. The gamma/sigma1 and alpha/sigma2 hemicomplexes of clathrin adaptors AP-1 and AP-2 harbor the dileucine recognition site. *Mol Biol Cell* (2007) **18**:1887–96. doi:10.1091/mbc.E07-01-0012
107. Janvier K, Kato Y, Boehm M, Rose JR, Martina JA, Kim BY, et al. Recognition of dileucine-based sorting signals from HIV-1 Nef and LIMP-II by the AP-1 gamma-sigma1 and AP-3 delta-sigma3 hemicomplexes. *J Cell Biol* (2003) **163**:1281–90. doi:10.1083/jcb.200307157
108. Doray B, Ghosh P, Griffith J, Geuze HJ, Kornfeld S. Cooperation of GGAs and AP-1 in packaging MPRs at the trans-Golgi network. *Science* (2002) **297**:1700–3. doi:10.1126/science.1075327
109. Hirst J, Lui WW, Bright NA, Totty N, Seaman MN, Robinson MS. A family of proteins with gamma-adaptin and VHS domains that facilitate trafficking between the trans-Golgi network and the vacuole/lysosome. *J Cell Biol* (2000) **149**:67–80. doi:10.1083/jcb.149.1.67
110. Page LJ, Sowerby PJ, Lui WW, Robinson MS. Gamma-synergin: an EH domain-containing protein that interacts with gamma-adaptin. *J Cell Biol* (1999) **146**:993–1004. doi:10.1083/jcb.146.5.993
111. Wasiak S, Legendre-Guillemin V, Puertollano R, Blondeau F, Girard M, de HE, et al. Enthoprotin: a novel clathrin-associated protein identified through subcellular proteomics. *J Cell Biol* (2002) **158**:855–62. doi:10.1083/jcb.200205078
112. Owen DJ, Vallis Y, Pearse BM, McMahon HT, Evans PR. The structure and function of the beta 2-adaptin appendage domain. *EMBO J* (2000) **19**:4216–27. doi:10.1093/emboj/19.16.4216
113. Gallusser A, Kirchhausen T. The beta 1 and beta 2 subunits of the AP complexes are the clathrin coat assembly components. *EMBO J* (1993) **12**:5237–44.
114. Dell'Angelica EC, Klumperman J, Stoorvogel W, Bonifacino JS. Association of the AP-3 adaptor

complex with clathrin. *Science* (1998) **280**:431–4. doi:10.1126/science.280.5362.431
115. Dell'Angelica EC, Ooi CE, Bonifacino JS. Beta3A-adaptin, a subunit of the adaptor-like complex AP-3. *J Biol Chem* (1997) **272**:15078–84. doi:10.1074/jbc.272.24.15078
116. Goodman OB Jr, Keen JH. The alpha chain of the AP-2 adaptor is a clathrin binding subunit. *J Biol Chem* (1995) **270**:23768–73. doi:10.1074/jbc.270.40.23768
117. Doray B, Kornfeld S. Gamma subunit of the AP-1 adaptor complex binds clathrin: implications for cooperative binding in coated vesicle assembly. *Mol Biol Cell* (2001) **12**:1925–35. doi:10.1091/mbc.12.7.1925
118. Heldwein EE, Macia E, Wang J, Yin HL, Kirchhausen T, Harrison SC. Crystal structure of the clathrin adaptor protein 1 core. *Proc Natl Acad Sci U S A* (2004) **101**:14108–13. doi:10.1073/pnas.0406102101
119. Robinson MS, Kreis TE. Recruitment of coat proteins onto Golgi membranes in intact and permeabilized cells: effects of brefeldin A and G protein activators. *Cell* (1992) **69**:129–38. doi:10.1016/0092-8674(92)90124-U
120. Ren X, Farias GG, Canagarajah BJ, Bonifacino JS, Hurley JH. Structural basis for recruitment and activation of the AP-1 clathrin adaptor complex by Arf1. *Cell* (2013) **152**:755–67. doi:10.1016/j.cell.2012.12.042
121. Stamnes MA, Rothman JE. The binding of AP-1 clathrin adaptor particles to Golgi membranes requires ADP-ribosylation factor, a small GTP-binding protein. *Cell* (1993) **73**:999–1005. doi:10.1016/0092-8674(93)90277-W
122. Traub LM, Ostrom JA, Kornfeld S. Biochemical dissection of AP-1 recruitment onto Golgi membranes. *J Cell Biol* (1993) **123**:561–73. doi:10.1083/jcb.123.3.561
123. Ghosh P, Kornfeld S. AP-1 binding to sorting signals and release from clathrin-coated vesicles is regulated by phosphorylation. *J Cell Biol* (2003) **160**:699–708. doi:10.1083/jcb.200211080
124. Collins BM, McCoy AJ, Kent HM, Evans PR, Owen DJ. Molecular architecture and functional model of the endocytic AP2 complex. *Cell* (2002) **109**:523–35. doi:10.1016/S0092-8674(02)00735-3
125. Molloy SS, Thomas L, VanSlyke JK, Stenberg PE, Thomas G. Intracellular trafficking and activation of the furin proprotein convertase: localization to the TGN and recycling from the cell surface. *EMBO J* (1994) **13**:18–33.
126. Bonifacino JS, Traub LM. Signals for sorting of transmembrane proteins to endosomes and lysosomes. *Annu Rev Biochem* (2003) **72**:395–447. doi:10.1146/annurev.biochem.72.121801.161800
127. Wan L, Molloy SS, Thomas L, Liu G, Xiang Y, Rybak SL, et al. PACS-1 defines a novel gene family of cytosolic sorting proteins required for trans-Golgi network localization. *Cell* (1998) **94**:205–16. doi:10.1016/S0092-8674(00)81420-8
128. Jones BG, Thomas L, Molloy SS, Thulin CD, Fry MD, Walsh KA, et al. Intracellular trafficking of furin is modulated by the phosphorylation state of a casein kinase II site in its cytoplasmic tail. *EMBO J* (1995) **14**:5869–83.
129. Crump CM, Xiang Y, Thomas L, Gu F, Austin C, Tooze SA, et al. PACS-1 binding to adaptors is required for acidic cluster motif-mediated protein traffic. *EMBO J* (2001) **20**:2191–201. doi:10.1093/emboj/20.9.2191
130. Scott GK, Fei H, Thomas L, Medigeshi GR, Thomas G. A PACS-1, GGA3 and CK2 complex regulates CI-MPR trafficking. *EMBO J* (2006) **25**:4423–35. doi:10.1038/sj.emboj.7601336
131. Scott GK, Gu F, Crump CM, Thomas L, Wan L, Xiang Y, et al. The phosphorylation state of an autoregulatory domain controls PACS-1-directed protein traffic. *EMBO J* (2003) **22**:6234–44. doi:10.1093/emboj/cdg596
132. Boman AL, Zhang C, Zhu X, Kahn RA. A family of ADP-ribosylation factor effectors that can alter membrane transport through the trans-Golgi. *Mol Biol Cell* (2000) **11**:1241–55. doi:10.1091/mbc.11.4.1241
133. Dell'Angelica EC, Puertollano R, Mullins C, Aguilar RC, Vargas JD, Hartnell LM, et al. GGAs: a family of ADP ribosylation factor-binding proteins related to adaptors and associated with the Golgi complex. *J Cell Biol* (2000) **149**:81–94. doi:10.1083/jcb.149.1.81
134. Bonifacino JS. The GGA proteins: adaptors on the move. *Nat Rev Mol Cell Biol* (2004) **5**:23–32. doi:10.1038/nrm1279
135. Poussu A, Lohi O, Lehto VP. Vear, a novel Golgi-associated protein with VHS and gamma-adaptin "ear" domains. *J Biol Chem* (2000) **275**:7176–83. doi:10.1074/jbc.275.10.7176
136. McCullough J, Row PE, Lorenzo O, Doherty M, Beynon R, Clague MJ, et al. Activation of the endosome-associated ubiquitin isopeptidase AMSH by STAM, a component of the multivesicular body-sorting machinery. *Curr Biol* (2006) **16**:160–5. doi:10.1016/j.cub.2005.11.073
137. Puertollano R, Aguilar RC, Gorshkova I, Crouch RJ, Bonifacino JS. Sorting of mannose 6-phosphate receptors mediated by the GGAs. *Science* (2001) **292**:1712–6. doi:10.1126/science.1060750
138. Bilodeau PS, Winistorfer SC, Allaman MM, Surendhran K, Kearney WR, Robertson AD, et al. The GAT domains of clathrin-associated GGA proteins have two ubiquitin binding motifs. *J Biol Chem* (2004) **279**:54808–16. doi:10.1074/jbc.M406654200
139. Puertollano R, Bonifacino JS. Interactions of GGA3 with the ubiquitin sorting machinery. *Nat Cell Biol* (2004) **6**:244–51. doi:10.1038/ncb1106
140. Shiba Y, Katoh Y, Shiba T, Yoshino K, Takatsu H, Kobayashi H, et al. GAT (GGA and Tom1) domain responsible for ubiquitin binding and ubiquitination. *J Biol Chem* (2004) **279**:7105–11. doi:10.1074/jbc.M311702200
141. Wang J, Sun HQ, Macia E, Kirchhausen T, Watson H, Bonifacino JS, et al. PI4P promotes the recruitment of the GGA adaptor proteins to the trans-Golgi network and regulates their recognition of the ubiquitin sorting signal. *Mol Biol Cell* (2007) **18**:2646–55. doi:10.1091/mbc.E06-10-0897
142. Scott PM, Bilodeau PS, Zhdankina O, Winistorfer SC, Hauglund MJ, Allaman MM, et al. GGA proteins bind ubiquitin to facilitate sorting at the trans-Golgi network. *Nat Cell Biol* (2004) **6**:252–9. doi:10.1038/ncb1107
143. Kim Y, Deng Y, Philpott CC. GGA2- and ubiquitin-dependent trafficking of Arn1, the ferrichrome transporter of *Saccharomyces cerevisiae*. *Mol Biol Cell* (2007) **18**:1790–802. doi:10.1091/mbc.E06-09-0861
144. Bai H, Doray B, Kornfeld S. GGA1 interacts with the adaptor protein AP-1 through a WNSF sequence in its hinge region. *J Biol Chem* (2004) **279**:17411–7. doi:10.1074/jbc.M401158200
145. Doray B, Bruns K, Ghosh P, Kornfeld SA. Autoinhibition of the ligand-binding site of GGA1/3 VHS domains by an internal acidic cluster-dileucine motif. *Proc Natl Acad Sci U S A* (2002) **99**:8072–7. doi:10.1073/pnas.082235699
146. Ghosh P, Kornfeld S. Phosphorylation-induced conformational changes regulate GGAs 1 and 3 function at the trans-Golgi network. *J Biol Chem* (2003) **278**:14543–9. doi:10.1074/jbc.M212543200
147. Cramer JF, Gustafsen C, Behrens MA, Oliveira CL, Pedersen JS, Madsen P, et al. GGA autoinhibition revisited. *Traffic* (2010) **11**:259–73. doi:10.1111/j.1600-0854.2009.01017.x
148. Takatsu H, Yoshino K, Nakayama K. Adaptor gamma ear homology domain conserved in gamma-adaptin and GGA proteins that interact with gamma-synergin. *Biochem Biophys Res Commun* (2000) **271**:719–25. doi:10.1006/bbrc.2000.2700
149. Mattera R, Arighi CN, Lodge R, Zerial M, Bonifacino JS. Divalent interaction of the GGAs with the rabaptin-5-rabex-5 complex. *EMBO J* (2003) **22**:78–88. doi:10.1093/emboj/cdg015
150. Zhu Y, Doray B, Poussu A, Lehto VP, Kornfeld S. Binding of GGA2 to the lysosomal enzyme sorting motif of the mannose 6-phosphate receptor. *Science* (2001) **292**:1716–8. doi:10.1126/science.1060896
151. Kakhlon O, Sakya P, Larijani B, Watson R, Tooze SA. GGA function is required for maturation of neuroendocrine secretory granules. *EMBO J* (2006) **25**:1590–602. doi:10.1038/sj.emboj.7601067
152. Hirst J, Borner GH, Antrobus R, Peden AA, Hodson NA, Sahlender DA, et al. Distinct and overlapping roles for AP-1 and GGAs revealed by the "knocksideways" system. *Curr Biol* (2012) **22**:1711–6. doi:10.1016/j.cub
153. Daboussi L, Costaguta G, Payne GS. Phosphoinositide-mediated clathrin adaptor progression at the trans-Golgi network. *Nat Cell Biol* (2012) **14**:239–48. doi:10.1038/ncb2427
154. Steegmaier M, Klumperman J, Foletti DL, Yoo JS, Scheller RH. Vesicle-associated membrane protein 4 is implicated in trans-Golgi network vesicle trafficking. *Mol Biol Cell* (1999) **10**:1957–72. doi:10.1091/mbc.10.6.1957
155. Braulke T, Bonifacino JS. Sorting of lysosomal proteins. *Biochim Biophys Acta* (2009) **1793**:605–14. doi:10.1016/j.bbamcr.2008.10.016

156. Glickman JN, Conibear E, Pearse BM. Specificity of binding of clathrin adaptors to signals on the mannose-6-phosphate/insulin-like growth factor II receptor. *EMBO J* (1989) **8**:1041–7.
157. Johnson KF, Chan W, Kornfeld S. Cation-dependent mannose 6-phosphate receptor contains two internalization signals in its cytoplasmic domain. *Proc Natl Acad Sci U S A* (1990) **87**:10010–4. doi:10.1073/pnas.87.24.10010
158. Meresse S, Ludwig T, Frank R, Hoflack B. Phosphorylation of the cytoplasmic domain of the bovine cation-independent mannose 6-phosphate receptor. Serines 2421 and 2492 are the targets of a casein kinase II associated to the Golgi-derived HAI adaptor complex. *J Biol Chem* (1990) **265**:18833–42.
159. Stockli J, Honing S, Rohrer J. The acidic cluster of the CK2 site of the cation-dependent mannose 6-phosphate receptor (CD-MPR) but not its phosphorylation is required for GGA1 and AP-1 binding. *J Biol Chem* (2004) **279**:23542–9. doi:10.1074/jbc.M313525200
160. Varlamov O, Fricker LD. Intracellular trafficking of metallocarboxypeptidase D in AtT-20 cells: localization to the trans-Golgi network and recycling from the cell surface. *J Cell Sci* (1998) **111**(Pt 7):877–85.
161. Varlamov O, Eng FJ, Novikova EG, Fricker LD. Localization of metallocarboxypeptidase D in AtT-20 cells. Potential role in prohormone processing. *J Biol Chem* (1999) **274**:14759–67. doi:10.1074/jbc.274.21.14759
162. Kalinina E, Varlamov O, Fricker LD. Analysis of the carboxypeptidase D cytoplasmic domain: implications in intracellular trafficking. *J Cell Biochem* (2002) **85**:101–11. doi:10.1002/jcb.10112
163. Waites CL, Mehta A, Tan PK, Thomas G, Edwards RH, Krantz DE. An acidic motif retains vesicular monoamine transporter 2 on large dense core vesicles. *J Cell Biol* (2001) **152**:1159–68. doi:10.1083/jcb.152.6.1159
164. Caromile LA, Oganesian A, Coats SA, Seifert RA, Bowen-Pope DF. The neurosecretory vesicle protein phogrin functions as a phosphatidylinositol phosphatase to regulate insulin secretion. *J Biol Chem* (2010) **285**:10487–96. doi:10.1074/jbc.M109.066563
165. Nykjaer A, Willnow TE. Sortilin: a receptor to regulate neuronal viability and function. *Trends Neurosci* (2012) **35**:261–70. doi:10.1016/j.tins.2012.01.003
166. Chen ZY, Ieraci A, Teng H, Dall H, Meng CX, Herrera DG, et al. Sortilin controls intracellular sorting of brain-derived neurotrophic factor to the regulated secretory pathway. *J Neurosci* (2005) **25**:6156–66. doi:10.1523/JNEUROSCI.1017-05.2005
167. Yang M, Lim Y, Li X, Zhong JH, Zhou XF. Precursor of brain-derived neurotrophic factor (proBDNF) forms a complex with Huntingtin-associated protein-1 (HAP1) and sortilin that modulates proBDNF trafficking, degradation, and processing. *J Biol Chem* (2011) **286**:16272–84. doi:10.1074/jbc.M110.195347
168. Nielsen MS, Madsen P, Christensen EI, Nykjaer A, Gliemann J, Kasper D, et al. The sortilin cytoplasmic tail conveys Golgi-endosome transport and binds the VHS domain of the GGA2 sorting protein. *EMBO J* (2001) **20**:2180–90. doi:10.1093/emboj/20.9.2180
169. Canuel M, Lefrancois S, Zeng J, Morales CR. AP-1 and retromer play opposite roles in the trafficking of sortilin between the Golgi apparatus and the lysosomes. *Biochem Biophys Res Commun* (2008) **366**:724–30. doi:10.1016/j.bbrc.2007.12.015
170. Asensio CS, Sirkis DW, Edwards RH. RNAi screen identifies a role for adaptor protein AP-3 in sorting to the regulated secretory pathway. *J Cell Biol* (2010) **191**:1173–87. doi:10.1083/jcb.201006131
171. Gauthier DJ, Sobota JA, Ferraro F, Mains RE, Lazure C. Flow cytometry-assisted purification and proteomic analysis of the corticotropes dense-core secretory granules. *Proteomics* (2008) **8**:3848–61. doi:10.1002/pmic.200700969
172. Wegrzyn JL, Bark SJ, Funkelstein L, Mosier C, Yap A, Kazemi-Esfarjani P, et al. Proteomics of dense core secretory vesicles reveal distinct protein categories for secretion of neuroeffectors for cell-cell communication. *J Proteome Res* (2010) **9**:5002–24. doi:10.1021/pr1003104
173. Katsumata O, Fujita-Yoshigaki J, Hara-Yokoyama M, Yanagishita M, Furuyama S, Sugiya H. Syntaxin6 separates from GM1a-rich membrane microdomain during granule maturation. *Biochem Biophys Res Commun* (2007) **357**:1071–7. doi:10.1016/j.bbrc.2007.04.053
174. Youker RT, Shinde U, Day R, Thomas G. At the crossroads of homoeostasis and disease: roles of the PACS proteins in membrane traffic and apoptosis. *Biochem J* (2009) **421**:1–15. doi:10.1042/BJ20081016

Conflict of Interest Statement: The authors declare that the research was conducted in the absence of any commercial or financial relationships that could be construed as a potential conflict of interest.

Received: 10 June 2013; accepted: 31 July 2013; published online: 14 August 2013.
*Citation: Bonnemaison ML, Eipper BA and Mains RE (2013) Role of adaptor proteins in secretory granule biogenesis and maturation. Front. Endocrinol. **4**:101. doi: 10.3389/fendo.2013.00101*
This article was submitted to Frontiers in Neuroendocrine Science, a specialty of Frontiers in Endocrinology.

frontiers in
ENDOCRINOLOGY

REVIEW ARTICLE
published: 21 October 2013
doi: 10.3389/fendo.2013.00153

The cortical acto-myosin network: from diffusion barrier to functional gateway in the transport of neurosecretory vesicles to the plasma membrane

Andreas Papadopulos, Vanesa M. Tomatis, Ravikiran Kasula and Frederic A. Meunier*

Queensland Brain Institute, The University of Queensland, St Lucia Campus, Brisbane, QLD, Australia

Edited by:
Stephane Gasman, Centre National de la Recherche Scientifique, France

Reviewed by:
Nicolas Vitale, Centre National de la Recherche Scientifique, France
Jose-Maria Trifaro, University of Ottawa, Canada

****Correspondence:***
Frederic A. Meunier, Queensland Brain Institute, The University of Queensland, St Lucia Campus, QBI Building #79, St Lucia, QLD 4072, Australia
e-mail: f.meunier@uq.edu.au

Dysregulation of regulated exocytosis is linked to an array of pathological conditions, including neurodegenerative disorders, asthma, and diabetes. Understanding the molecular mechanisms underpinning neuroexocytosis including the processes that allow neurosecretory vesicles to access and fuse with the plasma membrane and to recycle post-fusion, is therefore critical to the design of future therapeutic drugs that will efficiently tackle these diseases. Despite considerable efforts to determine the principles of vesicular fusion, the mechanisms controlling the approach of vesicles to the plasma membrane in order to undergo tethering, docking, priming, and fusion remain poorly understood. All these steps involve the cortical actin network, a dense mesh of actin filaments localized beneath the plasma membrane. Recent work overturned the long-held belief that the cortical actin network only plays a passive constraining role in neuroexocytosis functioning as a physical barrier that partly breaks down upon entry of Ca^{2+} to allow secretory vesicles to reach the plasma membrane. A multitude of new roles for the cortical actin network in regulated exocytosis have now emerged and point to highly dynamic novel functions of key myosin molecular motors. Myosins are not only believed to help bring about dynamic changes in the actin cytoskeleton, tethering and guiding vesicles to their fusion sites, but they also regulate the size and duration of the fusion pore, thereby directly contributing to the release of neurotransmitters and hormones. Here we discuss the functions of the cortical actin network, myosins, and their effectors in controlling the processes that lead to tethering, directed transport, docking, and fusion of exocytotic vesicles in regulated exocytosis.

Keywords: cortical actin, myosin, regulated exocytosis, cdc42, phosphoinositides, secretory vesicles

INTRODUCTION

Regulated exocytosis relies on the timely fusion of secretory vesicles or granules (SVs/SGs) with the plasma membrane. For this to occur, SVs need to be mobilized, translocated, docked, and primed at the plasma membrane. Translocation, docking/priming, and fusion of SGs rely on dynamic changes in the cortical actin network, a dense mesh of filamentous actin underneath the plasma membrane (**Figures 1A–C**) that is controlled by actin effectors and myosin motor proteins. The thick actin ring of the cortical actin network can be visualized in chromaffin cells by staining actin with a variety of methods ranging from classical immunofluorescence to phalloidin (covalently linked to fluorophores), a fungal alkaloid that preferentially binds actin filaments (**Figures 1B,C**). More recently, the development of lifeact-GFP, a 17-residue peptide from *S. cerevisiae* that selectively binds to actin without affecting neuroexocytosis (1, 2), has allowed the probing of the dynamic changes occurring during stimulation of exocytosis on the cortical actin network by time-lapse imaging (**Figures 1C,D**). Following secretagogue stimulation the cortical actin ring fragments, coinciding with a decrease in cortical F-actin labeling (**Figure 1B**). This process is Ca^{2+}-dependent and involves actin-severing proteins such as scinderin (3–6). Although actin reorganization helps vesicles reach the plasma membrane (7), F-actin also serves as an anchoring point for SGs and provides tracks for their directed motion toward fusion sites (8). Molecular motors associated with F-actin, such as myosins (9), are involved in additional functions (2, 10).

In nerve terminals, actin is a well-known modulator of neurotransmitter release. Actin is involved in synaptic vesicle mobilization as well as axonal vesicle trafficking and synaptic plasticity (11). It is the most abundant cytoskeletal protein in synapses and is highly enriched in dendritic spines, whose formation is initiated by dendritic filopodia formation (12–15), an actin-driven process facilitated by the action of myosin X (16, 17). Neurotransmitter release at central synapses is regulated by actin and depolymerization of F-actin by latrunculin A was found to transiently enhance neurotransmitter release indicating a restraining role of F-actin in active zones (18).

NEW ROLES FOR ACTIN IN EXOCYTOSIS

The cortical actin network plays an important and well-described role during vesicle exocytosis (5, 7, 9, 10), and in recent years new functions for actin and its associated proteins have emerged (2, 9, 10, 20–24). Ca^{2+}-dependent reorganization and remodeling of the cortical actin network help vesicles move toward the plasma membrane by partial disassembly of the cortical layer (**Figure 1B**) (3,

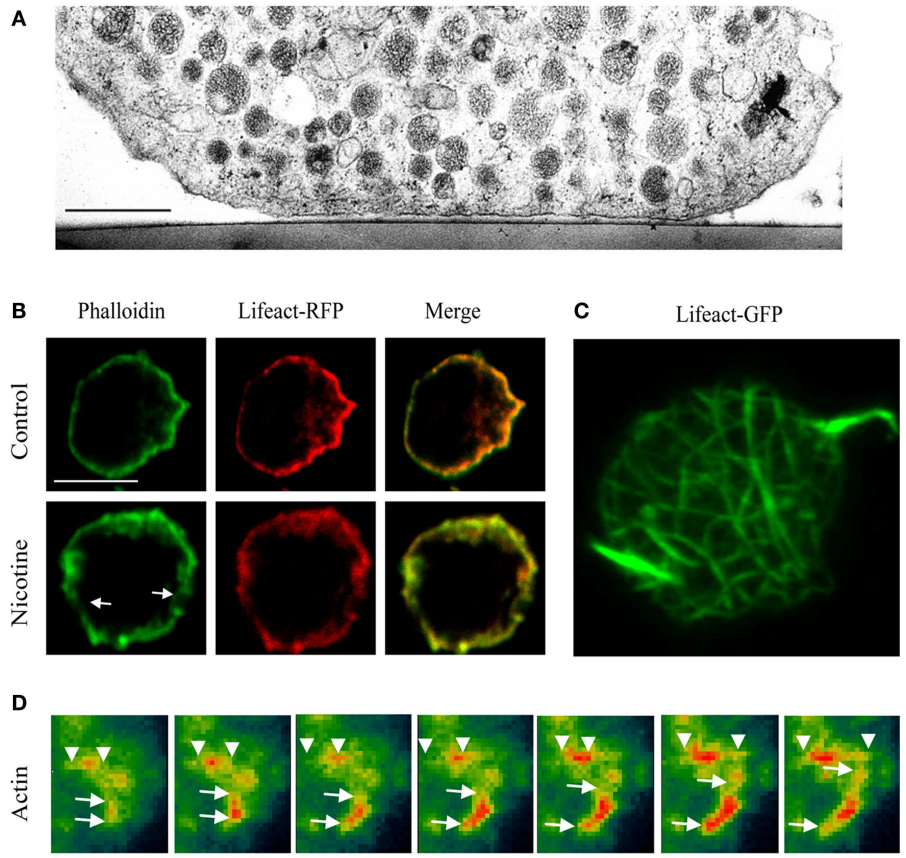

FIGURE 1 | Imaging the actin network in neurosecretory cells. **(A)** Electron micrograph of a bovine chromaffin cell region attached to the thermanox support. Note the presence of a filamentous cortical region that is devoid of SG. Bar, 1 μm [adapted from Ref. (19)]. **(B)** Confocal images showing the mid section of bovine chromaffin cells expressing lifeact-RFP and counter stained with FITC-conjugated phalloidin in the presence or absence of nicotine (50 μM). **(C)** Maximum intensity projection of the footprint of a chromaffin cell. **(D)** TIRF images showing actin lengthening in a chromaffin cell expressing lifeact-GFP (pseudocolor) after the addition of PI3Kδ inhibitor IC87114. **(B–D)** Adapted from Ref. (2).

6). At the same time, this remodeling provides tracks that extend further toward the center of the cell allowing the mobilization of SGs from the reserve pool (25) to their docking and fusion sites at the plasma membrane (4, 26, 27). Ca^{2+} regulates the cortical F-actin disassembly in chromaffin cells via two pathways (28, 29). The first involves stimulation-induced influx of extracellular Ca^{2+} through Ca^{2+} channels and results in activation of scinderin and ensuing F-actin severing. The second pathway is triggered by Ca^{2+} release from intracellular stores (30) and can be induced in the absence of secretagogue stimulation, by phorbol esters (3). Here actin disassembly is achieved through protein kinase C (PKC) activation followed by myristoylated alanine-rich C kinase substrate (MARCKS) phosphorylation that inhibits its F-actin-binding and cross-linking properties (28). The cortical actin network provides a layered structure that retains 2–4% of the total vesicles in close proximity to the cell surface that contribute to the burst of catecholamine release at the onset of stimulation (26, 31, 32). Indeed the majority of SGs in the vicinity of the plasma membrane are tethered to the cortical actin network (6), and newly arriving vesicles are also caught in this dense mesh of F-actin (33). Other studies point to the existence of F-actin cages that organize the SNARE proteins SNAP25 and syntaxin-1 as well as L- and P/Q-type calcium channels, creating sites in the cortical actin network where SGs fuse preferentially (34). Consistent with these data, studies using total internal reflection fluorescence (TIRF) microscopy revealed that vesicle motion becomes restricted in the vicinity of the plasma membrane (35, 36). Interestingly, both actin depolymerization (37) and N-WASP- and Cdc42-dependent actin polymerization (**Figure 1D**) potentiate exocytosis (2, 38). While these results may appear contradictory, such opposing role for actin is not unlikely. Partial actin depolymerization helps SGs to cross the actin layer that acts as barrier, and the remaining (10) as well as newly forming actin fibers provide tracks for vesicles to reach the plasma membrane (2, 38). The balance between actin polymerization and depolymerization is likely regulated by scinderin acting as a molecular switch capable of inducing both actin polymerization and depolymerization (39). An important link connecting membranes and actin during exocytosis is the glycerophospholipid phosphatidylinositol 4,5-bisphosphate (PIP_2). Although it is only a minor component of cellular membranes, microdomains, and

clusters of PIP_2 play a crucial role in exocytosis. PIP_2 is known to control actin polymerization by modulating the activity and targeting of actin regulatory proteins (40). PIP_2 involvement in SNARE-mediated exocytosis, i.e., its Ca^{2+}-dependent interaction with synaptotagmin-1 and syntaxin, has been described in numerous studies (41–44). Decreased levels of PIP_2 in the brain and impairment of its synthesis in nerve terminals lead to early postnatal lethality and synaptic defects in mice, including decreased frequency of miniature currents, enhanced synaptic depression, and a smaller ready release pool of synaptic vesicles, delayed endocytosis, and slower recycling kinetics (45). The formation of PIP_2 microdomains at syntaxin-1A clusters with docked SGs seems to be required for Ca^{2+}-dependent exocytosis (46). Both PIP_2 and syntaxin-1A have been found in punctate nanoclusters in isolated PC12 cell plasma membrane sheets, and similar PIP_2 clusters in PC12 cells have been reported to link synaptotagmin-1 and syntaxin-1A, thus providing a platform for SV recruitment (46, 47). Likewise, the clustering of syntaxin-1A in model membranes has been shown to be modulated by PIP_2 (48). PIP_2 also plays a role in regulated exocytosis by controlling several proteins involved in modifying the actin cytoskeleton (40), as well as stimulating actin polymerization (49). PIP_2 binds scinderin in a Ca^{2+} and pH-dependent manner (50). PIP_2 binding inhibits scinderin-induced actin depolymerization (51, 52), as well as the ADF/cofilin actin-severing activity (53) thereby promoting actin polymerization. A transient increase in PIP_2 levels is sufficient to promote the mobilization and recruitment of SVs to the plasma membrane via Cdc42-mediated actin reorganization (2). PIP_2 therefore links exocytosis and the actin cytoskeleton by coordinating the actin-based delivery of SVs to the plasma membrane (2). Likewise, decreasing PIP_2 levels in neuroendocrine cells by either ATP depletion or sequestering PIP_2 rapidly reduces the amount of cortical F-actin (54). In a similar study, nanomolar interaction of HIV-1 transcriptional activator with PIP_2 was found to prevent the actin reorganization necessary for bringing SVs to the plasma membrane and severely impaired neurosecretion in PC12 and chromaffin cells (55). Another actin-binding protein that PIP_2 has been found to interact with is vilin, with PIP_2-vilin association inhibiting actin depolymerization and enhancing actin cross-linking (56). The interplay of Rho GTPases such as Cdc42, RhoA, and Rac with PIP_2 and other actin regulatory proteins controls Ca^{2+}-regulated exocytosis in chromaffin cells (9, 22). Other small GTPases implicated in regulated secretion in neurosecretory and endocrine cells are Arf6 (57), Rab27A (58) as well as RalA and Rab3A. RalA has not only been shown to tether insulin granules to R- and L-type calcium channels (59) but also binds to the exocyst complex and regulates filopodia formation linking morphological changes and regulated exocytosis (60). RalA, which is present in GLUT4 vesicles in adipocytes, also interacts with the exocyst complex and its activation is required for insulin-stimulated GLUT4 trafficking. Impairment in the function of RalA in these cells attenuated insulin-stimulated glucose transport. RalA also interacts with Myo1C acting as a cargo receptor for this motor protein (61). In addition RalA has been found to control SG exocytosis in PC12 cells by interacting with phospholipase D1. It is activated during exocytosis and the expression of a constitutively active mutant was found to enhance neuroexocytosis whereas expression of an inactive mutant or silencing resulted in reduced secretion (62). Of the four homologs (A/B/C/D) Rab3A is the best characterized (63). Rab3A is involved in the late steps of exocytosis. Early studies showed that Rab3A is associated with SG in bovine chromaffin cells and rat PC12 cells (64, 65). Overexpression of Rab3A mutant proteins defective in either GTP hydrolysis or in guanine nucleotide-binding inhibited exocytosis (66). Similarly the perfusion of Rab3A and various guanine nucleotides into chromaffin cells resulted in delayed catecholamine secretion suggesting a negative regulatory role in secretion (67). Rab3A plays a role in vesicle priming, where it is involved in Munc13-1 activation and interacts with Munc18-1 to regulate priming and fusion (68). Furthermore, Munc13 and Rab3A localize in the acrosomal region in human sperm, where they stimulate acrosomal exocytosis and play an important role in membrane docking (69). In human spermatozoa Rab3A and Rab27 act in a cascade that regulates dense core granule exocytosis (70). Rab3 interaction with Munc18 has also been shown to regulate SG density at the periphery of PC12 cells (71) and Rab3 guanine cycling is required for Munc18-dependent SG docking (72). However, the high level of redundancy between the four Rab3 isoforms makes it difficult to fully assess their individual contributions and the lack of an obvious exocytic phenotype in double and triple knock-out animals points to a regulatory but not essential role of Rab3A in exocytosis (73).

A number of new functions are now being attributed to the interplay between actin and various myosins. Non-muscle myosin II, and the unconventional myosins 1c/e, Va, and VI are involved in different stages during regulated exocytosis of SGs.

MYOSINS

Myosins are a 17-member superfamily of actin-based molecular motor proteins (74) that are involved in many aspects of eukaryotic cell functions, including cell movement, establishment of cell shape and polarity (75–80), and vesicular trafficking (61, 81). Myosin function is not limited to that of a molecular motor, as myosins also regulate actin polymerization, serve as molecular anchors (33), and even play a role in signal transduction (82, 83). All myosins contain a heavy chain with a conserved ∼80 kDa N-terminal catalytic domain that includes the ATPase activity and actin-binding regions (**Figure 2**) (84). This domain is followed by an α-helical neck region containing one or more IQ motifs that allow binding of light chains and calmodulin (CaM). The C-terminal myosin tail contains cargo/membrane-binding domains, kinase activity, and/or mediates heavy chain dimerization depending on the myosin class (**Figure 2**) (83, 85).

MYOSIN I

Myosin I (**Figure 2**) is a single-headed membrane-associated protein that is expressed in all eukaryotic cells (84). Although there is currently no evidence for myosin I involvement in neurosecretion two isoforms of the human myosin 1C gene (86), myosin 1C (Myo1C), and myosin 1E (Myo1E) have been implicated in regulated exocytosis. All members of this unconventional myosin family interact with actin through their catalytic head domain (87). Myo1C is also capable of binding phosphoinositides (88) (**Figure 3**), thereby linking the actin cytoskeleton to the plasma membrane (89). Myo1C is recruited to GLUT4-containing vesicles

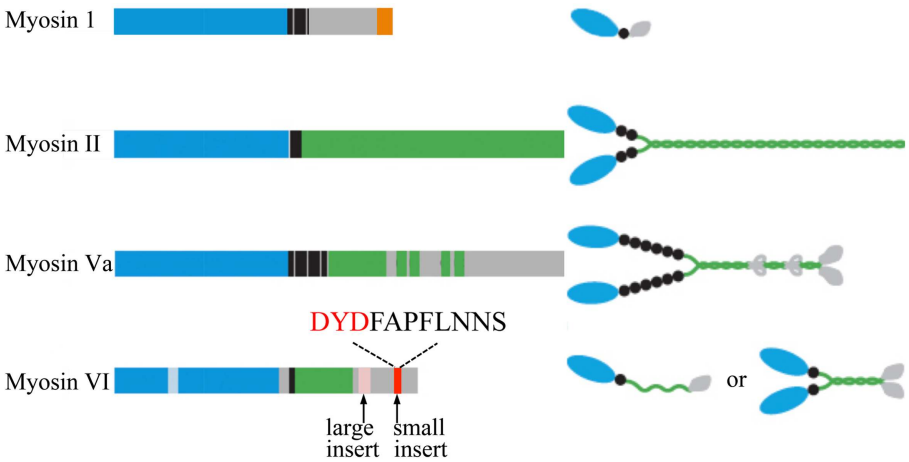

FIGURE 2 | Schematic diagrams of the myosin heavy chains involved in regulated exocytosis. All myosins consist of a head (motor) domain (blue), a neck that contains one or more IQ motifs for light chain and CaM binding (black), and a tail domain with coiled-coil regions (green) and membrane/cargo-binding domains (orange). The small insert of myosin VI, shown to be essential for the tethering of SGs to the cortical actin network, and the DYD-Src phosphorylation motif are highlighted. Cargo-binding induced dimerization of myosin VI is likely to be mediated by the coiled-coil regions and the cargo-binding domains. Adapted from Ref. (83).

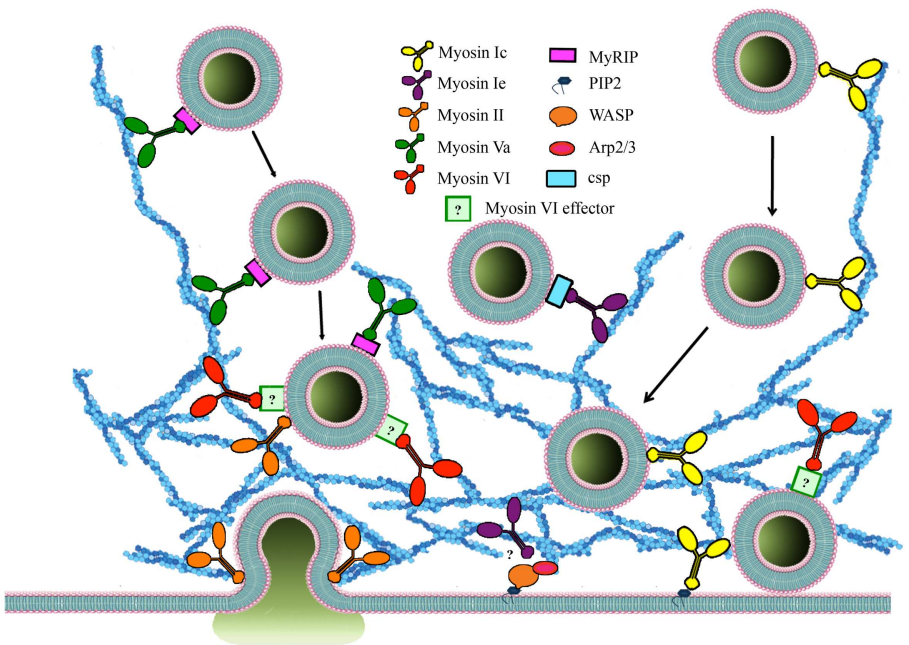

FIGURE 3 | The roles of myosins and accessory proteins involved in regulated exocytosis. Myosins are involved in several steps of regulated exocytosis. Myosin 1C (yellow), myosin 1E (burgundy), myosin II (orange), and myosin Va (green) are involved in secretory vesicle transport. In contrast, myosin VI (red) recruits SGs to the cortical actin network. Myosin 1C interacts with SG through cysteine string proteins and myosin Va binds to MyRIP (purple) on the membrane of SGs. Myosin 1C can be recruited to membranes through PIP_2 interaction. The effector that mediates binding between myosin VI and SGs (light green) is currently unknown. Myosin 1E is also involved in regulating actin polymerization through interaction with WASP/Arp 2/3. Cdc42 as well WASP/Arp 2/3 regulate actin polymerization in an activity-dependent manner. Myosin II also regulates size and duration of fusion pore opening.

that undergo regulated exocytosis in 3T3-L1 adipocytes in an insulin-dependent manner, and is involved in their transport to the plasma membrane (**Figure 3**) (61, 81). In addition, Myo1C also tethers GLUT4-containing vesicles to the cortical actin network (**Figure 3**) underneath the plasma membrane in response to insulin (90), and promotes GLUT4 insertion to the plasma membrane by fusion (91), thereby regulating glucose uptake in adipose and muscle tissue (92). Myo1C is required for vascular endothelial

growth factor receptor-2 (VEGFR2) delivery to the cell surface and for angiogenic signaling (93). VEGF stimulation promotes the recruitment of VEGFR2 to Myo1C and its delivery to the cell surface (93).

In *Xenopus* oocytes Myo1E, the only long-tailed myosin 1 class motor protein has been found to rapidly relocate from the cytosol to cortical SGs upon secretagogue stimulation and to bind to cysteine string proteins, components of cortical SGs that mediate vital steps in regulated exocytosis (94) by interacting with SNAP25 and the calcium sensor synaptotagmin 9 in pancreatic β-cells (95). While cortical granule exocytosis is enhanced by overexpression of Myo1E it is inhibited by injection of Myo1E antibodies (94). Myo1E has also been implicated in the recruitment of several actin-binding proteins leading to N-WASP recruitment and Arp2/3-mediated actin polymerization (**Figure 3**) (96).

MYOSIN II

Class II myosins are most abundant in muscle cells where their main function is to generate mechanical force. Non-muscle cells also contain a subset of myosin II molecules with distinct functionality. They all consist of two heavy chains (230 kDa), two regulatory light chains, and two essential light chains (**Figure 2**). In addition to actin cross-linking, bundling, and contractile properties, myosin II is known to regulate actin polymerization and is therefore linked to a great number of functions in eukaryotic cells including motility, adhesion (97), and regulated exocytosis (24, 98, 99). Non-muscle myosin II has been implicated in vesicle transport through the actin cytoskeleton (**Figure 3**). Expression of an inactive non-phosphorylatable regulatory light chain mutant myosin II fused to GFP drastically impairs granule mobility and influences actin dynamics, similar to blebbistatin treatment (100).

There is mounting evidence that myosin II is involved in controlling fusion pore dynamics and release kinetics (**Figure 3**). Expression of non-phosphorylatable regulatory light chain mutant myosin II that produces an inactive protein alters single vesicle fusion kinetics and slows fusion pore expansion (23, 24). Similarly, the release kinetics of fluorescently tagged tissue plasminogen activator and brain-derived neurotrophic (BDNF) factor are prolonged following overexpression of a wild-type form of the myosin II regulatory light chain and shortened by overexpression of a dominant-negative form (101). The use of a green fluorescent pH-sensitive protein (pHluorin) targeted inside the SVs revealed that the altered kinetics of release were caused by changes in the duration of fusion pore opening. Additional evidence indicates that myosin II affects catecholamine release by directly controlling the size of the fusion pore and the duration of its opening (20). Actin cortex disassembly elicited by high frequency stimulation promotes full fusion of SGs – an effect blocked by pharmacological inhibition of myosin II or myosin light chain (MLC) by preventing the fusion pore dilation (102). Inhibition of either actin polymerization with cytochalasin D or myosin II function with blebbistatin also slowed fusion pore expansion and increased its lifetime, suggesting that the interplay between actin and myosin II can accelerate catecholamine release (20). Similar results indicating that myosin II activity maintains an open fusion pore were obtained in exocrine pancreatic cells where myosin II (blebbistatin) and MLC (ML-9) inhibition did not alter the number of fusion events but resulted in a decreased fusion pore lifetime (103).

It has been suggested that myosin II contractility could also help to squeeze secretory cargo out of vesicles surrounded by an actin coat once they are connected to the plasma membrane through a fusion pore (104). Fusion pore opening and closing might not be enough to release large cargo from SVs and myosin II might provide an active extrusion mechanism (104). The direct involvement of MLC and myosin II was also observed in GLUT4-containing vesicle fusion following insulin-stimulated glucose uptake in 3T3-L1 adipocytes. Only active phosphorylated myosin II was recruited to GLUT4 vesicles in an activity-dependent manner. Interestingly, insulin specifically stimulates the myosin IIA isoform via MLC kinase phosphorylation of MLC (105, 106). Myosin II inhibition also increases the distance of SGs from the plasma membrane, and promotes the retraction of the cytoskeleton, suggesting its involvement in the final approach of vesicles toward the plasma membrane (107).

Myosin II involvement in integrin-mediated cell adhesion and exocytosis has been linked to changes in cell adhesion properties (108, 109). Glucose stimulation of pancreatic β-cells promotes the remodeling of integrin focal adhesions and phosphorylation of focal adhesion kinases and myosin II (108, 109). As myosin II is one of the main substrates of Rho-kinase 1/2, which stimulates myosin–actin interactions and induces reorganization of the actin cytoskeleton, this activity could modulate SG translocation and cargo release in response to secretagogue stimulation.

MYOSIN VA

Myosin Va (**Figure 2**) has been implicated in exocytosis and vesicle movement to the cell periphery. In melanocytes, in a complex with Rab27a and melanophilin, myosin Va regulates melanosome transport to the plasma membrane (110, 111). In pancreatic β-cells myosin Va also functions in the transport to and retention of insulin granules at the cortical actin network under stimulated conditions as well as their secretion (112–114). In neurosecretory cells, myosin Va is associated with SGs and plays distinctive roles during SG exocytosis (25, 115). Firstly, it assists the membrane remodeling required for SG maturation by promoting the removal of the transmembrane protein furin from maturing SGs (116). Secondly, in a complex with the SG-associated small GTPase Rab27 and its effector MyRIP, myosin Va regulates the interaction of SGs with the cortical actin network (**Figure 3**) (58). This complex has been implicated in exocytosis of SGs by modulating the transport of SGs and their retention in the cortical actin network on their way to the plasma membrane (117, 118). The interaction between myosin Va and MyRIP facilitates the dissociation of SGs from microtubules, enhancing their directed motion and the probability of SG docking to the plasma membrane (118). As a conventional processive molecular motor, myosin Va moves selective cargo along actin filaments (117). This feature strongly supports the key role of this protein in the translocation and tethering of SGs to the cell periphery. Blocking myosin Va function reduces the immobilization periods of SGs thereby decreasing the density of docked SGs near the plasma membrane and their exocytosis (117, 119). In resting conditions, myosin Va forms a stable complex with synaptic vesicle membrane proteins, synaptobrevin

II, and synaptophysin (120). This complex is rapidly disassembled upon Ca^{2+} increase in either intact nerve endings or *in vitro* assays (120). In chromaffin cells, influx of Ca^{2+} dissociates myosin V from chromaffin vesicles supporting a role for Ca^{2+} in the regulation of transient interactions between myosin V and its cargo (25). Furthermore, when an antibody against myosin V head was introduced in permeabilized chromaffin cells after a first stimulation of 40 s, the secretory response to a second stimulation several minutes after the first one, was greatly reduced. This points to a role for myosin V in providing SVs for the refilling of the release-ready pool following stimulation (25). The role of Ca^{2+} as a regulator of the interaction between myosin V and its cargo has also been demonstrated in melanosomes and *Xenopus* egg extracts (121). Released CaM activates CaM kinase II (CaMK-II), a myosin Va binding partner (122). CaMK-II activation leads to myosin Va phosphorylation and the release of melanosomes from F-actin (121). Similarly, microinjection of CaM antibodies into chromaffin cells resulted in reduced catecholamine output in response to stimulation (123). Ca^{2+}-regulated phosphorylation of myosin Va is believed to represent a universal mechanism that regulates the association between myosin Va and its cargo. These observations suggest that by regulating the interaction between myosin V and SGs, Ca^{2+} could also control the association between SGs and actin during SG mobilization in the cortical region (124). Importantly, the Ca^{2+}-regulated attachment/release of myosin Va from SGs could be finely coordinated by other molecular motors, such us myosin VI (33). This cooperative model would allow a highly organized and controlled mechanism that regulates SG transport, retention, and anchoring and ultimately SG fusion with the plasma membrane.

MYOSIN VI

Another member of the myosin family, myosin VI is critical for SV recruitment to the cortical actin network (**Figure 2**). The cellular functions of myosin VI are attributed to its unique ability to generate movement from the plus to the minus end of actin filaments. Myosin VI has an additional unique 53 aa insert, the "reverse gear," between the motor domain and the neck region that has been predicted to be responsible for this exceptional inverted movement directionality (**Figure 2**) (125, 126). Interestingly, this insert binds CaM even though it does not contain a recognizable IQ-CaM motif (127). The tail domain region is the most variable amongst the myosin VI isoforms. Four alternatively spliced isoforms are generated due to the presence of a large insert (21–31 aa), a small insert (9 aa), no insert, or both inserts in this domain (**Figure 2**) (128, 129).

The function of myosin VI depends on the ability of its cargo-binding domain (CBD) region to interact with different binding partners that target myosin VI to specific cellular compartments (130). Myosin VI undergoes cargo-mediated dimerization a potential regulatory pathway for all myosins (131, 132). Myosin VI has been linked to clathrin- and non-clathrin-mediated endocytosis, as well as maintenance of Golgi organization and cell polarity. The large and no insert isoforms are the main isoforms mediating these functions (128, 133–137). Myosin VI has also been implicated in autophagy (138), stereocilia maintenance (139), spermatid individualization (140–142), nuclear transcription (143), and cell–cell contacts (144, 145). Evidence of a role of myosin VI in secretion were highlighted by Warner et al. (146) using immortalized cells from Snell's waltzer mice, a strain of myosin VI knock-out mice (146–148). Immortalized fibroblastic cells from these mice have a reduced Golgi complex (∼40% smaller in comparison with that in normal cells) that is accompanied by a similar reduction in constitutive secretion (146). The down-regulation of myosin VI expression using small interfering RNA selectively reduces the secretion of prostate-specific antigen and vascular endothelial growth factor in the prostate cancer cell line LNCaP (149). Myosin VI together with its binding partner optineurin, regulates the final stage of constitutive exocytosis by mechanically controlling the formation of the fusion pore between the SV and the plasma membrane in HeLa cells (150). Less is known about the role of myosin VI in the nervous system (151). Myosin VI is widely and highly expressed in the brain; it is found in synapses and enriched at the postsynaptic density (151). In hippocampal neurons, myosin VI forms a complex with α-amino-3-hydroxy-5-methyl-4-isoxazolepropionic acid receptor (AMPAR), AP-2 and synaptic-associated protein 97 (SAP-97), and mediates AMPAR clathrin-mediated endocytosis. Importantly, myosin VI function underpins hippocampal neurons synapses and dendritic spines formation (151). Other work supports the role of myosin VI in neurotransmission by demonstrating that myosin VI; together with its binding partner GIPC1 is necessary for BDNF-TrkB-mediated synaptic plasticity (152).

Myosin VI has a very slow rate of release of ADP from its nucleotide-binding pocket, which therefore slows the dissociation of myosin VI from actin (153–155). Studies carried out in Snell's waltzer mice have shown that myosin VI allows the formation, maturation, and function of sensory hair cells by mediating the attachment of membrane compartments to the F-actin cytoskeleton (148). Together these lines of evidence point toward the possibility that myosin VI could regulate neuroexocytosis by anchoring/recruiting SVs to the actin network before they undergo fusion with the plasma membrane. Although little is known about the precise molecular mechanism(s) underpinning this role, the function of myosin VI in regulated in exocytosis in PC12 cells has been questioned (156). However, *Drosophila* mutants lacking myosin VI display altered neuromuscular junction morphology and synaptic vesicle localization resulting in impaired synaptic plasticity (157). Myosin VI could therefore mediate the mobilization of synaptic vesicles from different functional pools, by a yet to be elucidated mechanism. We recently described a novel role for the myosin VI small insert isoform (**Figure 2**) in regulated exocytosis in PC12 cells (33). Using purified SGs in a pull-down approach followed by mass spectrometry, we identified myosin VI as a cytosolic protein that interacts with SGs in a Ca^{2+}-dependent manner. We found that myosin VI maintains an active pool of SGs near the plasma membrane by tethering them to the cortical actin network (**Figure 3**). This allows the replenishment of the pool of SGs near the plasma membrane and is key to sustaining exocytosis during long periods of stimulation (33). Interestingly, we found that c-Src phosphorylation in a DYD motif located in the CBD of myosin VI small insert is one of the mechanisms controlling its function in regulated neuroexocytosis (33). The mechanisms that target myosin VI to SGs and the regulation of the isoform specific tethering function still need to be elucidated.

There are several other members of the myosin family that could potentially be involved in regulated secretion, including myosin X, a motor protein found predominantly at the tip of filopodia of many cell types including neurons (16, 17). Filopodia are important precursors for dendritic spine and synapse formation but more work is needed to assess whether neurosecretion can occur in these structures.

CONCLUSION

Understanding the detailed roles of myosins and other accessory proteins in regulated exocytosis is challenging. Although a great deal is known about the involvement of these proteins and their effectors during the different stages of secretion, there is still no comprehensive model of the interplay of the different myosin isoforms, e.g., the transition from myosin Va-mediated directed transport to myosin VI-dependent recruitment to the cortical actin network. Common pathways that are shared by other cellular functions, such as adhesion or migration should also be explored further. Future work should therefore aim at combining *in vitro* techniques with live cell microscopy experiments in order to explore the complex interplay between the different myosin molecular motors during neuroexocytosis. In particular, it will be necessary to address the nature of the pathways, which coordinate and control myosin functions in order to achieve such precise spatio-temporal trafficking of SVs en route to fusion with the plasma membrane.

ACKNOWLEDGMENTS

The authors thank Rowan Tweedale for critical reading of the manuscript.

REFERENCES

1. Jang Y, Soekmadji C, Mitchell JM, Thomas WG, Thorn P. Real-time measurement of F-actin remodelling during exocytosis using lifeact-EGFP transgenic animals. *PLoS One* (2012) **7**:e39815. doi:10.1371/journal.pone.0039815
2. Wen PJ, Osborne SL, Zanin M, Low PC, Wang HT, Schoenwaelder SM, et al. Phosphatidylinositol(4,5)bisphosphate coordinates actin-mediated mobilization and translocation of secretory vesicles to the plasma membrane of chromaffin cells. *Nat Commun* (2011) **2**:491. doi:10.1038/ncomms1500
3. Rose SD, Lejen T, Zhang L, Trifaro JM. Chromaffin cell F-actin disassembly and potentiation of catecholamine release in response to protein kinase C activation by phorbol esters is mediated through myristoylated alanine-rich C kinase substrate phosphorylation. *J Biol Chem* (2001) **276**:36757–63. doi:10.1074/jbc.M006518200
4. Trifaro JM. Scinderin and cortical F-actin are components of the secretory machinery. *Can J Physiol Pharmacol* (1999) **77**:660–71. doi:10.1139/y99-074
5. Trifaro JM, Rodriguez del Castillo A, Vitale ML. Dynamic changes in chromaffin cell cytoskeleton as prelude to exocytosis. *Mol Neurobiol* (1992) **6**:339–58. doi:10.1007/BF02757940
6. Vitale ML, Rodriguez Del Castillo A, Tchakarov L, Trifaro JM. Cortical filamentous actin disassembly and scinderin redistribution during chromaffin cell stimulation precede exocytosis, a phenomenon not exhibited by gelsolin. *J Cell Biol* (1991) **113**:1057–67. doi:10.1083/jcb.113.5.1057
7. Vitale ML, Seward EP, Trifaro JM. Chromaffin cell cortical actin network dynamics control the size of the release-ready vesicle pool and the initial rate of exocytosis. *Neuron* (1995) **14**:353–63. doi:10.1016/0896-6273(95)90291-0
8. Giner D, Neco P, Frances Mdel M, Lopez I, Viniegra S, Gutierrez LM. Real-time dynamics of the F-actin cytoskeleton during secretion from chromaffin cells. *J Cell Sci* (2005) **118**:2871–80. doi:10.1242/jcs.02419
9. Malacombe M, Bader M-F, Gasman SP. Exocytosis in neuroendocrine cells: new tasks for actin. *Biochim Biophys Acta* (2006) **1763**:1175–83. doi:10.1016/j.bbamcr.2006.09.004
10. Trifaro JM, Gasman S, Gutierrez LM. Cytoskeletal control of vesicle transport and exocytosis in chromaffin cells. *Acta Physiol (Oxf)* (2008) **192**:165–72. doi:10.1111/j.1748-1716.2007.01808.x
11. Cingolani LA, Goda Y. Actin in action: the interplay between the actin cytoskeleton and synaptic efficacy. *Nat Rev Neurosci* (2008) **9**:344–56. doi:10.1038/nrn2373
12. Fifkova E, Delay RJ. Cytoplasmic actin in neuronal processes as a possible mediator of synaptic plasticity. *J Cell Biol* (1982) **95**:345–50. doi:10.1083/jcb.95.1.345
13. Landis DM, Hall AK, Weinstein LA, Reese TS. The organization of cytoplasm at the presynaptic active zone of a central nervous system synapse. *Neuron* (1988) **1**:201–9. doi:10.1016/0896-6273(88)90140-7
14. Matus A. Actin-based plasticity in dendritic spines. *Science* (2000) **290**:754–8. doi:10.1126/science.290.5492.754
15. Matus A, Ackermann M, Pehling G, Byers HR, Fujiwara K. High actin concentrations in brain dendritic spines and postsynaptic densities. *Proc Natl Acad Sci U S A* (1982) **79**:7590–4. doi:10.1073/pnas.79.23.7590
16. Kerber ML, Cheney RE. Myosin-X: a MyTH-FERM myosin at the tips of filopodia. *J Cell Sci* (2011) **124**:3733–41. doi:10.1242/jcs.023549
17. Plantman S, Zelano J, Novikova LN, Novikov LN, Cullheim S. Neuronal myosin-X is upregulated after peripheral nerve injury and mediates laminin-induced growth of neurites. *Mol Cell Neurosci* (2013) **56C**:96–101. doi:10.1016/j.mcn.2013.04.001
18. Morales M, Colicos MA, Goda Y. Actin-dependent regulation of neurotransmitter release at central synapses. *Neuron* (2000) **27**:539–50. doi:10.1016/S0896-6273(00)00064-7
19. Plattner H, Artalejo AR, Neher E. Ultrastructural organization of bovine chromaffin cell cortex-analysis by cryofixation and morphometry of aspects pertinent to exocytosis. *J Cell Biol* (1997) **139**:1709–17. doi:10.1083/jcb.139.7.1709
20. Berberian K, Torres AJ, Fang Q, Kisler K, Lindau M. F-actin and myosin II accelerate catecholamine release from chromaffin granules. *J Neurosci* (2009) **29**:863–70. doi:10.1523/JNEUROSCI.2818-08.2009
21. Gasman S, Chasserot-Golaz S, Popoff MR, Aunis D, Bader MF. Trimeric G proteins control exocytosis in chromaffin cells. Go regulates the peripheral actin network and catecholamine secretion by a mechanism involving the small GTP-binding protein Rho. *J Biol Chem* (1997) **272**:20564–71. doi:10.1074/jbc.272.33.20564
22. Gasman S, Chasserot-Golaz S, Popoff MR, Aunis D, Bader MF. Involvement of Rho GTPases in calcium-regulated exocytosis from adrenal chromaffin cells. *J Cell Sci* (1999) **112**(Pt 24):4763–71.
23. Neco P, Fernandez-Peruchena C, Navas S, Gutierrez LM, de Toledo GA, Ales E. Myosin II contributes to fusion pore expansion during exocytosis. *J Biol Chem* (2008) **283**:10949–57. doi:10.1074/jbc.M709058200
24. Neco P, Giner D, Viniegra S, Borges R, Villarroel A, Gutierrez LM. New roles of myosin II during vesicle transport and fusion in chromaffin cells. *J Biol Chem* (2004) **279**:27450–7. doi:10.1074/jbc.M311462200
25. Rose SD, Lejen T, Casaletti L, Larson RE, Pene TD, Trifaro JM. Myosins II and V in chromaffin cells: myosin V is a chromaffin vesicle molecular motor involved in secretion. *J Neurochem* (2003) **85**:287–98. doi:10.1046/j.1471-4159.2003.01649.x
26. Neher E, Zucker RS. Multiple calcium-dependent processes related to secretion in bovine chromaffin cells. *Neuron* (1993) **10**:21–30. doi:10.1016/0896-6273(93)90238-M
27. Stevens DR, Schirra C, Becherer U, Rettig J. Vesicle pools: lessons from adrenal chromaffin cells. *Front Synaptic Neurosci* (2011) **3**:2. doi:10.3389/fnsyn.2011.00002
28. Trifaro J, Rose SD, Lejen T, Elzagallaai A. Two pathways control chromaffin cell cortical F-actin dynamics during exocytosis. *Biochimie* (2000) **82**:339–52. doi:10.1016/S0300-9084(00)00193-0
29. Trifaro JM, Lejen T, Rose SD, Pene TD, Barkar ND, Seward EP. Pathways that control cortical F-actin dynamics during secretion. *Neurochem Res* (2002) **27**:1371–85. doi:10.1023/A:1021627800918

30. Zhang L, Rodriguez Del Castillo A, Trifaro JM. Histamine-evoked chromaffin cell scinderin redistribution, F-actin disassembly, and secretion: in the absence of cortical F-actin disassembly, an increase in intracellular Ca2+ fails to trigger exocytosis. *J Neurochem* (1995) **65**:1297–308. doi:10.1046/j.1471-4159.1995.65031297.x
31. Gillis KD, Chow RH. Kinetics of exocytosis in adrenal chromaffin cells. *Semin Cell Dev Biol* (1997) **8**:133–40. doi:10.1006/scdb.1996.0132
32. Parsons TD, Coorssen JR, Horstmann H, Almers W. Docked granules, the exocytic burst, and the need for ATP hydrolysis in endocrine cells. *Neuron* (1995) **15**:1085–96. doi:10.1016/0896-6273(95)90097-7
33. Tomatis VM, Papadopulos A, Malintan NT, Martin S, Wallis T, Gormal RS, et al. Myosin VI small insert isoform maintains exocytosis by tethering secretory granules to the cortical actin. *J Cell Biol* (2013) **200**:301–20. doi:10.1083/jcb.201204092
34. Torregrosa-Hetland CJ, Villanueva J, Lopez-Font I, Garcia-Martinez V, Gil A, Gonzalez-Velez V, et al. Association of SNAREs and calcium channels with the borders of cytoskeletal cages organizes the secretory machinery in chromaffin cells. *Cell Mol Neurobiol* (2010) **30**:1315–9. doi:10.1007/s10571-010-9565-1
35. Johns LM, Levitan ES, Shelden EA, Holz RW, Axelrod D. Restriction of secretory granule motion near the plasma membrane of chromaffin cells. *J Cell Biol* (2001) **153**:177–90. doi:10.1083/jcb.153.1.177
36. Steyer JA, Almers W. Tracking single secretory granules in live chromaffin cells by evanescent-field fluorescence microscopy. *Biophys J* (1999) **76**:2262–71. doi:10.1016/S0006-3495(99)77382-0
37. Cuchillo-Ibanez I, Lejen T, Albillos A, Rose SD, Olivares R, Villarroya M, et al. Mitochondrial calcium sequestration and protein kinase C cooperate in the regulation of cortical F-actin disassembly and secretion in bovine chromaffin cells. *J Physiol* (2004) **560**:63–76. doi:10.1113/jphysiol.2004.064063
38. Gasman S, Chasserot-Golaz S, Malacombe M, Way M, Bader MF. Regulated exocytosis in neuroendocrine cells: a role for subplasmalemmal Cdc42/N-WASP-induced actin filaments. *Mol Biol Cell* (2004) **15**:520–31. doi:10.1091/mbc.E03-06-0402
39. Marcu MG, Zhang L, Elzagallaai A, Trifaro JM. Localization by segmental deletion analysis and functional characterization of a third actin-binding site in domain 5 of scinderin. *J Biol Chem* (1998) **273**:3661–8. doi:10.1074/jbc.273.6.3661
40. Yin HL, Janmey PA. Phosphoinositide regulation of the actin cytoskeleton. *Annu Rev Physiol* (2003) **65**:761–89. doi:10.1146/annurev.physiol.65.092101.142517
41. Bai J, Tucker WC, Chapman ER. PIP2 increases the speed of response of synaptotagmin and steers its membrane-penetration activity toward the plasma membrane. *Nat Struct Mol Biol* (2004) **11**:36–44. doi:10.1038/nsmb709
42. James DJ, Khodthong C, Kowalchyk JA, Martin TF. Phosphatidylinositol 4,5-bisphosphate regulates SNARE-dependent membrane fusion. *J Cell Biol* (2008) **182**:355–66. doi:10.1083/jcb.200801056
43. Kuo W, Herrick DZ, Cafiso DS. Phosphatidylinositol 4,5-bisphosphate alters synaptotagmin 1 membrane docking and drives opposing bilayers closer together. *Biochemistry* (2011) **50**:2633–41. doi:10.1021/bi200049c
44. van den Bogaart G, Meyenberg K, Diederichsen U, Jahn R. Phosphatidylinositol 4,5-bisphosphate increases Ca2+ affinity of synaptotagmin-1 by 40-fold. *J Biol Chem* (2012) **287**:16447–53. doi:10.1074/jbc.M112.343418
45. Di Paolo G, Moskowitz HS, Gipson K, Wenk MR, Voronov S, Obayashi M, et al. Impaired PtdIns(4,5)P2 synthesis in nerve terminals produces defects in synaptic vesicle trafficking. *Nature* (2004) **431**:415–22. doi:10.1038/nature02896
46. Aoyagi K, Sugaya T, Umeda M, Yamamoto S, Terakawa S, Takahashi M. The activation of exocytotic sites by the formation of phosphatidylinositol 4,5-bisphosphate microdomains at syntaxin clusters. *J Biol Chem* (2005) **280**:17346–52. doi:10.1074/jbc.M413307200
47. Honigmann A, van den Bogaart G, Iraheta E, Risselada HJ, Milovanovic D, Mueller V, et al. Phosphatidylinositol 4,5-bisphosphate clusters act as molecular beacons for vesicle recruitment. *Nat Struct Mol Biol* (2013) **20**:679–86. doi:10.1038/nsmb.2570
48. Murray DH, Tamm LK. Clustering of syntaxin-1A in model membranes is modulated by phosphatidylinositol 4,5-bisphosphate and cholesterol. *Biochemistry* (2009) **48**:4617–25. doi:10.1021/bi9003217
49. Lassing I, Lindberg U. Specific interaction between phosphatidylinositol 4,5-bisphosphate and profilactin. *Nature* (1985) **314**:472–4. doi:10.1038/314472a0
50. Rodriguez Del Castillo A, Vitale ML, Trifaro JM. Ca2+ and pH determine the interaction of chromaffin cell scinderin with phosphatidylserine and phosphatidylinositol 4,5,-biphosphate and its cellular distribution during nicotinic-receptor stimulation and protein kinase C activation. *J Cell Biol* (1992) **119**:797–810. doi:10.1083/jcb.119.4.797
51. Marcu MG, Rodriguez del Castillo A, Vitale ML, Trifaro JM. Molecular cloning and functional expression of chromaffin cell scinderin indicates that it belongs to the family of Ca(2+)-dependent F-actin severing proteins. *Mol Cell Biochem* (1994) **141**:153–65. doi:10.1007/BF00926179
52. Zhang L, Marcu MG, Nau-Staudt K, Trifaro JM. Recombinant scinderin enhances exocytosis, an effect blocked by two scinderin-derived actin-binding peptides and PIP2. *Neuron* (1996) **17**:287–96. doi:10.1016/S0896-6273(00)80160-9
53. Ojala PJ, Paavilainen V, Lappalainen P. Identification of yeast cofilin residues specific for actin monomer and PIP2 binding. *Biochemistry* (2001) **40**:15562–9. doi:10.1021/bi0117697
54. Bittner MA, Holz RW. Phosphatidylinositol-4,5-bisphosphate: actin dynamics and the regulation of ATP-dependent and -independent secretion. *Mol Pharmacol* (2005) **67**:1089–98. doi:10.1124/mol.104.008474
55. Tryoen-Toth P, Chasserot-Golaz S, Tu A, Gherib P, Bader MF, Beaumelle B, et al. HIV-1 Tat protein inhibits neurosecretion by binding to phosphatidylinositol 4,5-bisphosphate. *J Cell Sci* (2013) **126**:454–63. doi:10.1242/jcs.111658
56. Kumar N, Zhao P, Tomar A, Galea CA, Khurana S. Association of villin with phosphatidylinositol 4,5-bisphosphate regulates the actin cytoskeleton. *J Biol Chem* (2004) **279**:3096–110. doi:10.1074/jbc.M308878200
57. Galas MC, Helms JB, Vitale N, Thierse D, Aunis D, Bader MF. Regulated exocytosis in chromaffin cells. A potential role for a secretory granule-associated ARF6 protein. *J Biol Chem* (1997) **272**:2788–93. doi:10.1074/jbc.272.5.2788
58. Desnos C, Schonn JS, Huet S, Tran VS, El-Amraoui A, Raposo G, et al. Rab27A and its effector MyRIP link secretory granules to F-actin and control their motion towards release sites. *J Cell Biol* (2003) **163**:559–70. doi:10.1083/jcb.200302157
59. Xie L, Kang Y, Liang T, Dolai S, Xie H, Parsaud L, et al. RalA GTPase tethers insulin granules to L- and R-type calcium channels through binding alpha2 delta-1 subunit. *Traffic* (2013) **14**:428–39. doi:10.1111/tra.12047
60. Sugihara K, Asano S, Tanaka K, Iwamatsu A, Okawa K, Ohta Y. The exocyst complex binds the small GTPase RalA to mediate filopodia formation. *Nat Cell Biol* (2002) **4**:73–8. doi:10.1038/ncb720
61. Chen XW, Leto D, Chiang SH, Wang Q, Saltiel AR. Activation of RalA is required for insulin-stimulated Glut4 trafficking to the plasma membrane via the exocyst and the motor protein Myo1c. *Dev Cell* (2007) **13**:391–404. doi:10.1016/j.devcel.2007.07.007
62. Vitale N, Mawet J, Camonis J, Regazzi R, Bader MF, Chasserot-Golaz S. The small GTPase RalA controls exocytosis of large dense core secretory granules by interacting with ARF6-dependent phospholipase D1. *J Biol Chem* (2005) **280**:29921–8. doi:10.1074/jbc.M413748200
63. Lang T, Jahn R. Core proteins of the secretory machinery. *Handb Exp Pharmacol* (2008). **184**:107–27. doi:10.1007/978-3-540-74805-2_5
64. Darchen F, Senyshyn J, Brondyk WH, Taatjes DJ, Holz RW, Henry JP, et al. The GTPase Rab3a is associated with large dense core vesicles in bovine chromaffin cells and rat PC12 cells. *J Cell Sci* (1995) **108**(Pt 4):1639–49.
65. Darchen F, Zahraoui A, Hammel F, Monteils MP, Tavitian A, Scherman D. Association of the GTP-binding protein Rab3A with bovine adrenal chromaffin granules. *Proc Natl Acad Sci U S A* (1990) **87**:5692–6. doi:10.1073/pnas.87.15.5692

66. Lin CG, Pan CY, Kao LS. Rab3A delayed catecholamine secretion from bovine adrenal chromaffin cells. *Biochem Biophys Res Commun* (1996) **221**:675–81. doi:10.1006/bbrc.1996.0655
67. Johannes L, Lledo PM, Roa M, Vincent JD, Henry JP, Darchen F. The GTPase Rab3a negatively controls calcium-dependent exocytosis in neuroendocrine cells. *EMBO J* (1994) **13**:2029–37.
68. Huang CC, Yang DM, Lin CC, Kao LS. Involvement of Rab3A in vesicle priming during exocytosis: interaction with Munc13-1 and Munc18-1. *Traffic* (2011) **12**:1356–70. doi:10.1111/j.1600-0854.2011.01237.x
69. Bello OD, Zanetti MN, Mayorga LS, Michaut MA. RIM, Munc13, and Rab3A interplay in acrosomal exocytosis. *Exp Cell Res* (2012) **318**:478–88. doi:10.1016/j.yexcr.2012.01.002
70. Bustos MA, Lucchesi O, Ruete MC, Mayorga LS, Tomes CN. Rab27 and Rab3 sequentially regulate human sperm dense-core granule exocytosis. *Proc Natl Acad Sci U S A* (2012) **109**:E2057–66. doi:10.1073/pnas.1121173109
71. Graham ME, Handley MT, Barclay JW, Ciufo LF, Barrow SL, Morgan A, et al. A gain-of-function mutant of Munc18-1 stimulates secretory granule recruitment and exocytosis and reveals a direct interaction of Munc18-1 with Rab3. *Biochem J* (2008) **409**:407–16. doi:10.1042/BJ20071094
72. van Weering JR, Toonen RF, Verhage M. The role of Rab3a in secretory vesicle docking requires association/dissociation of guanidine phosphates and Munc18-1. *PLoS One* (2007) **2**:e616. doi:10.1371/journal.pone.0000616
73. Schluter OM, Schmitz F, Jahn R, Rosenmund C, Sudhof TC. A complete genetic analysis of neuronal Rab3 function. *J Neurosci* (2004) **24**:6629–37. doi:10.1523/JNEUROSCI.1610-04.2004
74. Berg JS, Powell BC, Cheney RE. A millennial myosin census. *Mol Biol Cell* (2001) **12**:780–94. doi:10.1091/mbc.12.4.780
75. Carlier MF, Valentin-Ranc C, Combeau C, Fievez S, Pantoloni D. Actin polymerization: regulation by divalent metal ion and nucleotide binding, ATP hydrolysis and binding of myosin. *Adv Exp Med Biol* (1994) **358**:71–81. doi:10.1007/978-1-4615-2578-3_7
76. Lechler T, Shevchenko A, Li R. Direct involvement of yeast type I myosins in Cdc42-dependent actin polymerization. *J Cell Biol* (2000) **148**:363–73. doi:10.1083/jcb.148.2.363
77. van den Boom F, Dussmann H, Uhlenbrock K, Abouhamed M, Bahler M. The myosin IXb motor activity targets the myosin IXb RhoGAP domain as cargo to sites of actin polymerization. *Mol Biol Cell* (2007) **18**:1507–18. doi:10.1091/mbc.E06-08-0771
78. Vicente-Manzanares M, Zareno J, Whitmore L, Choi CK, Horwitz AF. Regulation of protrusion, adhesion dynamics, and polarity by myosins IIA and IIB in migrating cells. *J Cell Biol* (2007) **176**:573–80. doi:10.1083/jcb.20061204320070302c
79. Win TZ, Gachet Y, Mulvihill DP, May KM, Hyams JS. Two type V myosins with non-overlapping functions in the fission yeast *Schizosaccharomyces pombe*: Myo52 is concerned with growth polarity and cytokinesis, Myo51 is a component of the cytokinetic actin ring. *J Cell Sci* (2001) **114**:69–79.
80. Yin H, Pruyne D, Huffaker TC, Bretscher A. Myosin V orientates the mitotic spindle in yeast. *Nature* (2000) **406**:1013–5. doi:10.1038/35023024
81. Bose A, Guilherme A, Robida SI, Nicoloro SM, Zhou QL, Jiang ZY, et al. Glucose transporter recycling in response to insulin is facilitated by myosin Myo1c. *Nature* (2002) **420**:821–4. doi:10.1038/nature01246
82. Bahler M. Myosins on the move to signal transduction. *Curr Opin Cell Biol* (1996) **8**:18–22. doi:10.1016/S0955-0674(96)80043-3
83. Mermall V, Post PL, Mooseker MS. Unconventional myosins in cell movement, membrane traffic, and signal transduction. *Science* (1998) **279**:527–33. doi:10.1126/science.279.5350.527
84. Sellers JR. Myosins: a diverse superfamily. *Biochim Biophys Acta* (2000) **1496**:3–22. doi:10.1016/S0167-4889(00)00005-7
85. Krendel M, Mooseker MS. Myosins: tails (and heads) of functional diversity. *Physiology (Bethesda)* (2005) **20**:239–51. doi:10.1152/physiol.00014.2005
86. Gillespie PG, Cyr JL. Myosin-1c, the hair cell's adaptation motor. *Annu Rev Physiol* (2004) **66**:521–45. doi:10.1146/annurev.physiol.66.032102.112842
87. Barylko B, Binns DD, Albanesi JP. Regulation of the enzymatic and motor activities of myosin I. *Biochim Biophys Acta* (2000) **1496**:23–35. doi:10.1016/S0167-4889(00)00006-9
88. Hokanson DE, Laakso JM, Lin T, Sept D, Ostap EM. Myo1c binds phosphoinositides through a putative pleckstrin homology domain. *Mol Biol Cell* (2006) **17**:4856–65. doi:10.1091/mbc.E06-05-0449
89. Tang N, Lin T, Yang J, Foskett JK, Ostap EM. CIB1 and CaBP1 bind to the myo1c regulatory domain. *J Muscle Res Cell Motil* (2007) **28**:285–91. doi:10.1007/s10974-007-9124-7
90. Boguslavsky S, Chiu T, Foley KP, Osorio-Fuentealba C, Antonescu CN, Bayer KU, et al. Myo1c binding to submembrane actin mediates insulin-induced tethering of GLUT4 vesicles. *Mol Biol Cell* (2012) **23**:4065–78. doi:10.1091/mbc.E12-04-0263
91. Bose A, Robida S, Furcinitti PS, Chawla A, Fogarty K, Corvera S, et al. Unconventional myosin Myo1c promotes membrane fusion in a regulated exocytic pathway. *Mol Cell Biol* (2004) **24**:5447–58. doi:10.1128/MCB.24.12.5447-5458.2004
92. Toyoda T, An D, Witczak CA, Koh HJ, Hirshman MF, Fujii N, et al. Myo1c regulates glucose uptake in mouse skeletal muscle. *J Biol Chem* (2011) **286**:4133–40. doi:10.1074/jbc.M110.174938
93. Tiwari A, Jung JJ, Inamdar SM, Nihalani D, Choudhury A. The myosin motor Myo1c is required for VEGFR2 delivery to the cell surface and for angiogenic signaling. *Am J Physiol Heart Circ Physiol* (2013) **304**:H687–96. doi:10.1152/ajpheart.00744.2012
94. Schietroma C, Yu HY, Wagner MC, Umbach JA, Bement WM, Gundersen CB. A role for myosin 1e in cortical granule exocytosis in *Xenopus* oocytes. *J Biol Chem* (2007) **282**:29504–13. doi:10.1074/jbc.M705825200
95. Boal F, Laguerre M, Milochau A, Lang J, Scotti PA. A charged prominence in the linker domain of the cysteine-string protein Cspalpha mediates its regulated interaction with the calcium sensor synaptotagmin 9 during exocytosis. *FASEB J* (2011) **25**:132–43. doi:10.1096/fj.09-152033
96. Cheng J, Grassart A, Drubin DG. Myosin 1E coordinates actin assembly and cargo trafficking during clathrin-mediated endocytosis. *Mol Biol Cell* (2012) **23**:2891–904. doi:10.1091/mbc.E11-04-0383
97. Vicente-Manzanares M, Ma X, Adelstein RS, Horwitz AR. Non-muscle myosin II takes centre stage in cell adhesion and migration. *Nat Rev Mol Cell Biol* (2009) **10**:778–90. doi:10.1038/nrm2786
98. Bond LM, Brandstaetter H, Sellers JR, Kendrick-Jones J, Buss F. Myosin motor proteins are involved in the final stages of the secretory pathways. *Biochem Soc Trans* (2011) **39**:1115–9. doi:10.1042/BST0391115
99. DePina AS, Wollert T, Langford GM. Membrane associated non-muscle myosin II functions as a motor for actin-based vesicle transport in clam oocyte extracts. *Cell Motil Cytoskeleton* (2007) **64**:739–55. doi:10.1002/cm.20219
100. Neco P, Gil A, Del Mar Frances M, Viniegra S, Gutierrez LM. The role of myosin in vesicle transport during bovine chromaffin cell secretion. *Biochem J* (2002) **368**:405–13. doi:10.1042/BJ20021090
101. Aoki R, Kitaguchi T, Oya M, Yanagihara Y, Sato M, Miyawaki A, et al. Duration of fusion pore opening and the amount of hormone released are regulated by myosin II during kiss-and-run exocytosis. *Biochem J* (2010) **429**:497–504. doi:10.1042/BJ20091839
102. Doreian BW, Fulop TG, Smith CB. Myosin II activation and actin reorganization regulate the mode of quantal exocytosis in mouse adrenal chromaffin cells. *J Neurosci* (2008) **28**:4470–8. doi:10.1523/JNEUROSCI.0008-08.2008
103. Bhat P, Thorn P. Myosin 2 maintains an open exocytic fusion pore in secretory epithelial cells. *Mol Biol Cell* (2009) **20**:1795–803. doi:10.1091/mbc.E08-10-1048
104. Miklavc P, Hecht E, Hobi N, Wittekindt OH, Dietl P, Kranz C, et al. Actin coating and compression of fused secretory vesicles are essential for surfactant secretion – a role for Rho, formins and myosin II. *J Cell Sci* (2012) **125**:2765–74. doi:10.1242/jcs.105262
105. Choi YO, Ryu HJ, Kim HR, Song YS, Kim C, Lee W, et al. Implication of phosphorylation of the myosin II regulatory light chain in insulin-stimulated GLUT4 translocation in 3T3-F442A adipocytes. *Exp Mol Med* (2006) **38**:180–9. doi:10.1038/emm.2006.22

106. Fulcher FK, Smith BT, Russ M, Patel YM. Dual role for myosin II in GLUT4-mediated glucose uptake in 3T3-L1 adipocytes. *Exp Cell Res* (2008) **314**:3264–74. doi:10.1016/j.yexcr.2008.08.007
107. Villanueva J, Torres V, Torregrosa-Hetland CJ, Garcia-Martinez V, Lopez-Font I, Viniegra S, et al. F-actin-myosin II inhibitors affect chromaffin granule plasma membrane distance and fusion kinetics by retraction of the cytoskeletal cortex. *J Mol Neurosci* (2012) **48**:328–38. doi:10.1007/s12031-012-9800-y
108. Arous C, Rondas D, Halban PA. Non-muscle myosin IIA is involved in focal adhesion and actin remodelling controlling glucose-stimulated insulin secretion. *Diabetologia* (2013) **56**:792–802. doi:10.1007/s00125-012-2800-1
109. Rondas D, Tomas A, Halban PA. Focal adhesion remodeling is crucial for glucose-stimulated insulin secretion and involves activation of focal adhesion kinase and paxillin. *Diabetes* (2011) **60**:1146–57. doi:10.2337/db10-0946
110. Deacon SW, Gelfand VI. Of yeast, mice, and men. Rab proteins and organelle transport. *J Cell Biol* (2001) **152**:F21–4. doi:10.1083/jcb.152.4.F21
111. Matesic LE, Yip R, Reuss AE, Swing DA, O'Sullivan TN, Fletcher CF, et al. Mutations in Mlph, encoding a member of the Rab effector family, cause the melanosome transport defects observed in leaden mice. *Proc Natl Acad Sci U S A* (2001) **98**:10238–43. doi:10.1073/pnas.181336698
112. Bizario JC, Castro FA, Sousa JF, Fernandes RN, Damiao AD, Oliveira MK, et al. Myosin-V colocalizes with MHC class II in blood mononuclear cells and is up-regulated by T-lymphocyte activation. *J Leukoc Biol* (2002) **71**:195–204.
113. Ivarsson R, Jing X, Waselle L, Regazzi R, Renstrom E. Myosin 5a controls insulin granule recruitment during late-phase secretion. *Traffic* (2005) **6**:1027–35. doi:10.1111/j.1600-0854.2005.00342.x
114. Wu X, Bowers B, Rao K, Wei Q, Hammer JA III. Visualization of melanosome dynamics within wild-type and dilute melanocytes suggests a paradigm for myosin V function in vivo. *J Cell Biol* (1998) **143**:1899–918. doi:10.1083/jcb.143.7.1899
115. Rudolf R, Kogel T, Kuznetsov SA, Salm T, Schlicker O, Hellwig A, et al. Myosin Va facilitates the distribution of secretory granules in the F-actin rich cortex of PC12 cells. *J Cell Sci* (2003) **116**:1339–48. doi:10.1242/jcs.00317
116. Kogel T, Rudolf R, Hodneland E, Hellwig A, Kuznetsov SA, Seiler F, et al. Distinct roles of myosin Va in membrane remodeling and exocytosis of secretory granules. *Traffic* (2010) **11**:637–50. doi:10.1111/j.1600-0854.2010.01048.x
117. Desnos C, Huet S, Fanget I, Chapuis C, Bottiger C, Racine V, et al. Myosin va mediates docking of secretory granules at the plasma membrane. *J Neurosci* (2007) **27**:10636–45. doi:10.1523/JNEUROSCI.1228-07.2007
118. Huet S, Fanget I, Jouannot O, Meireles P, Zeiske T, Larochette N, et al. Myrip couples the capture of secretory granules by the actin-rich cell cortex and their attachment to the plasma membrane. *J Neurosci* (2012) **32**:2564–77. doi:10.1523/JNEUROSCI.2724-11.2012
119. Varadi A, Tsuboi T, Rutter GA. Myosin Va transports dense core secretory vesicles in pancreatic MIN6 beta-cells. *Mol Biol Cell* (2005) **16**:2670–80. doi:10.1091/mbc.E04-11-1001
120. Prekeris R, Terrian DM. Brain myosin V is a synaptic vesicle-associated motor protein: evidence for a Ca2+-dependent interaction with the synaptobrevin-synaptophysin complex. *J Cell Biol* (1997) **137**:1589–601. doi:10.1083/jcb.137.7.1589
121. Karcher RL, Roland JT, Zappacosta F, Huddleston MJ, Annan RS, Carr SA, et al. Cell cycle regulation of myosin-V by calcium/calmodulin-dependent protein kinase II. *Science* (2001) **293**:1317–20. doi:10.1126/science.1061086
122. Costa MC, Mani F, Santoro W Jr, Espreafico EM, Larson RE. Brain myosin-V, a calmodulin-carrying myosin, binds to calmodulin-dependent protein kinase II and activates its kinase activity. *J Biol Chem* (1999) **274**:15811–9. doi:10.1074/jbc.274.22.15811
123. Kenigsberg RL, Trifaro JM. Microinjection of calmodulin antibodies into cultured chromaffin cells blocks catecholamine release in response to stimulation. *Neuroscience* (1985) **14**:335–47. doi:10.1016/0306-4522(85)90183-6
124. Rudolf R, Bittins CM, Gerdes HH. The role of myosin V in exocytosis and synaptic plasticity. *J Neurochem* (2011) **116**:177–91. doi:10.1111/j.1471-4159.2010.07110.x
125. Bryant Z, Altman D, Spudich JA. The power stroke of myosin VI and the basis of reverse directionality. *Proc Natl Acad Sci U S A* (2007) **104**:772–7. doi:10.1073/pnas.0610144104
126. Wells AL, Lin AW, Chen LQ, Safer D, Cain SM, Hasson T, et al. Myosin VI is an actin-based motor that moves backwards. *Nature* (1999) **401**:505–8. doi:10.1038/46835
127. Bahloul A, Chevreux G, Wells AL, Martin D, Nolt J, Yang Z, et al. The unique insert in myosin VI is a structural calcium-calmodulin binding site. *Proc Natl Acad Sci U S A* (2004) **101**:4787–92. doi:10.1073/pnas.0306892101
128. Au JS, Puri C, Ihrke G, Kendrick-Jones J, Buss F. Myosin VI is required for sorting of AP-1B-dependent cargo to the basolateral domain in polarized MDCK cells. *J Cell Biol* (2007) **177**:103–14. doi:10.1083/jcb.200608126
129. Buss F, Arden SD, Lindsay M, Luzio JP, Kendrick-Jones J. Myosin VI isoform localized to clathrin-coated vesicles with a role in clathrin-mediated endocytosis. *EMBO J* (2001) **20**:3676–84. doi:10.1093/emboj/20.14.3676
130. Buss F, Kendrick-Jones J. Multifunctional myosin VI has a multitude of cargoes. *Proc Natl Acad Sci U S A* (2011) **108**:5927–8. doi:10.1073/pnas.1103086108
131. Phichith D, Travaglia M, Yang Z, Liu X, Zong AB, Safer D, et al. Cargo binding induces dimerization of myosin VI. *Proc Natl Acad Sci U S A* (2009) **106**:17320–4. doi:10.1073/pnas.0909748106
132. Yu C, Feng W, Wei Z, Miyanoiri Y, Wen W, Zhao Y, et al. Myosin VI undergoes cargo-mediated dimerization. *Cell* (2009) **138**:537–48. doi:10.1016/j.cell.2009.05.030
133. Aschenbrenner L, Lee T, Hasson T. Myo6 facilitates the translocation of endocytic vesicles from cell peripheries. *Mol Biol Cell* (2003) **14**:2728–43. doi:10.1091/mbc.E02-11-0767
134. Buss F, Luzio JP, Kendrick-Jones J. Myosin VI, a new force in clathrin mediated endocytosis. *FEBS Lett* (2001) **508**:295–9. doi:10.1016/S0014-5793(01)03065-4
135. Hasson T. Myosin VI: two distinct roles in endocytosis. *J Cell Sci* (2003) **116**:3453–61. doi:10.1242/jcs.00669
136. Puri C. Loss of myosin VI no insert isoform (NoI) induces a defect in clathrin-mediated endocytosis and leads to caveolar endocytosis of transferrin receptor. *J Biol Chem* (2009) **284**:34998–5014. doi:10.1074/jbc.M109.012328
137. Roberts R, Lister I, Schmitz S, Walker M, Veigel C, Trinick J, et al. Myosin VI: cellular functions and motor properties. *Philos Trans R Soc Lond B Biol Sci* (2004) **359**:1931–44. doi:10.1098/rstb.2004.1563
138. Tumbarello DA, Waxse BJ, Arden SD, Bright NA, Kendrick-Jones J, Buss F. Autophagy receptors link myosin VI to autophagosomes to mediate Tom1-dependent autophagosome maturation and fusion with the lysosome. *Nat Cell Biol* (2012) **14**:1024–35. doi:10.1038/ncb2589
139. Hertzano R, Shalit E, Rzadzinska AK, Dror AA, Song L, Ron U, et al. A Myo6 mutation destroys coordination between the myosin heads, revealing new functions of myosin VI in the stereocilia of mammalian inner ear hair cells. *PLoS Genet* (2008) **4**:e1000207. doi:10.1371/journal.pgen.1000207
140. Hicks JL, Deng WM, Rogat AD, Miller KG, Bownes M. Class VI unconventional myosin is required for spermatogenesis in *Drosophila*. *Mol Biol Cell* (1999) **10**:4341–53. doi:10.1091/mbc.10.12.4341
141. Noguchi T, Frank DJ, Isaji M, Miller KG. Coiled-coil-mediated dimerization is not required for myosin VI to stabilize actin during spermatid individualization in *Drosophila melanogaster*. *Mol Biol Cell* (2009) **20**:358–67. doi:10.1091/mbc.E08-07-0776
142. Noguchi T, Lenartowska M, Miller KG. Myosin VI stabilizes an actin network during *Drosophila* spermatid individualization. *Mol Biol Cell* (2006) **17**:2559–71. doi:10.1091/mbc.E06-01-0031
143. Vreugde S, Ferrai C, Miluzio A, Hauben E, Marchisio PC, Crippa MP, et al. Nuclear myosin VI enhances RNA polymerase II-dependent transcription. *Mol Cell* (2006) **23**:749–55. doi:10.1016/j.molcel.2006.07.005
144. Maddugoda MP, Crampton MS, Shewan AM, Yap AS. Myosin VI and vinculin cooperate during the morphogenesis of cadherin cell cell contacts in mammalian epithelial cells. *J Cell Biol* (2007)

178:529–40. doi:10.1083/jcb.200612042
145. Millo H, Leaper K, Lazou V, Bownes M. Myosin VI plays a role in cell-cell adhesion during epithelial morphogenesis. *Mech Dev* (2004) **121**:1335–51. doi:10.1016/j.mod.2004.06.007
146. Warner CL, Stewart A, Luzio JP, Steel KP, Libby RT, Kendrick-Jones J, et al. Loss of myosin VI reduces secretion and the size of the Golgi in fibroblasts from Snell's waltzer mice. *EMBO J* (2003) **22**:569–79. doi:10.1093/emboj/cdg055
147. Avraham KB, Hasson T, Steel KP, Kingsley DM, Russell LB, Mooseker MS, et al. The mouse Snell's waltzer deafness gene encodes an unconventional myosin required for structural integrity of inner ear hair cells. *Nat Genet* (1995) **11**:369–75. doi:10.1038/ng1295-369
148. Self T, Sobe T, Copeland NG, Jenkins NA, Avraham KB, Steel KP. Role of myosin VI in the differentiation of cochlear hair cells. *Dev Biol* (1999) **214**:331–41. doi:10.1006/dbio.1999.9424
149. Puri C, Chibalina MV, Arden SD, Kruppa AJ, Kendrick-Jones J, Buss F. Overexpression of myosin VI in prostate cancer cells enhances PSA and VEGF secretion, but has no effect on endocytosis. *Oncogene* (2010) **29**:188–200. doi:10.1038/onc.2009.328
150. Bond LM, Peden AA, Kendrick-Jones J, Sellers JR, Buss F. Myosin VI and its binding partner optineurin are involved in secretory vesicle fusion at the plasma membrane. *Mol Biol Cell* (2011) **22**:54–65. doi:10.1091/mbc.E10-06-0553
151. Osterweil E, Wells DG, Mooseker MS. A role for myosin VI in postsynaptic structure and glutamate receptor endocytosis. *J Cell Biol* (2005) **168**:329–38. doi:10.1083/jcb.200410091
152. Yano H, Ninan I, Zhang H, Milner TA, Arancio O, Chao MV. BDNF-mediated neurotransmission relies upon a myosin VI motor complex. *Nat Neurosci* (2006) **9**:1009–18. doi:10.1038/nn1730
153. Iwaki M, Tanaka H, Iwane AH, Katayama E, Ikebe M, Yanagida T. Cargo-binding makes a wild-type single-headed myosin-VI move processively. *Biophys J* (2006) **90**:3643–52. doi:10.1529/biophysj.105.075721
154. Naccache SN, Hasson T. Myosin VI altered at threonine 406 stabilizes actin filaments in vivo. *Cell Motil Cytoskeleton* (2006) **63**:633–45. doi:10.1002/cm.20150
155. Rock RS, Rice SE, Wells AL, Purcell TJ, Spudich JA, Sweeney HL. Myosin VI is a processive motor with a large step size. *Proc Natl Acad Sci U S A* (2001) **98**:13655–9. doi:10.1073/pnas.191512398
156. Majewski L, Sobczak M, Redowicz MJ. Myosin VI is associated with secretory granules and is present in the nucleus in adrenal medulla chromaffin cells. *Acta Biochim Pol* (2010) **57**:109–14.
157. Kisiel M, Majumdar D, Campbell S, Stewart BA. Myosin VI contributes to synaptic transmission and development at the *Drosophila* neuromuscular junction. *BMC Neurosci* (2011) **12**:65. doi:10.1186/1471-2202-12-65

Conflict of Interest Statement: The authors declare that the research was conducted in the absence of any commercial or financial relationships that could be construed as a potential conflict of interest.

Received: 15 August 2013; accepted: 05 October 2013; published online: 21 October 2013.
*Citation: Papadopulos A, Tomatis VM, Kasula R and Meunier FA (2013) The cortical acto-myosin network: from diffusion barrier to functional gateway in the transport of neurosecretory vesicles to the plasma membrane. Front. Endocrinol. **4**:153. doi: 10.3389/fendo.2013.00153*
This article was submitted to Neuroendocrine Science, a section of the journal Frontiers in Endocrinology.

frontiers in
ENDOCRINOLOGY

ORIGINAL RESEARCH ARTICLE
published: 17 September 2013
doi: 10.3389/fendo.2013.00119

Munc13-1 translocates to the plasma membrane in a Doc2B- and calcium-dependent manner

Reut Friedrich[1], Irit Gottfried[1] and Uri Ashery[1,2]*

[1] *Department of Neurobiology, Wise Faculty of Life Sciences, Tel Aviv University, Tel Aviv, Israel*
[2] *Sagol School of Neuroscience, Tel Aviv University, Tel Aviv, Israel*

Edited by:
Stephane Gasman, Centre National de la Recherche Scientifique, France

Reviewed by:
Nicolas Vitale, Centre National de la Recherche Scientifique, France
Luis M. Gutiérrez, University Miguel Hernandez, Spain

***Correspondence:**
Uri Ashery, Department of Neurobiology, The George S. Wise Faculty of Life Sciences, Tel Aviv University, Ramat Aviv, Tel Aviv 69978, Israel
e-mail: uriashery@gmail.com

Munc13-1 is a presynaptic protein activated by calcium, calmodulin, and diacylglycerols (DAG) that is known to enhance vesicle priming. Doc2B is another presynaptic protein that translocates to the plasma membrane (PM) upon elevation of internal calcium concentration ($[Ca^{2+}]_i$) to the submicromolar range, and increases both spontaneous and asynchronous release in a calcium-dependent manner. We speculated that Doc2B also recruits Munc13-1 to the PM since these two proteins have been shown to interact physiologically and this interaction is enhanced by Ca^{2+}. However, this calcium-dependent co-translocation has never actually been shown. To examine this possibility, we expressed both proteins tagged to fluorescent proteins in PC12 cells and stimulated the cells to investigate the recruitment hypothesis using imaging techniques. We found that Munc13-1 does indeed translocate to the PM upon elevation in $[Ca^{2+}]_i$, but only when co-expressed with Doc2B. Interestingly, Munc13-1 co-translocates at a slower rate than Doc2B. Moreover, while Doc2B dislocates from the PM as soon as the $[Ca^{2+}]_i$ returns to basal levels, Munc13-1 dislocates at a slower rate and a fraction of it accumulates on the PM. This accumulation is more pronounced under subsequent stimulations, suggesting that Munc13-1 accumulation builds up as some other factors accumulate at the PM. Munc13-1 co-translocation and accumulation was reduced when its mutant Munc13-1^{H567K}, which is unable to bind DAG, was co-expressed with Doc2B, suggesting that Munc13-1 accumulation depends on DAG levels. These results suggest that Doc2B enables recruitment of Munc13-1 to the PM in a $[Ca^{2+}]_i$-dependent manner and offers another possible Munc13-1-regulatory mechanism that is both calcium- and Doc2B-dependent.

Keywords: Munc13, Doc2B, calcium, translocation, phorbol ester

INTRODUCTION

Munc13-1 is a key player in the final stages of exocytosis. It is a relatively large protein (1,735 aa) with several distinct domains (1). Its Mun domain (aa 859–1531) is responsible for the crucial role of Munc13-1 in exocytosis: the conversion of syntaxin to its open form. This open form of syntaxin interacts with SNAP-25 to form a heterodimer; the heterodimer then interacts with synaptobrevin to form the SNARE complex, which holds the vesicle in close proximity to the plasma membrane (PM) and enables efficient fusion. Munc13-1 has an active C1 domain [aa 567–616 (1, 2)] and has been shown to translocate to the PM upon TPA/PMA stimulation (3). Munc13-1 also has three active C2 domains (4–8), and it interacts with members of the double-C2 domain (Doc2) protein family via residues 851–1461 (3).

Doc2A and B are high-affinity sensors of internal calcium concentration ($[Ca^{2+}]_i$), containing tandem C2 domains that are responsible for their Ca^{2+}-dependent PM targeting and that promote priming and fusion (9, 10). Doc2A interacts with Munc13-1 through its Munc13-interacting domain (Mid, aa 13–37), which is highly conserved in Doc2B [92%, (3)]. The interaction between Munc13 and Doc2 has been demonstrated in both cell-free and intact cell systems. In the yeast two-hybrid system, Munc13-1 and Munc13-2 were shown to interact with both Doc2A and Doc2B (3). Co-immunoprecipitation of Munc13-1 with Doc2A from PC12 cells was markedly enhanced when the cells were stimulated by TPA or high K^+ in the presence of extracellular calcium (3). A growth hormone assay in PC12 suggested that this interaction has a physiological role; overexpression of the Doc2-interacting domain of Munc13 reduced the Ca^{2+}-dependent exocytosis from PC12 cells, and co-expression with Doc2 suppressed this reduction (3). However, expression of Mid alone in PC12 cells had no effect on the number of docked vesicles (11).

The physiological relevance of this interaction was then further tested in neurons. Introduction of the Mid peptide into presynaptic neurons of cholinergic synapses reversibly inhibited synaptic transmission evoked by action potentials (12). In contrast, the scrambled Mid peptide did not inhibit synaptic transmission. Recordings from the calyx of Held revealed that presynaptic loading of a synthetic Mid peptide significantly attenuates phorbol-ester (PE) induced synaptic potentiation, whereas the scrambled Mid peptide had no effect (13).

Imaging experiments revealed that Doc2B translocates to the PM when it is co-expressed with Munc13-1 following PE application (14). Doc2A and Munc13-4 relocated to the cell periphery

together with the secretory lysosome marker CD63 upon Ag stimulation in a calcium-free medium (15). This interaction depended on the Mid domain of Doc2A although C2B also seemed to play a role (15). Both Doc2B and Munc13-1 are expressed in chromaffin cells (10, 16). Based on the fact that Doc2B translocates to the PM upon calcium elevation and interacts with Munc13-1, and on the above data, we hypothesized that Doc2B will efficiently recruit Munc13-1 to the PM in a $[Ca^{2+}]_i$-dependent manner. We found that Munc13-1 co-translocates to and accumulates at the PM when co-expressed with Doc2B in a calcium-dependent manner.

MATERIALS AND METHODS

CELL LINES

PC12 cells (a generous gift from Dr. Nicolas Vitale, CNRS-UPR, Strasbourg, France) were grown in DMEM (Biological Industries, Beit Haemek, Israel) supplemented with glucose (4,500 mg/l) and L-glutamine (Gibco-BRL), and containing 5% (v/v) fetal calf serum, 10% (v/v) horse serum, and 100 U/ml penicillin/streptomycin (Biological Industries). The cells were split regularly to maintain confluence and were kept in a 37°C, 5% CO_2-humidified incubator. Transfection was performed using Lipofectamine™ 2000 (Invitrogen) according to the manufacturer's instructions at a 2:3 (DNA:reagent) ratio. Cells were imaged 16–32 h after transfection.

COS-7 cells were grown in DMEM supplemented with 10% fetal calf serum, 2 mM L-glutamine, and 100 U/ml penicillin-streptomycin. The cells were split regularly to maintain confluence and were kept in a 37°C, 5% CO_2-humidified incubator. Transfection was performed using Jet-PEI (PolyPlus Transfection, New York, NY, USA) according to the manufacturer's instructions at a 1:2 (DNA:reagent) ratio.

DNA CONSTRUCTS

All plasmids encoding fluorescently labeled Doc2B and the Doc2B–glutathione-*S*-transferase (GST) plasmids were a generous gift from Dr. Alexander J. Groffen (Vrije Universiteit, Amsterdam, The Netherlands) and the control GST construct was a generous gift from Prof. Joel Hirsch (Tel Aviv University, Israel). The sequences of all constructs were verified by automated DNA sequencing. Munc13-1 plasmids are a kind gift from Prof. N. Brose (Max-Plank institute, Gottingen, Germany).

WESTERN BLOTTING

Western blot experiments were performed according to standard procedures. In general, protein extracts (for overexpression experiments ∼10 μg protein, for endogenous experiments ∼100 μg protein) were loaded on an SDS-polyacrylamide (8 or 11%) gel and electrophoresed with a constant current of 30 mA for each gel. The proteins from the gel were transferred to a nitrocellulose membrane by electroblotting at a constant current of 400 mA for 1 h. The membrane was incubated in blocking solution (5% milk powder) overnight at 4°C with gentle agitation. After five washes, we incubated the membrane with primary rabbit anti-Doc2B antibody for 1 h at room temperature (diluted 1:500 in 1% BSA with 0.05% azide). The membrane was washed five times and incubated with the relevant secondary horseradish peroxidase-conjugated antibody for 45 min at room temperature (diluted 1:15,000 in milk). Then the membrane was washed six times, and detection was performed using enhanced chemiluminescence solution (Pierce) and exposure to Super RX film (Fuji).

CO-TRANSLOCATION EXPERIMENTS

For the translocation experiment, PC12 cells were plated on glass coverslips, transfected with different combinations of plasmids (see Results for details) encoding fluorescently tagged proteins – $Doc2B^{wt}$–mRFP, $Doc2B^{D218,220N}$–mRFP, $Doc2B^{Mid}$–mRFP, Munc13-1^{wt}–EGFP, Munc13-1^{H567K}–EGFP, or EGFP alone using Lipofectamine 2000. Imaging was performed 16–32 h post-transfection. Cells were perfused constantly with external solution and excited using a high K^+ solution (70 mM) as described in Groffen et al. (9). The imaging setup consisted of an Olympus IX-70 inverted microscope with a 60× total internal reflection fluorescence (TIRF) objective (Olympus), a TILL Photonics TIRF condenser (Gräfelfing, Germany), two solid-state lasers (Laser Quantum, Stockport, UK) emitting at 473 and 532 nm, an Andor Ixon 887 EMCCD camera (Belfast, Northern Ireland), and a dual-view beam-splitting device (Optical Insights, Roper Bioscience, Tucson, AZ, USA). Time-lapse images were taken every 300 ms. The equipment was controlled by Metamorph software (Molecular Devices, Downingtown, PA, USA), which was also used to perform the analysis. Confocal images were recorded using a 63× objective of Zeiss LSM 510 META microscope equipped with 30 mW 488 nm Argon laser and 15 mW 561 nm DPSS laser.

RESULTS

Doc2B AND Munc13-1 CO-TRANSLOCATE UPON ELEVATION OF $[Ca^{2+}]_i$

To investigate our hypothesis that co-expression of $Doc2B^{wt}$ and Munc13-1 results in co-translocation of both proteins to the PM upon $[Ca^{2+}]_i$ elevation, we expressed Munc13-1 fused to EGFP in PC12 cells together with $Doc2B^{wt}$ fused to mRFP. The cells were subjected to three short (20 s) KCl applications (with relaxation times between each application) which caused elevation of $[Ca^{2+}]_i$ and translocation of Doc2B and Munc13-1 to the PM (**Figure 1**). In the absence of calcium, the translocation of both proteins was abolished suggesting it is calcium dependent (Figure S1 in Supplementary Material). Munc13-1 translocated to the PM upon elevation in $[Ca^{2+}]_i$, but only when co-expressed with $Doc2B^{wt}$ (**Figures 1** and **2**). When Munc13-1 was expressed in PC12 cells without Doc2B it did not translocate to the PM upon high K^+ stimulation (Figure S2 in Supplementary Material). To establish a more quantitative connection between $Doc2B^{wt}$ translocation and that of Munc13-1^{wt}, we repeated this experimental protocol using TIRF microscopy, focusing on the fluorescence of the cell's lower PM (**Figure 2A**). Co-translocation of Munc13-1^{wt} and $Doc2B^{wt}$ was clearly seen in the TIRF plane (**Figure 2A**). Examining the translocation kinetics revealed that Munc13-1^{wt} translocates to the PM at a slower rate than $Doc2B^{wt}$ (**Figure 2B**; $n = 13$). Moreover, Munc13-1^{wt} translocation, at least in the second and third application, peaked when $Doc2B^{wt}$ was already in its dislocating phase (**Figure 2B**). Munc13-1 dislocation also seemed to occur at a slower rate than that of Doc2B. It is interesting to note that although $Doc2B^{wt}$ fluorescence returned to its initial level after each application, Munc13-1^{wt} started to accumulate at the PM after the first application, though this became more apparent after

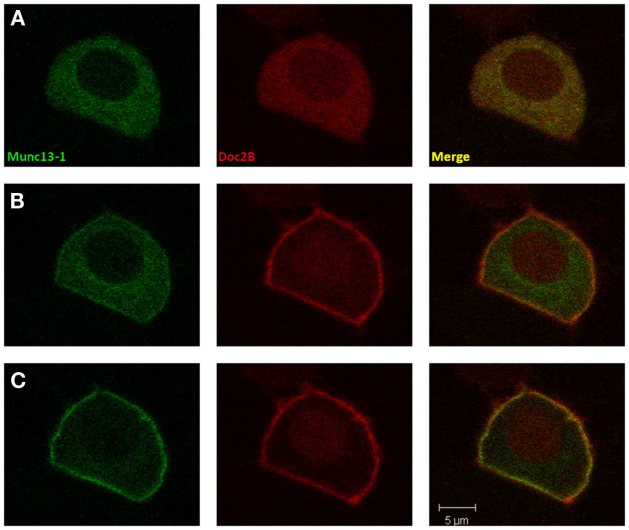

FIGURE 1 | Co-translocation of Doc2B^{wt} and Munc13-1^{wt}. Confocal images of a PC12 cell co-expressing Munc13-1^{wt}-EGFP (left) and Doc2B^{wt}-mRFP (middle). Merged images presented on the right. **(A)** At basal calcium both proteins have a cytoplasmic distribution. **(B)** At the initial phase of the calcium elevation (2–10 s after KCl application), translocation of Doc2B occurs, but Munc13-1 is still mainly cytoplasmic. **(C)** Munc13-1^{wt} translocation is seen only at later stages of the experiment when Doc2B concentration on the membrane is higher (10–20 s after KCl application).

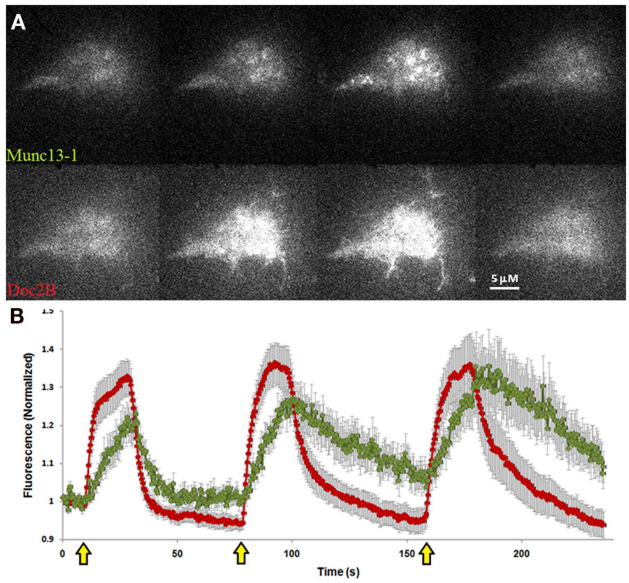

FIGURE 2 | Co-translocation of Doc2B^{wt}–mRFP and Munc13-1^{wt}–EGFP in the TIRF plane. **(A)** TIRF images of a PC12 cell expressing Munc13-1^{wt}–EGFP (upper panel) and Doc2B^{wt}–mRFP (lower panel). From left to right: basal state, beginning of translocation, maximum translocation, and back to basal state. **(B)** Quantification graph of the translocation kinetics observed in the cell's lower PM. Red line indicates Doc2B^{wt}–mRFP, green line indicates Munc13-1^{wt}–EGFP ($n = 13$). Yellow arrows indicate KCl application.

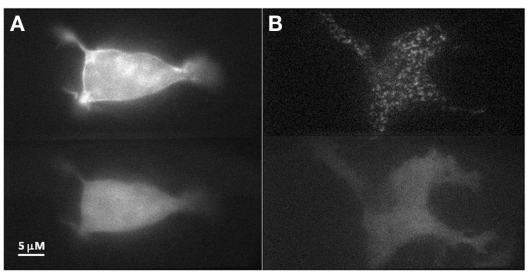

FIGURE 3 | PE stimulation of PC12 cell co-expressing Doc2B^{wt}–mRFP and Munc13-1^{wt}–EGFP. **(A)** Epi-fluorescence images of a PC12 cell co-expressing Munc13-1^{wt}–EGFP (upper panel) and Doc2B^{wt}–mRFP (lower panel) after PE application. Munc13-1^{wt} translocated to the PM while Doc2B^{wt} did not. **(B)** TIRF images of a PC12 cell co-expressing Munc13-1^{wt}–EGFP (upper panel) and Doc2B^{wt}–mRFP (lower panel) after PE application. Munc13-1^{wt} translocated to the PM while Doc2B^{wt} did not. Note the patchy nature of Munc13-1^{wt} 's translocation at the PM.

the second and third application. It is also interesting to note that although the translocation of Munc13^{wt} to the PM appeared rather uniform in the confocal images (**Figure 1**), it showed a patchy appearance in TIRF images (**Figure 2A**). This patchy pattern was not unique to Munc13-1^{wt}'s Doc2B^{wt}-dependent translocation; a similar dotted staining pattern appeared in PE-induced translocation of Munc13-1^{wt} (**Figure 3**). As PE mimics the interaction of Munc13-1 with diacylglycerol (DAG), it is possible that when on the PM, Munc13-1 interacts with DAG.

We have previously shown that a mutated form of Doc2B–Doc2B^{D218,220N} is constitutively associated with the PM. We therefore examined the effect of Doc2B^{D218,220N} on Munc13-1^{wt}'s distribution in the cell. Co-expression of these two proteins resulted in the constant translocation of both Doc2B^{D218,220N} and Munc13-1^{wt} (**Figure 4**). As in **Figure 2**, Munc13-1^{wt} showed a patchy pattern at the PM.

CO-TRANSLOCATION OF Munc13-1 AND Doc2B DEPENDS ON THE Doc2B–Munc13-1 INTERACTION AND ON Munc13-1s C1 DOMAIN

To determine whether the Mid domain of Doc2B is responsible for the co-translocation of Doc2B and Munc13-1, we repeated the translocation experiment with Doc2B harboring a scrambled Mid domain (Doc2B^{Mid}), and examined if this mutation abolishes translocation of Munc13-1^{wt}. Scrambling the Mid domain of Doc2B disrupted the interaction with Munc13-1^{wt} [Figure S3 in Supplementary Material; (12)]. Although the Mid mutation disrupted most of Munc13-1^{wt}'s translocation, some degree of translocation still existed (**Figure 5**). The translocation was barely detected in the first KCl application but in later applications, some Munc13-1 showed translocation and accumulation on the PM. These results suggest that the Mid domain is important for Munc13-1 co-translocation; however, Munc13-1 also accumulates slowly at the PM without the interaction with Doc2B Mid domain, possibly via its C1–DAG interaction.

The C1 domain of Munc13 is important for its membrane-attachment ability via its interaction with DAG (17, 18), and we therefore examined whether the C1 domain is also important for

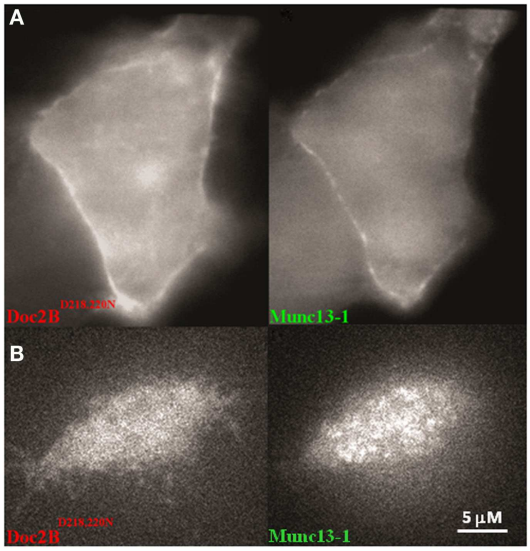

FIGURE 4 | A PC12 cell co-expressing Doc2B^{D218,220N}–mRFP and Munc13-1^{wt}. **(A)** Epi-fluorescence images of a PC12 cell co-expressing Doc2B^{D218,220N}–mRFP (left) and Munc13-1^{wt}–EGFP (right). **(B)** TIRF images of a PC12 cell co-expressing Doc2B^{D218,220N}–mRFP (left) and Munc13-1^{wt}–EGFP (right).

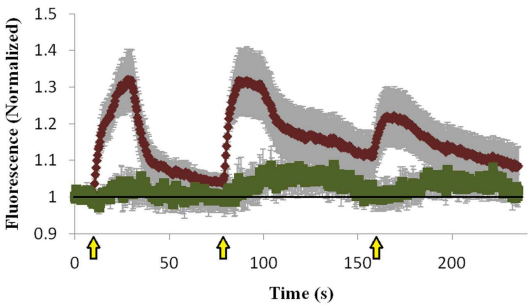

FIGURE 5 | Quantification of co-translocation of Doc2B^{Mid}–mRFP and Munc13-1^{wt}–EGFP. Quantification graph of the TIRF experiment demonstrating translocation of Doc2B^{Mid} and low translocation of Munc13-1^{wt} during the first KCl application ($n = 8$). Munc13-1^{wt} translocation becomes more pronounced at the second and third KCl application but still lower compared to co-expression with Doc2B^{wt}. Black line marks the value of 1 (no translocation). Yellow arrows indicate KCl application.

Doc2B-induced Munc13-1 translocation and accumulation. We used a Munc13-1 mutant that does not bind DAG (Munc13-1^{H567K}) and cannot translocate to the PM upon PE stimulation, and examined whether Doc2B could induce Munc13-1^{H567K} translocation. Munc13-1^{H567K} displayed lower translocation ability than Munc13-1^{wt} (**Figure 6** compared to **Figure 2**) and did not accumulate on the PM like its wild-type counterpart. Thus, it seems that the initial translocation of Munc13-1 depends on interaction with Doc2B and soon after, the C1–DAG interaction determines the accumulation of Munc13-1 at the PM.

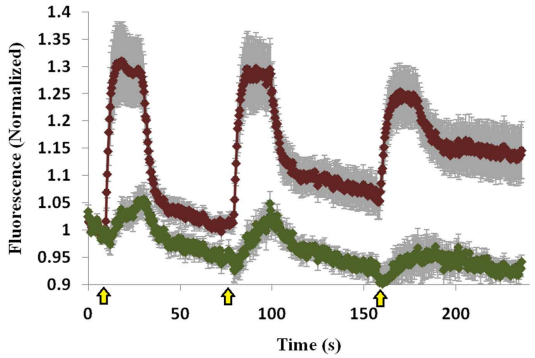

FIGURE 6 | Co-translocation of Doc2B^{wt}–mRFP and Munc13-1^{H567K}–EGFP. Quantification graph of the TIRF experiment demonstrating translocation of Doc2B^{wt} and low translocation of Munc13-1^{H567K} ($n = 14$). No accumulation of Munc13-1^{H567K} is detected. Yellow arrows indicate KCl application.

DISCUSSION

Munc13-1 is a key player in the synapse; the activity of this multidomain protein is tightly regulated by many factors, including calmodulin (5, 19, 20), DAG (18, 21), and Ca^{2+} in a PIP_2 dependent manner (7). We show here that Doc2B recruits Munc13-1 to the PM in a Ca^{2+}-dependent manner, thereby suggesting another possible Munc13-1-regulatory mechanism.

The Doc2 family of proteins interacts with the Munc13 family of proteins primarily via the Mid domain, located within the N-terminal domain of Doc2 (3, 12, 14, 15, 22). Doc2 translocates to the PM upon elevation of $[Ca^{2+}]_i$. Munc13-1, on the other hand, does not translocate to the PM upon calcium elevation. However, when co-expressed with Doc2B, Munc13-1 co-translocates to the PM following Doc2B. This translocation could not be detected with endogenous Doc2B and Munc13-1 as these proteins are expressed in low levels in neuroendocrine cells (10, 16, 19) and such translocation, if occurs might be undetectable under these conditions. Munc13-1's translocation is most likely mediated through the Mid domain as reflected by its reduction upon mutation in the Mid domain. When the elevation of calcium is brief, Munc13-1 translocation is reversible, dislocating back to the cytosol after Doc2B dislocation. However, following repeated stimulations, Munc13-1 starts to accumulate at the PM even after Doc2B has dislocated back to the cytosol. This accumulation was abolished when a Munc13-1 mutant that does not bind DAG (Munc13-1^{H567K}) was co-expressed with Doc2B suggesting that the C1–DAG interaction determines Munc13-1's accumulation at the PM. It is possible that during high-frequency activity, e.g., sustained or intermittent depolarization, the level of DAG increases (23). This would cause a more stable interaction of Munc13-1 with the PM via its C1 domain, anchoring it to the PM, and enabling its catalytic activity in the fusion step (2). Thus, according to this working model, the activity of Munc13-1 at the PM depends on the stimulation's frequency and on Doc2B translocation, becoming more prominent during periods of high activity. Doc2B has been recently shown to enhance neuronal network activity by specifically increasing the firing rate within a neuronal

burst (24). Therefore, it is possible that in addition to the direct effect of Doc2B on asynchronous release, it also recruits Munc13-1 during periods of intense activity, which might also contribute to the enhanced network activity. A similar mode of action has been suggested for protein kinase C (PKC) activity (25). Many receptor stimuli induce calcium signals prior to a more persistent increase in DAG concentration. These calcium signals have only a minimal effect on conventional PKC activity in the absence of DAG. However, in the presence of DAG, each calcium spike induces a more pronounced activation cycle of conventional PKC.

Our data suggest that the interaction between Doc2B and Munc13-1 depends on more than just the Mid domain of Doc2B since a small degree of translocation was still observed when Munc13-1 was co-expressed with $Doc2B^{Mid}$. We hypothesize that this interaction is also dependent on the C1 domain of Munc13-1 as it has been reported that deleting this domain increases Munc13-1's interaction with Doc2B (3). It is also possible that the C2B of Doc2B contributes to this interaction, as has been recently suggested for Doc2A and Munc13-4 (15).

A previous study described co-translocation of $Doc2B^{wt}$ and $Munc13\text{-}1^{wt}$ upon PE stimulation (14). Such translocation was not observed here, either in the epi-fluorescence or TIRF imaging. Hence, the interaction of Munc13-1's C1 domain with DAG at the PM may compete with Doc2B binding to Munc13-1. Therefore, stimulating the cells with PE caused Munc13-1's translocation but interfered with Doc2B translocation. These findings, together with the observation that Munc13-1 reaches maximal translocation when Doc2B is already dislocating from the PM due to a decrease in $[Ca^{2+}]_i$, suggest that the interaction of Munc13-1 with DAG at the PM cannot occur when it is in a complex with Doc2B. Therefore, DAG binding to Munc13-1 might disrupt Doc2B binding. These findings suggest that Doc2B recruits Munc13-1 to the PM but once there, Munc13-1 associates through its C1 domain with DAG and this reduces its interaction with Doc2B. Further experiments will be needed to validate this hypothesis.

Co-expression of $Doc2B^{D218,220N}$ with $Munc13\text{-}1^{wt}$ revealed that the two proteins are being constantly translocated to the PM, yet the $Doc2B^{D218,220N}$ mutant could not support refilling during repeated stimulations (10). Combining these two observations suggests a possible physiological effect of the Doc2B–Munc13-1 interaction: this complex needs to undergo an on–off cycle from the PM to achieve a full priming effect. Another possible explanation is that Munc13-1 needs to detach from Doc2B at the PM to enable its priming effect. Taken together, our data support the hypothesis that Doc2B serves as a calcium-dependent recruitment factor for Munc13-1 whereas at the PM, Munc13-1 interacts with DAG. This provides an activity-dependent recruitment mechanism for two major synaptic proteins, Doc2B and Munc13-1.

ACKNOWLEDGMENTS

We would like to thank Mrs. Lirin Michaeli for comments and assistance on the manuscript and Prof. Alexander J. Groffen for providing DNA constructs. This work was supported in part by the Israel Science Foundation (Grant no. 1211/07 and 730/11; Uri Ashery), the BSF (Grant no. 2009279; Uri Ashery) and the German-Israeli Foundation (GIF) (Grant no. 1125-145.1/2010; Uri Ashery).

SUPPLEMENTARY MATERIAL

The Supplementary Material for this article can be found online at: http://www.frontiersin.org/Neuroendocrine_Science/10.3389/fendo.2013.00119/abstract

Figure S1 | $Doc2B^{wt}$ and $Munc13\text{-}1^{wt}$ do not translocate to the PM in the absence of calcium. Epi-fluorescence images of a PC12 cell co-expressing $Doc2B^{wt}$-mRFP (left) and $Munc13\text{-}1^{wt}$-EGFP (center). Merged images presented on the right. In the upper panel, the cell in its basal state. In the lower panel, the cell after application of depolarizing high K^+ solution without calcium (containing 0.1 mM EGTA). Note there is no evident change in the proteins distribution in the cell.

Figure S2 | $Munc13\text{-}1^{wt}$ does not translocate to the PM in the absence of Doc2B. Epi-fluorescence images of a PC12 cell expressing $Munc13\text{-}1^{wt}$–EGFP, before (left) and after (right) application of depolarizing high K^+ solution. Note there is no evident change in the protein's distribution in the cell.

Figure S3 | GST pull-down assay of Doc2B N-terminal with Munc13-1. GST fusion of the N-terminal of $Doc2B^{wt}$ and N-terminal of $Doc2B^{Mid}$ binding to $Munc13\text{-}1^{wt}$ (Upper panel) and $Munc13\text{-}1^{H567K}$ (lower panel). $Munc13\text{-}1^{wt}$ and $Munc13\text{-}1^{H567K}$ show binding only to N-terminal of $Doc2B^{wt}$ and not to N-terminal of $Doc2B^{Mid}$.

REFERENCES

1. Stevens DR, Wu Z, Matti U, Junge HJ, Schirra C, Becherer U, et al. Identification of the minimal protein domain required for priming activity of Munc13-1. *Curr Biol* (2005) **15**:2243–8. doi:10.1016/j.cub.2005.10.055
2. Basu J, Betz A, Brose N, Rosenmund C. Munc13-1 C1 domain activation lowers the energy barrier for synaptic vesicle fusion. *J Neurosci* (2007) **27**:1200–10. doi:10.1523/JNEUROSCI.4908-06.2007
3. Orita S, Naito A, Sakaguchi G, Maeda M, Igarashi H, Sasaki T, et al. Physical and functional interactions of Doc2 and Munc13 in Ca^{2+}-dependent exocytotic machinery. *J Biol Chem* (1997) **272**:16081–4. doi:10.1074/jbc.272.26.16081
4. Betz A, Thakur P, Junge HJ, Ashery U, Rhee JS, Scheuss V, et al. Functional interaction of the active zone proteins Munc13-1 and RIM1 in synaptic vesicle priming. *Neuron* (2001) **30**:183–96. doi:10.1016/S0896-6273(01)00272-0
5. Junge HJ, Rhee JS, Jahn O, Varoqueaux F, Spiess J, Waxham MN, et al. Calmodulin and Munc13 form a Ca^{2+} sensor/effector complex that controls short-term synaptic plasticity. *Cell* (2004) **118**:389–401. doi:10.1016/j.cell.2004.06.029
6. Lu J, Machius M, Dulubova I, Dai H, Südhof TC, Tomchick DR, et al. Structural basis for a Munc13-1 homodimer to Munc13-1/RIM heterodimer switch. *PLoS Biol* (2006) **4**:e192. doi:10.1371/journal.pbio.0040192
7. Shin O, Lu J, Rhee J, Tomchick DR, Pang ZP, Wojcik SM, et al. Munc13 C2B domain is an activity-dependent Ca^{2+} regulator of synaptic exocytosis. *Nat Struct Mol Biol* (2010) **17**:280–8. doi:10.1038/nsmb.1758
8. Deng L, Kaeser PS, Xu W, Südhof TC. RIM proteins activate vesicle priming by reversing autoinhibitory homodimerization of Munc13. *Neuron* (2011) **69**:317–31. doi:10.1016/j.neuron.2011.01.005
9. Groffen A, Friedrich R, Brian E, Ashery U, Verhage M. Doc2A and Doc2B are sensors for neuronal activity with unique calcium-dependent and kinetic properties. *J Neurochem* (2006) **97**:818–33. doi:10.1111/j.1471-4159.2006.03755.x
10. Friedrich R, Groffen A, Connell E, van Weering J, Gutman O, Henis Y, et al. Doc2B acts as a calcium switch and enhances vesicle fusion. *J Neurosci* (2008) **28**:6794–806. doi:10.1523/JNEUROSCI.0538-08.2008
11. Sato M, Mori Y, Matsui T, Aoki R, Oya M, Yanagihara Y, et al. Role of the polybasic sequence in the Doc2alpha C2B domain in dense-core vesicle exocytosis in PC12 cells. *J Neurochem* (2010) **114**:171–81. doi:10.1111/j.1471-4159.2010.06739.x

12. Mochida S, Orita S, Sakaguchi G, Sasaki T, Takai Y. Role of the Doc2 alpha-Munc13-1 interaction in the neurotransmitter release process. *Proc Natl Acad Sci U S A* (1998) **95**:11418–22. doi:10.1073/pnas.95.19.11418
13. Hori T, Takai Y, Takahashi T. Presynaptic mechanism for phorbol ester-induced synaptic potentiation. *J Neurosci* (1999) **19**:7262–7.
14. Duncan R, Betz A, Shipston M, Brose N, Chow R. Transient, phorbol ester-induced Doc2-Munc13 interactions in vivo. *J Biol Chem* (1999) **274**:27347–50. doi:10.1074/jbc.274.39.27347
15. Higashio H, Nishimura N, Ishizaki H, Miyoshi J, Orita S, Sakane A, et al. Doc2 alpha and Munc13-4 regulate $Ca^{(2+)}$-dependent secretory lysosome exocytosis in mast cells. *J Immunol* (2008) **180**:4774–84.
16. Ashery U, Varoqueaux F, Voets T, Betz A, Thakur P, Koch H, et al. Munc13-1 acts as a priming factor for large dense-core vesicles in bovine chromaffin cells. *EMBO J* (2000) **19**:3586–96. doi:10.1093/emboj/19.14.3586
17. Betz A, Ashery U, Rickmann M, Augustin I, Neher E, Südhof TC, et al. Munc13-1 is a presynaptic phorbol ester receptor that enhances neurotransmitter release. *Neuron* (1998) **21**:123–36. doi:10.1016/S0896-6273(00)80520-6
18. Rhee J, Betz A, Pyott S, Reim K, Varoqueaux F, Augustin I, et al. Beta phorbol ester- and diacylglycerol-induced augmentation of transmitter release is mediated by Munc13s and not by PKCs. *Cell* (2002) **108**:121–33. doi:10.1016/S0092-8674(01)00635-3
19. Zikich D, Mezer A, Varoqueaux F, Sheinin A, Junge H, Nachliel E, et al. Vesicle priming and recruitment by ubMunc13-2 are differentially regulated by calcium and calmodulin. *J Neurosci* (2008) **28**:1949–60. doi:10.1523/JNEUROSCI.5096-07.2008
20. Rodríguez-Castañeda F, Maestre-Martínez M, Coudevylle N, Dimova K, Junge H, Lipstein N, et al. Modular architecture of Munc13/calmodulin complexes: dual regulation by Ca^{2+} and possible function in short-term synaptic plasticity. *EMBO J* (2010) **29**:680–91. doi:10.1038/emboj.2009.373
21. Lou X, Korogod N, Brose N, Schneggenburger R. Phorbol esters modulate spontaneous and Ca2+-evoked transmitter release via acting on both Munc13 and protein kinase C. *J Neurosci* (2008) **28**:8257–67. doi:10.1523/JNEUROSCI.0550-08.2008
22. Abdullah LH, Bundy JT, Ehre C, Davis CW. Mucin secretion and PKC isoforms in SPOC1 goblet cells: differential activation by purinergic agonist and PMA. *Am J Physiol Lung Cell Mol Physiol* (2003) **285**:L149–60.
23. Wakade T, Bhave S, Bhave A, Malhotra R, Wakade A. Depolarizing stimuli and neurotransmitters utilize separate pathways to activate protein kinase C in sympathetic neurons. *J Biol Chem* (1991) **266**:6424–8.
24. Lavi A, Sheinin A, Shapira R, Zelmanoff D, Ashery U. Doc2B and Munc13-1 differentially regulate neuronal network activity. *Cereb Cortex* (2013) [Epub ahead of print]. doi:10.1093/cercor/bht081
25. Oancea E, Meyer T. Protein kinase C as a molecular machine for decoding calcium and diacylglycerol signals. *Cell* (1998) **95**:307–18. doi:10.1016/S0092-8674(00)81763-8

Conflict of Interest Statement: The authors declare that the research was conducted in the absence of any commercial or financial relationships that could be construed as a potential conflict of interest.

Received: 15 June 2013; accepted: 27 August 2013; published online: 17 September 2013.
*Citation: Friedrich R, Gottfried I and Ashery U (2013) Munc13-1 translocates to the plasma membrane in a Doc2B- and calcium-dependent manner. Front. Endocrinol. **4**:119. doi: 10.3389/fendo.2013.00119*
This article was submitted to Neuroendocrine Science, a section of the journal Frontiers in Endocrinology.

frontiers in
ENDOCRINOLOGY

REVIEW ARTICLE
published: 04 December 2013
doi: 10.3389/fendo.2013.00187

CAPS and Munc13: CATCHRs that SNARE vesicles

Declan J. James [†] ***and Thomas F. J. Martin*** [*†]

Department of Biochemistry, University of Wisconsin, Madison, WI, USA

Edited by:
Stephane Gasman, Centre national de la recherche scientifique, France

Reviewed by:
Thomas Söllner, University of Heidelberg, Germany
Jingshi Shen, University of Colorado Boulder, USA

***Correspondence:**
Thomas F. J. Martin, Department of Biochemistry, University of Wisconsin, 433 Babcock Drive, Madison, WI 53706, USA
e-mail: tfmartin@wisc.edu

[†] *Declan J. James and Thomas F. J. Martin have contributed equally to this work.*

CAPS (Calcium-dependent Activator Protein for Secretion, aka CADPS) and Munc13 (Mammalian Unc-13) proteins function to prime vesicles for Ca^{2+}-triggered exocytosis in neurons and neuroendocrine cells. CAPS and Munc13 proteins contain conserved C-terminal domains that promote the assembly of SNARE complexes for vesicle priming. Similarities of the C-terminal domains of CAPS/Munc13 proteins with Complex Associated with Tethering Containing Helical Rods domains in multi-subunit tethering complexes (MTCs) have been reported. MTCs coordinate multiple interactions for SNARE complex assembly at constitutive membrane fusion steps. We review aspects of these diverse tethering and priming factors to identify common operating principles.

Keywords: CAPS (aka CADPS), Munc13, priming factors, vesicle fusion, SNAREs, multi-subunit tethering complexes

TRAFFICKING IN THE SECRETORY AND ENDOSOMAL PATHWAYS

The transport of proteins and membranes in the secretory pathway is vectorial with vesicle formation in a donor compartment coupled to vesicle transport and subsequent fusion in an acceptor compartment. Vesicle delivery to an acceptor membrane involves several layers of interaction that confer targeting specificity involving tethering, docking, and priming of vesicles. These lead to SNARE pairing that mediates fusion of the vesicle with the acceptor membrane. In exocytic vesicle fusion with the plasma membrane, as well as for intracellular membrane fusion events, a diverse set of accessory (tethering and priming) factors are required to prime vesicles for fusion. Accessory factors commonly interact with vesicle and target membrane constituents that are characteristic of a membrane compartment such as Rab proteins (1, 2) and phosphoinositides (3, 4). Accessory factors also interact with SNARE proteins to promote SNARE protein complex assembly usually in association with proteins of the Sec1/Munc18 (SM) family. Accessory factors for constitutive trafficking include the tethering factor complexes Dsl1 for Golgi to ER transport, HOPS for late endosome fusion, and exocyst for exocytic fusion. Accessory factors for regulated vesicle exocytosis include the priming factors CAPS and Munc13. These exhibit sequence and structural similarity with tethering factor subunits (e.g., exocyst Sec6) (5, 6), which suggests there may be common features for these diverse accessory factors. We review aspects of tethering and priming factor function at several trafficking stations attempting to identify common operating principles.

SNARE PROTEINS IN MEMBRANE FUSION

Biochemical reconstitution studies of membrane trafficking in the Golgi led to the discovery of SNARE (soluble *N*-ethylmaleimide sensitive factor attachment protein receptor) proteins as the general machinery for membrane fusion (7). The initial identification of neuronal syntaxin-1, SNAP-25, and VAMP2 (aka synaptobrevin2) as SNARE proteins in brain membrane extracts prompted advances for understanding Ca^{2+}-triggered vesicle fusion events for neurotransmitter and peptide secretion (8, 9). An essential role for neuronal SNAREs in regulated vesicle exocytosis was indicated by finding them to be the substrates for the *Clostridial* zinc endopeptidase toxins (10–14). The further characterization of proteins in the SNARE protein superfamily generally facilitated research on membrane trafficking throughout the secretory and endosomal pathways (15). Much current research in membrane fusion is focused on understanding how accessory factors prime vesicles for fusion by regulating SNARE complex assembly.

SNARE proteins, usually C-terminal tail-anchored membrane proteins with membrane-proximal helical SNARE motifs, are grouped into syntaxin, SNAP-25, and VAMP families based on sequence relatedness, and referred to as "Q" or "R" SNAREs based on highly conserved glutamine or arginine residues in the zero layer of the SNARE motif (e.g., syntaxin-1 as Qa-, SNAP-25 as Qbc-, VAMP2 as R-SNARE) (16). The reconstitution of SNARE proteins into liposomes demonstrated that SNAREs are sufficient for mediating membrane fusion (17). Although the details of how SNARE proteins fuse membranes is emerging, structural, and biochemical analyses indicate that SNARE proteins present on two apposed membranes form a trans-SNARE complex to pin membranes close together (18, 19). Membrane fusion ensues when trans-SNARE complexes zipper-up through coiled-coil interactions in helical SNARE motifs (16, 20). The formation of a tight coiled-coil bundle, characteristically containing 3Q (Qa, Qb and Qc, or Qa and Qbc) and 1R SNARE motifs, is coupled to membrane fusion events throughout the secretory pathway (21). For regulated vesicle exocytosis, SNARE complex assembly is thought to proceed by a two-stage process with the initial formation of heterodimeric QaQbc complexes of plasma membrane syntaxin-1 with SNAP-25 followed by the insertion of the vesicle R-SNARE

VAMP2 to form heterotrimeric (RQaQbc) SNARE complexes (8). Alternative assembly pathways have been suggested (22–25).

At least 44 SNARE protein isoforms in vertebrate cells are distributed throughout membrane trafficking pathways (15). It was proposed that unique cognate SNARE pairing contributes to specificity for vesicle targeting to acceptor membranes (26, 27). However, it has been noted that SNARE pairing can be promiscuous and may not be the sole determinant of vesicle targeting specificity (28, 29). Targeting specificity is likely combinatorial consisting of multiple levels of interaction requiring accessory factors that are recruited to membranes by interactions with Rabs, phosphoinositides, and SNAREs (26). Accessory factors acting with SM proteins promote stages of SNARE complex assembly and enable specific SNARE pairing for fusion. For example, recent studies revealed differential effects of the SM proteins Munc18-1 and Munc18c for enabling fusion on cognate but not on non-cognate SNARE proteins (30, 31).

SM PROTEINS IN MEMBRANE FUSION

The SM (Sec1/Munc18) protein family consists of soluble proteins that are required for membrane trafficking (32–34). SM proteins are grouped into four highly conserved subfamilies across eukaryotes. In spite of their sequence homology, SM proteins encode a high degree of specificity for SNARE protein interactions. A common theme is SM protein-directed interaction with Q-SNAREs at exocytic (Munc18/Sec1), ER-Golgi (Sly1), endosomal-lysosomal (Vps33), and endosomal (Vps45) membrane trafficking stations (32, 35–38). The mode of Q-SNARE-binding by different SM proteins appears to differ but the SM proteins may generally function in stabilizing SNARE protein complexes (39). Studies on the interaction of the neuronal SM protein Munc18-1 with the Qa-SNARE syntaxin-1 have played a prominent role in understanding SM protein function even though Munc18-1 has unique features that distinguish it from other SM proteins (32). Munc18-1 chaperones syntaxin-1 to the plasma membrane (32, 39). At the plasma membrane, Munc18-1 stabilizes a closed form of syntaxin-1, which is unable to form heterodimeric complexes with the Qbc-SNARE SNAP-25 (40). The closed configuration of syntaxin-1 may prevent unwanted interactions with SNARE proteins as the complex traffics to the plasma membrane (41). Eliminating Munc18-1 reduces syntaxin-1 delivery to the plasma membrane, abrogates dense-core vesicle (DCV) docking, and abolishes triggered exocytosis (42).

Recent findings that Munc18-1 accelerates SNARE-catalyzed liposome fusion help to reconcile the role of Munc18-1 as a chaperone with its essential role in regulated exocytosis (30). Munc18-1 stimulates trans-SNARE complex formation and membrane fusion but does so by switching from an inhibitory to a stimulatory mode. The switch from an inhibitory to a stimulatory mode in liposome fusion for Munc18-1 requires pre-incubation with both R- and Q- SNARE proteins (VAMP2 and syntaxin-1/SNAP-25) (43), which suggests that Munc18-1 utilizes specific interaction sites on the SNARE proteins. Recent studies have identified some of these sites on VAMP2 (C-terminal) and syntaxin-1 (N- and C-terminal) (30, 31). Interestingly, Munc18c appeared to operate differently on its cognate SNAREs lacking an inhibitory mode on syntaxin-4. In addition, recognition sites on shared cognate VAMP2 differed with C-terminal sites for Munc18-1 and N-terminal sites for Munc18c (30, 31). While both Munc18-1 and Munc18c promote the assembly of cognate SNARE protein complexes, they appear to do so by distinct sets of interactions that play a role in establishing specific SNARE protein pairing.

Tethering and priming factors act with SM proteins to promote SNARE complex assembly. Munc13-1 is proposed to enhance the switching of Munc18-1 from an inhibitory to stimulatory mode for regulated vesicle exocytosis (44) as discussed below. At other fusion events, cognate SM proteins also function in concert with accessory factors. In vacuolar fusion, the SM protein Vps33 operates as a subunit of a HOPS (homotypic fusion and vacuole protein sorting) complex, a multi-subunit tethering complex that promotes trans-SNARE complex assembly (45). At other trafficking stations where SM proteins are not formally part of complexes, it is likely that tethering and priming factors cooperate with SM proteins in the assembly of SNARE complexes as noted below.

TETHERING FACTORS INTEGRATE SNARE PROTEIN FUNCTION FOR CONSTITUTIVE FUSION

Tethering is considered to be a long-range interaction of a vesicle near a target membrane independent of cytoskeletal anchoring. Tethering factors may also operate to bring vesicles into closer proximity for trans-SNARE complex assembly (docking). Tethering factors have been classified as either long coiled-coil proteins or multi-subunit tethering complexes (MTCs). Several MTCs that function at distinct membrane trafficking steps have been identified (46) where they function as important interfaces between Rabs, phosphoinositides, and SNARE proteins (47). Tethering factors are very diverse but sequence comparisons indicate a subtle relatedness among subunits of a subset of MTCs in predicted coiled coils (48). Structural analysis of several MTC subunits from COG, Dsl, exocyst, and GARP complexes indicate a homologous tertiary structure composed of an extended rod-like domain made up of helical bundles (49, 50). MTCs with this structural signature were termed members of a Complex Associated with Tethering Containing Helical Rods (CATCHR) family (50). The CATCHR homology is not restricted to MTC subunits and is found in Myo2p (Myosin V) and in CAPS and Munc13 proteins (see below) (5). In the following, we discuss a well-studied MTC (HOPS) whose subunits lacks CATCHR homology followed by two other well-studied MTCs (exocyst and Dsl1p) that contain subunits with CATCHR homology.

The HOPS complex is an MTC of ∼663 kDa comprised of six subunits Vps41, Vps11, Vps18, Vps16, Vps33, and Vps39 (**Figure 1**, upper) (45). Conserved across eukaryotes, HOPS was initially identified for its role in yeast vacuole fusion, which is a correlate of endo-lysosomal fusion in vertebrate cells (48). The HOPS complex interacts with lipids, Rabs, and SNARE proteins (45). As a complex, HOPS mediates vesicle tethering as well as membrane fusion (51). Ultra-structural analysis of purified HOPS by EM-reconstruction techniques revealed that the holo-complex is a 30 nm long molecular monolith (52, 53). A combination of biochemical and structural reconstruction indicated that its Rab-interacting subunits Vps41 and Vps39 are positioned at either end of the complex (53). This arrangement of Rab-binding domains may mediate HOPS-dependent vesicle tethering. The SM protein Vps33 and nearby Rab-binding Vps39 are juxtaposed toward the

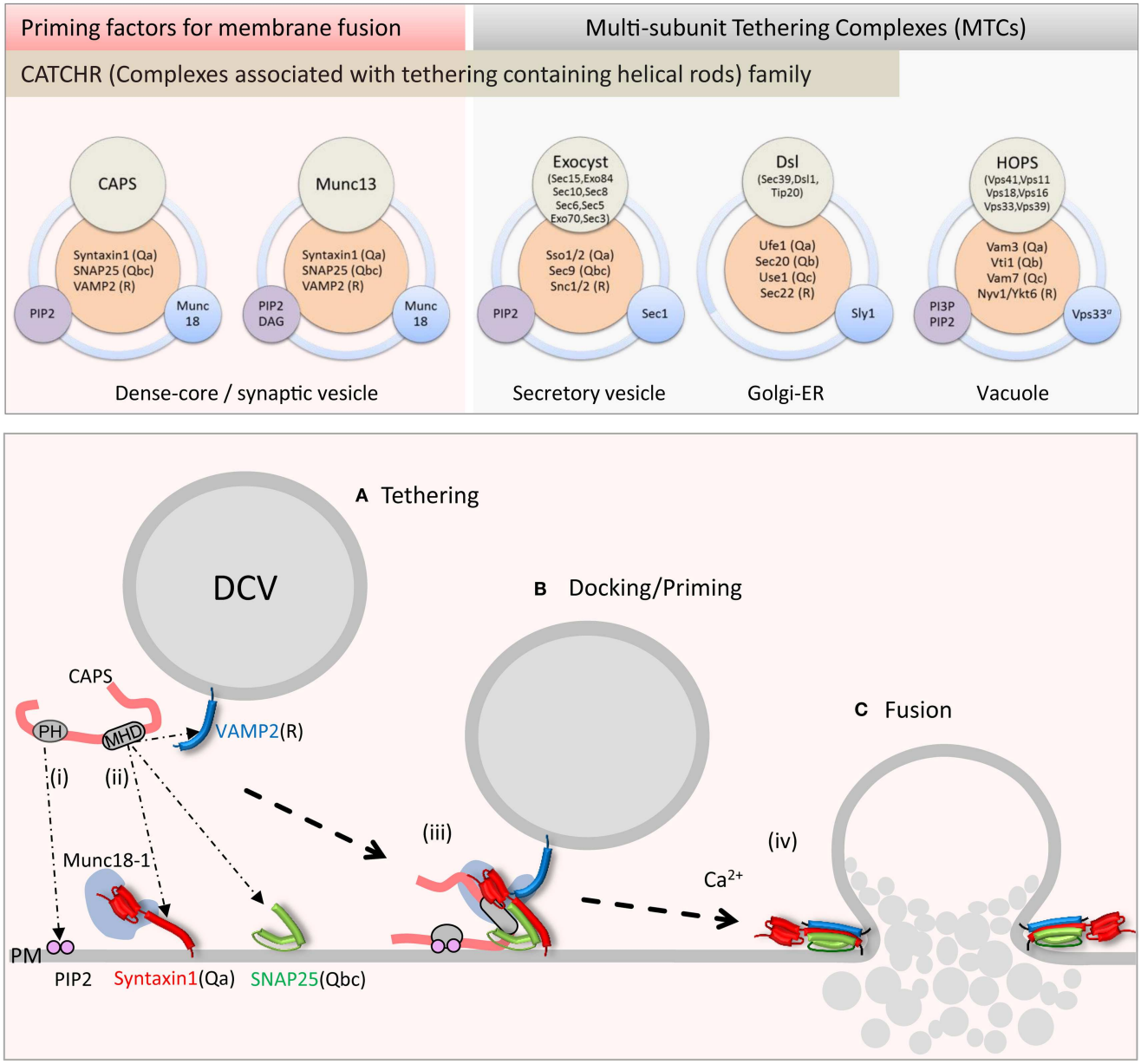

FIGURE 1 | Upper panel: schematic of priming factor (CAPS, Munc13) and tethering complex (exocyst, Dsl1, HOPS) composition and interactions. Multi-domain CAPS and Munc13 proteins interact with neuronal SNAREs and PIP_2 and co-function with the SM Munc18-1. The exocyst complex with eight subunits interacts with cognate SNAREs, PIP_2, and the SM Sec1. The Dsl1 complex with three subunits interacts with cognate SNAREs and co-functions with the SM protein Sly1. The HOPS complex with six subunits interacts with cognate SNAREs, PI3P, and PIP_2, and contains the SM protein Vps33. Lower panel: schematic of CAPS function in vesicle priming depicting **(i)** PH domain binding to PIP_2 and **(ii)** MHD1-mediated SNARE binding. Simultaneous binding of vesicle and plasma membrane constituents by CAPS might tether vesicles **(A)** in proximity to the SNARE proteins. These interactions could lead to **(iii)** syntaxin-1/SNAP-25 heterodimer formation followed by VAMP2 insertion to form trans-SNARE complexes in priming **(B)**. **(iv)** Full SNARE complex zippering in response to elevations of intracellular calcium mediated by synaptotagmin and complexin triggers vesicle fusion **(C)** and contents release into the extracellular space.

membrane where HOPS may couple vesicle tethering with SNARE complex assembly. The monolith-like HOPS would stand like Stonehenge coordinating vacuole–vacuole fusion sites arranged around a vertex ring (45). Fusion between large organelles such as vacuoles likely requires solid tethering foundations provided by the HOPS complex for coordinating large surface area membrane fusion events. HOPS also requires the phosphoinositides PI3P and $PI(4,5)P_2$ to coordinate its function (45). Overall, HOPS promotes the formation of a 3Q:1R trans-SNARE complex consisting of Vam3(Qa), Vti1(Qb), Vam7(Qc), and Nyv1(R) (54). Besides the

requirement of the SM protein subunit Vps33 in SNARE complex formation, Vps16 and Vps18 interact with the soluble Qc-SNARE Vam7 and mediate a rate-limiting step for Qc-SNARE entry into a fusion-competent SNARE complex (55). The SM protein subunit Vps33 also interacts with the SNARE-binding Vps16 subunit (56), which may together with Vps18 form a SNARE-binding interface for the HOPS complex. The HOPS complex lacks the CATCHR domain homology but is an example of an MTC that integrates Rab, phosphoinositide, and SNARE interactions for tethering and compartment-specific SNARE complex assembly.

The exocyst complex, originally discovered in yeast, is a conserved multi-subunit complex ∼750 kDa composed of eight subunits Sec3, Sec5, Sec6, Sec8, Sec10, Sec15, Exo70, and Exo84 (**Figure 1**, upper) (57). Exocyst functions in polarized constitutive exocytosis in budding yeast, plants, and vertebrate cells, and is thought to tether vesicles to exocytic sites at the plasma membrane. Ablation of exocyst components in yeast results in the mis-localization of the complex and an accumulation of vesicles within the cell interior. At the plasma membrane, the exocyst is an octomeric holo-complex but the exact pathway for assembly of the complex is under active study. Studies in yeast suggest that vesicle tethering is achieved by complex assembly initiated between vesicle-bound Sec4 (Rab)-Sec15 and plasma membrane-targeted Exo70 and Sec3 subunits (58). The fully assembled exocyst complex localizes to growth cones in neurons where it plays an important role in membrane addition (59). The plasma membrane recruitment of exocyst is mediated through interactions of exocyst subunits Exo70 and Sec3 with GTPases (Rho and cdc42 family) and the phosphoinositide lipid $PI(4,5)P_2$ (60, 61).

Structural studies indicate that Sec6, Sec15, Exo70, and Exo84 subunits contain homologous CATCHR domains. These CATCHR domains mediate inter-subunit interactions to provide an elongated structure for tethering as well as interactions with other proteins (GTPases) (62). Besides a role in tethering, exocyst subunits interact with SNARE and SM proteins to control SNARE complex assembly (57). The exocyst subunit Sec6, as a dimer, interacts with the Qbc-SNARE Sec9 and inhibits the formation of Qabc acceptor SNARE complexes (63). In addition, Sec6 interacts with the SM protein Sec1 when it is part of the exocyst complex mediated by N-terminal sites in Sec6, which functionally overlap with Sec9 binding sites (64). Truncation of these N-terminal sites in Sec6 (the CATCHR domain is C-terminal) inhibits dimerization as well as Sec9 and Sec1 binding. In contrast, mutations in the Sec6 CATCHR domain disrupt exocytosis and polarized localization of exocyst but not exocyst complex formation or Sec6-Sec9 interactions (64). It is not known whether these Sec6 CATCHR domain mutations impair exocyst-Sec1 interactions. Nevertheless, it appears that Sec6 mediates interactions that anchor the exocyst to sites of polarized exocytosis (65). One speculation is that Sec6-Sec9 interactions may help stage the assembly of a Qabc-SNARE complex concomitant with arrival of the vesicle containing other exocyst components to promote trans-SNARE complex formation mediated by exocyst-Sec1 interactions. Notably the formation of a Q-SNARE complex by exocyst is similar to the HOPS recruitment of Vam7. In summary, the exocyst complex tethers through vesicle Rab (Sec4) and plasma membrane phosphoinositide and GTPase interactions, and associates with the SM protein Sec1 and SNAREs to promote or stabilize SNARE complex assembly.

The Dsl1 complex is the smallest of the MTCs at ∼250 kDa and is composed of three subunits Dsl1, Tip20, and Sec39 (**Figure 1**, upper) (66, 67). As an essential protein complex in yeast, it is required for the fusion of Golgi-derived vesicles with the ER. Two of the three subunits have homologs in humans that are involved in retrograde trafficking pathways between the Golgi and ER (48). Structural studies of the yeast Dsl1 complex indicate that Sec39 and Tip20 subunits are bridged by Dsl1 through interactions of the CATCHR domain of Dsl1 with that of Tip20 to assemble a 20 nm structure (68). The Dsl1 subunit interacts with the COP1 coat complex and may serve as a direct link securing incoming Golgi-derived COP1 vesicles at the ER membrane (69). The Dsl1 complex interacts with ER resident SNAREs Ufe1(Qa), Sec20(Qb), and Use1(Qc) to stabilize a Qabc-SNARE complex (66, 70) in conjunction with the SM protein Sly1 (71). Interestingly, interactions with the Qb-SNARE Sec20 appear to be mediated by the CATCHR domain of the Tip20 subunit (68). The recruitment of the Qc-SNARE Use1 into SNARE complexes depends on Sec39 and Dsl1 subunits interacting with Tip20 (66). Sly1 interactions with Ufe1 and SNARE complexes are part of a larger complex that includes Dsl1 representing a complex that coordinates Golgi to ER retrograde traffic (38, 71). Overall, the Dsl1 complex links vesicle tethering to SNARE complex assembly and fusion at sites in the ER.

Tethering factors are essential coordinators linking vesicle arrival with SNARE complex assembly. Individual MTC subunits mediate a number of protein and phospholipid interactions. CATCHR domains in MTC subunits that possess them appear to generally mediate interactions with other subunits or with other proteins including SNAREs. One common theme illustrated by tethering factors at several vesicle trafficking stations is the on-demand assembly of Q-SNARE complexes with vesicle arrival. Recent studies (29) suggested that Qc-SNAREs are a particularly important determinant for selectivity in SNARE pairing for fusion. Thus, it is notable that an interaction specific for the Qc-SNARE is found for HOPS (55), and that exocyst and Dsl1 complexes bind Sec9 Qbc- or Use1p Qc- SNAREs, respectively. Overall this suggests an important role for tethering factors in promoting the entry of Qc-SNAREs into SNARE complexes to enable appropriately paired, compartment-specific fusion.

PRIMING FACTORS INTEGRATE SNARE PROTEIN FUNCTION FOR REGULATED FUSION

The release of neurotransmitters from synaptic vesicles (SVs) at the neuronal synapse or peptides from DCVs of neuroendocrine cells occurs by regulated exocytosis. Pools of SVs and DCVs are stored near the plasma membrane in various states prior to fusion (72). Traditionally, vesicles are viewed as progressing through states of tethering, docking, and priming prior to Ca^{2+}-triggered fusion (73). Recent high-pressure freeze EM (74) and fluorescence microscopy mobility studies of vesicles (75) indicate that docking and priming may be closely linked steps. Physiological and genetic studies suggest that SNARE complex assembly occurs during priming (76, 77). SV exocytosis is strongly inhibited in mice lacking Munc13-1 (78, 79) and CAPS (80). DCV exocytosis is also

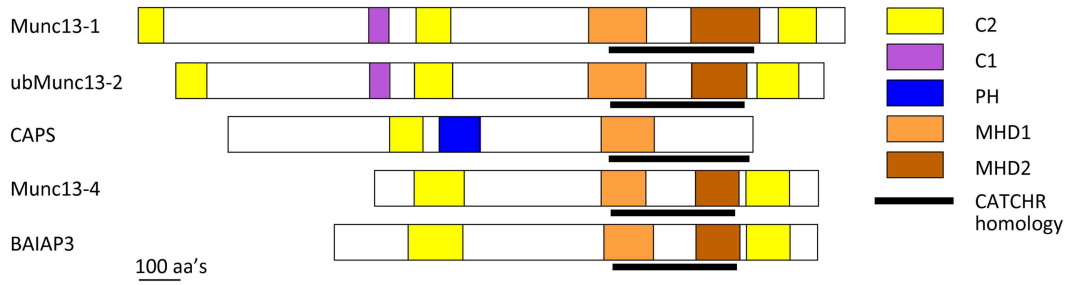

FIGURE 2 | Schematic of CAPS/Munc13 family of priming factors. Colored boxes indicate relative location of C2, C1, PH, MHD1, and MHD2 domains. The CATCHR homology region is indicated by black line.

strongly impaired in cells lacking Munc13-1 or CAPS (78, 81–83). Thus, major accessory factors for SV and DCV priming are the related CAPS and Munc13 proteins. Munc18-1 is also involved in SV and DCV priming but its role in priming in cells is difficult to separate from its upstream role as a syntaxin-1 chaperone that influences vesicle docking (42, 84). It is likely that CAPS and Munc13 proteins co-function with Munc18-1 in vesicle priming.

CAPS and Munc13 proteins are related in sequence (**Figure 2**) (6, 85). CAPS and Munc13-1 exhibit ∼40% sequence similarity in a C-terminal region that contains the MHD1 homology domain. All Munc13 proteins (including Munc13-4 and BAIAP3) but not CAPS proteins also share a more C-terminal MHD2 domain. Overall the C-terminal region of CAPS and Munc13 proteins exhibits weak sequence homology to the CATCHR domain of exocyst, COG, GARP, and Dsl1 complex subunits (**Figure 2**) (6). More convincingly, crystallographic studies of a Munc13-1(1148–1531) protein indicated strong structural similarity to the CATCHR region of the Sec6 subunit of the exocyst complex (5). This homology across diverse proteins implies an evolutionary relatedness but could also indicate a conserved functional role for the CATCHR domain. In MTCs, an inherent structural role for CATCHR domains was seen to be adapted to mediate protein–protein interactions that include SNARE-binding (50). Studies of the CAPS and Munc13 proteins indicate a role for this region in scaffolding SNARE proteins as well as for other protein interactions. In the following, we discuss membrane- and SNARE-binding features of CAPS and Munc13 proteins that have counterparts in MTCs.

PRIMING FACTORS FOR REGULATED VESICLE EXOCYTOSIS: CAPS

CAPS (aka CADPS) was discovered for its activity in regulating DCV exocytosis in neuroendocrine cells (86) and was found to correspond to the *Caenorhabditis elegans* UNC31 protein (87). Unc-31 deletion mutants exhibit a strong loss of DCV exocytosis and neuropeptide secretion (88–90) with moderate reductions in SV exocytosis and synaptic transmission (88, 89, 91, 92), which matches the conditional uncoordinated phenotype. By contrast, the phenotypes for *C. elegans* UNC13 mutants are much more severe. Unc-13 hypomorphs are paralyzed, and exhibit a strong loss of synaptic transmission with lesser impact on DCV exocytosis and neuropeptide secretion (89, 93, 94). Thus, *C. elegans* CAPS/UNC31 is essential for DCV exocytosis whereas Munc13/UNC13 plays a dominant role in SV exocytosis. In vertebrates, the requirements for vesicle priming are more complex in requiring both CAPS and Munc13 proteins. Vertebrates possess two CAPS genes (CAPS/CADPS and CAPS2/CADPS2) that control DCV exocytosis in chromaffin cells, pancreatic β cells, and neurons (83, 95–100). Munc13 proteins are encoded by five genes (Munc13-1, -2, -3, -4, BAIAP3). Munc13-1 is required for DCV exocytosis in pancreatic β cells (101, 102), which indicates that both CAPS and Munc13-1 are required for regulated insulin secretion. CAPS localizes to DCVs but not SVs in brain tissue (103). In spite of this, studies indicate that CAPS-1/2 KO mice exhibit as complete loss of synaptic transmission as reported for Munc13-1 KO mice (78, 80). Thus, it appears that CAPS and Munc13 proteins are both required for SV and DCV priming in vertebrate nervous and endocrine systems.

Recent studies have revealed CAPS to be a regulator of SNARE complex assembly. Attempts to detect direct CAPS interactions with soluble SNARE proteins were of limited success indicating only very low affinity interactions; however, recent studies revealed direct CAPS interactions with membrane-associated SNARE proteins (**Figure 1**, lower) (104–107). Liposomes containing syntaxin-1/SNAP-25 heterodimers or VAMP2 were found to retain CAPS in liposome flotation studies (104). CAPS interacted independently with either syntaxin-1 or SNAP-25 suggesting that CAPS might promote QaQbc-SNARE heterodimer formation. CAPS binding to syntaxin-1 was mediated by the membrane-proximal C-terminal SNARE motif (H3) and membrane linker domain sequences of syntaxin-1 (104). CAPS interactions with N-terminal regions of the SNARE motif of VAMP2 were also detected, which suggests that CAPS might recruit VAMP2 into syntaxin-1/SNAP-25 heterodimers for RQaQbc-SNARE complex assembly. As a SNARE-binding protein, CAPS stimulated the formation of SNARE complexes on liposomes (106) and promoted VAMP2 liposome docking on supported bilayer membranes containing syntaxin-1/SNAP-25 heterodimers indicating that stable trans-SNARE complex formation had occurred. These studies utilized pre-formed syntaxin-1/SNAP-25 heterodimers, and indicated that CAPS could promote VAMP2 insertion into QaQbc-SNARE heterodimers to assemble heterotrimeric SNARE complexes (**Figure 1**, lower). The activity of CAPS in promoting SNARE complex formation was also evident in studies

of SNARE-dependent liposome fusion where CAPS markedly increased the rate and extent of fusion between donor VAMP2 liposomes and syntaxin-1/SNAP-25 acceptor liposomes (105, 106). These results also suggested that CAPS acts to promote the insertion of the R-SNARE VAMP2 into Qabc-SNARE syntaxin-1/SNAP-25 acceptors (**Figure 1**, lower) but it is not yet known if CAPS utilizes direct interactions with syntaxin-1/SNAP-25, with VAMP2, or with both to enable SNARE complex assembly. Additional studies are needed to determine the detailed mechanism of how CAPS enhances SNARE complex assembly.

A key issue is which CAPS domains mediate SNARE protein binding and SNARE complex assembly. The C-terminal region of CAPS/Munc13 proteins contains numerous α-helices, which makes standard recombinant protein analysis or yeast two-hybrid interaction studies very challenging (5, 108). We produced a set of recombinant proteins across the CAPS sequence based on secondary structure predictions and proteolysis studies, and tested these proteins for moderate-to-high affinity (0.2 μM) SNARE-binding (107). Only one protein fragment corresponding to rat CAPS(859-1073) was retained in flotation studies by syntaxin-1/SNAP-25 liposomes (107). CAPS(859-1073), which brackets the MHD1 homology region (**Figure 2**), exhibited submicromolar binding affinity for SNARE proteins and effectively competed with full-length CAPS(1-1289) for binding indicating that this region contains the major SNARE-binding domain of CAPS. Further studies with protein fragments suggested that the major SNARE-binding segment may consist of a helix in the center of MHD1 that contains a VAMP2 homology region. This corresponds to the N-terminal helix of the CATCHR homology region (**Figure 2**) (5, 6, 107). These studies did not exclude the possibility that other helices within the CATCHR homology domain provide additional lower affinity SNARE-binding. Thus, this region consisting of stacked α-helices could function as a scaffold to organize helical SNARE motifs. A recent report suggested that syntaxin-1 binding by CAPS was mediated by more C-terminal sequences within CATCHR; however, these studies employed constructs in yeast two-hybrid studies that may have encoded unfolded proteins (109). Studies on CAPS are consistent with a SNARE scaffolding role for the CATCHR homology region. However, other CAPS-protein interactions have also been reported for this region (110), which could indicate a more general role for the CATCHR domain as a protein interaction domain.

For MTCs, numerous membrane interactions can be achieved by multiple subunits. As a large multi-domain protein, CAPS may instead utilize multiple domains to mediate protein and lipid interactions. CAPS exhibits low affinity but functionally significant interactions with plasma membrane PIP_2 via its central PH (pleckstrin homology) domain (82, 111). PIP_2 enhanced CAPS stimulation of SNARE-dependent liposome fusion with wild-type but not with mutant PH domain CAPS proteins (105). Inclusion of PIP_2 in the syntaxin-1/SNAP-25-containing acceptor liposomes was much more effective than inclusion in the VAMP2-containing donor membranes, which suggests that PIP_2 is an important co-factor for CAPS in acting on plasma membrane SNARE proteins (**Figure 1**, lower). PIP_2 may promote conformational or oligomerization changes in CAPS to enhance its SNARE interactions (111). In addition, because CAPS interacts with syntaxin-1 near its C-terminal linker that binds PIP_2, this might allow CAPS to regulate the conformation of syntaxin-1 (104, 105). These results suggest a framework for understanding the actions of priming factors. CAPS utilizes two contacts with the membrane – one with membrane phospholipids via its PH domain and the other with SNAREs via its MHD1 domain – to promote the assembly of SNARE protein complexes.

CAPS localizes to DCVs (103, 112) and also interacts with plasma membrane PIP_2, which could provide a trans-membrane interaction for vesicle tethering. However, such a tethering mechanism would likely be transient because of the low affinity PIP_2 interactions. The basis for CAPS anchoring to DCVs via C-terminal interactions (112) remains to be clarified. Possible interactions with the DCV constituents phogrin (113), VMAT (114), ARF4/5 (115, 116), and RRP17 (110) have been suggested.

Tethering factors are thought to engage in long-range capture of vesicles (tethering) at the target membrane involving distances (>20 nm) at which SNARE complexes cannot assemble. MTC tethering complexes likely bring vesicles into closer proximity to enable SNARE complex formation and docking. CAPS functions in vesicle priming to promote the assembly of SNARE complexes that bridge vesicles to the plasma membrane, which may be expected to mediate vesicle docking. Indeed, *in vitro* studies of VAMP2 liposome docking onto syntaxin-1/SNAP-25-containing membranes revealed that CAPS could promote a stable docking complex (106). EM studies in *C. elegans* also indicated that CAPS/Unc31 was required for DCV docking to the plasma membrane (88). Although DCV docking defects were not reported for chromaffin cells from CAPS KO mice, this may be attributable to the small percentage of total vesicles that are primed in these cells (83).

PRIMING FACTORS FOR REGULATED VESICLE EXOCYTOSIS: Munc13

Munc13 proteins are thought to function in vesicle priming by interacting with SNARE proteins (44). Munc13-4, a short Munc13 isoform with N- and C-terminal C2 domains (C2A and C2B, respectively) bracketing the MHD1-MHD2 region (**Figure 2**), functions in the priming as well as the maturation of lysosome-related secretory granules for fusion in secretory cells of hematopoietic origin (117). Munc13-4 appears to function as a tether for granule-plasma membrane interactions mediated by vesicle-associated Rab27 (118, 119). Recent biochemical studies revealed that Munc13-4 exhibits Ca^{2+}-regulated SNARE interactions modulated by its C2A domain and Ca^{2+}-dependent membrane interactions mediated by its C2B domain (120). Munc13-4 promoted the fusion of VAMP2 donor liposomes with syntaxin-1/SNAP-25 acceptor liposomes that was dependent on Ca^{2+} and Ca^{2+}-binding residues in each C2 domain (120). These results indicated that Ca^{2+}-activated Munc13-4 can function similarly to CAPS by promoting the recruitment of the R-SNARE VAMP2 into Qabc-SNARE syntaxin-1/SNAP-25 acceptors for RQaQbc-SNARE complex assembly. The central MHD1-MHD2 region of Munc13-4 with CATCHR homology may mediate SNARE-binding but this has yet to be demonstrated. For Munc13-4 as for CAPS, it appeared that anchoring the protein to the membrane (via the Ca^{2+}-dependent C2B domain) coupled to SNARE-binding was

required to promote SNARE complex assembly and liposome fusion (120).

C-terminal regions of Munc13-1 were reported to interact with N-terminal domains of syntaxin-1 in yeast two-hybrid interaction studies (121, 122). Solution binding studies with recombinant Munc13-1 protein fragments localized N-terminal syntaxin-1 binding to Munc13-1(1181–1736), which corresponds to sequences beginning in MHD1 (**Figure 2**). This interaction was proposed to counteract Munc18-1-mediated stabilization of a "closed" form of syntaxin-1 to "open" it to enable syntaxin-1/SNAP-25 heterodimer formation. However, subsequent studies reported that Munc13-1(859–1531) (termed MUN domain) failed to interact with SNARE proteins in solution but did interact with liposome-integrated SNARE protein complexes (108, 123, 124). Munc13-1(859–1531) bound to syntaxin-1/SNAP-25 or syntaxin-1/SNAP-25/VAMP2 liposomes but not to syntaxin-1 liposomes, which suggested that Munc13-1 stabilizes SNARE complexes (123). Consistent with this, other studies provided evidence that Munc13-1(859–1531) stabilized parallel conformations of syntaxin-1/SNAP-25 heterodimers (124). Recent NMR studies with Munc13-1(859–1531) and soluble SNARE proteins indicated that Munc13-1(859–1531) interacts very weakly with the C-terminal SNARE domain of syntaxin-1 and with Munc18-1-bound syntaxin-1 (125). By contrast, a structurally defined Munc13-1(1148–1531) protein fragment exhibited further attenuated SNARE protein interactions possibly because this fragment lacked more N-terminal sequences (5).

In recent studies, a Munc13-1(529–1531) protein that contained C1 and C2B domains (**Figure 2**) was shown to operate on liposomal syntaxin-1-Munc18-1 to enable Ca^{2+}-bound synaptotagmin C2AB to promote SNARE-dependent liposome fusion (126). It was proposed that the Munc13-1 fragment catalyzed a transition of Munc18-1-bound syntaxin-1 into syntaxin-1/SNAP-25 heterodimers to serve as acceptor complexes for VAMP2. This model for Munc13-1 action retains the feature of syntaxin-1 "opening" but proposes that the Munc13-1 C-terminal domain interacts with C-terminal rather than N-terminal regions of syntaxin-1 (126). In addition, these studies with a Munc13-1 fragment plus Munc18-1 suggested a possible exchange of the Qbc-SNARE SNAP-25 into Q-SNARE complexes as an important regulated step (126).

These studies suggest a mode of action for Munc13-1 in promoting the transition of closed syntaxin-1 monomers to syntaxin-1/SNAP-25 heterodimers. Similar effects for Munc13-4 and CAPS have not yet been demonstrated. Actual differences in the mechanisms of Munc13-1 and CAPS action on SNAREs could help to account for the non-redundancy of these factors for vesicle priming. However, future study will be needed to assess whether these apparent differences result from the use of different assays for CAPS and Munc13-1 proteins. Genetic studies in *C. elegans* have found that expression of an "open" syntaxin mutant by-passes DCV docking defects in CAPS/Unc-31 mutants (88) and SV docking defects in Unc-13 mutants (127) possibly indicating that both proteins enable a transition of syntaxin-1/Munc18-1 complexes to syntaxin-1/SNAP-25 complexes. Overall, the studies on Munc13-1 are compatible with a SNARE scaffolding role for the CATCHR homology region but the detailed mechanics of SNARE-binding remain to be worked out.

Munc13-1/2 proteins are also reported to exhibit Ca^{2+}-dependent, high affinity PIP_2 interactions via a central C2B domain (128). This interaction was significant for SV exocytosis in response to high frequency stimulation rather than for responses to single action potentials. The importance of C2B-mediated phosphoinositide interactions for DCV exocytosis in neuroendocrine cells has not been determined but could play a role in recruiting cytosolic Munc13-1/2 to sites of DCV exocytosis. The adjacent DAG-binding C1 domain of Munc13-1 mediates the membrane recruitment of Munc13-1 in response to DAG, however, a functional C1 domain in Munc13-1 is not required for Ca^{2+}-stimulated vesicle exocytosis but rather for potentiated responses (129).

In contrast to the cytoplasmic localization of Munc13-1/2 in neuroendocrine cells, Munc13-1 localizes to the active zone in synapses where it associates with at least four other active zone proteins (RIM, bassoon, aczonin/piccolo, and CAST) via its N-terminal domain (130). This molecular complex likely serves a tethering role mediated by proteins anchored to both the presynaptic membrane and to SVs (130). Interactions with SVs may be mediated by a complex of RIM and Munc13-1 with Rab3 on the vesicle (131). Studies suggest that RIM activates Munc13-1 by converting it from an inactive dimer to active monomer (42). Standard chemical fixation methods had failed to reveal decreased SV docking in neurons from Munc13-1 KO mice, but high-pressure freezing techniques with EM tomography indicated that SVs were tethered but not docked in the absence of Munc13-1 (74). Similarly, high-pressure freezing followed by low-temperature fixation in *C. elegans* revealed a requirement for UNC13 in SV docking (88). Although the studies might suggest that priming and docking are functional and morphological aspects of the same process, more studies are needed in vertebrate neurons and endocrine cells where CAPS and Munc13 are co-required for vesicle priming.

SUMMARY

At multiple trafficking stations in secretory and endosomal pathways, diverse tethering and priming factors integrate multiple protein and lipid interactions to achieve compartment-specific SNARE complex assembly for fusion. The MTCs promote SNARE complex assembly by direct interactions of MTC subunits with Q-SNAREs and collaborative interactions with SM proteins. A subset of MTC subunits utilize structurally similar CATCHR domains to mediate inter-subunit interactions as well as SNARE protein interactions. At sites of regulated vesicle exocytosis in neurons and endocrine cells, homologous CAPS and Munc13 proteins play a similar role in mediating SNARE complex assembly for vesicle priming, however they may do so by distinct mechanisms. SNARE-binding in the CAPS and Munc13 proteins appears to reside within the CATCHR domain, which may also mediate additional protein interactions. CAPS and Munc13-1 collaborate with the SM protein Munc18-1 but the details of integration remain to be worked out. Studies are needed to determine whether accessory factors and SM proteins operate in concert or sequentially to assemble SNARE complexes, and to determine how these interactions occur within the confined space of juxtaposed membranes.

ACKNOWLEDGMENTS

The Martin lab is supported by USPHS grants DK040428 and DK025861.

REFERENCES

1. Fukuda M. Regulation of secretory vesicle traffic by Rab small GTPases. *Cell Mol Life Sci* (2008) **65**:2801–13. doi:10.1007/s00018-008-8351-4
2. Hutagalung AH, Novick PJ. Role of Rab GTPases in membrane traffic and cell physiology. *Physiol Rev* (2011) **91**:119–49. doi:10.1152/physrev.00059.2009
3. Di Paolo G, De Camilli P. Phosphoinositides in cell regulation and membrane dynamics. *Nature* (2006) **443**:651–7. doi:10.1038/nature05185
4. Martin TF. PI(4,5)P(2) regulation of surface membrane traffic. *Curr Opin Cell Biol* (2001) **13**:493–9. doi:10.1016/S0955-0674(00)00241-6
5. Li W, Ma C, Guan R, Xu Y, Tomchick DR, Rizo J. The crystal structure of a Munc13 C-terminal module exhibits a remarkable similarity to vesicle tethering factors. *Structure* (2011) **19**:1443–55. doi:10.1016/j.str.2011.07.012
6. Pei J, Ma C, Rizo J, Grishin NV. Remote homology between Munc13 MUN domain and vesicle tethering complexes. *J Mol Biol* (2009) **391**:509–17. doi:10.1016/j.jmb.2009.06.054
7. Sollner T, Whiteheart SW, Brunner M, Erdjument-Bromage H, Geromanos S, Tempst P, et al. SNAP receptors implicated in vesicle targeting and fusion. *Nature* (1993) **362**:318–24. doi:10.1038/362318a0
8. Jahn R, Fasshauer D. Molecular machines governing exocytosis of synaptic vesicles. *Nature* (2012) **490**:201–7. doi:10.1038/nature11320
9. Malsam J, Kreye S, Sollner TH. Membrane fusion: SNAREs and regulation. *Cell Mol Life Sci* (2008) **65**:2814–32. doi:10.1007/s00018-008-8352-3
10. Blasi J, Chapman ER, Link E, Binz T, Yamasaki S, De Camilli P, et al. Botulinum neurotoxin A selectively cleaves the synaptic protein SNAP-25. *Nature* (1993) **365**:160–3. doi:10.1038/365160a0
11. Blasi J, Chapman ER, Yamasaki S, Binz T, Niemann H, Jahn R. Botulinum neurotoxin C1 blocks neurotransmitter release by means of cleaving HPC-1/syntaxin. *EMBO J* (1993) **12**:4821–8.
12. Hayashi T, McMahon H, Yamasaki S, Binz T, Hata Y, Sudhof TC, et al. Synaptic vesicle membrane fusion complex: action of clostridial neurotoxins on assembly. *EMBO J* (1994) **13**:5051–61.
13. Link E, Edelmann L, Chou JH, Binz T, Yamasaki S, Eisel U, et al. Tetanus toxin action: inhibition of neurotransmitter release linked to synaptobrevin proteolysis. *Biochem Biophys Res Commun* (1992) **189**:1017–23. doi:10.1016/0006-291X(92)92305-H
14. Schiavo G, Benfenati F, Poulain B, Rossetto O, Polverino de Laureto P, DasGupta BR, et al. Tetanus and botulinum-B neurotoxins block neurotransmitter release by proteolytic cleavage of synaptobrevin. *Nature* (1992) **359**:832–5. doi:10.1038/359832a0
15. Kienle N, Kloepper TH, Fasshauer D. Differences in the SNARE evolution of fungi and metazoa. *Biochem Soc Trans* (2009) **37**:787–91. doi:10.1042/BST0370787
16. Fasshauer D, Sutton RB, Brunger AT, Jahn R. Conserved structural features of the synaptic fusion complex: SNARE proteins reclassified as Q- and R-SNAREs. *Proc Natl Acad Sci U S A* (1998) **95**:15781–6. doi:10.1073/pnas.95.26.15781
17. Weber T, Zemelman BV, McNew JA, Westermann B, Gmachl M, Parlati F, et al. SNAREpins: minimal machinery for membrane fusion. *Cell* (1998) **92**:759–72. doi:10.1016/S0092-8674(00)81404-X
18. Brunger AT. Structure and function of SNARE and SNARE-interacting proteins. *Q Rev Biophys* (2005) **38**:1–47. doi:10.1017/S0033583505004051
19. Fasshauer D. Structural insights into the SNARE mechanism. *Biochim Biophys Acta* (2003) **1641**:87–97. doi:10.1016/S0167-4889(03)00090-9
20. Sutton RB, Fasshauer D, Jahn R, Brunger AT. Crystal structure of a SNARE complex involved in synaptic exocytosis at 2.4 A resolution. *Nature* (1998) **395**:347–53. doi:10.1038/26412
21. Jahn R, Scheller RH. SNAREs – engines for membrane fusion. *Nat Rev Mol Cell Biol* (2006) **7**:631–43. doi:10.1038/nrm2002
22. Chen YA, Scales SJ, Scheller RH. Sequential SNARE assembly underlies priming and triggering of exocytosis. *Neuron* (2001) **30**:161–70. doi:10.1016/S0896-6273(01)00270-7
23. Halemani ND, Bethani I, Rizzoli SO, Lang T. Structure and dynamics of a two-helix SNARE complex in live cells. *Traffic* (2010) **11**:394–404. doi:10.1111/j.1600-0854.2009.01020.x
24. Kasai H, Takahashi N, Tokumaru H. Distinct initial SNARE configurations underlying the diversity of exocytosis. *Physiol Rev* (2012) **92**:1915–64. doi:10.1152/physrev.00007.2012
25. Takamori S, Holt M, Stenius K, Lemke EA, Gronborg M, Riedel D, et al. Molecular anatomy of a trafficking organelle. *Cell* (2006) **127**:831–46. doi:10.1016/j.cell.2006.10.030
26. McNew JA, Parlati F, Fukuda R, Johnston RJ, Paz K, Paumet F, et al. Compartmental specificity of cellular membrane fusion encoded in SNARE proteins. *Nature* (2000) **407**:153–9. doi:10.1038/35025000
27. Parlati F, McNew JA, Fukuda R, Miller R, Sollner TH, Rothman JE. Topological restriction of SNARE-dependent membrane fusion. *Nature* (2000) **407**:194–8. doi:10.1038/35025076
28. Brandhorst D, Zwilling D, Rizzoli SO, Lippert U, Lang T, Jahn R. Homotypic fusion of early endosomes: SNAREs do not determine fusion specificity. *Proc Natl Acad Sci U S A* (2006) **103**:2701–6. doi:10.1073/pnas.0511138103
29. Izawa R, Onoue T, Furukawa N, Mima J. Distinct contributions of vacuolar Qabc- and R-SNARE proteins to membrane fusion specificity. *J Biol Chem* (2012) **287**:3445–53. doi:10.1074/jbc.M111.307439
30. Shen J, Tareste DC, Paumet F, Rothman JE, Melia TJ. Selective activation of cognate SNAREpins by Sec1/Munc18 proteins. *Cell* (2007) **128**:183–95. doi:10.1016/j.cell.2006.12.016
31. Yu H, Rathore SS, Lopez JA, Davis EM, James DE, Martin JL, et al. Comparative studies of Munc18c and Munc18-1 reveal conserved and divergent mechanisms of Sec1/Munc18 proteins. *Proc Natl Acad Sci U S A* (2013) **110**:E3271–80. doi:10.1073/pnas.1311232110
32. Hata Y, Slaughter CA, Sudhof TC. Synaptic vesicle fusion complex contains unc-18 homologue bound to syntaxin. *Nature* (1993) **366**:347–51. doi:10.1038/366347a0
33. Hosono R, Hekimi S, Kamiya Y, Sassa T, Murakami S, Nishiwaki K, et al. The unc-18 gene encodes a novel protein affecting the kinetics of acetylcholine metabolism in the nematode *Caenorhabditis elegans*. *J Neurochem* (1992) **58**:1517–25. doi:10.1111/j.1471-4159.1992.tb11373.x
34. Novick P, Field C, Schekman R. Identification of 23 complementation groups required for post-translational events in the yeast secretory pathway. *Cell* (1980) **21**:205–15. doi:10.1016/0092-8674(80)90128-2
35. Bryant NJ, James DE. Vps45p stabilizes the syntaxin homologue Tlg2p and positively regulates SNARE complex formation. *EMBO J* (2001) **20**:3380–8. doi:10.1093/emboj/20.13.3380
36. Dulubova I, Yamaguchi T, Gao Y, Min SW, Huryeva I, Sudhof TC, et al. How Tlg2p/syntaxin 16 'snares' Vps45. *EMBO J* (2002) **21**:3620–31. doi:10.1093/emboj/cdf381
37. Lobingier BT, Merz AJ. Sec1/Munc18 protein Vps33 binds to SNARE domains and the quaternary SNARE complex. *Mol Biol Cell* (2012) **23**:4611–22. doi:10.1091/mbc.E12-05-0343
38. Yamaguchi T, Dulubova I, Min SW, Chen X, Rizo J, Sudhof TC. Sly1 binds to Golgi and ER syntaxins via a conserved N-terminal peptide motif. *Dev Cell* (2002) **2**:295–305. doi:10.1016/S1534-5807(02)00125-9
39. Dulubova I, Yamaguchi T, Arac D, Li H, Huryeva I, Min SW, et al. Convergence and divergence in the mechanism of SNARE binding by Sec1/Munc18-like proteins. *Proc Natl Acad Sci U S A* (2003) **100**:32–7. doi:10.1073/pnas.232701299
40. Misura KM, Scheller RH, Weis WI. Three-dimensional structure of the neuronal-Sec1-syntaxin 1a complex. *Nature* (2000) **404**:355–62. doi:10.1038/35006120
41. Dulubova I, Sugita S, Hill S, Hosaka M, Fernandez I, Sudhof TC, et al. A conformational switch in syntaxin during exocytosis: role of munc18. *EMBO J* (1999) **18**:4372–82. doi:10.1093/emboj/18.16.4372
42. Verhage M, Maia AS, Plomp JJ, Brussaard AB, Heeroma JH, Vermeer H, et al. Synaptic assembly of the brain in the absence of neurotransmitter secretion. *Science* (2000) **287**:864–9. doi:10.1126/science.287.5454.864
43. Schollmeier Y, Krause JM, Kreye S, Malsam J, Sollner TH. Resolving the function of distinct Munc18-1/SNARE protein interaction modes in a reconstituted membrane fusion assay. *J Biol Chem* (2011) **286**:30582–90. doi:10.1074/jbc.M111.269886
44. Rizo J, Sudhof TC. The membrane fusion enigma: SNAREs, Sec1/Munc18 proteins, and their accomplices – guilty as charged? *Annu Rev Cell Dev Biol* (2012) **28**:279–308. doi:10.1146/annurev-cellbio-101011-155818
45. Wickner W. Membrane fusion: five lipids, four SNAREs, three chaperones, two nucleotides, and a Rab, all dancing in a ring on yeast vacuoles. *Annu Rev Cell Dev Biol* (2010) **26**:115–36. doi:10.1146/annurev-cellbio-100109-104131

46. Whyte JR, Munro S. Vesicle tethering complexes in membrane traffic. *J Cell Sci* (2002) **115**:2627–37.
47. Cai H, Reinisch K, Ferro-Novick S. Coats, tethers, Rabs, and SNAREs work together to mediate the intracellular destination of a transport vesicle. *Dev Cell* (2007) **12**:671–82. doi:10.1016/j.devcel.2007.04.005
48. Koumandou VL, Dacks JB, Coulson RM, Field MC. Control systems for membrane fusion in the ancestral eukaryote; evolution of tethering complexes and SM proteins. *BMC Evol Biol* (2007) **7**:29. doi:10.1186/1471-2148-7-29
49. Bonifacino JS, Hierro A. Transport according to GARP: receiving retrograde cargo at the trans-Golgi network. *Trends Cell Biol* (2011) **21**:159–67. doi:10.1016/j.tcb.2010.11.003
50. Yu IM, Hughson FM. Tethering factors as organizers of intracellular vesicular traffic. *Annu Rev Cell Dev Biol* (2010) **26**:137–56. doi:10.1146/annurev.cellbio.042308.113327
51. Hickey CM, Wickner W. HOPS initiates vacuole docking by tethering membranes before trans-SNARE complex assembly. *Mol Biol Cell* (2010) **21**:2297–305. doi:10.1091/mbc.E10-01-0044
52. Balderhaar HJ, Ungermann C. CORVET and HOPS tethering complexes – coordinators of endosome and lysosome fusion. *J Cell Sci* (2013) **126**:1307–16. doi:10.1242/jcs.107805
53. Brocker C, Kuhlee A, Gatsogiannis C, Balderhaar HJ, Honscher C, Engelbrecht-Vandre S, et al. Molecular architecture of the multisubunit homotypic fusion and vacuole protein sorting (HOPS) tethering complex. *Proc Natl Acad Sci U S A* (2012) **109**:1991–6. doi:10.1073/pnas.1117797109
54. Alpadi K, Kulkarni A, Comte V, Reinhardt M, Schmidt A, Namjoshi S, et al. Sequential analysis of trans-SNARE formation in intracellular membrane fusion. *PLoS Biol* (2012) **10**:e1001243. doi:10.1371/journal.pbio.1001243
55. Kramer L, Ungermann C. HOPS drives vacuole fusion by binding the vacuolar SNARE complex and the Vam7 PX domain via two distinct sites. *Mol Biol Cell* (2011) **22**:2601–11. doi:10.1091/mbc.E11-02-0104
56. Baker RW, Jeffrey PD, Hughson FM. Crystal structures of the Sec1/Munc18 (SM) protein Vps33, alone and bound to the homotypic fusion and vacuolar protein sorting (HOPS) subunit Vps16*. *PLoS One* (2013) **8**:e67409. doi:10.1371/journal.pone.0067409
57. Heider MR, Munson M. Exorcising the exocyst complex. *Traffic* (2012) **13**:898–907. doi:10.1111/j.1600-0854.2012.01353.x
58. Boyd C, Hughes T, Pypaert M, Novick P. Vesicles carry most exocyst subunits to exocytic sites marked by the remaining two subunits, Sec3p and Exo70p. *J Cell Biol* (2004) **167**:889–901. doi:10.1083/jcb.200408124
59. Hazuka CD, Foletti DL, Hsu SC, Kee Y, Hopf FW, Scheller RH. The sec6/8 complex is located at neurite outgrowth and axonal synapse-assembly domains. *J Neurosci* (1999) **19**:1324–34.
60. He B, Xi F, Zhang X, Zhang J, Guo W. Exo70 interacts with phospholipids and mediates the targeting of the exocyst to the plasma membrane. *EMBO J* (2007) **26**:4053–65. doi:10.1038/sj.emboj.7601834
61. Liu J, Zuo X, Yue P, Guo W. Phosphatidylinositol 4,5-bisphosphate mediates the targeting of the exocyst to the plasma membrane for exocytosis in mammalian cells. *Mol Biol Cell* (2007) **18**:4483–92. doi:10.1091/mbc.E07-05-0461
62. Dong G, Hutagalung AH, Fu C, Novick P, Reinisch KM. The structures of exocyst subunit Exo70p and the Exo84p C-terminal domains reveal a common motif. *Nat Struct Mol Biol* (2005) **12**:1094–100.
63. Sivaram MV, Saporita JA, Furgason ML, Boettcher AJ, Munson M. Dimerization of the exocyst protein Sec6p and its interaction with the t-SNARE Sec9p. *Biochemistry* (2005) **44**:6302–11. doi:10.1021/bi048008z
64. Morgera F, Sallah MR, Dubuke ML, Gandhi P, Brewer DN, Carr CM, et al. Regulation of exocytosis by the exocyst subunit Sec6 and the SM protein Sec1. *Mol Biol Cell* (2012) **23**:337–46. doi:10.1091/mbc.E11-08-0670
65. Songer JA, Munson M. Sec6p anchors the assembled exocyst complex at sites of secretion. *Mol Biol Cell* (2009) **20**:973–82. doi:10.1091/mbc.E08-09-0968
66. Kraynack BA, Chan A, Rosenthal E, Essid M, Umansky B, Waters MG, et al. Dsl1p, Tip20p, and the novel Dsl3(Sec39) protein are required for the stability of the Q/t-SNARE complex at the endoplasmic reticulum in yeast. *Mol Biol Cell* (2005) **16**:3963–77. doi:10.1091/mbc.E05-01-0056
67. Spang A. The DSL1 complex: the smallest but not the least CATCHR. *Traffic* (2012) **13**:908–13. doi:10.1111/j.1600-0854.2012.01362.x
68. Ren Y, Yip CK, Tripathi A, Huie D, Jeffrey PD, Walz T, et al. A structure-based mechanism for vesicle capture by the multisubunit tethering complex Dsl1. *Cell* (2009) **139**:1119–29. doi:10.1016/j.cell.2009.11.002
69. Andag U, Schmitt HD. Dsl1p, an essential component of the Golgi-endoplasmic reticulum retrieval system in yeast, uses the same sequence motif to interact with different subunits of the COPI vesicle coat. *J Biol Chem* (2003) **278**:51722–34. doi:10.1074/jbc.M308740200
70. Meiringer CT, Rethmeier R, Auffarth K, Wilson J, Perz A, Barlowe C, et al. The Dsl1 protein tethering complex is a resident endoplasmic reticulum complex, which interacts with five soluble NSF (*N*-ethylmaleimide-sensitive factor) attachment protein receptors (SNAREs): implications for fusion and fusion regulation. *J Biol Chem* (2011) **286**:25039–46. doi:10.1074/jbc.M110.215327
71. Hirose H, Arasaki K, Dohmae N, Takio K, Hatsuzawa K, Nagahama M, et al. Implication of ZW10 in membrane trafficking between the endoplasmic reticulum and Golgi. *EMBO J* (2004) **23**:1267–78. doi:10.1038/sj.emboj.7600135
72. Martin TF. Stages of regulated exocytosis. *Trends Cell Biol* (1997) **7**:271–6. doi:10.1016/S0962-8924(97)01060-X
73. Rettig J, Neher E. Emerging roles of presynaptic proteins in Ca++-triggered exocytosis. *Science* (2002) **298**:781–5. doi:10.1126/science.1075375
74. Siksou L, Varoqueaux F, Pascual O, Triller A, Brose N, Marty S. A common molecular basis for membrane docking and functional priming of synaptic vesicles. *Eur J Neurosci* (2009) **30**:49–56. doi:10.1111/j.1460-9568.2009.06811.x
75. Nofal S, Becherer U, Hof D, Matti U, Rettig J. Primed vesicles can be distinguished from docked vesicles by analyzing their mobility. *J Neurosci* (2007) **27**:1386–95. doi:10.1523/JNEUROSCI.4714-06.2007
76. Walter AM, Wiederhold K, Bruns D, Fasshauer D, Sorensen JB. Synaptobrevin N-terminally bound to syntaxin-SNAP-25 defines the primed vesicle state in regulated exocytosis. *J Cell Biol* (2010) **188**:401–13. doi:10.1083/jcb.200907018
77. Xu T, Binz T, Niemann H, Neher E. Multiple kinetic components of exocytosis distinguished by neurotoxin sensitivity. *Nat Neurosci* (1998) **1**:192–200. doi:10.1038/642
78. Augustin I, Rosenmund C, Sudhof TC, Brose N. Munc13-1 is essential for fusion competence of glutamatergic synaptic vesicles. *Nature* (1999) **400**:457–61. doi:10.1038/22768
79. Varoqueaux F, Sigler A, Rhee JS, Brose N, Enk C, Reim K, et al. Total arrest of spontaneous and evoked synaptic transmission but normal synaptogenesis in the absence of Munc13-mediated vesicle priming. *Proc Natl Acad Sci U S A* (2002) **99**:9037–42. doi:10.1073/pnas.122623799
80. Jockusch WJ, Speidel D, Sigler A, Sorensen JB, Varoqueaux F, Rhee JS, et al. CAPS-1 and CAPS-2 are essential synaptic vesicle priming proteins. *Cell* (2007) **131**:796–808. doi:10.1016/j.cell.2007.11.002
81. Ashery U, Varoqueaux F, Voets T, Betz A, Thakur P, Koch H, et al. Munc13-1 acts as a priming factor for large dense-core vesicles in bovine chromaffin cells. *EMBO J* (2000) **19**:3586–96. doi:10.1093/emboj/19.14.3586
82. Grishanin RN, Kowalchyk JA, Klenchin VA, Ann K, Earles CA, Chapman ER, et al. CAPS acts at a prefusion step in dense-core vesicle exocytosis as a PIP2 binding protein. *Neuron* (2004) **43**:551–62. doi:10.1016/j.neuron.2004.07.028
83. Liu Y, Schirra C, Stevens DR, Matti U, Speidel D, Hof D, et al. CAPS facilitates filling of the rapidly releasable pool of large dense-core vesicles. *J Neurosci* (2008) **28**:5594–601. doi:10.1523/JNEUROSCI.5672-07.2008
84. Voets T, Toonen RF, Brian EC, de Wit H, Moser T, Rettig J, et al. Munc18-1 promotes large dense-core vesicle docking. *Neuron* (2001) **31**:581–91. doi:10.1016/S0896-6273(01)00391-9
85. Koch H, Hofmann K, Brose N. Definition of Munc13-homology-domains and characterization of a novel ubiquitously expressed Munc13 isoform. *Biochem J* (2000) **349**:247–53. doi:10.1042/0264-6021:3490247
86. Walent JH, Porter BW, Martin TF. A novel 145 kd brain cytosolic protein reconstitutes Ca(2+)-regulated secretion in permeable neuroendocrine cells. *Cell* (1992) **70**:765–75. doi:10.1016/0092-8674(92)90310-9
87. Ann K, Kowalchyk JA, Loyet KM, Martin TF. Novel Ca2+-binding protein (CAPS) related to UNC-31 required for Ca2+-activated exocytosis. *J Biol Chem* (1997) **272**:19637–40. doi:10.1074/jbc.272.32.19637
88. Hammarlund M, Watanabe S, Schuske K, Jorgensen EM. CAPS and syntaxin dock dense core vesicles to the plasma membrane in neurons. *J Cell Biol* (2008) **180**:483–91. doi:10.1083/jcb.200708018
89. Speese S, Petrie M, Schuske K, Ailion M, Ann K, Iwasaki K, et al. UNC-31 (CAPS) is required for dense-core vesicle but not synaptic vesicle exocytosis in *Caenorhabditis elegans*. *J Neurosci* (2007) **27**:6150–62. doi:10.1523/JNEUROSCI.1466-07.2007
90. Zhou KM, Dong YM, Ge Q, Zhu D, Zhou W, Lin XG, et al. PKA activation bypasses the requirement for UNC-31 in the docking of dense core vesicles from

C. elegans neurons. *Neuron* (2007) **56**:657–69. doi:10.1016/j.neuron.2007.09.015
91. Charlie NK, Schade MA, Thomure AM, Miller KG. Presynaptic UNC-31 (CAPS) is required to activate the G alpha(s) pathway of the *Caenorhabditis elegans* synaptic signaling network. *Genetics* (2006) **172**:943–61. doi:10.1534/genetics.105.049577
92. Gracheva EO, Burdina AO, Touroutine D, Berthelot-Grosjean M, Parekh H, Richmond JE. Tomosyn negatively regulates CAPS-dependent peptide release at *Caenorhabditis elegans* synapses. *J Neurosci* (2007) **27**:10176–84. doi:10.1523/JNEUROSCI.2339-07.2007
93. Richmond JE, Davis WS, Jorgensen EM. UNC-13 is required for synaptic vesicle fusion in *C. elegans*. *Nat Neurosci* (1999) **2**:959–64. doi:10.1038/12160
94. Sieburth D, Madison JM, Kaplan JM. PKC-1 regulates secretion of neuropeptides. *Nat Neurosci* (2007) **10**:49–57. doi:10.1038/nn1810
95. Fujita Y, Xu A, Xie L, Arunachalam L, Chou TC, Jiang T, et al. Ca2+-dependent activator protein for secretion 1 is critical for constitutive and regulated exocytosis but not for loading of transmitters into dense core vesicles. *J Biol Chem* (2007) **282**:21392–403. doi:10.1074/jbc.M703699200
96. Nojiri M, Loyet KM, Klenchin VA, Kabachinski G, Martin TF. CAPS activity in priming vesicle exocytosis requires CK2 phosphorylation. *J Biol Chem* (2009) **284**:18707–14. doi:10.1074/jbc.M109.017483
97. Olsen HL, Hoy M, Zhang W, Bertorello AM, Bokvist K, Capito K, et al. Phosphatidylinositol 4-kinase serves as a metabolic sensor and regulates priming of secretory granules in pancreatic beta cells. *Proc Natl Acad Sci U S A* (2003) **100**:5187–92. doi:10.1073/pnas.0931282100
98. Sadakata T, Mizoguchi A, Sato Y, Katoh-Semba R, Fukuda M, Mikoshiba K, et al. The secretory granule-associated protein CAPS2 regulates neurotrophin release and cell survival. *J Neurosci* (2004) **24**:43–52. doi:10.1523/JNEUROSCI.2528-03.2004
99. Speidel D, Salehi A, Obermueller S, Lundquist I, Brose N, Renstrom E, et al. CAPS1 and CAPS2 regulate stability and recruitment of insulin granules in mouse pancreatic beta cells. *Cell Metab* (2008) **7**:57–67. doi:10.1016/j.cmet.2007.11.009
100. Waselle L, Gerona RR, Vitale N, Martin TF, Bader MF, Regazzi R. Role of phosphoinositide signaling in the control of insulin exocytosis. *Mol Endocrinol* (2005) **19**:3097–106. doi:10.1210/me.2004-0530
101. Kang L, He Z, Xu P, Fan J, Betz A, Brose N, et al. Munc13-1 is required for the sustained release of insulin from pancreatic beta cells. *Cell Metab* (2006) **3**:463–8. doi:10.1016/j.cmet.2006.04.012
102. Kwan EP, Xie L, Sheu L, Nolan CJ, Prentki M, Betz A, et al. Munc13-1 deficiency reduces insulin secretion and causes abnormal glucose tolerance. *Diabetes* (2006) **55**:1421–9. doi:10.2337/db05-1263
103. Berwin B, Floor E, Martin TF. CAPS (mammalian UNC-31) protein localizes to membranes involved in dense-core vesicle exocytosis. *Neuron* (1998) **21**:137–45. doi:10.1016/S0896-6273(00)80521-8
104. Daily NJ, Boswell KL, James DJ, Martin TF. Novel interactions of CAPS (Ca2+-dependent activator protein for secretion) with the three neuronal SNARE proteins required for vesicle fusion. *J Biol Chem* (2010) **285**:35320–9. doi:10.1074/jbc.M110.145169
105. James DJ, Khodthong C, Kowalchyk JA, Martin TF. Phosphatidylinositol 4,5-bisphosphate regulation of SNARE function in membrane fusion mediated by CAPS. *Adv Enzyme Regul* (2010) **50**:62–70. doi:10.1016/j.advenzreg.2009.10.012
106. James DJ, Kowalchyk J, Daily N, Petrie M, Martin TF. CAPS drives trans-SNARE complex formation and membrane fusion through syntaxin interactions. *Proc Natl Acad Sci U S A* (2009) **106**:17308–13. doi:10.1073/pnas.0900755106
107. Khodthong C, Kabachinski G, James DJ, Martin TF. Munc13 homology domain-1 in CAPS/UNC31 mediates SNARE binding required for priming vesicle exocytosis. *Cell Metab* (2011) **14**:254–63. doi:10.1016/j.cmet.2011.07.002
108. Basu J, Shen N, Dulubova I, Lu J, Guan R, Guryev O, et al. A minimal domain responsible for Munc13 activity. *Nat Struct Mol Biol* (2005) **12**:1017–8.
109. Parsaud L, Li L, Jung CH, Park S, Saw NM, Park S, et al. Calcium-dependent activator protein for secretion 1 (CAPS1) binds to syntaxin-1 in a distinct mode from Munc13-1. *J Biol Chem* (2013) **288**(32):23050–63. doi:10.1074/jbc.M113.494088
110. Rybkin II, Kim MS, Bezprozvannaya S, Qi X, Richardson JA, Plato CF, et al. Regulation of atrial natriuretic peptide secretion by a novel Ras-like protein. *J Cell Biol* (2007) **179**:527–37. doi:10.1083/jcb.200707101
111. Loyet KM, Kowalchyk JA, Chaudhary A, Chen J, Prestwich GD, Martin TF. Specific binding of phosphatidylinositol 4,5-bisphosphate to calcium-dependent activator protein for secretion (CAPS), a potential phosphoinositide effector protein for regulated exocytosis. *J Biol Chem* (1998) **273**:8337–43. doi:10.1074/jbc.273.14.8337
112. Grishanin RN, Klenchin VA, Loyet KM, Kowalchyk JA, Ann K, Martin TF. Membrane association domains in Ca2+-dependent activator protein for secretion mediate plasma membrane and dense-core vesicle binding required for Ca2+-dependent exocytosis. *J Biol Chem* (2002) **277**:22025–34. doi:10.1074/jbc.M201614200
113. Cai T, Fukushige T, Notkins AL, Krause M. Insulinoma-associated protein IA-2, a vesicle transmembrane protein, genetically interacts with UNC-31/CAPS and affects neurosecretion in *Caenorhabditis elegans*. *J Neurosci* (2004) **24**:3115–24. doi:10.1523/JNEUROSCI.0101-04.2004
114. Brunk I, Blex C, Speidel D, Brose N, Ahnert-Hilger G. Ca2+-dependent activator proteins of secretion promote vesicular monoamine uptake. *J Biol Chem* (2009) **284**:1050–6. doi:10.1074/jbc.M805328200
115. Sadakata T, Sekine Y, Oka M, Itakura M, Takahashi M, Furuichi T. Calcium-dependent activator protein for secretion 2 interacts with the class II ARF small GTPases and regulates dense-core vesicle trafficking. *FEBS J* (2012) **279**:384–94. doi:10.1111/j.1742-4658.2011.08431.x
116. Sadakata T, Shinoda Y, Sekine Y, Saruta C, Itakura M, Takahashi M, et al. Interaction of calcium-dependent activator protein for secretion 1 (CAPS1) with the class II ADP-ribosylation factor small GTPases is required for dense-core vesicle trafficking in the trans-Golgi network. *J Biol Chem* (2010) **285**:38710–9. doi:10.1074/jbc.M110.137414
117. Feldmann J, Callebaut I, Raposo G, Certain S, Bacq D, Dumont C, et al. Munc13-4 is essential for cytolytic granules fusion and is mutated in a form of familial hemophagocytic lymphohistiocytosis (FHL3). *Cell* (2003) **115**:461–73. doi:10.1016/S0092-8674(03)00855-9
118. Elstak ED, Neeft M, Nehme NT, Voortman J, Cheung M, Goodarzifard M, et al. The munc13-4-rab27 complex is specifically required for tethering secretory lysosomes at the plasma membrane. *Blood* (2011) **118**:1570–8. doi:10.1182/blood-2011-02-339523
119. Neeft M, Wieffer M, de Jong AS, Negroiu G, Metz CH, van Loon A, et al. Munc13-4 is an effector of rab27a and controls secretion of lysosomes in hematopoietic cells. *Mol Biol Cell* (2005) **16**:731–41. doi:10.1091/mbc.E04-10-0923
120. Boswell KL, James DJ, Esquibel JM, Bruinsma S, Shirakawa R, Horiuchi H, et al. Munc13-4 reconstitutes calcium-dependent SNARE-mediated membrane fusion. *J Cell Biol* (2012) **197**:301–12. doi:10.1083/jcb.201109132
121. Betz A, Okamoto M, Benseler F, Brose N. Direct interaction of the rat unc-13 homologue Munc13-1 with the N terminus of syntaxin. *J Biol Chem* (1997) **272**:2520–6. doi:10.1074/jbc.272.4.2520
122. Stevens DR, Wu ZX, Matti U, Junge HJ, Schirra C, Becherer U, et al. Identification of the minimal protein domain required for priming activity of Munc13-1. *Curr Biol* (2005) **15**:2243–8. doi:10.1016/j.cub.2005.10.055
123. Guan R, Dai H, Rizo J. Binding of the Munc13-1 MUN domain to membrane-anchored SNARE complexes. *Biochemistry* (2008) **47**:1474–81. doi:10.1021/bi702345m
124. Weninger K, Bowen ME, Choi UB, Chu S, Brunger AT. Accessory proteins stabilize the acceptor complex for synaptobrevin, the 1:1 syntaxin/SNAP-25 complex. *Structure* (2008) **16**:308–20. doi:10.1016/j.str.2007.12.010
125. Ma C, Li W, Xu Y, Rizo J. Munc13 mediates the transition from the closed syntaxin-Munc18 complex to the SNARE complex. *Nat Struct Mol Biol* (2011) **18**:542–9. doi:10.1038/nsmb.2047
126. Ma C, Su L, Seven AB, Xu Y, Rizo J. Reconstitution of the vital functions of Munc18 and Munc13 in neurotransmitter release. *Science* (2013) **339**:421–5. doi:10.1126/science.1230473
127. Hammarlund M, Palfreyman MT, Watanabe S, Olsen S, Jorgensen EM. Open syntaxin docks synaptic vesicles. *PLoS Biol* (2007) **5**:e198. doi:10.1371/journal.pbio.0050198
128. Shin OH, Lu J, Rhee JS, Tomchick DR, Pang ZP, Wojcik SM, et al. Munc13 C2B domain is an activity-dependent Ca2+ regulator of synaptic exocytosis. *Nat Struct Mol Biol* (2010) **17**:280–8. doi:10.1038/nsmb.1758
129. Bauer CS, Woolley RJ, Teschemacher AG, Seward EP. Potentiation of exocytosis by phospholipase C-coupled G-protein-coupled receptors requires the priming protein Munc13-1. *J Neurosci* (2007) **27**:212–9. doi:10.1523/JNEUROSCI.4201-06.2007

130. Wang X, Hu B, Zieba A, Neumann NG, Kasper-Sonnenberg M, Honsbein A, et al. A protein interaction node at the neurotransmitter release site: domains of Aczonin/Piccolo, Bassoon, CAST, and rim converge on the N-terminal domain of Munc13-1. *J Neurosci* (2009) **29**:12584–96. doi:10.1523/JNEUROSCI.1255-09.2009
131. Dulubova I, Lou X, Lu J, Huryeva I, Alam A, Schneggenburger R, et al. A Munc13/RIM/Rab3 tripartite complex: from priming to plasticity? *EMBO J* (2005) **24**:2839–50. doi:10.1038/sj.emboj.7600753

Conflict of Interest Statement: The authors declare that the research was conducted in the absence of any commercial or financial relationships that could be construed as a potential conflict of interest.

Received: 03 September 2013; accepted: 18 November 2013; published online: 04 December 2013.
*Citation: James DJ and Martin TFJ (2013) CAPS and Munc13: CATCHRs that SNARE vesicles. Front. Endocrinol. **4**:187. doi: 10.3389/fendo.2013.00187*
This article was submitted to Neuroendocrine Science, a section of the journal Frontiers in Endocrinology.

frontiers in
ENDOCRINOLOGY

MINI REVIEW ARTICLE
published: 18 September 2013
doi: 10.3389/fendo.2013.00124

The functional significance of synaptotagmin diversity in neuroendocrine secretion

Paanteha K. Moghadam and Meyer B. Jackson*

Department of Neuroscience, University of Wisconsin, Madison, WI, USA

Edited by:
Stephane Gasman, Centre national de la recherche scientifique, France

Reviewed by:
Ling-Gang Wu, National Institute of Neurological Disorders and Stroke (NINDS), USA
Ralf Schneggenburger, Ecole Polytechnique Fédérale de Lausanne, Switzerland

***Correspondence:**
Meyer B. Jackson, Department of Neuroscience, University of Wisconsin, 1300 University Avenue, Madison, WI 53706-1510, USA
e-mail: mbjackso@wisc.edu

Synaptotagmins (syts) are abundant, evolutionarily conserved integral membrane proteins that play essential roles in regulated exocytosis in nervous and endocrine systems. There are at least 17 syt isoforms in mammals, all with tandem C-terminal C2 domains with highly variable capacities for Ca^{2+} binding. Many syts play roles in neurotransmitter release or hormone secretion or both, and a growing body of work supports a role for some syts as Ca^{2+} sensors of exocytosis. Work in many types of endocrine cells has documented the presence of a number of syt isoforms on dense-core vesicles containing various hormones. Syts can influence the kinetics of exocytotic fusion pores and the choice of release mode between kiss-and-run and full-fusion. Vesicles harboring different syt isoforms can preferentially undergo distinct modes of exocytosis with different forms of stimulation. The diverse properties of syt isoforms enable these proteins to shape Ca^{2+} sensing in endocrine cells, thus contributing to the regulation of hormone release and the organization of complex endocrine functions.

Keywords: exocytosis, neuropeptides, dense-core vesicle, norepinephrine, insulin, calcium, fusion pores, kiss-and-run

INTRODUCTION

Nature employs the same basic molecular machinery for the release of both hormones and neurotransmitters (1–4). Several protein families function broadly in regulated exocytosis, including SNAREs, synaptotagmins (syts), and complexins (5–7). The rich molecular diversity within these families provides a platform for variations in the release process, enabling different cell types to tune and tailor release by blending the different molecular variants of the fusion apparatus. In this way endocrine cells can optimize secretory responses elicited by widely varying signals that are unique to each system. The rates of hormone release from different cell types vary by over two orders of magnitude (8). Endocrine cells secrete an extraordinary variety of hormones by exocytosis from dense-core vesicles (DCVs), and DCVs usually co-package collections of molecules ranging in size from small catecholamines to large peptides (9, 10). The nature of the stimulus can determine which packaged molecules will be released (11, 12), and a single DCV can release both catecholamines and neuropeptides simultaneously (13). Cells also can sort different hormones to different DCVs (14, 15). The diverse forms of storage and release raise questions as to how the exocytotic machinery can be called upon to modulate release rates and enable different types of Ca^{2+} signals to trigger the release of different substances from the same cell or even the same vesicle. One can hope to gain a better understanding of these problems by studying functional variations within the diverse families of exocytotic proteins.

Exocytosis proceeds through a sequence of distinct steps. Release can start once a fusion pore has formed to create a continuous fluid pathway from the vesicle interior to the extracellular space. The fusion pore is initially very small and can allow only small molecules such as norepinephrine to pass, but after it expands larger molecules such as chromogranins, insulin, and glucagon can escape. It is well established that DCVs of endocrine cells undergo two modes of exocytosis, kiss-and-run, and full-fusion (16–19). In kiss-and-run the pore opens transiently, and closes so that vesicles maintain their integrity as they retreat from the plasma membrane. The fusion pore formed during kiss-and-run can act as a filter to expel small molecules and retain larger molecules. The small molecules can be rapidly restored by vesicular transporters so DCVs can recycle. By contrast, in full-fusion the pore expands and the vesicle membrane collapses into the plasma membrane. After full-fusion a DCV is lost; replacing these DCVs requires the entire production sequence beginning with peptide hormone translation in the endoplasmic reticulum, DCV processing in the trans-Golgi network, and maturation (20). The choice between full-fusion and kiss-and-run thus plays a decisive role in determining the fate of the DCV as well as in selecting what molecules are released.

Ca^{2+} triggers exocytosis by binding to syt (21–23), but Ca^{2+} can also influence the kinetics of fusion pores in a variety of ways (24–26), thus raising the possibility that syt isoforms play roles not only in triggering exocytosis, but also in regulating release in subtle ways. Syts regulate the stability of fusion pores (26–30), and fusion pore stability in turn is intimately related to release mode, with the relative frequency of kiss-and-run versus full-fusion described quantitatively in terms of the kinetic rates of fusion pore closure and dilation (26). There are many examples of syts influencing the choice between kiss-and-run and full-fusion (26, 29, 31–33). Syts are conserved proteins with well established functions in membrane trafficking and exocytosis. They contain two C2 domains, and in syt 1, the first isoform to be characterized, each C2 domain binds two or three Ca^{2+} ions through

interactions with key aspartate side chains (34). Syts interact with lipid membranes containing specific phospholipids including phosphatidylserine and phosphatidylinositol-4,5-biphosphate, as well as SNARE proteins. These interactions are regulated by Ca^{2+}, but it remains unclear how binding to these targets enables syts to serve as Ca^{2+} sensors in exocytosis (21, 22, 30).

The mouse and human genomes encode 17 syt isoforms (35), and the functional significance of syt diversity is a subject of considerable interest (22, 36, 37). Syts vary widely in their Ca^{2+}-dependent lipid binding, with syts 1, 2, and 3 binding rapidly, syts 5, 6, 9, and 10 binding at an intermediate rate, and syt 7 binding slowly (38). The isoforms also vary in their activity in Ca^{2+}-stimulated liposome fusion: Ca^{2+} concentrations that trigger responses range widely between the isoforms, and many syts completely fail to confer Ca^{2+} sensitivity on SNARE-mediated liposome fusion *in vitro* (32, 39, 40). Variations in Ca^{2+} sensitivity and fusion pore regulation make these proteins ideal candidates for modifying the release apparatus and tuning responses as Ca^{2+} concentrations rise and fall in distinct spatiotemporal patterns. Here, we survey relevant work on syt functions in hormone release, and where possible draw parallels between syt isoform properties, Ca^{2+} signals, and forms of secretion.

SYT FUNCTION IN ENDOCRINE CELLS

Synaptotagmins appear broadly throughout the endocrine system, with essentially every cell type examined expressing multiple isoforms (**Table 1**). Expression varies between cell types and not all reports agree. No effort was made here to distinguish between isoforms untested versus undetected, and the number of isoforms found in endocrine cells will grow as reagents are developed and improved, and as proteomics methods advance. A large body of work supports the expression of syts 1, 4, 7, and 9 in many endocrine systems, and it is remarkable that these four molecules appear in so many different cell types. Syts 1, 4, and 7 are ancient, conserved proteins distributed widely through metazoan genomes (35). These isoforms presumably perform fundamental biological functions, and evidence is accumulating for their roles in a wide range of endocrine and non-endocrine systems.

Table 1 | Syt isoform expression in various endocrine systems.

Cells	Syt isoforms	Reference
PC12 cells	1, 4, 7, 9	Tucker et al. (55)
	1, 9	Lynch and Martin (44), Fukuda et al. (54)
	3	Mizuta et al. (82)
	3, 5, 6, 10	Saegusa et al. (83)
	8	Monterrat et al. (68)
Chromaffin cells	1, 4, 7, 9	Matsuoka et al. (84)
	1, 7	Schonn et al. (47)
	1	Voets et al. (46)
Hypothalamus	1–4	Xi et al. (71)
Anterior pituitary	1, 3, 4	Xi et al. (71)
LβT2	1, 4	Hu et al. (85)
AtT20	3	Mizuta et al. (82)
	4	Eaton et al. (65)
GH3	3	Mizuta et al. (82)
Posterior pituitary	1, 4	Zhang et al. (63)
Intermediate pituitary (melanotrophs)	1, 3, 4, 7, 9	Kreft et al. (86)
Pancreatic islets	3, 4, 7	Gao et al. (87)
	3	Mizuta et al. (88)
	5, 9	Iezzi et al. (89)
	7	Gustavsson et al. (51)
Pancreatic β-cells	3	Brown et al. (90)
	4	Gut et al. (67)
	7	Gustavsson et al. (50)
β-Cell lines[a]	1–4, 7, 8	Gao et al. (87)
	1, 2	Lang et al. (91)
	3	Gut et al. (67), Mizuta et al. (82), Mizuta et al. (88)
	4, 7, 11, 13	Andersson et al. (69)
	5, 9	Iezzi et al. (89)
	8	Monterrat et al. (68)
Pancreatic α cells	7	Gustavsson et al. (51)

In most cases the localization and expression was based on immunocytochemistry (see text).

[a]*β-Cell lines include RINm5F, INS1, MN6, HT-T15, TC6-F7.*

SYT 1

Syt 1 is the most widely distributed syt isoform in nervous and endocrine systems. This low-affinity Ca^{2+} sensor (32, 39, 41, 42) generally triggers rapid exocytosis. The very tight temporal coupling between Ca^{2+} entry and fusion, within milliseconds, has prompted investigators to use the term "synchronous" to describe this form of release, particularly in the context of synaptic transmission. An early syt 1 knock-down study suggested that PC12 cells can secrete without syt 1 (43), but subsequent work showed that this was due to redundancy with another syt isoform of PC12 cells, syt 9 (33, 44). Overexpression of wild type syt 1 in PC12 cells left the overall time course of secretion unchanged, but overexpression of either wild type syt 1 or a number of syt 1 mutants altered fusion pore kinetics (26–28, 30, 45). Overexpressing syt 1 in PC12 cells also produced more kiss-and-run events than syt 7 and 9 (32).

Deletion of the syt 1 gene in mouse selectively abolished the initial rapid phase of exocytosis in chromaffin cells (33, 46, 47), but had no deleterious effects on slower Ca^{2+}-triggered release. For a given concentration of Ca^{2+}, exocytosis was much slower in chromaffin cells lacking syt 1 than in control cells (46). Mutation of a residue that reduces Ca^{2+} binding slowed exocytosis in chromaffin cells (48). In PC12 cells syt 1 sorted preferentially to smaller DCVs (32), raising the interesting possibility that hormones packaged in smaller vesicles will be released more rapidly than hormones packaged in larger vesicles.

SYT 7

In contrast to syt 1, syt 7 acts as a high affinity Ca^{2+} sensor (32, 39, 49). Syt 7 is more abundant on larger DCVs in PC12 cells (32).

Syt 7 overexpression in PC12 cells prolonged fusion pore lifetimes more than syt 1 overexpression (30), and favored full-fusion (32). Syt 7 knock-down in zebra fish reduced delayed synaptic release, indicating it is a slow Ca^{2+} sensor (49). Syt 7 deletion in chromaffin cells reduced Ca^{2+}-triggered release by 50%, also selectively impairing the slow phase of exocytosis, and deletion of both syt 1 and 7 nearly abolished Ca^{2+}-triggered exocytosis. Thus, in chromaffin cells syt 1 and 7 are the primary Ca^{2+} sensors for the fast and slow kinetic phases of exocytosis, respectively (47). Syt 7 gene ablation also reduced Ca^{2+}-triggered exocytosis of insulin secretion from pancreatic β-cells and of glucagon secretion from pancreatic α-cells (50, 51). It is intriguing that syt 7 also functions in insulin responsive cells (fat and muscle), promoting glucose uptake through Ca^{2+}-stimulated translocation of type-4 glucose transporter to the plasma membrane (52). In syt 7 knock-out α cells, ω-conotoxin further inhibited glucagon secretion to baseline levels, revealing the presence of an N-type Ca^{2+} channel-dependent component of residual glucagon secretion triggered by another protein (51).

SYT 9

Syt 9 is closely related to syt 1 but exhibits intermediate Ca^{2+} sensitivity in fusion assays (32, 39). This protein has also been referred to as syt 5 (35, 53); here syt 9 refers to a 386 amino acid isoform. It is abundant on DCVs of PC12 cells (32, 54, 55), and overexpressing it produces fusion pore lifetimes intermediate between those seen with syt 1 and 7 (30). Down-regulating syt 9 alone produced a small, insignificant reduction of fusion rate in PC12 cells, but as noted above, because of the redundancy of syt 1 and 9 as Ca^{2+} sensors, both must be down-regulated to reduce secretion (33, 44). Silencing of syt 9 strongly inhibited insulin release from islet β-cells and INS-1E cells (56). However, mice with a pancreas-specific knock-out of syt 9 had normal glucose homeostasis and showed no changes in other insulin-dependent functions (57).

CA^{2+} NON-BINDERS

Slightly more than half of the mammalian syts have non-acidic amino acids at some of the positions engaged in Ca^{2+} binding (35), and these isoforms fail to act as Ca^{2+} sensors in liposome fusion assays (40). The best characterized of these, syt 4, harbors an evolutionarily conserved serine-for-aspartate substitution at a Ca^{2+} ligand in the C2A domain (58). Syt 4 is widely expressed in endocrine cells and its expression rises and falls depending on electrical activity (59) and reproductive state (60). Syt 4 negatively regulates both release and Ca^{2+}-dependent liposome fusion (28, 32, 40) and does not bind Ca^{2+} (61). Syt 4 overexpression reduced exocytosis in PC12 cells (28, 32, 62). Although syt 4 overexpression in PC12 cells shortened the lifetimes of fusion pores capable of dilating to full-fusion (28), another form of release was enhanced in which very small fusion pores could open exclusively as kiss-and-run events with exceptionally long lifetimes. Many but not all of the effects of syt 4 overexpression were mimicked by syt 1 harboring the serine-for-alanine Ca^{2+} ligand replacement seen in syt 4 (29). Syt 4 overexpression also favored kiss-and-run in MIN6 β-cells (31). Ablation of the syt 4 gene altered exocytosis and fusion pore properties in posterior pituitary nerve terminals. These results suggested that syt 4 reduced exocytosis in response to modest Ca^{2+} rises but enhanced exocytosis in response to large Ca^{2+} rises (63). Syt 4 also contributes to the maturation of DCVs (64, 65), and altering syt 4 levels changes DCV size (62, 63, 66).

The Ca^{2+} non-binding isoforms syt 4, 8, and 13 have been detected in insulin-secreting cells (67–69). Silencing syt 4 and 13 reduced glucose stimulated insulin secretion in INS1 cells (69). Glucose stimulated expression of the syt 8 gene in human islets and syt 8 knock-down impaired both basal and evoked insulin release (70). Since syt 8 fails to stimulate liposome fusion in a Ca^{2+}-dependent manner (40) the precise role of syt 8 in insulin secretion remains unclear. One intriguing possibility is that syt 8 increases the relative proportion of full-fusion events so that fusion pores can grow large enough to allow insulin to escape. It is likely that the Ca^{2+} non-binders interact with other components of the release machinery in ways that remain to be elucidated. These interactions could allow syts to regulate release in ways that cannot as yet be explained in terms of their biochemical properties.

Reports vary regarding the expression of other syt isoforms in endocrine cells (**Table 1**) and little is known about their localization and functions in hormone release. Syt 2 has been reported in the hypothalamus (71) but is absent from endocrine cells, and its primary function is likely to be as a synaptic Ca^{2+} sensor (72, 73).

SPECIFICITY OF CA^{2+} SIGNALING

The differences in performance of syts as Ca^{2+} sensors gives a special significance to the spatiotemporal character of Ca^{2+} signals in different cell types and with different forms of stimuli. Ca^{2+} can enter cells through a variety of routes so that the dynamics and spatial extent of changes in cytosolic Ca^{2+} can vary enormously. This creates a scenario in which differences in Ca^{2+} sensing properties can have a major impact on responses (74). Intracellular Ca^{2+} rises and falls as Ca^{2+} enters through Ca^{2+} channels, diffuses away from these sources into the cytoplasm, binds Ca^{2+} binding proteins, and is sequestered into stores or pumped out of the cytoplasm (75–77). The opening of one voltage gated Ca^{2+} channel allows approximately 10^3 ions to enter per msec. This localized flux sets up a steep gradient to create a domain of high local Ca^{2+} concentration. In the immediate vicinity of the channel mouth (within tens of nanometer) Ca^{2+} can rise to $>100\,\mu M$, which is substantially higher than the average bulk cytoplasmic level, even under conditions of intense stimulation (75, 78). These Ca^{2+} domains around a Ca^{2+} channel can form and collapse rapidly (within a few ms) so that the activation of a Ca^{2+} sensor will depend critically on the kinetics of Ca^{2+} association and dissociation. A low-affinity sensor can detect this high local Ca^{2+} as long as it binds with rapid kinetics. A high affinity Ca^{2+} sensor may fail to respond if it binds too slowly. Syt 1 has properties suited for responding to transient domains with high Ca^{2+}. Syt 7 has properties suited for responding to modest but prolonged rises in bulk Ca^{2+} concentration (38).

The idea of localized Ca^{2+} signals leads to two types of Ca^{2+} concentration profile illustrated in **Figure 1**. When an endocrine cell fires at a moderate rate, Ca^{2+} domains form and collapse around a few open Ca^{2+} channels as shown in **Figure 1A**. The resulting brief period of high Ca^{2+} concentration will only affect vesicles near the open channels, and will preferentially activate syt 1 over slower isoforms. Basal firing rates corresponding to the resting state of an animal (feed and breed) have been shown

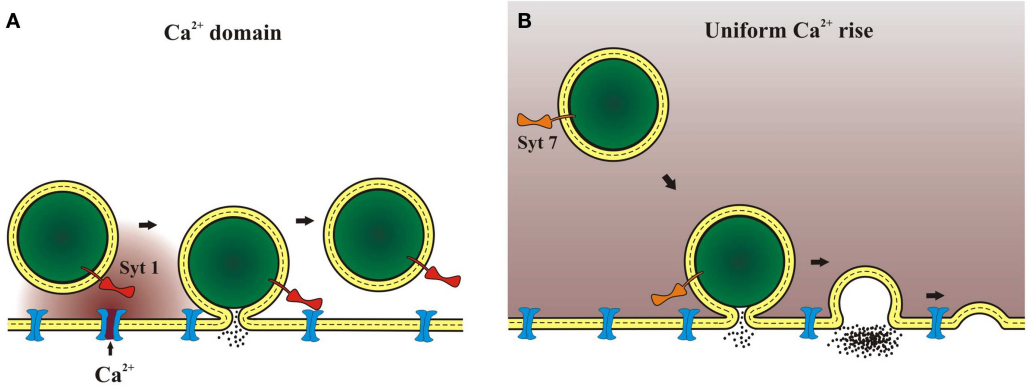

FIGURE 1 | Ca^{2+} domains and release mechanisms. **(A)** Weak stimulation opens Ca^{2+} channels less frequently. One isolated channel can open and as Ca^{2+} flows a domain of high Ca^{2+} concentration will form around the channel mouth. This will lead to a highly localized Ca^{2+} signal that will persist for milliseconds. A Ca^{2+} sensor such as syt 1, with its rapid kinetics and low affinity, can be activated by a Ca^{2+} signal of this form. **(B)** Strong stimulation opens many Ca^{2+} channels to raise bulk Ca^{2+}. Bulk Ca^{2+} can also rise as a result of Ca^{2+} release from internal stores. After the stimulus ends the Ca^{2+} gradients around individual vesicles will collapse as Ca^{2+} diffuses through the cytoplasm away from the membrane. This will lead to a more uniform, moderate concentration that can persist for seconds. A Ca^{2+} sensor such as syt 7, with its slow kinetics and high affinity, can be activated by a Ca^{2+} signal of this form.

to trigger norepinephrine release from chromaffin cells without triggering chromogranin release (11). This implicates exocytosis by kiss-and-run, which is preferentially triggered by syt 1 (32). By contrast, with vigorous electrical activity during stress (fight and flight) the bulk Ca^{2+} concentration will rise to moderate levels (well under 50 μM) for longer times on the order of seconds (**Figure 1B**). These signals will activate slow, low-affinity Ca^{2+} sensors such as syt 7. This form of [Ca^{2+}] signal has been shown to trigger full-fusion (79), with release of both norepinephrine and chromogranin (11). This can be explained by the tendency of syt 7 to trigger full-fusion preferentially (32). Different spatiotemporal patterns of cytosolic Ca^{2+} can thus target different syt isoforms to modulate fusion kinetics. Furthermore, because syt isoforms favor different modes of exocytosis, by selectively promoting kiss-and-run or full-fusion, Ca^{2+} signals that activate different syts will determine the relative release of small and large molecules. The sorting of syts to different sized vesicles may also serve as a mechanism for allowing different Ca^{2+} signals to select different substances for release if content is also found to vary with vesicle size (32).

CONCLUSION

Studies of how different syt isoforms influence the kinetics of exocytosis are starting to resolve functionally relevant distinctions in the mechanisms by which Ca^{2+} regulates exocytosis. More studies like these will expand our understanding of the diversity of endocrine release mechanisms, but rigorous assessments of syt isoform function in cells face a number of challenges. (1) It is important to address the expression of multiple isoforms, either by ablating endogenous proteins or varying each isoform individually with careful assessment of protein levels. Overexpression of proteins can result in high protein concentrations, possibly leading to mis-targeting and artificial functions. (2) Experiments need to address the different Ca^{2+} sensitivities of syt isoforms. This requires measurement and control of Ca^{2+} concentration. (3) Biophysical techniques for measuring exocytosis are very sensitive but often measure surrogates of release and detect events on different time scales. Amperometry measures release and can detect rapid processes but its greatest sensitivity is realized with biogenic amines, and is not nearly as powerful in the measurement of peptides. Furthermore, after content expulsion the closure of a fusion pore can no longer be detected, and the mode of release as kiss-and-run or full-fusion can no longer be ascertained. Capacitance measures membrane area, and single-vesicle capacitance steps provide strong evidence for kiss-and-run. Total internal reflectance microscopy of fluorescent tracers follows the fate of the vesicle content or membrane (80). Like capacitance recording, this method can reveal kiss-and-run but its time resolution is poor. Furthermore, the fate of fluorescent cargo can vary with the design of the fusion construct, raising concerns about experimental artifacts (81). Amperometry, capacitance, and total internal reflectance microscopy are very powerful techniques but they do not always agree and these differences can complicate interpretations and comparisons (62).

Given the functional versatility within the syt protein family, the studies to date probably have only scratched the surface in addressing the roles of syt isoforms in the complex and varied forms of hormone release. By selecting among the different syt isoforms and regulating their expression, and by sorting to different vesicles containing different hormones, cells can regulate the response to diverse forms of Ca^{2+} signals. The syt isoforms present on a vesicle will determine what form of Ca^{2+} signal will trigger fusion, how different Ca^{2+} signals direct the choice between kiss-and-run and full-fusion, and what proportion of small and large molecules are released.

ACKNOWLEDGMENTS

This research was supported by NIH grants NS044057 and NS072905. We thank Drs. Xuelin Lou and Edwin Chapman for helpful discussions and comments.

REFERENCES

1. De Camilli P, Jahn R. Pathways to regulated exocytosis in neurons. *Annu Rev Physiol* (1990) **52**:625–45. doi:10.1146/annurev.ph.52.030190.003205
2. Walch-Solimena C, Takei K, Marek KL, Midyett K, Südhof TC, De Camilli P, et al. Synaptotagmin: a membrane constituent of neuropeptide-containing large dense-core vesicles. *J Neurosci* (1993) **13**:3895–903.
3. Brunner Y, Coute Y, Iezzi M, Foti M, Fukuda M, Hochstrasser DF, et al. Proteomics analysis of insulin secretory granules. *Mol Cell Proteomics* (2007) **6**:1007–17. doi:10.1074/mcp.M600443-MCP200
4. Wegrzyn JL, Bark SJ, Funkelstein L, Mosier C, Yap A, Kazemi-Esfarjani P, et al. Proteomics of dense core secretory vesicles reveal distinct protein categories for secretion of neuroeffectors for cell-cell communication. *J Proteome Res* (2010) **9**:5002–24. doi:10.1021/pr1003104
5. Sudhof TC, Rothman JE. Membrane fusion: grappling with SNARE and SM proteins. *Science* (2009) **323**:474–7. doi:10.1126/science.1161748
6. Jahn R, Scheller RH. SNAREs – engines for membrane fusion. *Nat Rev Mol Cell Biol* (2006) **7**:631–43. doi:10.1038/nrm2002
7. Jahn R, Fasshauer D. Molecular machines governing exocytosis of synaptic vesicles. *Nature* (2012) **490**:201–7. doi:10.1038/nature11320
8. Martin TF. Tuning exocytosis for speed: fast and slow modes. *Biochim Biophys Acta* (2003) **1641**:157–65. doi:10.1016/S0167-4889(03)00093-4
9. Winkler H, Westhead E. The molecular organization of adrenal chromaffin granules. *Neuroscience* (1980) **5**:1803–23. doi:10.1016/0306-4522(80)90031-7
10. Hokfelt T, Broberger C, Xu ZQ, Sergeyev V, Ubink R, Diez M. Neuropeptides – an overview. *Neuropharmacology* (2000) **39**:1337–56. doi:10.1016/S0028-3908(00)00010-1
11. Fulop T, Radabaugh S, Smith C. Activity-dependent differential transmitter release in mouse adrenal chromaffin cells. *J Neurosci* (2005) **25**:7324–32. doi:10.1523/JNEUROSCI.2042-05.2005
12. MacDonald PE, Braun M, Galvanovskis J, Rorsman P. Release of small transmitters through kiss-and-run fusion pores in rat pancreatic beta cells. *Cell Metab* (2006) **4**:283–90. doi:10.1016/j.cmet.2006.08.011
13. Whim MD. Near simultaneous release of classical and peptide cotransmitters from chromaffin cells. *J Neurosci* (2006) **26**:6637–42. doi:10.1523/JNEUROSCI.5100-05.2006
14. Perello M, Stuart R, Nillni EA. Prothyrotropin-releasing hormone targets its processing products to different vesicles of the secretory pathway. *J Biol Chem* (2008) **283**:19936–47. doi:10.1074/jbc.M800732200
15. Sossin WS, Scheller RH. Biosynthesis and sorting of neuropeptides. *Curr Opin Neurobiol* (1991) **1**:79–83. doi:10.1016/0959-4388(91)90013-W
16. Alvarez de Toledo G, Fernández-Chacón R, Fernández JM. Release of secretory products during transient vesicle fusion. *Nature* (1993) **363**:554–8. doi:10.1038/363554a0
17. Fernandez JM, Neher E, Gomperts BD. Capacitance measurements reveal stepwise fusion events in degranulating mast cells. *Nature* (1984) **312**:453–5. doi:10.1038/312453a0
18. Klyachko VA, Jackson MB. Capacitance steps and fusion pores of small and large-dense-core vesicles in nerve terminals. *Nature* (2002) **418**:89–92. doi:10.1038/nature00852
19. Neher E, Marty A. Discrete changes of cell membrane capacitance observed under conditions of enhanced secretion in bovine adrenal chromaffin cells. *Proc Natl Acad Sci U S A* (1982) **79**:6712–6. doi:10.1073/pnas.79.21.6712
20. Kim T, Gondré-Lewis MC, Arnaoutova I, Loh YP. Dense-core secretory granule biogenesis. *Physiology (Bethesda)* (2006) **21**:124–33. doi:10.1152/physiol.00043.2005
21. Augustine GJ. How does calcium trigger neurotransmitter release? *Curr Opin Neurobiol* (2001) **11**:320–6. doi:10.1016/S0959-4388(00)00214-2
22. Chapman ER. How does synaptotagmin trigger neurotransmitter release? *Annu Rev Biochem* (2008) **77**:615–41. doi:10.1146/annurev.biochem.77.062005.101135
23. Koh TW, Bellen HJ. Synaptotagmin I, a Ca2+ sensor for neurotransmitter release. *Trends Neurosci* (2003) **26**:413–22. doi:10.1016/S0166-2236(03)00195-4
24. Ales E, Tabares L, Poyato JM, Valero V, Lindau M, Alvarez de Toledo G. High calcium concentrations shift the mode of exocytosis to the kiss-and-run mechanism. *Nat Cell Biol* (1999) **1**:40–4. doi:10.1038/9012
25. Fernandez-Chacon R, Alvarez de Toledo G. Cytosolic calcium facilitates release of secretory products after exocytotic vesicle fusion. *FEBS Lett* (1995) **363**:221–5. doi:10.1016/0014-5793(95)00319-5
26. Wang CT, Bai J, Chang PY, Chapman ER, Jackson MB. Synaptotagmin-Ca^{2+} triggers two sequential steps in regulated exocytosis in rat PC12 cells: fusion pore opening and fusion pore dilation. *J Physiol* (2006) **570**:295–307.
27. Bai J, Wang CT, Richards DA, Jackson MB, Chapman ER. Fusion pore dynamics are regulated by synaptotagmin*t-SNARE interactions. *Neuron* (2004) **41**:929–42. doi:10.1016/S0896-6273(04)00117-5
28. Wang CT, Grishanin R, Earles CA, Chang PY, Martin TF, Chapman ER, et al. Synaptotagmin modulation of fusion pore kinetics in regulated exocytosis of dense-core vesicles. *Science* (2001) **294**:1111–5. doi:10.1126/science.1064002
29. Wang CT, Lu JC, Bai J, Chang PY, Martin TF, Chapman ER, et al. Different domains of synaptotagmin control the choice between kiss-and-run and full fusion. *Nature* (2003) **424**:943–7. doi:10.1038/nature01857
30. Zhang Z, Hui E, Chapman ER, Jackson MB. Regulation of exocytosis and fusion pores by synaptotagmin-effector interactions. *Mol Biol Cell* (2010) **21**:2821–31. doi:10.1091/mbc.E10-04-0285
31. Tsuboi T, Rutter GA. Multiple forms of "kiss-and-run" exocytosis revealed by evanescent wave microscopy. *Curr Biol* (2003) **13**:563–7. doi:10.1016/S0960-9822(03)00176-3
32. Zhang Z, Wu Y, Wang Z, Dunning FM, Rehfuss J, Ramanan D, et al. Release mode of large and small dense-core vesicles specified by different synaptotagmin isoforms in PC12 cells. *Mol Biol Cell* (2011) **22**:2324–36. doi:10.1091/mbc.E11-02-0159
33. Zhu D, Zhou W, Liang T, Yang F, Zhang RY, Wu ZX, et al. Synaptotagmin I and IX function redundantly in controlling fusion pore of large dense core vesicles. *Biochem Biophys Res Commun* (2007) **361**:922–7. doi:10.1016/j.bbrc.2007.07.083
34. Ubach J, Zhang X, Shao X, Sudhof TC, Rizo J. Ca2+ binding to synaptotagmin: how many Ca2+ ions bind to the tip of a C2-domain? *EMBO J* (1998) **17**:3921–30. doi:10.1093/emboj/17.14.3921
35. Craxton M. A manual collection of Syt, Esyt, Rph3a, Rph3al, Doc2, and Dblc2 genes from 46 metazoan genomes – an open access resource for neuroscience and evolutionary biology. *BMC Genomics* (2010) **11**:37. doi:10.1186/1471-2164-11-37
36. Marqueze B, Berton F, Seagar M. Synaptotagmins in membrane traffic: which vesicles do the tagmins tag? *Biochimie* (2000) **82**:409–20. doi:10.1016/S0300-9084(00)00220-0
37. Sudhof TC. Synaptotagmins: why so many? *J Biol Chem* (2002) **277**:7629–32. doi:10.1074/jbc.R100052200
38. Hui E, Bai J, Wang P, Sugimori M, Llinas RR, Chapman ER. Three distinct kinetic groupings of the synaptotagmin family: candidate sensors for rapid and delayed exocytosis. *Proc Natl Acad Sci U S A* (2005) **102**:5210–4. doi:10.1073/pnas.0500941102
39. Bhalla A, Tucker WC, Chapman ER. Synaptotagmin isoforms couple distinct ranges of Ca^{2+}, Ba^{2+}, and Sr^{2+} concentration to SNARE-mediated membrane fusion. *Mol Biol Cell* (2005) **16**:4755–64. doi:10.1091/mbc.E05-04-0277
40. Bhalla A, Chicka MC, Chapman ER. Analysis of the synaptotagmin family during reconstituted membrane fusion. Uncovering a class of inhibitory isoforms. *J Biol Chem* (2008) **283**:21799–807. doi:10.1074/jbc.M709628200
41. Li C, Ullrich B, Zhang JZ, Anderson RG, Brose N, Südhof TC. Ca(2+)-dependent and -independent activities of neural and non-neural synaptotagmins. *Nature* (1995) **375**:594–9. doi:10.1038/375594a0
42. Sugita S, Shin OH, Han W, Lao Y, Sudhof TC. Synaptotagmins form a hierarchy of exocytotic Ca(2+) sensors with distinct Ca(2+) affinities. *EMBO J* (2002) **21**:270–80. doi:10.1093/emboj/21.3.270
43. Shoji-Kasai Y, Yoshida A, Sato K, Hoshino T, Ogura A, Kondo S, et al. Neurotransmitter release from synaptotagmin-deficient clonal variants of PC12 cells. *Science* (1992) **256**:1821–3.
44. Lynch KL, Martin TF. Synaptotagmins I and IX function redundantly in regulated exocytosis but not endocytosis in PC12 cells. *J Cell Sci* (2007) **120**:617–27. doi:10.1242/jcs.03375

45. Lynch KL, Gerona RR, Kielar DM, Martens S, McMahon HT, Martin TF. Synaptotagmin-1 utilizes membrane bending and SNARE binding to drive fusion pore expansion. *Mol Biol Cell* (2008) **19**:5093–103. doi:10.1091/mbc.E08-03-0235
46. Voets T, Moser T, Lund PE, Chow RH, Geppert M, Sudhof TC, et al. Intracellular calcium dependence of large dense-core vesicle exocytosis in the absence of synaptotagmin I. *Proc Natl Acad Sci U S A* (2001) **98**:11680–5. doi:10.1073/pnas.201398798
47. Schonn JS, Maximov A, Lao Y, Sudhof TC, Sorensen JB. Synaptotagmin-1 and -7 are functionally overlapping Ca2+ sensors for exocytosis in adrenal chromaffin cells. *Proc Natl Acad Sci U S A* (2008) **105**:3998–4003. doi:10.1073/pnas.0712373105
48. Sorensen JB, Fernandez-Chacon R, Sudhof TC, Neher E. Examining synaptotagmin 1 function in dense core vesicle exocytosis under direct control of Ca2+. *J Gen Physiol* (2003) **122**:265–76. doi:10.1085/jgp.200308855
49. Wen H, Linhoff MW, McGinley MJ, Li GL, Corson GM, Mandel G, et al. Distinct roles for two synaptotagmin isoforms in synchronous and asynchronous transmitter release at zebrafish neuromuscular junction. *Proc Natl Acad Sci U S A* (2010) **107**:13906–11. doi:10.1073/pnas.1008598107
50. Gustavsson N, Lao Y, Maximov A, Chuang JC, Kostromina E, Repa JJ, et al. Impaired insulin secretion and glucose intolerance in synaptotagmin-7 null mutant mice. *Proc Natl Acad Sci U S A* (2008) **105**:3992–7. doi:10.1073/pnas.0711700105
51. Gustavsson N, Wei SH, Hoang DN, Lao Y, Zhang Q, Radda GK, et al. Synaptotagmin-7 is a principal Ca^{2+} sensor for Ca^{2+}-induced glucagon exocytosis in pancreas. *J Physiol* (2009) **587**:1169–78. doi:10.1113/jphysiol.2008.168005
52. Li Y, Wang P, Xu J, Gorelick F, Yamazaki H, Andrews N, et al. Regulation of insulin secretion and GLUT4 trafficking by the calcium sensor synaptotagmin VII. *Biochem Biophys Res Commun* (2007) **362**:658–64. doi:10.1016/j.bbrc.2007.08.023
53. Fukuda M, Sagi-Eisenberg R. Confusion in the nomenclature of synaptotagmins V and IX. *Calcium Bind Proteins* (2008) **3**:1–4.
54. Fukuda M, Kowalchyk JA, Zhang X, Martin TF, Mikoshiba K. Synaptotagmin IX regulates Ca2+-dependent secretion in PC12 cells. *J Biol Chem* (2002) **277**:4601–4. doi:10.1074/jbc.C100588200
55. Tucker WC, Edwardson JM, Bai J, Kim HJ, Martin TF, Chapman ER. Identification of synaptotagmin effectors via acute inhibition of secretion from cracked PC12 cells. *J Cell Biol* (2003) **162**:199–209. doi:10.1083/jcb.200302060
56. Iezzi M, Eliasson L, Fukuda M, Wollheim CB. Adenovirus-mediated silencing of synaptotagmin 9 inhibits Ca2+-dependent insulin secretion in islets. *FEBS Lett* (2005) **579**:5241–6. doi:10.1016/j.febslet.2005.08.047
57. Gustavsson N, Wang X, Wang Y, Seah T, Xu J, Radda GK, et al. Neuronal calcium sensor synaptotagmin-9 is not involved in the regulation of glucose homeostasis or insulin secretion. *PLoS One* (2010) **5**:e15414. doi:10.1371/journal.pone.0015414
58. von Poser C, Ichtchenko K, Shao X, Rizo J, Sudhof TC. The evolutionary pressure to inactivate. A subclass of synaptotagmins with an amino acid substitution that abolishes Ca2+ binding. *J Biol Chem* (1997) **272**:14314–9. doi:10.1074/jbc.272.22.14314
59. Vician L, Lim IK, Ferguson G, Tocco G, Baudry M, Herschman HR. Synaptotagmin IV is an immediate early gene induced by depolarization in PC12 cells and in brain. *Proc Natl Acad Sci U S A* (1995) **92**:2164–8. doi:10.1073/pnas.92.6.2164
60. Poopatanapong A, Teramitsu I, Byun JS, Vician LJ, Herschman HR, White SA. Singing, but not seizure, induces synaptotagmin IV in zebra finch song circuit nuclei. *J Neurobiol* (2006) **66**:1613–29. doi:10.1002/neu.20329
61. Dai H, Shin OH, Machius M, Tomchick DR, Sudhof TC, Rizo J. Structural basis for the evolutionary inactivation of Ca^{2+} binding to synaptotagmin 4. *Nat Struct Mol Biol* (2004) **11**:844–9. doi:10.1038/nsmb817
62. Zhang Z, Zhang Z, Jackson MB. Synaptotagmin IV modulation of vesicle size and fusion pores in PC12 cells. *Biophys J* (2010) **98**:968–78. doi:10.1016/j.bpj.2009.11.024
63. Zhang Z, Bhalla A, Dean C, Chapman ER, Jackson MB. Synaptotagmin IV: a multifunctional regulator of peptidergic nerve terminals. *Nat Neurosci* (2009) **12**:163–71. doi:10.1038/nn.2252
64. Ahras M, Otto GP, Tooze SA. Synaptotagmin IV is necessary for the maturation of secretory granules in PC12 cells. *J Cell Biol* (2006) **173**(2):242–51. doi:10.1083/jcb.200506163
65. Eaton BA, Haugwitz M, Lau D, Moore HP. Biogenesis of regulated exocytotic carriers in neuroendocrine cells. *J Neurosci* (2000) **20**:7334–44.
66. Wang P, Wang CT, Bai J, Jackson MB, Chapman ER. Mutations in the effector binding loops in the C2A and C2B domains of synaptotagmin I disrupt exocytosis in a nonadditive manner. *J Biol Chem* (2003) **278**:47030–7. doi:10.1074/jbc.M306728200
67. Gut A, Kiraly CE, Fukuda M, Mikoshiba K, Wollheim CB, Lang J. Expression and localisation of synaptotagmin isoforms in endocrine beta-cells: their function in insulin exocytosis. *J Cell Sci* (2001) **114**:1709–16.
68. Monterrat C, Boal F, Grise F, Hemar A, Lang J. Synaptotagmin 8 is expressed both as a calcium-insensitive soluble and membrane protein in neurons, neuroendocrine and endocrine cells. *Biochim Biophys Acta* (2006) **1763**:73–81. doi:10.1016/j.bbamcr.2005.11.008
69. Andersson SA, Olsson AH, Esguerra JL, Heimann E, Ladenvall C, Edlund A, et al. Reduced insulin secretion correlates with decreased expression of exocytotic genes in pancreatic islets from patients with type 2 diabetes. *Mol Cell Endocrinol* (2012) **364**:36–45. doi:10.1016/j.mce.2012.08.009
70. Xu Z, Wei G, Chepelev I, Zhao K, Felsenfeld G. Mapping of INS promoter interactions reveals its role in long-range regulation of SYT8 transcription. *Nat Struct Mol Biol* (2011) **18**:372–8. doi:10.1038/nsmb.1993
71. Xi D, Chin H, Gainer H. Analysis of synaptotagmin I-IV messenger RNA expression and developmental regulation in the rat hypothalamus and pituitary. *Neuroscience* (1999) **88**:425–35. doi:10.1016/S0306-4522(98)00234-6
72. Kochubey O, Schneggenburger R. Synaptotagmin increases the dynamic range of synapses by driving Ca(2)+-evoked release and by clamping a near-linear remaining Ca(2)+ sensor. *Neuron* (2011) **69**:736–48. doi:10.1016/j.neuron.2011.01.013
73. Sun J, Pang ZP, Qin D, Fahim AT, Adachi R, Südhof TC. A dual-Ca2+-sensor model for neurotransmitter release in a central synapse. *Nature* (2007) **450**:676–82. doi:10.1038/nature06308
74. Kasai H. Comparative biology of Ca2+-dependent exocytosis: implications of kinetic diversity for secretory function. *Trends Neurosci* (1999) **22**:88–93. doi:10.1016/S0166-2236(98)01293-4
75. Neher E. Vesicle pools and Ca2+ microdomains: new tools for understanding their roles in neurotransmitter release. *Neuron* (1998) **20**:389–99. doi:10.1016/S0896-6273(00)80983-6
76. Neher E. Usefulness and limitations of linear approximations to the understanding of Ca++ signals. *Cell Calcium* (1998) **24**:345–57. doi:10.1016/S0143-4160(98)90058-6
77. Augustine GJ, Santamaria F, Tanaka K. Local calcium signaling in neurons. *Neuron* (2003) **40**:331–46. doi:10.1016/S0896-6273(03)00639-1
78. Yamada WM, Zucker RS. Time course of transmitter release calculated from simulations of a calcium diffusion model. *Biophys J* (1992) **61**:671–82. doi:10.1016/S0006-3495(92)81872-6
79. Elhamdani A, Azizi F, Artalejo CR. Double patch clamp reveals that transient fusion (kiss-and-run) is a major mechanism of secretion in calf adrenal chromaffin cells: high calcium shifts the mechanism from kiss-and-run to complete fusion. *J Neurosci* (2006) **26**:3030–6. doi:10.1523/JNEUROSCI.5275-05.2006
80. Michael DJ, Cai H, Xiong W, Ouyang J, Chow RH. Mechanisms of peptide hormone secretion. *Trends Endocrinol Metab* (2006) **17**:408–15. doi:10.1016/j.tem.2006.10.011
81. Michael DJ, Geng X, Cawley NX, Loh YP, Rhodes CJ, Drain P, et al. Fluorescent cargo proteins in pancreatic beta-cells: design determines secretion kinetics at exocytosis. *Biophys J* (2004) **87**:L03–5. doi:10.1529/biophysj.104.052175
82. Mizuta M, Inagaki N, Nemoto Y, Matsukura S, Takahashi M, Seino S. Synaptotagmin III is a novel isoform of rat synaptotagmin expressed in endocrine and neuronal cells. *J Biol Chem* (1994) **269**:11675–8.
83. Saegusa C, Fukuda M, Mikoshiba K. Synaptotagmin V is targeted to dense-core vesicles that undergo calcium-dependent exocytosis in PC12 cells. *J Biol*

Chem (2002) **277**:24499–505. doi:10.1074/jbc.M202767200
84. Matsuoka H, Harada K, Nakamura J, Fukuda M, Inoue M. Differential distribution of synaptotagmin-1, -4, -7, and -9 in rat adrenal chromaffin cells. *Cell Tissue Res* (2011) **344**:41–50. doi:10.1007/s00441-011-1131-8
85. Hu ZT, Chen MR, Ping Z, Dong YM, Zhang RY, Xu T, et al. Synaptotagmin IV regulates dense core vesicle (DCV) release in LbetaT2 cells. *Biochem Biophys Res Commun* (2008) **371**:781–6. doi:10.1016/j.bbrc.2008.04.174
86. Kreft M, Kuster V, Grilc S, Rupnik M, Milisav I, Zorec R. Synaptotagmin I increases the probability of vesicle fusion at low [Ca2+] in pituitary cells. *Am J Physiol Cell Physiol* (2003) **284**:C547–54. doi:10.1152/ajpcell.00333.2002
87. Gao Z, Reavey-Cantwell J, Young RA, Jegier P, Wolf BA. Synaptotagmin III/VII isoforms mediate Ca2+-induced insulin secretion in pancreatic islet beta-cells. *J Biol Chem* (2000) **275**:36079–85. doi:10.1074/jbc.M004284200
88. Mizuta M, Kurose T, Miki T, Shoji-Kasai Y, Takahashi M, Seino S, et al. Localization and functional role of synaptotagmin III in insulin secretory vesicles in pancreatic beta-cells. *Diabetes* (1997) **46**:2002–6. doi:10.2337/diabetes.46.12.2002
89. Iezzi M, Kouri G, Fukuda M, Wollheim CB. Synaptotagmin V and IX isoforms control Ca2+-dependent insulin exocytosis. *J Cell Sci* (2004) **117**:3119–27. doi:10.1242/jcs.01179
90. Brown H, Meister B, Deeney J, Corkey BE, Yang SN, Larsson O, et al. Synaptotagmin III isoform is compartmentalized in pancreatic beta-cells and has a functional role in exocytosis. *Diabetes* (2000) **49**:383–91. doi:10.2337/diabetes.49.3.383
91. Lang J, Fukuda M, Zhang H, Mikoshiba K, Wollheim CB. The first C2 domain of synaptotagmin is required for exocytosis of insulin from pancreatic beta-cells: action of synaptotagmin at low micromolar calcium. *EMBO J* (1997) **16**:5837–46. doi:10.1093/emboj/16.19.5837

Conflict of Interest Statement: The authors declare that the research was conducted in the absence of any commercial or financial relationships that could be construed as a potential conflict of interest.

Received: 23 June 2013; accepted: 31 August 2013; published online: 18 September 2013.
*Citation: Moghadam PK and Jackson MB (2013) The functional significance of synaptotagmin diversity in neuroendocrine secretion. Front. Endocrinol. **4**:124. doi: 10.3389/fendo.2013.00124*
This article was submitted to Neuroendocrine Science, a section of the journal Frontiers in Endocrinology.

frontiers in
ENDOCRINOLOGY

REVIEW ARTICLE
published: 17 September 2013
doi: 10.3389/fendo.2013.00125

Lipids in regulated exocytosis: what are they doing?

Mohamed Raafet Ammar, Nawal Kassas, Sylvette Chasserot-Golaz, Marie-France Bader and Nicolas Vitale*

Institut des Neurosciences Cellulaires et Intégratives (INCI), UPR-3212 Centre National de la Recherche Scientifique, Université de Strasbourg, Strasbourg, France

Edited by:
Stephane Gasman, Centre National de la Recherche Scientifique, France

Reviewed by:
Thomas F. J. Martin, University of Wisconsin, USA
Frederic A. Meunier, University of Queensland, Australia

***Correspondence:**
Nicolas Vitale, Institut des Neurosciences Cellulaires et Intégratives (INCI), UPR-3212 Centre National de la Recherche Scientifique, Université de Strasbourg, 5 rue Blaise Pascal, 67084 Strasbourg, France
e-mail: vitalen@inci-cnrs.unistra.fr

The regulated secretory pathway in neuroendocrine cells ends with the release of hormones and neurotransmitters following a rise in cytosolic calcium. This process known as regulated exocytosis involves the assembly of soluble *N*-ethylmaleimide-sensitive factor attachment protein receptor (SNARE) proteins, the synaptic vesicle VAMP (synaptobrevin), and the plasma membrane proteins syntaxin and SNAP-25. Although there is much evidence suggesting that SNARE proteins play a key role in the fusion machinery, other cellular elements regulating the kinetics, the extent of fusion, and the preparation of vesicle for release have received less attention. Among those factors, lipids have also been proposed to play important functions both at the level of secretory vesicle recruitment and late membrane fusion steps. Here, we will review the latest evidence supporting the concept of the fusogenic activity of lipids, and also discuss how this may be achieved. These possibilities include the recruitment and sequestration of the components of the exocytotic machinery, regulation of protein function, and direct effects on membrane topology.

Keywords: cholesterol, phosphatidic acids, phosphoinositides, exocytosis, membrane fusion, chromaffin cell

INTRODUCTION: A ROLE FOR LIPID IN EXOCYTOSIS?

Release of hormones from neuroendocrine cells occurs through exocytosis, a process in which specialized vesicles (secretory granules) fuse with the plasma membrane in response to extrinsic stimuli leading to elevated cytosolic calcium. Chromaffin cells have proven to be a valuable model for unraveling the molecular mechanisms underlying this fundamental membrane fusion event (1). In these cells, secretory granules are first transported from the Golgi area to the cell periphery where they are then docked at the plasma membrane in two apparent stages: a non-primed (fusion incompetent) and a primed (fusion competent) state. Details of the molecular machinery underlying some of these steps have been described (2). For instance, once tethered to the plasma membrane, docking of granules is mediated by soluble *N*-ethylmaleimide-sensitive factor (NSF) attachment protein receptors (SNAREs) found on granules (v-SNAREs) and on the plasma membrane (t-SNAREs). Through coiled-coil interactions, these proteins form a stable complex that provides the energy necessary to pull membranes into close proximity rendering them fusion competent (3). The mechanism of membrane fusion *per se* is however an aspect that continues to be debated. SNAREs are able to drive membrane fusion *in vitro* (4), but with relatively slow kinetics suggesting that additional factors are required for physiological membrane fusion. Recently, the SNARE accessory protein Munc18 was shown to increase the speed of SNARE-mediated fusion (5). Lipids, the prime constituents of the fusing membranes, are also obvious candidates to accelerate the fusion process. The first lipid firmly demonstrated to be critical for exocytosis was phosphatidylinositol-4,5-bisphosphate [PtdIns(4,5)P_2], for review, see Ref. (6), and more recently fatty acids have been suggested to play an important function in neurotransmitter release from synaptic vesicles (7). Growing evidence also support a role for cholesterol and phosphatidic acid (PA) during exocytosis, for review, see Ref. (8). Hence, many observations are in agreement with the notion that lipids contribute at different levels to exocytosis. The issues now arising concern the precise step in the dynamic exocytotic process in which a given lipid actually functions.

LIPIDS ARE INVOLVED THROUGHOUT THE SEQUENTIAL STAGES UNDERLYING EXOCYTOSIS

CHOLESTEROL AND PHOSPHATIDYLSERINE FOR DEFINING EXOCYTOSIS SITES

Cholesterol and sphingolipids cluster into discrete microdomains in cellular membranes to form lipid ordered domains. This clustering is triggered by secretagogues at the level of exocytotic sites in chromaffin cells (9). Although cholesterol depletion by methyl-β-cyclodextrin provided the initial evidence for a positive role of cholesterol in exocytosis (10), these experiments are subjected to caution because of the brought structural role of cholesterol in most cellular functions. More compelling evidence supporting a direct role for cholesterol relies on both biochemical and high-resolution imaging observations indicating that SNAREs concentrate in cholesterol-dependent clusters (11). Additionally, a cholesterol-sequestering agent, the polyene antibiotic filipin, that is supposed to have less dramatic effects on membrane structures than methyl-β-cyclodextrin, induces a dose-dependent inhibition of catecholamine secretion and the release from the plasma membrane of annexin A2 which participates in the formation and/or stabilization of GM1-PtdIns(4,5)P_2 enriched domains required for granule recruitment (9, 12). Altogether these findings support the notion that cholesterol is involved in the spatial definition of exocytotic sites.

In the plasma membrane, phosphatidylserine (PS) mostly resides in the inner cytoplasmic leaflet. In non-apoptotic cells, several biological functions are accompanied by a disruption of this phospholipid asymmetry resulting in the externalization of

PS on the outer leaflet of the plasma membrane. This is the case for calcium-regulated exocytosis in neuroendocrine chromaffin and PC12 cells (13, 14). However the functional importance of PS scrambling for secretion is still under debate and the precise kinetics of this translocation is not established. An interesting possibility lies in the fact that PS contributes substantially to the negative charge of the inner leaflet of the plasma membrane. Consequently, PS scrambling at exocytotic sites could modify the protein/lipid interactions occurring during either the course of exocytosis or the early phases of endocytosis, as suggested recently (15).

PHOSPHOINOSITIDES FOR PRIMING SECRETORY VESICLES

Phosphoinositides are a class of phospholipids characterized by an inositol head group that can be phosphorylated on the three, four, and five positions to generate seven distinct species key in cell signaling and trafficking. Much of the work carried out on exocytosis has focused on the role played by PtdIns(4,5)P_2. Indeed a number of pioneer studies indicated that PtdIns(4,5)P_2 positively modulates secretion in neuroendocrine cells (16–18). Using patch clamp experiments on intact chromaffin cells and in parallel analyzing images of plasma membrane lawns, it was subsequently shown that over-expression of the kinase that generates PtdIns(4,5)P_2 causes an increase in the plasmalemmal PtdIns(4,5)P_2 level and secretion, whereas over-expression of a membrane-tagged PtdIns(4,5)P_2 phosphatase eliminates plasmalemmal PtdIns(4,5)P_2 and inhibits secretion (19). Thus, the balance between the generation and degradation rates of the plasmalemmal PtdIns(4,5)P_2 directly regulates the extent of exocytosis from chromaffin cell. Using the phosphatidylinositol 3-kinase inhibitor LY294002, a correlation between the level of the plasma membrane PtdIns(4,5)P_2 and the size of the primed vesicle pool was found (19, 20). Wen et al. (21) further demonstrated that selective inhibition of phosphatidylinositol 3-kinase delta isoform was responsible for this effect. Importantly, such an inhibition promotes a transient rise in PtdIns(4,5)P2 that was sufficient to mobilize secretory vesicles to the plasma membrane via activation of the small GTPase Cdc42 and actin polymerization. More recently, a functional link between PtdIns(4,5)P_2 signaling and secretory vesicle dynamics through *de novo* remodeling of the actin cytoskeleton was also described (22). These observations are consistent with a function of PtdIns(4,5)P_2 as an acute regulator of secretion. PtdIns(4,5)P_2 seems to lie in a key position controlling the size and refilling rate of the primed vesicle pools, but not the fusion rate constants *per se*. In line with this model, we recently reported that the HIV PtdIns(4,5)P_2-binding protein Tat is able to penetrate neuroendocrine cells and accumulate at the plasma membrane through its binding to PtdIns(4,5)P_2. By sequestering plasma membrane PtdIns(4,5)P_2, Tat alters neurosecretion, reducing the number of exocytotic events without significantly affecting kinetic parameters (fusion pore opening, dilatation, and closure) of individual events (23).

Other phosphoinositides seem to act as signaling or recruitment factors to prime secretory vesicles for exocytosis. For instance, experiments carried out on permeabilized chromaffin cells reveal that PtdIns(3)P located on a subpopulation of chromaffin granules positively regulates secretion (21, 24). Extending these observations, PIKfyve kinase that produces PtdIns(3,5)P_2 from PtdIns(3)P on secretory granules was shown to negatively affect exocytosis (25). Hence, these studies highlight a complex regulation of neuroexocytosis by phosphoinositides, with PtdIns(4,5)P_2 and PtdIns(3)P being essential factors promoting ATP-dependent priming in neurosecretory cells. It is intriguing that PtdIns(3,5)P_2 displays an opposite effect, but reveals how fine-tuning of exocytosis by phosphoinositides could potentially control the number of vesicles undergoing priming in response to a stimulation.

PHOSPHATIDIC ACID FOR FUSION

The local formation of PA is a recurring theme in intracellular membrane traffic and its involvement in regulated exocytosis has been suggested in various models, including neuroendocrine cells (14, 26). The development of molecular tools has enabled the identification of phospholipase D1 (PLD1) as the key enzyme responsible for PA synthesis during exocytosis (14, 27). Capacitance recordings from chromaffin cells silenced for PLD1 suggest that PLD1 controls the number of fusion competent secretory granules at the plasma membrane without affecting earlier recruitment or docking steps, leading to the idea that PA acts directly in membrane fusion (28). In agreement with this concept, a molecular sensor for PA revealed local PA accumulation at the plasma membrane near morphologically docked granules at sites of active exocytosis (28).

OTHER LIPIDS

Various other lipids are suspected to take part in regulated exocytosis. Although most of them have been implicated based on *in vitro* membrane fusion assays, some have also been studied in neuroendocrine cells. For instance, diacylglycerol (DAG) increases stimulus-coupled secretion by recruiting vesicles to the immediately releasable pool through the regulation of the vesicle priming protein Munc13-1 (29). Furthermore by activating protein kinase C, DAG may modulate the phosphorylation level of various proteins contributing or regulating the exocytotic machinery, including SNAP-25 and Munc18 (30, 31). Modulating PS levels also directly affects the rate of exocytosis in PC12 cells. Although it is likely that long term provision of high level of PS (incubation with 100 μM for 48 h or over-expression of PS synthase) may affect numerous key cellular functions altogether, it was shown that PS influences exocytosis by enhancing fusion pore opening and slowing fusion pore dilatation in PC12 cells (32). The kinetic changes in exocytosis resulting from elevated PS levels were shown to be unlikely the reflection of an indirect action of PS on Ca^{2+} channels, or vesicle size or number, or the levels of some of the major exocytosis proteins, but may be the consequence of synaptotagmin binding to PS (32). Finally, arachidonic acid produced from different phospholipids by phospholipase A2 and from DAG by DAG-lipase potentiates exocytosis from chromaffin cells (33, 34).

LIPIDS AS RECRUITING COMPONENTS OF THE EXOCYTOTIC MACHINERY

Within membranes, the ability of microdomains to sequester specific proteins and exclude others makes them ideally suited to spatially organize cellular pathways. Cholesterol-enriched microdomains seem to concentrate components of the exocytotic/fusion machinery. For instance, numerous studies of the

distribution of SNARE proteins in various cell types suggest that SNAREs partially associate with detergent resistant, cholesterol-enriched microdomains (11). Palmitoylation appears to be the major targeting signal in these microdomains, as in the case of SNAP-25, although it is likely that other elements contribute to the enrichment of constituents of the exocytotic machinery within these cholesterol microdomains. However despite intense research there is still little known about what lipid or protein molecules are actually present at sites of exocytosis.

Up to 20 proteins potentially involved in regulated exocytosis have been reported to bind PtdIns(4,5)P_2 (35). These include synaptotagmin (36), syntaxin (37), Ca^{2+}-dependent activator protein for secretion (CAPS) (38), and members of the PLD signaling pathway (16, 39, 40). Using immunogold labeling of plasma membrane sheets combined with spatial point pattern analysis, we recently observed that PtdIns(4,5)P_2 microdomains co-localize with SNARE clusters and docked secretory granules (12). Translocation of the PtdIns(4,5)P_2-binding protein annexin A2 to the plasma membrane following cell stimulation is a hallmark of chromaffin cell exocytosis (41). Annexin A2 plays an essential role in calcium-regulated exocytosis by promoting PtdIns(4,5)P_2 and cholesterol-enriched domains containing SNAREs in the vicinity of docked granules (9, 12). Altogether these observation raise the notion that functional exocytotic sites defined by specific lipids such as cholesterol, GM1, and PtdIns(4,5)P_2 are able to recruit and sequester components to build a machine that drives fast and efficient membrane fusion (**Figure 1**).

Molecular details of how PtdIns(4,5)P_2 forms a platform for vesicle recruitment have recently been proposed (42). In this study, synaptotagmin-1 was shown to interact independently of Ca^{2+} with the polybasic linker region of syntaxin-1A already associated with PtdIns(4,5)P_2 at the plasma membrane. When then triggered by Ca^{2+}, this interaction allows the Ca^{2+}-binding sites of synaptotagmin-1 to bind PS in the vesicle membrane, thereby bridging the vesicle membrane close enough for SNARE assembly and subsequent membrane fusion. Interestingly, this polybasic juxtamembrane domain of syntaxin-1A which binds PtdIns(4,5)P_2 has also been shown to tightly bind both PA (37) and PtdIns(3,4,5)P_3 (43). Like PtdIns(4,5)P_2, these anionic lipids can probably recruit syntaxin-1A, and it is tempting to propose that the recruitment of syntaxin isoforms may depend on the type of lipid present. Furthermore, the fact that these lipids can be quickly converted into different forms using kinases, lipases, and phosphatases, such a protein-recruiting mechanism offers a supplementary level of control to adapt the exocytotic machinery to the physiological demands put on the cell. Finally, using super-resolution optical techniques and fluorescence lifetime imaging microscopy, it was shown that distinct t-SNARE intermediate states on the plasma membrane can be patterned by the underlying lipid environment (44). Undoubtedly these high-resolution imaging techniques will be useful to determine how lipids contribute to the organization of the exocytotic platform.

LIPIDS AS REGULATORS OF THE EXOCYTOTIC MACHINERY

PtdIns(4,5)P_2 directly binds to a large subset of proteins from the exocytotic machinery. *In vitro* experiments revealed that at physiological concentrations PtdIns(4,5)P_2 regulates exocytosis by recruiting priming factors such as CAPS, which facilitate SNARE-dependent liposome fusion (45). PtdIns(4,5)P_2 is also a necessary cofactor for PLD1 activity and PA synthesis during exocytosis (39). Finally, PtdIns(4,5)P_2 controls actin polymerization by modulating the activity and targeting of actin regulatory proteins. Indeed the activity of the actin-binding proteins scinderin and gelsolin, two F-actin severing proteins that are constituents of the exocytotic machinery, is regulated by PtdIns(4,5)P_2 (46). A transient increase in PIP2 levels is sufficient to promote the mobilization and recruitment of secretory vesicles to the plasma membrane (22). PIP2 therefore links exocytosis and the actin cytoskeleton by

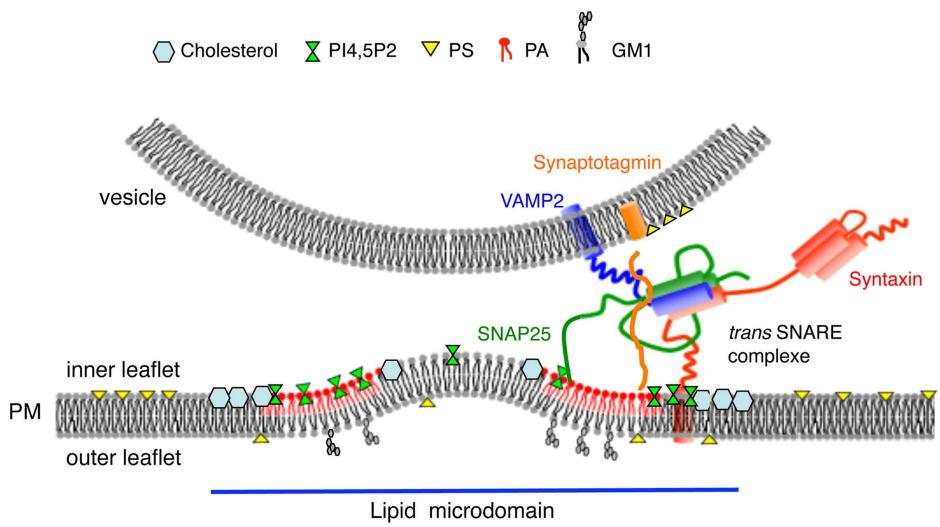

FIGURE 1 | Model highlighting the importance of lipids for membrane fusion. Exocytotic sites defined as cholesterol, GM1, PtdIns(4,5)P_2, and PA enriched microdomains recruit constituents of the docking/fusion machinery and create membrane curvature of the inner leaflet of the plasma membrane prior to promote membrane merging. PtdIns(4,5)P_2 and PA may also regulate SNARE complex assembly and structure.

coordinating the actin-based delivery of secretory vesicles to the exocytotic sites.

Diacylglycerol production through hydrolysis of PtdIns(4,5)P_2 by phospholipase C is mandatory for exocytosis (47). DAG is essential in the priming of exocytosis, owing to the activation of protein kinase C and Munc13, which then modulate the function of syntaxin-1A (29). It is worth to mention that up to 10 different DAG-kinases may also produce DAG from various subcellular pools of PA during exocytosis. Finally DAG is further hydrolyzed by DAG lipases to liberate fatty acids and monoacylglycerols. This pathway is essential for exocytosis as inhibition of DAG lipase blocks exocytosis (48).

Several constituents and regulators of the exocytotic machinery have also been shown to bind to PA, including small GTPases, NSF, and syntaxin-1A (49). PA directly activates these proteins, but evidence that this activation directly contributes to exocytosis remains scarce. PA is also an essential cofactor of phosphatidylinositol-4-phosphate 5-kinase, which produces PtdIns(4,5)P_2, suggesting a possible positive feedback loop in the synthesis of PA and PtdIns(4,5)P_2 (50). Although no direct evidence in neuroendocrine systems have shown that PA directly regulates the assembly or the function of the minimal fusion machinery, *in vitro* reconstituted fusion assays with purified yeast vacuolar SNAREs do so. Indeed experiments performed in a complex reconstituted system including the SNARE chaperones Sec17p/Sec18p, the multifunctional HOPS complex including a subunit of the Sec1-Munc18 family and vacuolar lipids suggest that PA is equally essential for SNARE complex assembly and for fusion. PA has been proposed to facilitate functional interactions among SNAREs and SNARE chaperones (**Figure 1**). Interestingly, in this system, PA could not be replaced by either lipids with small headgroups, such as DAG or acidic lipids, like PS or PI (51).

Arachidonic acid has been described to directly promote the assembly of syntaxin-3 with SNAP-25 and the formation of the ternary SNARE complex (52). Interestingly, omega-3 and omega-6 fatty acids, which play important roles in human health, have be shown to recapitulate this *in vitro* effect of arachidonic acid on SNARE complex formation, suggesting that syntaxins may represent crucial targets of polyunsaturated lipids (52). In other words, polyunsaturated lipids may physiologically regulate SNARE complex assembly and thus exocytosis. Along this same line, sphingosine a releasable backbone of sphingolipids, activates vesicular synaptobrevin facilitating the assembly of SNARE complexes required for membrane fusion (53). It is however important to note that the effects of arachidonic acid and sphingosine observed in these studies are all achieved near or at the CMC value for these lipids, treatments that may also lead to membrane disorganization like detergent action.

LIPIDS AFFECT MEMBRANE TOPOLOGY DURING MEMBRANE FUSION: THE CONCEPT OF FUSOGENIC LIPIDS

The most widely accepted model for membrane fusion, the stalk pore model proposes that the merging of *cis* contacting monolayers gives rise to a negatively curved lipid structure called a stalk. The structure of this stalk depends on the composition of the *cis* monolayers (the outer leaflet of the vesicle and the inner leaflet of the plasma membrane). This model implies that cone-shaped lipids such as cholesterol, DAG, or PA, which have intrinsic negative curvatures, in the *cis* leaflets of contacting bilayers would enhance membrane fusion (54). *Vice versa* inverted cone-shaped lipids (such as PS, gangliosides, or lysophospholipids) should prevent membrane fusion in the *cis* leaflets, but promote fusion when present in the outer leaflets (54). Interestingly, GM1 was found enriched in the outer leaflet of the plasma membrane at the sites of exocytosis in stimulated chromaffin cells (9). These GM1 domains may induce positive membrane curvature in the outer leaflet (55), thereby promoting fusion (**Figure 1**). Reconstituted fusion assays and direct addition of lipids on cultured cells validate the concept that PA, DAG, and cholesterol might promote membrane fusion by changing the spontaneous curvature of membranes [reviewed in (8)]. At physiological concentrations, PtdIns(4,5)P_2 inhibits SNARE-dependent liposome fusion (45), most likely due to its intrinsic positive curvature-promoting properties. However, PtdIns(4,5)P_2 has been described to be converted from an inverted cone-shaped structure to a cone-shaped form in the presence of calcium (56). Thus, in stimulated cells, a local accumulation of PA and PtdIns(4,5)P_2 at granule docking sites where GM1 is in the outer leaflets may well have a synergistic effect on membrane curvature and promote fusion (**Figure 1**). In an alternate mode of changing membrane topology, synaptotagmin has been proposed to facilitate membrane fusion by phase separating PS, a process that is expected to locally buckle bilayers and disorder lipids due to the curvature tendencies of PS (57). It is worth to mention that most of lipid mentioned in this review, also have the ability to flip from one leaflet to another. How this flipping is regulated and how it affects curvature remains an unsolved issue. However, it is likely that the ability of these lipids to interact with the fusion machinery largely controls these flipping properties.

CONCLUSION

As genuine components of the exocytotic machinery, lipids have several advantages over proteins for this task: lipids can directly change the intrinsic fusion properties of membranes, recruit, and/or activate a large number of different proteins to create a local environment in which exocytosis takes place (**Figure 1**). As illustrated in this review, a given lipid can play multiple functions, acting either individually or successively or even simultaneously in concert with other lipids. At the same time, the rapid enzymatic production and degradation of lipids at exocytotic sites allows the cell to remain flexible: by changing the lipid levels, physiological function can be modified within seconds or minutes without the need for protein synthesis or degradation. Over the last decade, *in vitro* reconstituted membrane fusion combined with precise methods to quantify specific lipid species and improved molecular and pharmacological tools to manipulate cellular levels of a given lipid, have lead to a better understanding of the capacities of lipids to promote exocytosis at different steps of the process. For different kinds of vesicles in different cell types, it is likely that the local lipid environment may differentially regulate fusion pore formation, enlargement, and duration, which may in part explain the great variety of fusion kinetics observed *in vivo*. Finally, lipids could also contribute to the tight coupling between exocytosis and the early

stages of membrane retrieval and endocytosis as highlighted in a review of this issue (Houy et al., submitted). Undoubtedly, the next challenge will be to follow individual lipid dynamics at the speed of pore formation and expansion.

ACKNOWLEDGMENTS

We wish to thank Dr. Nancy Grant for critical reading of the manuscript. This work is supported by Agence Nationale pour la Recherche (ANR-09-BLAN-0264-01 grant) to Nicolas Vitale.

REFERENCES

1. Bader MF, Doussau F, Chasserot-Golaz S, Vitale N, Gasman S. Coupling actin and membrane dynamics during calcium-regulated exocytosis: a role for Rho and ARF GTPases. *Biochim Biophys Acta* (2004) **1742**:37–49. doi:10.1016/j.bbamcr.2004.09.028
2. Jahn R, Fasshauer D. Molecular machines governing exocytosis of synaptic vesicles. *Nature* (2012) **490**:201–7. doi:10.1038/nature11320
3. Sutton RB, Fasshauer D, Jahn R, Brunger AT. Crystal structure of a SNARE complex involved in synaptic exocytosis at 2.4 A resolution. *Nature* (1998) **395**:347–53. doi:10.1038/26412
4. Weber T, Zemelman BV, McNew JA, Westermann B, Gmachl M, Parlati F, et al. SNAREpins: minimal machinery for membrane fusion. *Cell* (1998) **92**:759–72. doi:10.1016/S0092-8674(00)81404-X
5. Ma C, Su L, Seven AB, Xu Y, Rizo J. Reconstitution of the vital functions of Munc18 and Munc13 in neurotransmitter release. *Science* (2013) **339**:421–5. doi:10.1126/science.1230473
6. Martin TF. Role of PI(4,5)P(2) in vesicle exocytosis and membrane fusion. *Subcell Biochem* (2012) **59**:111–30. doi:10.1007/978-94-007-3015-1_4
7. Darios F, Connell E, Davletov B. Phospholipases and fatty acid signalling in exocytosis. *J Physiol* (2007) **585**:699–704. doi:10.1113/jphysiol.2007.136812
8. Chasserot-Golaz S, Coorssen JR, Meunier FA, Vitale N. Lipid dynamics in exocytosis. *Cell Mol Neurobiol* (2010) **30**:1335–42. doi:10.1007/s10571-010-9577-x
9. Chasserot-Golaz S, Vitale N, Umbrecht-Jenck E, Knight D, Gerke V, Bader MF. Annexin 2 promotes the formation of lipid microdomains required for calcium-regulated exocytosis of dense-core vesicles. *Mol Biol Cell* (2005) **16**:1108–19. doi:10.1091/mbc.E04-07-0627
10. Chamberlain LH, Burgoyne RD, Gould GW. SNARE proteins are highly enriched in lipid rafts in PC12 cells: implications for the spatial control of exocytosis. *Proc Natl Acad Sci U S A* (2001) **98**:5619–24. doi:10.1073/pnas.091502398
11. Lang T. SNARE proteins and "membrane rafts". *J Physiol* (2007) **585**:693–8. doi:10.1113/jphysiol.2007.134346
12. Umbrecht-Jenck E, Demais V, Calco V, Bailly Y, Bader MF, Chasserot-Golaz S. S100A10-mediated translocation of annexin-A2 to SNARE proteins in adrenergic chromaffin cells undergoing exocytosis. *Traffic* (2010) **11**:958–71. doi:10.1111/j.1600-0854.2010.01065.x
13. Ceridono M, Ory S, Momboisse F, Chasserot-Golaz S, Houy S, Calco V, et al. Selective recapture of secretory granule components after full collapse exocytosis in neuroendocrine chromaffin cells. *Traffic* (2011) **12**:72–88. doi:10.1111/j.1600-0854.2010.01125.x
14. Vitale N, Caumont AS, Chasserot-Golaz S, Du G, Wu S, Sciorra VA, et al. Phospholipase D1: a key factor for the exocytotic machinery in neuroendocrine cells. *EMBO J* (2001) **20**:2424–34. doi:10.1093/emboj/20.10.2424
15. Ory S, Ceridono M, Momboisse F, Houy S, Chasserot-Golaz S, Heintz D, et al. Phospholipid scramblase-1-induced lipid reorganization regulates compensatory endocytosis in neuroendocrine cells. *J Neurosci* (2013) **33**:3545–56. doi:10.1523/JNEUROSCI.3654-12.2013
16. Aikawa Y, Martin TF. ARF6 regulates a plasma membrane pool of phosphatidylinositol(4,5)bisphosphate required for regulated exocytosis. *J Cell Biol* (2003) **162**:647–59. doi:10.1083/jcb.200212142
17. Eberhard DA, Cooper CL, Low MG, Holz RW. Evidence that the inositol phospholipids are necessary for exocytosis. Loss of inositol phospholipids and inhibition of secretion in permeabilized cells caused by a bacterial phospholipase C and removal of ATP. *Biochem J* (1990) **268**:15–25.
18. Holz RW, Hlubek MD, Sorensen SD, Fisher SK, Balla T, Ozaki S, et al. A pleckstrin homology domain specific for phosphatidylinositol 4, 5-bisphosphate (PtdIns-4,5-P2) and fused to green fluorescent protein identifies plasma membrane PtdIns-4,5-P2 as being important in exocytosis. *J Biol Chem* (2000) **275**:17878–85. doi:10.1074/jbc.M000925200
19. Milosevic I, Sorensen JB, Lang T, Krauss M, Nagy G, Haucke V, et al. Plasmalemmal phosphatidylinositol-4,5-bisphosphate level regulates the releasable vesicle pool size in chromaffin cells. *J Neurosci* (2005) **25**:2557–65. doi:10.1523/JNEUROSCI.3761-04.2005
20. Chasserot-Golaz S, Hubert P, Thierse D, Dirrig S, Vlahos CJ, Aunis D, et al. Possible involvement of phosphatidylinositol 3-kinase in regulated exocytosis: studies in chromaffin cells with inhibitor LY294002. *J Neurochem* (1998) **70**:2347–56. doi:10.1046/j.1471-4159.1998.70062347.x
21. Wen PJ, Osborne SL, Morrow IC, Parton RG, Domin J, Meunier FA. Ca2+-regulated pool of phosphatidylinositol-3-phosphate produced by phosphatidylinositol 3-kinase C2alpha on neurosecretory vesicles. *Mol Biol Cell* (2008) **19**:5593–603. doi:10.1091/mbc.E08-06-0595
22. Wen PJ, Osborne SL, Zanin M, Low PC, Wang HT, Schoenwaelder SM, et al. Phosphatidylinositol(4,5)bisphosphate coordinates actin-mediated mobilization and translocation of secretory vesicles to the plasma membrane of chromaffin cells. *Nat Commun* (2011) **2**:491. doi:10.1038/ncomms1500
23. Tryoen-Toth P, Chasserot-Golaz S, Tu A, Gherib P, Bader MF, Beaumelle B, et al. HIV-1 Tat protein inhibits neurosecretion by binding to phosphatidylinositol 4,5-bisphosphate. *J Cell Sci* (2013) **126**:454–63. doi:10.1242/jcs.111658
24. Meunier FA, Osborne SL, Hammond GR, Cooke FT, Parker PJ, Domin J, et al. Phosphatidylinositol 3-kinase C2alpha is essential for ATP-dependent priming of neurosecretory granule exocytosis. *Mol Biol Cell* (2005) **210**:4841–51. doi:10.1091/mbc.E05-02-0171
25. Osborne SL, Wen PJ, Boucheron C, Nguyen HN, Hayakawa M, Kaizawa H, et al. PIKfyve negatively regulates exocytosis in neurosecretory cells. *J Biol Chem* (2008) **283**:2804–13. doi:10.1074/jbc.M704856200
26. Bader MF, Vitale N. Phospholipase D in calcium-regulated exocytosis: lessons from chromaffin cells. *Biochim Biophys Acta* (2009) **1791**:936–41. doi:10.1016/j.bbalip.2009.02.016
27. Waselle L, Gerona RR, Vitale N, Martin TF, Bader MF, Regazzi R. Role of phosphoinositide signaling in the control of insulin exocytosis. *Mol Endocrinol* (2005) **19**:3097–106. doi:10.1210/me.2004-0530
28. Zeniou-Meyer M, Zabari N, Ashery U, Chasserot-Golaz S, Haeberle AM, Demais V, et al. Phospholipase D1 production of phosphatidic acid at the plasma membrane promotes exocytosis of large dense-core granules at a late stage. *J Biol Chem* (2007) **282**:21746–57. doi:10.1074/jbc.M702968200
29. Bauer CS, Woolley RJ, Teschemacher AG, Seward EP. Potentiation of exocytosis by phospholipase C-coupled G-protein-coupled receptors requires the priming protein Munc13-1. *J Neurosci* (2007) **27**:212–9. doi:10.1523/JNEUROSCI.4201-06.2007
30. Barclay JW, Craig TJ, Fisher RJ, Ciufo LF, Evans GJ, Morgan A, et al. Phosphorylation of Munc18 by protein kinase C regulates the kinetics of exocytosis. *J Biol Chem* (2003) **278**:10538–45. doi:10.1074/jbc.M211114200
31. Yang Y, Craig TJ, Chen X, Ciufo LF, Takahashi M, Morgan A, et al. Phosphomimetic mutation of Ser-187 of SNAP-25 increases both syntaxin binding and highly Ca2+-sensitive exocytosis. *J Gen Physiol* (2007) **129**:233–44. doi:10.1085/jgp.200609685
32. Zhang Z, Hui E, Chapman ER, Jackson MB. Phosphatidylserine regulation of Ca2+-triggered exocytosis and fusion pores in PC12 cells. *Mol Biol Cell* (2009) **20**:5086–95. doi:10.1091/mbc.E09-08-0691
33. Latham CF, Osborne SL, Cryle MJ, Meunier FA. Arachidonic acid potentiates exocytosis and allows neuronal SNARE complex to interact with Munc18a. *J Neurochem* (2007) **100**:1543–54.
34. Vitale N. Synthesis of fusogenic lipids through activation of phospholipase D1 by GTPases and the kinase RSK2 is required for calcium-regulated exocytosis in neuroendocrine cells. *Biochem Soc Trans* (2010) **38**:167–71. doi:10.1042/BST0380167

35. Koch M, Holt M. Coupling exo- and endocytosis: an essential role for PIP(2) at the synapse. *Biochim Biophys Acta* (2012) **1821**:1114–32. doi:10.1016/j.bbalip.2012.02.008
36. Schiavo G, Gu QM, Prestwich GD, Sollner TH, Rothman JE. Calcium-dependent switching of the specificity of phosphoinositide binding to synaptotagmin. *Proc Natl Acad Sci U S A* (1996) **93**:13327–32. doi:10.1073/pnas.93.23.13327
37. Lam AD, Tryoen-Toth P, Tsai B, Vitale N, Stuenkel EL. SNARE-catalyzed fusion events are regulated by syntaxin1A-lipid interactions. *Mol Biol Cell* (2008) **19**:485–97. doi:10.1091/mbc.E07-02-0148
38. Loyet KM, Kowalchyk JA, Chaudhary A, Chen J, Prestwich GD, Martin TF. Specific binding of phosphatidylinositol 4,5-bisphosphate to calcium-dependent activator protein for secretion (CAPS), a potential phosphoinositide effector protein for regulated exocytosis. *J Biol Chem* (1998) **273**:8337–43. doi:10.1074/jbc.273.14.8337
39. Du G, Altshuller YM, Vitale N, Huang P, Chasserot-Golaz S, Morris AJ, et al. Regulation of phospholipase D1 subcellular cycling through coordination of multiple membrane association motifs. *J Cell Biol* (2003) **162**:305–15. doi:10.1083/jcb.200302033
40. Liao H, Ellena J, Liu L, Szabo G, Cafiso D, Castle D. Secretory carrier membrane protein SCAMP2 and phosphatidylinositol 4,5-bisphosphate interactions in the regulation of dense core vesicle exocytosis. *Biochemistry* (2007) **46**:10909–20. doi:10.1021/bi701121j
41. Chasserot-Golaz S, Vitale N, Sagot I, Delouche B, Dirrig S, Pradel LA, et al. Annexin II in exocytosis: catecholamine secretion requires the translocation of p36 to the subplasmalemmal region in chromaffin cells. *J Cell Biol* (1996) **133**:1217–36. doi:10.1083/jcb.133.6.1217
42. Honigmann A, van den Bogaart G, Iraheta E, Risselada HJ, Milovanovic D, Mueller V, et al. Phosphatidylinositol 4,5-bisphosphate clusters act as molecular beacons for vesicle recruitment. *Nat Struct Mol Biol* (2013) **20**:679–86. doi:10.1038/nsmb.2570
43. Khuong TM, Habets RL, Kuenen S, Witkowska A, Kasprowicz J, Swerts J, et al. Synaptic PI(3,4,5)P3 is required for syntaxin1A clustering and neurotransmitter release. *Neuron* (2013) **77**:1097–108. doi:10.1016/j.neuron.2013.01.025
44. Rickman C, Medine CN, Dun AR, Moulton DJ, Mandula O, Halemani ND, et al. t-SNARE protein conformations patterned by the lipid microenvironment. *J Biol Chem* (2010) **285**:13535–41. doi:10.1074/jbc.M109.091058
45. James DJ, Khodthong C, Kowalchyk JA, Martin TF. Phosphatidylinositol 4,5-bisphosphate regulates SNARE-dependent membrane fusion. *J Cell Biol* (2008) **182**:355–66. doi:10.1083/jcb.200801056
46. Trifaro JM, Gasman S, Gutierrez LM. Cytoskeletal control of vesicle transport and exocytosis in chromaffin cells. *Acta Physiol (Oxf)* (2008) **192**:165–72. doi:10.1111/j.1748-1716.2007.01808.x
47. Hammond GR, Dove SK, Nicol A, Pinxteren JA, Zicha D, Schiavo G. Elimination of plasma membrane phosphatidylinositol (4,5)-bisphosphate is required for exocytosis from mast cells. *J Cell Sci* (2006) **119**:2084–94. doi:10.1242/jcs.02912
48. Sheu L, Pasyk EA, Ji J, Huang X, Gao X, Varoqueaux F, et al. Regulation of insulin exocytosis by Munc13-1. *J Biol Chem* (2003) **278**:27556–63. doi:10.1074/jbc.M303203200
49. Jang JH, Lee CS, Hwang D, Ryu SH. Understanding of the roles of phospholipase D and phosphatidic acid through their binding partners. *Prog Lipid Res* (2011) **51**:71–81. doi:10.1016/j.plipres.2011.12.003
50. Honda A, Nogami M, Yokozeki T, Yamazaki M, Nakamura H, Watanabe H, et al. Phosphatidylinositol 4-phosphate 5-kinase alpha is a downstream effector of the small G protein ARF6 in membrane ruffle formation. *Cell* (1999) **99**:521–32. doi:10.1016/S0092-8674(00)81540-8
51. Mima J, Wickner W. Complex lipid requirements for SNARE- and SNARE chaperone-dependent membrane fusion. *J Biol Chem* (2009) **284**:27114–22. doi:10.1074/jbc.M109.010223
52. Darios F, Davletov B. Omega-3 and omega-6 fatty acids stimulate cell membrane expansion by acting on syntaxin 3. *Nature* (2006) **440**:813–7. doi:10.1038/nature04598
53. Darios F, Wasser C, Shakirzyanova A, Giniatullin A, Goodman K, Munoz-Bravo JL, et al. Sphingosine facilitates SNARE complex assembly and activates synaptic vesicle exocytosis. *Neuron* (2009) **62**:683–94. doi:10.1016/j.neuron.2009.04.024
54. Chernomordik LV, Kozlov MM. Membrane hemifusion: crossing a chasm in two leaps. *Cell* (2005) **123**:375–82. doi:10.1016/j.cell.2005.10.015
55. Mrowczynska L, Lindqvist C, Iglic A, Hagerstrand H. Spontaneous curvature of ganglioside GM1 – effect of cross-linking. *Biochem Biophys Res Commun* (2012) **422**:776–9. doi:10.1016/j.bbrc.2012.05.083
56. Zimmerberg J, Chernomordik LV. Membrane fusion. *Adv Drug Deliv Rev* (1999) **38**:197–205. doi:10.1016/S0169-409X(99)00029-0
57. Lai AL, Tamm LK, Ellena JF, Cafiso DS. Synaptotagmin 1 modulates lipid acyl chain order in lipid bilayers by demixing phosphatidylserine. *J Biol Chem* (2011) **286**:25291–300. doi:10.1074/jbc.M111.258848

Conflict of Interest Statement: The authors declare that the research was conducted in the absence of any commercial or financial relationships that could be construed as a potential conflict of interest.

Received: 18 June 2013; accepted: 31 August 2013; published online: 17 September 2013.
*Citation: Ammar MR, Kassas N, Chasserot-Golaz S, Bader M-F and Vitale N (2013) Lipids in regulated exocytosis: what are they doing? Front. Endocrinol. **4**:125. doi: 10.3389/fendo.2013.00125*
This article was submitted to Neuroendocrine Science, a section of the journal Frontiers in Endocrinology.

frontiers in
ENDOCRINOLOGY

MINI REVIEW ARTICLE
published: 27 August 2013
doi: 10.3389/fendo.2013.00109

Intersectin: the crossroad between vesicle exocytosis and endocytosis

Olga Gubar[1,2,3], Dmytro Morderer[1,2], Lyudmila Tsyba[2], Pauline Croisé[3], Sébastien Houy[3], Stéphane Ory[3], Stéphane Gasman[3] and Alla Rynditch[1,2]*

[1] State Key Laboratory of Molecular and Cellular Biology, Institute of Molecular Biology and Genetics, Kyiv, Ukraine
[2] Department of Functional Genomics, Institute of Molecular Biology and Genetics, Kyiv, Ukraine
[3] Institut des Neurosciences Cellulaires et Intégratives, Centre National de la Recherche Scientifique-Unité Propre de Recherche 3212, Université de Strasbourg, Strasbourg, France

Edited by:
Rafael Vazquez-Martinez, University of Cordoba, Spain

Reviewed by:
Pedro A. Jose, Georgetown University, USA
Sanda Predescu, Rush University Medical Center, USA

***Correspondence:**
Alla Rynditch, Department of Functional Genomics, Institute of Molecular Biology and Genetics, 150, Zabolotnogo Street, 03680 Kyiv-143, Ukraine
e-mail: rynditch@imbg.org.ua

Intersectins (ITSNs) are a family of highly conserved proteins with orthologs from nematodes to mammals. In vertebrates, ITSNs are encoded by two genes (*itsn1* and *itsn2*), which act as scaffolds that were initially discovered as proteins involved in endocytosis. Further investigation demonstrated that ITSN1 is also implicated in several other processes including regulated exocytosis, thereby suggesting a role for ITSN1 in the coupling between exocytosis and endocytosis in excitatory cells. Despite a high degree of conservation amongst orthologs, ITSN function is not so well preserved as they have acquired new properties during evolution. In this review, we will discuss the role of ITSN1 and its orthologs in exo- and endocytosis, in particular in neurons and neuroendocrine cells.

Keywords: intersectin, exocytosis, endocytosis, neurons, neuroendocrine cells, Cdc42, scaffold

ITSN FAMILY OF SCAFFOLD PROTEINS

Intersectins (ITSNs) are multifunctional scaffold proteins implicated in several cellular mechanisms, including membrane trafficking (clathrin- and caveolin-mediated endocytosis, secretagogue-evoked exocytosis) and receptor-dependent signaling (Ras-MAPK and Rho GTPase regulation, EGF receptor ubiquitylation) to name a few [extensively reviewed in (1–3)]. Based on the high involvement of ITSNs in membrane trafficking, this mini review will focus on the role of these proteins in exocytosis and endocytosis in neurosecretory cells such as neurons and neuroendocrine cells, and will discuss how ITSNs could be key players in coupling exocytosis to endocytosis.

Intersectin is highly conserved in all metazoans examined so far and ITSN orthologs have been found in nematodes (*Caenorhabditis elegans*) (4), arthropods (*Drosophila melanogaster* Dap160 – Dynamin-associated protein 160 kDa) (5), fish (*Danio rerio*) (6), amphibians (*Xenopus laevis*) (7), and mammals (*Mus musculus*, *Rattus norvegicus*, *Homo sapiens*) (8–10) (**Figure 1**). ITSN is encoded by one gene in invertebrates. Its molecular organization consists of two N-terminal EH (Eps15 homology) domains followed by a coiled-coil region and four or five SH3 (Src homology 3) domains (5). In vertebrates, two genes encode ITSN proteins (ITSN1 and ITSN2). In addition, ITSNs exist in two main isoforms generated by alternative splicing: a short form (ITSN-S) that harbors the same domain organization as invertebrate ITSN and is ubiquitously expressed and a long form (ITSN-L) which has three additional domains in its C-terminal part [tandem of Dbl (DH) and pleckstrin homology (PH) domains and a C2 domain] (10). This extension has guanine nucleotide exchange factor (GEF) properties for Cdc42 (11), a small GTPase of the Rho family. The ITSN1-L is enriched in neurons (10, 12).

ITSN1 IN NEURONAL ENDOCYTOSIS

Multimodular ITSN1 has been shown to interact with numerous endocytic proteins, including dynamin, AP2 (adaptor protein 2), proteins from the Epsin family, and the synaptojanin phosphatase; its function in the control of endocytosis has been described in different cell types and organisms [reviewed in (1, 2)]. The role of ITSN1 in endocytosis in neurons was further demonstrated in functional assays performed in various model organisms. *C. elegans* containing deletions in the *itsn-1* gene were hypersensitive to the acetylcholine esterase inhibitor aldicarb that is widely used for unmasking neurotransmission defects. It causes rapid hypercontraction and eventual death of wild-type worms. This *itsn-1*-null aldicarb-hypersensitive phenotype could be rescued by expressing ITSN-1 in neurons, but not in muscles, indicating a pre-synaptic dysfunction in mutant animals (4). Another study revealed a decrease in the number of vesicles in neuromuscular junctions (NMJ) of *itsn-1*-null worms, implying that ITSN-1 was required for synaptic vesicle (SV) recycling (13). In both cases, the mutant worms were viable and exhibited no changes in growth and locomotor activity, implying that the nervous system functioned normally. This suggests that ITSN-1 is not essential for neuronal endocytosis in nematodes, but rather plays a regulatory role increasing the efficiency of this process. Worm ITSN-1 has been shown to form a complex with the Eps15 ortholog EHS-1 (13) and a mutation in the *ehs-1* gene also leads to SV depletion. However, *ehs-1*/*itsn-1* double mutants develop a phenotype similar to that of single

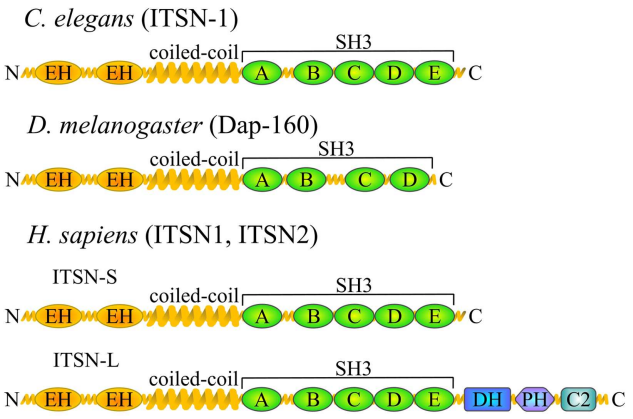

FIGURE 1 | ITSN orthologs and domain composition. Schematic representation of the ITSN proteins in different species depicting the position of various functional domains. EH, Eps15 homology domain; SH3, Src homology 3 domain; DH, Dbl homology domain; PH, pleckstrin homology domain; C2, Ca^{2+}-binding domain. Vertebrates usually have two ITSN genes, both of which give rise to two major isoforms.

mutants, supporting the idea that these proteins act in the same process (13, 14). Intriguingly, *itsn-1* and *ehs-1* mutants have opposite sensitivities to aldicarb, indicating that they have different effects on cholinergic neurotransmission, most likely at the pre-synaptic level (4). Finally, in addition to pre-synaptic functions, ITSN-1 is required for internalization of the GLR-1 (glutamate receptor 1) subunit of the α-amino-3-hydroxy-5-methyl-4-isoxazolepropionic acid-type glutamate (AMPA) receptors in the post-synaptic terminals of nematode command interneurons (15). Thus ITSN-1 seems to be important for both pre- and post-synaptic endocytosis in worms.

In contrast to nematodes, the loss-of-function mutation of the *ITSN* ortholog *Dap160* in *Drosophila* is lethal at late larval stages. Functional studies on the NMJ of mutant flies did not reveal significant changes in stimuli-evoked SV exocytosis; however, prolonged stimulation led to a severe decline in the excitatory post-synaptic potential (EPSP), indicating impairment of compensatory endocytosis (16, 17). As in nematodes, the number of vesicles in the active zones decreased in the NMJ of mutant *Drosophila* (16). In agreement with a function of ITSN in tethering endocytic proteins to the sites of endocytosis, the loss of Dap160 leads to mislocalization of dynamin, endophilin, and synaptojanin, resulting in decreased levels of these proteins in periactive synaptic zones (16, 17). Interestingly, overexpression of Dap160 also leads to a decrease in the level of synaptojanin, a 5′-phosphoinositide phosphatase involved in late stages of endocytosis, in NMJ synaptic terminals (18), indicating that Dap160/ITSN1 functions as a scaffold in endocytosis and is required to maintain endocytic proteins in synaptic terminals at levels necessary for efficient retrieval of SVs.

Studies on lamprey giant reticulospinal synapse have confirmed the data obtained in invertebrates concerning the involvement of ITSN1 in SV endocytosis. Perturbation of ITSN1 function by injecting either anti-ITSN1 antibodies or the SH3C domain into the pre-synaptic terminal resulted in an accumulation of clathrin-coated pits and a reduction in SV number, suggesting a defect in compensatory endocytosis (19, 20). It has also been shown that ITSN1 binds the AP2 clathrin adaptor both in lamprey and mammalian brain, suggesting that ITSN1 participates in the early steps of clathrin-mediated SV endocytosis. Moreover, such an interaction prevents ITSN1 from associating with synaptojanin 1 (20). These findings imply that ITSN1 temporally regulates SV endocytosis.

The data regarding the role of ITSN1 in SV endocytosis in mammals remain contradictory. ITSN1 along with Eps15 have been shown to form a complex with FCHo (Fer/Cip4 homology domain-only) proteins, that promotes the initiation of clathrin-coated pit formation – the step required for clathrin-mediated endocytosis of different cargo in various cell types, including SV endocytosis in neurons (21). ITSN1 isoforms have also been identified as members of the synaptotagmin I-associated endocytic complex in the synaptosomal fraction of rat brain, and were subsequently shown to co-localize with other members of this complex in the pre-synaptic transmitter-release face of the giant calyx-type synapse of the chick ciliary ganglion (22). Knockout of *ITSN1* in mice slows down SV endocytosis in neurons, although the animals are viable (23). However, another group found that SV endocytosis remains normal following ITSN1 knock-down in rat primary hippocampal neurons. This was demonstrated by the absence of a decrease in the uptake of FM4-64 membrane dye after KCl stimulation (24). Moreover, using capacitance measurements of plasma membrane in knockout mouse calyx of Held synapse, Sakaba and co-workers have recently shown that ITSN1 is not essential for endocytic SV recovery after pulse stimulation (25). Furthermore, several authors have reported that ITSN1 is mostly localized post-synaptically in hippocampal neurons, (24, 26), although some data indicating a pre-synaptic localization in mammalian synapses also exist (20, 25). Finally, recent electrophysiological studies did not reveal abnormalities in synaptic transmission either in ITSN1 knockout mice or in ITSN1/ITSN2 double knockout mice using a wide range of stimulation protocols, indicating that under the conditions tested SV recycling is not perturbed (27). Therefore it seems possible that in mammals, in contrast to invertebrates, ITSN1 acts predominantly post-synaptically; however, we cannot totally exclude it is an accessory protein in SV recycling.

Thus the role of ITSN in neuronal endocytosis apparently has not been conserved during evolution. In some groups of organisms (e.g., arthropods) ITSN is indispensable for normal SV recycling, whereas in higher evolved organisms it has become non-essential probably due to the development of alternative or compensatory mechanisms. In lower organisms, these functions are fulfilled by the short isoform, whereas in higher organisms (e.g., vertebrates) ITSN1-L is the likely candidate as it is the main isoform in neurons.

ITSN1 FUNCTION IN EXOCYTOSIS IN NEUROENDOCRINE CELLS

There is much less evidence about the implication of ITSN in exocytosis. One of the first studies reported the interaction of ITSN1 with t-SNAREs [target Soluble NSF Attachment Protein (SNAP) Receptor] SNAP-23 and SNAP-25, but no functional consequence was demonstrated (9). A new specific function of ITSN1-L as GEF

for Cdc42 in exocytosis was described in neuroendocrine cells. In regulated exocytosis, remodeling of the dense actin cortical network is an important step that is controlled by small GTPases. The key players in this process are the Rho family GTPases [reviewed in (28, 29)]. In the PC12 rat pheochromocytoma secretory model, Cdc42 was shown to be activated near the plasma membrane during exocytosis, where it recruits Neural Wiskott–Aldrich syndrome protein (N-WASP) and induces actin polymerization (30). ITSN1-L appeared to be an ideal candidate for Cdc42 activation at docking sites for secretory granules, because it is a specific GEF for Cdc42 and at the same time binds to its effector N-WASP (11). This leads to local polymerization of actin, thereby facilitating exocytosis. ITSN1-L was observed to co-localize with exocytic sites in PC12 and primary bovine chromaffin cells (31). Moreover, silencing of ITSN1 (as well as of Cdc42) significantly inhibits regulated exocytosis in PC12 cells, whereas overexpression of the C-terminal part of ITSN1-L (DH-PH-C2 domains) promotes exocytosis and peripheral actin polymerization in neuroendocrine cells (31, 32). These results were confirmed in *ITSN1*-null mice where exocytosis is also reduced in chromaffin cells (23). Finally, ITSN1 was very recently shown to regulate the replenishment of the fast-releasing SV pool in mouse calyx of Held synapse, possibly together with dynamin 1 and as a GEF for Cdc42 (25). Thus ITSN1-L displays novel properties in membrane trafficking distinct from those of ITSN1-S that were probably acquired during evolution.

ITSN AS A PLAUSIBLE LINK BETWEEN EXO- AND ENDOCYTOSIS

Since ITSN1, especially the isoform ITSN1-L, is strongly implicated in both endo- and exocytosis it is an ideal protein for the coupling of these processes. Regulated exocytosis is always followed by compensatory endocytosis, which is also Ca^{2+}-dependent and is stimulated together with exocytosis (33). Thus the presence of a calcium-binding C2 domain in ITSN-L may be a key for its implication in both exo- and endocytosis. Moreover, in studies on the chick ciliary ganglion ITSN1-S and ITSN1-L have been reported to be associated with the CaV2.2 calcium channels at transmitter-release sites (34).

In neurons, the active zone is highly structured to provide maximum secretory efficiency. The protein matrix, which consists of the cytoskeleton and scaffold proteins, ensures efficient SV docking, whereas electron-dense projections from this matrix serve to tether and maintain the ready-to-use SV pool (35). It is surrounded by a periactive zone that serves for SV recycling by endocytosis. A tight connection and coordination of SV release and recycling is provided by scaffolds [reviewed in (36)]. ITSN1 is a perfect candidate to fulfill this role. During synaptic activity, Dap160 has recently been shown to shuttle between active and periactive zones, ensuring the delivery of dynamin to the periactive zone for efficient bulk membrane retrieval (37). In the lamprey giant reticulospinal synapse, ITSN1 is also localized in the active zone of resting synapses, but re-localizes with its major

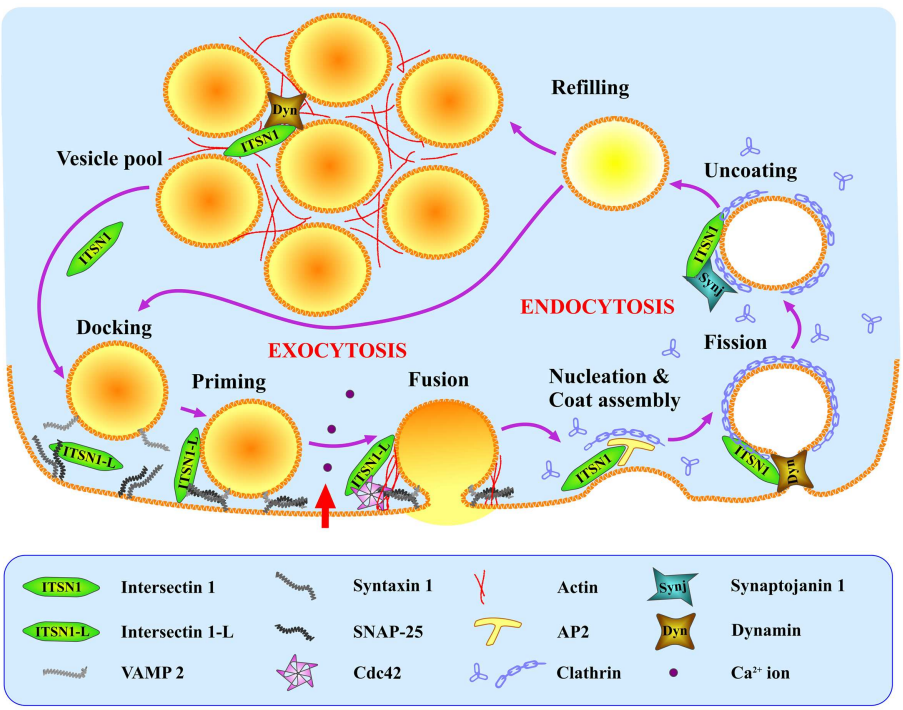

FIGURE 2 | Hypothetical model of ITSN1 coupling exo- and endocytosis in neuroendocrine cells. SNAP-25 recruits ITSN1-L to the SNARE complex (VAMP2, SNAP-25, syntaxin 1) at the exocytic sites where ITSN1-L facilitates regulated exocytosis by activating Cdc42. Immediately after vesicle fusion and hormone release, ITSN1 promotes clathrin-mediated endocytosis of the granule membrane via AP2, and facilitates later stages of endocytosis together with dynamin and synaptojanin. ITSN1 then stays in the vesicle cluster (probably with dynamin) to be recruited back to the membrane for the next release cycle. ITSN1, total ITSN1(both short and long isoforms); ITSN1-L, long isoform of ITSN1.

binding partner dynamin to the periactive zone upon stimulation (19). These results support the idea that ITSN1 acts as a scaffold coupling vesicle fusion and internalization events.

Although to date there is currently no direct evidence that ITSN1 plays a role in compensatory endocytosis in neuroendocrine cells, such data do exist for other cell types (including neurons). Based on these data and the presence of ITSN1 partners in neuroendocrine cells, we propose the following hypothetical model of ITSN1 functioning in exo- and endocytosis in these cells (**Figure 2**). ITSN1 may function in both the release and retrieval of the dense-core granules. SNAP-25 could recruit ITSN1-L to exocytic sites where the latter activates Cdc42 thereby inducing actin polymerization and facilitating the late stages of secretion (9, 31, 32). After release, ITSN1-L remaining on the vesicle membrane could directly promote assembly of the endocytic complex, because the vesicle membrane has been shown to be preserved as an entity during the compensatory endocytosis in neuroendocrine cells (38). Otherwise, ITSN1 could be recruited *de novo* and induce clathrin coat assembly via AP2 (20). Then ITSN1, in turn, can recruit dynamin to provoke vesicle scission (8, 9). After vesicle dissociation from the membrane, AP2 could be replaced by synaptojanin 1, which takes part in the uncoating and dephosphorylation of PIP_2 (phosphatidylinositol 4,5-bisphosphate) (20). The vesicle is then refilled and can be tethered ready for another cycle of exocytosis or added to the releasable vesicle pool. ITSN1 may accompany the vesicle throughout this cycle and remain in the releasable pool as it does in neurons (19). Thus ITSN1 could be a multipurpose player providing the crossroad between exo- and endocytosis in neurosecretory cells and an important regulator of these processes.

ACKNOWLEDGMENTS

We thank Dr. A.-L. Haenni and Dr. N. Grant for helpful discussions and comments on the manuscript.

REFERENCES

1. O'Bryan JP. Intersecting pathways in cell biology. *Sci Signal* (2010) **3**(152):re10. doi:10.1126/scisignal.3152re10
2. Tsyba L, Nikolaienko O, Dergai O, Dergai M, Novokhatska O, Skrypkina I, et al. Intersectin multidomain adaptor proteins: regulation of functional diversity. *Gene* (2011) **473**(2):67–75. doi:10.1016/j.gene.2010.11.016
3. Hunter MP, Russo A, O'Bryan JP. Emerging roles for intersectin (ITSN) in regulating signaling and disease pathways. *Int J Mol Sci* (2013) **14**(4):7829–52. doi:10.3390/ijms14047829
4. Rose S, Malabarba MG, Krag C, Schultz A, Tsushima H, Di Fiore PP, et al. *Caenorhabditis elegans* intersectin: a synaptic protein regulating neurotransmission. *Mol Biol Cell* (2007) **18**(12):5091–9. doi:10.1091/mbc.E07-05-0460
5. Roos J, Kelly RB. Dap160, a neural-specific Eps15 homology and multiple SH3 domain-containing protein that interacts with *Drosophila* dynamin. *J Biol Chem* (1998) **273**(30):19108–19. doi:10.1074/jbc.273.30.19108
6. Dergai M, Tsyba L, Dergai O, Zlatskii I, Skrypkina I, Kovalenko V, et al. Microexon-based regulation of ITSN1 and Src SH3 domains specificity relies on introduction of charged amino acids into the interaction interface. *Biochem Biophys Res Commun* (2010) **399**(2):307–12. doi:10.1016/j.bbrc.2010.07.080
7. Yamabhai M, Hoffman NG, Hardison NL, McPherson PS, Castagnoli L, Cesareni G, et al. Intersectin, a novel adaptor protein with two Eps15 homology and five Src homology 3 domains. *J Biol Chem* (1998) **273**(47):31401–7. doi:10.1074/jbc.273.47.31401
8. Sengar AS, Wang W, Bishay J, Cohen S, Egan SE. The EH and SH3 domain Ese proteins regulate endocytosis by linking to dynamin and Eps15. *EMBO J* (1999) **18**(5):1159–71. doi:10.1093/emboj/18.5.1159
9. Okamoto M, Schoch S, Südhof TC. EHSH1/intersectin, a protein that contains EH and SH3 domains and binds to dynamin and SNAP-25. A protein connection between exocytosis and endocytosis? *J Biol Chem* (1999) **274**(26):18446–54. doi:10.1074/jbc.274.26.18446
10. Guipponi M, Scott HS, Hattori M, Ishii K, Sakaki Y, Antonarakis SE. Genomic structure, sequence, and refined mapping of the human intersectin gene (ITSN), which encompasses 250 kb on chromosome 21q22.1–>q22.2. *Cytogenet Cell Genet* (1998) **83**(3–4):218–20. doi:10.1159/000015182
11. Hussain NK, Jenna S, Glogauer M, Quinn CC, Wasiak S, Guipponi M, et al. Endocytic protein intersectin-l regulates actin assembly via Cdc42 and N-WASP. *Nat Cell Biol* (2001) **3**(10):927–32. doi:10.1038/ncb1001-927
12. Hussain NK, Yamabhai M, Ramjaun AR, Guy AM, Baranes D, O'Bryan JP, et al. Splice variants of intersectin are components of the endocytic machinery in neurons and nonneuronal cells. *J Biol Chem* (1999) **274**(22):15671–7. doi:10.1074/jbc.274.22.15671
13. Wang W, Bouhours M, Gracheva EO, Liao EH, Xu K, Sengar AS, et al. ITSN-1 controls vesicle recycling at the neuromuscular junction and functions in parallel with DAB-1. *Traffic* (2008) **9**(5):742–54. doi:10.1111/j.1600-0854.2008.00712.x
14. Salcini AE, Hilliard MA, Croce A, Arbucci S, Luzzi P, Tacchetti C, et al. The Eps15 *C. elegans* homologue EHS-1 is implicated in synaptic vesicle recycling. *Nat Cell Biol* (2001) **3**(8):755–60. doi:10.1038/35087075
15. Glodowski DR, Chen CC, Schaefer H, Grant BD, Rongo C. RAB-10 regulates glutamate receptor recycling in a cholesterol-dependent endocytosis pathway. *Mol Biol Cell* (2007) **18**(11):4387–96. doi:10.1091/mbc.E07-05-0486
16. Koh TW, Verstreken P, Bellen HJ. Dap160/intersectin acts as a stabilizing scaffold required for synaptic development and vesicle endocytosis. *Neuron* (2004) **43**(2):193–205. doi:10.1016/j.neuron.2004.06.029
17. Marie B, Sweeney ST, Poskanzer KE, Roos J, Kelly RB, Davis GW. Dap160/intersectin scaffolds the periactive zone to achieve high-fidelity endocytosis and normal synaptic growth. *Neuron* (2004) **43**(2):207–19. doi:10.1016/j.neuron.2004.07.001
18. Chang KT, Min KT. Upregulation of three *Drosophila* homologs of human chromosome 21 genes alters synaptic function: implications for down syndrome. *Proc Natl Acad Sci U S A* (2009) **106**(40):17117–22. doi:10.1073/pnas.0904397106
19. Evergren E, Gad H, Walther K, Sundborger A, Tomilin N, Shupliakov O. Intersectin is a negative regulator of dynamin recruitment to the synaptic endocytic zone in the central synapse. *J Neurosci* (2007) **27**(2):379–90. doi:10.1523/JNEUROSCI.4683-06.2007
20. Pechstein A, Bacetic J, Vahedi-Faridi A, Gromova K, Sundborger A, Tomlin N, et al. Regulation of synaptic vesicle recycling by complex formation between intersectin 1 and the clathrin adaptor complex AP2. *Proc Natl Acad Sci U S A* (2010) **107**(9):4206–11. doi:10.1073/pnas.0911073107
21. Henne WM, Boucrot E, Meinecke M, Evergren E, Vallis Y, Mittal R, et al. FCHo proteins are nucleators of clathrin-mediated endocytosis. *Science* (2010) **328**(5983):1281–4. doi:10.1126/science.1188462
22. Khanna R, Li Q, Stanley EF. "Fractional recovery" analysis of a presynaptic synaptotagmin 1-anchored endocytic protein complex. *PLoS ONE* (2006) **1**:e67. doi:10.1371/journal.pone.0000067
23. Yu Y, Chu PY, Bowser DN, Keating DJ, Dubach D, Harper I, et al. Mice deficient for the chromosome 21 ortholog Itsn1 exhibit vesicle-trafficking abnormalities. *Hum Mol Genet* (2008) **17**(21):3281–90. doi:10.1093/hmg/ddn224
24. Thomas S, Ritter B, Verbich D, Sanson C, Bourbonnière L, McKinney RA, et al. Intersectin regulates dendritic spine development and somatodendritic endocytosis but not synaptic vesicle recycling in hippocampal neurons. *J Biol Chem* (2009) **284**(18):12410–9. doi:10.1074/jbc.M809746200
25. Sakaba T, Kononenko NL, Bacetic J, Pechstein A, Schmoranzer J, Yao L, et al. Fast neurotransmitter release regulated by the endocytic scaffold intersectin. *Proc Natl Acad Sci U S A* (2013) **110**(20):8266–71. doi:10.1073/pnas.1219234110
26. Nishimura T, Yamaguchi T, Tokunaga A, Hara A, Hamaguchi T, Kato K, et al. Role of numb in dendritic spine development with a Cdc42 GEF intersectin and EphB2. *Mol Biol Cell* (2006) **17**(3):1273–85. doi:10.1091/mbc.E05-07-0700

27. Sengar AS, Ellegood J, Yiu AP, Wang H, Wang W, Juneja SC, et al. Vertebrate intersectin1 is repurposed to facilitate cortical midline connectivity and higher order cognition. *J Neurosci* (2013) **33**(9):4055–65. doi:10.1523/JNEUROSCI.4428-12.2013
28. Ory S, Gasman S. Rho GTPases and exocytosis: what are the molecular links? *Semin Cell Dev Biol* (2011) **22**(1):27–32. doi:10.1016/j.semcdb.2010.12.002
29. Momboisse F, Houy S, Ory S, Calco V, Bader MF, Gasman S. How important are Rho GTPases in neurosecretion? *J Neurochem* (2011) **117**(4):623–31. doi:10.1111/j.1471-4159.2011.07241.x
30. Gasman S, Chasserot-Golaz S, Malacombe M, Way M, Bader MF. Regulated exocytosis in neuroendocrine cells: a role for subplasmalemmal Cdc42/N-WASP-induced actin filaments. *Mol Biol Cell* (2004) **15**(2):520–31. doi:10.1091/mbc.E03-06-0402
31. Malacombe M, Ceridono M, Calco V, Chasserot-Golaz S, McPherson PS, Bader MF, et al. Intersectin-1L nucleotide exchange factor regulates secretory granule exocytosis by activating Cdc42. *EMBO J* (2006) **25**(15):3494–503. doi:10.1038/sj.emboj.7601247
32. Momboisse F, Ory S, Calco V, Malacombe M, Bader MF, Gasman S. Calcium-regulated exocytosis in neuroendocrine cells: intersectin-1L stimulates actin polymerization and exocytosis by activating Cdc42. *Ann N Y Acad Sci* (2009) **1152**:209–14. doi:10.1111/j.1749-6632.2008.03998.x
33. Barg S, Machado JD. Compensatory endocytosis in chromaffin cells. *Acta Physiol (Oxf)* (2008) **192**(2):195–201. doi:10.1111/j.1748-1716.2007.01813.x
34. Khanna R, Li Q, Schlichter LC, Stanley EF. The transmitter release-site CaV2.2 channel cluster is linked to an endocytosis coat protein complex. *Eur J Neurosci* (2007) **26**(3):560–74. doi:10.1111/j.1460-9568.2007.05681.x
35. Zhai RG, Bellen HJ. The architecture of the active zone in the presynaptic nerve terminal. *Physiology (Bethesda)* (2004) **19**:262–70. doi:10.1152/physiol.00014.2004
36. Haucke V, Neher E, Sigrist SJ. Protein scaffolds in the coupling of synaptic exocytosis and endocytosis. *Nat Rev Neurosci* (2011) **12**(3):127–38. doi:10.1038/nrn2948
37. Winther AM, Jiao W, Vorontsova O, Rees KA, Koh TW, Sopova E, et al. The dynamin-binding domains of Dap160/intersectin affect bulk membrane retrieval in synapses. *J Cell Sci* (2013) **126**(Pt 4):1021–31. doi:10.1242/jcs.118968
38. Ceridono M, Ory S, Momboisse F, Chasserot-Golaz S, Houy S, Calco V, et al. Selective recapture of secretory granule components after full collapse exocytosis in neuroendocrine chromaffin cells. *Traffic* (2011) **12**(1):72–88. doi:10.1111/j.1600-0854.2010.01125.x

Conflict of Interest Statement: The authors declare that the research was conducted in the absence of any commercial or financial relationships that could be construed as a potential conflict of interest.

Received: 01 July 2013; accepted: 09 August 2013; published online: 27 August 2013.
*Citation: Gubar O, Morderer D, Tsyba L, Croisé P, Houy S, Ory S, Gasman S and Rynditch A (2013) Intersectin: the crossroad between vesicle exocytosis and endocytosis. Front. Endocrinol. **4**:109. doi: 10.3389/fendo.2013.00109*
This article was submitted to Neuroendocrine Science, a section of the journal Frontiers in Endocrinology.

frontiers in
ENDOCRINOLOGY

MINI REVIEW ARTICLE
published: 02 October 2013
doi: 10.3389/fendo.2013.00135

Exocytosis and endocytosis in neuroendocrine cells: inseparable membranes!

Sébastien Houy, Pauline Croisé, Olga Gubar, Sylvette Chasserot-Golaz, Petra Tryoen-Tóth, Yannick Bailly, Stéphane Ory, Marie-France Bader and Stéphane Gasman*

Institut des Neurosciences Cellulaires et Intégratives (INCI), Centre National de la Recherche Scientifique (CNRS UPR 3212), Université de Strasbourg, Strasbourg, France

Edited by:
Rafael Vazquez-Martinez, University of Cordoba, Spain

Reviewed by:
Silvio O. Rizzoli, European Neuroscience Institute Göttingen, Germany
Corey Smith, Case Western Reserve University, USA

****Correspondence:***
Stéphane Gasman, Institut des Neurosciences Cellulaires et Intégratives (INCI), Centre National de la Recherche Scientifique (CNRS UPR 3212), Université de Strasbourg, 5 rue Blaise Pascal, Strasbourg 67084, France
e-mail: gasman@inci-cnrs.unistra.fr

Although much has been learned concerning the mechanisms of secretory vesicle formation and fusion at donor and acceptor membrane compartments, relatively little attention has been paid toward understanding how cells maintain a homeostatic membrane balance through vesicular trafficking. In neurons and neuroendocrine cells, release of neurotransmitters, neuropeptides, and hormones occurs through calcium-regulated exocytosis at the plasma membrane. To allow recycling of secretory vesicle components and to preserve organelles integrity, cells must initiate and regulate compensatory membrane uptake. This review relates the fate of secretory granule membranes after full fusion exocytosis in neuroendocrine cells. In particular, we focus on the potential role of lipids in preserving and sorting secretory granule membranes after exocytosis and we discuss the potential mechanisms of membrane retrieval.

Keywords: exocytosis, compensatory endocytosis, membrane lipids, neuroendocrine cells, chromaffin cells

INTRODUCTION

Mammalian cells exhibit complex and dynamic patterns of intracellular membrane traffic between various organelles. Although much has been learned concerning the mechanisms of vesicle transport and vesicle fusion at donor and acceptor compartments, relatively little attention has been paid to understanding how organelle homeostasis is maintained. This aspect is particularly important in neurosecretory cells in which intense membrane trafficking and mixing occurs between secretory vesicles and the plasma membrane during secretion of various transmitters, peptides, and hormones. Calcium-regulated exocytosis, i.e., fusion of secretory vesicles with the plasma membrane results in the merging of these two membrane compartments, hence triggering an increase in plasma membrane surface and loss of identity. As a consequence, exocytosis must be coupled to a compensatory endocytotic process allowing the plasma membrane to recover its integrity and the granule membrane to be recycled. In neurons, molecular mechanisms of synaptic vesicle recycling and coupling with exocytosis have been intensively studied, but is still debated [for reviews see (1–3)]. However, the equivalent process for large dense core granules in neuroendocrine cells remains largely unexplored.

In neuroendocrine cells, secretion can occur through different modes of exocytosis depending on the physiological demand (see **Figure 1** for details). The "kiss-and-run" mode allows only the release of catecholamines and other small molecules through a narrow fusion pore (4, 5). During "cavicapture" (granule cavity capture) mode, expansion of the fusion pore triggers partial release of the small proteins (6–9). During kiss-and-run and cavicapture processes, the granule shape remains almost intact, whereas during "full collapse" or "full fusion" exocytosis, granules lose their round shape, flatten out in the plane of the plasma membrane leading to the merging of these two compartments and the complete release of the granular content (10–12). Whereas the molecular mechanisms of the various exocytotic modes (secretory vesicle recruitment, docking, priming, and fusion processes) have been largely explored, how granule and plasma membranes maintain their composition and recover their integrity after full fusion exocytosis is poorly known. Two types of retrieval have been described after full fusion exocytosis: clathrin-mediated endocytosis and bulk endocytosis. Bulk endocytosis occurs during elevated secretory activity when clathrin-mediated endocytosis is unable to fully compensate the large increase in membrane surface. To rapidly reverse this excess of plasma membrane, bulk endocytosis internalizes large invaginations of plasma membrane, which then form endosomal-like compartments. Bulk endocytosis has been described in several reviews (13, 14). Here, we focus on potential mechanisms that allow neuroendocrine cells to compensate full fusion exocytosis of large dense core vesicles through clathrin-mediated endocytosis.

THE FATE OF THE SECRETORY GRANULE MEMBRANE AFTER FUSION

For a long time, it was believed that after full fusion exocytosis vesicular components diffuse into the plasma membrane and are subsequently randomly internalized. This model implies that both the secretory vesicle and plasma membranes lose their identities and that exocytosis is not directly coupled to endocytosis. In contradiction with this model, synaptic activity in neurons results neither in the overall dispersion of vesicle components in the plasma membrane nor in the enrichment of

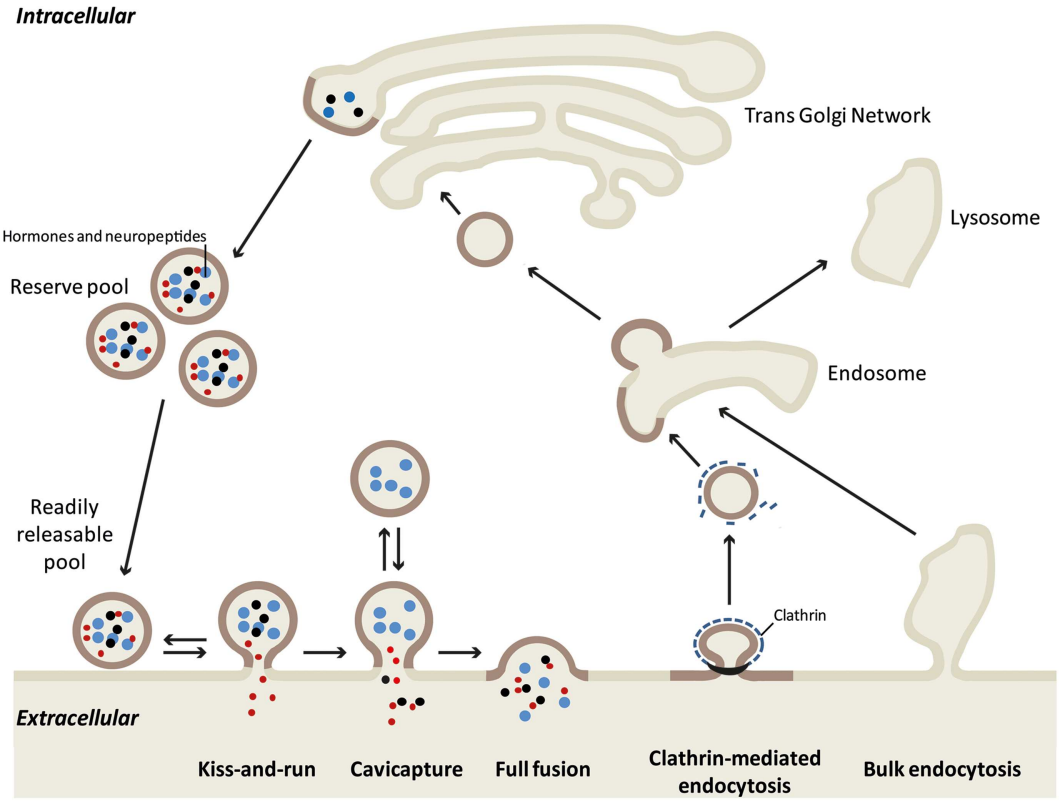

FIGURE 1 | Different models of exo-endocytosis coupling in neuroendocrine cells. Hormone sorting and large dense core granule biogenesis occurs at the trans-Golgi network. Mature granules either constitute the reserve pool or are recruited to the plasma membrane as a readily releasable pool. Large proteins (blue dots), small neuropeptides (black dots), and small molecules like catecholamines (red dots) can be released differentially according to the exo-endocytosis mode. During "kiss-and-run" mode, only small molecules are released through a narrow fusion pore, whereas cavicapture (granule cavity capture) allow the partial release of small neuropeptides (7). Note that for these two modes, retrieval of intact granules is easily conceived as the granule shape remains almost intact. During full fusion exocytosis, the intra-granular contents are all released and the granule membrane collapses into the plasma membrane. This membrane incorporation is compensated by clathrin-mediated endocytosis that specifically retrieves granule membrane piece by piece [see **Figure 2** and (19)]. After uncoating, the endocytic granule membrane reaches early endosome where granule components remain clustered (12), before being re-maturated at the Golgi network. During intense exocytotic activity, bulk endocytosis supports clathrin-mediated endocytosis by internalizing large plasma membrane invaginations that most likely follow the lysosomal degradation pathway.

plasma membrane components in synaptic vesicles (2). Similarly, despite full fusion exocytosis in neuroendocrine cells, granules, and plasma membranes seem to maintain their specific protein composition.

Early evidence for exo-endocytosis coupling came from morphological studies in the 80s suggesting that large dense core granule membrane-bound components could be retrieved after exocytosis (10, 15). At the same time, Geisow and co-workers observed an important increase in the number of coated pits containing secretory granule components in secretagogue-stimulated chromaffin cells (16). Later on patch-clamp and imaging studies suggested a fast temporal coupling between exocytosis and endocytosis processes (17, 18).

Using electron microscopy of cultured chromaffin cells, our group has recently described clustering of secretory granule proteins on the plasma membrane after full fusion exocytosis, arguing against the idea that granule components are dispersed in the plasma membrane (12). The group of Holz recently confirmed that chromaffin granule markers remain associated after fusion (19). Additionally, we have shown that these granule-bound proteins are subsequently internalized through vesicles devoid of plasma membrane makers (12). In other words, granule membranes are maintained together as "microdomains" after exocytosis and are subsequently recaptured without intermixing with the plasma membrane. How do neuroendocrine cells preserve granule membrane integrity after full collapse and precisely sort granule membrane lipids and associated proteins?

LIPIDS AS CENTRAL ORGANIZERS OF EXO-ENDOCYTOSIS COUPLING?

CREATING MEMBRANE DOMAINS TO PRESERVE GRANULE IDENTITY

The preservation of secretory granule identity after fusion with the plasma membrane implies that both proteins and lipids do not diffuse in the plasma membrane. Lateral segregation of membrane lipids would in this case represent an obvious sorting mechanism. Interestingly, we and others have shown that exocytosis requires several types of lipid remodeling processes (described in the present "Research Topic" by Amar et al. (28)). Some of

these processes might contribute to prevent granular component from diffusing. For instance, secretagogue-evoked stimulation of chromaffin cells triggers the formation of lipid raft microdomains at the plasma membrane enriched in ganglioside GM1, cholesterol, and phosphatidylinositol 4,5 bisphosphate [$PI(4,5)P_2$]. Such lipid rafts correspond to membrane areas stabilized by the presence of cholesterol within a liquid-ordered phase in which lateral diffusion of proteins and lipids is limited, resulting in the clustering of specific components (20). In neuroendocrine and various other secretory cells, lipid raft formation is necessary for the spatial organization of the exocytotic machinery including SNARE proteins (21–23). As a consequence, it is tempting to imagine that this lipid confinement at the exocytotic sites would help to prevent granular lipids and proteins from diffusing after secretory granules fusion with the plasma membrane.

Of particular interest, the formation of membrane domains corresponding to exocytotic sites is regulated by annexin-A2 (21, 24), a calcium- and phospholipid-binding protein involved in both exo- and endocytosis (25). Annexin-A2 has been described on clathrin-coated vesicles in the adrenal gland (26). The protein displays two typical YXX∅ endocytic motifs allowing its interaction with the μ2-subunit of the AP-2 complex that triggers clathrin recruitment (27). Therefore, annexin-A2 constitutes a strong candidate to participate in the coupling of secretory granule exocytosis with the subsequent compensatory endocytosis.

PI(4,5)P2: ORCHESTRATING EXO-ENDOCYTOSIS COUPLING

Phosphatidylinositol 4,5 bisphosphate [$PI(4,5)P_2$] has been largely described as an important regulator in exocytosis (28, 29) but it is also known to recruit and regulate multiple components involved in clathrin-mediated endocytosis. Therefore, the $PI(4,5)P_2$-enriched membrane microdomains where exocytosis occurs is likely to constitute preferential spots for endocytosis, a perfect way to couple these two processes. For example, interaction of the adaptor protein AP-2 with YXX∅ endocytic motifs is driven by its interaction with $PI(4,5)P_2$ (30). Local $PI(4,5)P_2$ concentration regulates the membrane binding and deformation capacity of proteins containing Bin/amphiphysin/Rvs (BAR) domains including endophilin, syndapin, and amphiphysin, three membrane-deforming scaffold proteins that have been implicated in endocytotic processes (31, 32). Interestingly, it has been proposed that BAR domains participate in the fission of budding vesicles by synergistically cooperating with dynamin, a GTPase also sensitive to $PI(4,5)P_2$ (33). Moreover, in collaboration with the group of Dr. Cardenas, we have recently demonstrated that dynamin-2 controls both exocytosis, by regulating fusion pore expansion, and the subsequent endocytosis of secretory granules in chromaffin cells (34). Finally, $PI(4,5)P_2$ also regulates the dynamics of actin filaments, which are believed to limit plasma membrane protein diffusion and/or to directly participate in endocytosis (35, 36). Accordingly, we have previously demonstrated that actin filaments are formed at a post-docking step of exocytosis (37) and disruption of actin filament organization inhibits compensatory endocytosis after full fusion. These data suggest that actin remodeling is also implicated in the process of internalization *per se* (12).

PHOSPHOLIPID SCRAMBLING: A SIGNAL TO TRIGGER COMPENSATORY ENDOCYTOSIS?

One key feature of cell membranes is the asymmetric distribution of phospholipids between the leaflets. In the plasma membrane, phosphatidylserine (PS) and phosphatidylethanolamine (PE) reside in the inner cytoplasmic leaflet while phosphatidylcholine and sphingomyelin are located in the outer leaflet (38). In non-apoptotic cells, several biological functions are accompanied by a disruption of this phospholipid asymmetry resulting in the externalization of PS in the outer leaflet of the plasma membrane (39). This phenomenon has been observed during regulated exocytosis in mast cells (40), nerve terminals (41), and the neuroendocrine PC12 and chromaffin cells (12, 42, 43). More recently, we have shown that PS externalization occurs in specific domains at the frontier between the fused granule membrane and the plasma membrane and is triggered by the calcium-sensitive phospholipid scramblase-1 (PLSCR1). Interestingly, in chromaffin cells cultured from PLSCR1 knock-out mice, surface exposure of PS is not involved in exocytosis, but is required for granule membrane compensatory endocytosis (44).

To date no current evidence is available to explain the mechanism by which PS externalization is linked to compensatory endocytosis. However, two scenarios are possible. Firstly, as loss of phospholipid asymmetry can modify the mechanical stability of membranes (45), this might facilitates local reorganization of lipids surrounding the granule membrane transiently inserted within the plasma membrane and preserve the integrity of the granule membrane. Secondly, as an anionic phospholipid, PS confers negative charges and directly binds various proteins involved in exocytosis like annexin-A2, rabphilin, DOC 2, or synaptotagmin (46). PLSCR1-induced local decrease in PS concentration in the inner leaflet of the plasma membrane could therefore represent a signal to switch from exocytosis to endocytosis, thereby permitting the release of exocytotic components and/or the recruitment of the endocytic machinery.

However, whether externalization of PS simply reflects the loss of PS asymmetry or reveals more profound lipid reorganization is basically unknown and requires further investigation.

HOW TO RECAPTURE A LARGE DENSE CORE VESICLE?

In chromaffin cells, we have found that clathrin is rapidly recruited to the granule membrane right after merging with the plasma membrane and that knocking-down clathrin expression drastically blocks compensatory endocytosis (12). The clathrin dependency of large dense core granule endocytosis raises the question of the mechanism by which a granule displaying a mean diameter of about 250 nm may be recaptured by a clathrin coat? Energetic constraints indicate that *in vitro* clathrin baskets assemble with a mean diameter of 100 nm or even less (80 nm) in the presence of adaptor proteins (47). In INS-1 insulinoma cells for example, the mean diameter of secretory granule ranges from 110 to 170 nm but the endocytotic events detected by capacitance measurements correspond to vesicles of 70 nm diameter (48). In mouse chromaffin cells, the average size of endocytic vesicles calculated from endocytic capacitance step sizes is 122 nm (49). Accordingly, recent electron microscopy experiments performed on chromaffin cells demonstrated that clathrin-coated vesicles size increases

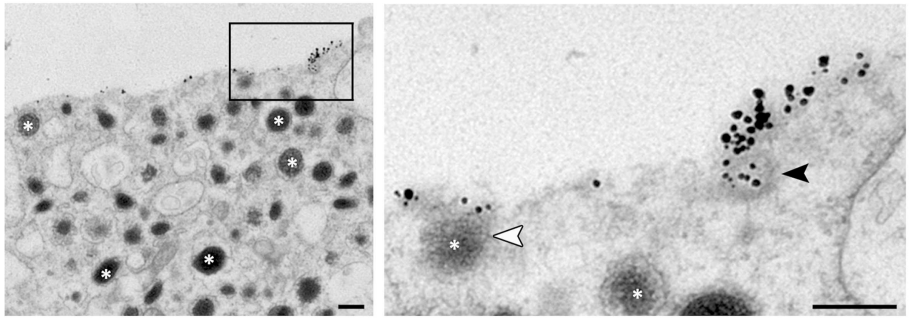

FIGURE 2 | Ultrastructural observation of budding vesicle from exocytotic spots in stimulated chromaffin cells. To stain specifically the granule membrane fused with plasma membrane, stimulated cells are incubated in the presence of antibodies raised against the luminal region of dopamine-beta hydroxylase (DBH), a transmembrane marker of secretory granules (asterisks). Note that small vesicles budding can be observed from the DBH antibodies clusters (black arrowhead in enlarged view) suggesting a partial recapture of the granule membrane. The white arrowhead shows a granule fusing with the plasma membrane. Bar = 100 nm.

upon potassium stimulation (mean diameter of 87 nm) compared to resting cells (19). Altogether, these observations tend to demonstrate that large granule membranes may be recaptured as small pieces rather than a whole. Indeed, direct observations of the internalization of fused granule membranes allowed us to reveal early endocytotic events corresponding to 50–80 nm coated vesicles budding from granular membrane-bound proteins clusters (**Figure 2**).

ENDOCYTIC PATHWAY

The intracellular route followed by the post-exocytotic internalized granules has not been fully characterized. The main difference with synaptic vesicle recycling is that, to be reused, large dense core granules need to be reloaded with matrix proteins, which most likely implies a re-maturation process involving the Golgi apparatus. The transient accessibility of granule-bound proteins at the cell surface during full fusion exocytosis has been exploited to label and follow post-fusion granules with specific antibodies or biotinylation. This approach was widely used in the 80s in order to demonstrate that granule-bound proteins transit through the Golgi region before being recycled in newly mature granules (10, 15, 50, 51). Alternatively, granule markers have been proposed to be degraded through a lysosomal pathway (52, 53). Both recycling and degradation pathways coexist and their proportion may depend on cell secretory activity. The recycling pathway leading to releasable granules is more predominant upon mild stimulation whereas above a certain threshold of membrane incorporation during intense exocytotic activity, the occurrence of bulk endocytosis will lead to the degradation of the internalized membrane (54, 55). Altogether, these data do not provide any information concerning the immediate fate of internalized granule membrane. Our group has observed that internalized granule-bound markers rapidly co-localize with the early endosomal marker EEA1, suggesting that chromaffin granule components might be retrieved through early endosomes after regulated exocytosis (12). Since clathrin is likely to retrieve the collapsed granule membrane as pieces and not as a whole, the early endosomes might constitute a transient sorting station that would sort the retrieved pieces to reconstitute a functional granule prior to entering the retrograde transport pathway to the TGN. Accordingly, we have observed budding of the immunogold-labeled DBH clusters present on endosomes (unpublished data).

CONCLUSION

New evidence is now emerging to support the idea that, in neuroendocrine cells but also in neurons, vesicle/granule membranes do not intermix with the plasma membrane following full fusion exocytosis (56, 57). Compensation of membrane incorporation by endocytosis is a critical process and selective recapture of secretory organelles is required to maintain cellular homeostasis. Resolving the mechanisms that specifically preserve the granule membrane platform and retain granular components together after its incorporation in the plasma membrane to is the next challenging question to answer. Highly resolutive biophotonic approaches are now required to precisely investigate the dynamic behavior of secretory granules merged with the plasma membrane during and after exocytosis. Lipids clearly play a central role in this process, but attention should also be given to bi-functional proteins regulating both exo- and endocytosis, in particular annexin, synaptotagmin, and BAR domain-containing proteins.

ACKNOWLEDGMENTS

We wish to thank Dr. Nancy Grant for critical reading of the manuscript. We thank V. Calco and A. M. Haeberlé for setting up preliminary experiments and T. Thahouly for technical assistance. Part of the work from our group discussed in this review was supported by various grant to Stéphane Gasman: ANR grant (ANR-07-JCJC-088-01), "Association pour la Recherche sur le Cancer" grant (ARC #1055), and EMMA service (under the EU contract Grant Agreement Number 227490) of the EC FP7 Capacities Specific Programme. We acknowledge the Plateforme "Imagerie in vitro" (NeuroPôle; Strasbourg). Especially A. M. Haeberlé and V. Demais for their excellent technical assistance in electron microscopy.

REFERENCES

1. Gundelfinger ED, Kessels MM, Qualmann B. Temporal and spatial coordination of exocytosis and endocytosis. *Nat Rev Mol Cell Biol* (2003) **4**:127–39. doi:10.1038/nrm1016
2. Rizzoli SO, Jahn R. Kiss-and-run, collapse and 'readily retrievable' vesicles. *Traffic* (2007) **8**:1137–44. doi:10.1111/j.1600-0854.2007.00614.x
3. Haucke V, Neher E, Sigrist SJ. Protein scaffolds in the coupling of synaptic exocytosis and endocytosis. *Nat Rev Neurosci* (2011) **12**:127–38. doi:10.1038/nrn2948
4. Henkel AW, Kang G, Kornhuber J. A common molecular machinery for exocytosis and the 'kiss-and-run' mechanism in chromaffin cells is controlled by phosphorylation. *J Cell Sci* (2001) **114**:4613–20.
5. Hanna ST, Pigeau GM, Galvanovskis J, Clark A, Rorsman P, Macdonald PE. Kiss-and-run exocytosis and fusion pores of secretory vesicles in human beta-cells. *Pflugers Arch* (2009) **457**:1343–50. doi:10.1007/s00424-008-0588-0
6. Taraska JW, Perrais D, Ohara-Imaizumi M, Nagamatsu S, Almers W. Secretory granules are recaptured largely intact after stimulated exocytosis in cultured endocrine cells. *Proc Natl Acad Sci U S A* (2003) **100**:2070–5. doi:10.1073/pnas.0337526100
7. Perrais D, Kleppe IC, Taraska JW, Almers W. Recapture after exocytosis causes differential retention of protein in granules of bovine chromaffin cells. *J Physiol* (2004) **560**:413–28. doi:10.1113/jphysiol.2004.064410
8. Fulop T, Radabaugh S, Smith C. Activity-dependent differential transmitter release in mouse adrenal chromaffin cells. *J Neurosci* (2005) **25**:7324–32. doi:10.1523/JNEUROSCI.2042-05.2005
9. Llobet A, Wu M, Lagnado L. The mouth of a dense-core vesicle opens and closes in a concerted action regulated by calcium and amphiphysin. *J Cell Biol* (2008) **182**:1017–28. doi:10.1083/jcb.200807034
10. Patzak A, Winkler H. Exocytotic exposure and recycling of membrane antigens of chromaffin granules: ultrastructural evaluation after immunolabeling. *J Cell Biol* (1986) **102**:510–5. doi:10.1083/jcb.102.2.510
11. Wick PF, Trenkle JM, Holz RW. Punctate appearance of dopamine-beta-hydroxylase on the chromaffin cell surface reflects the fusion of individual chromaffin granules upon exocytosis. *Neuroscience* (1997) **80**:847–60. doi:10.1016/S0306-4522(97)00062-6
12. Ceridono M, Ory S, Momboisse F, Chasserot-Golaz S, Houy S, Calco V, et al. Selective recapture of secretory granule components after full collapse exocytosis in neuroendocrine chromaffin cells. *Traffic* (2011) **12**:72–88. doi:10.1111/j.1600-0854.2010.01125.x
13. Clayton EL, Cousin MA. The molecular physiology of activity-dependent bulk endocytosis of synaptic vesicles. *J Neurochem* (2009) **111**:901–14. doi:10.1111/j.1471-4159.2009.06384.x
14. Cardenas AM, Marengo FD. Rapid endocytosis and vesicle recycling in neuroendocrine cells. *Cell Mol Neurobiol* (2010) **30**:1365–70. doi:10.1007/s10571-010-9579-8
15. Patzak A, Bock G, Fischer-Colbrie R, Schauenstein K, Schmidt W, Lingg G, et al. Exocytotic exposure and retrieval of membrane antigens of chromaffin granules: quantitative evaluation of immunofluorescence on the surface of chromaffin cells. *J Cell Biol* (1984) **98**:1817–24. doi:10.1083/jcb.98.5.1817
16. Geisow MJ, Childs J, Burgoyne RD. Cholinergic stimulation of chromaffin cells induces rapid coating of the plasma membrane. *Eur J Cell Biol* (1985) **38**:51–6.
17. Smith C, Neher E. Multiple forms of endocytosis in bovine adrenal chromaffin cells. *J Cell Biol* (1997) **139**:885–94. doi:10.1083/jcb.139.4.885
18. Tsuboi T, Zhao C, Terakawa S, Rutter GA. Simultaneous evanescent wave imaging of insulin vesicle membrane and cargo during a single exocytotic event. *Curr Biol* (2000) **10**:1307–10. doi:10.1016/S0960-9822(00)00756-9
19. Bittner MA, Aikman RL, Holz RW. A nibbling mechanism for clathrin-mediated retrieval of secretory granule membrane after exocytosis. *J Biol Chem* (2013) **288**:9177–88. doi:10.1074/jbc.M113.450361
20. Lingwood D, Simons K. Lipid rafts as a membrane-organizing principle. *Science* (2010) **327**:46–50. doi:10.1126/science.1174621
21. Chasserot-Golaz S, Vitale N, Umbrecht-Jenck E, Knight D, Gerke V, Bader MF. Annexin 2 promotes the formation of lipid microdomains required for calcium-regulated exocytosis of dense-core vesicles. *Mol Biol Cell* (2005) **16**:1108–19. doi:10.1091/mbc.E04-07-0627
22. Salaun C, Gould GW, Chamberlain LH. Lipid raft association of SNARE proteins regulates exocytosis in PC12 cells. *J Biol Chem* (2005) **280**:19449–53. doi:10.1074/jbc.M501923200
23. Puri N, Roche PA. Ternary SNARE complexes are enriched in lipid rafts during mast cell exocytosis. *Traffic* (2006) **7**:1482–94. doi:10.1111/j.1600-0854.2006.00490.x
24. Umbrecht-Jenck E, Demais V, Calco V, Bailly Y, Bader MF, Chasserot-Golaz S. S100A10-mediated translocation of annexin-A2 to SNARE proteins in adrenergic chromaffin cells undergoing exocytosis. *Traffic* (2010) **11**:958–71. doi:10.1111/j.1600-0854.2010.01065.x
25. Futter CE, White IJ. Annexins and endocytosis. *Traffic* (2007) **8**:951–8. doi:10.1111/j.1600-0854.2007.00590.x
26. Turpin E, Russo-Marie F, Dubois T, De Paillerets C, Alfsen A, Bomsel M. In adrenocortical tissue, annexins II and VI are attached to clathrin coated vesicles in a calcium-independent manner. *Biochim Biophys Acta* (1998) **1402**:115–30. doi:10.1016/S0167-4889(97)00151-1
27. Creutz CE, Snyder SL. Interactions of annexins with the mu subunits of the clathrin assembly proteins. *Biochemistry* (2005) **44**:13795–806. doi:10.1021/bi051160w
28. Ammar MR, Kassas N, Chasserot-Golaz S, Bader M-F, Vitale N. Lipids in regulated exocytosis: what are they doing? *Front Endocrinol* (2013) **4**:125. doi:10.3389/fendo.2013.00125
29. Chasserot-Golaz S, Coorssen JR, Meunier FA, Vitale N. Lipid dynamics in exocytosis. *Cell Mol Neurobiol* (2010) **30**:1335–42. doi:10.1007/s10571-010-9577-x
30. Jackson LP, Kelly BT, Mccoy AJ, Gaffry T, James LC, Collins BM, et al. A large-scale conformational change couples membrane recruitment to cargo binding in the AP2 clathrin adaptor complex. *Cell* (2010) **141**:1220–9. doi:10.1016/j.cell.2010.05.006
31. Rao Y, Haucke V. Membrane shaping by the Bin/amphiphysin/Rvs (BAR) domain protein superfamily. *Cell Mol Life Sci* (2011) **68**:3983–93. doi:10.1007/s00018-011-0768-5
32. Yoon Y, Zhang X, Cho W. Phosphatidylinositol 4,5-bisphosphate (PtdIns(4,5)P2) specifically induces membrane penetration and deformation by Bin/amphiphysin/Rvs (BAR) domains. *J Biol Chem* (2012) **287**:34078–90. doi:10.1074/jbc.M112.372789
33. Meinecke M, Boucrot E, Camdere G, Hon WC, Mittal R, Mcmahon HT. Cooperative recruitment of dynamin and BIN/amphiphysin/Rvs (BAR) domain-containing proteins leads to GTP-dependent membrane scission. *J Biol Chem* (2013) **288**:6651–61. doi:10.1074/jbc.M112.444869
34. González-Jamett AM, Momboisse F, Guerra MJ, Ory S, Báez-Matus X, Barraza N, et al. Dynamin-2 regulates fusion pore expansion and quantal release through a mechanism that involves actin dynamics in neuroendocrine chromaffin cells. *PLoS One* (2013) **8**:e70638. doi:10.1371/journal.pone.0070638
35. Winckler B, Forscher P, Mellman I. A diffusion barrier maintains distribution of membrane proteins in polarized neurons. *Nature* (1999) **397**:698–701. doi:10.1038/17806
36. Mooren OL, Galletta BJ, Cooper JA. Roles for actin assembly in endocytosis. *Annu Rev Biochem* (2012) **81**:661–86. doi:10.1146/annurev-biochem-060910-094416
37. Gasman S, Chasserot-Golaz S, Malacombe M, Way M, Bader MF. Regulated exocytosis in neuroendocrine cells: a role for subplasmalemmal Cdc42/N-WASP-induced actin filaments. *Mol Biol Cell* (2004) **15**:520–31. doi:10.1091/mbc.E03-06-0402
38. van Meer G, Voelker DR, Feigenson GW. Membrane lipids: where they are and how they behave. *Nat Rev Mol Cell Biol* (2008) **9**:112–24. doi:10.1038/nrm2330
39. Ikeda M, Kihara A, Igarashi Y. Lipid asymmetry of the eukaryotic plasma membrane: functions and related enzymes. *Biol Pharm Bull* (2006) **29**:1542–6. doi:10.1248/bpb.29.1542
40. Demo SD, Masuda E, Rossi AB, Throndset BT, Gerard AL, Chan EH, et al. Quantitative measurement of mast cell degranulation using a novel flow cytometric annexin-V binding assay. *Cytometry* (1999) **36**:340–8. doi:10.1002/(SICI)1097-0320(19990801)36:4<340::AID-CYTO9>3.0.CO;2-C
41. Lee D, Hirashima N, Kirino Y. Rapid transbilayer phospholipid redistribution associated with exocytotic

release of neurotransmitters from cholinergic nerve terminals isolated from electric ray *Narke japonica*. *Neurosci Lett* (2000) **291**: 21–4. doi:10.1016/S0304-3940(00)01365-3

42. Vitale N, Caumont AS, Chasserot-Golaz S, Du G, Wu S, Sciorra VA, et al. Phospholipase D1: a key factor for the exocytotic machinery in neuroendocrine cells. *EMBO J* (2001) **20**:2424–34. doi:10.1093/emboj/20.10.2424
43. Malacombe M, Ceridono M, Calco V, Chasserot-Golaz S, Mcpherson PS, Bader MF, et al. Intersectin-1L nucleotide exchange factor regulates secretory granule exocytosis by activating Cdc42. *EMBO J* (2006) **25**:3494–503. doi:10.1038/sj.emboj.7601247
44. Ory S, Ceridono M, Momboisse F, Houy S, Chasserot-Golaz S, Heintz D, et al. Phospholipid scramblase-1-induced lipid reorganization regulates compensatory endocytosis in neuroendocrine cells. *J Neurosci* (2013) **33**:3545–56. doi:10.1523/JNEUROSCI.3654-12.2013
45. Manno S, Takakuwa Y, Mohandas N. Identification of a functional role for lipid asymmetry in biological membranes: phosphatidylserine-skeletal protein interactions modulate membrane stability. *Proc Natl Acad Sci U S A* (2002) **99**:1943–8. doi:10.1073/pnas.042688399
46. Stace CL, Ktistakis NT. Phosphatidic acid- and phosphatidylserine-binding proteins. *Biochim Biophys Acta* (2006) **1761**:913–26. doi:10.1016/j.bbalip.2006.03.006
47. Nossal R. Energetics of clathrin basket assembly. *Traffic* (2001) **2**:138–47. doi:10.1034/j.1600-0854.2001.020208.x
48. MacDonald PE, Eliasson L, Rorsman P. Calcium increases endocytotic vesicle size and accelerates membrane fission in insulin-secreting INS-1 cells. *J Cell Sci* (2005) **118**:5911–20. doi:10.1242/jcs.02685
49. Yao LH, Rao Y, Varga K, Wang CY, Xiao P, Lindau M, et al. Synaptotagmin 1 is necessary for the Ca2+ dependence of clathrin-mediated endocytosis. *J Neurosci* (2012) **32**:3778–85. doi:10.1523/JNEUROSCI.3540-11.2012
50. Hunter A, Phillips JH. The recycling of a secretory granule membrane protein. *Exp Cell Res* (1989) **182**:445–60. doi:10.1016/0014-4827(89)90249-8
51. Hurtley SM. Recycling of a secretory granule membrane protein after stimulated secretion. *J Cell Sci* (1993) **106**(Pt 2): 649–55.
52. Benedeczky I, Somogyi P. Cytochemical localization of exogenous peroxidase in adrenal medullary cells of hamster. *Acta Biol Acad Sci Hung* (1978) **29**:155–63.
53. Patzak A, Aunis D, Langley K. Membrane recycling after exocytosis: an ultrastructural study of cultured chromaffin cells. *Exp Cell Res* (1987) **171**:346–56. doi:10.1016/0014-4827(87)90167-4
54. Perez Bay AE, Ibanez LI, Marengo FD. Rapid recovery of releasable vesicles and formation of nonreleasable endosomes follow intense exocytosis in chromaffin cells. *Am J Physiol Cell Physiol* (2007) **293**:C1509–22. doi:10.1152/ajpcell.00632.2006
55. Perez Bay AE, Belingheri AV, Alvarez YD, Marengo FD. Membrane cycling after the excess retrieval mode of rapid endocytosis in mouse chromaffin cells. *Acta Physiol (Oxf)* (2012) **204**:403–18. doi:10.1111/j.1748-1716.2011.02340.x
56. Opazo F, Punge A, Buckers J, Hoopmann P, Kastrup L, Hell SW, et al. Limited intermixing of synaptic vesicle components upon vesicle recycling. *Traffic* (2010) **11**:800–12. doi:10.1111/j.1600-0854.2010.01058.x
57. Opazo F, Rizzoli SO. The fate of synaptic vesicle components upon fusion. *Commun Integr Biol* (2010) **3**:427–9. doi:10.4161/cib.3.5.12132

Conflict of Interest Statement: The authors declare that the research was conducted in the absence of any commercial or financial relationships that could be construed as a potential conflict of interest.

Received: 10 July 2013; accepted: 13 September 2013; published online: 02 October 2013.

*Citation: Houy S, Croisé P, Gubar O, Chasserot-Golaz S, Tryoen-Tóth P, Bailly Y, Ory S, Bader M-F and Gasman S (2013) Exocytosis and endocytosis in neuroendocrine cells: inseparable membranes! Front. Endocrinol. **4**:135. doi: 10.3389/fendo.2013.00135*

This article was submitted to Neuroendocrine Science, a section of the journal Frontiers in Endocrinology.

frontiers in
ENDOCRINOLOGY

REVIEW ARTICLE
published: 18 September 2013
doi: 10.3389/fendo.2013.00126

Dynamin-2 function and dysfunction along the secretory pathway

Arlek M. González-Jamett[1], Fanny Momboisse[1], Valentina Haro-Acuña[1], Jorge A. Bevilacqua[2], Pablo Caviedes[3] and Ana María Cárdenas[1]*

[1] *Facultad de Ciencias, Centro Interdisciplinario de Neurociencia de Valparaíso, Universidad de Valparaíso, Valparaíso, Chile*
[2] *Programa de Anatomía y Biología del Desarrollo, ICBM, Facultad de Medicina, Departamento de Neurología y Neurocirugía, Hospital Clínico Universidad de Chile, Universidad de Chile, Santiago, Chile*
[3] *Programa de Farmacología Molecular y Clínica, ICBM, Facultad de Medicina, Universidad de Chile, Santiago, Chile*

Edited by:
Stephane Gasman, Centre national de la Recherche Scientifique, France

Reviewed by:
Jocelyn Laporte, Institut National de la Santé et de la Recherche Médicale, France
Fernando Diego Marengo, Universidad de Buenos Aires, Argentina

***Correspondence:**
Ana María Cárdenas, Facultad de Ciencias, Centro Interdisciplinario de Neurociencia de Valparaíso, Universidad de Valparaíso, Gran Bretaña 1111, Playa Ancha 2360102, Valparaíso, Chile
e-mail: ana.cardenas@uv.cl

Dynamin-2 is a ubiquitously expressed mechano-GTPase involved in different stages of the secretory pathway. Its most well-known function relates to the scission of nascent vesicles from the plasma membrane during endocytosis; however, it also participates in the formation of new vesicles from the Golgi network, vesicle trafficking, fusion processes and in the regulation of microtubule, and actin cytoskeleton dynamics. Over the last 8 years, more than 20 mutations in the dynamin-2 gene have been associated to two hereditary neuromuscular disorders: Charcot–Marie–Tooth neuropathy and centronuclear myopathy. Most of these mutations are grouped in the pleckstrin homology domain; however, there are no common mutations associated with both disorders, suggesting that they differently impact on dynamin-2 function in diverse tissues. In this review, we discuss the impact of these disease-related mutations on dynamin-2 function during vesicle trafficking and endocytotic processes.

Keywords: dynamin-2, endocytosis, exocytosis, actin, microtubules, mutations, Charcot–Marie–Tooth neuropathy, centronuclear myopathy

INTRODUCTION

Dynamin was identified for the first time almost 25 years ago as a 100 kDa microtubule-associated protein that induced microtubule bundles and promoted microtubule sliding *in vivo* (1). As described by the same authors, the motor activity of dynamin required ATP and other co-purified polypeptides (1). A year later, the same group cloned and sequenced dynamin, and found that it contained a consensus GTP-binding site (2), and subsequently characterized its GTPase activity (3). At present, three dynamin isoforms encoded by three distinct genes (*DNM1*, *DNM2*, and *DNM3*) have been described in mammals (4). These exhibit approximately 80% homology in their sequences, yet they differ in their tissue expression pattern; dynamin-1 is mainly expressed in neuronal tissue, dynamin-2 is ubiquitously expressed, and dynamin-3 is expressed in brain, testis, and lungs (5). Of these three dynamin isoforms, only dynamin-2 appears to play a pleiotropic role during embryonic development (6). In fact, studies in knock-out animals show that deletion of dynamin-1 or -3 can be compensated by the other dynamin isoforms (7), while the deletion of dynamin-2 causes early embryonic lethality (8). Moreover, as discussed below, mutations in *DMN2* result in severe hereditary neuropathies and myopathies in humans, strongly suggesting that dynamin-2 has more susceptible functions in the nervous and skeletal muscle tissues.

All dynamin isoforms exhibit at least four alternatively spliced variants, resulting in different dynamin proteins (5) that share a primary structure comprising: a large amino-terminal GTPase domain (G-domain) that binds and hydrolyzes GTP; a middle and a GTPase effector domains (GED) that form a "stalk" structurally essential region; a pleckstrin homology domain (PH) that binds inositol phospholipids and a carboxy-terminal proline and arginine rich-domain (PRD) that allows interaction with SH3-domain-containing-proteins (5) (**Figure 1**).

Dynamin function relies on its ability to form high order oligomers, and its self-assembly is necessary to promote its catalytic activity. Purified dynamin has been shown to spontaneously polymerize in the presence of negatively charged tubular templates such as lipid membranes (11), microtubules (3, 12), or actin bundles (13, 14) as well as after incubation in low ionic strength solutions (15). Over the last years several cryo-electron microscopy (16–18) and X-ray crystallographic studies (19, 20) of dynamin and its domains (21–24) have allowed a better understanding of the mechanisms mediating dynamin oligomerization. It appears that the stable dimers formed by the crossed interaction between the "stalk" regions of monomeric dynamins (20, 25) are the basic unit that allows dynamin polymerization (18), thus promoting the GTPase activation required for membrane remodeling and scission in different cellular processes.

In the present review, we discuss the different roles of dynamin during endocytosis, vesicle trafficking, and exocytosis, specially focusing in dynamin-2, and how disease-linked mutations in dynamin-2 gene alter such cellular processes.

DYNAMIN AS A KEY COMPONENT OF ENDOCYTOSIS AND VESICLE RECYCLING

Dynamin is a GTPase that plays a crucial role in the recycling of secretory vesicle in neuroendocrine cells (26).

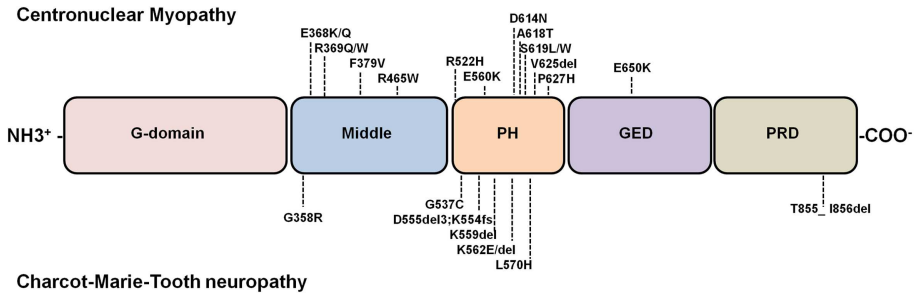

FIGURE 1 | Diagram of dynamin structure and localization of dynamin-2 mutations linked to CNM and CMT. Dynamins are multimodular proteins comprising five highly conserved structural domains: a large N-terminal GTPase domain (G-domain), a middle domain, a PH domain that bind phosphoinositides, a GTPase effector domain (GED), and a C-terminal proline rich domain (PRD) that interacts with SH3-domain containing proteins. Most common disease-related dynamin-2 mutations are represented. Note that almost all dynamin-2 mutations identified in CNM and CMT patients are clustered into the PH domains; only one CNM-linked mutation has been found in GED, and one related to CMT has been identified in the PRD. The D555del3 mutation is one of the products of a 9-bp deletion in the exon 14 (1652_1659 + 1delATGAGGAGg) of the dynamin-2 gene (9). This gene deletion also results in a 65-kDa truncated protein (9). For that reason here is described as D555del3, K554fs. An updated database of DNM2 mutations is at the website www.umd.be/DNM2/ (10).

The first evidence suggesting a role for dynamin in endocytosis came from the mapping and characterization of the *Drosophila shibire* gene, which was identified to be the *Drosophila* homolog of mammal dynamin (27, 28). *Drosophila* bearing mutations in the *shibire* gene exhibited a rapid and reversible paralysis at temperatures exceeding 29°C (29). The first ultrastructural analyses of synaptic terminals of *shibire* mutants showed a decreased number of synaptic vesicles and accumulation of "collared pits" suggesting a blocked step in the endocytotic process (30, 31). These ultrastructural changes were also observed in garland cells, a type of cell considered to be very active in endocytosis, where horseradish peroxidase uptake activity was also reduced, thus confirming an alteration in endocytosis in the *shibire* mutants (32). The role of dynamin in endocytosis in mammalian cells was later demonstrated using dynamin mutants with reduced GTPase activity (33, 34). The use of the non-hydrolyzable GTP analog GTP-γ-S allowed the visualization of endocytotic pits with elongated necks, decorated by electron-dense rings positive for dynamin immunoreactivity, showing that dynamin oligomerizes around the neck of endocytotic pits (35). Moreover, the fact that the dynamin mutant K44A, defective in GTP binding and hydrolysis, specifically blocked the coated vesicle formation without affecting the coat assembly and invagination revealed that dynamin is required for the constriction and subsequent budding of the coated vesicles (36). However, later studies suggested that dynamin also plays a role during a pre-collar stage, when the clathrin lattice is growing (37, 38). In this stage, dynamin may function as a scaffolding molecule that interacts with SH3 domain-containing proteins that control coated pit assembly and maturation (37). The recruitment of dynamin at endocytosis sites (39) also depends on its interaction with SH3-domain-containing proteins and phosphoinositides present at the plasma membrane via its PRD (40) and PH domain, respectively (41).

Regarding the mechanism by which dynamin catalyzes membrane fission, it has been proposed that the assembly of dynamin into helical oligomers around the neck of clathrin-coated pit promotes the dimerization of G domains of adjacent helical rungs, leading to the hydrolysis of GTP (18). The GTP hydrolysis triggers a conformational change in the dynamin polymer, allowing the constriction of the dynamin ring (18, 42, 43). The ring constriction strength then drives the constriction of the membrane neck, increasing membrane curvature (44). Such change in membrane curvature raises the local elastic energy, reducing the energy barrier to fission, and subsequently triggering the spontaneous fission at the boundary between the dynamin ring and the bare membranes (44).

The ability of dynamin to catalyze membrane fission is not only required in CME, but is also needed in other types of endocytotic pathways that are independent of clathrin. For instance, dynamin is required for caveolae-mediated endocytosis (45), which is essential for the uptake of molecules such as the complement C5b-9 complex (46). Dynamin also participates in the internalization of the β-chain of the interleukin-2 receptor through a clathrin independent, but RhoA dependent process, which is inhibited by the overexpression of a dominant negative mutant of dynamin GTPase activity (47). The entry in host cells of many pathogens and toxins such as anthrax toxin (48), Ebola virus (49), HIV (50), or Hepatitis C virus (51) also require the participation of dynamin.

Finally, the role of dynamin in vesicle formation is not only restricted to the plasma membrane and, as discussed below; its function is also needed in intracellular compartments.

ROLE OF DYNAMIN IN VESICLE TRAFFICKING AND GOLGI FUNCTION

Dynamin-mediated vesicle budding and membrane fission has also been reported in intracellular compartments such as endosomes (52, 53) and Golgi complex (54). Regarding dynamin-2 participation in vesicle trafficking from endosomes, this protein appears to play a role in two different steps: (1) the vesicle transport from late endosomes to the Golgi compartment (52) and (2) the recycling pathways from early endosomes (53). However, the establishment of dynamin-2 participation in the post-Golgi vesicle trafficking has been more controversial. Pioneer reports showed that the transport of vesicles from the Golgi to the cell surface or to lysosomes was independent of dynamin (36), and according to these results, no evidence of endogenous dynamin-2

localization in the Trans-Golgi network (TGN) nor of its participation in vesicle formation from this compartment were observed using different cell lines (55). Nevertheless, contemporary studies showed that ectopically expressed dynamin-2 localizes in the TGN in hepatocytes (54) and that the formation of clathrin-coated pits from Golgi membranes, in a cell-free assay, was inhibited in the presence of anti-dynamin antibodies, thus indicating the importance of dynamin at this level (54). Furthermore, canine kidney cells expressing a GTPase defective dynamin-2 mutant showed a restricted traffic of the protein p75 from the Golgi to the apical membrane (56). Also, the overexpression of a dominant negative mutant of dynamin-2 was shown to lead to the retention of proteins and accumulation of cisternae at the Golgi compartment, suggesting a role of dynamin-2 in keeping both the structure and function of the TGN (57).

In agreement with a role of dynamin-2 in Golgi vesicle formation, it was demonstrated that endogenous dynamin-2 localizes in the TGN in neuroendocrine mouse pituitary corticotrope cells (58), where it interacts with the βγ subunit of G-proteins via its PH domain. Interestingly, the overexpression of the purified PH domain induced the translocation of dynamin-2 from the Golgi complex to the plasma membrane, increasing receptor-mediated endocytosis but inhibiting basal and CRH-induced secretion of β-endorphins, suggesting a key role of dynamin-2 in the secretory pathway (58). Several studies have highlighted the importance of dynamin-2 to the proper traffic of nascent proteins from the TGN to the plasma membrane, a process that seems to be dependent on the actin cytoskeleton. In this regard, a subset of actin filaments anchored to the Golgi membrane via the small GTPase Arf-1 appears to form complexes with dynamin-2 and the actin-binding-protein cortactin, allowing the emergence and post-Golgi trafficking of secretory vesicles (59). Other proteins such as LimK1 and its substrate cofilin (60), syndapin, and the Wiskott–Aldrich-Syndrome-protein (WASP) (61) have been also involved in the regulation of the peri-Golgi actin cytoskeleton and in the dynamin-mediated transport of secretory vesicles from Golgi to the plasma membrane. Additionally, dynamin-2 function is necessary for the Golgi fragmentation and vesicle segregation induced by cholesterol in HeLa cells (62) and for the Golgi vesiculation induced by the c-SRC kinase activation (63) further supporting a pivotal role of dynamin in the Golgi dynamics along the secretory pathway.

DYNAMIN AS A FACILITATOR OF MEMBRANE FUSION

Dynamins have been involved in different types of fusion processes. Among them regulated exocytosis in neuroendocrine cells (64–69), acrosomal reaction (70), cell-to-cell fusion (71, 72), and fusion of virus with host cells (73, 74).

The first evidences showing the involvement of dynamin in exocytosis came from experiments performed at the beginning of 2000, which suggested that dynamin was involved in kiss-and-run, a transient mode of exocytosis, in neuroendocrine cells (64–66). In this type of exocytosis, the vesicle partially releases its content, and then it is recovered intact (75, 76). It was then hypothesized that dynamin would allow the reclosure of the vesicle mouth, acting through a mechanism similar to that described for vesicle formation during endocytosis (77). However, the mechanism by which dynamin controls the quantal release of hormones still remains unclear. More intriguing is the mechanism by which dynamin facilitates the fusion process during exocytosis. For instance, dynamin-2 reportedly favors granule secretion in both natural killer (78) and insulin-secreting cells (79). More recently, it was reported that, in chromaffin cells, dynamin-1 speeds up the expansion of the fusion pore, an intermediate structure formed during exocytosis, in a GTPase activity-dependent fashion (68). Therefore, both dynamin-1 and -2 appear to be involved in fusion processes. A possible explanation for this function is that dynamin interacts with SNARE proteins or SNARE-interacting proteins. In this regard, dynamin-2 has been shown to associate to secretory granules in chromaffin cells (80) via its interaction with syntaxin (80) and synaptophysin (67). In mammalian sperm, dynamin-2 associates with the SNARE regulatory protein complexin I (81), where it favors membrane fusion events during acrosomal exocytosis (70). In yeast, the dynamin homolog Vps1p interacts with the t-SNARE Vamp3; the disruption of this association with an antibody against Vps1p inhibits the fusion reaction (82). More recently, Peters' lab has demonstrated that Vps1 binds to the Qa SNARE Vamp3 and controls trans-SNARE formation, which is essential for membrane fusion in yeasts (83).

An alternative explanation is that dynamin controls fusion events via actin cytoskeleton dynamics. In this regard, cortical actin is dynamically rearranged during regulated exocytosis in neuroendocrine cells acting as a barrier as well as a carrier for the access of the secretory granules to the plasma membrane (84–86). Actin filaments also control the fusion pore expansion (87), as dynamin does (68). As we discuss below, given that dynamin regulates actin organization (13, 14, 88), it is plausible to assume that its actions on fusion processes relay on its ability to modulate actin dynamics. According to this idea, we have recently demonstrated that endogenous dynamin-2 directs a Ca^{2+}-dependent polymerization of cortical actin in adrenal chromaffin cells. Interestingly, both cortical actin and dynamin-2 regulate the initial fusion pore expansion and quantal release of transmitters, suggesting a synergistic action during exocytosis (89). Corey Smith and Collaborators found that the fusion pore expansion in chromaffin cells is controlled by the association of dynamin-1 with syndapin (69), a protein that modulates actin polymerization through neural-Wiskott–Aldrich-syndrome-protein (N-WASP) (90).

The role of dynamin-2 in fusion processes has also been extended to the fusion of myoblasts to form multinucleated myotubes (71). Interestingly, the GTPase activity of dynamin-2 is required at a stage that follows hemifusion but precedes the expansion of the fusion pores (71). The underlying mechanism is still unclear, but it could explain the muscular dysfunction in centronuclear myopathies caused by dynamin-2 mutations. Dynamin-2 has also been involved in the cell-to-cell fusion triggered by HIV-1 virus infection (72) and in fusion between HIV-1 virus and endosomes (73, 74). The latter authors proposed that dynamin promotes the expansion of the fusion pore that connects the HIV-1 envelope and the endosomal membrane, but the possible mechanism remains to be clarified.

Taken together, these findings indicate a pleiotropic role of dynamin in membrane fusion. Although dynamin does not promote membrane fusion by itself, it seems to act after a hemifusion state, facilitating the expansion of the fusion pore (71). The

underlying mechanism probably relies on dynamin ability to sense membrane curvature and remodel membranes (91).

DYNAMIN AS A REGULATOR OF MICROTUBULE INSTABILITY

Although dynamin was first identified as a microtubules-associated protein (1) its specific role in microtubule integrity and dynamics is still unclear. Using papain-digestion experiments *in vitro*, Herskovits and Co-workers observed that the entire PRD constituted a microtubule-binding site (34). Later, it was demonstrated that only the PRD amino-terminal region was necessary for the association of dynamin to microtubules, whereas its C-terminus appeared to negatively regulate this interaction (92). Pioneering studies also described that dynamin polymerized around microtubules, interconnecting them and allowing bundle formation (1), and in turn, microtubules seemed to stimulate dynamin GTPase activity (12). Other findings showed that the middle domain of dynamin-2 binds to γ-tubulin (93) locating dynamin-2 to the centrosome, therefore suggesting its participation during centrosome cohesion (93). More recently, dynamin-2 was found to be enriched in microtubule bundles at the mitotic spindle of mitotic cells, playing a key role during the cell cycle progression (94). In 2009, Tanabe and Takei observed that depletion of dynamin-2 in COS-7 cells, led to an abnormal accumulation of stable microtubules, consequently inducing disturbance of the microtubules-dependent membrane trafficking. These authors did not find alterations in microtubule assembly in cells that expressed a specific interfering RNA against dynamin-2, but they did report increased stability of pre-existing microtubules, suggesting a role of dynamin-2 in microtubule dynamics instability (95). This dynamin role appears to be independent of its GTPase activity. On the other hand, a deletion of three amino acid residues located at the β3/β4 loops of the PH domain induced decoration of microtubules and accumulation of acetylated tubulin, indicating that this region is required for the correct bundling of microtubules (95). The authors also proposed that this action of dynamin-2 on microtubule instability is necessary for a proper formation of Golgi network and vesicle trafficking.

DYNAMIN AS A DIRECTOR OF ACTIN CYTOSKELETON DYNAMICS

Dynamin-2 is recruited to different actin-rich structures such as phagocytic cups (96), podosomes (97), *Listeria* actin (98), lamellipodia (99), and filopodia (88), supporting a connection between dynamin-2 function and actin cytoskeleton polymerization. Moreover, both actin and dynamin-2 have regulatory functions during T cells activation (100), phagocytosis (101), and clathrin-dependent endocytosis (102). In the latter, actin and dynamin-2 have been shown to exhibit a synergistic action, where one modulates the recruitment of the other, and both participate in membrane remodeling and scission (103, 104).

In all these processes, dynamin appears to promote actin assembly in a manner dependent on its GTPase activity (14). The mechanism is still unclear, yet it is probably a consequence of its association with several nucleation promoting factors (NPF) via a PRD-SH3 interaction; among them Abp1 (105), the N-WASP (106), and cortactin (13, 88), all of which have been described as dynamin-partners during actin polymerization.

In 2010, Gu and Co-workers reported a direct interaction between dynamin and short actin filaments (F-actin). The latter promoted dynamin oligomerization, and in turn dynamin induced F-actin elongation (14). These authors suggested a model wherein dynamin would favor actin polymerization by removing the "caping"-protein gelsolin of the "barbed" ends (14). More recently, Yamada et al. (88) demonstrated that dynamin induces actin bundle stabilization in a way dependent on its association with cortactin in growth cone filopodia, where they seem to form ring-structures along actin filaments that stabilize F-actin bundles (88). Since dynamin oligomerization enhances its catalytic activity (14), its association with cortactin during actin polymerization fits better with its role as a GTPase than that of a mere "uncapping" protein.

IMPACT OF DISEASE-RELATED DYNAMIN-2 MUTATIONS IN VESICLE TRAFFICKING AND ENDOCYTOSIS

Specific missense mutations and short deletions into the structural domains of dynamin-2 have been associated with two congenital autosomic neuromuscular disorders: Charcot–Marie–Tooth neuropathy (CMT) (9) and centronuclear myopathy (CNM) (107). While CMT is a demyelinating disease affecting peripheral nerves (108), CNM is characterized by a progressive weakness and atrophy of distal muscles, usually involving facial and extraocular musculature (109–111). Although most dynamin-2 mutations linked to CMT and CNM are located in the middle and PH domains, there are no common mutations to both disorders (112) and the molecular mechanisms that lead to the neuropathy or myopathy remain obscure. **Figure 1** shows the localization of the CMT and CNM dynamin-2 mutations described until now, and **Table 1** summarizes their impacts on different cellular processes.

Regarding how these disease-related mutations affect dynamin-2 oligomerization and catalytic properties, *in vitro* studies have revealed that the CNM-linked mutations E368K/Q, R369Q/W, and R465W located into the middle domain of dynamin-2 (107) as well as the mutations A618T, S619L/W, and V625del clustered into the PH domain (118) exhibit an increased stability of the oligomers and an enhanced GTPase activity (119, 120). However, how these and other dynamin-2 mutations impact on dynamin-dependent cellular processes is still under discussion.

Given that the best-known role of dynamin-2 is to catalyze membrane scission during endocytosis, most of the studies regarding the mechanism underlying CNM associated to mutations in dynamin-2 have been focused in this cellular process. However, the findings are contradictory. The overexpression of the CNM-linked mutants R465W, R522H, S619L, P627H V625del, and E650K impaired CME in COS-1 and COS-7 cells (112, 115). The fact that the CNM mutant D614N causes intracellular mislocalization of both dynamin-2 and clathrin (121) suggests that an impairment in CME could be a consequence of the anomalous distribution of dynamin-2 and other endocytotic proteins. In opposition to the aforementioned findings, fibroblasts from patients harboring the mutations R465W or S619L reportedly display normal CME (112). In a similar manner, embryonic fibroblasts from heterozygous knock-in (KI) mice carrying the mutation R465W exhibited no defects in CME (113). Unlike the heterozygous R465W KI mice, the homozygous animals displayed impaired receptor-mediated

Table 1 | Cellular function alterations induced by CNM and CMT mutants.

Cellular process impaired	CNM mutations	CMT mutations
Intracellular calcium concentration in KI mice myofibers (113)	R465W	
Protein export from Golgi to plasma membrane in dynamin-2 (114)	E368K, R465W	D555del3, L570H
Clathrin-mediated endocytosis in:		
COS-1 and/or COS-7 cells (95, 112, 115)	R465W, R522H, E560K, S619L/W, V625del, P627H	K558E, K562E
RT4 Schwann cells and NSC-34 motor neurons (116)		G358R, G537C, K562E, K559del, L570H
Embryonic fibroblasts from homozygous KI mice (117)	R465W	
Clathrin-independent endocytosis (114)	E368K, R465W	D555del3, L570H
Raft-dependent endocytosis (114)	E368K, R465W	D555del3, L570H
Myelination in dorsal root ganglia (116)		G358R, G537C, K559del K562E, K562del, L570H
Demyelination in dorsal root ganglia (116)		G358R, K562E
Autophagy and autophagosome maturation (117)	R465W	

endocytosis, indicating that this mutation differentially impacts on CME according to the heterozygous or homozygous carrier state. In this regard, fibroblasts from patients harboring the homozygous mutation F379V, the first one linked to a lethal congenital syndrome, also exhibited dysfunctional endocytosis (6). In order to compare the effects of dynamin-2 mutations associated to CNM in a context that mimics the homozygous and heterozygous states, Schmid and Collaborators (114) established stable cell lines from dynamin-2 conditional null mouse fibroblasts and expressed two CNM-linked dynamin-2 mutants (E368K and R465W). Cells expressing comparable levels of wild-type dynamin-2 and the given mutant were selected to evaluate clathrin-dependent and independent endocytosis, and also vesicle trafficking. The authors showed that none of these mutations affected CME in the condition that mimics the heterozygous state; and they were able to fully rescue transferrin uptake in dynamin-2 KO cells. Nevertheless, all these mutants impaired clathrin-independent endocytosis of epidermal grow factor receptors and raft-dependent endocytosis of cholera toxin. Furthermore, also in the condition that mimics the heterozygous state, all the mutants disrupted trafficking of p75/neurotrophin receptor from Golgi to plasma membrane. It seems therefore plausible that the physiological dysfunctions in CNM patients harboring heterozygous mutations in dynamin-2 are not a consequence of defective CME, but other dynamin-2-dependent processes, such as clathrin-independent endocytosis or vesicle trafficking could be affected in these conditions.

Regarding the mechanism underlying CMT associated to dynamin-2 mutations, Sidiropoulos and Co-workers (116) suggested that an impairment of CME in Schwanm cells plays an important role in the pathogenesis of CMT neuropathy. They showed that the CMT mutants K562E, G358R, G537C, and L570H, but not the CNM mutants R465W and E560K, strongly reduced myelination in dorsal root ganglia explant cultures derived from heterozygous embryos carrying a dynamin-2 null allele, thus mimicking the heterozygous state. These CMT mutants also reduced transferrin internalization in Schwann cells and motor neurons. Conversely, none of the 11 CNM mutations evaluated in that work had any effect on transferrin internalization, neither in Schwann cells nor in motor neurons, suggesting that CMT and CNM mutations affect different cellular processes.

The aforementioned cellular impairments induced by CNM- and CMT-mutations, as well as others not previously mentioned, are summarized in the **Table 1**.

CONCLUDING REMARKS

The secretory pathway plays a pivotal role in mammalian cell function. Its disruption underlies many known diseases, such as those described herein. Dynamin-2 is critical in such mechanisms, as it regulates Golgi structure and function, cytoskeletal integrity, vesicle trafficking, and most interestingly, membrane fusion.

In the last 10 years, more than 20 disease-linked mutations have been reported in the dynamin-2 gene, affecting different dynamin-mediated cellular processes. Nevertheless, their impact on neuroendocrine tissues remains obscure. Also elusive are the mechanisms by which the said mutations affect actin cytoskeleton dynamics and exocytosis, processes which are dynamin-dependent and critical in the course of the secretory pathway. The latter opens an interesting research field that could prove useful to understand the mechanisms involved in the pathogenesis of dynamin-2 disease-related mutations.

Several diseases caused by genetic modifications remain as the final frontier in medicine, and although pivotal hallmarks such as the sequencing of the human genome have been attained, we still have much to learn about the cellular and molecular consequences of diverse gene mutations, specially, those that are common in many tissues. In this regard, dynamin-2 is a ubiquitous protein with diverse pleiotropic roles, whose mutations cause tissue-specific phenotypes. The existence of pertinent cell and animal models will be extremely useful for better understanding

how dynamin-2 mutations impact on its properties and related functions, and consequently in the identification of potential therapeutic targets.

ACKNOWLEDGMENTS

Fondecyt 1110552 (Chile); Proyecto Anillo ACT-1121 (CONICYT); Fondos ICM-ECONOMIA Project P09-022-F (Chile).

REFERENCES

1. Shpetner HS, Vallee RB. Identification of dynamin, a novel mechanochemical enzyme that mediates interactions between microtubules. *Cell* (1989) **59**:421–32. doi:10.1016/0092-8674(89)90027-5
2. Obar RA, Collins CA, Hammarback JA, Shpetner HS, Vallee RB. Molecular cloning of the microtubule-associated mechanochemical enzyme dynamin reveals homology with a new family of GTP-binding proteins. *Nature* (1990) **347**:256–61. doi:10.1038/347256a0
3. Shpetner HS, Vallee RB. Dynamin is a GTPase stimulated to high levels of activity by microtubules. *Nature* (1992) **355**:733–5. doi:10.1038/355733a0
4. Praefcke GJ, McMahon HT. The dynamin superfamily: universal membrane tubulation and fission molecules? *Nat Rev Mol Cell Biol* (2004) **5**:133–47. doi:10.1038/nrm1313
5. Cao H, Garcia F, McNiven MA. Differential distribution of dynamin isoforms in mammalian cells. *Mol Biol Cell* (1998) **9**:2595–609. doi:10.1091/mbc.9.9.2595
6. Koutsopoulos OS, Kretz C, Weller CM, Roux A, Mojzisova H, Böhm J, et al. Dynamin 2 homozygous mutation in humans with a lethal congenital syndrome. *Eur J Hum Genet* (2012) **21**:637–42. doi:10.1038/ejhg.2012.226
7. Raimondi A, Ferguson SM, Lou X, Armbruster M, Giovedi S, Messa M, et al. Overlapping role of dynamin isoforms in synaptic vesicle endocytosis. *Neuron* (2011) **70**: 100–14. doi:10.1016/j.neuron.2011.04.031
8. Ferguson SM, Raimondi A, Paradise S, Mesaki K, Ferguson A, Destaing O, et al. Coordinated actions of actin and BAR proteins upstream of dynamin at endocytic clathrin-coated pits. *Dev Cell* (2009) **17**:811–22. doi:10.1016/j.devcel.2009.11.005.coordinated
9. Züchner S, Noureddine M, Kennerson M, Verhoeven K, Claeys K, De Jonghe P, et al. Mutations in the pleckstrin homology domain of dynamin 2 cause dominant intermediate Charcot-Marie-Tooth disease. *Nat Genet* (2005) **37**:289–94. doi:10.1002/mrd.20660
10. Böhm J, Biancalana V, Dechene ET, Bitoun M, Pierson CR, Schaefer E, et al. Mutation spectrum in the large GTPase dynamin 2, and genotype-phenotype correlation in autosomal dominant centronuclear myopathy. *Hum Mutat* (2012) **33**:949–59. doi:10.1002/humu.22067
11. Tuma PL, Stachniak MC, Collins CA. Activation of dynamin GTPase by acidic phospholipids and endogenous rat brain vesicles. *J Biol Chem* (1993) **268**:17240–6.
12. Maeda K, Nakata T, Noda Y, Sato-Yoshitake R, Hirokawa N. Interaction of dynamin with microtubules: its structure and GTPase activity investigated by using highly purified dynamin. *Mol Biol Cell* (1992) **3**:1181–94. doi:10.1091/mbc.3.10.1181
13. Mooren OL, Kotova TI, Moore AJ, Schafer DA. Dynamin2 GTPase and cortactin remodel actin filaments. *J Biol Chem* (2009) **284**:23995–4005. doi:10.1074/jbc.M109.024398
14. Gu C, Yaddanapudi S, Weins A, Osborn T, Reiser J, Pollak M, et al. Direct dynamin-actin interactions regulate the actin cytoskeleton. *EMBO J* (2010) **29**:3593–606. doi:10.1038/emboj.2010.249
15. Hinshaw JE, Schmid SL. Dynamin self-assembles into rings suggesting a mechanism for coated vesicle budding. *Nature* (1995) **374**:190–2. doi:10.1038/374190a0
16. Zhang P, Hinshaw JE. Three-dimensional reconstruction of dynamin in the constricted state. *Nat Cell Biol* (2001) **3**:922–6. doi:10.1038/ncb1001-922
17. Danino D, Moon KH, Hinshaw JE. Rapid constriction of lipid bilayers by the mechanochemical enzyme dynamin. *J Struct Biol* (2004) **147**:259–67. doi:10.1016/j.jsb.2004.04.005
18. Chappie JS, Mears JA, Fang S, Leonard M, Schmid SL, Milligan RA, et al. A pseudoatomic model of the dynamin polymer identifies a hydrolysis-dependent powerstroke. *Cell* (2011) **147**:209–22. doi:10.1016/j.cell.2011.09.003
19. Ford MG, Jenni S, Nunnari J. The crystal structure of dynamin. *Nature* (2011) **477**:561–6. doi:10.1038/nature10441
20. Faelber K, Posor Y, Gao S, Held M, Roske Y, Schulze D, et al. Crystal structure of nucleotide-free dynamin. *Nature* (2011) **477**:556–60. doi:10.1038/nature10369
21. Timm D, Salim K, Gout I, Guruprasad L, Waterfield M, Blundell T. Crystal structure of the pleckstrin homology domain from dynamin. *Nat Struct Biol* (1994) **1**:782–8. doi:10.1038/nsb1194-782
22. Niemann HH, Knetsch ML, Scherer A, Manstein DJ, Kull FJ. Crystal structure of a dynamin GTPase domain in both nucleotide-free and GDP-bound forms. *EMBO J* (2001) **20**:5813–21. doi:10.1093/emboj/20.21.5813
23. Reubold TF, Eschenburg S, Becker A, Leonard M, Schmid SL, Vallee RB, et al. Crystal structure of the GTPase domain of rat dynamin 1. *Proc Natl Acad Sci U S A* (2005) **102**:13093–8. doi:10.1073/pnas.0506491102
24. Chappie JS, Acharya S, Liu Y, Leonard M, Pucadyil TJ, Schmid SL. An intramolecular signaling element that modulates dynamin function in vitro and in vivo. *Mol Biol Cell* (2009) **20**:3561–71. doi:10.1091/mbc.E09
25. Chappie JS, Acharya S, Leonard M, Schmid SL, Dyda F. G domain dimerization controls dynamin's assembly-stimulated GTPase activity. *Nature* (2010) **465**:43540. doi:10.1038/nature09032
26. Cárdenas AM, Marengo FD. Rapid endocytosis and vesicle recycling in neuroendocrine cells. *Cell Mol Neurobiol* (2010) **30**:1365–70. doi:10.1007/s10571-010-9579-8
27. van der Bliek AM, Meyerowitz EM. Dynamin-like protein encoded by the *Drosophila* shibire gene associated with vesicular traffic. *Nature* (1991) **351**:411–4. doi:10.1038/351411a0
28. Chen MS, Obar RA, Schroeder CC, Austin TW, Poodry CA, Wadsworth SC, et al. Multiple forms of dynamin are encoded by shibire, a *Drosophila* gene involved in endocytosis. *Nature* (1991) **351**:583–6. doi:10.1038/351583a0
29. Grigliatti TA, Hall L, Rosenbluth R, Suzuki DT. Temperature-sensitive mutations in *Drosophila melanogaster*. XIV. A selection of immobile adults. *Mol Gen Genet* (1973) **120**:107–14. doi:10.1007/BF00267238
30. Poodry CA, Edgar L. Reversible alteration in the neuromuscular junctions of *Drosophila melanogaster* bearing a temperature-sensitive mutation, shibire. *J Cell Biol* (1979) **81**:520–7. doi:10.1083/jcb.81.3.520
31. Kosaka T, Ikeda K. Possible temperature-dependent blockage of synaptic vesicle recycling induced by a single gene mutation in *Drosophila*. *J Neurobiol* (1983) **14**:207–25. doi:10.1002/neu.480140305
32. Kosaka T, Ikeda K. Reversible blockage of membrane retrieval and endocytosis in the garland cell of the temperature-sensitive mutant of *Drosophila melanogaster*, shibirets1. *J Cell Biol* (1983) **97**:499–507. doi:10.1083/jcb.97.2.499
33. van der Bliek AM, Redelmeier TE, Damke H, Tisdale EJ, Meyerowitz EM, Schmid SL. Mutations in human dynamin block an intermediate stage in coated vesicle formation. *J Cell Biol* (1993) **122**:553–63. doi:10.1083/jcb.122.3.553
34. Herskovits JS, Burgess CC, Obar RA, Vallee RB. Effects of mutant rat dynamin on endocytosis. *J Cell Biol* (1993) **122**:565–78. doi:10.1083/jcb.122.3.565
35. Takei K, McPherson PS, Schmid SL, De Camilli P. Tubular membrane invaginations coated by dynamin rings are induced by GTP-gamma S in nerve terminals. *Nature* (1995) **374**:186–90. doi:10.1038/374186a0
36. Damke H, Baba T, Warnock DE, Schmid SL, Jolla L. Induction of mutant dynamin specifically blocks endocytic coated vesicle formation. *J Cell Biol* (1994) **127**:915–34. doi:10.1083/jcb.127.4.915
37. Narayanan R, Leonard M, Song BD, Schmid SL, Ramaswami M. An internal GAP domain negatively regulates presynaptic dynamin in vivo: a two-step model for dynamin function. *J Cell Biol* (2005) **169**:117–26. doi:10.1083/jcb.200502042
38. Macia E, Ehrlich M, Massol R, Boucrot E, Brunner C, Kirchhausen T. Dynasore, a cell-permeable inhibitor of dynamin. *Dev Cell* (2006) **10**:839–50. doi:10.1016/j.devcel.2006.04.002

39. Merrifield CJ, Perrais D, Zenisek D. Coupling between clathrin-coated-pit invagination, cortactin recruitment, and membrane scission observed in live cells. *Cell* (2005) **121**:593–606. doi:10.1016/j.cell.2005.03.015
40. Shpetner HS, Herskovits JS, Vallee RB. A binding site for SH3 domains targets dynamin to coated pits. *J Biol Chem* (1996) **271**:13–6. doi:10.1074/jbc.271.1.13
41. Lee A, Frank DW, Marks MS, Lemmon MA. Dominant-negative inhibition of receptor-mediated endocytosis by a dynamin-1 mutant with a defective pleckstrin homology domain. *Curr Biol* (1999) **9**:261–4. doi:10.1016/S0960-9822(99)80115-8
42. Roux A, Uyhazi K, Frost A, De Camilli P. GTP-dependent twisting of dynamin implicates constriction and tension in membrane fission. *Nature* (2006) **441**:528–31. doi:10.1038/nature04718
43. Mears JA, Ray P, Hinshaw JE. A corkscrew model for dynamin constriction. *Structure* (2007) **15**:1190–202. doi:10.1016/j.str.2007.08.012
44. Morlot S, Galli V, Klein M, Chiaruttini N, Manzi J, Humbert F, et al. Membrane shape at the edge of the dynamin helix sets location and duration of the fission reaction. *Cell* (2012) **151**:619–29. doi:10.1016/j.cell.2012.09.017
45. Henley JR, Krueger EW, Oswald BJ, McNiven MA. Dynamin-mediated Internalization of caveolae. *J Cell Biol* (1998) **141**:85–99. doi:10.1083/jcb.141.1.85
46. Moskovich O, Herzog LO, Ehrlich M, Fishelson Z. Caveolin-1 and dynamin-2 are essential for removal of the complement C5b-9 complex via endocytosis. *J Biol Chem* (2012) **287**:19904–15. doi:10.1074/jbc.M111.333039
47. Lamaze C, Dujeancourt A, Baba T, Lo CG, Benmerah A, Dautry-Varsat A. Interleukin 2 receptors and detergent-resistant membrane domains define a clathrin-independent endocytic pathway. *Mol Cell* (2001) **7**:661–71. doi:10.1016/S1097-2765(01)00212-X
48. Abrami L, Liu S, Cosson P, Leppla SH, van der Goot FG. Anthrax toxin triggers endocytosis of its receptor via a lipid raft-mediated clathrin-dependent process. *J Cell Biol* (2003) **160**:321–8. doi:10.1083/jcb.200211018
49. Mulherkar N, Raaben M, de la Torre JC, Whelan SP, Chandran K. The Ebola virus glycoprotein mediates entry via a non-classical dynamin-dependent macropinocytic pathway. *Virology* (2011) **419**:72–83. doi:10.1016/j.virol.2011.08.009
50. Carter GC, Bernstone L, Baskaran D, James W. HIV-1 infects macrophages by exploiting an endocytic route dependent on dynamin, Rac1 and Pak1. *Virology* (2011) **409**:234–50. doi:10.1128/JVI.01051-12
51. Abdulkarim AS, Cao H, Huang B, McNiven MA. The large GTPase dynamin is required for hepatitis B virus protein secretion from hepatocytes. *J Hepatol* (2003) **38**:76–83. doi:10.1016/S0168-8278(02)00326-4
52. Nicoziani P, Vilhardt F, Llorente A, Hilout L, Courtoy PJ, Sandvig K, et al. Role for dynamin in late endosome dynamics and trafficking of the cation-independent mannose 6-phosphate receptor. *Mol Biol Cell* (2000) **11**:481–95. doi:10.1091/mbc.11.2.481
53. Mesaki K, Tanabe K, Obayashi M, Oe N, Takei K. Fission of tubular endosomes triggers endosomal acidification and movement. *PLoS One* (2011) **6**:e19764. doi:10.1371/journal.pone.0019764
54. Jones SM, Howell KE, Henley JR, Cao H, McNiven MA. Role of dynamin in the formation of transport vesicles from the trans-Golgi network. *Science* (1998) **279**:573–7. doi:10.1126/science.279.5350.573
55. Kasai K, Shin HW, Shinotsuka C, Murakami K, Nakayama K. Dynamin II is involved in endocytosis but not in the formation of transport vesicles from the trans-Golgi network. *J Biochem* (1999) **125**:780–9. doi:10.1093/oxfordjournals.jbchem.a022349
56. Kreitzer G, Marmorstein A, Okamoto P, Vallee R, Rodriguez-Boulan E. Kinesin and dynamin are required for post-Golgi transport of a plasma-membrane protein. *Nat Cell Biol* (2000) **2**:125–7. doi:10.1038/35000081
57. Cao H, Thompson HM, Krueger EW, McNiven MA. Disruption of Golgi structure and function in mammalian cells expressing a mutant dynamin. *J Cell Sci* (2000) **113**:1993–2002.
58. Yang Z, Li H, Chai Z, Fullerton MJ, Cao Y, Toh BH, et al. Dynamin II regulates hormone secretion in neuroendocrine cells. *J Biol Chem* (2001) **276**:4251–60. doi:10.1074/jbc.M006371200
59. Cao H, Weller S, Orth JD, Chen J, Huang B, Chen JL, et al. Actin and Arf1-dependent recruitment of a cortactin-dynamin complex to the Golgi regulates post-Golgi transport. *Nat Cell Biol* (2005) **7**:483–92. doi:10.1038/ncb1246
60. Salvarezza SB, Deborde S, Schreiner R, Campagne F, Kessels MM, Qualmann B, et al. LIM kinase 1 and cofilin regulate actin filament population required for dynamin-dependent apical carrier fission from the trans-Golgi network. *Mol Biol Cell* (2009) **20**:438–51. doi:10.1091/mbc.E08-08-0891
61. Kessels MM, Dong J, Leibig W, Westermann P, Qualmann B. Complexes of syndapin II with dynamin II promote vesicle formation at the trans-Golgi network. *J Cell Sci* (2006) **119**:1504–16. doi:10.1242/jcs.02877
62. Grimmer S, Ying M, Wälchli S, van Deurs B, Sandvig K. Golgi vesiculation induced by cholesterol occurs by a dynamin and cPLA2-dependent mechanism. *Traffic* (2005) **6**:144–56. doi:10.1111/j.1600-0854.2005.00258.x
63. Weller SG, Capitani M, Cao H, Micaroni M, Luini A, Sallese M, et al. Src kinase regulates the integrity and function of the Golgi apparatus via activation of dynamin 2. *Proc Natl Acad Sci U S A* (2010) **107**:5863–8. doi:10.1073/pnas.0915123107
64. Artalejo CR, Elhamdani A, Palfrey HC. Sustained stimulation shifts the mechanism of endocytosis from dynamin-1-dependent rapid endocytosis to clathrin and dynamin-2-mediated slow endocytosis in chromaffin cells. *Proc Natl Acad Sci U S A* (2002) **99**:6358–63. doi:10.1073/pnas.082658499
65. Graham ME, O'Callaghan DW, McMahon HT, Burgoyne RD. Dynamin-dependent and dynamin-independent processes contribute to the regulation of single vesicle release kinetics and quantal size. *Proc Natl Acad Sci U S A* (2002) **99**:7124–9. doi:10.1073/pnas.102645099
66. Holroyd P, Lang T, Wenzel D, De Camilli P, Jahn R. Imaging direct, dynamin-dependent recapture of fusing secretory granules on plasma membrane lawns from PC12 cells. *Proc Natl Acad Sci U S A* (2002) **99**:16806–11. doi:10.1073/pnas.222677399
67. González-Jamett AM, Báez-Matus X, Hevia MA, Guerra MJ, Olivares MJ, Martínez AD, et al. The association of dynamin with synaptophysin regulates quantal size and duration of exocytotic events in chromaffin cells. *J Neurosci* (2010) **30**:10683–91. doi:10.1523/JNEUROSCI.5210-09.2010
68. Anantharam A, Bittner MA, Aikman RL, Stuenkel EL, Schmid SL, Axelrod D, et al. A new role for the dynamin GTPase in the regulation of fusion pore expansion. *Mol Biol Cell* (2011) **22**:1907–18. doi:10.1091/mbc.E11-02-0101
69. Samasilp P, Chan SA, Smith C. Activity-dependent fusion pore expansion regulated by a calcineurin-dependent dynamin-syndapin pathway in mouse adrenal chromaffin cells. *J Neurosci* (2012) **32**:10438–47. doi:10.1523/JNEUROSCI.1299-12.2012
70. Reid AT, Lord T, Stanger SJ, Roman SD, McCluskey A, Robinson PJ, et al. Dynamin regulates specific membrane fusion events necessary for acrosomal exocytosis in mouse spermatozoa. *J Biol Chem* (2012) **287**:37659–72. doi:10.1074/jbc.M112.392803
71. Leikina E, Melikov K, Sanyal S, Verma SK, Eun B, Gebert C, et al. Extracellular annexins and dynamin are important for sequential steps in myoblast fusion. *J Cell Biol* (2013) **200**:109–23. doi:10.1083/jcb.201207012
72. Lai W, Huang L, Ho P, Montefiori D, Chen CH. The role of dynamin in HIV type 1 Env-mediated cell-cell fusion. *AIDS Res Hum Retroviruses* (2011) **27**:1013–7. doi:10.1089/AID.2010.0259
73. Miyauchi K, Kim Y, Latinovic O, Morozov V, Melikyan GB. HIV enters cell via endocytosis and dynamin-dependent fusion with endosomes. *Cell* (2010) **137**:433–44. doi:10.1016/j.cell.2009.02.046.HIV
74. de la Vega M, Marin M, Kondo N, Miyauchi K, Kim Y, Epand RF, et al. Inhibition of HIV-1 endocytosis allows lipid mixing at the plasma membrane, but not complete fusion. *Retrovirology* (2011) **8**:99. doi:10.1186/1742-4690-8-99
75. Alés E, Tabares L, Poyato JM, Valero V, Lindau M, Alvarez de Toledo G. High calcium concentrations shift the mode of exocytosis to the kiss-and-run mechanism. *Nat Cell Biol* (1999) **1**:40–4. doi:10.1038/9012
76. Perrais D, Kleppe IC, Taraska JW, Almers W. Recapture after exocytosis causes differential retention of protein in granules of bovine

chromaffin cells. *J Physiol* (2004) **560**:413–28. doi:10.1113/jphysiol.2004.064410
77. Tsuboi T, McMahon HT, Rutter GA. Mechanisms of dense core vesicle recapture following "kiss and run" ("cavicapture") exocytosis in insulin-secreting cells. *J Biol Chem* (2004) **279**:47115–24. doi:10.1074/jbc.M408179200
78. Arneson LN, Segovis CM, Gomez TS, Schoon RA, Dick J, Lou Z, et al. Dynamin 2 regulates granule exocytosis during NK cell-mediated cytotoxicity. *J Immunol* (2008) **181**:6995–7001.
79. Min L, Leung YM, Tomas A, Watson RT, Gaisano HY, Halban PA, et al. Dynamin is functionally coupled to insulin granule exocytosis. *J Biol Chem* (2007) **282**:33530–6. doi:10.1074/jbc.M703402200
80. Galas M, Chasserot-golaz S, Dirrig-grosch S, Bader M. Presence of dynamin – syntaxin complexes associated with secretory granules in adrenal chromaffin cells. *J Neurochem* (2000) **75**:1511–9. doi:10.1046/j.1471-4159.2000.0751511.x
81. Zhao L, Shi X, Li L, Miller DJ. Dynamin 2 associates with complexins and is found in the acrosomal region of mammalian sperm. *Mol Reprod Dev* (2007) **74**:750–7. doi:10.1002/mrd.20660
82. Peters C, Baars TL, Bühler S, Mayer A. Mutual control of membrane fission and fusion proteins. *Cell* (2004) **119**:667–78. doi:10.1016/j.cell.2004.11.023
83. Alpadi K, Kulkarni A, Namjoshi S, Srinivasan S, Sippel KH, Ayscough K, et al. Dynamin-SNARE interactions control trans-SNARE formation in intracellular membrane fusion. *Nat Commun* (2013) **4**:1704. doi:10.1038/ncomms2724
84. Gasman S, Chasserot-Golaz S, Malacombe M, Way M, Bader MF. Regulated exocytosis in neuroendocrine cells: a role for subplasmalemmal Cdc42/N-WASP-induced actin filaments. *Mol Biol Cell* (2004) **15**:520–31. doi:10.1091/mbc.E03-06-0402
85. Malacombe M, Bader MF, Gasman S. Exocytosis in neuroendocrine cells: new tasks for actin. *Biochim Biophys Acta* (2006) **1763**:1175–83. doi:10.1016/j.bbamcr.2006.09.004
86. Wollman R, Meyer T. Coordinated oscillations in cortical actin and Ca2+ correlate with cycles of vesicle secretion. *Nat Cell Biol* (2012) **14**:1261–9. doi:10.1038/ncb2614
87. Berberian K, Torres AJ, Fang Q, Kisler K, Lindau M. F-actin and myosin II accelerate catecholamine release from chromaffin granules. *J Neurosci* (2009) **29**:863–70. doi:10.1523/JNEUROSCI.2818-08.2009
88. Yamada H, Abe T, Satoh A, Okazaki N, Tago S, Kobayashi K, et al. Stabilization of actin bundles by a dynamin 1/cortactin ring complex is necessary for growth cone filopodia. *J Neurosci* (2013) **33**:4514–26. doi:10.1523/JNEUROSCI.2762-12.2013
89. González-Jamett AM, Momboisse F, Guerra MJ, Ory S, Báez-Matus X, Barraza N, et al. Dynamin-2 regulates fusion pore expansion and quantal release through a mechanism that involves actin dynamics in neuroendocrine chromaffin cells. *PLoS One* (2013) **8**:70638. doi:10.1371/journal.pone.0070638
90. Dharmalingam E, Haeckel A, Pinyol R, Schwintzer L, Koch D, Kessels MM, et al. F-BAR proteins of the syndapin family shape the plasma membrane and are crucial for neuromorphogenesis. *J Neurosci* (2009) **29**:13315–27. doi:10.1523/JNEUROSCI.3973-09.2009
91. Anantharam A, Axelrod D, Holz RW. Real-time imaging of plasma membrane deformations reveals pre-fusion membrane curvature changes and a role for dynamin in the regulation of fusion pore expansion. *J Neurochem* (2012) **122**:661–71. doi:10.1111/j.1471-4159.2012.07816.x
92. Hamao K, Morita M, Hosoya H. New function of the proline rich domain in dynamin-2 to negatively regulate its interaction with microtubules in mammalian cells. *Exp Cell Res* (2009) **315**:1336–45. doi:10.1016/j.yexcr.2009.01.025
93. Thompson HM, Cao H, Chen J, Euteneuer U, McNiven MA. Dynamin 2 binds gamma-tubulin and participates in centrosome cohesion. *Nat Cell Biol* (2004) **6**:335–42. doi:10.1038/ncb1112
94. Ishida N, Nakamura Y, Tanabe K, Li S, Takei K. Dynamin 2 associates with microtubules at mitosis and regulates cell cycle progression. *Cell Struct Funct* (2011) **36**:145–54. doi:10.1247/csf.10016
95. Tanabe K, Takei K. Dynamic instability of microtubules requires dynamin 2 and is impaired in a Charcot-Marie-Tooth mutant. *J Cell Biol* (2009) **185**:939–48. doi:10.1083/jcb.200803153
96. Gold ES, Underhill DM, Morrissette NS, Guo J, McNiven MA, Aderem A. Dynamin 2 is required for phagocytosis in macrophages. *J Exp Med* (1999) **190**:1849–56. doi:10.1084/jem.190.12.1849
97. Ochoa G, Slepnev VI, Neff L, Ringstad N, Takei K, Daniell L, et al. A functional link between dynamin and the actin cytoskeleton at podosomes. *J Cell Biol* (2000) **150**:377–89. doi:10.1083/jcb.150.2.377
98. Lee E, De Camilli P. Dynamin at actin tails. *Proc Natl Acad Sci U S A* (2002) **99**:161–6. doi:10.1073/pnas.012607799
99. Yamada H, Abe T, Li SA, Masuoka Y, Isoda M, Watanabe M, et al. Dynasore, a dynamin inhibitor, suppresses lamellipodia formation and cancer cell invasion by destabilizing actin filaments. *Biochem Biophys Res Commun* (2009) **390**:1142–8. doi:10.1016/j.bbrc.2009.10.105
100. Gomez TS, Hamann MJ, McCarney S, Savoy DN, Lubking CM, Heldebrant MP, et al. Dynamin 2 regulates T cell activation by controlling actin polymerization at the immunological synapse. *Nat Immunol* (2005) **6**:261–70. doi:10.1038/ni1168
101. Otsuka A, Abe T, Watanabe M, Yagisawa H, Takei K, Yamada H. Dynamin 2 is required for actin assembly in phagocytosis in sertoli cells. *Biochem Biophys Res Commun* (2009) **378**:478–82. doi:10.1016/j.bbrc.2008.11.066
102. Merrifield CJ, Feldman ME, Wan L, Almers W. Imaging actin and dynamin recruitment during invagination of single clathrin-coated pits. *Nat Cell Biol* (2002) **4**:691–8. doi:10.1038/ncb837
103. Itoh T, Erdmann KS, Roux A, Habermann B, Werner H, De Camilli P. Dynamin and the actin cytoskeleton cooperatively regulate plasma membrane invagination by BAR and F-BAR proteins. *Dev Cell* (2005) **9**:791–804. doi:10.1016/j.devcel.2005.11.005
104. Taylor MJ, Lampe M, Merrifield CJ. A feedback loop between dynamin and actin recruitment during clathrin-mediated endocytosis. *PLoS Biol* (2012) **10**:e1001302. doi:10.1371/journal.pbio.1001302
105. Kessels MM, Engqvist-Goldstein AE, Drubin DG, Qualmann B. Mammalian Abp1, a signal-responsive F-actin-binding protein, links the actin cytoskeleton to endocytosis via the GTPase dynamin. *Sci Signal* (2001) **153**:351–66. doi:10.1083/jcb.153.2.35
106. Shin N, Lee S, Ahn N, Kim SA, Ahn SG, YongPark Z, et al. Sorting nexin 9 interacts with dynamin 1 and N-WASP and coordinates synaptic vesicle endocytosis. *J Biol Chem* (2007) **282**:28939–50. doi:10.1074/jbc.M700283200
107. Bitoun M, Maugenre S, Jeannet PY, Lacène E, Ferrer X, Laforêt P, et al. Mutations in dynamin 2 cause dominant centronuclear myopathy. *Nat Genet* (2005) **37**:1207–9. doi:10.1038/ng1657
108. Tanabe K, Takei K. Dynamin 2 in Charcot-Marie-Tooth disease. *Acta Med Okayama* (2012) **66**:183–90.
109. Jeannet PY, Bassez G, Eymard B, Laforêt P, Urtizberea JA, Rouche A, et al. Clinical and histologic findings in autosomal centronuclear myopathy. *Neurology* (2004) **62**:1484–90. doi:10.1212/01.WNL.0000124388.67003.56
110. Fisher J, Towfighi J, Darvish D, Simmons Z. A case of hereditary inclusion body myopathy: 1 patient, 2 novel mutations. *J Clin Neuromuscul Dis* (2006) **7**:179–84. doi:10.1097/01.cnd.0000211406.94445.f0
111. Susman RD, Quijano-Roy S, Yang N, Webster R, Clarke NF, Dowling J, et al. Expanding the clinical, pathological and MRI phenotype of DNM2-related centronuclear myopathy. *Neuromuscul Disord* (2010) **20**:229–37. doi:10.1016/j.nmd.2010.02.016
112. Koutsopoulos OS, Koch C, Tosch V, Böhm J, North KN, Laporte J. Mild functional differences of dynamin 2 mutations associated to centronuclear myopathy and Charcot-Marie Tooth peripheral neuropathy. *PLoS One* (2011) **6**:e27498. doi:10.1371/journal.pone.0027498
113. Durieux AC, Vignaud A, Prudhon B, Viou MT, Beuvin M, Vassilopoulos S, et al. A centronuclear myopathy-dynamin 2 mutation impairs skeletal muscle structure and function in mice. *Hum Mol Genet* (2010) **19**:4820–36. doi:10.1093/hmg/ddq413
114. Liu YW, Lukiyanchuk V, Schmid SL. Common membrane trafficking defects of disease-associated dynamin 2 mutations. *Traffic* (2011) **12**:1620–33. doi:10.1111/j.1600-0854.2011.01250.x
115. Bitoun M, Durieux AC, Prudhon B, Bevilacqua JA, Herledan A, Sakanyan V, et al. Dynamin 2 mutations associated with human diseases impair clathrin-mediated receptor endocytosis. *Hum Mutat* (2009) **30**:1419–27. doi:10.1002/humu.21086

116. Sidiropoulos NM, Miehe M, Bock T, Tinelli E, Oertli CI. Dynamin 2 mutations in Charcot-Marie-Tooth clathrin-mediated endocytosis in myelination. *Brain* (2012) **135**:1395–411. doi:10.1093/brain/aws061
117. Durieux AC, Vassilopoulos S, Lainé J, Fraysse B, Briñas L, Prudhon B, et al. A centronuclear myopathy – dynamin 2 mutation impairs autophagy in mice. *Traffic* (2012) **13**:869–79. doi:10.1111/j.1600-0854.2012.01348.x
118. Bitoun M, Bevilacqua JA, Prudhon B, Maugenre S, Taratuto AL, Monges S, et al. Dynamin 2 mutations cause sporadic centronuclear myopathy with neonatal onset. *Ann Neurol* (2007) **62**:666–70. doi:10.1002/ana.21235
119. Wang L, Barylko B, Byers C, Ross JA, Jameson DM, Albanesi JP. Dynamin 2 mutants linked to centronuclear myopathies form abnormally stable polymers. *J Biol Chem* (2010) **285**:22753–7. doi:10.1074/jbc.C110.130013
120. Kenniston JA, Lemmon MA. Dynamin GTPase regulation is altered by PH domain mutations found in centronuclear myopathy patients. *EMBO J* (2010) **29**:3054–67. doi:10.1038/emboj.2010.187
121. Kierdaszuk B, Berdynski M, Karolczak J, Redowicz MJ, Zekanowski C, Kaminska AM. A novel mutation in the DNM2 gene impairs dynamin 2 localization in skeletal muscle of a patient with late onset centronuclear myopathy. *Neuromuscul Disord* (2013) **23**:219–28. doi:10.1016/j.nmd.2012.12.007

Conflict of Interest Statement: The authors declare that the research was conducted in the absence of any commercial or financial relationships that could be construed as a potential conflict of interest.

Received: 29 May 2013; accepted: 31 August 2013; published online: 18 September 2013.
*Citation: González-Jamett AM, Momboisse F, Haro-Acuña V, Bevilacqua JA, Caviedes P and Cárdenas AM (2013) Dynamin-2 function and dysfunction along the secretory pathway. Front. Endocrinol. **4**:126. doi: 10.3389/fendo.2013.00126*
This article was submitted to Neuroendocrine Science, a section of the journal Frontiers in Endocrinology.

frontiers in
ENDOCRINOLOGY

REVIEW ARTICLE
published: 30 September 2013
doi: 10.3389/fendo.2013.00127

GnRH-induced Ca^{2+} signaling patterns and gonadotropin secretion in pituitary gonadotrophs. Functional adaptations to both ordinary and extraordinary physiological demands

Maria Luisa Durán-Pastén[1†] and Tatiana Fiordelisio[2*†]

[1] *Departamento de Neurociencia Cognitiva, Instituto de Fisiología Celular, Universidad Nacional Autónoma de México (UNAM), México DF, México*
[2] *Departamento de Ecología y Recursos Naturales, Facultad de Ciencias, Universidad Nacional Autónoma de México (UNAM), México DF, México*

Edited by:
Stephane Gasman, Centre National de la Recherche Scientifique, France

Reviewed by:
Gustavo M. Somoza, Instituto de Investigaciones Biotecnologicas-Instituto Tecnologico de Chascomus, Argentina
Stanko S. Stojilkovic, National Institutes of Health, USA

****Correspondence:***
Tatiana Fiordelisio, Departamento de Ecología y Recursos Naturales, Facultad de Ciencias, Universidad Nacional Autónoma de México (UNAM), Circuito exterior s/n. Ciudad Universitaria, C.P. 04510 México DF, México
e-mail: tfiorde@ciencias.unam.mx

[†] Maria Luisa Durán-Pastén and Tatiana Fiordelisio have contributed equally to this work.

Pituitary gonadotrophs are a small fraction of the anterior pituitary population, yet they synthesize gonadotropins: luteinizing (LH) and follicle-stimulating (FSH), essential for gametogenesis and steroidogenesis. LH is secreted via a regulated pathway while FSH release is mostly constitutive and controlled by synthesis. Although gonadotrophs fire action potentials spontaneously, the intracellular Ca^{2+} rises produced do not influence secretion, which is mainly driven by Gonadotropin-Releasing Hormone (GnRH), a decapeptide synthesized in the hypothalamus and released in a pulsatile manner into the hypophyseal portal circulation. GnRH binding to G-protein-coupled receptors triggers Ca^{2+} mobilization from $InsP_3$-sensitive intracellular pools, generating the global Ca^{2+} elevations necessary for secretion. Ca^{2+} signaling responses to increasing (GnRH) vary in stereotyped fashion from subthreshold to baseline spiking (oscillatory), to biphasic (spike-oscillatory or spike-plateau). This progression varies somewhat in gonadotrophs from different species and biological preparations. Both baseline spiking and biphasic GnRH-induced Ca^{2+} signals control LH/FSH synthesis and exocytosis. Estradiol and testosterone regulate gonadotropin secretion through feedback mechanisms, while FSH synthesis and release are influenced by activin, inhibin, and follistatin. Adaptation to physiological events like the estrous cycle, involves changes in GnRH sensitivity and LH/FSH synthesis: in proestrus, estradiol feedback regulation abruptly changes from negative to positive, causing the pre-ovulatory LH surge. Similarly, when testosterone levels drop after orquiectomy the lack of negative feedback on pituitary and hypothalamus boosts both GnRH and LH secretion, gonadotrophs GnRH sensitivity increases, and Ca^{2+} signaling patterns change. In addition, gonadotrophs proliferate and grow. These plastic changes denote a more vigorous functional adaptation in response to an extraordinary functional demand.

Keywords: pituitary, gonadotrophs, calcium, gonadotropins, GnRH, secretion

GONADOTROPHS FUNCTION AND CHARACTERISTICS

The reproductive function and sexual maturation is under the control of the hypothalamic-pituitary-gonadal axis. Pituitary gonadotrophs, which constitute 7–15% of the anterior pituitary gland secrete two dimeric glycoproteins, gonadotropins, luteinizing (LH) and follicle-stimulating (FSH) hormones that play an essential role in the control of steroidogenesis, gametogenesis, and ovulation (1). The regulation of their synthesis and secretion are under control of hypothalamic stimulation (gonadotropin-releasing hormone; GnRH), gonadal sex steroids (estradiol, progesterone, testosterone) and peptides (inhibins), and paracrine factors (inhibins, activins, and follistatin). The pituitary gland must adapt to different physiological changes from prepubertal to mature sexual life, therefore gonadotrophs plasticity and gonadotropins secretion are essential to produce the changes needed in different situations, for example the rapid daily hormonal variations along the reproductive female cycle. Integration of the different regulatory signals by the gonadotrophs results in the coordinated control of synthesis, packaging, and differential secretion of gonadotropins to accurately respond and control sexual maturation and normal reproductive function.

Immunocytochemical studies have demonstrated the presence of bihormonal (70%) and monohormonal (15%) gonadotrophs whose percentage shifts under different physiological conditions, such as castration or estrous cycle (2). LH and FSH have a common alpha (α) and distinct beta (β) subunit. After its synthesis in the endoplasmic reticulum (ER) and its passage trough the Golgi apparatus, hormones are delivered to the plasma membrane trough a constitutively or regulated secretory pathway; in the latter, fusion of secretory vesicles to the plasma membrane is arrested waiting for specific signals to be secreted. Gonadotropin synthesis and secretion diverges under a range of physiological and experimental conditions (3), indicating that GnRH and other regulators of gonadotropins selectively activate this pathways.

Exocytosis in excitable cells is a process highly dependent of intracellular calcium concentration ($[Ca^{2+}]_i$) rise, gonadotrophs as other pituitary endocrine cells display spontaneous intracellular Ca^{2+} transients in dependence of changes in the membrane

electrical activity. However, this membrane potential oscillations are small and do not produce the necessary $[Ca^{2+}]_i$ increase to generate hormonal secretion (4, 5), as a result, basal secretion is low and not affected by extracellular Ca^{2+} (4, 6). In both cases, the principal regulation is done by GnRH, a decapeptide that is synthesized in the hypothalamus, stored in axon terminals in the median eminence, and released in a pulsatile manner into the hypophyseal portal circulation (7). Numerous studies have shown that isolated gonadotrophs in primary culture (and more recently, also gonadotrophs *in situ*) present robust and stereotyped dose-dependent intracellular Ca^{2+} signals in response to suprathreshold concentrations of GnRH (8–11), the rise produced in cytosolic $[Ca^{2+}]$ triggers gonadotropins exocytosis and synthesis.

Understanding the origin and meaning of these intracellular Ca^{2+} signals are essential to the knowledge of the physiology of normal reproduction, as well as reproductive function disorders. This review outlines different regulators of the gonadotrophs biology with special regard in the recent progress on GnRH-induced Ca^{2+} signaling and secretion in pituitary gonadotrophs, both at the cellular and tissue level.

Ca^{2+} SIGNALS INDUCED BY GnRH AND OTHER SECRETAGOGUES

In order to mediate multiple effects such as secretion, synthesis, and phenotype maintenance, the GnRH variants in different species interact with their receptor (GnRHR), which is a member of the rhodopsin-like G-protein-coupled receptors (GPCR) superfamily (12). Upon GnRH binding to the GnRHRs in the gonadotroph membrane, the α subunit of the $Gq/_{11}$ protein dissociates and activates phospholipase C (PLC-β), resulting in the rapid hydrolysis of phosphatidylinositol 4, 5-biphosphate (PIP2) and the production of two second messengers: diacylglycerol (DAG) and inositol 1,4,5-trisphosphate ($InsP_3$); long lasting GnRH stimulation (∼5–10 min) could also activate phospholipase D (PLD) and phospholipase A_2 (PLA_2) (12). $InsP_3$ generates Ca^{2+} mobilization from intracellular pools, and DAG triggers protein kinase C (PKC) activation which in turn reduces depolarization-mediated Ca^{2+} influx, while increasing gonadotropin secretion (13) (**Figure 1**). PKC sensitizes the secretory machinery to Ca^{2+} (14), which explain why GnRH application is more effective to induce secretion than membrane depolarization or caged Ca^{2+} photolysis (5). PKC activation is also involved in other exocytosis-associated processes, like GnRH self-priming and cytoskeletal rearrangement (3).

In the lumen of the ER, $[Ca^{2+}]$ is maintained higher (between 10 and 250 μM free) than in the cytosol (50–250 nM) by the pumping activity of the sarco-ER Ca^{2+} ATPase (SERCA) located in the ER membrane (15). This membrane holds intracellular channel that allow Ca^{2+} efflux from the ER down its concentration gradient; the $InsP_3$ receptor ($InsP_3R$), a ligand-gated Ca^{2+} channel

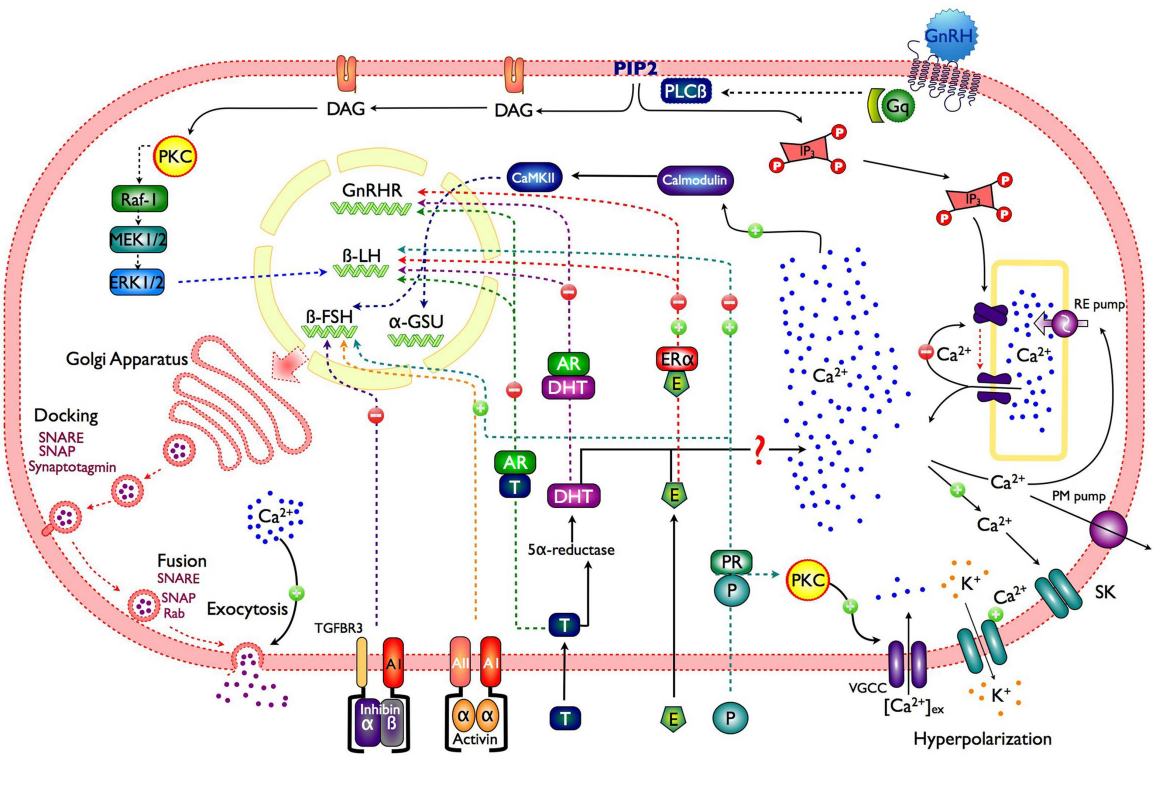

FIGURE 1 | Schematic representation of a gonadotroph illustrating the main control pathways of gonadotropin synthesis and secretion. GnRH, gonadotropin-releasing hormone; Gq, protein $Gq/_{11}$; PLCβ, phospholipase C; PIP2, phosphatidylinositol 4,5 bisphosphate; DAG, diacylglycerol; IP_3, inositol 1,4,5-trisphosphate; PKC, protein kinase C; VGCC, voltage-gated calcium channels; CaMKII, calcium calmodulin type II kinase; RE pump, endoplasmic reticulum Ca^{2+} pump; PM pump, plasma membrane Ca^{2+} pump; SK, small conductance calcium-activated potassium channels; P, progesterone; PR, progesterone receptor; E, estradiol; ERα, estrogen receptor α; T, testosterone; AR, androgen receptor; Raf, serine/threonine kinase; MEK, mitogen-activated protein kinase; ERK, extracellular-signal-regulated kinases.

that opens after $InsP_3$ binding (16). Besides $InsP_3$ binding, Ca^{2+} interaction with high-affinity (activation) sites on the cytoplasmic side of the $InsP_3R$ is essential for channel opening. In fact, Ca^{2+} and $InsP_3$ operate as co-agonists. Ca^{2+} signal amplification and spreading phenomena, involving assemblies of $InsP_3Rs$ originate from this synergistic role of Ca^{2+} (17). The large and abrupt $[Ca^{2+}]_i$ increase, triggered by $InsP_3Rs$ activation results from the combination of Ca^{2+} released and its amplification by Ca^{2+} induced Ca^{2+} release [CICR; (18)]. Even if cytosolic $InsP_3$ remains high, Ca^{2+} efflux often ceases because Ca^{2+} binds to a low-affinity (inactivating) site of the receptor, which closes the $InsP_3R$ channel. This occurs when cytosolic Ca^{2+} close to the $InsP_3Rs$ is high, i.e., after an episode of fast release. As in most pituitary cells, agonist stimulation in gonadotrophs produce a $[Ca^{2+}]_i$ peak which decays to sustained Ca^{2+} level (plateau phase). At intermediate GnRH concentration the initial Ca^{2+} spike is often followed by large $[Ca^{2+}]_i$ oscillations resulting from opening and closing cycles of the $InsP_3R$ channels as a consequence of $[Ca^{2+}]_i$ fluctuations near its cytoplasmic side (19). The frequency of these Ca^{2+} oscillations is determined by the dose of GnRH applied and the intracellular ($InsP_3$) reached (20) (**Figure 1**).

Gonadotropin-releasing hormone-induced $[Ca^{2+}]_i$ oscillations can be reproduced with mathematical models that include a Ca^{2+} gradient between the ER lumen and the cytosol maintained by a SERCA Ca^{2+} pump, Ca^{2+} influx trough voltage-gated Ca^{2+} channels, and $InsP_3R$ channels co-activated by $InsP_3$ and low $[Ca^{2+}]_i$, and inactivated by high $[Ca^{2+}]_i$ (8, 15, 21, 22). Nonetheless, Ca^{2+} oscillations in real cells requires the precise coordination of Ca^{2+} mobilization/uptake/extrusion mechanisms, it is for it that immortalized gonadotroph cell lines αT3–1 (21) and LβT2 (23) are not good cell models for studies on GnRH-induced calcium signaling and modulation of voltage-gated calcium influx, as well as goldfish (24, 25) and immature mammalian gonadotrophs, since these cells respond to GnRH with non-oscillatory amplitude-modulated Ca^{2+} signals. When SERCA pumps in gonadotrophs are blocked by thapsigargin, the agonist-induced Ca^{2+} oscillations become non-oscillatory biphasic responses (8, 26). Therefore different factors, i.e., the amount and speed of $InsP_3$ production, the total number of $InsP_3R$ channels available for activation, the rate of Ca^{2+} leakage from the store and the efficiency of the SERCA Ca^{2+} pump vary from cell to cell, and they ultimately determine the characteristics of gonadotrophs Ca^{2+} signaling patterns. It is important to note that the oscillatory behavior is intrinsic to the Ca^{2+} handling properties of gonadotrophs (17).

Gonadotropin-releasing hormone produces Ca^{2+} oscillations: i.e., large Ca^{2+} spikes, arising from a flat baseline as well as smaller sinusoidal Ca^{2+} oscillations superimposed on an elevated plateau. Under sustained GnRH stimulation, the amplitude of these Ca^{2+} spikes gradually diminishes, probably due to intracellular Ca^{2+} pool depletion, until a "plateau" without oscillations is reached. Ca^{2+} influx through voltage-gated Ca^{2+} channels is essential to maintain this plateau, and also for the replenishment of intracellular Ca^{2+} pools. GnRH induces continuous AP firing periodically interrupted by hyperpolarizations, which occur in phase with each Ca^{2+} elevation, and resulting from the opening of Ca^{2+} dependent SK-type K^+ channels (6, 27). Immediately after each hyperpolarization, the cell fires a burst of APs, which open Ca^{2+} channels allowing Ca^{2+} influx, predominantly high-voltage – activated L-type calcium channels. This Ca^{2+} entry does not contribute to Ca^{2+} elevation or gonadotropin secretion, but is crucial for refilling the intracellular Ca^{2+} pools (20) (**Figure 1**).

Oscillatory Ca^{2+} signals in gonadotrophs can also be elicited by endothelin (ET) (28, 29), pituitary adenylate cyclase-activating polypeptide, (PACAP) (30), and substance P (SP) (31). Conversely, neuropeptide Y (NPY) and melatonin, in neonatal gonadotrophs, inhibit GnRH-induced Ca^{2+} signals and gonadotropin secretion. Lactotrophs, gonadotrophs, and somatotrophs produce ETs, and gonadotrophs express ET receptors (32) under the control of ovarian steroid hormones, suggesting a paracrine function. ET binding, leads to $Gq/_{11}$ activation, intracellular Ca^{2+} fluctuations, and gonadotropin secretion (29). SP, which is a weaker agonist than GnRH, produces amplitude-modulated $[Ca^{2+}]_i$ responses and secretion in gonadotrophs (31), being the first phase of secretion dependent of intracellular Ca^{2+} release, and the second phase Ca^{2+} influx-dependent. The hypothalamic factor PACAP which stimulates cAMP production and potentiates gonadotropin release (33), also induces Ca^{2+} oscillations in rat gonadotrophs through activation of PVR1, a G-protein-coupled receptor and $InsP_3$ production (30). The activation of coupled $G_{i/o}$ melatonin receptors MT1 and MT2, expressed in gonadotrophs only at neonatal stage, inhibits both calcium influx through voltage-gated calcium channels and calcium mobilization from intracellular stores, decreasing intracellular cAMP production and protein kinase A (PKA) activity, with a consequent diminution on gonadotropin secretion (34–36); tonic melatonin inhibition of immature gonadotrophs prevents premature initiation of puberty. NPY inhibits GnRH-induced Ca^{2+} signaling and LH release (37); its receptors Y1 and Y5 expression on gonadotrophs is regulated by estrogens (38).

Ca^{2+} SIGNALING PATTERNS AND SECRETION IN GONADOTROPHS IS DEPENDENT ON GnRH CONCENTRATION

Dissociated pituitary gonadotrophs respond to increasing doses of GnRH with a stereotyped progression of intracellular Ca^{2+} signaling: i.e., subthreshold GnRH concentrations produce either small monophasic Ca^{2+} transients or irregular, small Ca^{2+} spikes. With higher GnRH concentrations (0.1–10 nM) regular, oscillatory, frequency-modulated, large Ca^{2+} transients (baseline Ca^{2+} spiking) are produced. Eventually (∼50–100 nM GnRH), these Ca^{2+} spikes fuse into an amplitude-modulated biphasic Ca^{2+} response (9, 10, 39) which comprises two variants; biphasic oscillatory and biphasic non-oscillatory, also known as spike-plateau (40). It is reasonable to assume that different Ca^{2+} release patterns observed with increasing doses of GnRH underlie the dose-dependent increase of gonadotropin secretion. Nonetheless, it has also been suggested that these patterns encode other cell functions. For instance, spike-plateau Ca^{2+} responses were associated to LH secretion and oscillatory Ca^{2+} responses to the synthesis of LH β-subunits (9). Later, it was established that GnRH-induced Ca^{2+} oscillations trigger exocytosis (41) and that both oscillatory and spike-plateau Ca^{2+} signals can initiate LH release (10, 40). Furthermore, gonadotrophs do not respond in the same way to the secretagogue: i.e., individual cells can respond with different patterns of activity to the same GnRH concentration

(40). Conversely, when the same dose of GnRH is applied repetitively, individual cells respond with similar latency and signaling pattern (11). It remains to be established which cellular aspects determine the Ca^{2+} signals displayed by individual gonadotrophs in response to GnRH and how these different patterns affect gonadotropin synthesis and secretion. Moreover, LH and FSH are secreted through parallel pathways (see below) and hormones that alter their synthesis, release, and/or storage can dynamically regulate their output.

GONADOTROPIN EXOCYTOSIS. CONTRIBUTION OF VGCC-MEDIATED Ca^{2+} INFLUX AND INTRACELLULAR Ca^{2+} RELEASE

A rise in $[Ca^{2+}]_i$ is the key signal to trigger regulated exocytosis in neuronal and endocrine tissues. Endocrine cell models used to study the role of Ca^{2+} in exocytosis include adrenal chromaffin and PC12 cells (42–46), pancreatic β cells (47–49), and pituitary cells (6, 50). Cytosolic Ca^{2+} levels regulate several maturation steps that secretory vesicles must undergo prior to fusion, like priming of secretory vesicles (51). An entirely different phenomena occurs when $[Ca^{2+}]_i$ rises abruptly, promoting the fusion of docked secretory vesicles with the plasma membrane (47, 52). In contrast to nerve synapses, where Ca^{2+} influx is primarily responsible for this abrupt $[Ca^{2+}]_i$ rise, exocytosis in endocrine cells is triggered to a large extent by Ca^{2+} released from intracellular stores (17, 53).

Ca^{2+} controls the fusion of secretory vesicles with the plasma membrane to release neurotransmitters and hormones when is needed [regulated exocytosis, (51)]. The first phase of GnRH-induced exocytosis in gonadotrophs is mediated by $InsP_3$-sensitive Ca^{2+} pools, while the second "plateau" phase of secretion involves voltage-gated Ca^{2+} influx (54). GnRH-$InsP_3$ induced Ca^{2+} oscillations produce much greater exocytosis than the simple general rise in $[Ca^{2+}]_i$ induced by micropipette injection or uncaging $[Ca^{2+}]_i$ (5, 41). This suggests that in contrast with other pituitary cell types, the formation of sub-plasmalemmal microdomains of high Ca^{2+} in gonadotrophs is insufficient to induce vesicular fusion. Instead large Ca^{2+} signals that propagate across the entire cell are needed to accomplish this task (6). Exocytosis can be directly monitored electrically as changes in membrane capacitance due to the addition of new plasma membrane. Using capacitance measurements, exocytosis is detected in gonadotrophs whenever $[Ca^{2+}]$ rises above 300 nM (55), but for strong exocytosis high $[Ca^{2+}]_i$ with half maximal concentration of 16 μM are required (6). When the responses induced by GnRH are oscillatory, step increases in membrane capacitance can be seen in each Ca^{2+} spike (40, 41, 55). The first Ca^{2+} oscillations elicit the largest exocytosis events, returning to full capacity within about 2 min (5). GnRH-induced secretion continues in the absence of external Ca^{2+}, but ceases when $[Ca^{2+}]$ rises are blocked by the introduction of a strong intracellular Ca^{2+} buffer (41).

Secretory granules must undergo a well-defined series of events: (1) recruitment, (2) tethering at the plasma membrane, (3) priming, and (4) vesicle fusion with the plasma membrane. Regulated hormone secretion is a Ca^{2+}-dependent exocytosis that uses the secretory vesicle synaptotagmin as the Ca^{2+} sensor and is mediated by SNARE (soluble *N*-ethylmaleimide-sensitive factor attachment protein receptors) proteins as effectors. Syntaxin, SNAP25 (synaptosome-associated protein of 25 kDa in molecular weight), and synaptobrevin (vesicle-associated membrane protein, VAMP, also termed vSNARE) constitute SNARE proteins. Syntaxin and SNAP25 (also known as "target" tSNAREs) are the plasma membrane proteins to which VAMP couples (**Figure 1**). Then, vSNAREs and tSNAREs form trans-SNARE complexes, which join secretory vesicles and plasma membrane (56–58). Vesicle priming, another Ca^{2+}-dependent step in exocytosis probably involves early SNARE complex formation (particularly tSNARE), before its association to the trans-SNAREs. Finally, synaptotagmin detects the $[Ca^{2+}]$ elevation and provides the extra drive needed to overcome the energy barrier of lipid-to-lipid interaction, allowing membrane fusion (58). The use of high-resolution microscopy techniques have allowed to demonstrate in PC12 cells that tSNARE molecules are distributed on the plasma membrane in areas of low and high density, and in contrast to current models of SNARE-driven membrane fusion (59), this data suggest that secretory vesicles are targeted over areas of low tSNARE density as sites of docking, hence a relatively low number of tSNAREs close to the secretory vesicle (less than seven) are sufficient to drive membrane fusion. Moreover, using atomic forces microscopy and scanning electron microscopy it has been described that gonadotrophs mainly present "single and simple fusion pore" with diameter ranging from 100 to 500 nm, which appear more frequently after stimulation with GnRH; this pore configuration supports the idea of a "kiss and stay" mechanism for the exocytosis process (60), in addition pores of 20–40 nm diameter have also been found, probably representing the constitutive pathway of gonadotropins (60).

FSH AND LH DIFFERENTIAL SECRETION UNDER PHYSIOLOGICAL CONDITIONS

Along the follicular phase of the estrus cycle, LH secretion is maximal while FSH secretion is reduced; even though gonadotrophs secrete both hormones, the mechanisms underlying this differential release are unclear. FSH appears to be released mostly through the constitutive pathway in accordance to its rate of synthesis. Conversely, LH-containing granules are released through the regulated pathway in response to GnRH, with no effect on LHβ mRNA production (61). Moreover, LH and FSH appear to be packaged into different secretory granules (62). Large, moderately electron-dense granules show antigenicity for FSH, LH, and chromogranin A (CgA), while smaller, electron-dense storage granules released by GnRH contain LH and secretogranin II (SgII) (3); thereby protein sorting domains in the β subunit of gonadotropins and the association with certain proteins may be responsible for differential sorting and packaging of LH and FSH into different secretory granules (3). The movement of these granules toward the membrane defining a secretory pathway and differential exocytosis could explain the disparity on the gonadotropins secretion (63). Accordingly, in LβT2 mouse cells, FSH released in response to activin/GnRH is constitutively secreted via a granin-independent pathway; while LH is released in response to GnRH is co-released with SgII via a regulated, granin-dependent pathway (64).

Gonadotropin subunits (α-GSU, FSHβ, and LHβ) mRNAs levels, which reflect changes in gene transcription in pituitary gonadotrophs, are GnRH pulse frequency modulated (65–67). GnRH pulses (30–60 min interval), preferentially increases

synthesis and secretion of LH by the mediation of the transcription factor Egr-1 (68–71); whereas slower GnRH pulsing (120–240 min interval) favors FSH secretion (65–67, 72) by the activation of PKA (73–75). There is no a definitive explanation to how GnRH pulses can activate in a different manner gonadotropin subunit gene transcription; nevertheless several routes have been proposed which may contribute to this regulation; one is through the increase on Ca^{2+} levels and PKC activation, which as a consequence activated mitogen-activated protein kinase (MAPK) cascade, culminating in an activation of extracellular-signal-regulated kinase (ERK) 1/2, cJun NH2-terminale kinase (JNK), p38 MAPK, and ERK 5 (76–80), it is also believe that the rise in $[Ca^{2+}]_i$, activates a calcium/calmodulin-dependent kinase II (CAMK2), whose autophosphorylation could be important in transmitting Ca^{2+} pulse frequency and amplitude signals, as fast and high-amplitude Ca^{2+} influxes, which results in greater and/or sustained Ca^{2+}/CALM1 levels (79, 81) (**Figure 1**). GnRH pulses at lower frequency selectively increase the expression of PACAP and its receptor (PAC1-R) in gonadotrophs (82), where they subsequently stimulate the synthesis of gonadotropin subunits (83).

Gonadotropin-releasing hormone-induced LH and FSH synthesis and secretion are modulated by steroid hormones, such as estrogen, progesterone, and testosterone, in addition to peptide hormones, such as activin, inhibin, and follistatin (**Figures 1** and **2**). This modulation occurs principally through gonadal feedback at the pituitary and hypothalamus level (84–86). During most part of the female reproductive cycle and in males, pulsatile GnRH release drives tonic gonadotropin secretion (84, 87) while steroids and inhibins provide negative feedback to limit further gonadotropin stimulation and maintaining low circulating levels of gonadotropins; in females, this happens until the pre-ovulatory surge when, in response to low levels of progesterone (88) and an increase in estrogen, feedback switches to positive (89), producing changes on GnRHergic neurons (90) and gonadotrophs (91), which results in increased LH and FSH secretion (**Figure 2**). In some female species a secondary FSH surge occurs after ovulation when LH levels are already low, this rise produces the recruitment of the next cohort of follicles and it is GnRH independent (92) and more likely depends on the reduction of circulating inhibin (93).

Estradiol (E) exerts a direct action at the pituitary level through its α-receptor (94–97), increasing gonadotroph responsiveness to GnRH (98–100) raising synthesis and insertion of GnRH receptor into gonadotroph membrane (86, 91, 101–104) and decreasing the concentration of GnRH needed to produce the threshold response and frequency of Ca^{2+} spiking (101, 105, 106). Nevertheless, these actions seems to be and indirect action that depends of the increased expression produced by GnRH on its own receptor (101, 103, 107–109). Besides these changes, during the gonadotropin surge, the pituitary gland shows cellular modifications, implying an augmentation on the number of secreting gonadotrophs (98, 104) and hypertrophy and re-organization of its intracellular organelles (110–112). However, it has been documented that

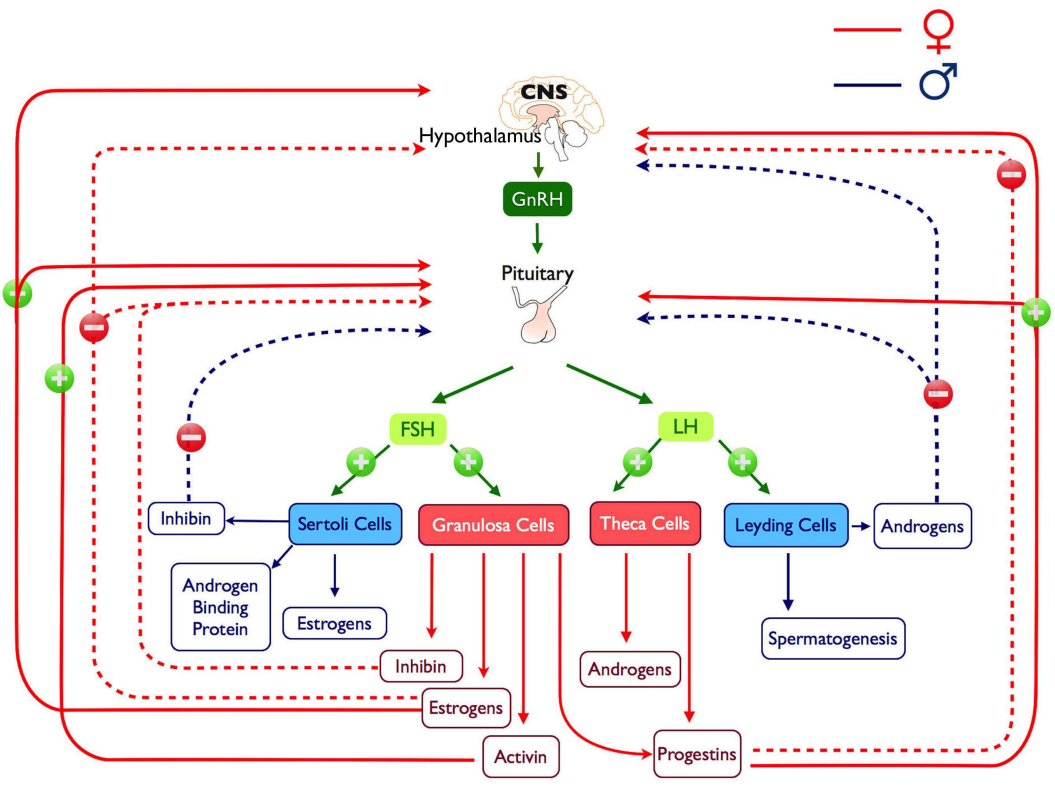

FIGURE 2 | Representation of the hypothalamus-pituitary-gonadal axis, positive and negatives feedback loops and products are illustrated.

E can act to suppress the transcriptional rate of LH subunit genes. Controversial results have been reported for FSHβ synthesis (113–117), although serum levels of both hormones increased markedly.

Progesterone (P) exerts some of its effects at hypothalamic level, decreasing GnRH secretion and pulse frequency (91, 103) contributing to the abrupt decline in gonadotropin levels. P does not inhibit LH secretion induced by GnRH (100, 118) but it can stimulate murine FSHβ promoter activity alone or in synergy with activins (103). In dependence with the time of exposition, P can either inhibit or facilitate the estrogen-induced LH surge during the rat estrous cycle (100, 103, 119). P modulates the E effect on GnRH production of LH surge by the modulation of Ca^{2+} mobilization and Ca^{2+} entry to gonadotrophs. In E-primed cells P alters the intracellular Ca^{2+} signaling patterns produced by GnRH. In the short-term P treatment shifts subthreshold $[Ca^{2+}]_i$ responses to oscillatory, and oscillatory to biphasic responses; in contrast, long-term P exposure led to decreased GnRH sensitivity, changing oscillatory response into subthreshold $[Ca^{2+}]_i$ response profiles (105, 106).

Androgens [testosterone (T) and 5α-dihydrotestosterone (DHT)] are important component of the male gonadal feedback and they act either at the hypothalamic level by regulating the secretion of GnRH into the hypophyseal portal circulation (120–122), directly at the pituitary level (99) or by the combination of both sites (123) (**Figure 2**).

At hypothalamic level, T reduce GnRH synthesis (122, 124–127) and pulsatile patterns of GnRH release (128–131). At pituitary level, it is known that testosterone and more dramatically DHT inhibits LH synthesis and GnRH-induced LH secretion in a concentration and time dependent manner (132–137), but increase basal FSH secretion and synthesis (138, 139). In castrated rats it has been shown that LH secretion increase (140, 141) as well as gonadotrophs size and number (140, 142, 143). These hypertrophied cells are called castration cells (144–146), and they present a dilated rough ER and an extended Golgi complex (147, 148). On these cells, the secretion granules content are progressively diminished (149) and their cisternae fused to form large vacuoles that originated the typical "signet ring cell" (148, 150, 151).

It is widely accepted that in gonadotrophs an increase in $[Ca^{2+}]_i$ is essential for the transduction of GnRH signal; T but specially DHT regulate GnRH-induced $[Ca^{2+}]_i$ variations (152) changing the type of calcium patterns (153), these effects are not seen in all species (145) and it could be related with the influence of this hormone on the regulation of the GnRH receptor density (154–156) and the change in their sensitivity to the GnRH stimulus (134).

Tobin and collaborators (153) demonstrated that in cultured gonadotrophs of gonadectomized male rats, the relationship between GnRH concentration and the type of intracellular Ca^{2+} response is altered, most gonadotrophs (∼70%) show oscillatory responses regardless of the GnRH concentration. Correlated with this results it has been demonstrated that in T or DHT treated cells, there is an inhibition of the GnRH increase in $[Ca^{2+}]_i$; at low GnRH doses (0.1 nM) 30% of gonadotrophs were unable to initiated threshold spiking and in the residual cells the frequency of oscillations decreased, as in controls, androgen treated cells, respond with a spike-plateau type of signal to 1 nM GnRH, but the frequency of spiking was also reduced (134, 152). Finally at high dose GnRH (100 nM) induce biphasic elevations of $[Ca^{2+}]_i$ with a minor reduction in the amplitude (134). Testosterone inhibits both phases of GnRH-stimulated LH secretory responses, the early extracellular Ca^{2+}-independent spike phase and the sustained Ca^{2+} and extracellular Ca^{2+}-dependent plateau phase (134). These results suggest that androgens act on the efficacy of the agonist to release Ca^{2+}, leading to a decrease in the secretory output.

As it has been previously established, secretion of FSH and LH are not co-ordinately regulated, their discordant regulation must be related to differential intracellular responses to several stimuli, factors as activins, inhibins, and follistatin, may play a key role on establishing such differences. In this regard, activins which are produced in a variety of tissues, including gonadotrophs, stimulates FSHβ transcription (132, 157–159) and enhance its sensitivity to GnRH by up-regulation of the GnRH receptor expression (92, 160). Contrary, inhibins which are produced in Sertoli and granulosa cells as well as in gonadotrophs (161), have been shown to rapidly reduce FSHβ synthesis and secretion independently of GnRH (162), by binding to activin receptors on gonadotrophs preventing the assembly of active signaling complexes (92).

Follistatins, which are glycoprotein ubiquitously expressed (including gonadotrophs and follicle stellated cells) bind to activins with high-affinity modulating its actions (92, 132, 160, 163). Activin and follistatin function in a reciprocal feedback loop altering their secretion, internalization, and degradation (92, 114, 160, 163), modifying the rise and fall of biosynthesis and secretion across the reproductive cycle (160, 163).

One mechanism that contributes to differential FSH and LH production may be related to the observation that different patterns of GnRH pulses produce differential effects on inhibin/activin and follistatin mRNA levels (160). Estrogen, progesterone, testosterone, inhibin, activin, follistatin, and hypothalamic GnRH, may combine to distinct regulate LH and FSH during the reproductive cycle (97).

GONADOTROPHS ACTIVITY AT THE TISSUE LEVEL

Endocrine cells are organized in three-dimensional networks, which facilitate the coordination of the activity of thousands of individual cells to respond to different regulation factors and achieve hormone output (164, 165). The magnitude of the hormone pulses into the systemic circulation is apparently not just the simple addition of the individual endocrine activity, instead, biophysical and biochemical interactions in the whole tissue must be essential for *in vivo* organization. However, as it has been described in this and other works, most of the studies have been done in individual cell activity where this networks and relations are disrupted, due to methodological difficulties, just few recently approaches has been done in the understanding of the endocrine activity in a tissue context.

In this regard, the distribution of gonadotrophs in fixed and live slices at different female reproductive stages has been analyzed (166). Across different physiological stages, pituitary gonadotrophs shows changes in their distribution within the gland and in response to GnRH stimulation (166), this might represent and adaptation to better respond at different conditions.

The possibility of changes in gonadotrophs activity within its tissue context and physiological conditions was recently addressed using Ca^{2+} imaging in male mouse acute pituitary slices (11, 145). Cells in this preparation are amenable to functional studies in their native environment. We showed that rather than a constant number of gonadotrophs responding to GnRH stimulus, the number of responding cells grew with increasing GnRH concentration (GnRH), and in general, gonadotrophs Ca^{2+} signaling resembled that recorded in primary cultures (11, 145). However, Ca^{2+} imaging in acute mouse pituitary slices revealed Ca^{2+} signaling patterns unique to *in situ* conditions, gonadotrophs (58%) under increasing doses of GnRH stimulation exhibited a progression of Ca^{2+} signaling patterns termed "non-canonical" [i.e., oscillatory responses at a given (GnRH) and transient responses at both lower and higher concentrations as described before in this review; **Figure 3**], and some of them (3.6%) even showed atypical (non-oscillatory) responses, regardless of the (GnRH) used (145). Furthermore, responses to a given dose of GnRH varied considerably from one cell to another, reflecting a range of dose-response properties in the *in situ* gonadotroph population.

As it has been described in this review, following the removal of the gonads, the population of pituitary gonadotrophs undergoes drastic functional and morphological modifications concomitantly with the large (five to sixfold) increase in gonadotropin secretion that characterizes this condition (123, 154, 167, 168) some changes as amplitude and frequency of GnRH-induced Ca^{2+} signaling has been reported in dissociated cells (10) and there is no difference with respect of what it has been reported in acute pituitary slices from 15 and 45 days castrated male mice (GnX) (145). Nevertheless, other characteristics on the intracellular Ca^{2+} signaling appear to be different; gonadotrophs of pituitary slices from GnX responding with "non-canonical" sequences of Ca^{2+} signaling (described earlier in this review) to increasing GnRH were significantly augmented (80% of GnRH responding gonadotrophs) and "canonical" sequences were significantly reduced (145) (**Figure 3**), indicating that probably this sequences of Ca^{2+} signaling in response to GnRH are modulated by paracrine and systemic factors as testosterone, allowing gonadotrophs to adapt to different physiological requirements. Additionally, median effective dose (ED50) for GnRH decreased from 0.17 nM (control) to 0.07 nM after GnX, suggesting an increased GnRH responsiveness of the gonadotroph population (145). Different sizes of gonadotrophs are present in intact mice pituitary gland, most gonadotrophs (97%) were smaller than 60 μm^2 with a mean of $31.3 \pm 0.6\,\mu m^2$ in area and even if large interindividual variation on the peak amplitude of Ca^{2+} transients (Max DF) was seen, no matter the size of the cell, they generated intracellular Ca^{2+} signals smaller than 40 fluorescence arbitrary units (a.u.) poorly correlated with the cell size (**Figure 4**). By contrast it is reported that 15-day castrated male mouse pituitary gonadotrophs, whose size increase to a mean of $54.4 \pm 1.24\,\mu m^2$ and 26% of cells larger than 60 μm^2 present less variation on the Ca^{2+} peak amplitude and significantly higher correlation of this with the cell size (i.e., hypertrophied gonadotrophs tended to generate Ca^{2+} signals of greater amplitude) (145) (**Figure 4**), suggesting that in this condition, Ca^{2+} peak amplitude correlated with cell size, and that hypertrophied gonadotrophs tended to produce stronger GnRH-induced Ca^{2+} signals.

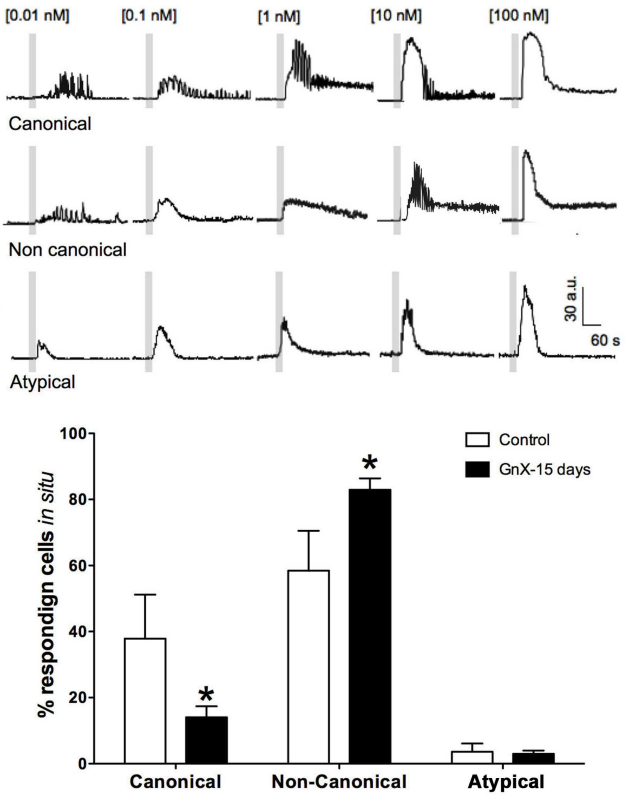

FIGURE 3 | Percentage of gonadotrophs that display different GnRH dose-response intracellular Ca^{2+} signaling patterns rises in response to increasing GnRH: canonical ($[Ca^{2+}]_i$ oscillations of increasing frequency at low-medium GnRH concentration and spike-plateau at saturating GnRH concentration), non-canonical (disordered sequence of oscillatory and spike-plateau $[Ca^{2+}]_i$ signals in response to increasing GnRH concentrations), and atypical (non-oscillatory, transient $[Ca^{2+}]_i$); open bars represent data from intact mice and black bars those of castrated mice after 15 post-GnX. After orchidectomy, non-canonical responses increased, while the fraction of cells with canonical responses declined. Differences between intact and post-GnX, for both canonical and non-canonical responses are significant. $*p < 0.05$ versus the control (two way ANOVA with Bonferroni *post hoc* test). Parts of this figure were originally published in Durán-Pastén et al., (145).

Functional adaptation of the gonadotrophs in the pituitary gland to different external and internal conditions may involucrate not just alterations in cell number, size, and morphology, as it has been considered for many years, recent methodological techniques allowed us to understand that it is a more complicated process that involucrates different aspects at the cellular physiology level but in coordination with the whole tissue environment.

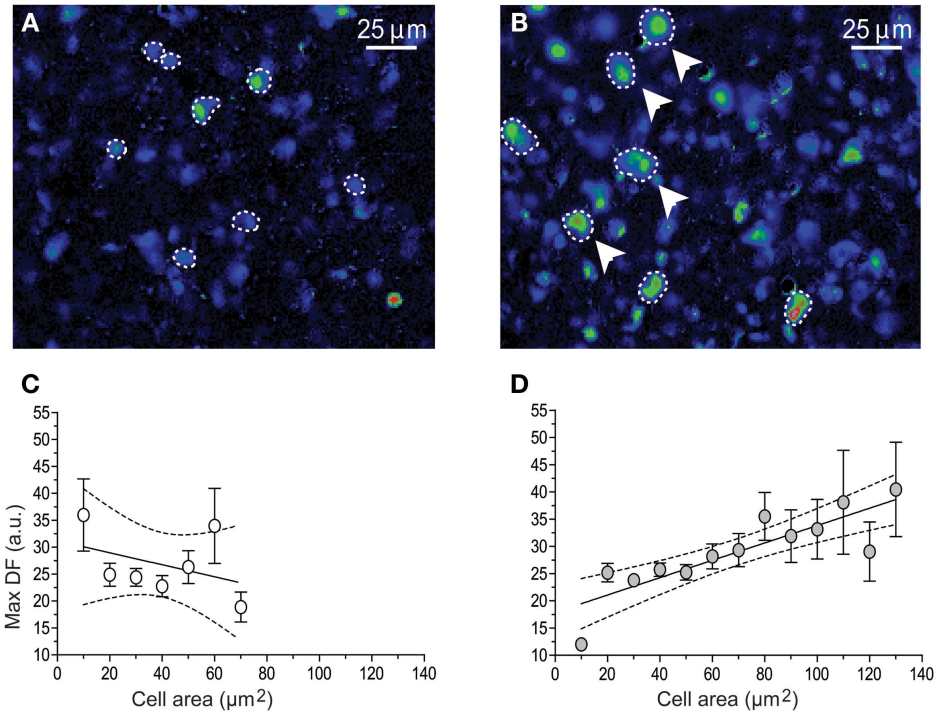

FIGURE 4 | Graphs illustrating the relation between gonadotrophs area size versus the peak amplitude of GnRH-induced Ca^{2+} transients. Fluo-4 fluorescence images of 100 nM GnRH responding gonadotrophs (dashed lines) in intact **(A)** and 15 days post-GnX **(B)** mice pituitary slice, arrows pointed bigger gonadotrophs. **(C,D)** shows the relationship between $[Ca^{2+}]_i$ transients peak amplitude (Max DF) and cell area (Mean ± SE). **(C)** Intact ($n = 6$) and **(D)** 15 days post-GnX ($n = 6$) mice pituitary slices are represented; dashed line represent the confidence interval. **(C)** $y = -0.11^* \pm 0.11x + 31.1 \pm 5.1$, $R_2 = 0.15$, $p > 0.05$, Pearson $r = 0.38$, $p > 0.05$ and **(D)** $y = 0.16^* \pm 0.02x + 17.88 \pm 2.3$, $R_2 = 0.73$, $p < 0.05$, Pearson $r = 0.85$, $p < 0.05$. Parts of this figure were originally published in Durán-Pastén et al., (145).

ACKNOWLEDGMENTS

The authors are indebted to Dr. Arturo Hernández who provided invaluable insights throughout this work. We are also grateful with Daniel Diaz for his support on data analysis and figure design. Grant support: PAPIIT IN222613 and IN222413, CONACYT 166430.

REFERENCES

1. Kaiser UB. Gonadotropin hormones. In: Melmed S, editor. *The Pituitary*. Amsterdam: Academic Press (2011). 731 p.
2. Moriarty GC. Immunocytochemistry of the pituitary glycoprotein hormones. *J Histochem Cytochem* (1976) **24**:846–63. doi:10.1177/24.7.60435
3. Anderson L. Intracellular mechanisms triggering gonadotropin secretion. *Rev Reprod* (1996) **1**:193–202. doi:10.1530/ror.0.0010193
4. Stojilkovic SS, Zemkova H, Van Goor F. Biophysical basis of pituitary cell type-specific Ca2+ signaling-secretion coupling. *Trends Endocrinol Metab* (2005) **16**:152–9. doi:10.1016/j.tem.2005.03.003
5. Tse FW, Tse A, Hille B, Horstmann H, Almers W. Local Ca2+ release from internal stores controls exocytosis in pituitary gonadotrophs. *Neuron* (1997) **18**:121–32. doi:10.1016/S0896-6273(01)80051-9
6. Stojilkovic SS. Pituitary cell type-specific electrical activity, calcium signaling and secretion. *Biol Res* (2006) **39**:403–23. doi:10.4067/S0716-97602006000300004
7. Stojilkovic SS, Krsmanovic LZ, Spergel DJ, Catt KJ. Gonadotropin-releasing hormone neurons: intrinsic pulsatility and receptor-mediated regulation. *Trends Endocrinol Metab* (1994) **5**:201–9. doi:10.1016/1043-2760(94)90078-7
8. Iida T, Stojilkovic SS, Izumi S, Catt KJ. Spontaneous and agonist-induced calcium oscillations in pituitary gonadotrophs. *Mol Endocrinol* (1991) **5**:949–58. doi:10.1210/mend-5-7-949
9. Leong DA, Thorner MO. A potential code of luteinizing hormone-releasing hormone-induced calcium ion responses in the regulation of luteinizing hormone secretion among individual gonadotrophs. *J Biol Chem* (1991) **266**:9016–22.
10. Tomic M, Cesnajaj M, Catt KJ, Stojilkovic SS. Developmental and physiological aspects of Ca2+ signaling in agonist-stimulated pituitary gonadotrophs. *Endocrinology* (1994) **135**:1762–71. doi:10.1210/en.135.5.1762
11. Sanchez-Cardenas C, Hernandez-Cruz A. GnRH-induced [Ca2+]i-signalling patterns in mouse gonadotrophs recorded from acute pituitary slices in vitro. *Neuroendocrinology* (2010) **91**:239–55. doi:10.1159/000274493
12. Naor Z. Signaling by G-protein-coupled receptor (GPCR): studies on the GnRH receptor. *Front Neuroendocrinol* (2009) **30**:10–29. doi:10.1016/j.yfrne.2008.07.001
13. Stojilkovic SS, Iida T, Merelli F, Torsello A, Krsmanovic LZ, Catt KJ. Interactions between calcium and protein kinase C in the control of signaling and secretion in pituitary gonadotrophs. *J Biol Chem* (1991) **266**:10377–84.
14. Zhu H, Hille B, Xu T. Sensitization of regulated exocytosis by protein kinase C. *Proc Natl Acad Sci U S A* (2002) **99**:17055–9. doi:10.1073/pnas.232588899

15. Li YX, Keizer J, Stojilkovic SS, Rinzel J. Ca2+ excitability of the ER membrane: an explanation for IP3-induced Ca2+ oscillations. *Am J Physiol* (1995) **269**:C1079–92.
16. Stojilkovic SS, Tabak J, Bertram R. Ion channels and signaling in the pituitary gland. *Endocr Rev* (2010) **31**:845–915. doi:10.1210/er.2010-0005
17. Stojilkovic SS. Molecular mechanisms of pituitary endocrine cell calcium handling. *Cell Calcium* (2012) **51**:212–21. doi:10.1016/j.ceca.2011.11.003
18. Stojilkovic SS, He ML, Koshimizu TA, Balik A, Zemkova H. Signaling by purinergic receptors and channels in the pituitary gland. *Mol Cell Endocrinol* (2010) **314**:184–91. doi:10.1016/j.mce.2009.05.008
19. Tse A, Hille B. GnRH-induced Ca2+ oscillations and rhythmic hyperpolarizations of pituitary gonadotrophs. *Science* (1992) **255**:462–4. doi:10.1126/science.1734523
20. Stojilkovic SS, Kukuljan M, Tomic M, Rojas E, Catt KJ. Mechanism of agonist-induced [Ca2+]i oscillations in pituitary gonadotrophs. *J Biol Chem* (1993) **268**:7713–20.
21. Li YX, Rinzel J, Keizer J, Stojilkovic SS. Calcium oscillations in pituitary gonadotrophs: comparison of experiment and theory. *Proc Natl Acad Sci U S A* (1994) **91**:58–62. doi:10.1073/pnas.91.1.58
22. De Young GW, Keizer J. A single-pool inositol 1,4,5-trisphosphate-receptor-based model for agonist-stimulated oscillations in Ca2+ concentration. *Proc Natl Acad Sci U S A* (1992) **89**:9895–9. doi:10.1073/pnas.89.20.9895
23. Thomas P, Mellon PL, Turgeon J, Waring DW. The L beta T2 clonal gonadotrope: a model for single cell studies of endocrine cell secretion. *Endocrinology* (1996) **137**:2979–89. doi:10.1210/en.137.7.2979
24. Strandabo RA, Hodne K, Ager-Wick E, Sand O, Weltzien FA, Haug TM. Signal transduction involved in GnRH2-stimulation of identified LH-producing gonadotrophs from lhb-GFP transgenic medaka (*Oryzias latipes*). *Mol Cell Endocrinol* (2013) **372**:128–39. doi:10.1016/j.mce.2013.03.022
25. Mollard P, Kah O. Spontaneous and gonadotropin-releasing hormone-stimulated cytosolic calcium rises in individual goldfish gonadotrophs. *Cell Calcium* (1996) **20**:415–24. doi:10.1016/S0143-4160(96)90004-4
26. Tse A, Tse FW, Hille B. Calcium homeostasis in identified rat gonadotrophs. *J Physiol* (1994) **477**(Pt 3):511–25.
27. Kukuljan M, Vergara L, Stojilkovic SS. Modulation of the kinetics of inositol 1,4,5-trisphosphate-induced [Ca2+]i oscillations by calcium entry in pituitary gonadotrophs. *Biophys J* (1997) **72**:698–707. doi:10.1016/S0006-3495(97)78706-X
28. Kanyicska B, Burris TP, Freeman ME. Endothelin-3 inhibits prolactin and stimulates LH, FSH and TSH secretion from pituitary cell culture. *Biochem Biophys Res Commun* (1991) **174**:338–43. doi:10.1016/0006-291X(91)90525-C
29. Stojilkovic SS, Merelli F, Iida T, Krsmanovic LZ, Catt KJ. Endothelin stimulation of cytosolic calcium and gonadotropin secretion in anterior pituitary cells. *Science* (1990) **248**:1663–6. doi:10.1126/science.2163546
30. Rawlings SR, Demaurex N, Schlegel W. Pituitary adenylate cyclase-activating polypeptide increases [Ca2]i in rat gonadotrophs through an inositol trisphosphate-dependent mechanism. *J Biol Chem* (1994) **269**:5680–6.
31. Mau SE, Witt MR, Saermark T, Vilhardt H. Substance P increases intracellular Ca2+ in individual rat pituitary lactotrophs, somatotrophs, and gonadotrophs. *Mol Cell Endocrinol* (1997) **126**:193–201. doi:10.1016/S0303-7207(96)03988-3
32. Kanyicska B, Lerant A, Freeman ME. Endothelin-like immunoreactivity in lactotrophs, gonadotrophs, and somatotrophs of rat anterior pituitary gland are affected differentially by ovarian steroid hormones. *Endocrine* (2001) **14**:263–8. doi:10.1385/ENDO:14:2:263
33. Culler MD, Paschall CS. Pituitary adenylate cyclase-activating polypeptide (PACAP) potentiates the gonadotropin-releasing activity of luteinizing hormone-releasing hormone. *Endocrinology* (1991) **129**:2260–2. doi:10.1210/endo-129-4-2260
34. Balik A, Kretschmannova K, Mazna P, Svobodova I, Zemkova H. Melatonin action in neonatal gonadotrophs. *Physiol Res* (2004) **53**(Suppl 1):S153–66.
35. Zemkova H, Vanecek J. Inhibitory effect of melatonin on gonadotropin-releasing hormone-induced Ca2+ oscillations in pituitary cells of newborn rats. *Neuroendocrinology* (1997) **65**:276–83. doi:10.1159/000127185
36. Zemkova H, Vanecek J. Dual effect of melatonin on gonadotropin-releasing-hormone-induced Ca(2+) signaling in neonatal rat gonadotropes. *Neuroendocrinology* (2001) **74**:262–9. doi:10.1159/000054693
37. Shangold GA, Miller RJ. Direct neuropeptide Y-induced modulation of gonadotrope intracellular calcium transients and gonadotropin secretion. *Endocrinology* (1990) **126**:2336–42. doi:10.1210/endo-126-5-2336
38. Hill JW, Urban JH, Xu M, Levine JE. Estrogen induces neuropeptide Y (NPY) Y1 receptor gene expression and responsiveness to NPY in gonadotrope-enriched pituitary cell cultures. *Endocrinology* (2004) **145**:2283–90. doi:10.1210/en.2003-1368
39. Stojilkovic SS, Tomic M. GnRH-induced calcium and current oscillations in gonadotrophs. *Trends Endocrinol Metab* (1996) **7**:379–84. doi:10.1016/S1043-2760(96)00189-0
40. Thomas P, Waring DW. Modulation of stimulus-secretion coupling in single rat gonadotrophs. *J Physiol* (1997) **504**(Pt 3):705–19. doi:10.1111/j.1469-7793.1997.705bd.x
41. Tse A, Tse FW, Almers W, Hille B. Rhythmic exocytosis stimulated by GnRH-induced calcium oscillations in rat gonadotropes. *Science* (1993) **260**:82–4. doi:10.1126/science.8385366
42. Alvarez YD, Marengo FD. The immediately releasable vesicle pool: highly coupled secretion in chromaffin and other neuroendocrine cells. *J Neurochem* (2011) **116**:155–63. doi:10.1111/j.1471-4159.2010.07108.x
43. Garcia AG, Padin F, Fernandez-Morales JC, Maroto M, Garcia-Sancho J. Cytosolic organelles shape calcium signals and exo-endocytotic responses of chromaffin cells. *Cell Calcium* (2012) **51**:309–20. doi:10.1016/j.ceca.2011.12.004
44. Weiss JL. Ca(2+) signaling mechanisms in bovine adrenal chromaffin cells. *Adv Exp Med Biol* (2012) **740**:859–72. doi:10.1007/978-94-007-2888-2_38
45. Marengo FD. Calcium gradients and exocytosis in bovine adrenal chromaffin cells. *Cell Calcium* (2005) **38**:87–99. doi:10.1016/j.ceca.2005.06.006
46. Neher E. A comparison between exocytic control mechanisms in adrenal chromaffin cells and a glutamatergic synapse. *Pflugers Arch* (2006) **453**:261–8. doi:10.1007/s00424-006-0143-9
47. Dolensek J, Skelin M, Rupnik MS. Calcium dependencies of regulated exocytosis in different endocrine cells. *Physiol Res* (2011) **60**(Suppl 1):S29–38.
48. Hoppa MB, Jones E, Karanauskaite J, Ramracheya R, Braun M, Collins SC, et al. Multivesicular exocytosis in rat pancreatic beta cells. *Diabetologia* (2012) **55**:1001–12. doi:10.1007/s00125-011-2400-5
49. Wan QF, Dong Y, Yang H, Lou X, Ding J, Xu T. Protein kinase activation increases insulin secretion by sensitizing the secretory machinery to Ca2+. *J Gen Physiol* (2004) **124**:653–62. doi:10.1085/jgp.200409082
50. Tse A, Lee AK, Tse FW. Ca2+ signaling and exocytosis in pituitary corticotropes. *Cell Calcium* (2012) **51**:253–9. doi:10.1016/j.ceca.2011.12.007
51. Martin TF. Tuning exocytosis for speed: fast and slow modes. *Biochim Biophys Acta* (2003) **1641**:157–65. doi:10.1016/S0167-4889(03)00093-4
52. Voets T. Dissection of three Ca2+-dependent steps leading to secretion in chromaffin cells from mouse adrenal slices. *Neuron* (2000) **28**:537–45. doi:10.1016/S0896-6273(00)00131-8
53. Tse FW, Tse A. Regulation of exocytosis via release of Ca(2+) from intracellular stores. *Bioessays* (1999) **21**:861–5. doi:10.1002/(SICI)1521-1878(199910)21:10<861::AID-BIES8>3.3.CO;2-0
54. Naor Z, Harris D, Shacham S. Mechanism of GnRH receptor signaling: combinatorial cross-talk of Ca2+ and protein kinase C. *Front Neuroendocrinol* (1998) **19**:1–19. doi:10.1006/frne.1997.0162
55. Hille B, Tse A, Tse FW, Almers W. Calcium oscillations and exocytosis in pituitary gonadotropes. *Ann N Y Acad Sci* (1994) **710**:261–70. doi:10.1111/j.1749-6632.1994.tb26634.x
56. Stojilkovic SS. Ca2+-regulated exocytosis and SNARE function. *Trends Endocrinol Metab* (2005) **16**:81–3. doi:10.1016/j.tem.2005.02.002
57. Jahn R, Scheller RH. SNAREs – engines for membrane fusion. *Nat*

Rev Mol Cell Biol (2006) **7**:631–43. doi:10.1038/nrm2002
58. Martens S, McMahon HT. Mechanisms of membrane fusion: disparate players and common principles. *Nat Rev Mol Cell Biol* (2008) **9**:543–56. doi:10.1038/nrm2417
59. Yang L, Dun AR, Martin KJ, Qiu Z, Dunn A, Lord GJ, et al. Secretory vesicles are preferentially targeted to areas of low molecular SNARE density. *PLoS ONE* (2012) **7**:e49514. doi:10.1371/journal.pone.0049514
60. Savigny P, Evans J, McGrath KM. Cell membrane structures during exocytosis. *Endocrinology* (2007) **148**:3863–74. doi:10.1210/en.2006-1644
61. Farnworth PG. Gonadotrophin secretion revisited. How many ways can FSH leave a gonadotroph? *J Endocrinol* (1995) **145**:387–95. doi:10.1677/joe.0.1450387
62. Childs GV. Functional ultrastructure of gonadotropes: a review. *Curr Top Neuroendocrinol* (1986) **7**:49–97. doi:10.1007/978-3-642-71461-0_2
63. McNeilly AS, Crawford JL, Taragnat C, Nicol L, McNeilly JR. The differential secretion of FSH and LH: regulation through genes, feedback and packaging. *Reprod Suppl* (2003) **61**:463–76.
64. Nicol L, McNeilly JR, Stridsberg M, McNeilly AS. Differential secretion of gonadotrophins: investigation of the role of secretogranin II and chromogranin A in the release of LH and FSH in LbetaT2 cells. *J Mol Endocrinol* (2004) **32**:467–80. doi:10.1677/jme.0.0320467
65. Haisenleder DJ, Dalkin AC, Ortolano GA, Marshall JC, Shupnik MA. A pulsatile gonadotropin-releasing hormone stimulus is required to increase transcription of the gonadotropin subunit genes: evidence for differential regulation of transcription by pulse frequency in vivo. *Endocrinology* (1991) **128**:509–17. doi:10.1210/endo-128-1-509
66. Martinez de la Escalera G, Choi AL, Weiner RI. Generation and synchronization of gonadotropin-releasing hormone (GnRH) pulses: intrinsic properties of the GT1-1 GnRH neuronal cell line. *Proc Natl Acad Sci U S A* (1992) **89**:1852–5. doi:10.1073/pnas.89.5.1852
67. Shupnik MA. Effects of gonadotropin-releasing hormone on rat gonadotropin gene transcription in vitro: requirement for pulsatile administration for luteinizing hormone-beta gene stimulation. *Mol Endocrinol* (1990) **4**:1444–50. doi:10.1210/mend-4-10-1444
68. Halvorson LM, Ito M, Jameson JL, Chin WW. Steroidogenic factor-1 and early growth response protein 1 act through two composite DNA binding sites to regulate luteinizing hormone beta-subunit gene expression. *J Biol Chem* (1998) **273**:14712–20. doi:10.1074/jbc.273.24.14712
69. Halvorson LM, Kaiser UB, Chin WW. The protein kinase C system acts through the early growth response protein 1 to increase LHbeta gene expression in synergy with steroidogenic factor-1. *Mol Endocrinol* (1999) **13**:106–16. doi:10.1210/me.13.1.106
70. Tremblay JJ, Drouin J. Egr-1 is a downstream effector of GnRH and synergizes by direct interaction with Ptx1 and SF-1 to enhance luteinizing hormone beta gene transcription. *Mol Cell Biol* (1999) **19**:2567–76.
71. Wolfe MW, Call GB. Early growth response protein 1 binds to the luteinizing hormone-beta promoter and mediates gonadotropin-releasing hormone-stimulated gene expression. *Mol Endocrinol* (1999) **13**:752–63. doi:10.1210/me.13.5.752
72. Wildt L, Hausler A, Marshall G, Hutchison JS, Plant TM, Belchetz PE, et al. Frequency and amplitude of gonadotropin-releasing hormone stimulation and gonadotropin secretion in the rhesus monkey. *Endocrinology* (1981) **109**:376–85. doi:10.1210/endo-109-2-376
73. Thompson IR, Ciccone NA, Xu S, Zaytseva S, Carroll RS, Kaiser UB. GnRH pulse frequency-dependent stimulation of FSHbeta transcription is mediated via activation of PKA and CREB. *Mol Endocrinol* (2013) **27**:606–18. doi:10.1210/me.2012-1281
74. Garrel G, Simon V, Thieulant ML, Cayla X, Garcia A, Counis R, et al. Sustained gonadotropin-releasing hormone stimulation mobilizes the cAMP/PKA pathway to induce nitric oxide synthase type 1 expression in rat pituitary cells in vitro and in vivo at proestrus. *Biol Reprod* (2010) **82**:1170–9. doi:10.1095/biolreprod.109.082925
75. Ciccone NA, Xu S, Lacza CT, Carroll RS, Kaiser UB. Frequency-dependent regulation of follicle-stimulating hormone beta by pulsatile gonadotropin-releasing hormone is mediated by functional antagonism of bZIP transcription factors. *Mol Cell Biol* (2010) **30**:1028–40. doi:10.1128/MCB.00848-09
76. Melamed P, Savulescu D, Lim S, Wijeweera A, Luo Z, Luo M, et al. Gonadotrophin-releasing hormone signalling downstream of calmodulin. *J Neuroendocrinol* (2012) **24**:1463–75. doi:10.1111/j.1365-2826.2012.02359.x
77. Pnueli L, Luo M, Wang S, Naor Z, Melamed P. Calcineurin mediates the gonadotropin-releasing hormone effect on expression of both subunits of the follicle-stimulating hormone through distinct mechanisms. *Mol Cell Biol* (2011) **31**:5023–36. doi:10.1128/MCB.06083-11
78. Lim S, Pnueli L, Tan JH, Naor Z, Rajagopal G, Melamed P. Negative feedback governs gonadotrope frequency-decoding of gonadotropin releasing hormone pulse-frequency. *PLoS ONE* (2009) **4**:e7244. doi:10.1371/journal.pone.0007244
79. Burger LL, Haisenleder DJ, Aylor KW, Marshall JC. Regulation of intracellular signaling cascades by GNRH pulse frequency in the rat pituitary: roles for CaMK II, ERK, and JNK activation. *Biol Reprod* (2008) **79**:947–53. doi:10.1095/biolreprod.108.070987
80. Haisenleder DJ, Yasin M, Marshall JC. Gonadotropin subunit and gonadotropin-releasing hormone receptor gene expression are regulated by alterations in the frequency of calcium pulsatile signals. *Endocrinology* (1997) **138**:5227–30. doi:10.1210/en.138.12.5227
81. De Koninck P, Schulman H. Sensitivity of CaM kinase II to the frequency of Ca2+ oscillations. *Science* (1998) **279**:227–30. doi:10.1126/science.279.5348.227
82. Purwana IN, Kanasaki H, Oride A, Mijiddorj T, Shintani N, Hashimoto H, et al. GnRH-induced PACAP and PAC1 receptor expression in pituitary gonadotrophs: a possible role in the regulation of gonadotropin subunit gene expression. *Peptides* (2010) **31**:1748–55. doi:10.1016/j.peptides.2010.05.012
83. Kanasaki H, Purwana IN, Miyazaki K. Possible role of PACAP and its PAC1 receptor in the differential regulation of pituitary LHbeta- and FSHbeta-subunit gene expression by pulsatile GnRH stimulation. *Biol Reprod* (2013) **88**:35. doi:10.1095/biolreprod.112.105601
84. Levine JE. New concepts of the neuroendocrine regulation of gonadotropin surges in rats. *Biol Reprod* (1997) **56**:293–302. doi:10.1095/biolreprod56.2.293
85. Herbison AE. Multimodal influence of estrogen upon gonadotropin-releasing hormone neurons. *Endocr Rev* (1998) **19**:302–30. doi:10.1210/er.19.3.302
86. Gregg DW, Schwall RH, Nett TM. Regulation of gonadotropin secretion and number of gonadotropin-releasing hormone receptors by inhibin, activin-A, and estradiol. *Biol Reprod* (1991) **44**:725–32. doi:10.1095/biolreprod44.4.725
87. Steiner RA, Bremner WJ, Clifton DK. Regulation of luteinizing hormone pulse frequency and amplitude by testosterone in the adult male rat. *Endocrinology* (1982) **111**:2055–61. doi:10.1210/endo-111-6-2055
88. Hooley RD, Baxter RW, Chamley WA, Cumming IA, Jonas HA, Findlay JK. FSH and LH response to gonadotropin-releasing hormone during the ovine estrous cycle and following progesterone administration. *Endocrinology* (1974) **95**:937–42. doi:10.1210/endo-95-4-937
89. Smith MS, Freeman ME, Neill JD. The control of progesterone secretion during the estrous cycle and early pseudopregnancy in the rat: prolactin, gonadotropin and steroid levels associated with rescue of the corpus luteum of pseudopregnancy. *Endocrinology* (1975) **96**:219–26. doi:10.1210/endo-96-1-219
90. Libertun C, Orias R, McCann SM. Biphasic effect of estrogen on the sensitivity of the pituitary to luteinizing hormone-releasing factor (LRF). *Endocrinology* (1974) **94**:1094–100. doi:10.1210/endo-94-4-1094
91. Nett TM, Turzillo AM, Baratta M, Rispoli LA. Pituitary effects of steroid hormones on secretion of follicle-stimulating hormone and luteinizing hormone. *Domest Anim Endocrinol* (2002) **23**:33–42. doi:10.1016/S0739-7240(02)00143-1
92. Bernard DJ, Fortin J, Wang Y, Lamba P. Mechanisms of FSH synthesis: what we know, what we don't, and why you should care. *Fertil Steril* (2010) **93**:2465–85.

doi:10.1016/j.fertnstert.2010.03.034
93. Schwartz NB, Channing CP. Evidence. *Proc Natl Acad Sci U S A* (1977) **74**:5721–4. doi:10.1073/pnas.74.12.5721
94. Wersinger SR, Haisenleder DJ, Lubahn DB, Rissman EF. Steroid feedback on gonadotropin release and pituitary gonadotropin subunit mRNA in mice lacking a functional estrogen receptor alpha. *Endocrine* (1999) **11**:137–43. doi:10.1385/ENDO:11:2:137
95. Mercer JE, Phillips DJ, Clarke IJ. Short-term regulation of gonadotropin subunit mRNA levels by estrogen: studies in the hypothalamo-pituitary intact and hypothalamo-pituitary disconnected ewe. *J Neuroendocrinol* (1993) **5**:591–6. doi:10.1111/j.1365-2826.1993.tb00526.x
96. Mercer JE, Clements JA, Funder JW, Clarke IJ. Regulation of follicle-stimulating hormone beta and common alpha-subunit messenger ribonucleic acid by gonadotropin-releasing hormone and estrogen in the sheep pituitary. *Neuroendocrinology* (1989) **50**:321–6. doi:10.1159/000125240
97. Glidewell-Kenney C, Weiss J, Hurley LA, Levine JE, Jameson JL. Estrogen receptor alpha signaling pathways differentially regulate gonadotropin subunit gene expression and serum follicle-stimulating hormone in the female mouse. *Endocrinology* (2008) **149**:4168–76. doi:10.1210/en.2007-1807
98. Smith PF, Frawley LS, Neill JD. Detection of LH release from individual pituitary cells by the reverse hemolytic plaque assay: estrogen increases the fraction of gonadotropes responding to GnRH. *Endocrinology* (1984) **115**:2484–6. doi:10.1210/endo-115-6-2484
99. Drouin J, Labrie F. Selective effect of androgens on LH and FSH release in anterior pituitary cells in culture. *Endocrinology* (1976) **98**:1528–34. doi:10.1210/endo-98-6-1528
100. Batra SK, Miller WL. Progesterone decreases the responsiveness of ovine pituitary cultures to luteinizing hormone-releasing hormone. *Endocrinology* (1985) **117**:1436–40. doi:10.1210/endo-117-4-1436
101. Clarke IJ, Cummins JT, Crowder ME, Nett TM. Pituitary receptors for gonadotropin-releasing hormone in relation to changes in pituitary and plasma gonadotropins in ovariectomized hypothalamo/pituitary-disconnected ewes. II. A marked rise in receptor number during the acute feedback effects of estradiol. *Biol Reprod* (1988) **39**:349–54.
102. Clayton RN, Solano AR, Garcia-Vela A, Dufau ML, Catt KJ. Regulation of pituitary receptors for gonadotropin-releasing hormone during the rat estrous cycle. *Endocrinology* (1980) **107**:699–706. doi:10.1210/endo-107-3-699
103. Bauer-Dantoin AC, Weiss J, Jameson JL. Roles of estrogen, progesterone, and gonadotropin-releasing hormone (GnRH) in the control of pituitary GnRH receptor gene expression at the time of the preovulatory gonadotropin surges. *Endocrinology* (1995) **136**:1014–9. doi:10.1210/en.136.3.1014
104. Ghosh BR, Wu JC, Strahl BD, Childs GV, Miller WL. Inhibin and estradiol alter gonadotropes differentially in ovine pituitary cultures: changing gonadotrope numbers and calcium responses to gonadotropin-releasing hormone. *Endocrinology* (1996) **137**:5144–54. doi:10.1210/en.137.11.5144
105. Ortmann O, Stojilkovic SS, Cesnjaj M, Emons G, Catt KJ. Modulation of cytoplasmic calcium signaling in rat pituitary gonadotrophs by estradiol and progesterone. *Endocrinology* (1992) **131**:1565–7. doi:10.1210/en.131.3.1565
106. Ortmann O, Merelli F, Stojilkovic SS, Schulz KD, Emons G, Catt KJ. Modulation of calcium signaling and LH secretion by progesterone in pituitary gonadotrophs and clonal pituitary cells. *J Steroid Biochem Mol Biol* (1994) **48**:47–54. doi:10.1016/0960-0760(94)90249-6
107. Clayton RN, Channabasavaiah K, Stewart JM, Catt KJ. Hypothalamic regulation of pituitary gonadotropin-releasing hormone receptors: effects of hypothalamic lesions and a gonadotropin-releasing hormone antagonist. *Endocrinology* (1982) **110**:1108–15. doi:10.1210/endo-110-4-1116
108. Naik SI, Young LS, Charlton HM, Clayton RN. Pituitary gonadotropin-releasing hormone receptor regulation in mice. II: females. *Endocrinology* (1984) **115**:114–20. doi:10.1210/endo-115-1-114
109. Nett TM, Crowder ME, Moss GE, Duello TM. GnRH-receptor interaction. V. Down-regulation of pituitary receptors for GnRH in ovariectomized ewes by infusion of homologous hormone. *Biol Reprod* (1981) **24**:1145–55.
110. Shupnik MA, Gharib SD, Chin WW. Estrogen suppresses rat gonadotropin gene transcription in vivo. *Endocrinology* (1988) **122**:1842–6. doi:10.1210/endo-122-5-1842
111. Gharib SD, Wierman ME, Badger TM, Chin WW. Sex steroid hormone regulation of follicle-stimulating hormone subunit messenger ribonucleic acid (mRNA) levels in the rat. *J Clin Invest* (1987) **80**:294–9. doi:10.1172/JCI113072
112. Sanchez-Criado JE, de Las Mulas JM, Bellido C, Navarro VM, Aguilar R, Garrido-Gracia JC, et al. Gonadotropin-secreting cells in ovariectomized rats treated with different oestrogen receptor ligands: a modulatory role for ERbeta in the gonadotrope? *J Endocrinol* (2006) **188**:167–77. doi:10.1677/joe.1.06377
113. Prendergast KA, Burger LL, Aylor KW, Haisenleder DJ, Dalkin AC, Marshall JC. Pituitary follistatin gene expression in female rats: evidence that inhibin regulates transcription. *Biol Reprod* (2004) **70**:364–70. doi:10.1095/biolreprod.103.021733
114. Kaiser UB, Chin WW. Regulation of follistatin messenger ribonucleic acid levels in the rat pituitary. *J Clin Invest* (1993) **91**:2523–31. doi:10.1172/JCI116488
115. Baratta M, West LA, Turzillo AM, Nett TM. Activin modulates differential effects of estradiol on synthesis and secretion of follicle-stimulating hormone in ovine pituitary cells. *Biol Reprod* (2001) **64**:714–9. doi:10.1095/biolreprod64.2.714
116. Strahl BD, Huang HJ, Sebastian J, Ghosh BR, Miller WL. Transcriptional activation of the ovine follicle-stimulating hormone beta-subunit gene by gonadotropin-releasing hormone: involvement of two activating protein-1-binding sites and protein kinase C. *Endocrinology* (1998) **139**:4455–65. doi:10.1210/en.139.11.4455
117. Miller CD, Miller WL. Transcriptional repression of the ovine follicle-stimulating hormone-beta gene by 17 beta-estradiol. *Endocrinology* (1996) **137**:3437–46. doi:10.1210/en.137.8.3437
118. Lagace L, Massicotte J, Labrie F. Acute stimulatory effects of progesterone on luteinizing hormone and follicle-stimulating hormone release in rat anterior pituitary cells in culture. *Endocrinology* (1980) **106**:684–9. doi:10.1210/endo-106-3-684
119. Everett JW. Progesterone and estrogen in the experimental control of ovulation time and other features of the estrous cycle in the rat. *Endocrinology* (1948) **43**:389–405. doi:10.1210/endo-43-6-389
120. Urbanski HF, Pickle RL, Ramirez VD. Simultaneous measurement of gonadotropin-releasing hormone, luteinizing hormone, and follicle-stimulating hormone in the orchidectomized rat. *Endocrinology* (1988) **123**:413–9. doi:10.1210/endo-123-1-413
121. Shivers BD, Harlan RE, Morrell JI, Pfaff DW. Immunocytochemical localization of luteinizing hormone-releasing hormone in male and female rat brains. Quantitative studies on the effect of gonadal steroids. *Neuroendocrinology* (1983) **36**:1–12. doi:10.1159/000123522
122. Toranzo D, Dupont E, Simard J, Labrie C, Couet J, Labrie F, et al. Regulation of progonadotropin-releasing hormone gene expression by sex steroids in the brain of male and female rats. *Mol Endocrinol* (1989) **3**:1748–56. doi:10.1210/mend-3-11-1748
123. Lindzey J, Wetsel WC, Couse JF, Stoker T, Cooper R, Korach KS. Effects of castration and chronic steroid treatments on hypothalamic gonadotropin-releasing hormone content and pituitary gonadotropins in male wild-type and estrogen receptor-alpha knockout mice. *Endocrinology* (1998) **139**:4092–101. doi:10.1210/en.139.10.4092
124. Wetsel WC, Negro-Vilar A. Testosterone selectively influences protein kinase-C-coupled secretion of proluteinizing hormone-releasing hormone-derived peptides. *Endocrinology* (1989) **125**:538–47. doi:10.1210/endo-125-1-538
125. Selmanoff M, Shu C, Petersen SL, Barraclough CA, Zoeller RT. Single cell levels of hypothalamic messenger ribonucleic acid

encoding luteinizing hormone-releasing hormone in intact, castrated, and hyperprolactinemic male rats. *Endocrinology* (1991) **128**:459–66. doi:10.1210/endo-128-1-459

126. Roselli CE, Kelly MJ, Ronnekleiv OK. Testosterone regulates progonadotropin-releasing hormone levels in the preoptic area and basal hypothalamus of the male rat. *Endocrinology* (1990) **126**:1080–6. doi:10.1210/endo-126-2-1080
127. Culler MD, Valenca MM, Merchenthaler I, Flerko B, Negro-Vilar A. Orchidectomy induces temporal and regional changes in the processing of the luteinizing hormone-releasing hormone prohormone in the rat brain. *Endocrinology* (1988) **122**:1968–76. doi:10.1210/endo-122-5-1968
128. Zanisi M, Celotti F, Ferraboschi P, Motta M. Testosterone metabolites do not participate in the control of hypothalamic LH-releasing hormone. *J Endocrinol* (1986) **109**:291–6. doi:10.1677/joe.0.1090291
129. Levine JE, Pau KY, Ramirez VD, Jackson GL. Simultaneous measurement of luteinizing hormone-releasing hormone and luteinizing hormone release in unanesthetized, ovariectomized sheep. *Endocrinology* (1982) **111**:1449–55. doi:10.1210/endo-111-5-1449
130. Jackson GL, Kuehl D, Rhim TJ. Testosterone inhibits gonadotropin-releasing hormone pulse frequency in the male sheep. *Biol Reprod* (1991) **45**:188–94. doi:10.1095/biolreprod45.1.188
131. Giri M, Kaufman JM. Effects of long-term orchidectomy on in vitro pulsatile gonadotropin-releasing hormone release from the medial basal hypothalamus of the adult guinea pig. *Endocrinology* (1994) **134**:1621–6. doi:10.1210/en.134.4.1621
132. Burger LL, Haisenleder DJ, Wotton GM, Aylor KW, Dalkin AC, Marshall JC. The regulation of FSHbeta transcription by gonadal steroids: testosterone and estradiol modulation of the activin intracellular signaling pathway. *Am J Physiol Endocrinol Metab* (2007) **293**:E277–85. doi:10.1152/ajpendo.00447.2006
133. Gharib SD, Leung PC, Carroll RS, Chin WW. Androgens positively regulate follicle-stimulating hormone beta-subunit mRNA levels in rat pituitary cells. *Mol Endocrinol* (1990) **4**:1620–6. doi:10.1210/mend-4-11-1620
134. Ortmann O, Tomic M, Weiss JM, Diedrich K, Stojilkovic SS. Dual action of androgen on calcium signaling and luteinizing hormone secretion in pituitary gonadotrophs. *Cell Calcium* (1998) **24**:223–31. doi:10.1016/S0143-4160(98)90131-2
135. Kalra SP, Kalra PS. Neural regulation of luteinizing hormone secretion in the rat. *Endocr Rev* (1983) **4**:311–51. doi:10.1210/edrv-4-4-311
136. Liang T, Brady EJ, Cheung A, Saperstein R. Inhibition of luteinizing hormone (LH)-releasing hormone-induced secretion of LH in rat anterior pituitary cell culture by testosterone without conversion to 5 alpha-dihydrotestosterone. *Endocrinology* (1984) **115**:2311–7. doi:10.1210/endo-115-6-2311
137. Wierman ME, Gharib SD, LaRovere JM, Badger TM, Chin WW. Selective failure of androgens to regulate follicle stimulating hormone beta messenger ribonucleic acid levels in the male rat. *Mol Endocrinol* (1988) **2**:492–8. doi:10.1210/mend-2-6-492
138. Kennedy J, Chappel S. Direct pituitary effects of testosterone and luteinizing hormone-releasing hormone upon follicle-stimulating hormone: analysis by radioimmuno and radioreceptor assay. *Endocrinology* (1985) **116**:741–8. doi:10.1210/endo-116-2-741
139. Winters SJ, Ishuizaka K, Kitahara S, Troen P, Attardi B, Ghooray D, et al. Effects of testosterone on gonadotropin subunit messenger ribonucleic acids in the presence or absence of gonadotropin releasing hormone. *Endocrinology* (1992) **130**:726–34. doi:10.1210/en.130.2.726
140. Inoue K, Kurosumi K. Mode of proliferation of gonadotrophic cells of the anterior pituitary after castration – immunocytochemical and autoradiographic studies. *Arch Histol Jpn* (1981) **44**:71–85. doi:10.1679/aohc1950.44.71
141. Childs GV, Lloyd JM, Unabia G, Gharib SD, Wierman ME, Chin WW. Detection of luteinizing hormone beta messenger ribonucleic acid (RNA) in individual gonadotropes after castration: use of a new in situ hybridization method with a photobiotinylated complementary RNA probe. *Mol Endocrinol* (1987) **1**:926–32. doi:10.1210/mend-1-12-926
142. Hymer WC, Mastro A, Griswold E. DNA synthesis in the anterior pituitary of the male rat: effect of castration and photoperiod. *Science* (1970) **167**:1629–31. doi:10.1126/science.167.3925.1629
143. Inoue K, Tanaka S, Kurosumi K. Mitotic activity of gonadotropes in the anterior pituitary of the castrated male rat. *Cell Tissue Res* (1985) **240**:271–6. doi:10.1007/BF00222334
144. Ishikawa H, Totsuka S. Histological and histometrical studies on the adeno-hypophyseal cells in castrated male rats, with special emphasis on a contradiction of classifying the gonadotroph and the thyrotroph. *Endocrinol Jpn* (1968) **15**:457–79. doi:10.1507/endocrj1954.15.457
145. Duran-Pasten ML, Fiordelisio-Coll T, Hernandez-Cruz A. Castration-induced modifications of GnRH-elicited [Ca2+](i) signaling patterns in male mouse pituitary gonadotrophs in situ: studies in the acute pituitary slice preparation. *Biol Reprod* (2013) **88**:38. doi:10.1095/biolreprod.112.103812
146. Arimura A, Shino M, de la Cruz KG, Rennels EG, Schally AV. Effect of active and passive immunization with luteinizing hormone-releasing hormone on serum luteinizing hormone and follicle-stimulating hormone levels and the ultrastructure of the pituitary gonadotrophs in castrated male rats. *Endocrinology* (1976) **99**:291–303. doi:10.1210/endo-99-1-291
147. Yoshimura F, Harumiya K. Electron microscopy of the anterior lobe of pituitary in normal and castrated rats. *Endocrinol Jpn* (1965) **12**:119–52. doi:10.1507/endocrj1954.12.119
148. Console GM, Jurado SB, Rulli SB, Calandra RS, Gomez Dumm CL. Ultrastructural and quantitative immunohistochemical changes induced by nonsteroid antiandrogens on pituitary gonadotroph population of prepubertal male rats. *Cells Tissues Organs* (2001) **169**:64–72. doi:10.1159/000047862
149. Gomez-Dumm CL, Echave-Llanos JM. Further studies on the ultrastructure of the pars distalis of castrated male mice pituitary. *Virchows Arch B Cell Pathol* (1973) **13**:145–52.
150. Tixier-Vidal A, Tougard C, Kerdelhue B, Jutisz M. Light and electron microscopic studies on immunocytochemical localization of gonadotropic hormones in the rat pituitary gland with antisera against ovine FSH, LH, LHalpha, and LHbeta. *Ann N Y Acad Sci* (1975) **254**:433–61. doi:10.1111/j.1749-6632.1975.tb29193.x
151. Ibrahim SN, Moussa SM, Childs GV. Morphometric studies of rat anterior pituitary cells after gonadectomy: correlation of changes in gonadotropes with the serum levels of gonadotropins. *Endocrinology* (1986) **119**:629–37. doi:10.1210/endo-119-2-629
152. Tobin VA, Canny BJ. The regulation of gonadotropin-releasing hormone-induced calcium signals in male rat gonadotrophs by testosterone is mediated by dihydrotestosterone. *Endocrinology* (1998) **139**:1038–45. doi:10.1210/en.139.3.1038
153. Tobin VA, Canny BJ. Testosterone regulates gonadotropin-releasing hormone-induced calcium signals in male rat gonadotrophs. *Endocrinology* (1996) **137**:1299–305. doi:10.1210/en.137.4.1299
154. Clayton RN, Detta A, Naik SI, Young LS, Charlton HM. Gonadotrophin releasing hormone receptor regulation in relationship to gonadotrophin secretion. *J Steroid Biochem* (1985) **23**:691–702. doi:10.1016/S0022-4731(85)80004-2
155. Sonntag WE, Forman LJ, Fiori JM, Hylka VW, Meites J. Decreased ability of old male rats to secrete luteinizing hormone (LH) is not due to alterations in pituitary LH-releasing hormone receptors. *Endocrinology* (1984) **114**:1657–64. doi:10.1210/endo-114-5-1657
156. Garcia A, Schiff M, Marshall JC. Regulation of pituitary gonadotropin-releasing hormone receptors by pulsatile gonadotropin-releasing hormone injections in male rats. Modulation by testosterone. *J Clin Invest* (1984) **74**:920–8. doi:10.1172/JCI111510
157. Weiss J, Guendner MJ, Halvorson LM, Jameson JL. Transcriptional activation of the follicle-stimulating hormone beta-subunit gene by activin. *Endocrinology*

(1995) **136**:1885–91. doi:10.1210/en.136.5.1885

158. Dalkin AC, Knight CD, Shupnik MA, Haisenleder DJ, Aloi J, Kirk SE, et al. Ovariectomy and inhibin immunoneutralization acutely increase follicle-stimulating hormone-beta messenger ribonucleic acid concentrations: evidence for a nontranscriptional mechanism. *Endocrinology* (1993) **132**:1297–304. doi:10.1210/en.132.3.1297
159. Gregory SJ, Lacza CT, Detz AA, Xu S, Petrillo LA, Kaiser UB. Synergy between activin A and gonadotropin-releasing hormone in transcriptional activation of the rat follicle-stimulating hormone-beta gene. *Mol Endocrinol* (2005) **19**:237–54. doi:10.1210/me.2003-0473
160. Bilezikjian LM, Blount AL, Leal AM, Donaldson CJ, Fischer WH, Vale WW. Autocrine/paracrine regulation of pituitary function by activin, inhibin and follistatin. *Mol Cell Endocrinol* (2004) **225**:29–36. doi:10.1016/j.mce.2004.02.010
161. Roberts V, Meunier H, Vaughan J, Rivier J, Rivier C, Vale W, et al. Production and regulation of inhibin subunits in pituitary gonadotropes. *Endocrinology* (1989) **124**:552–4. doi:10.1210/endo-124-1-552
162. de Kretser DM, Hedger MP, Loveland KL, Phillips DJ. Inhibins, activins and follistatin in reproduction. *Hum Reprod Update* (2002) **8**:529–41. doi:10.1093/humupd/8.6.529
163. Kaiser UB, Lee BL, Carroll RS, Unabia G, Chin WW, Childs GV. Follistatin gene expression in the pituitary: localization in gonadotropes and folliculostellate cells in diestrous rats. *Endocrinology* (1992) **130**:3048–56. doi:10.1210/en.130.5.3048
164. Mollard P, Hodson DJ, Lafont C, Rizzoti K, Drouin J. A tridimensional view of pituitary development and function. *Trends Endocrinol Metab* (2012) **23**:261–9. doi:10.1016/j.tem.2012.02.004
165. Hodson DJ, Romano N, Schaeffer M, Fontanaud P, Lafont C, Fiordelisio T, et al. Coordination of calcium signals by pituitary endocrine cells in situ. *Cell Calcium* (2012) **51**:222–30. doi:10.1016/j.ceca.2011.11.007
166. Alim Z, Hartshorn C, Mai O, Stitt I, Clay C, Tobet S, et al. Gonadotrope plasticity at cellular and population levels. *Endocrinology* (2012) **153**:4729–39. doi:10.1210/en.2012-1360
167. Ramirez VD, McCann SM. Inhibitory effect of testosterone on luteinizing hormone secretion in immature and adult rats. *Endocrinology* (1965) **76**:412–7. doi:10.1210/endo-76-3-412
168. Brown-Grant K, Greig F. A comparison of changes in the peripheral plasma concentrations of luteinizing hormone and follicle-stimulating hormone in the rat. *J Endocrinol* (1975) **65**:389–97. doi:10.1677/joe.0.0650389

Conflict of Interest Statement: The authors declare that the research was conducted in the absence of any commercial or financial relationships that could be construed as a potential conflict of interest.

Received: 06 July 2013; accepted: 31 August 2013; published online: 30 September 2013.

*Citation: Durán-Pastén ML and Fiordelisio T (2013) GnRH-induced Ca^{2+} signaling patterns and gonadotropin secretion in pituitary gonadotrophs. Functional adaptations to both ordinary and extraordinary physiological demands. Front. Endocrinol. **4**:127. doi: 10.3389/fendo.2013.00127*

This article was submitted to Neuroendocrine Science, a section of the journal Frontiers in Endocrinology.

frontiers in
ENDOCRINOLOGY

MINI REVIEW ARTICLE
published: 06 August 2013
doi: 10.3389/fendo.2013.00096

The regulated secretory pathway and human disease: insights from gene variants and single nucleotide polymorphisms

Wei-Jye Lin*[1] *and Stephen R. Salton*[1,2,3]

[1] *Department of Neuroscience, Icahn School of Medicine at Mount Sinai, New York, NY, USA*
[2] *Friedman Brain Institute, Icahn School of Medicine at Mount Sinai, New York, NY, USA*
[3] *Department of Geriatrics, Icahn School of Medicine at Mount Sinai, New York, NY, USA*

Edited by:
Rafael Vazquez-Martinez, University of Cordoba, Spain

Reviewed by:
Paolo Magni, Università degli Studi di Milano, Italy
T. Rajendra Kumar, University of Kansas Medical Center, USA

****Correspondence:***
Stephen R. Salton, Department of Neuroscience, Icahn School of Medicine at Mount Sinai, One Gustave L. Levy Place, Box 1065, New York, NY 10029, USA
e-mail: stephen.salton@mssm.edu

The regulated secretory pathway provides critical control of peptide, growth factor, and hormone release from neuroendocrine and endocrine cells, and neurons, maintaining physiological homeostasis. Propeptides and prohormones are packaged into dense core granules (DCGs), where they frequently undergo tissue-specific processing as the DCG matures. Proteins of the granin family are DCG components, and although their function is not fully understood, data suggest they are involved in DCG formation and regulated protein/peptide secretion, in addition to their role as precursors of bioactive peptides. Association of gene variation, including single nucleotide polymorphisms (SNPs), with neuropsychiatric, endocrine, and metabolic diseases, has implicated specific secreted proteins and peptides in disease pathogenesis. For example, a SNP at position 196 (G/A) of the human brain-derived neurotrophic factor gene dysregulates protein processing and secretion and leads to cognitive impairment. This suggests more generally that variants identified in genes encoding secreted growth factors, peptides, hormones, and proteins involved in DCG biogenesis, protein processing, and the secretory apparatus, could provide insight into the process of regulated secretion as well as disorders that result when it is impaired.

Keywords: single nucleotide polymorphism (SNP), dense core granule (DCG), insulin, brain-derived neurotrophic factor (BDNF), chromogranin, neurotrophin, proopiomelanocortin (POMC), prohormone convertase

GENERAL OVERVIEW OF REGULATED SECRETION

Neuronal and endocrine peptides, growth factors, and hormones maintain physiological homeostasis. Their release is therefore tightly controlled by regulated secretion (1). Messenger RNAs (mRNAs) are translated and secreted proteins enter the cisternae of the rough endoplasmic reticulum (RER), are transported to the trans-Golgi network (TGN), are targeted into immature dense core granules (DCGs), and are retained in mature DCGs (also called large dense core vesicles or LDCVs), in endocrine and neuronal cells. Proteins including members of the granin family, such as chromogranin A (CgA), chromogranin B (CgB), secretogranin II (SgII), and secretogranin III (SgIII), the exopeptidase carboxypeptidase E (CPE), and prohormone convertases 1/3 and 2 (PC1/3 and PC2), are also sorted into DCGs, which in addition, increase the diversity of biologically active peptides through processing of granin precursor proteins (2).

Although the sorting of proteins into DCGs is not fully understood, interaction of DCG cargo proteins with TGN lipid raft-anchoring or membrane-spanning proteins (SgIII, CPE, sortilin) plays an essential role in docking and concentrating of DCG components and is critical for the correct sorting of cargo proteins and for vesicle biogenesis (3, 4). DCG sorting domains have been identified in prohormones, propeptides, and granins, and although not highly conserved, these polypeptide motifs are required for regulated secretion. After budding from the TGN, immature DCGs undergo acidification, mediated by the DCG membrane-spanning proton pump, leading to activation of resident prohormone convertases and carboxypeptidases. All granin members and most other propeptides, prohormones, and prohormone convertases are known to undergo proteolytic processing during granule maturation, which is essential for enzymatic activation and the generation of biologically active peptides.

Granin family members, including CgA, CgB, SgII, and SgIII, are the most abundant DCG components, with CgA, for example, constituting almost half of the soluble protein content of the adrenal chromaffin cell secretory granule (5). The importance of granin proteins in vesicle biogenesis has been demonstrated by overexpression of CgA or CgB in cells that lack a classical regulated secretory pathway, such as fibroblasts, which results in the production of granule-like structures and the regulated release of vesicle contents (6, 7). Moreover, gene silencing studies demonstrate reciprocal effects on DCG biogenesis, with decreased DCG number reported in PC12 cells that contain reduced levels of CgA or SgII, and in the adrenal medulla of CgA knockout mouse (8–10). Other CgA and CgB knockout mouse models, although showing no change in DCG number in adrenal medulla and other endocrine tissues, were found to have increased levels of other granin proteins, which is likely due to compensatory mechanisms (11, 12).

MECHANISMS BY WHICH GENETIC VARIANTS CAN IMPACT SECRETED PROTEINS

Single nucleotide polymorphisms (SNPs) are the most common genetic variations in genomic DNA, occurring 1/1200 bp on average (13). Individual SNPs submitted to the Single Nucleotide Polymorphism Database (dbSNP), a service provided by the National Center for Biotechnology Information (NCBI), are assigned a unique reference SNP ID number (rs#) to map the SNP to other external databases. Many SNPs are silent variations and their occurrence does not affect gene expression or protein function. However, a single nucleotide change has the potential to modulate protein level or function if the SNP is located: (1) in the promoter region, which may alter transcriptional activity, (2) in intronic regions, which may interfere with splicing efficiency if the SNP is found at exon-intron boundaries in splice donor sites, regulatory sequences, or splice acceptor sites, (3) in the 3′ untranslated region (3′UTR), which may affect the expression levels of either mRNA or protein due to altered *cis*-elements including mRNA destabilization sequences, AU-rich elements, and translational repressor binding sites, including miRNA targeting sites, and (4) in the protein coding region, which can cause missense or nonsense mutations. Nonsense mutations can result in premature termination of translation and the production of truncated proteins, while missense mutations can lead to loss-of-function or gain-of-function. With respect to proteins in the regulated secretory pathway, missense SNPs could impact enzymatic catalytic activity, alter peptide affinity for receptors, impair protein sorting when found in targeting motif(s) of secretory proteins, or block peptide processing when located in the cleavage sites of prohormones or propeptides (**Figure 1**).

REPORTED SNPs IN GENES ENCODING SECRETED PROTEINS THAT ARE ASSOCIATED WITH NEUROPSYCHIATRIC OR ENDOCRINE/METABOLIC DISEASE

Neurotrophic growth factors, hormones, peptide precursors, prohormone convertases, granins, and other DCG proteins are secreted through the regulated or constitutive secretory pathways. Even relatively subtle changes in protein processing, levels, or regulated secretion, due to specific SNPs that impact a variety of proteins in the secretory pathway, have been reported to be associated with neuropsychiatric or metabolic disease, and these studies are reviewed below.

NEUROTROPHINS

Brain-derived neurotrophic factor

Brain-derived neurotrophic factor (BDNF) is well known for its role in regulating neuroplasticity and neurogenesis in the brain. A functional variant in the propeptide domain of BDNF, SNP rs6265 (G- to A-allele, Val66Met), was found to affect the secretion of BDNF (14). Previous biochemical studies have shown that BDNF (Met66, encoded by minor A-allele) fails to bind to sortilin through its pro-domain region, and this lowers its activity-dependent secretion due to failed DCG sorting and localization (14, 15). BDNF (Met66) is associated with reduced brain volume, impaired episodic memory (16), and high trait anxiety (17). Two other SNPs located at the protease cleavage site of the proBDNF protein, SNPs rs1048220 (G- to T-allele, Arg125Met) and rs1048221 (G- to T-allele, Arg127Leu), partially impair proBDNF cleavage but not DCG sorting and secretion (18). The minor alleles of SNP rs1048220 (T-allele) and SNP rs1048218 (T-allele) have also been associated with familial and sporadic Alzheimer's disease (19).

Nerve growth factor

Mature nerve growth factor (NGF) binds to tropomyosin-related kinase A (TrkA) receptor tyrosine kinase and activates signaling pathways that regulate neuronal differentiation and survival. Unprocessed proNGF, however, has higher binding affinity for the p75NTR neurotrophin receptor, and can stimulate either cell survival or programed cell death (20). SNP rs6330 (C- to T-allele, Ala35Val) was previously identified in the pro-domain region of NGF, which has the potential to alter the efficiency of proNGF sorting or processing. The nucleotide variant of SNP rs6330 was found to be associated with increased anxiety in women (C-allele) (21), was over-transmitted in Attention Deficit Hyperactivity Disorder (ADHD)-affected children (C-allele) (22), and was associated with Alzheimer's disease onset (both C- and minor T-alleles) (19, 23).

NEUROPEPTIDES

Proopiomelanocortin

Expression of proopiomelanocortin (POMC), the precursor of several processed neuropeptides [α-MSH, adrenocorticotrophic hormone (ACTH), β-MSH, and β-endorphin], is regulated by the adipocyte-derived hormone leptin, which signals by binding receptors on neurons in the hypothalamic arcuate nucleus. The POMC-derived peptide α-MSH activates the melanocortin 4-receptor (MC4R) and suppresses food intake. Lack of POMC in humans and mouse models leads to the development of severe obesity, ACTH deficiency, and hypopigmentation (24, 25). A missense amino acid substitution by SNP rs28932472 (G- to C-allele, Arg236Gly) in the *POMC* gene was reported to disrupt the dibasic processing site between β-MSH and β-endorphin. The minor C-allele that encodes POMC (Gly236) results in an aberrant fusion peptide of β-MSH and β-endorphin, which still binds to the MC4R but antagonizes its activation. As a consequence, the Gly236 variation is associated with early onset obesity in several ethnic groups (26).

Agouti-related peptide

Expressed in the arcuate nucleus of the hypothalamus, agouti-related peptide (AgRP) is an endogenous antagonist of the MC4R that increases feeding behavior. The amino acid substitution of Ala67 to Thr67 caused by SNP rs5030980 (G- to A-allele) in the *AgRP* gene is associated with Anorexia Nervosa and leanness (27). In healthy subjects, homozygosity for the Thr67 allele is associated with low body fat mass and low lean body mass, while the Ala67 allele is associated with late-onset obesity. Although the Thr67 variation results in no detectable change in binding to the MC4R or sorting efficiency into and secretion from DCGs, the polarity of the amino acid substitution may cause a conformational change in AgRP, affecting other peptide functions that need further characterization (28).

Neuropeptide Y

Neuropeptide Y (NPY) is a potent orexigenic peptide that is also expressed in the hypothalamus. It regulates energy balance

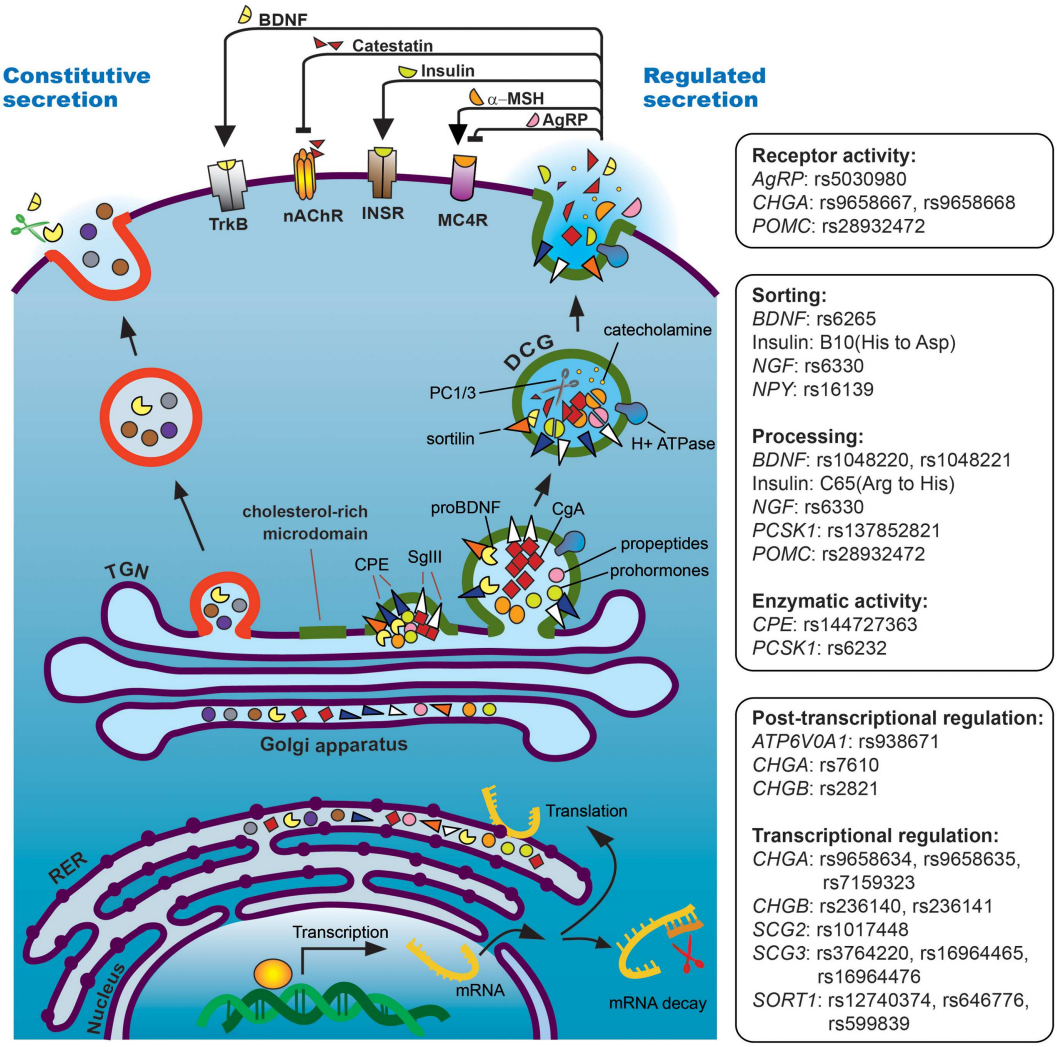

FIGURE 1 | Regulated secretory pathway of a model neuroendocrine cell. Single nucleotide polymorphisms (SNPs) can affect granule biogenesis and release through these mechanisms: (1) SNPs in the promoter or 3′UTR of granule-associated genes modulate gene expression levels, resulting in altered granule biogenesis, (2) SNPs in the pro-domain of peptides or hormones block their processing and/or sorting into the regulated pathway, (3) SNPs in convertase/peptidase catalytic or regulatory domains reduce enzymatic activity and lead to aberrant propeptide processing, (4) SNPs in the signal peptide and/or sorting domain(s) disrupt regulated secretion, and (5) SNPs that change the processing or sequence of neuropeptides modulate membrane receptor binding affinity. TrkB, tropomyosin-related kinase B receptor; INSR, insulin receptor.

through effects on energy intake, expenditure, and partitioning. A non-synonymous SNP rs16139 that leads to an amino acid change (T- to C-allele, Leu7Pro) in the signal peptide domain of preproNPY has been reported to cause a tertiary structural change in its sorting domain, and this Pro7 substitution alters intracellular proNPY packaging, processing, and secretion (29–31). NPY (Pro7) is associated with elevated food intake, altered free fatty acid (FFA) metabolism and high serum cholesterol and LDL cholesterol levels, but doesn't affect insulin sensitivity, insulin secretion, or glucose metabolism (30, 32, 33). Lower plasma NPY and norepinephrine concentrations, and lower insulin but higher glucose concentrations in plasma, were also reported in the population with the Pro7 substitution (34).

HORMONES

Insulin

A nucleotide variation in the proinsulin gene is located at the C-peptide-A-chain junction (C65, causes Arg to His), and the His65 substitution prevents processing of the dibasic cleavage site, resulting in hyperproinsulinemia that is caused by the accumulation of a circulating, biologically defective form of the proinsulin intermediate peptide, which fails to be metabolized via receptor-mediated endocytosis (35). The other identified proinsulin nucleotide variation results in an amino acid substitution of B10 (His to Asp), resulting in aberrant proinsulin sorting into the constitutive secretory pathway and a subsequent failure in peptide processing, which is also associated with hyperproinsulinemia in affected individuals (36, 37).

GRANINS

Proteins of the granin family, including the chromogranins and secretogranins, have been demonstrated to play an important role in DCG biogenesis, in neural, neuroendocrine, and endocrine cells (2). It is not too surprising, then, that a number of SNPs which alter granin expression levels have been associated with metabolic diseases or neurological disorders, because physiological homeostasis is tightly regulated by neuropeptides, growth factors, and hormones, all of which are processed and stored in DCGs.

Chromogranin A (CHGA)

The combination of SNPs that are inherited together is called a haplotype, which can be used for studying genetic linkage of diseases. Two haplotype polymorphism carriers, haplotype (A-T-C) of SNPs rs9658634–rs9658635–rs7159323 in the *CHGA* promoter region, and haplotype (T-C) of SNPs rs7610–rs875395 in the *CHGA* 3′UTR and downstream regions, are linked to hypertensive renal disease (38). SNP rs9658634 in the *CHGA* promoter was found to be located in a predicted PPARγ/RXRα binding motif, and the nucleotide variant A-allele disrupted reporter expression that was co-stimulated by PPARγ/RXRα and their cognate ligands. Physiologically, the minor A-allele is associated with lower leptin secretion, as well as lower BMI, especially in women (39). SNP rs7610 (minor T-allele) has been identified in *CHGA*, showed decreased reporter expression in PC12 pheochromocytoma cells, and was associated with lower plasma chromogranin A levels and blood pressure (BP) in a sex-dependent manner (40). Other polymorphisms identified in *CHGA* coding sequence (rs9658667, G- to A-allele, Gly364Ser, and rs9658668, C- to T-allele, Pro370Leu) result in altered catestatin activity, changing its potency to inhibit nicotinic acetylcholine receptor (nAChR)-stimulated catecholamine release from chromaffin cells, and likely linking these SNPs to an increased risk of developing hypertension (41, 42). SNP rs9658635 and haplotype (C-T) of SNPs rs9658635–rs729940 are both linked to the onset of schizophrenia in the Japanese population, but their effect on *CHGA* gene expression remains to be determined (43).

Chromogranin B (CHGB)

Reduced chromogranin B levels have been observed in the thalamic subregion, the mediodorsal nucleus, parvocellular division (MDNp; *CHGB* mRNA levels), and cerebrospinal fluid (both CgA and CgB protein levels) of schizophrenic patients (44, 45). Two polymorphisms identified in the *CHGB* coding sequence, rs236152 (C- to G-allele, Arg353Gly) and rs236153 (A- to G-allele, Glu368Glu), are associated with schizophrenia in a Japanese population study, although the functional consequences of these two SNP variants are unknown (46). A haplotype (A-T) of SNPs rs236140–rs236141 identified in the *CHGB* gene promoter region shows the highest transcriptional strength in reporter assays carried out in PC12 cells, and interestingly, the (A-T) haplotype is strongly associated with hypertension (47). The SNP rs2821 (minor A-allele) found in an RNA-destabilizing A/U-rich motif of the *CHGB* 3′UTR was reportedly associated with lower plasma chromogranin B levels in population studies, likely due to shortened *CHGB* mRNA half-life (48).

Secretogranin II and secretogranin III (SCG2 and SCG3)

Single nucleotide polymorphism rs1017448 (minor A-allele) was found in the first intron of the *SCG2* gene. It is significantly associated with elevated BP, and likely increases *SCG2* gene expression by facilitating the recruitment of paired-like homeobox transcriptional factor 2a (Phox2a) (49). SNP rs3764220 (A-allele), which is found in the promoter region of the *SCG3* gene, is associated with metabolic syndrome-related physiological changes, including dyslipidemia, hypertension, and impaired glucose tolerance, with increased risk of cardiovascular disease-related morbidity and mortality (50). SNP rs16964465 (minor C-allele) in the *SCG3* promoter region and minor G-allele of rs16964476 in the first intron, both enhanced transcriptional activity of a reporter in the neuroblastoma cell line SH-SY5Y (51). Interestingly, in hypothalamus, SgIII protein is detected in both POMC and NPY neurons in the arcuate nucleus, and in orexin-expressing and melanin-concentrating hormone (MCH)-expressing neurons in the lateral hypothalamus; all these neuropeptides regulate food intake (51). Notably, these two minor alleles, both associated with increased SgIII expression, seemed to confer resistance to the onset of obesity, suggesting the possibility that decreased SgIII levels could reciprocally increase the risk of obesity.

PEPTIDASES AND CONVERTASES

Prohormone convertase 1/3

Prohormone convertases are a family of endopeptidases that cleave proteins at internal sites, generally paired or clustered basic lysine, and/or arginine residues. PC1 is encoded by the proprotein convertase, subtilisin/kexin-type 1 (*PCSK1*) gene. Two functionally relevant SNPs, originally identified in different *PCSK1* alleles of a female patient with childhood early onset obesity, are associated with abnormal glucose homeostasis, and elevated plasma proinsulin and POMC levels (52, 53). SNP rs137852821 (G- to A-allele) changes an amino acid from Gly483 to Arg483, which prevents processing of proPC1 and favors its retention in the RER. Another C-allele variant found in the intron-5 donor splice site of *PCSK1* gene also causes exon 5 skipping and results in premature termination of PC1 translation in the catalytic region. Yet another identified non-synonymous allele substitution that is associated with early onset obesity is SNP rs6232 (A- to G-allele), which changes Asn221 to Asp221 and causes impaired catalytic function of PC1 (54).

Carboxypeptidase E

Carboxypeptidase E trims C-terminal lysine and arginine residues from peptides that are generated by prohormone convertase cleavage of precursor proteins at paired dibasic residues (55). Notably, CPE is also a sorting/retention receptor for proinsulin and proBDNF trafficking to the regulated secretory pathway (56, 57). The SNP rs144727363 (C- to T-allele, Arg189Trp) in the *CPE* coding region changes arginine to tryptophan, which reduces enzymatic activity of CPE, and is associated with hyperproinsulinemia and type II diabetes mellitus in affected Ashkenazi Jewish families (58). Similarly, a missense mutation in the *CPE* gene (Ser202Pro), identified from the mouse *fat/fat* model, which generates an enzymatically inactive and unprocessed protein product,

results in impaired processing of proinsulin and other propeptides, chronic hyperproinsulinaemia, and obesity (59–61).

OTHER PROTEINS THAT REGULATE SECRETORY PATHWAY FUNCTION

ATP6V0A1

ATP6V0A1 encodes the α1 subunit of the vacuolar H^+-translocating ATPase complex, which functions in acidification of intracellular organelles. Bafilomycin A1, a chemical inhibitor of the vacuolar H^+ ATPase, impairs DCG formation, and the sorting of secretory proteins into the regulated pathway (62). A reported SNP rs938671 (minor C-allele, 3246 T/C) in the 3′UTR of *ATP6V0A1* gene creates a binding motif for the micro-RNA hsa-miR-637, which decreases overall gene expression of *ATP6V0A1*. Its clinical association with hypertension may be due to altered DCG acidification by the risk C-allele, and as a consequence, decreased sorting, retention, and/or processing of DCG components (63).

Sortilin (SORT1)

Sortilin, a Vps10p domain protein, binds to proBDNF, and other polypeptides and facilitates their trafficking into the regulated secretory pathway (15). Plasma membrane sortilin also functions as an internalization receptor for apolipoprotein A-V and progranulin uptake (64, 65). Several SNPs are located in a non-coding region downstream of the *SORT1* allele and strongly correlate with increased sortilin expression, including SNP rs12740374 (minor T-allele), which creates a C/EBPα binding site, SNP rs646776 (minor C-allele), and SNP rs599839 (minor G-allele). Increased sortilin expression is reported to associate with reduced ApoB secretion, enhanced LDL uptake in the liver, and increased uptake of plasma progranulin (66–69). How these existing SNPs affect other known function of sortilin, including propeptide sorting, is still unclear.

FUTURE PERSPECTIVES

Protein secretion from neuroendocrine, neural, and endocrine cells is a complex, highly regulated process. Due to the nature of the cargo, which includes critical growth factors, hormones, peptide precursors, the enzymes that process them, and proteins that function in secretory vesicle biogenesis, subtle alterations in the regulated secretory pathway, and/or the proteins transiting through it, can have a significant physiological impact. Many studies reviewed here describe the association of specific, discrete SNPs in the genes of secreted proteins with the risk or onset of human disease. Neuropsychiatric disorders such as schizophrenia, metabolic disorders including obesity and diabetes, and hypertension are strongly associated with a number of well-characterized SNPs. These identified SNPs together with genome-wide association studies (GWAS) and molecular and cellular analyses of SNP function will advance our understanding of the process of regulated secretion and the important roles that secreted and secretory proteins play in maintaining physiological homeostasis.

ACKNOWLEDGMENTS

Research in the authors' laboratory is supported by NIH grants MH086499 and DE021996, and by the Diabetes Action Research and Education Foundation.

REFERENCES

1. Kelly RB. Pathways of protein secretion in eukaryotes. *Science* (1985) **230**:25–32. doi:10.1126/science.2994224
2. Bartolomucci A, Possenti R, Mahata SK, Fischer-Colbrie R, Loh YP, Salton SR. The extended granin family: structure, function, and biomedical implications. *Endocr Rev* (2011) **32**:755–97. doi:10.1210/er.2010-0027
3. Dikeakos JD, Reudelhuber TL. Sending proteins to dense core secretory granules: still a lot to sort out. *J Cell Biol* (2007) **177**:191–6. doi:10.1083/jcb.200701024
4. Kim T, Gondre-Lewis MC, Arnaoutova I, Loh YP. Dense-core secretory granule biogenesis. *Physiology* (2006) **21**:124–33. doi:10.1152/physiol.00043.2005
5. O'Connor DT, Frigon RP. Chromogranin A, the major catecholamine storage vesicle soluble protein. Multiple size forms, subcellular storage, and regional distribution in chromaffin and nervous tissue elucidated by radioimmunoassay. *J Biol Chem* (1984) **259**:3237–47.
6. Huh YH, Jeon SH, Yoo SH. Chromogranin B-induced secretory granule biogenesis: comparison with the similar role of chromogranin A. *J Biol Chem* (2003) **278**:40581–9. doi:10.1074/jbc.M304942200
7. Kim T, Tao-Cheng JH, Eiden LE, Loh YP. Chromogranin A, an "on/off" switch controlling dense-core secretory granule biogenesis. *Cell* (2001) **106**:499–509. doi:10.1016/S0092-8674(01)00459-7
8. Kim T, Zhang CF, Sun Z, Wu H, Loh YP. Chromogranin A deficiency in transgenic mice leads to aberrant chromaffin granule biogenesis. *J Neurosci* (2005) **25**:6958–61. doi:10.1523/JNEUROSCI.1058-05.2005
9. Courel M, Soler-Jover A, Rodriguez-Flores JL, Mahata SK, Elias S, Montero-Hadjadje M, et al. Prohormone secretogranin II regulates dense core secretory granule biogenesis in catecholaminergic cells. *J Biol Chem* (2010) **285**:10030–43. doi:10.1074/jbc.M109.064196
10. Mahapatra NR, O'Connor DT, Vaingankar SM, Hikim AP, Mahata M, Ray S, et al. Hypertension from targeted ablation of chromogranin A can be rescued by the human ortholog. *J Clin Invest* (2005) **115**:1942–52. doi:10.1172/JCI24354
11. Hendy GN, Li T, Girard M, Feldstein RC, Mulay S, Desjardins R, et al. Targeted ablation of the chromogranin a (Chga) gene: normal neuroendocrine dense-core secretory granules and increased expression of other granins. *Mol Endocrinol* (2006) **20**:1935–47. doi:10.1210/me.2005-0398
12. Obermuller S, Calegari F, King A, Lindqvist A, Lundquist I, Salehi A, et al. Defective secretion of islet hormones in chromogranin-B deficient mice. *PLoS ONE* (2010) **5**:e8936. doi:10.1371/journal.pone.0008936
13. Sherry ST, Ward MH, Kholodov M, Baker J, Phan L, Smigielski EM, et al. dbSNP: the NCBI database of genetic variation. *Nucleic Acids Res* (2001) **29**:308–11. doi:10.1093/nar/29.1.308
14. Egan MF, Kojima M, Callicott JH, Goldberg TE, Kolachana BS, Bertolino A, et al. The BDNF val66met polymorphism affects activity-dependent secretion of BDNF and human memory and hippocampal function. *Cell* (2003) **112**:257–69. doi:10.1016/S0092-8674(03)00035-7
15. Chen ZY, Ieraci A, Teng H, Dall H, Meng CX, Herrera DG, et al. Sortilin controls intracellular sorting of brain-derived neurotrophic factor to the regulated secretory pathway. *J Neurosci* (2005) **25**:6156–66. doi:10.1523/JNEUROSCI.1017-05.2005
16. Hariri AR, Goldberg TE, Mattay VS, Kolachana BS, Callicott JH, Egan MF, et al. Brain-derived neurotrophic factor val66met polymorphism affects human memory-related hippocampal activity and predicts memory performance. *J Neurosci* (2003) **23**:6690–4.
17. Montag C, Basten U, Stelzel C, Fiebach CJ, Reuter M. The BDNF Val66Met polymorphism and anxiety: support for animal knock-in studies from a genetic association study in humans. *Psychiatry Res* (2010) **179**:86–90. doi:10.1016/j.psychres.2008.08.005
18. Koshimizu H, Kiyosue K, Hara T, Hazama S, Suzuki S, Uegaki K, et al. Multiple functions of precursor BDNF to CNS neurons: negative regulation of neurite growth, spine formation and cell survival. *Mol Brain* (2009) **2**:27. doi:10.1186/1756-6606-2-27
19. Cozza A, Melissari E, Iacopetti P, Mariotti V, Tedde A, Nacmias B, et al. SNPs in neurotrophin system genes and Alzheimer's disease in an Italian population. *J Alzheimers Dis* (2008) **15**:61–70.

20. Capsoni S, Cattaneo A. On the molecular basis linking nerve growth factor (NGF) to Alzheimer's disease. *Cell Mol Neurobiol* (2006) **26**:619–33. doi:10.1007/s10571-006-9112-2
21. Lang UE, Hellweg R, Bajbouj M, Gaus V, Sander T, Gallinat J. Gender-dependent association of a functional NGF polymorphism with anxiety-related personality traits. *Pharmacopsychiatry* (2008) **41**:196–9. doi:10.1055/s-0028-1082070
22. Syed Z, Dudbridge F, Kent L. An investigation of the neurotrophic factor genes GDNF, NGF, and NT3 in susceptibility to ADHD. *Am J Med Genet B Neuropsychiatr Genet* (2007) **144B**:375–8. doi:10.1002/ajmg.b.30459
23. Di Maria E, Giorgio E, Uliana V, Bonvicini C, Faravelli F, Cammarata S, et al. Possible influence of a non-synonymous polymorphism located in the NGF precursor on susceptibility to late-onset Alzheimer's disease and mild cognitive impairment. *J Alzheimers Dis* (2012) **29**:699–705. doi:10.3233/JAD-2012-112006
24. Krude H, Biebermann H, Luck W, Horn R, Brabant G, Gruters A. Severe early-onset obesity, adrenal insufficiency and red hair pigmentation caused by POMC mutations in humans. *Nat Genet* (1998) **19**:155–7. doi:10.1038/509
25. Yaswen L, Diehl N, Brennan MB, Hochgeschwender U. Obesity in the mouse model of pro-opiomelanocortin deficiency responds to peripheral melanocortin. *Nat Med* (1999) **5**:1066–70. doi:10.1038/12506
26. Challis BG, Pritchard LE, Creemers JW, Delplanque J, Keogh JM, Luan J, et al. A missense mutation disrupting a dibasic prohormone processing site in pro-opiomelanocortin (POMC) increases susceptibility to early-onset obesity through a novel molecular mechanism. *Hum Mol Genet* (2002) **11**:1997–2004. doi:10.1093/hmg/11.17.1997
27. Vink T, Hinney A, van Elburg AA, van Goozen SH, Sandkuijl LA, Sinke RJ, et al. Association between an agouti-related protein gene polymorphism and anorexia nervosa. *Mol Psychiatry* (2001) **6**:325–8. doi:10.1038/sj.mp.4000854
28. de Rijke CE, Jackson PJ, Garner KM, van Rozen RJ, Douglas NR, Kas MJ, et al. Functional analysis of the Ala67Thr polymorphism in agouti related protein associated with anorexia nervosa and leanness. *Biochem Pharmacol* (2005) **70**:308–16. doi:10.1016/j.bcp.2005.04.033
29. Kallio J, Pesonen U, Karvonen MK, Kojima M, Hosoda H, Kangawa K, et al. Enhanced exercise-induced GH secretion in subjects with Pro7 substitution in the prepro-NPY. *J Clin Endocrinol Metab* (2001) **86**:5348–52. doi:10.1210/jc.86.11.5348
30. Ding B, Kull B, Liu Z, Mottagui-Tabar S, Thonberg H, Gu HF, et al. Human neuropeptide Y signal peptide gain-of-function polymorphism is associated with increased body mass index: possible mode of function. *Regul Pept* (2005) **127**:45–53. doi:10.1016/j.regpep.2004.10.011
31. Mitchell GC, Wang Q, Ramamoorthy P, Whim MD. A common single nucleotide polymorphism alters the synthesis and secretion of neuropeptide Y. *J Neurosci* (2008) **28**:14428–34. doi:10.1523/JNEUROSCI.0343-08.2008
32. Karvonen MK, Pesonen U, Koulu M, Niskanen L, Laakso M, Rissanen A, et al. Association of a leucine(7)-to-proline(7) polymorphism in the signal peptide of neuropeptide Y with high serum cholesterol and LDL cholesterol levels. *Nat Med* (1998) **4**:1434–7. doi:10.1038/4027
33. Pihlajamaki J, Karhapaa P, Vauhkonen I, Kekalainen P, Kareinen A, Viitanen L, et al. The Leu7Pro polymorphism of the neuropeptide Y gene regulates free fatty acid metabolism. *Metabolism* (2003) **52**:643–6. doi:10.1053/meta.2003.50098
34. Kallio J, Pesonen U, Jaakkola U, Karvonen MK, Helenius H, Koulu M. Changes in diurnal sympathoadrenal balance and pituitary hormone secretion in subjects with Leu7Pro polymorphism in the prepro-neuropeptide Y. *J Clin Endocrinol Metab* (2003) **88**:3278–83. doi:10.1210/jc.2002-021957
35. Robbins DC, Blix PM, Rubenstein AH, Kanazawa Y, Kosaka K, Tager HS. A human proinsulin variant at arginine 65. *Nature* (1981) **291**:679–81. doi:10.1038/291679a0
36. Gruppuso PA, Gorden P, Kahn CR, Cornblath M, Zeller WP, Schwartz R. Familial hyperproinsulinemia due to a proposed defect in conversion of proinsulin to insulin. *N Engl J Med* (1984) **311**:629–34. doi:10.1056/NEJM198409063111003
37. Chan SJ, Seino S, Gruppuso PA, Schwartz R, Steiner DF. A mutation in the B chain coding region is associated with impaired proinsulin conversion in a family with hyperproinsulinemia. *Proc Natl Acad Sci U S A* (1987) **84**:2194–7. doi:10.1073/pnas.84.8.2194
38. Salem RM, Cadman PE, Chen Y, Rao F, Wen G, Hamilton BA, et al. Chromogranin A polymorphisms are associated with hypertensive renal disease. *J Am Soc Nephrol* (2008) **19**:600–14. doi:10.1681/ASN.2007070754
39. Rao F, Chiron S, Wei Z, Fung MM, Chen Y, Wen G, et al. Genetic variation within a metabolic motif in the chromogranin a promoter: pleiotropic influence on cardiometabolic risk traits in twins. *Am J Hypertens* (2012) **25**:29–40. doi:10.1038/ajh.2011.163
40. Chen Y, Rao F, Rodriguez-Flores JL, Mahata M, Fung MM, Stridsberg M, et al. Naturally occurring human genetic variation in the 3'-untranslated region of the secretory protein chromogranin A is associated with autonomic blood pressure regulation and hypertension in a sex-dependent fashion. *J Am Coll Cardiol* (2008) **52**:1468–81. doi:10.1016/j.jacc.2008.07.047
41. Wen G, Mahata SK, Cadman P, Mahata M, Ghosh S, Mahapatra NR, et al. Both rare and common polymorphisms contribute functional variation at CHGA, a regulator of catecholamine physiology. *Am J Hum Genet* (2004) **74**:197–207. doi:10.1086/381399
42. Rao F, Wen G, Gayen JR, Das M, Vaingankar SM, Rana BK, et al. Catecholamine release-inhibitory peptide catestatin (chromogranin A(352-372)): naturally occurring amino acid variant Gly364Ser causes profound changes in human autonomic activity and alters risk for hypertension. *Circulation* (2007) **115**:2271–81. doi:10.1161/CIRCULATIONAHA.106.628859
43. Takahashi N, Ishihara R, Saito S, Maemo N, Aoyama N, Ji X, et al. Association between chromogranin A gene polymorphism and schizophrenia in the Japanese population. *Schizophr Res* (2006) **83**:179–83. doi:10.1016/j.schres.2005.12.854
44. Landen M, Grenfeldt B, Davidsson P, Stridsberg M, Regland B, Gottfries CG, et al. Reduction of chromogranin A and B but not C in the cerebrospinal fluid in subjects with schizophrenia. *Eur Neuropsychopharmacol* (1999) **9**:311–5. doi:10.1016/S0924-977X(98)00042-X
45. Chu TT, Liu Y. An integrated genomic analysis of gene-function correlation on schizophrenia susceptibility genes. *J Hum Genet* (2010) **55**:285–92. doi:10.1038/jhg.2010.24
46. Iijima Y, Inada T, Ohtsuki T, Senoo H, Nakatani M, Arinami T. Association between chromogranin b gene polymorphisms and schizophrenia in the Japanese population. *Biol Psychiatry* (2004) **56**:10–7. doi:10.1016/j.biopsych.2004.03.012
47. Zhang K, Rao F, Wang L, Rana BK, Ghosh S, Mahata M, et al. Common functional genetic variants in catecholamine storage vesicle protein promoter motifs interact to trigger systemic hypertension. *J Am Coll Cardiol* (2010) **55**:1463–75. doi:10.1016/j.jacc.2009.11.064
48. Rao F, Zhang K, Khandrika S, Mahata M, Fung MM, Ziegler MG, et al. Isoprostane, an "intermediate phenotype" for oxidative stress heritability, risk trait associations, and the influence of chromogranin B polymorphism. *J Am Coll Cardiol* (2010) **56**:1338–50. doi:10.1016/j.jacc.2010.03.092
49. Wen G, Wessel J, Zhou W, Ehret GB, Rao F, Stridsberg M, et al. An ancestral variant of secretogranin II confers regulation by PHOX2 transcription factors and association with hypertension. *Hum Mol Genet* (2007) **16**:1752–64. doi:10.1093/hmg/ddm123
50. Hotta K, Kitamoto T, Kitamoto A, Mizusawa S, Matsuo T, Nakata Y, et al. Association of variations in the FTO, SCG3 and MTMR9 genes with metabolic syndrome in a Japanese population. *J Hum Genet* (2011) **56**:647–51. doi:10.1038/jhg.2011.74
51. Tanabe A, Yanagiya T, Iida A, Saito S, Sekine A, Takahashi A, et al. Functional single-nucleotide polymorphisms in the secretogranin III (SCG3) gene that form secretory granules with appetite-related neuropeptides are associated with obesity. *J Clin Endocrinol Metab* (2007) **92**:1145–54. doi:10.1210/jc.2006-1808
52. O'Rahilly S, Gray H, Humphreys PJ, Krook A, Polonsky KS, White A, et al. Brief report: impaired processing of prohormones associated with abnormalities of glucose homeostasis and adrenal function. *N Engl J Med* (1995) **333**:1386–90. doi:10.1056/NEJM199511233332104
53. Jackson RS, Creemers JW, Ohagi S, Raffin-Sanson ML, Sanders L, Montague CT, et al. Obesity and impaired prohormone processing associated with mutations in the human prohormone convertase 1 gene. *Nat Genet* (1997) **16**:303–6. doi:10.1038/ng0797-303
54. Benzinou M, Creemers JW, Choquet H, Lobbens S, Dina C, Durand E, et al. Common nonsynonymous

variants in PCSK1 confer risk of obesity. *Nat Genet* (2008) **40**:943–5. doi:10.1038/ng.177
55. Fricker LD, Snyder SH. Enkephalin convertase: purification and characterization of a specific enkephalin-synthesizing carboxypeptidase localized to adrenal chromaffin granules. *Proc Natl Acad Sci U S A* (1982) **79**:3886–90. doi:10.1073/pnas.79.12.3886
56. Cawley NX, Rodriguez YM, Maldonado A, Loh YP. Trafficking of mutant carboxypeptidase E to secretory granules in a beta-cell line derived from Cpe(fat)/Cpe(fat) mice. *Endocrinology* (2003) **144**:292–8. doi:10.1210/en.2002-220588
57. Lou H, Kim SK, Zaitsev E, Snell CR, Lu B, Loh YP. Sorting and activity-dependent secretion of BDNF require interaction of a specific motif with the sorting receptor carboxypeptidase e. *Neuron* (2005) **45**:245–55. doi:10.1016/j.neuron.2004.12.037
58. Chen H, Jawahar S, Qian Y, Duong Q, Chan G, Parker A, et al. Missense polymorphism in the human carboxypeptidase E gene alters enzymatic activity. *Hum Mutat* (2001) **18**:120–31. doi:10.1002/humu.1161
59. Naggert JK, Fricker LD, Varlamov O, Nishina PM, Rouille Y, Steiner DF, et al. Hyperproinsulinaemia in obese fat/fat mice associated with a carboxypeptidase E mutation which reduces enzyme activity. *Nat Genet* (1995) **10**:135–42. doi:10.1038/ng0695-135
60. Rovere C, Viale A, Nahon J, Kitabgi P. Impaired processing of brain proneurotensin and promelanin-concentrating hormone in obese fat/fat mice. *Endocrinology* (1996) **137**:2954–8. doi:10.1210/en.137.7.2954
61. Friis-Hansen L, Lacourse KA, Samuelson LC, Holst JJ. Attenuated processing of proglucagon and glucagon-like peptide-1 in carboxypeptidase E-deficient mice. *J Endocrinol* (2001) **169**:595–602. doi:10.1677/joe.0.1690595
62. Taupenot L, Harper KL, O'Connor DT. Role of H+-ATPase-mediated acidification in sorting and release of the regulated secretory protein chromogranin A: evidence for a vesiculogenic function. *J Biol Chem* (2005) **280**:3885–97. doi:10.1074/jbc.M408197200
63. Wei Z, Biswas N, Wang L, Courel M, Zhang K, Soler-Jover A, et al. A common genetic variant in the 3'-UTR of vacuolar H+-ATPase ATP6V0A1 creates a micro-RNA motif to alter chromogranin A processing and hypertension risk. *Circ Cardiovasc Genet* (2011) **4**:381–9. doi:10.1161/CIRCGENETICS.111.959767
64. Nilsson SK, Christensen S, Raarup MK, Ryan RO, Nielsen MS, Olivecrona G. Endocytosis of apolipoprotein A-V by members of the low density lipoprotein receptor and the VPS10p domain receptor families. *J Biol Chem* (2008) **283**:25920–7. doi:10.1074/jbc.M802721200
65. Hu F, Padukkavidana T, Vaegter CB, Brady OA, Zheng Y, Mackenzie IR, et al. Sortilin-mediated endocytosis determines levels of the frontotemporal dementia protein, progranulin. *Neuron* (2010) **68**:654–67. doi:10.1016/j.neuron.2010.09.034
66. Carrasquillo MM, Nicholson AM, Finch N, Gibbs JR, Baker M, Rutherford NJ, et al. Genome-wide screen identifies rs646776 near sortilin as a regulator of progranulin levels in human plasma. *Am J Hum Genet* (2010) **87**:890–7. doi:10.1016/j.ajhg.2010.11.002
67. Linsel-Nitschke P, Heeren J, Aherrahrou Z, Bruse P, Gieger C, Illig T, et al. Genetic variation at chromosome 1p13.3 affects sortilin mRNA expression, cellular LDL-uptake and serum LDL levels which translates to the risk of coronary artery disease. *Atherosclerosis* (2010) **208**:183–9. doi:10.1016/j.atherosclerosis.2009.06.034
68. Musunuru K, Strong A, Frank-Kamenetsky M, Lee NE, Ahfeldt T, Sachs KV, et al. From noncoding variant to phenotype via SORT1 at the 1p13 cholesterol locus. *Nature* (2010) **466**:714–9. doi:10.1038/nature09266
69. Strong A, Ding Q, Edmondson AC, Millar JS, Sachs KV, Li X, et al. Hepatic sortilin regulates both apolipoprotein B secretion and LDL catabolism. *J Clin Invest* (2012) **122**:2807–16. doi:10.1172/JCI63563

Conflict of Interest Statement: The authors declare that the research was conducted in the absence of any commercial or financial relationships that could be construed as a potential conflict of interest.

Received: 29 May 2013; accepted: 23 July 2013; published online: 06 August 2013.
*Citation: Lin W-J and Salton SR (2013) The regulated secretory pathway and human disease: insights from gene variants and single nucleotide polymorphisms. Front. Endocrinol. **4**:96. doi: 10.3389/fendo.2013.00096*
This article was submitted to Frontiers in Neuroendocrine Science, a specialty of Frontiers in Endocrinology.

frontiers in
ENDOCRINOLOGY

REVIEW ARTICLE
published: 26 June 2013
doi: 10.3389/fendo.2013.00077

Platelet granule exocytosis: a comparison with chromaffin cells

Jennifer L. Fitch-Tewfik and Robert Flaumenhaft*

Division of Hemostasis and Thrombosis, Department of Medicine, BIDMC, Harvard Medical School, Boston, MA, USA

Edited by:
Rafael Vazquez-Martinez, University of Cordoba, Spain

Reviewed by:
Ricardo Borges, University of La Laguna, Spain
Joshua J. Park, University of Toledo College of Medicine, USA

****Correspondence:***
Robert Flaumenhaft, Center for Life Science, Beth Israel Deaconess Medical Center, Room 939, 3 Blackfan Circle, Boston, MA 02215, USA
e-mail: rflaumen@bidmc.harvard.edu

The rapid secretion of bioactive amines from chromaffin cells constitutes an important component of the fight or flight response of mammals to stress. Platelets respond to stresses within the vasculature by rapidly secreting cargo at sites of injury, inflammation, or infection. Although chromaffin cells derive from the neural crest and platelets from bone marrow megakaryocytes, both have evolved a heterogeneous assemblage of granule types and a mechanism for efficient release. This article will provide an overview of granule formation and exocytosis in platelets with an emphasis on areas in which the study of chromaffin cells has influenced that of platelets and on similarities between the two secretory systems. Commonalities include the use of transporters to concentrate bioactive amines and other cargos into granules, the role of cytoskeletal remodeling in granule exocytosis, and the use of granules to provide membrane for cytoplasmic projections. The SNAREs and SNARE accessory proteins used by each cell type will also be considered. Finally, we will discuss the newly appreciated role of dynamin family proteins in regulated fusion pore formation. This evaluation of the comparative cell biology of regulated exocytosis in platelets and chromaffin cells demonstrates a convergence of mechanisms between two disparate cell types both tasked with responding rapidly to physiological stimuli.

Keywords: exocytosis, granules, platelets, chromaffin system, cytoskeleton, dynamins, SNAREs

INTRODUCTION

Platelets are small, anucleate blood cells derived from bone marrow megakaryocytes. They are best known for their central role in maintaining the integrity of the vasculature (hemostasis) and for their pathological role in clotting arteries and veins (thrombosis) during myocardial infarction, stroke, peripheral vascular disease, and deep vein thrombosis. In addition to their role in hemostasis, platelets have also been proposed to function in many other aspects of host defense. Stimulus-induced release of platelet granules contributes to nearly all platelet functions including hemostasis and thrombosis, inflammation, angiogenesis, and anti-microbial activities (Blair and Flaumenhaft, 2009). Platelets contain three granule types: α-granules, dense granules, and lysosomes (**Figure 1**; **Table 1**). Absence of dense granules, as observed in inherited syndromes such as Hermansky–Pudlak syndrome or Chediak–Higashi syndrome, results in a bleeding diathesis (Hermansky and Pudlak, 1959). Absence of α-granules, as observed in gray platelet syndrome, also increases bleeding (Buchanan and Handin, 1976; Costa et al., 1976). The bleeding phenotype associated with these disorders underscores the importance of platelet granules in hemostasis.

Despite the functional importance of platelet granule secretion in maintaining vascular integrity and promoting host defense, the molecular basis of platelet granule secretion remained poorly studied until the late 1990s, despite transformative advances in secretion biology that had occurred over the preceding decade (Rothman and Orci, 1992; Sollner et al., 1993). This knowledge deficit was due in part to the fact that platelets are anucleate, complicating the use of standard molecular biological approaches that have been widely used to study regulated secretion in nucleated cells. In addition, the small size (2–3 μm in diameter) and unusual membrane system of the platelet prevented application of classic electrophysical approaches such as patch-clamp studies. Earlier studies evaluating the molecular mechanisms of platelet granule secretion relied on applying knowledge derived from other systems to the study of platelets. The chromaffin cell has been influential in this regard. Although these two cell types have different embryonic derivations and functions, both cells store bioactive amines and peptides at high concentrations and release their cargos rapidly in response to stress signals (**Table 1**). The study of platelet granule secretion has matured considerably over the past decade, making relevant a comparison of the mechanisms by which platelets and chromaffin cells store and release their granule contents in response to environmental signals.

PLATELET GRANULE TYPES

α-GRANULES

α-Granules are by far the most abundant platelet granule type (**Figure 1**). There are ∼50–80 α-granules/platelet, ranging in size from 200 to 500 nm. They comprise roughly 10% of the platelet volume, 10-fold more than dense granules. α-Granules contain a variety of membrane proteins and soluble cargo that give them a distinct appearance when stained with osmium and viewed by transmission electron microscopy (TEM). Proteomic analyses indicate that these granules contain hundreds of different types of proteins (Coppinger et al., 2004; Piersma et al., 2009). Protein cargos found in α-granules include neuroactive peptides that are more typically associated with chromaffin cells, including tachykinins

and enkephalins (Graham et al., 2004). Conversely, proteomic studies suggest that chromaffin large dense-core vesicles (LDCVs) contain several major constituents of α-granules that can act in the vasculature, including platelet basic protein precursor, TGF-β, collagen isoforms, and metalloproteases (**Table 2**) (Wegrzyn et al., 2010). As with chromaffin cells, the mechanisms by which proteins are packaged in platelet storage granules are incompletely understood.

Platelet α-granule cargos can include coagulants and anticoagulants, angiogenic and antiangiogenic factors, proteases and proteases inhibitors, and proinflammatory and anti-inflammatory mediators. This observation has raised the question of how α-granules are able to efficiently mediate their biological functions when they contain so many proteins with opposing functions (Italiano et al., 2008; Blair and Flaumenhaft, 2009). One possibility is that there are different α-granule subpopulations that store distinct cargo. However, the number of discrete types of α-granule is not known. Evidence that α-granules are heterogeneous comes from several sources. Immunofluorescence microscopy demonstrated that the two α-granule cargos von Willebrand factor and fibrinogen do not localize to the same granule (Sehgal and Storrie, 2007). Subsequent studies showed that angiogenic factors localize to distinct compartments and were differentially released by different agonists (Italiano et al., 2008). The molecular mechanisms that mediate differential release are unclear. Differential distribution of SNAREs among subpopulations of α-granules may account for differential release. For example, Peters et al. (2012) showed that a population of granules containing vesicle-associated membrane protein-7 (VAMP-7) physically separated from VAMP-3 and VAMP-8-containing granules during spreading. However, the idea of α-granule heterogeneity remains controversial and some investigators in the field believe that granule cargos are stochastically distributed and that differential release either does not occur or is controlled at the level of pore expansion.

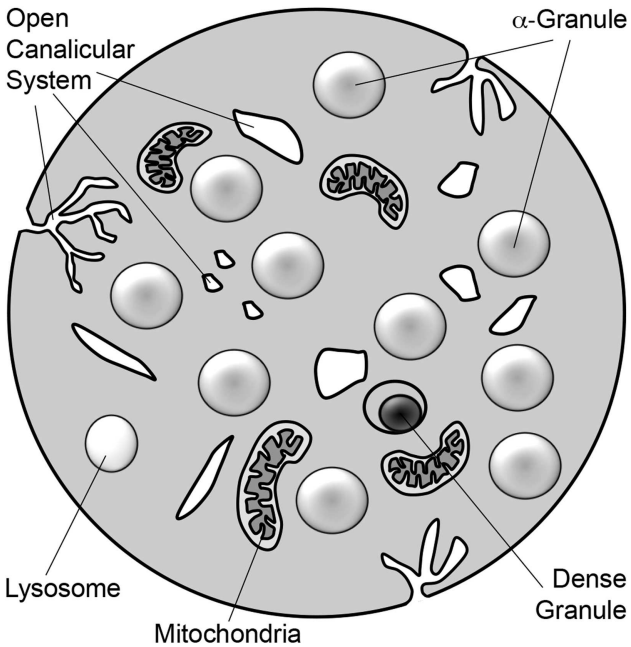

FIGURE 1 | Schematic diagram of platelet. The platelet is a 2–3 μm discoid cell that contains α-granules, dense granules, and lysosomes. Platelets also contain mitochondria. Tunnel invaginations of the plasma membrane forms a complex membrane network, termed the open canalicular system, that courses throughout the platelet interior. Platelet granule secretion is thought to occur through fusion of granules with either the plasma membrane or the open canalicular system.

Granule heterogeneity and differential release have also been evaluated in chromaffin cells. Morphologic studies demonstrate heterogeneity among both LDCVs and synaptic-like microvesicles (SLMVs) (Koval et al., 2001). Studies using carbon-fiber amperometry to measure catecholamine release from individual granules indicated distinct granule populations on the basis of release kinetics (Tang et al., 2005). Different SNAREs and SNARE chaperones may associate with different granule populations and facilitate differential release. For example, different synaptotagmin isoforms associated with LDCVs and SLMVs and this observation could account for their differential secretion in response to calcium (Matsuoka et al., 2011). Other factors influencing chromaffin granule release include pore expansion kinetics and degree. Basal levels of catecholamine release may occur through a restricted fusion pore, while in response to excitation dynamin and myosin-mediated mechanisms may elicit fusion pore expansion (Chan et al., 2010). In addition, large aggregates of chromogranin A require complete fusion to facilitate release (Perrais et al., 2004; Felmy, 2007).

Table 1 | Comparison of platelets and chromaffin cells.

	Platelets	Chromaffin cells
Distribution	Intravascular	Adrenal medulla
Size	2–3 μm	∼20 μm
Functions	Hemostasis/thrombosis Inflammation Angiogenesis Anti-microbial host defense Mitogenesis	Blood pressure modulation Paracrine signaling Anti-microbial host defense Immune regulation Analgesia
Granule types	α-Granules, dense granules, and lysosomes	Large dense-core vesicles (LDCVs) and synaptic-like microvesicles (SLMVs)

Table 2 | Comparison of granule types contained in platelets and chromaffin cells.

	α-Granules	Dense granules	LDCVs
Diameter	200–500 nm	150 nm	150–300 nm
Number	50–80 per platelet	3–8 per platelet	∼10,000 per cell
Percentage of cell volume	10	∼1	13.5
Contents	Integral membrane proteins (e.g., P-selectin, αIIbβ3, GPIbα) Coagulants/anticoagulants and fibrinolytic proteins (e.g., factor V, factor IX, plasminogen) Adhesion proteins (e.g., fibrinogen, vWF) Chemokines [e.g., CXCL4 (PF4), CXCL12 (SDF-1α)] Growth factors (e.g., EGF, IGF) Angiogenic factors/inhibitors (e.g., VEGF, PDGF, angiostatins) Immune mediators (e.g., IgG, complement precursors)	Cations (e.g., Ca^{2+}, Mg^{2+}) Polyphosphates Bioactive amines (e.g., serotonin, histamine) Nucleotides (e.g., ADP, ATP)	Structural proteins (e.g., granins, glycoproteins) Vasoregulators (e.g., catecholamines, vasostatins, renin-angiotensin) Paracrine signaling factors (e.g., guanylin, neurotensin, chromogranin B) Immune mediators (e.g., enkelytin, ubiquitin) Opioids (e.g., enkephalins, endorphins) Ions (e.g., Ca^{2+}, Na^{+}, Cl^{-}) Nucleotides (e.g., AMP, GDP, UTP) Nucleotides Polyphosphates

DENSE GRANULES

Dense granules are a subtype of lysosome-related organelle (LRO). There are ∼3–6 dense granules/platelet (Flaumenhaft, 2013). These granules are so electron dense that they can be detected by whole mount electron microscopy in the absence of staining. They are highly osmophilic when viewed by TEM. Dense granules play a critical role in hemostasis and thrombosis, releasing factors such as ADP and epinephrine that act in an autocrine and paracrine manner to stimulate platelets at sites of vascular injury. Dense granules also contain factors that are vasoconstrictive such as serotonin (Flaumenhaft, 2013).

Dense granules and LDCVs have been compared based on their unusually high concentrations of cations, polyphosphates, adenine nucleotides, and bioactive amines such as serotonin and histamine (Sigel and Corfu, 1996) (**Figure 2**; **Table 2**). In platelets, adenine nucleotides are concentrated at ∼653 mM ADP and ∼436 mM ATP (Holmsen and Weiss, 1979). Calcium is at 2.2 M. Chromaffin granules and platelet dense granules are among the few mammalian granule types to contain polyphosphates (Aikawa et al., 1971; Ruiz et al., 2004). Active transport mechanisms are thought to contribute to efficient concentration of these constituents in platelets (**Figure 2**). A vesicular H^{+}-ATPase proton pump maintains the dense-granule lumen at pH ∼5.4 (Dean et al., 1984), similar to the pH of LDCVs. The multidrug transporter MRP4, a multidrug resistance protein, is found on platelet dense granules and is proposed to transport adenine nucleotides into these granules (Jedlitschky et al., 2004). Uptake of serotonin from platelet cytosol into dense granules is mediated by vesicular monoamine transporter 2 (VMAT2). Transport is driven by an electrochemical proton gradient across the granule membrane. VMAT2 also appears to mediate histamine transport into dense granules (Fukami et al., 1984). The primary nucleotide transporter in chromaffin cells is Slc17A/VNUT (Sawada et al., 2008). Whether or not platelets use Slc17 family transporters to concentrate dense-granule cargo has yet to be evaluated. Like platelets, chromaffin cells use VMAT2, in addition to VMAT1, to pump monoamines from the cytosol into their granules.

LYSOSOMES

Platelets contain few primary and secondary lysosomes. These lysosomes contain many acid hydrolases and cathepsins as cargo and express CD63 and LAMP-2 in their membrane. Platelet lysosome function is not well-studied. They may serve a role in endosomal digestion, as observed in nucleated cells (Flaumenhaft, 2013).

AN OVERVIEW OF PLATELET GRANULE RELEASE

Platelets are uniform discoid cells that circulate in a quiescent state and undergo a dramatic morphological change when activated. Their plasma membrane surface area is ∼19 μm^2 and the total surface area of their granules is ∼14 μm^2. They have an unusual membrane system, including an open canalicular system (OCS), which is a system of tunneling invaginations of the plasma membrane that is unique to platelets and is estimated to have a surface area of ∼14 μm^2 (Flaumenhaft, 2013). The OCS tracks through the platelet, but is topologically similar to the plasma membrane in that it possesses both an extracellular and a cytosolic face. Platelets also have a dense tubular system (DTS), which is a membrane system thought to be derived from the megakaryocytic endoplasmic reticulum. The DTS serves as an intracellular calcium storage site, but is not directly connected to either the plasma membrane or the OCS (van Nispen tot Pannerden et al., 2010).

Ultrastructural studies have demonstrated several atypical features of the platelet release reaction. In the resting state, platelet α-granules and dense granules are distributed throughout the platelet. With activation-induced shape change, granules become localized in a central granulomere. As with chromaffin granules, platelet granules may fuse with one another in a process termed

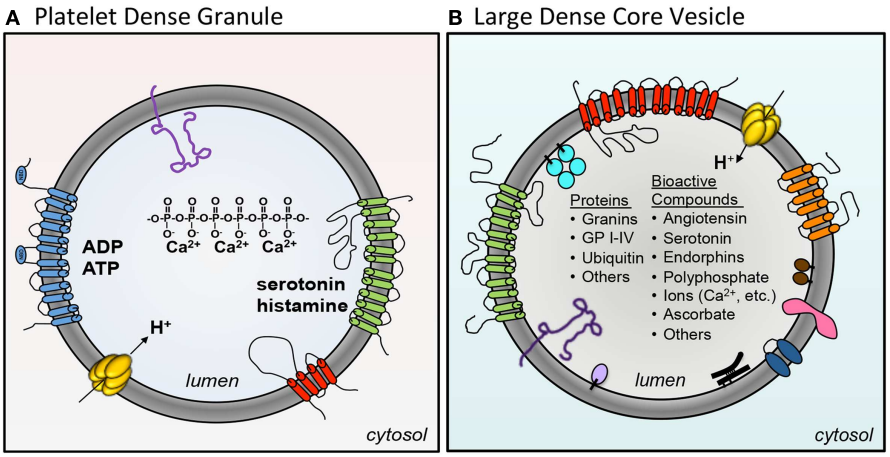

FIGURE 2 | A comparison of platelet dense granules and chromaffin LDCVs. **(A)** Several membrane pumps concentration granule contents in the maturing granule. VMAT2 concentrates serotonin (*green*). An H^+-ATPase proton pump maintains the granule at pH ∼5.4 (*yellow*). MRP4 (*blue*) is thought to concentrate adenine nucleotides into dense granules. Dense granules also express the tetraspanin CD63 (*red*) and the lysosomal marker LAMP-2 (*purple*). Dense granules contain a core of calcium chelated by polyphosphate. **(B)** The chromaffin large dense-core vesicle (LDCV) express a variety of membrane proteins including VMAT1 amine transporter (*red*), H^+-ATPase (*yellow*), Cytochrome b561 (*orange*), p65 (*pink*), peptidyl α-amidation monooxygenase (PAM) (*blue*), LAMP-1 (*dark purple*), and VNUT/Slc17a nucleotide carrier (*green*). In addition, the following peripheral proteins are associated with the LDCV membrane: endopeptidases PC1/PC2 (*brown*), GPIII/SGP2/clusterin (*black*), carboxypeptidase H (*lavender*), and Dopamine β-hydroxylase (DβH) (*turquoise*). The LDCV core contains a large number of different proteins and bioactive compounds.

homotypic fusion (Ginsberg et al., 1980). However, during exocytosis platelet granules then fuse with the OCS (Stenberg et al., 1984; Escolar and White, 1991). Granule contents are released into the OCS and diffuse out into the extracellular environment (Escolar and White, 1991). Exocytosis via fusion directly with plasmalemma has also been described (Morgenstern et al., 1987). SNAREs are localized on platelet membranes in a manner to support fusion of granules with OCS, plasma membrane, or other granules (Feng et al., 2002). Despite the morphological differences between exocytosis in platelets and chromaffin cells, similarities in the release mechanism have enabled platelet biologists to use chromaffin cells as a model in studying platelet granule release. For example, both platelets and chromaffin cells require Ca^{2+} influx as a mediator of exocytosis via different mechanisms. Upon platelet activation by agonists, the concentration of cytosolic Ca^{2+} increases activating protein kinase c (PKC), which is important for granule secretion (Knight et al., 1988; Flaumenhaft, 2013). Formation of an action potential in chromaffin cells triggers Ca^{2+} influx via Ca^{2+} channels thereby triggering exocytosis (Knight and Scrutton, 1980; Knight et al., 1982; Knight and Baker, 1985; Penner and Nicher, 1988; Cheek and Barry, 1993; Livett, 1993; Aunis, 1998; Garcia et al., 2006).

THE CYTOSKELETAL AS BOTH BARRIER AND FACILITATOR IN EXOCYTOSIS

The observation that platelet granule secretion occurs concurrently with a dramatic change in the shape of the platelet has prompted investigators to evaluate the role of the cytoskeleton in granule release. Platelets are rich in actin, which is the most abundant platelet protein. The resting platelet contains 40% filamentous actin (F-actin). Upon platelet activation, the percentage of F-actin increases to 80%. Studies using cytochalasins (Cox, 1988), latrunculin A (Flaumenhaft et al., 2005), Ca^{2+}-mediated stimulation of the F-actin severing protein scinderin (Marcu et al., 1996), and PKC-mediated stimulation of MARCKS (Trifaro et al., 2002) demonstrate increased dense-granule release with inhibition of actin polymerization or with cleavage of F-actin. Inhibition of actin polymerization also augments the kinetics and degree of α-granule release (Flaumenhaft et al., 2005). These results suggest that F-actin disassembly might actually be required for normal granule secretion and that activation-mediated granule release is related to actin.

In contrast to the barrier function that the cytoskeleton serves in the resting state, *de novo* actin polymerization during platelet activation contributes to granule release as evidenced by the observation that high concentrations of inhibitors of actin polymerization block α-granule release (Woronowicz et al., 2010). These studies led to speculation that an actin barrier helps prevent inappropriate α-granule exocytosis, but that some *de novo* actin polymerization is required for α-granule release. Woronowicz et al. (2010) demonstrated that the target membrane SNARE (t-SNARE) SNAP-23 associates with the actin cytoskeleton of resting and activated platelets. In a cell-free platelet granule secretory system, inhibition of F-actin formation blocks release of SNARE-dependent α-granule contents, whereas actin polymerization stimulates α-granule release (Woronowicz et al., 2010). Yet the molecular mechanism by which the binding of SNAREs to the platelet cytoskeleton facilitates granule release is unknown. Overall, actin polymerization appears to serve a bipartite role in platelet granule secretion, both as a barrier to prevent inadvertent loss of thrombogenic cargo and as a facilitator of secretion.

Actin has been shown to serve a barrier function in chromaffin cells. The most well-studied pathways for disrupting the cortical F-actin barrier during chromaffin exocytosis include Ca^{2+}-mediated

stimulation of scinderin and PKC-mediated stimulation of MARCKS (Trifaro et al., 2002). Scinderin also potentiates Ca^{2+}-induced granule secretion in a permeabilized platelet system and inhibitory peptides directed at scinderin inhibited granule release in this same assay (Marcu et al., 1996). MARCKS-derived inhibitory peptides blocks phorbol ester-induced platelet granule release, invoking MARCKS phosphorylation and deactivation in facilitating the disruption of F-actin required for granule release (Elzagallaai et al., 2000, 2001).

SNARE FUNCTION IN PLATELET AND CHROMAFFIN GRANULE EXOCYTOSIS

Soluble NSF attachment protein receptors, or SNAREs, assemble into complexes to form a universal membrane fusion apparatus (Jahn and Scheller, 2006). Although all cells use SNAREs for membrane fusion, different cells possess different SNARE isoforms. Neurons and neuroendocrine cells use a set of SNAREs that is distinct from those used in non-neuronal cells. In contrast, platelets and chromaffin cells use many of the same chaperone proteins to regulate SNARE-mediated secretion (**Table 3**).

VAMP-8 (endobrevin) is the primary and most abundant vesicular SNARE (v-SNARE) in platelets (Ren et al., 2007; Graham et al., 2009). It is required for activation-induced release of α-granules, dense granules, and lysosomes (Ren et al., 2007) as evidenced by studies using permeabilized human platelets exposed to anti-VAMP-8 antibodies and by evaluation of secretion from VAMP-$8^{-/-}$ platelets (Ren et al., 2007). Platelet-mediated thrombus formation relies on ADP and other factors released from platelet granules. VAMP-$8^{-/-}$ mice demonstrate decreased thrombus formation upon vascular injury (Graham et al., 2009). Electron microscopy indicates that platelet VAMPs localize primarily to granule membranes (Feng et al., 2002). VAMP-2, -3, -5, and -7 are also present in platelets. VAMPs 2 and 3 mediate granule release in VAMP-8 deficiency (Ren et al., 2007). VAMP-7 contains a profilin-like longin domain, has been shown to function in neurite extension, and associates with F-actin during cell spreading (Alberts et al., 2006). Granules expressing VAMP-7 move to the periphery of the platelet during spreading and may represent a distinct granule type that functions to provide membrane to cover growing cytoskeletal structures following activation (Peters et al., 2012). Future studies will evaluate the respective roles of VAMP-8 and VAMP-7 in mediating granule release during spreading and identify the participating membrane compartments.

Synaptosomal-associated protein 23 (SNAP-23), a t-SNARE, is required for release from all three types of granules in platelets (Chen et al., 2000; Lemons et al., 2000). Nearly 2/3rds of SNAP-23 associates with the platelet plasma membrane, with the remaining SNAP-23 distributed between the granule membrane and membranes of the OCS (Feng et al., 2002). SNAP-23 contains five palmitoylation sites in its membrane-binding domain. Cleavage of palmitate by acyl-protein thioesterase 1 releases SNAP-23 from platelet membranes demonstrating that SNAP-23 associates with membranes via these palmitoylation sites (Sim et al., 2007). In addition, SNAP-23 associates with the actin cytoskeleton in both resting and activated platelets (Woronowicz et al., 2010). Antibodies to SNAP-23 or addition of an inhibitory C-terminal peptide against SNAP-23 both block dense-granule release in human platelets (Chen et al., 2000). In addition, overexpression of dominant negative SNAP-23 inhibits dense-granule release in murine platelets (Gillitzer et al., 2008).

Table 3 | SNAREs and SM proteins in platelets and chromaffin cells.

	Platelets	Chromaffin cells
v-SNARES	Vamp-2	**VAMP-2**
	Vamp-3	VAMP-3
	Vamp-4	VAMP-7 (TI-VAMP)
	Vamp-5	
	Vamp-7 (TI-VAMP)	
	Vamp-8	
t-SNARES	**SNAP-23**	SNAP-23
	SNAP-25	**SNAP-25a**
	SNAP-29	**SNAP-25b**
	Syntaxin-1	**Syntaxin-1A**
	Syntaxin-2	**Syntaxin-1B**
	Syntaxin-4	Syntaxin-2
	Syntaxin-7	Syntaxin-3
	Syntaxin-8	Syntaxin-4
	Syntaxin-11	
	Syntaxin-12	
Munc13 family	**Munc13-4**	Munc13-1
		Munc13-4
Munc18 family	Munc18-1	**Munc18-1**
	Munc18-2	Munc18-2
	Munc18-3	Munc18-3

Essential components of the secretory machinery are highlighted.
Criteria: platelets: Vamp-8, murine knockout; SNAP-23, inhibitory antibodies, inhibitory peptides, overexpression of dominant negative construct; syntaxin-11, FLH4; Munc13-4, murine knockout, FLH3; Munc18-2, FLH5.
Chromaffin: VAMP-2, neurotoxin cleavage; SNAP-25, deletion of C terminus; Syntaxin 1, botulinum neurotoxin C1 and inhibitory antibodies; Munc18-1, murine knockout.

Our understanding of the role of syntaxins, another family of t-SNAREs, in platelet granule release has recently evolved. Platelets express syntaxin-2, -4, -7, -8, -11, and -12. Whiteheart's group identified a patient with Familial Hemophagocytic Lymphohistiocytosis type four (FHL-4) who was deficient in syntaxin-11 and exhibited a significant granule secretion defect. An inhibitory antibody that this group had previously used to demonstrate a role for syntaxin-2 in granule release was found to cross-react with syntaxin-11, further suggesting a role for syntaxin-11 in platelet exocytosis (Ye et al., 2012). They also demonstrated that syntaxin-$2^{-/-}$ mice, syntaxin-$4^{-/-}$ mice, and double knockout mice all demonstrated normal granule release. On the basis of these results, syntaxin-11 appears to be the primary syntaxin involved in platelet granule release.

In chromaffin cells, VAMP-2 is the primary v-SNARE and is required for efficient, rapid release of granule constituents in response to agonists (**Table 3**). Proteolytic cleavage of VAMP-2 by botulinum neurotoxins A through G or tetanus neurotoxin results in decreased DCV secretion in chromaffin cells (Knight

et al., 1985; Schiavo et al., 1992; Xu et al., 1998). VAMP-3 is less efficient than and plays a subordinate role to VAMP-2, only functioning in its absence (Borisovska et al., 2005). VAMP-7 serves a central role in neurite outgrowth in chromaffin-like cells (Coco et al., 1999; Martinez-Arca et al., 2000, 2001), analogous to its putative role in providing membrane for platelet spreading (Peters et al., 2012). Studies in PC12 cells indicate that the NH2-terminal domain of VAMP-7 negatively regulates neurite outgrowth since neurite outgrowth is blocked by overexpression of this domain and enhanced by its deletion (Martinez-Arca et al., 2000, 2001). SNAP-25a has established roles in both docking and priming of DCVs and participates in agonist-dependent fusion of secretory vesicles in complex with both VAMP-2 and syntaxin-1A. Deletion of the C-terminal synaptotagmin-interacting residues of SNAP-25 in PC12 cells results in decreased DCV secretion (Zhang et al., 2002). Adrenal chromaffin cells express syntaxins-1A, -1B, -2, -3, and -4. Viral infection with botulinum neurotoxin C1 cleaves syntaxin-1A, 1B, 2, and 3 resulting in reduced DCV docking at the plasma membrane (de Wit et al., 2006) and an inhibitory antibody to syntaxin-1 decreases catecholamine release in bovine chromaffin cells (Gutierrez et al., 1995).

SNARE CHAPERONE FUNCTION IN PLATELET AND CHROMAFFIN GRANULE EXOCYTOSIS

Although not members of the exocytic core complex, another important group of proteins involved in degranulation in secretory cells are the Sec1/Munc18-like (SM) proteins which function as SNARE chaperones (Carr and Rizo, 2010). Platelets and chromaffin cells possess a similar repertoire of SM proteins, including members of the Munc13 and Munc18 families. These proteins are SNARE regulators that have no apparent membrane-binding domain, but bind syntaxin upon phosphorylation by PKC (Houng et al., 2003; Schraw et al., 2003) and interact with the regulatory N-terminal sequence of syntaxins (Ashery et al., 2000; Rosenmund et al., 2002). Munc13 family members include Muncs13-1, -2, -3, and 4. These proteins have two C2 (Ca^{2+}-binding) and one C1 (DAG/phorbol ester-binding) domains (**Figure 3**). They interact with SNARE proteins via two Munc13 (mammalian) homology domains, MHDs 1 and 2 (Guan et al., 2008), which are involved in dissociating Munc18 protein/syntaxin interactions (Sassa et al., 1999), thereby promoting *trans* SNARE complex assembly.

Munc13-4 is the only Munc13 family member found in platelets. It lacks the N-terminal C1 domain present in Munc13-1, -2, and -3 and the MHD2 domain present in the other Munc13 family members, but has a central MHD1 domain and binds directly to syntaxins in platelets via interaction with the syntaxin H3 domain (Boswell et al., 2012). It is ubiquitously expressed, but enriched in cells of the hematopoietic lineage (Song et al., 1998; Feldmann et al., 2003). In platelets, the Munc13-4 interaction with activated Rab27a/b is important for SNARE binding (via MHD1 interaction), granule formation and plasma membrane interaction (**Figure 3**) (Song et al., 1998; Shirakawa et al., 2004; Ishii et al., 2005; Boswell et al., 2012). Boswell et al. (2012) determined that the C2A domain of Munc13-4 is required for Ca^{2+}-dependent SNARE interaction, whereas the C2B domain mediates Ca^{2+}-dependent membrane association. Mutation of Munc13-4 results in another form of familial hemophagocytic lymphohistiocytosis (FHL3) (Feldmann et al., 2003) and Munc13-4 deletion from murine platelets results in complete ablation of dense-granule release and impaired release from α-granules *in vitro* indicating its importance in Ca^{2+} regulation of SNARE interactions with the plasma membrane (Ren et al., 2010).

Munc13-4 is a rate-limiting protein for granule exocytosis in both platelets and chromaffin cells. As with platelet granule release, Munc13-4 triggers rapid and efficient release of catecholamines from chromaffin-like PC12 cells (Boswell et al., 2012). Munc13-4 promotes trans-exocytic core complex formation in a Ca^{2+}-dependent manner in both chromaffin cells and platelets. In addition to Munc13-4, Munc13-1 serves a role in DCV secretion in chromaffin cells. Overexpression of Munc13-1 results in increased DCV secretion (Ashery et al., 2000; Stevens et al., 2005) and its interaction with syntaxin-1 is important for DCV priming (Stevens et al., 2005).

Platelets express three Munc18 isoforms: Munc18-1, 18-2 and 18-3. All three isoforms are associated with granule and OCS membranes in resting platelets (Schraw et al., 2003). Al Hawas et al. (2012) recently demonstrated that defects in the Munc18-2 gene result in familial hemophagocytic lymphohistiocytosis type

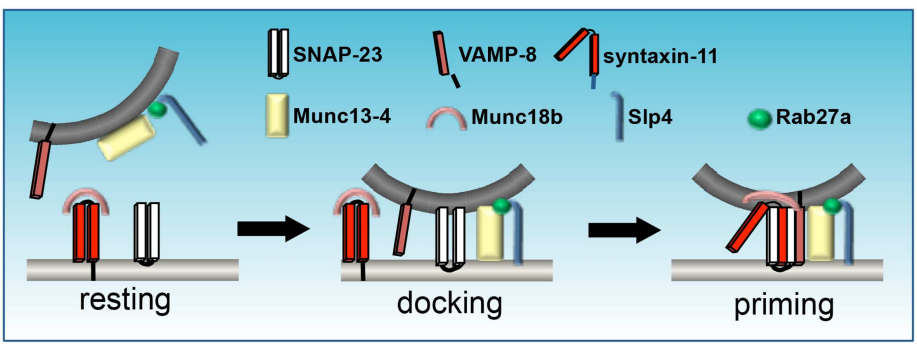

FIGURE 3 | Assemblage of SNAREs and SM proteins during platelet granule exocytosis. Munc18b sequesters syntaxin in an inactive state. Munc13-4 docks opposing membranes via interactions with Rab27a, which also binds Slp1. Activation promotes a conformational change in Munc18b that enables the coiled-coil domain of syntaxin to form a four-helical bundle with SNAP-23 and VAMP. Mutations in Munc13-4, as in familial hemophagocytic lymphohistiocytosis (FHL)-3, syntaxin-11 (FHL-4), Munc18b (FHL-5), or Rab27a (Griscelli syndrome) result in defective secretion (figure adapted from Flaumenhaft, 2013).

5 (FHL5). These patients demonstrate decreased α- and dense-granule secretion and levels of both Munc18-2 and syntaxin-11 were diminished, indicating that Munc18-2 plays a key role in platelet exocytosis and, potentially, a regulatory role toward syntaxin-11.

In chromaffin cells, Munc18-1 participates in granule docking/priming and SNARE engagement via its interaction with syntaxin 1 (Hata et al., 1993; Pevsner et al., 1994). Munc18-1 knock out in embryonic cells results in decreased DCV docking at the plasma membrane (Voets et al., 2001; Gulyas-Kovacs et al., 2007). In addition, syntaxin 1 expression is decreased by 50% in Munc18-1 deficient neurons and chromaffin cells (Voets et al., 2001; Gulyas-Kovacs et al., 2007). Munc18-1 interaction with the "closed" conformation of syntaxin 1 appears to be important for docking of the secretory vesicle at the plasma membrane (Dulubova et al., 1999; Yang et al., 2000; Schutz et al., 2005; Gulyas-Kovacs et al., 2007). However, Munc18-1 interactions with the N-terminal peptide of syntaxin-1 (in the "open" conformation) is required for membrane fusion to occur (Khvotchev et al., 2007; Gerber et al., 2008; Rathore et al., 2010), indicating that Munc18-1 is important in both early and late stages of exocytosis. Munc18-2 also shows affinity for syntaxins-1, -2, and -3 in chromaffin cells. While Munc18-2 rescued the reduced docking phenotype in Munc18-1$^{-/-}$ animals, they continued to exhibit impaired vesicle priming (Gulyas-Kovacs et al., 2007). Munc18-3 is ubiquitously expressed and has been implicated in secretion in chromaffin cells. However, Munc18-3 only partially rescued the Munc18-1$^{-/-}$ secretion defect in chromaffin cells and deletion of Munc18-3 from chromaffin cells did not cause defects in granule secretion (Gulyas-Kovacs et al., 2007).

THE PLATELET FUSION PORE

Although there are many methods to evaluate platelet granule release, platelet secretion assays are largely restricted to bulk assays of cargo release (e.g., ADP, serotonin, platelet factor 4) or granule membrane receptor surface expression (e.g., P-selectin, CD63). These assays are inadequate for evaluation of the release of single granules and unable to detect membrane fusion events that occur in the millisecond time frame. Standard electrophysiology using patch-clamp techniques are difficult to apply to the platelet because of their small size and atypical membrane system. More recently, however, platelet investigators are applying some of the same approaches used to evaluate fusion pore dynamics in chromaffin cells. In particular, investigators are using single-cell amperometry to evaluate the release kinetics of single granules from platelets. Carbon-fiber microelectrode amperometry is being used to detect serotonin release from platelets stimulated with thrombin (Ge et al., 2008, 2009, 2010). Tracings indicate previously unrecognized fusion events such as "kiss and run" fusion and foot process formation (Wightman and Haynes, 2004) (**Figure 4**). This approach has enabled an appreciation of nuances of membrane fusion in platelets that have previously gone unrecognized and, more importantly, have enabled investigators to begin to evaluate the molecular mechanisms of pore formation in platelets. Amperometry has recently been used to evaluate the role of dynamin family proteins in platelet and chromaffin cell granule release.

Dynamins are a family of large GTPases that act as mechanoenzymes, demonstrating both oligomerization-dependent GTPase and membrane modeling activities (Piersma et al., 2009). Although originally described as mediators of membrane scission during vesicle endocytosis (Graham et al., 2004; Wegrzyn et al., 2010), dynamin GTPases are now recognized to function in exocytosis (Graham et al., 2002; Tsuboi et al., 2004; Fulop et al., 2008; Anantharam et al., 2010, 2011; Gonzalez-Jamett et al., 2010). In particular, dynamins act immediately upon membrane fusion to regulate the release of granule content. Dynamin and dynamin-related proteins are found in platelets. Dynamin 3 is upregulated during megakaryopoiesis (Reems et al., 2008; Gieger et al., 2011; Wang et al., 2011). Dynamin 2 and dynamin-related protein 1 (Drp1) are present in platelets, but dynamin 1 is not.

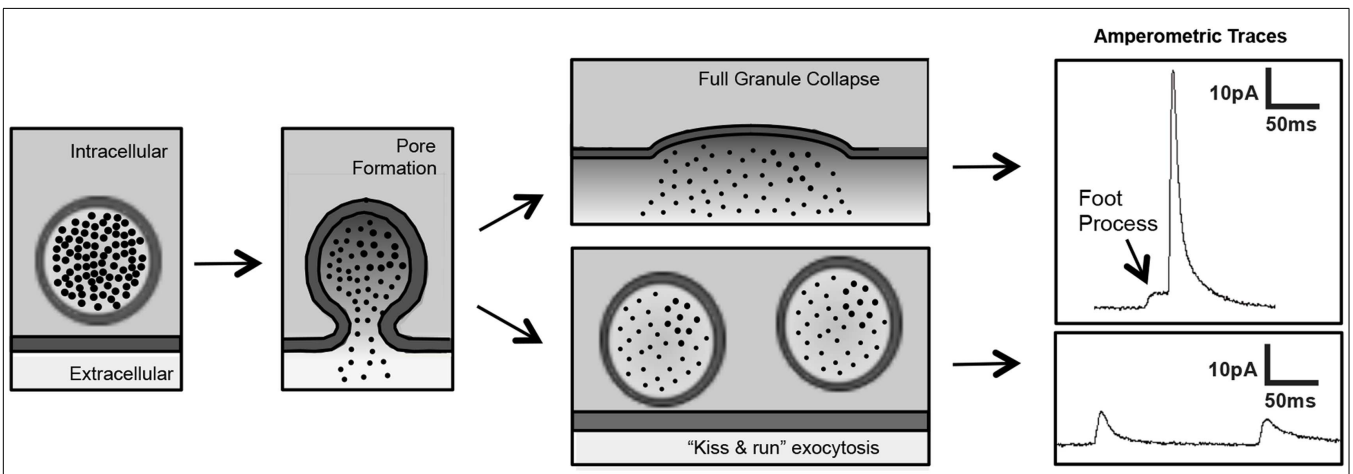

FIGURE 4 | Single-cell amperometry to measure dense-granule release from platelets. Amperometry demonstrates pore formation progressing through a foot process (*left panels*) to full granule collapse (*upper panels*) and pore formation reversing in a "kiss and run" exocytotic event (*lower panels*) (figure adapted from Koseoglu et al., 2013).

Drp1 is phosphorylated upon platelet activation (Koseoglu et al., 2013). Inhibition of platelets using dynasore or MiTMAB, which inhibit the activity of dynamin family proteins, block agonist-induced platelet granule secretion (Koseoglu et al., 2013). The Drp1 inhibitor, mdivi-1, also blocks platelet granule exocytosis. Studies using single-cell amperometry demonstrate that mdivi-1 exposure results in fusion pore instability as evidenced by decreased foot process formation and inefficient pore expansion as evidenced by an increased $T_{1/2}$ (Koseoglu et al., 2013). These observations implicate dynamin and dynamin-related proteins in platelet fusion pore dynamics. However, the mechanism by which Drp1, which is typically associated with mitochondrial fission, impacts platelet granule release remains to be determined.

Dynamin-mediated pore expansion in chromaffin has been evaluated using total internal reflection fluorescence microscopy and amperometry. In chromaffin cells overexpressing a dynamin I mutant with low GTPase activity, deformations in the membrane associated with fusion are long-lived, indicating defective pore expansion (Anantharam et al., 2011). Chromaffin cells overexpressing a dynamin I mutant with enhanced GTPase activity demonstrate increased pore expansion. These observations have led to a model in which dynamin restricts fusion pore expansion until GTPase activity is stimulated. The higher the GTPase activity, the faster the expansion of the fusion pore (Gerber et al., 2008). Dynamins appear to associate with actin, SNAREs, and synaptotagmin family proteins to participate in fusion pore expansion (Chan et al., 2010; Gu et al., 2010; Anantharam et al., 2012). However, the importance of these associations is poorly understood.

CONCLUSION

Some characteristics of regulated secretion shared between platelets and chromaffin cells are common to all secretory systems. However, these secretory systems also share some unusual features that, if not unique to these cells, are not universally observed among secretory systems. These special commonalities may provide avenues for researchers investigating these cells types to further define these secretory systems. For example, the unusual density of LDCVs and platelet dense granules and their ability to concentrate nucleotides, bioactive amines, and polyphosphates raises the possibility that may use similar transporters. Some similarities in transporters such as VMAT2 have already been described. Further probing could reveal further overlap (e.g., Scl17A transporters in platelet dense granules, multidrug resistance transporters in chromaffin cells, or yet undiscovered transporters that are common to both cells). The ability of chromaffin-like PC12 cells to use VAMP-7 for neurite outgrowth and platelets to use VAMP-7 during spreading speaks to potential underlying similarities between the molecular mechanisms of membrane utilization during shape change. The role of dynamin family proteins in exocytosis is an emerging area of interest in secretion biology and further studies of these two cell types may reveal how they use these mechanoenzymes to regulate fusion pore formation during exocytosis. Historically, the study of the chromaffin cell has advanced more quickly than that of the platelet and has helped direct how platelet biologists have approached the study of granule exocytosis. As the study of platelet exocytosis progresses, understanding this secretory system may help chromaffin cell biologists better understand elements of granule formation and exocytosis in neuroendocrine cells.

REFERENCES

Aikawa, M., Schoenbechler, M. J., Barbaro, J. F., and Sadun, E. H. (1971). Interaction of rabbit platelets and leukocytes in the release of histamine. Electron microscopic observations. *Am. J. Pathol.* 63, 85–98.

Al Hawas, R., Ren, Q., Ye, S., Karim, Z. A., Filipovich, A. H., and Whiteheart, S. W. (2012). Munc18b/STXBP2 is required for platelet secretion. *Blood* 120, 2493–2500. doi:10.1182/blood-2012-05-430629

Alberts, P., Rudge, R., Irinopoulou, T., Danglot, L., Gauthier-Rouvière, C., and Galli, T. (2006). Cdc42 and actin control polarized expression of TI-VAMP vesicles to neuronal growth cones and their fusion with the plasma membrane. *Mol. Biol. Cell* 17, 1194–1203. doi:10.1091/mbc.E05-07-0643

Anantharam, A., Axelrod, D., and Holz, R. W. (2012). Polarized TIRFM reveals changes in plasma membrane topology before and during granule fusion. *Cell. Mol. Neurobiol.* 30, 1343–1349. doi:10.1007/s10571-010-9590-0

Anantharam, A., Bittner, M. A., Aikman, R. L., Stuenkel, E. L., Schmid, S. L., Axelrod, D., et al. (2011). A new role for the dynamin GTPase in the regulation of fusion pore expansion. *Mol. Biol. Cell* 22, 1907–1918. doi:10.1091/mbc.E11-02-0101

Anantharam, A., Onoa, B., Edwards, R. H., Holz, R. W., and Axelrod, D. (2010). Localized topological changes of the plasma membrane upon exocytosis visualized by polarized TIRFM. *J. Cell Biol.* 188, 415–428. doi:10.1083/jcb.200908010

Ashery, U., Varoqueaux, F., Voets, T., Betz, A., Thakur, P., Koch, H., et al. (2000). Munc13-1 acts as a priming factor for large dense-core vesicles in bovine chromaffin cells. *EMBO J.* 19, 3586–3596. doi:10.1093/emboj/19.14.3586

Aunis, D. (1998). Exocytosis in chromaffin cells of the adrenal medulla. *Int. Rev. Cytol.* 181, 213–320. doi:10.1016/S0074-7696(08)60419-2

Blair, P., and Flaumenhaft, R. (2009). Platelet alpha-granules: basic biology and clinical correlates. *Blood Rev.* 23, 177–189. doi:10.1016/j.blre.2009.04.001

Borisovska, M., Zhao, Y., Tsytsyura, Y., Glyvuk, N., Takamori, S., Matti, U., et al. (2005). v-SNAREs control exocytosis of vesicles from priming to fusion. *EMBO J.* 24, 2114–2126. doi:10.1038/sj.emboj.7600696

Boswell, K. L., James, D. J., Esquibel, J. M., Bruinsma, S., Shirakawa, R., Horiuchi, H., et al. (2012). Munc13-4 reconstitutes calcium-dependent SNARE-mediated membrane fusion. *J. Cell Biol.* 197, 301–312. doi:10.1083/jcb.201109132

Buchanan, G. R., and Handin, R. I. (1976). Platelet function in the Chediak-Higashi syndrome. *Blood* 47, 941–948.

Carr, C. M., and Rizo, J. (2010). At the junction of SNARE and SM protein function. *Curr. Opin. Cell Biol.* 22, 488–495. doi:10.1016/j.ceb.2010.04.006

Chan, S. A., Doreian, B., and Smith, C. (2010). Dynamin and myosin regulate differential exocytosis from mouse adrenal chromaffin cells. *Cell. Mol. Neurobiol.* 30, 1351–1357. doi:10.1007/s10571-010-9591-z

Cheek, T. R., and Barry, V. A. (1993). Stimulus-secretion coupling in excitable cells: a central role for calcium. *J. Exp. Biol.* 184, 183–196.

Chen, D., Lemons, P. P., Schraw, T., and Whiteheart, S. W. (2000). Molecular mechanisms of platelet exocytosis: role of SNAP-23 and syntaxin 2 and 4 in lysosome release. *Blood* 96, 1782–1788.

Coco, S., Raposo, G., Martinez, S., Fontaine, J. J., Takamori, S., Zahraoui, A., et al. (1999). Subcellular localization of tetanus neurotoxin-insensitive vesicle-associated membrane protein (VAMP)/VAMP7 in neuronal cells: evidence for a novel membrane compartment. *J. Neurosci.* 19, 9803–9812.

Coppinger, J. A., Cagney, G., Toomey, S., Kislinger, T., Belton, O., McRedmond, J. P., et al. (2004). Characterization of the proteins released from activated platelets leads to localization of novel platelet proteins in human atherosclerotic lesions. *Blood* 103, 2096–2104. doi:10.1182/blood-2003-08-2804

Costa, J. L., Fauci, A. S., and Wolff, S. M. (1976). A platelet abnormality in the Chediak-Higashi syndrome of man. *Blood* 48, 517–520.

Cox, A. C. (1988). Cytochalasin E enhances the protein kinase C-dependent process of secretion. *Biochem. Biophys. Res. Commun.* 150, 745–751. doi:10.1016/0006-291X(88)90454-8

de Wit, H., Cornelisse, L. N., Toonen, R. F., and Verhage, M. (2006). Docking of secretory vesicles is syntaxin dependent. *PLoS ONE* 1:e126. doi:10.1371/journal.pone.0000126

Dean, G. E., Fishkes, H., Nelson, P. J., and Rudnick, G. (1984). The hydrogen ion-pumping adenosine triphosphatase of platelet dense granule membrane. Differences from F1F0- and phosphoenzyme-type ATPases. *J. Biol. Chem.* 259, 9569–9574.

Dulubova, I., Sugita, S., Hill, S., Hosaka, M., Fernandez, I., Sudhof, T. C., et al. (1999). A conformational switch in syntaxin during exocytosis: role of munc18. *EMBO J.* 18, 4372–4382. doi:10.1093/emboj/18.16.4372

Elzagallaai, A., Rose, S. D., Brandan, N. C., and Trifaro, J. M. (2001). Myristoylated alanine-rich C kinase substrate phosphorylation is involved in thrombin-induced serotonin release from platelets. *Br. J. Haematol.* 112, 593–602. doi:10.1046/j.1365-2141.2001.02642.x

Elzagallaai, A., Rose, S. D., and Trifaro, J. M. (2000). Platelet secretion induced by phorbol esters stimulation is mediated through phosphorylation of MARCKS: a MARCKS-derived peptide blocks MARCKS phosphorylation and serotonin release without affecting pleckstrin phosphorylation. *Blood* 95, 894–902.

Escolar, G., and White, J. G. (1991). The platelet open canalicular system: a final common pathway. *Blood Cells* 17, 467–485. discussion 486-495,

Feldmann, J., Callebaut, I., Raposo, G., Certain, S., Bacq, D., Dumont, C., et al. (2003). Munc13-4 is essential for cytolytic granules fusion and is mutated in a form of familial hemophagocytic lymphohistiocytosis (FHL3). *Cell* 115, 461–473. doi:10.1016/S0092-8674(03)00855-9

Felmy, F. (2007). Modulation of cargo release from dense core granules by size and actin network. *Traffic* 8, 983–997. doi:10.1111/j.1600-0854.2007.00583.x

Feng, D., Crane, K., Rozenvayn, N., Dvorak, A. M., and Flaumenhaft, R. (2002). Subcellular distribution of 3 functional platelet SNARE proteins: human cellubrevin, SNAP-23, and syntaxin 2. *Blood* 99, 4006–4014. doi:10.1182/blood.V99.11.4006

Flaumenhaft, R. (2013). "Platelet secretion," in *Platelets*, 3rd Edn, ed. A. D. Michelson (London: Academic Press), 343–366.

Flaumenhaft, R., Dilks, J. R., Rozenvayn, N., Monahan-Earley, R. A., Feng, D., and Dvorak, A. M. (2005). The actin cytoskeleton differentially regulates platelet alpha-granule and dense-granule secretion. *Blood* 105, 3879–3887. doi:10.1182/blood-2004-04-1392

Fukami, M. H., Holmsen, H., and Ugurbil, K. (1984). Histamine uptake in pig platelets and isolated dense granules. *Biochem. Pharmacol.* 33, 3869–3874. doi:10.1016/0006-2952(84)90053-4

Fulop, T., Doreian, B., and Smith, C. (2008). Dynamin I plays dual roles in the activity-dependent shift in exocytic mode in mouse adrenal chromaffin cells. *Arch. Biochem. Biophys.* 477, 146–154. doi:10.1016/j.abb.2008.04.039

Garcia, A. G., Garcia-de-Diego, A. M., Gandia, L., Borges, R., and Garcia-Sancho, J. (2006). Calcium signaling and exocytosis in adrenal chromaffin cells. *Physiol. Rev.* 86, 1093–1131. doi:10.1152/physrev.00039.2005

Ge, S., White, J. G., and Haynes, C. L. (2009). Quantal release of serotonin from platelets. *Anal. Chem.* 81, 2935–2943. doi:10.1021/ac8024202

Ge, S., White, J. G., and Haynes, C. L. (2010). Critical role of membrane cholesterol in exocytosis revealed by single platelet study. *ACS Chem. Biol.* 5, 819–828. doi:10.1021/cb100130b

Ge, S., Wittenberg, N. J., and Haynes, C. L. (2008). Quantitative and real-time detection of secretion of chemical messengers from individual platelets. *Biochemistry* 47, 7020–7024. doi:10.1021/bi800792m

Gerber, S. H., Rah, J. C., Min, S. W., Liu, X., de Wit, H., Dulubova, I., et al. (2008). Conformational switch of syntaxin-1 controls synaptic vesicle fusion. *Science* 321, 1507–1510. doi:10.1126/science.1163174

Gieger, C., Radhakrishnan, A., Cvejic, A., Tang, W., Porcu, E., Pistis, G., et al. (2011). New gene functions in megakaryopoiesis and platelet formation. *Nature* 480, 201–208. doi:10.1038/nature10659

Gillitzer, A., Peluso, M., Bultmann, A., Munch, G., Gawaz, M., and Ungerer, M. (2008). Effect of dominant negative SNAP-23 expression on platelet function. *J. Thromb. Haemost.* 6, 1757–1763. doi:10.1111/j.1538-7836.2008.03108.x

Ginsberg, M. H., Taylor, L., and Painter, R. G. (1980). The mechanism of thrombin-induced platelet factor 4 secretion. *Blood* 55, 661–668.

Gonzalez-Jamett, A. M., Baez-Matus, X., Hevia, M. A., Guerra, M. J., Olivares, M. J., Martinez, A. D., et al. (2010). The association of dynamin with synaptophysin regulates quantal size and duration of exocytotic events in chromaffin cells. *J. Neurosci.* 30, 10683–10691. doi:10.1523/JNEUROSCI.5210-09.2010

Graham, G. J., Ren, Q., Dilks, J. R., Blair, P., Whiteheart, S. W., and Flaumenhaft, R. (2009). Endobrevin/VAMP-8-dependent dense granule release mediates thrombus formation in vivo. *Blood* 114, 1083–1090. doi:10.1182/blood-2009-03-210211

Graham, G. J., Stevens, J. M., Page, N. M., Grant, A. D., Brain, S. D., Lowry, P. J., et al. (2004). Tachykinins regulate the function of platelets. *Blood* 104, 1058–1065. doi:10.1182/blood-2003-11-3979

Graham, M. E., O'Callaghan, D. W., McMahon, H. T., and Burgoyne, R. D. (2002). Dynamin-dependent and dynamin-independent processes contribute to the regulation of single vesicle release kinetics and quantal size. *Proc. Natl. Acad. Sci. U.S.A.* 99, 7124–7129. doi:10.1073/pnas.102645099

Gu, C., Yaddanapudi, S., Weins, A., Osborn, T., Reiser, J., Pollak, M., et al. (2010). Direct dynamin-actin interactions regulate the actin cytoskeleton. *EMBO J.* 29, 3593–3606. doi:10.1038/emboj.2010.249

Guan, R., Dai, H., and Rizo, J. (2008). Binding of the Munc13-1 MUN domain to membrane-anchored SNARE complexes. *Biochemistry* 47, 1474–1481. doi:10.1021/bi702345m

Gulyas-Kovacs, A., de Wit, H., Milosevic, I., Kochubey, O., Toonen, R., Klingauf, J., et al. (2007). Munc18-1: sequential interactions with the fusion machinery stimulate vesicle docking and priming. *J. Neurosci.* 27, 8676–8686. doi:10.1523/JNEUROSCI.0658-07.2007

Gutierrez, L. M., Quintanar, J. L., Viniegra, S., Salinas, E., Moya, F., and Reig, J. A. (1995). Anti-syntaxin antibodies inhibit calcium-dependent catecholamine secretion from permeabilized chromaffin cells. *Biochem. Biophys. Res. Commun.* 206, 1–7. doi:10.1006/bbrc.1995.1001

Hata, Y., Slaughter, C. A., and Sudhof, T. C. (1993). Synaptic vesicle fusion complex contains unc-18 homologue bound to syntaxin. *Nature* 366, 347–351. doi:10.1038/366347a0

Hermansky, F., and Pudlak, P. (1959). Albinism associated with hemorrhagic diathesis and unusual pigmented reticular cells in the bone marrow: report of two cases with histochemical studies. *Blood* 14, 162–169.

Holmsen, H., and Weiss, H. J. (1979). Secretable storage pools in platelets. *Annu. Rev. Med.* 30, 119–134. doi:10.1146/annurev.me.30.020179.001003

Houng, A., Polgar, J., and Reed, G. L. (2003). Munc18-syntaxin complexes and exocytosis in human platelets. *J. Biol. Chem.* 278, 19627–19633. doi:10.1074/jbc.M212465200

Ishii, E., Ueda, I., Shirakawa, R., Yamamoto, K., Horiuchi, H., Ohga, S., et al. (2005). Genetic subtypes of familial hemophagocytic lymphohistiocytosis: correlations with clinical features and cytotoxic T lymphocyte/natural killer cell functions. *Blood* 105, 3442–3448. doi:10.1182/blood-2004-08-3296

Italiano, J. E. Jr., Richardson, J. L., Patel-Hett, S., Battinelli, E., Zaslavsky, A., Short, S., et al. (2008). Angiogenesis is regulated by a novel mechanism: pro- and antiangiogenic proteins are organized into separate platelet {alpha} granules and differentially released. *Blood* 111, 1227–1233. doi:10.1182/blood-2007-09-113837

Jahn, R., and Scheller, R. H. (2006). SNAREs – engines for membrane fusion. *Nat. Rev. Mol. Cell Biol.* 7, 631–643. doi:10.1038/nrm2002

Jedlitschky, G., Tirschmann, K., Lubenow, L. E., Nieuwenhuis, H. K., Akkerman, J. W., Greinacher, A., et al. (2004). The nucleotide transporter MRP4 (ABCC4) is highly expressed in human platelets and present in dense granules, indicating a role in mediator storage. *Blood* 104, 3603–3610. doi:10.1182/blood-2003-12-4330

Khvotchev, M., Dulubova, I., Sun, J., Dai, H., Rizo, J., and Sudhof, T. C. (2007). Dual modes of Munc18-1/SNARE interactions are coupled by functionally critical binding to syntaxin-1 N terminus. *J. Neurosci.* 27, 12147–12155. doi:10.1523/JNEUROSCI.3655-07.2007

Knight, D. E., and Baker, P. F. (1985). The chromaffin granule proton pump and calcium-dependent exocytosis in bovine adrenal medullary cells. *J. Membr. Biol.* 83, 147–156. doi:10.1007/BF01868746

Knight, D. E., Hallam, T. J., and Scrutton, M. C. (1982). Agonist selectivity and second messenger concentration in Ca2+-mediated

secretion. *Nature* 296, 256–257. doi:10.1038/296256a0

Knight, D. E., and Scrutton, M. C. (1980). Direct evidence for a role for Ca2+ in amine storage granule secretion by human platelets. *Thromb. Res.* 20, 437–446. doi:10.1016/0049-3848(80)90282-0

Knight, D. E., Sugden, D., and Baker, P. F. (1988). Evidence implicating protein kinase C in exocytosis from electropermeabilized bovine chromaffin cells. *J. Membr. Biol.* 104, 21–34. doi:10.1007/BF01871899

Knight, D. E., Tonge, D. A., and Baker, P. F. (1985). Inhibition of exocytosis in bovine adrenal medullary cells by botulinum toxin type D. *Nature* 317, 719–721. doi:10.1038/317719a0

Koseoglu, S., Dilks, J. R., Peters, C. G., Fitch, J. L., Fadel, N. A., Jasuja, R., et al. (2013). Dynamin-related protein-1 controls fusion pore dynamics during platelet granule exocytosis. *Arterioscler. Thromb. Vasc. Biol.* 33, 481–488. doi:10.1161/ATVBAHA.112.255737

Koval, L. M., Yavorskaya, E. N., and Lukyanetz, E. A. (2001). Electron microscopic evidence for multiple types of secretory vesicles in bovine chromaffin cells. *Gen. Comp. Endocrinol.* 121, 261–277. doi:10.1006/gcen.2000.7592

Lemons, P. P., Chen, D., and Whiteheart, S. W. (2000). Molecular mechanisms of platelet exocytosis: requirements for alpha-granule release. *Biochem. Biophys. Res. Commun.* 267, 875–880. doi:10.1006/bbrc.1999.2039

Livett, B. G. (1993). Chromaffin cells: roles for vesicle proteins and Ca2+ in hormone secretion and exocytosis. *Trends Pharmacol. Sci.* 14, 345–348. doi:10.1016/0165-6147(93)90090-7

Marcu, M. G., Zhang, L., Nau-Staudt, K., and Trifaro, J. M. (1996). Recombinant scinderin, an F-actin severing protein, increases calcium-induced release of serotonin from permeabilized platelets, an effect blocked by two scinderin-derived actin-binding peptides and phosphatidylinositol 4,5-bisphosphate. *Blood* 87, 20–24.

Martinez-Arca, S., Alberts, P., Zahraoui, A., Louvard, D., and Galli, T. (2000). Role of tetanus neurotoxin insensitive vesicle-associated membrane protein (TI-VAMP) in vesicular transport mediating neurite outgrowth. *J. Cell Biol.* 149, 889–900. doi:10.1083/jcb.149.4.889

Martinez-Arca, S., Coco, S., Mainguy, G., Schenk, U., Alberts, P., Bouille, P., et al. (2001). A common exocytotic mechanism mediates axonal and dendritic outgrowth. *J. Neurosci.* 21, 3830–3838.

Matsuoka, H., Harada, K., Nakamura, J., Fukuda, M., and Inoue, M. (2011). Differential distribution of synaptotagmin-1, -4, -7, and -9 in rat adrenal chromaffin cells. *Cell Tissue Res.* 344, 41–50. doi:10.1007/s00441-011-1131-8

Morgenstern, E., Neumann, K., and Patscheke, H. (1987). The exocytosis of human blood platelets. A fast freezing and freeze-substitution analysis. *Eur. J. Cell Biol.* 43, 273–282.

Penner, R., and Nicher, E. (1988). The role of calcium in stimulus-secretion coupling in excitable and non-excitable cells. *J. Exp. Biol.* 139, 329–345.

Perrais, D., Kleppe, I., Taraska, J., and Almers, W. (2004). Recapture after exocytosis causes differential retention of protein in granules of bovine chromaffin cells. *J. Physiol.* 560, 413–428. doi:10.1113/jphysiol.2004.064410

Peters, C. G., Michelson, A. D., and Flaumenhaft, R. (2012). Granule exocytosis is required for platelet spreading: differential sorting of alpha-granules expressing VAMP-7. *Blood* 120, 199–206. doi:10.1182/blood-2011-10-389247

Pevsner, J., Hsu, S. C., and Scheller, R. H. (1994). n-Sec1: a neural-specific syntaxin-binding protein. *Proc. Natl. Acad. Sci. U.S.A.* 91, 1445–1449. doi:10.1073/pnas.91.4.1445

Piersma, S. R., Broxterman, H. J., Kapci, M., de Haas, R. R., Hoekman, K., Verheul, H. M., et al. (2009). Proteomics of the TRAP-induced platelet releasate. *J. Proteomics* 72, 91–109. doi:10.1016/j.jprot.2008.10.009

Rathore, S. S., Bend, E. G., Yu, H., Hammarlund, M., Jorgensen, E. M., and Shen, J. (2010). Syntaxin N-terminal peptide motif is an initiation factor for the assembly of the SNARE-Sec1/Munc18 membrane fusion complex. *Proc. Natl. Acad. Sci. U.S.A.* 107, 22399–22406. doi:10.1073/pnas.1012997108

Reems, J. A., Wang, W., Tsubata, K., Abdurrahman, N., Sundell, B., Tijssen, M. R., et al. (2008). Dynamin 3 participates in the growth and development of megakaryocytes. *Exp. Hematol.* 36, 1714–1727. doi:10.1016/j.exphem.2008.08.010

Ren, Q., Barber, H. K., Crawford, G. L., Karim, Z. A., Zhao, C., Choi, W., et al. (2007). Endobrevin/VAMP-8 is the primary v-SNARE for the platelet release reaction. *Mol. Biol. Cell* 18, 24–33. doi:10.1091/mbc.E06-09-0785

Ren, Q., Wimmer, C., Chicka, M. C., Ye, S., Ren, Y., Hughson, F. M., et al. (2010). Munc13-4 is a limiting factor in the pathway required for platelet granule release and hemostasis. *Blood* 116, 869–877. doi:10.1182/blood-2010-02-270934

Rosenmund, C., Sigler, A., Augustin, I., Reim, K., Brose, N., and Rhee, J. S. (2002). Differential control of vesicle priming and short-term plasticity by Munc13 isoforms. *Neuron* 33, 411–424. doi:10.1016/S0896-6273(02)00568-8

Rothman, J. E., and Orci, L. (1992). Molecular dissection of the secretory pathway. *Nature* 355, 409–415. doi:10.1038/355409a0

Ruiz, F. A., Lea, C. R., Oldfield, E., and Docampo, R. (2004). Human platelet dense granules contain polyphosphate and are similar to acidocalcisomes of bacteria and unicellular eukaryotes. *J. Biol. Chem.* 279, 44250–44257. doi:10.1074/jbc.M406261200

Sassa, T., Harada, S., Ogawa, H., Rand, J. B., Maruyama, I. N., and Hosono, R. (1999). Regulation of the UNC-18-*Caenorhabditis elegans* syntaxin complex by UNC-13. *J. Neurosci.* 19, 4772–4777.

Sawada, K., Echigo, N., Juge, N., Miyaji, T., Otsuka, M., Omote, H., et al. (2008). Identification of a vesicular nucleotide transporter. *Proc. Natl. Acad. Sci. U.S.A.* 105, 5683–5686. doi:10.1073/pnas.0800141105

Schiavo, G., Benfenati, F., Poulain, B., Rossetto, O., Polverino de Laureto, P., DasGupta, B. R., et al. (1992). Tetanus and botulinum-B neurotoxins block neurotransmitter release by proteolytic cleavage of synaptobrevin [see comments]. *Nature* 359, 832–835. doi:10.1038/359832a0

Schraw, T. D., Lemons, P. P., Dean, W. L., and Whiteheart, S. W. (2003). A role for Sec1/Munc18 proteins in platelet exocytosis. *Biochem. J.* 374, 207–217. doi:10.1042/BJ20030610

Schutz, D., Zilly, F., Lang, T., Jahn, R., and Bruns, D. (2005). A dual function for Munc-18 in exocytosis of PC12 cells. *Eur. J. Neurosci.* 21, 2419–2432. doi:10.1111/j.1460-9568.2005.04095.x

Sehgal, S., and Storrie, B. (2007). Evidence that differential packaging of the major platelet granule proteins von Willebrand factor and fibrinogen can support their differential release. *J. Thromb. Haemost.* 5, 2009–2016. doi:10.1111/j.1538-7836.2007.02698.x

Shirakawa, R., Higashi, T., Tabuchi, A., Yoshioka, A., Nishioka, H., Fukuda, M., et al. (2004). Munc13-4 is a GTP-Rab27-binding protein regulating dense core granule secretion in platelets. *J. Biol. Chem.* 279, 10730–10737. doi:10.1074/jbc.M309426200

Sigel, H., and Corfu, N. A. (1996). The assisted self-association of ATP4- by a poly(amino acid) [poly(Lys)] and its significance for cell organelles that contain high concentrations of nucleotides. *Eur. J. Biochem.* 240, 508–517. doi:10.1111/j.1432-1033.1996.0508h.x

Sim, D. S., Dilks, J. R., and Flaumenhaft, R. (2007). Platelets possess and require an active protein palmitoylation pathway for agonist-mediated activation and in vivo thrombus formation. *Arterioscler. Thromb. Vasc. Biol.* 27, 1478–1485. doi:10.1161/ATVBAHA.106.139287

Sollner, T., Whiteheart, S. W., Brunner, M., Erdjument-Bromage, H., Geromanos, S., Tempst, P., et al. (1993). SNAP receptors implicated in vesicle targeting and fusion [see comments]. *Nature* 362, 318–324. doi:10.1038/362318a0

Song, Y., Ailenberg, M., and Silverman, M. (1998). Cloning of a novel gene in the human kidney homologous to rat munc13s: its potential role in diabetic nephropathy. *Kidney Int.* 53, 1689–1695. doi:10.1046/j.1523-1755.1998.00942.x

Stenberg, P. E., Shuman, M. A., Levine, S. P., and Bainton, D. F. (1984). Redistribution of alpha-granules and their contents in thrombin-stimulated platelets. *J. Cell Biol.* 98, 748–760. doi:10.1083/jcb.98.2.748

Stevens, D. R., Wu, Z. X., Matti, U., Junge, H. J., Schirra, C., Becherer, U., et al. (2005). Identification of the minimal protein domain required for priming activity of Munc13-1. *Curr. Biol.* 15, 2243–2248. doi:10.1016/j.cub.2005.10.055

Tang, K. S., Tse, A., and Tse, F. W. (2005). Differential regulation of multiple populations of granules in rat adrenal chromaffin cells by culture duration and cyclic AMP. *J. Neurochem.* 92, 1126–1139. doi:10.1111/j.1471-4159.2004.02944.x

Trifaro, J. M., Lejen, T., Rose, S. D., Pene, T. D., Barkar, N. D., and Seward, E. P. (2002). Pathways that control cortical F-actin dynamics during secretion. *Neurochem. Res.* 27, 1371–1385. doi:10.1023/A:1021627800918

Tsuboi, T., McMahon, H. T., and Rutter, G. A. (2004). Mechanisms of dense core vesicle recapture following "kiss and run" ("cavicapture")

exocytosis in insulin-secreting cells. *J. Biol. Chem.* 279, 47115–47124. doi:10.1074/jbc.M408179200

van Nispen tot Pannerden, H., De Haas, F., Geerts, W., Posthuma, G., Van Dijk, S., and Heijnen, H. F. G. (2010). The platelet interior revisited: electron tomography reveals tubular alpha-granule subtypes. *Blood* 116, 1147–1156. doi:10.1182/blood-2010-02-268680

Voets, T., Toonen, R. F., Brian, E. C., de Wit, H., Moser, T., Rettig, J., et al. (2001). Munc18-1 promotes large dense-core vesicle docking. *Neuron* 31, 581–591. doi:10.1016/S0896-6273(01)00391-9

Wang, W., Gilligan, D. M., Sun, S., Wu, X., and Reems, J. A. (2011). Distinct functional effects for dynamin 3 during megakaryocytopoiesis. *Stem Cells Dev.* 20, 2139–2151. doi:10.1089/scd.2011.0159

Wegrzyn, J. L., Bark, S. J., Funkelstein, L., Mosier, C., Yap, A., Kazemi-Esfarjani, P., et al. (2010). Proteomics of dense core secretory vesicles reveal distinct protein categories for secretion of neuroeffectors for cell-cell communication. *J. Proteome Res.* 9, 5002–5024. doi:10.1021/pr1003104

Wightman, R. M., and Haynes, C. L. (2004). Synaptic vesicles really do kiss and run. *Nat. Neurosci.* 7, 321–322. doi:10.1038/nn0404-321

Woronowicz, K., Dilks, J. R., Rozenvayn, N., Dowal, L., Blair, P. S., Peters, C. G., et al. (2010). The platelet actin cytoskeleton associates with SNAREs and participates in alpha-granule secretion. *Biochemistry* 49, 4533–4542. doi:10.1021/bi100541t

Xu, T., Binz, T., Niemann, H., and Neher, E. (1998). Multiple kinetic components of exocytosis distinguished by neurotoxin sensitivity. *Nat. Neurosci.* 1, 192–200. doi:10.1038/642

Yang, B., Steegmaier, M., Gonzalez, L. C. Jr., and Scheller, R. H. (2000). nSec1 binds a closed conformation of syntaxin1A. *J. Cell Biol.* 148, 247–252. doi:10.1083/jcb.148.2.247

Ye, S., Karim, Z. A., Al Hawas, R., Pessin, J. E., Filipovich, A. H., and Whiteheart, S. W. (2012). Syntaxin-11, but not syntaxin-2 or syntaxin-4, is required for platelet secretion. *Blood* 120, 2484–2492. doi:10.1182/blood-2012-05-430603

Zhang, X., Kim-Miller, M. J., Fukuda, M., Kowalchyk, J. A., and Martin, T. F. (2002). Ca2+-dependent synaptotagmin binding to SNAP-25 is essential for Ca2+-triggered exocytosis. *Neuron* 34, 599–611. doi:10.1016/S0896-6273(02)00671-2

Conflict of Interest Statement: The authors declare that the research was conducted in the absence of any commercial or financial relationships that could be construed as a potential conflict of interest.

Received: 17 April 2013; accepted: 11 June 2013; published online: 26 June 2013.
*Citation: Fitch-Tewfik JL and Flaumenhaft R (2013) Platelet granule exocytosis: a comparison with chromaffin cells. Front. Endocrinol. **4**:77. doi: 10.3389/fendo.2013.00077*
This article was submitted to Frontiers in Neuroendocrine Science, a specialty of Frontiers in Endocrinology.

frontiers in
ENDOCRINOLOGY

REVIEW ARTICLE
published: 18 September 2013
doi: 10.3389/fendo.2013.00129

Regulated mucin secretion from airway epithelial cells

***Kenneth B. Adler*[1], *Michael J. Tuvim*[2] *and Burton F. Dickey*[2]*

[1] Department of Molecular Biomedical Sciences, North Carolina State University College of Veterinary Medicine, Raleigh, NC, USA
[2] Department of Pulmonary Medicine, The University of Texas MD Anderson Cancer Center, Houston, TX, USA

Edited by:
Rafael Vazquez-Martinez, University of Cordoba, Spain

Reviewed by:
Ricardo Borges, University of La Laguna, Spain
Gunnar C. Hansson, University of Gothenburg, Sweden

***Correspondence:**
Burton F. Dickey, Department of Pulmonary Medicine, University of Texas MD Anderson Cancer Center, Unit 1462, 1515 Holcombe Boulevard, Houston, TX 77030-4009, USA
e-mail: bdickey@mdanderson.org

Secretory epithelial cells of the proximal airways synthesize and secrete gel-forming polymeric mucins. The secreted mucins adsorb water to form mucus that is propelled by neighboring ciliated cells, providing a mobile barrier which removes inhaled particles and pathogens from the lungs. Several features of the intracellular trafficking of mucins make the airway secretory cell an interesting comparator for the cell biology of regulated exocytosis. Polymeric mucins are exceedingly large molecules (up to 3×10^6 Da per monomer) whose folding and initial polymerization in the ER requires the protein disulfide isomerase Agr2. In the Golgi, mucins further polymerize to form chains and possibly branched networks comprising more than 20 monomers. The large size of mucin polymers imposes constraints on their packaging into transport vesicles along the secretory pathway. Sugar side chains account for >70% of the mass of mucins, and their attachment to the protein core by O-glycosylation occurs in the Golgi. Mature polymeric mucins are stored in large secretory granules ~1 μm in diameter. These are translocated to the apical membrane to be positioned for exocytosis by cooperative interactions among myristoylated alanine-rich C kinase substrate, cysteine string protein, heat shock protein 70, and the cytoskeleton. Mucin granules undergo exocytic fusion with the plasma membrane at a low basal rate and a high stimulated rate. Both rates are mediated by a regulated exocytic mechanism as indicated by phenotypes in both basal and stimulated secretion in mice lacking Munc13-2, a sensor of the second messengers calcium and diacylglycerol (DAG). Basal secretion is induced by low levels of activation of P_2Y_2 purinergic and A3 adenosine receptors by extracellular ATP released in paracrine fashion and its metabolite adenosine. Stimulated secretion is induced by high levels of the same ligands, and possibly by inflammatory mediators as well. Activated receptors are coupled to phospholipase C by Gq, resulting in the generation of DAG and of IP_3 that releases calcium from apical ER. Stimulated secretion requires activation of the low affinity calcium sensor Synaptotagmin-2, while a corresponding high affinity calcium sensor in basal secretion is not known. The core exocytic machinery is comprised of the SNARE proteins VAMP8, SNAP23, and an unknown Syntaxin protein, together with the scaffolding protein Munc18b. Common and distinct features of this exocytic system in comparison to neuroendocrine cells and neurons are highlighted.

Keywords: secretion, exocytosis, mucin, mucus, MARCKS, Munc18, Munc13, synaptotagmin

BIOLOGY AND PATHOPHYSIOLOGY OF AIRWAY MUCUS

Mucus has physical characteristics on the border between a viscous fluid and a soft and elastic solid (1). These characteristics are conferred by a semi-dilute network of polymerized mucins in water. The secreted, polymeric mucins expressed in the airways are Muc5ac and Muc5b (2, 3). (Note, lower case letters are used to designate non-human mammalian mucins, while MUC5AC and MUC5B designate the human orthologs. In this review, we use lower case letters to designate all mammalian mucins, and only use upper case letters when referring specifically to human data.) In healthy airway mucus, water accounts for about 98% of the mass, mucins for about 0.7%, and salts and small amounts of other macromolecules for the rest. The mucus layer lies atop a denser periciliary layer containing membrane-tethered glycoconjugates, including glycosaminoglycans and membrane-spanning mucins (Muc 1, 4, and 16) (4–6). The mucus layer is continually swept from distal to proximal airways by beating cilia, and is eventually propelled out of the lungs into the pharynx and swallowed, removing entrapped particles, pathogens, and dissolved chemicals. The critical importance of the mucus layer in airway defense is shown by the spontaneous inflammatory lung and nasal disease that develops in mice in which the constitutively produced mucin, Muc5b, has been deleted (1).

In order to replenish the mucus layer, mucins are continuously synthesized and released by secretory cells that form a mosaic with ciliated cells, with similar numbers of both cell types (**Figure 1**, left). In allergic lung inflammation, which appears to be a parasitic defense gone awry (4, 7), the second polymeric airway mucin, Muc5ac, is produced in large quantities (**Figure 1**, center and right). Whereas increased mucin production alone does not appear

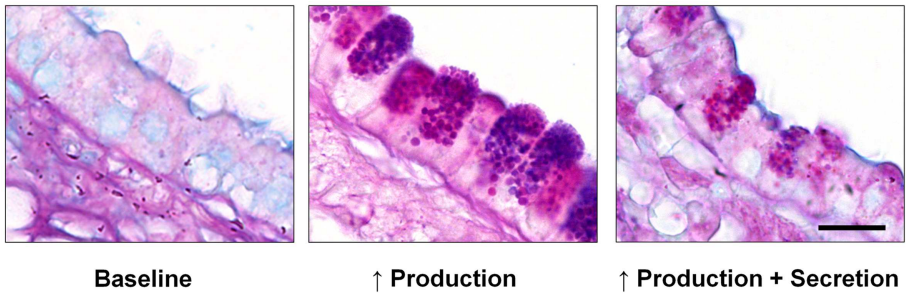

FIGURE 1 | Mucin production and secretion in the mouse airway. Left – In the healthy baseline state, alternating ciliated and domed secretory cells are seen, with no mucin granules visible by Alcian blue and periodic acid Schiff (AB-PAS) staining. Center – Numerous large mucin granules are visible in secretory cells 3 days after mucin production is increased by IL-13-dependent allergic inflammation as described (51). Right – Exocytic secretion of the intraepithelial mucin stored in inflamed airway epithelium induced by brief exposure to an ATP aerosol as described (51). Scale bar is 10 μm.

to lead to pathology (8), the production of large amounts of mucin together with its rapid secretion ("mucus hypersecretion") can overwhelm available liquid resulting in formation of excessively viscoelastic mucus that is poorly cleared by ciliary action or cough. When coupled with airway narrowing due to bronchoconstriction in asthma, this can lead to widespread airway closure with serious consequences. Mucus hypersecretion is also an important feature of chronic obstructive pulmonary disease (COPD), cystic fibrosis (CF), and idiopathic bronchiectasis (1).

A key event in mucus secretion is its hydration immediately after exocytosis (4, 9, 10). Mucins are packaged dehydrated in secretory granules, and must adsorb more than 100-fold their mass of water soon after secretion in order to attain the appropriate viscoelasticity for ciliary clearance. Water in the airway lumen is controlled both by the release of chloride through CFTR, CaCC, and Slc26A9, and by the absorption of sodium by ENaC, with water passively following the flux of ions (11–13). Coupling of the secretion of chloride and mucins is accomplished by paracrine signaling through ATP, adenosine, and other extracellular signaling molecules. In CF, mutation of the principal chloride channel, CFTR, results in insufficient luminal water that causes the formation of underhydrated mucus which is excessively viscoelastic and difficult to clear. The underhydration is exacerbated because CFTR is also a channel for bicarbonate, which is needed to chelate calcium (9, 14). In acidic secretory granules of the intestinal epithelium, calcium binds to the N-terminus of MUC2, which is the secreted mucin most similar to MUC5AC in structure, and organizes the mucin in such a way that it can be secreted without entanglement (15). Too little bicarbonate at mucin release prevents normal mucin unfolding and leads to formation of abnormally dense mucus (16); similar mechanisms likely operate in the airway.

In summary, the mucus layer forms a mobile, essential barrier that protects the lungs when it is functioning properly, but dysfunction of the mucus layer plays a prominent role in all of the common diseases of the airways.

MUCIN SYNTHESIS, PROCESSING, AND PACKAGING

Muc5b/MUC5B is transcribed constitutively throughout the conducting airways from the trachea down to but not including terminal bronchioles (1, 17, 18). Muc5ac is produced in low amounts or not at all in healthy mice, although in humans MUC5AC is produced constitutively in proximal airways (trachea and bronchi) (1). In allergic inflammation the production of Muc5ac increases dramatically (40- to 200-fold) in the airways of mice and in cultured human airway epithelial cells (19–21). Both mucins are produced in the same secretory cells, but even in conditions of severe inflammation they are not produced in small airways, which makes teleologic sense in that their small luminal diameters (<200 μm) make them highly susceptible to occlusion.

After translation at the ER, Muc5ac, and Muc5b undergo initial polymerization as homodimers (3). These are among the largest macromolecules encoded in the mammalian genome, and their processing induces a stress response in the ER (22). Proper folding and polymerization require the protein disulfide isomerase Agr2, whose deletion in mice results in absent intestinal mucin (23) and in reduced airway mucin in the setting of allergic lung inflammation (24). The transport of polymeric mucins from the ER to the Golgi and through the Golgi has been little studied, but likely involves modulation of COP-II transport vesicle size to accommodate large cargoes as has been described for collagen (25). In the Golgi, Muc5b undergoes further polymerization in linear chains up to 20 monomers in length (3, 26). The structure of Muc5ac is less well studied, but appears to be more similar to Muc2 that forms branched polymers resulting in formation of a covalent net (9). Both mucins undergo O-glycosylation in the Golgi that result in mature glycoproteins that are more than 70% carbohydrate with a general negative charge due to sulfation or sialylation of many terminal sugars (27).

Export of polymeric mucins from the trans-Golgi and lateral fusion of post-Golgi vesicles to form secretory granules are additional transport steps that have been poorly studied. Similar to the case of COP-II vesicles, post-Golgi clathrin-coated vesicles have recently been shown to be capable of size variation to accommodate large cargo proteins (28). It is probable this mechanism is also utilized for mammalian mucins because, in fruit flies, assembly of large salivary mucin granules requires clathrin and the adaptor AP-1 (29). Mature mucin secretory granules are very large, with a mean diameter of 1 μm. Their exocytic fusion is highly regulated by extracellular secretagogues (**Table 1**), as described below. It should be noted that even though additional secretory pathways

Table 1 | Ligands shown to induce mucin secretion.

Ligand	Receptor; site of action	Reference
ATP, UTP	P_2Y_2; epithelium	Chen et al. (68), Danahay et al. (49), Ehre et al. (37), Kemp et al. (69), and Kim and Lee (70)
Adenosine	A3AR; epithelium (in mice but not humans, dogs, or guinea pigs)	Young et al. (62)
Proteases	PAR1, PAR2, other; epithelium	Breuer et al. (71), Jones et al. (47), Liu et al. (72), and Park et al. (39)
Acetylcholine	Unknown; may be indirect	Singer et al. (34)
Histamine	Unknown; may be indirect	Huang et al. (73)
Serotonin	Unknown; may be indirect	Foster et al. (36)
Capsaicin (substance P)	NK1; may be indirect	Guo et al. (74) and Kuo et al. (75)
Ionomycin (calcium)	Syt2, Munc13, PKC, other; epithelium (intracellular)	Danahay et al. (49), Ehre et al. (37), Tuvim et al. (46), and Zhu et al. (18)
PMA	Munc13-2, PKC; epithelium (intracellular)	Danahay et al. (49), Ehre et al. (37), and Zhu et al. (18)

In the left column are ligands reported to induce secretion of mucin from airway surface epithelial cells. In the middle column are receptors for these ligands and whether they act directly on epithelial cells. In the right column are selected references that offer evidence for the activity of the ligands, their receptors, and their cellular localization. The first three rows (white background) show ligands that appear to act directly on epithelial cell surface receptors based upon in vitro and/or in vivo studies; the next four rows (gray background) show ligands that generally act on cell surface receptors, but may activate cells in the airway other than epithelial cells that in turn activate epithelial cells; the last two rows show ligands that act on intracellular targets. PMA, phorbol 12-myristate 13-acetate.

have been described in other cell types, such as a minor regulated pathway for secretion of immature granules and the compound exocytosis of mature granules (30), these are not well-described in airway secretory cells and will not be addressed in this review.

MUCIN GRANULE POSITIONING FOR SECRETION

The movement of mature mucin granules to the plasma membrane for exocytosis has been the subject of work in numerous laboratories for many years. In the 1990s, work in the Adler laboratory turned to the Myristoylated Alanine-Rich C Kinase Substrate (MARCKS) protein. MARCKS was a known actin-binding protein and protein kinase C (PKC) substrate (31), and it was known that PKC activation enhanced mucin secretion (32), so MARCKS was a logical candidate regulator of mucin granule movement.

MARCKS is a rod-shaped 87 kDa protein that is ubiquitously expressed. Three domains of MARCKS are conserved evolutionarily. First is the Phosphorylation Site Domain (PSD), also known as the "effector domain," a highly basic 25 amino acid stretch containing a number of serine residues that are phosphorylated by PKC. This domain also binds calcium/calmodulin and crosslinks actin filaments. Second is the Multiple Homology (MH2) domain, whose function is unknown. Third is the N-terminal region containing 24 amino acids and a myristic acid moiety involved in binding to membranes. MARCKS knockout mice die at birth or soon afterward, so peptides that might compete with native MARCKS to inhibit its function were generated by the Adler laboratory in collaboration with the Blackshear laboratory. These were tested using normal human bronchial epithelial (NHBE) cells grown in air-liquid interface culture to maintain their well-differentiated state. Peptides identical to the PSD site tended to induce a toxic response, but a peptide identical to the N-terminus had a strong inhibitory effect on mucin secretion induced by a combination of phorbol ester, a PKC activator, and 8-bromo-cyclic GMP, a protein kinase G (PKG) activator (33), or by the more physiologically relevant stimulus UTP. This peptide was named Myristoylated N-terminal Sequence (MANS), and a control missense peptide was named Random N-terminal Sequence (RNS). In contrast to MANS, RNS was without effect on mucin secretion. Additional studies showed that MARCKS phosphorylation in response to protein kinase activation, followed by dephosphorylation catalyzed by a protein phosphatase type 2A (PP2A), were critical to MARCKS function. This was the first publication to show a specific biological function for MARCKS, and suggested a mechanism whereby MARCKS came off the inner face of the plasma membrane when phosphorylated by PKC, then bound to mucin granules at the N-terminus and the cytoskeleton at the PSD site, serving as a bridge for granule transport to the plasma membrane by the cytoskeleton (33).

To examine the function of MARCKS *in vivo*, mice with mucous metaplasia induced by allergic inflammation (see Mucin Exocytosis, below) were then exposed to aerosolized methacholine to induce mucin secretion. Intratracheal pretreatment with MANS dose-dependently inhibited mucin secretion (34), and it attenuated airflow obstruction about 40% (35). Gold-labeling of stimulated cells revealed MARCKS to be morphologically associated with mucin granules, and treatment with MANS but not RNS blocked the association (34). Additional studies performed in mice with human neutrophil elastase instilled in the airways to induce mucous metaplasia showed similar results, with MANS but not RNS attenuating both mucin secretion and airway hyperreactivity in response to serotonin (36).

Subsequent studies have revealed that PKC δ and ε isoforms are involved in stimulated mucin secretion (37, 38), and that PKCδ-provoked secretion depends on phosphorylation of MARCKS (38, 39). Another question was the mechanism of translocation of MARCKS from the plasma membrane to mucin granules. Co-immunoprecipitation studies revealed an association between MARCKS and two previously described chaperones – Heat Shock

Protein 70 (HSP70) and Cysteine String Protein (CSP) (40). Of interest, there was previously known to be direct and specific interaction of HSP70 with CSP (41). Western blotting and proteomic analysis of mucin granule membranes, ultrastructural immunohistochemistry, and immunoprecipitation experiments showed that MARCKS, HSP70, and CSP form a trimeric complex associated with the granule membrane (42, 43). Functional studies in a bronchial epithelial cell line using siRNA to knock down expression of MARCKS, HSP70, or CSP resulted in the attenuation of stimulated mucin secretion (42).

Additional studies have examined interactions among MARCKS, the chaperones, and cytoskeletal proteins. Treatment of NHBE cells with the pyrimidinone MAL3-101, an HSP70 inhibitor, or siRNA against HSP70, attenuated phorbol ester-stimulated mucin secretion, and blocked trafficking of fluorescent-tagged MARCKS (42, 44). In preliminary studies, cell-permeant peptides that target different domains of CSP were utilized to show that the C-terminus of CSP, rather than the more frequently studied "J" domain, appears to be involved in attachment of MARCKS to mucin granule membranes and resultant secretion. MARCKS has been found to bind both actin and myosin (33), and recent experiments showed that the myosin family involved is Myosin V (45). A possible contributing mechanism of MARCKS action besides granule transport could be the remodeling of apical actin (30). Exocytic Rab GTPases of the 3 and 27 subfamilies interact with the cytoskeleton and catalyze loose tethering of secretory granules to the plasma membrane in other cell types; Rab3D and Rab27A are expressed in airway secretory cells (30, 46), though they have not yet been functionally implicated in mucin secretion or MARCKS interaction. Another possibly important interaction is with VAMP8 that has been identified as the principal t-SNARE in mucin secretion (47) (see Core Exocytic Machinery, below). Preliminary studies from the Adler laboratory show that MARCKS and CSP bind VAMP8 on mucin granules. In summary, MARCKS engages in multiple protein interactions that together help position mucin secretory granules for exocytotic release. For a listing of proteins known to localize to the mucin granule membrane, see **Table 2**.

Table 2 | Proteins associated with airway epithelial mucin granules.

Protein	Reference
ClCa3	Leverkoehne and Gruber (76), Lin et al. (45), Park et al. (40), Raiford et al. (43), and Singer et al. (34)
CFTR	Lesimple et al. (77)
CSP	Fang et al. (44), Lin et al. (45), Park et al. (40), and Raiford et al. (43)
HSP70	Fang et al. (44), Lin et al. (45), Park et al. (40), and Raiford et al. (43)
MARCKS	Fang et al. (44), Li et al. (33), Lin et al. (45), Park et al. (40), Park et al. (38), Raiford et al. (43), and Singer et al. (34)
Myosin V	Lin et al. (45) and Raiford et al. (43)
Rab3D	Evans et al. (51) and Tuvim et al. (46)
Syt2	Tuvim et al. (46)
VAMP8	Jones et al. (47)
VNUT	Sesma et al. (78)

Proteins that have been found to be associated with mucin granules of airway surface epithelial cells are listed alphabetically in the first column, and references for the association are reported in the second column. See Table 1 in Ref. (43) for a full listing of all proteins found by LC/MS to associate with mucin granules, though not all of these have been validated. ClCa, calcium-activated chloride channel; CFTR, cystic fibrosis transmembrane conductance regulator; CSP, cysteine string protein; HSP, heat shock protein; VNUT, vesicular nucleotide transporter.

MUCIN EXOCYTOSIS

Mucins are secreted into the airway lumen at a low basal rate and a high stimulated rate (1, 30). It is difficult to precisely define the difference in these rates because their measurement depends upon intracellular mucin content, the time interval of observation, and the post-exocytic release of mucins and their maturation to mucus for most assays. Despite these limitations, the rate of stimulated secretion has been generally found to exceed the rate of basal secretion by ∼5-fold over durations of 1 h or less by a variety of techniques (18, 37, 48, 49). The basal rate of secretion matches the basal rate of mucin synthesis in the distal airways of humans and all the airways of mice so that there is little intracellular mucin accumulation in the healthy state (**Figure 1**, left). Small amounts of intracellular mucin in this setting can be detected by sensitive immunohistochemical techniques that involve signal amplification (18, 50), but generally are not detectable by histochemical stains (51). The proximal airways of humans do contain histochemically apparent mucin associated with the constitutive expression of MUC5AC (1), but most functional studies of the exocytic machinery have been performed in mouse models so these will be the focus of further discussion. For comparison with *in vitro* systems studied by electrophysiologic (49) and videomicroscopic (52) techniques, the reader is referred to the referenced articles.

A regulated exocytic mechanism mediates both basal and stimulated mucin secretion as indicated by abnormal phenotypes in both basal and stimulated secretion when Munc13-2, a sensor of second messengers (see Extracellular Signaling and the Exocytic Regulatory Machinery), is deleted in mice (18). A defect in basal mucin secretion can be detected as the spontaneous accumulation of intracellular mucin in the absence of increased mucin synthesis (53). To measure stimulated secretion, it is useful to first induce increased mucin production and accumulation (mucous metaplasia) with allergic inflammation (**Figure 1**, center), such as by IL-13 instillation or ovalbumin immunization and challenge (51, 53). A defect in stimulated mucin secretion can then be detected as the failure to release intracellular mucin in response to a strong agonist such as ATP (**Figure 1**, right). Differential effects of the deletion of genes encoding various exocytic proteins on basal and stimulated mucin secretion indicate which proteins participate in which secretory state. In general, deletion of components of the core exocytic machinery give phenotypes in both basal and stimulated secretion, indicating that there is a single core exocytic machine, whereas deletion of components of the regulatory machinery give variable phenotypes, as described below.

CORE EXOCYTIC MACHINERY

Every step of vesicular transport on the exocytic and endocytic pathways involves the interactions of a four helix SNARE bundle with an SM protein (30, 54, 55). The SNARE proteins impart specificity to the pairing of transport vesicles with target membranes, mediate tight docking of vesicles to target membranes, and induce fusion of vesicle and target membranes when they fully coil. SM proteins provide an essential platform for sequential interactions of SNARE proteins, and also mediate interactions of the SNARE complex with tethering proteins (**Figure 2**). Three of the SNARE helices localize to the target membrane (called t-SNAREs for target SNAREs, or Q-SNAREs since the ionic amino acid of their SNARE domains is generally glutamine), and one SNARE helix is localized on the vesicle membrane (v-SNARE for vesicle SNARE, or R-SNARE since the ionic amino acid is generally arginine).

Syntaxins are Qa SNAREs that can be considered the central component of the core machinery since they initiate formation of the SNARE complex and their structure is ordered even in the absence of interaction with the other SNARE components. The Syntaxin that mediates mucin granule exocytosis remains unknown. Candidates are Stx 2, 3, and 11, all of which have been shown to functionally pair with Munc18b in other cell types since Munc18b has been definitively implicated in airway mucin exocytosis (56) (see below). Efforts are underway in the Dickey laboratory using genetically modified mice to test the roles of these Syntaxins in mucin secretion.

In both yeast and neurons, the Qb and Qc SNAREs involved in exocytosis are contributed by a single protein with two SNARE domains connected by a linker region. In yeast this protein is Sec9, which is essential for cell viability. In neurons the cognate protein mediating axonal synaptic vesicle release is SNAP25 (57). While SNAP25 is essential for post-natal life, brain development to the time of birth is nearly normal. In unpublished work, the Dickey laboratory has obtained evidence that SNAP23 mediates both basal and stimulated airway mucin secretion. SNAP23 is expressed ubiquitously, and knockout mice experience early embryonic lethality (58, 59). However heterozygous knockout mice show spontaneous airway epithelial cell mucin accumulation, indicating a defect in basal mucin secretion, as well as epithelial mucin retention after stimulation with aerosolized ATP, indicating a defect in stimulated secretion. Thus, SNAP23 appears to mediate most or all Qbc function in both basal and stimulated mucin secretion.

Recently, the R-SNARE (v-SNARE) in airway mucin secretion was identified as VAMP8 by immunolocalization to mucin secretory granules, *in vitro* functional analysis by RNA interference, and *in vivo* analysis of knockout mice (47). Both basal and stimulated mucin secretion were reduced by loss of VAMP8, though the defects were not as severe as from the loss of some other exocytic proteins, consistent with the viability of knockout mice, and suggesting that other v-SNAREs also participate in mucin secretion.

The scaffolding function of SM proteins in exocytosis in different cell types is mediated by three Munc18 proteins (54, 56). Munc18a (Stxbp1) and Munc18b (Stxbp2) appear to be paralogs functioning in axonal/apical secretion, whereas Munc18c (Stxbp3) is a ubiquitous isoform functioning in dendritic/basolateral secretion. Munc18a is expressed in neurons and neuroendocrine

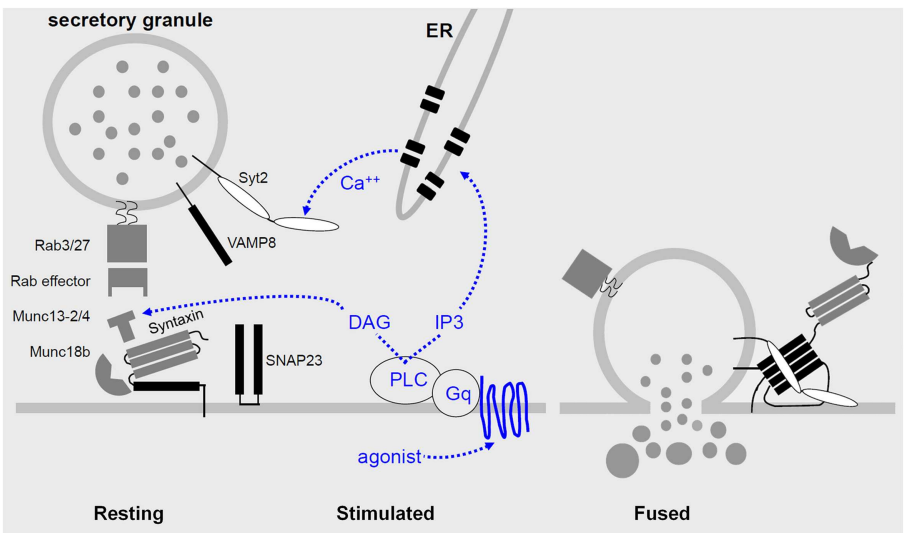

FIGURE 2 | Regulated airway mucin secretion. Left – In the basal state, mucin granules are thought to become tethered to the plasma membrane by Rab proteins and effectors that have not yet been identified, in the vicinity of components of the exocytic machinery. Center – Activation of heptahelical receptors such as those for ATP (P_2Y_2) and adenosine (A3R) leads to activation of the trimeric G-protein, Gq, and phospholipase C (PLC), resulting in generation of the second messengers diacylglycerol (DAG) and inositol trisphosphate (IP_3). Diacylglycerol activates the priming protein Munc13-2, and IP_3 induces the release of calcium from apical ER to activate Synaptotagmin-2 (Syt2). Munc13-4 also participates in granule priming, and an unknown high affinity calcium sensor likely functions in basal secretion rather than Syt2. Right – Activation of the regulatory Munc13 and Syt proteins leads to full coiling of the SNARE proteins (SNAP23, VAMP8, and an unknown Syntaxin, all shown in black) to induce fusion of the granule and plasma membranes. The interactions of the SNARE proteins take place on a scaffold provided by Munc18b. In other secretory cells that form the basis for this model, exocytic Syntaxins contain four hydrophobic coiled-coil domains that must be opened to initiate secretion (left panel), and during fusion the associated Munc18 protein remains associated only by an interaction at the Syntaxin N-terminus (right panel).

cells, whereas Munc18b is expressed in polarized epithelia. Together, these data suggested that Munc18b mediates airway mucin secretion, and localization and functional data support this. Munc18b is highly expressed in airway secretory cells where it localizes to the apical plasma membrane (56). Munc18b knockout mice are not viable postnatally, but heterozygous knockout mice show an ∼50% reduction in stimulated mucin secretion, indicating that Munc18b is a limiting component of the exocytic machinery (56). These heterozygous mutant mice do not show spontaneous mucin accumulation, unlike heterozygous SNAP23 mutant mice, suggesting that another SM protein besides Munc18b also plays a scaffolding role in basal mucin secretion whereas no other protein besides SNAP23 appears to function as a Qbc SNARE in mucin exocytosis. Ruling out the possibility that Munc18b functions only in stimulated and not basal mucin secretion, conditional mutant mice with Munc18b deleted only in airway secretory cells are viable and show spontaneous mucin accumulation, although preliminary results suggest that the accumulation is less than in Munc13-2 mice.

EXTRACELLULAR SIGNALING AND THE EXOCYTIC REGULATORY MACHINERY

The extracellular ligands and signal transduction pathways controlling mucin secretion have been studied for longer and in more depth than the exocytic machinery itself (30). The best-studied ligand is ATP that acts on the P_2Y_2 receptor to activate Gq and PLC-β1, resulting in generation of the second messengers IP_3 and diacylglycerol (DAG). ATP is released in a paracrine fashion from ciliated cells in response to mechanical shear stress and in an autocrine fashion along with uridine nucleotides from secretory granules (60, 61). The ATP metabolite adenosine acting on the A3 adenosine receptor appears to activate the same Gq-PLC pathway (62). It is possible that other G-protein coupled receptors, such as those sensing serotonin or acetylcholine, also function on airway secretory cells since those ligands induce mucin secretion *in vivo* (34, 36), however they may be acting in a paracrine fashion by inducing contraction of smooth muscle cells leading to the release of ATP that in turn induces mucin release (**Table 1**).

In airway secretory cells, the second messenger IP_3 activates receptors on apical ER to induce the release of calcium. In contrast to excitable cells in which calcium enters the cytoplasm from outside through voltage-gated channels, or secretory hematopoietic cells such as mast cells in which an initial release of calcium from intracellular stores triggers further calcium entry from outside through ICRAC, all of the cytoplasmic calcium involved in exocytic signaling in airway secretory cells appears to come from intracellular stores (30). This may be an adaptation to the fact that the calcium concentration in the thin layer of airway surface liquid is not stable due to the variable release of mucins that carry calcium as a counterion and the variable secretion via CFTR of bicarbonate that chelates calcium. Calcium does enter airway secretory cells from the basolateral surface to maintain intracellular stores, presumably by communication between the basolateral and apical ER since mitochondrial barriers segregate cytoplasmic calcium signals (63). Nonetheless, the chelation of extracellular calcium *in vitro* does not acutely affect mucin secretion. Rough ER at the apical pole of airway secretory cells lies in close apposition to mucin granules (46, 64), which should allow localized calcium signaling to the exocytic machinery through proteins such as Synaptotagmins and Munc13s.

Synaptotagmins are a family of proteins containing two C2 domains capable of calcium-dependent phospholipid binding, of which several members mediate calcium-dependent exocytosis. Using Syt2 knockout mice, we have found that Syt2 serves as a critical sensor of stimulated but not of basal mucin secretion (46). There was no spontaneous mucin accumulation in these mice, consistent with the fact that Syt2 and its close homolog Syt1 inhibit rather than promote synaptic vesicle release at baseline levels of cytoplasmic calcium (65). In contrast, there was a complete failure of ATP-stimulated mucin release in homozygous knockout mice and a dose-dependent failure in heterozygous knockout mice (46). This was a surprising result for several reasons. First, there is no impairment of synaptic vesicle release in heterozygous mutant Syt1 or Syt2 mice, indicating that some structural or functional feature of stimulated exocytosis in airway secretory cells differs from that in neurons to make Syt2 levels limiting, such as the difference in size of the secretory vesicles (50 nm in neurons versus 1000 nm in airway secretory cells) or the concentration of exocytic proteins at the active zone. Second, Syt2 is the fastest among the low affinity, fast calcium exocytic sensors Syt 1, 2, and 9, yet mucin secretion is a slow exocytic process (measured in hundreds of milliseconds) compared to synaptic vesicle release (measured in milliseconds). This suggests that some other feature of Syt2 besides its kinetics makes it a suitable regulator of mucin release. The calcium-sensing protein in basal mucin secretion that performs a role comparable to that of Syt2 in stimulated secretion is not yet known. Nonetheless such a protein likely exists since a second, high affinity calcium sensor functions in neurons and neuroendocrine cells, and basal mucin secretion has been shown to be calcium dependent (66).

Munc13 comprises a family of four calcium and lipid sensing proteins with variable numbers of C1 and C2 domains that function in the priming of secretory vesicles. As mentioned above, Munc13-2 knockout mice show defects in both basal and stimulated mucin secretion, with the basal defect being more dramatic than the stimulated defect (18). Munc13-2 contains a C1 domain that binds the second messenger DAG. Another member of this family, Munc13-4, is also expressed in airway secretory cells (67). Munc13-4 does not contain a C1 domain, though it does contain two C2 domains that may bind phospholipids in a calcium-dependent manner. In unpublished results, the Dickey laboratory has found that deletion of Munc13-4 causes a mild defect in stimulated secretion, and that deletion of both Munc13-2 and Munc13-4 together causes a severe (though incomplete) defect in stimulated secretion. Whether a third protein also functions in mucin granule priming to account for the residual secretion or whether mucin granule exocytosis depends only partially on priming function is not yet known.

There are additional targets of the regulation of mucin secretion besides Synaptotagmin and Munc13 proteins, such as PKC that also binds DAG and calcium (37, 38). Here we have focused on components of the exocytic machinery. A full accounting of the regulation of mucin secretion will require further knowledge of second messengers and their targets, together with analysis of their integrated function.

SUMMARY

Airway secretory cells continuously synthesize and secrete polymeric mucins that form a protective mucus layer. Both the synthesis and secretion of mucins are highly regulated, with low basal rates and high stimulated rates for each. Mature mucin granules are positioned for secretion by interactions of MARCKS, CSP, HSP70, Rab proteins, and the cytoskeleton. A core exocytic machine consisting of the SNARE proteins VAMP8, SNAP23, and an unknown Syntaxin, along with the scaffolding protein Munc18b, mediates both basal and stimulated mucin secretion. Regulatory proteins including Munc13-2, Munc13-4, and Syt2 respond to second messengers to control the rate of mucin secretion in response to extracellular signals. These regulatory proteins show differential activities in basal and stimulated secretion, suggesting that they variably associate with the core machinery depending on the levels of second messengers. Close coordination of mucin production and secretion with physiologic need are essential to lung health since either a deficiency or excess of airway mucus causes disease. The medical importance of airway mucin secretion and its scientific value as a model of large-granule exocytosis in polarized epithelia insure its continued study.

ACKNOWLEDGMENTS

This work was supported by grants from the U.S. National Institutes of Health HL36982 (Kenneth B. Adler) and HL097000 and HL094848 (Michael J. Tuvim and Burton F. Dickey).

REFERENCES

1. Fahy JV, Dickey BF. Airway mucus function and dysfunction. *N Engl J Med* (2010) **363**:2233–47. doi:10.1056/NEJMra0910061
2. Rose MC, Voynow JA. Respiratory tract mucin genes and mucin glycoproteins in health and disease. *Physiol Rev* (2006) **86**:245–78. doi:10.1152/physrev.00010.2005
3. Thornton DJ, Rousseau K, McGuckin MA. Structure and function of the polymeric mucins in airways mucus. *Annu Rev Physiol* (2008) **70**:459–86. doi:10.1146/annurev.physiol.70.113006.100702
4. Button B, Cai LH, Ehre C, Kesimer M, Hill DB, Sheehan JK, et al. A periciliary brush promotes the lung health by separating the mucus layer from airway epithelia. *Science* (2012) **337**:937–41. doi:10.1126/science.1223012
5. Dickey BF. Walking on solid ground: a gel-on-brush model of airway mucosal surfaces. *Science* (2012) **337**:924–5. doi:10.1126/science.1227091
6. Hattrup CL, Gendler SJ. Structure and function of the cell surface (tethered) mucins. *Annu Rev Physiol* (2008) **70**:431–57. doi:10.1146/annurev.physiol.70.113006.100659
7. Dickey BF. Exoskeletons and exhalation. *N Engl J Med* (2007) **357**:2082–4. doi:10.1056/NEJMe0706634
8. Ehre C, Worthington EN, Liesman RM, Grubb BR, Barbier D, O'Neal WK, et al. Overexpressing mouse model demonstrates the protective role of Muc5ac in the lungs. *Proc Natl Acad Sci U S A* (2012) **109**:16528–33. doi:10.1073/pnas.1206552109
9. Ambort D, Johansson ME, Gustafsson JK, Ermund A, Hansson GC. Perspectives on mucus properties and formation – lessons from the biochemical world. *Cold Spring Harb Perspect Med* (2012) **2**(11):a014159. doi:10.1101/cshperspect.a014159
10. Verdugo P. Supramolecular dynamics of mucus. *Cold Spring Harb Perspect Med* (2012) **2**(11):a009597. doi:10.1101/cshperspect.a009597
11. Anagnostopoulou P, Riederer B, Duerr J, Michel S, Binia A, Agrawal R, et al. SLC26A9-mediated chloride secretion prevents mucus obstruction in airway inflammation. *J Clin Invest* (2012) **122**:3629–34. doi:10.1172/JCI60429
12. Boucher RC. Cystic fibrosis: a disease of vulnerability to airway surface dehydration. *Trends Mol Med* (2007) **13**:231–40. doi:10.1016/j.molmed.2007.05.001
13. Garcia GJ, Boucher RC, Elston TC. Biophysical model of ion transport across human respiratory epithelia allows quantification of ion permeabilities. *Biophys J* (2013) **104**:716–26. doi:10.1016/j.bpj.2012.12.040
14. Quinton PM. Role of epithelial HCO3 transport in mucin secretion: lessons from cystic fibrosis. *Am J Physiol Cell Physiol* (2010) **299**:C1222–33. doi:10.1152/ajpcell.00362.2010
15. Ambort D, Johansson ME, Gustafsson JK, Nilsson HE, Ermund A, Johansson BR, et al. Calcium and pH-dependent packing and release of the gel-forming MUC2 mucin. *Proc Natl Acad Sci U S A* (2012) **109**:5645–50. doi:10.1073/pnas.1120269109
16. Gustafsson JK, Ermund A, Ambort D, Johansson ME, Nilsson HE, Thorell K, et al. Bicarbonate and functional CFTR channel are required for proper mucin secretion and link cystic fibrosis with its mucus phenotype. *J Exp Med* (2012) **209**:1263–72. doi:10.1084/jem.20120562
17. Wickstrom C, Davies JR, Eriksen GV, Veerman EC, Carlstedt I. MUC5B is a major gel-forming, oligomeric mucin from human salivary gland, respiratory tract and endocervix: identification of glycoforms and C-terminal cleavage. *Biochem J* (1998) **334**(Pt 3):685–93.
18. Zhu Y, Ehre C, Abdullah LH, Sheehan JK, Roy M, Evans CM, et al. Munc13-2-/- baseline secretion defect reveals source of oligomeric mucins in mouse airways. *J Physiol* (2008) **586**:1977–92. doi:10.1113/jphysiol.2007.149310
19. Alevy YG, Patel AC, Romero AG, Patel DA, Tucker J, Roswit WT, et al. IL-13-induced airway mucus production is attenuated by MAPK13 inhibition. *J Clin Invest* (2012) **122**:4555–68. doi:10.1172/JCI64896
20. Young HW, Williams OW, Chandra D, Bellinghausen LK, Perez G, Suarez A, et al. Central role of Muc5ac expression in mucous metaplasia and its regulation by conserved 5' elements. *Am J Respir Cell Mol Biol* (2007) **37**:273–90. doi:10.1165/rcmb.2005-0460OC
21. Zhen G, Park SW, Nguyenvu LT, Rodriguez MW, Barbeau R, Paquet AC, et al. IL-13 and epidermal growth factor receptor have critical but distinct roles in epithelial cell mucin production. *Am J Respir Cell Mol Biol* (2007) **36**:244–53. doi:10.1165/rcmb.2006-0180OC
22. Martino MB, Jones L, Brighton B, Ehre C, Abdulah L, Davis CW, et al. The ER stress transducer IRE1beta is required for airway epithelial mucin production. *Mucosal Immunol* (2013) **6**:639–54. doi:10.1038/mi.2012.105
23. Park SW, Zhen G, Verhaeghe C, Nakagami Y, Nguyenvu LT, Barczak AJ, et al. The protein disulfide isomerase AGR2 is essential for production of intestinal mucus. *Proc Natl Acad Sci U S A* (2009) **106**:6950–5. doi:10.1073/pnas.0808722106
24. Schroeder BW, Verhaeghe C, Park SW, Nguyenvu LT, Huang X, Zhen G, et al. AGR2 is induced in asthma and promotes allergen-induced mucin overproduction. *Am J Respir Cell Mol Biol* (2012) **47**:178–85. doi:10.1165/rcmb.2011-0421OC
25. Stephens DJ. Cell biology: collagen secretion explained. *Nature* (2012) **482**:474–5. doi:10.1038/482474a
26. Kesimer M, Makhov AM, Griffith JD, Verdugo P, Sheehan JK. Unpacking a gel-forming mucin: a view of MUC5B organization after granular release. *Am J Physiol Lung Cell Mol Physiol* (2010) **298**:L15–22. doi:10.1152/ajplung.00194.2009
27. Bennett EP, Mandel U, Clausen H, Gerken TA, Fritz TA, Tabak LA. Control of mucin-type O-glycosylation: a classification of the polypeptide GalNAc-transferase gene family. *Glycobiology* (2012) **22**:736–56. doi:10.1093/glycob/cwr182
28. Philippe M, Leger T, Desvaux R, Walch L. Discs large 1 (dlg1) scaffolding protein participates with clathrin and adaptor protein complex 1 (AP-1) in forming Weibel-Palade bodies of endothelial cells. *J Biol Chem* (2013) **288**:13046–56. doi:10.1074/jbc.M112.441261
29. Burgess J, Jauregui M, Tan J, Rollins J, Lallet S, Leventis PA, et al. AP-1 and clathrin are essential for secretory granule biogenesis in *Drosophila*. *Mol Biol Cell* (2011) **22**:2094–105. doi:10.1091/mbc.E11-01-0054
30. Davis CW, Dickey BF. Regulated airway goblet cell mucin secretion. *Annu Rev Physiol* (2008) **70**:487–512. doi:10.1146/annurev.physiol.70.113006.100638
31. Stumpo DJ, Graff JM, Albert KA, Greengard P, Blackshear PJ. Molecular cloning, characterization, and expression of a cDNA encoding the "80- to 87-kDa" myristoylated alanine-rich C kinase substrate: a major cellular substrate for protein kinase C. *Proc Natl Acad Sci U S A* (1989) **86**:4012–6. doi:10.1073/pnas.86.11.4012

32. Abdullah LH, Conway JD, Cohn JA, Davis CW. Protein kinase C and Ca2+ activation of mucin secretion in airway goblet cells. *Am J Physiol* (1997) **273**:L201–10.
33. Li Y, Martin LD, Spizz G, Adler KB. MARCKS protein is a key molecule regulating mucin secretion by human airway epithelial cells in vitro. *J Biol Chem* (2001) **276**:40982–90. doi:10.1074/jbc.M105614200
34. Singer M, Martin LD, Vargaftig BB, Park J, Gruber AD, Li Y, et al. A MARCKS-related peptide blocks mucus hypersecretion in a mouse model of asthma. *Nat Med* (2004) **10**:193–6. doi:10.1038/nm983
35. Agrawal A, Rengarajan S, Adler KB, Ram A, Ghosh B, Fahim M, et al. Inhibition of mucin secretion with MARCKS-related peptide improves airway obstruction in a mouse model of asthma. *J Appl Physiol* (2007) **102**:399–405. doi:10.1152/japplphysiol.00630.2006
36. Foster WM, Adler KB, Crews AL, Potts EN, Fischer BM, Voynow JA. MARCKS-related peptide modulates in vivo the secretion of airway Muc5ac. *Am J Physiol Lung Cell Mol Physiol* (2010) **299**:L345–52. doi:10.1152/ajplung.00067.2010
37. Ehre C, Zhu Y, Abdullah LH, Olsen J, Nakayama KI, Nakayama K, et al. nPKCepsilon, a P2Y2-R downstream effector in regulated mucin secretion from airway goblet cells. *Am J Physiol Cell Physiol* (2007) **293**:C1445–54. doi:10.1152/ajpcell.00051.2007
38. Park JA, Crews AL, Lampe WR, Fang S, Park J, Adler KB. Protein kinase C delta regulates airway mucin secretion via phosphorylation of MARCKS protein. *Am J Pathol* (2007) **171**:1822–30. doi:10.2353/ajpath.2007.070318
39. Park JA, He F, Martin LD, Li Y, Chorley BN, Adler KB. Human neutrophil elastase induces hypersecretion of mucin from well-differentiated human bronchial epithelial cells in vitro via a protein kinase C{delta}-mediated mechanism. *Am J Pathol* (2005) **167**:651–61. doi:10.1016/S0002-9440(10)62040-8
40. Park J, Fang S, Crews AL, Lin KW, Adler KB. MARCKS regulation of mucin secretion by airway epithelium in vitro: interaction with chaperones. *Am J Respir Cell Mol Biol* (2008) **39**:68–76. doi:10.1165/rcmb.2007-0139OC
41. Stahl B, Tobaben S, Sudhof TC. Two distinct domains in hsc70 are essential for the interaction with the synaptic vesicle cysteine string protein. *Eur J Cell Biol* (1999) **78**:375–81. doi:10.1016/S0171-9335(99)80079-X
42. Park J, Fang S, Adler KB. Regulation of airway mucin secretion by MARCKS protein involves the chaperones heat shock protein 70 and cysteine string protein. *Proc Am Thorac Soc* (2006) **3**:493. doi:10.1513/pats.200603-067MS
43. Raiford KL, Park J, Lin KW, Fang S, Crews AL, Adler KB. Mucin granule-associated proteins in human bronchial epithelial cells: the airway goblet cell "granulome". *Respir Res* (2011) **12**:118. doi:10.1186/1465-9921-12-118
44. Fang S, Crews AL, Chen W, Park J, Yin Q, Ren XR, et al. MARCKS and HSP70 interactions regulate mucin secretion by human airway epithelial cells in vitro. *Am J Physiol Lung Cell Mol Physiol* (2013) **304**:L511–8. doi:10.1152/ajplung.00337.2012
45. Lin KW, Fang S, Park J, Crews AL, Adler KB. MARCKS and related chaperones bind to unconventional myosin V isoforms in airway epithelial cells. *Am J Respir Cell Mol Biol* (2010) **43**:131–6. doi:10.1165/rcmb.2010-0016RC
46. Tuvim MJ, Mospan AR, Burns KA, Chua M, Mohler PJ, Melicoff E, et al. Synaptotagmin 2 couples mucin granule exocytosis to Ca2+ signaling from endoplasmic reticulum. *J Biol Chem* (2009) **284**:9781–7. doi:10.1074/jbc.M807849200
47. Jones LC, Moussa L, Fulcher ML, Zhu Y, Hudson EJ, O'Neal WK, et al. VAMP8 is a vesicle SNARE that regulates mucin secretion in airway goblet cells. *J Physiol* (2012) **590**:545–62.
48. Abdullah LH, Davis SW, Burch L, Yamauchi M, Randell SH, Nettesheim P, et al. P2u purinoceptor regulation of mucin secretion in SPOC1 cells, a goblet cell line from the airways. *Biochem J* (1996) **316**(Pt 3):943–51.
49. Danahay H, Atherton HC, Jackson AD, Kreindler JL, Poll CT, Bridges RJ. Membrane capacitance and conductance changes parallel mucin secretion in the human airway epithelium. *Am J Physiol Lung Cell Mol Physiol* (2006) **290**:L558–69. doi:10.1152/ajplung.00351.2005
50. Nguyen LP, Omoluabi O, Parra S, Frieske JM, Clement C, Ammar-Aouchiche Z, et al. Chronic exposure to beta-blockers attenuates inflammation and mucin content in a murine asthma model. *Am J Respir Cell Mol Biol* (2008) **38**:256–62. doi:10.1165/rcmb.2007-0279RC
51. Evans CM, Williams OW, Tuvim MJ, Nigam R, Mixides GP, Blackburn MR, et al. Mucin is produced by clara cells in the proximal airways of antigen-challenged mice. *Am J Respir Cell Mol Biol* (2004) **31**:382–94. doi:10.1165/rcmb.2004-0060OC
52. Davis CW, Dowell ML, Lethem M, Van Scott M. Goblet cell degranulation in isolated canine tracheal epithelium: response to exogenous ATP, ADP, and adenosine. *Am J Physiol* (1992) **262**:C1313–23.
53. Piccotti L, Dickey BF, Evans CM. Assessment of intracellular mucin content in vivo. *Methods Mol Biol* (2012) **842**:279–95. doi:10.1007/978-1-61779-513-8_17
54. Carr CM, Rizo J. At the junction of SNARE and SM protein function. *Curr Opin Cell Biol* (2010) **22**:488–95. doi:10.1016/j.ceb.2010.04.006
55. Sudhof TC, Rothman JE. Membrane fusion: grappling with SNARE and SM proteins. *Science* (2009) **323**:474–7. doi:10.1126/science.1161748
56. Kim K, Petrova YM, Scott BL, Nigam R, Agrawal A, Evans CM, et al. Munc18b is an essential gene in mice whose expression is limiting for secretion by airway epithelial and mast cells. *Biochem J* (2012) **446**:383–94. doi:10.1042/BJ20120057
57. Washbourne P, Thompson PM, Carta M, Costa ET, Mathews JR, Lopez-Bendito G, et al. Genetic ablation of the t-SNARE SNAP-25 distinguishes mechanisms of neuroexocytosis. *Nat Neurosci* (2002) **5**:19–26.
58. Suh YH, Terashima A, Petralia RS, Wenthold RJ, Isaac JT, Roche KW, et al. A neuronal role for SNAP-23 in postsynaptic glutamate receptor trafficking. *Nat Neurosci* (2010) **13**:338–43. doi:10.1038/nn.2488
59. Suh YH, Yoshimoto-Furusawa A, Weih KA, Tessarollo L, Roche KW, Mackem S, et al. Deletion of SNAP-23 results in pre-implantation embryonic lethality in mice. *PLoS One* (2011) **6**:e18444. doi:10.1371/journal.pone.0018444
60. Lazarowski ER, Boucher RC. Purinergic receptors in airway epithelia. *Curr Opin Pharmacol* (2009) **9**:262–7. doi:10.1016/j.coph.2009.02.004
61. Tarran R, Button B, Boucher RC. Regulation of normal and cystic fibrosis airway surface liquid volume by phasic shear stress. *Annu Rev Physiol* (2006) **68**:543–61. doi:10.1146/annurev.physiol.68.072304.112754
62. Young HW, Sun CX, Evans CM, Dickey BF, Blackburn MR. A3 adenosine receptor signaling contributes to airway mucin secretion after allergen challenge. *Am J Respir Cell Mol Biol* (2006) **35**:549–58. doi:10.1165/rcmb.2006-0060OC
63. Ribeiro CM, Paradiso AM, Livraghi A, Boucher RC. The mitochondrial barriers segregate agonist-induced calcium-dependent functions in human airway epithelia. *J Gen Physiol* (2003) **122**:377–87. doi:10.1085/jgp.200308893
64. Perez-Vilar J, Ribeiro CM, Salmon WC, Mabolo R, Boucher RC. Mucin granules are in close contact with tubular elements of the endoplasmic reticulum. *J Histochem Cytochem* (2005) **53**:1305–9. doi:10.1369/jhc.5B6713.2005
65. Pang ZP, Melicoff E, Padgett D, Liu Y, Teich AF, Dickey BF, et al. Synaptotagmin-2 is essential for survival and contributes to Ca2+ triggering of neurotransmitter release in central and neuromuscular synapses. *J Neurosci* (2006) **26**:13493–504. doi:10.1523/JNEUROSCI.3519-06.2006
66. Rossi AH, Sears PR, Davis CW. Ca2+ dependency of 'Ca2+-independent' exocytosis in SPOC1 airway goblet cells. *J Physiol* (2004) **559**:555–65. doi:10.1113/jphysiol.2004.070433
67. Koch H, Hofmann K, Brose N. Definition of Munc13-homology-domains and characterization of a novel ubiquitously expressed Munc13 isoform. *Biochem J* (2000) **349**:247–53. doi:10.1042/0264-6021:3490247
68. Chen Y, Zhao YH, Wu R. Differential regulation of airway mucin gene expression and mucin secretion by extracellular nucleotide triphosphates. *Am J Respir Cell Mol Biol* (2001) **25**:409–17. doi:10.1165/ajrcmb.25.4.4413
69. Kemp PA, Sugar RA, Jackson AD. Nucleotide-mediated mucin secretion from differentiated human bronchial epithelial cells. *Am J Respir Cell Mol Biol* (2004) **31**:446–55. doi:10.1165/rcmb.2003-0211OC
70. Kim KC, Lee BC. P2 purinoceptor regulation of mucin release by airway goblet cells in primary culture. *Br J Pharmacol* (1991) **103**:1053–6. doi:10.1111/j.1476-5381.1991.tb12299.x

71. Breuer R, Christensen TG, Lucey EC, Stone PJ, Snider GL. An ultrastructural morphometric analysis of elastase-treated hamster bronchi shows discharge followed by progressive accumulation of secretory granules. *Am Rev Respir Dis* (1987) **136**:698–703. doi:10.1164/ajrccm/136.3.698
72. Liu C, Li Q, Zhou X, Kolosov VP, Perelman JM. Human airway trypsin-like protease induces mucin5AC hypersecretion via a protease-activated receptor 2-mediated pathway in human airway epithelial cells. *Arch Biochem Biophys* (2013) **535**:234–40. doi:10.1016/j.abb.2013.02.013
73. Huang HT, Guo JJ, Huang YH, Fu YS. Histamine-induced changes in rat tracheal goblet cell mucin store and mucosal edema. *Histochem Cell Biol* (2013) **139**:717–26. doi:10.1007/s00418-012-1060-y
74. Guo JJ, Wang DS, Huang HT. Spontaneous remission of edema and regranulation of goblet cells in rat tracheae after capsaicin-induced acute inflammation. *Anat Embryol (Berl)* (2003) **206**:301–9.
75. Kuo HP, Rohde JA, Tokuyama K, Barnes PJ, Rogers DF. Capsaicin and sensory neuropeptide stimulation of goblet cell secretion in guinea-pig trachea. *J Physiol* (1990) **431**:629–41.
76. Leverkoehne I, Gruber AD. The murine mCLCA3 (alias gob-5) protein is located in the mucin granule membranes of intestinal, respiratory, and uterine goblet cells. *J Histochem Cytochem* (2002) **50**:829–38. doi:10.1177/002215540205000609
77. Lesimple P, Goepp J, Palmer ML, Fahrenkrug SC, O'Grady SM, Ferraro P, et al. CFTR is expressed in mucin granules from Calu-3 and primary human airway epithelial cells. *Am J Respir Cell Mol Biol* (2013) **49**. doi:10.1165/rcmb.2012-0419RC
78. Sesma JI, Kreda SM, Okada SF, van Heusden C, Moussa L, Jones LC, et al. Vesicular nucleotide transporter regulates the nucleotide content in airway epithelial mucin granules. *Am J Physiol Cell Physiol* (2013) **304**:C976–84. doi:10.1152/ajpcell.00371.2012

Conflict of Interest Statement: Kenneth B. Adler has an ownership interest in BioMarck Pharmaceuticals that is developing the MANS peptide for commercial use. Michael J. Tuvim and Burton F. Dickey have no potential conflicts of interest.

Received: 04 June 2013; accepted: 03 September 2013; published online: 18 September 2013.
*Citation: Adler KB, Tuvim MJ and Dickey BF (2013) Regulated mucin secretion from airway epithelial cells. Front. Endocrinol. **4**:129. doi: 10.3389/fendo.2013.00129*
This article was submitted to Neuroendocrine Science, a section of the journal Frontiers in Endocrinology.

frontiers in
NEUROSCIENCE

MINI REVIEW ARTICLE
published: 25 November 2013
doi: 10.3389/fnins.2013.00222

Super-resolution microscopy in studying neuroendocrine cell function

Anneka Bost[1], Mathias Pasche[2], Claudia Schirra[1] and Ute Becherer[1]*

[1] *Physiologisches Institut, Universität des Saarlandes, Homburg/Saar, Germany*
[2] *Division of Neurobiology, MRC Laboratory of Molecular Biology, Cambridge, UK*

Edited by:
Stephane Gasman, CNRS, France

Reviewed by:
Valentin Nägerl, Université Bordeaux Segalen, France
Corey Smith, Case Western Reserve University, USA

****Correspondence:***
Ute Becherer, Physiologisches Institut, Universität des Saarlandes, Kirrberger Strasse, Geb. 59, D-66421 Homburg/Saar, Germany
e-mail: ute.becherer@uks.eu

The last two decades have seen a tremendous development in high resolution microscopy techniques giving rise to acronyms such as TIRFM, SIM, PALM, STORM, and STED. The goal of all these techniques is to overcome the physical resolution barrier of light microscopy in order to resolve precise protein localization and possibly their interaction in cells. Neuroendocrine cell function is to secrete hormones and peptides on demand. This fine-tuned multi-step process is mediated by a large array of proteins. Here, we review the new microscopy techniques used to obtain high resolution and how they have been applied to increase our knowledge of the molecular mechanisms involved in neuroendocrine cell secretion. Further the limitations of these methods are discussed and insights in possible new applications are provided.

Keywords: chromaffin cell, membrane capacitance, amperometry, TIRFM, SIM, PALM, STORM, STED

INTRODUCTION

The main function of neuroendocrine cells, e.g., chromaffin cells, is the regulated release of hormones or peptides into the blood stream. This function is well documented in several reviews (Becherer and Rettig, 2006; Stevens et al., 2011; Jahn and Fasshauer, 2012; Kasai et al., 2012). Briefly, regulated exocytosis is a multi-step process controlled by calcium (**Figure 1A**). In order to fuse, large dense core vesicles (LDCVs) containing catecholamines approach the plasma membrane (PM) along actin filaments (Villanueva et al., 2012). They dock to the PM to the target-SNARE (t-SNARE) acceptor complex composed of syntaxin1 and SNAP-25, via synaptotagmin (de Wit, 2010). This process is controlled by Munc18 which acts at several steps during exocytosis (Rizo and Sudhof, 2012). After docking LDCVs undergo maturation reactions in which the vesicular SNAREs, vesicle associated membrane protein 2 and 3, also called synaptobrevin and cellubrevin, associate with the t-SNAREs to form the SNARE core complex. This reaction, that stably binds LDCVs to the PM, is regulated by a variety of proteins such as Ca^{2+}-dependent activator protein for secretion (CAPS), complexin, snapin or tomosyn (Becherer and Rettig, 2006). Upon increase of Ca^{2+} above a concentration of 0.5–0.9 μM, fusion is initiated by the interaction of synaptotagmin with the SNARE complex and the PM (Sudhof, 2012). Proteins such as complexin control this reaction. After exocytosis, the LDCV membrane and protein components are taken up via clathrin dependent endocytosis and processed through poorly understood recycling (Becherer et al., 2012). The development of this rather complex model of the exocytosic pathway was enabled by an array of innovative measurement methods that were applied to neuroendocrine cells.

METHODS TO STUDY CHROMAFFIN CELL FUNCTION

In neuroendocrine cells, regulated exocytosis has been studied since the late 1960s using biochemical methods (Schneider et al., 1967). Among other important findings, researchers were able to describe the Ca^{2+}-dependency of exocytosis (Pollard et al., 1982). The pace of research in this field greatly picked up with the launch of high time resolution measurement methods. In 1982 using patch-clamp electrophysiology, Neher and Marty (1982) were able to measure changes in the membrane capacitance of chromaffin cells that corresponded to either the addition (exocytosis) or subtraction (endocytosis) of vesicular membrane to the PM. Using complex depolarization protocols (Gillis et al., 1996; Voets et al., 1999) or flash photolysis of caged Ca^{2+} (Kaplan and Ellis-Davies, 1988; Neher and Zucker, 1993) it was possible to dissect four main functional pools of LDCVs termed reserve pool, unprimed pool (UPP), slowly releasable pool (SRP) and readily releasable pool (RRP) (**Figure 1B**1). It was hypothesized that LDCVs dock to join the UPP and that while priming occurs, LDCVs proceed in a sequential manner through SRP and RRP (Sorensen, 2004). The molecular machinery mediating these reactions was dissected using gain or loss of function assays (Becherer and Rettig, 2006). Ten years after establishing membrane capacitance recording, carbon fiber amperometry was developed (Wightman et al., 1991). With this technique the release of oxidizable neurotransmitters or hormones such as catecholamines from individual LDCVs can be measured with very high temporal resolution (Bruns and Jahn, 2002). The derived kinetics of release were used to identify proteins such as synaptobrevin, that play a role in fusion pore opening during exocytosis (Borisovska et al., 2005) (**Figure 1B**2). By combining carbon fiber amperometry with membrane capacitance recording, it was then possible to discriminate between exo- and endocytosis when they occur simultaneously (Borges et al., 2008). Furthermore, this combination was instrumental in uncovering the role of for example CAPS in loading LDCVs with catecholamines (Speidel et al., 2005).

The main limitation of both methods is that they measure directly the very last step of exocytosis and they provide only little

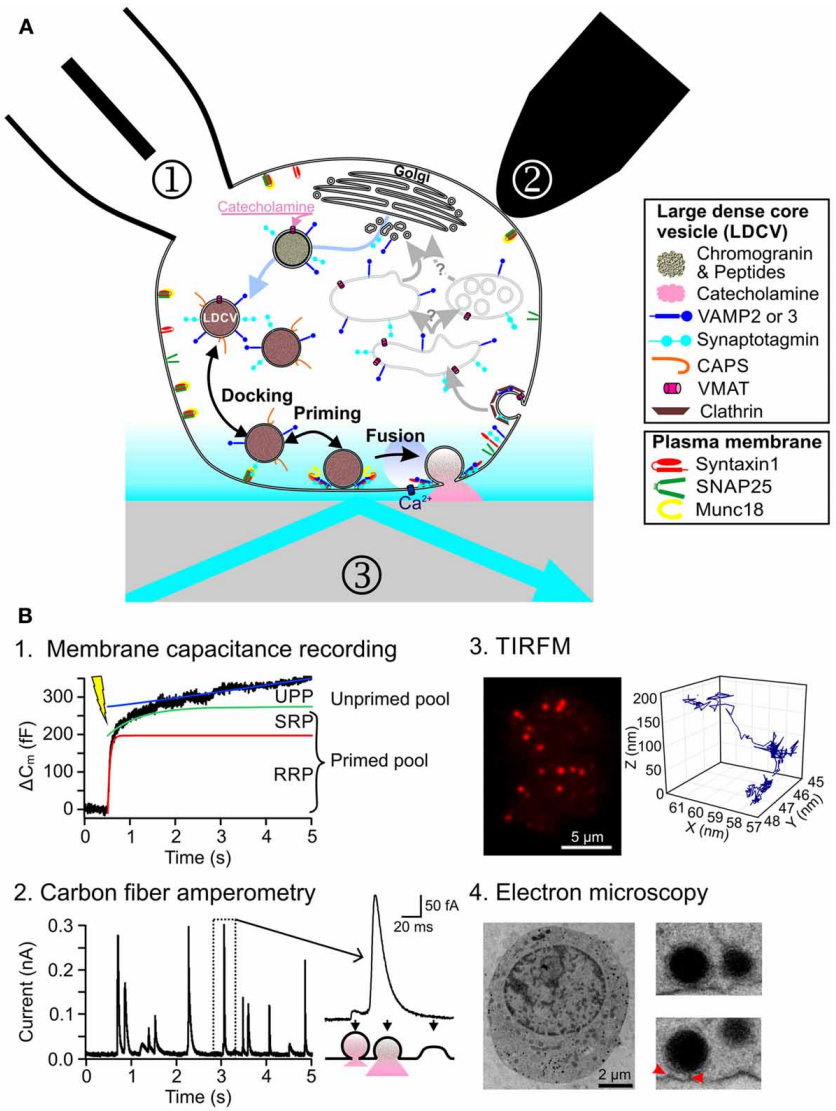

FIGURE 1 | Current methods to study regulated exocytosis in chromaffin cells. (A) Model of regulated exocytosis in chromaffin cells depicting a number of proteins involved in the process. Exocytosis of LDCVs can be monitored by ① membrane capacitance through patch clamp electrophysiology, ② carbon fiber amperometry and ③ TIRFM. **(B)** Example of exocytosis measurement in chromaffin cells. (B1) Representative trace of a membrane capacitance recording in which exocytosis was induced by flash photolysis of caged Ca^{2+}. Three functional pools can be determined by fitting the data with 3 components: a fast exponential (RRP, red line), a slow exponential (SRP, green line) and a linear regression (UPP, blue line). (B2) Release of catecholamines from single LDCVs can be observed as individual spikes by carbon fiber amperometry (left). The spike shape provides information about the fusion pore opening (right). (B3) TIRFM picture of a bovine chromaffin cell expressing NPY-mCherry (left). Due to the high signal to noise ratio, the LDCVs can easily be seen as individual spots. They can be tracked over time thus revealing a complex behavior (right). (B4) Electron micrograph of an embryonic mouse chromaffin cell, fixed using high-pressure freezing method (left). The close up of some LDCVs shows astounding morphological details (right). Red arrows indicate fine tethers that appear to bridge the LDCV and the plasma membrane.

information about docking. Electron microscopy (EM) is therefore often used to complement this information (Ashery et al., 2000; Yizhar et al., 2004; de Wit et al., 2009). Vesicles are considered morphologically docked if they are touching the PM or located within 30 nm distance to the PM (Verhage and Sorensen, 2008; de Wit, 2010). These vesicles can belong to all three functional pools UPP, SRP or RRP. The development of a fixation method involving high-pressure freezing produced nearly artifact free, highly preserved cell morphology (Studer et al., 2001; Vanhecke et al., 2008). Electron micrographs of chromaffin cells fixed with this method, revealed fine structures at the contact regions between LDCVs and the PM, which might correspond to assembled SNARE proteins (**Figure 1B**4). Due to this increased resolution a new morphological classification was introduced of docked and tethered vesicles (Verhage and Sorensen, 2008). Until now it was not possible to clearly associate a functional pool to those two morphologically different pools of LDCVs, thereby generating quite some confusion in the field.

In the 1990s total internal reflection fluorescence microscopy (TIRFM) was first introduced in the field of exocytosis (Axelrod, 1981; Steyer et al., 1997; Oheim et al., 1998; Oheim and Stuhmer, 2000). It is used to visualize individual LDCVs approaching the PM and their fusion. The principal feature of TIRFM is that a thin evanescent field of light with decaying exponential excitation energy is generated at the interface of the glass coverslip and the cell. Thus, excitation of fluorophores is restricted to a shallow layer close to the PM (**Figure 1B**3). This technique provides an axial (z) resolution well below 100 nm, while the lateral (x, y) resolution is about 250 nm. The highly contrasted pictures of individual fluorescently labeled LDCVs and the possibility to follow them over time raised very high expectations that TIRFM would provide profound insights in the molecular machinery of docking and priming (Steyer et al., 1997; Oheim and Stuhmer, 2000; Johns et al., 2001). This turned out to be much more complex than originally anticipated (Oheim and Stuhmer, 2000; Nofal et al., 2007). TIRFM helped to understand the role of Munc18-1 (Toonen et al., 2006) and Ca^{2+} (Pasche et al., 2012) during docking, and the function of tomosyn in priming (Yizhar and Ashery, 2008).

Taken together, using a combination of membrane capacitance recording, carbon fiber amperometry and EM very effectively uncovered the function of several proteins, such as the SNARE proteins or Munc13, which play a role at only one step of exocytosis in chromaffin cells. TIRFM helped to examine the function of certain proteins or substances, such as Munc18 or Ca^{2+}, that mediate several steps of exocytosis. However, the results of these studies become more and more complex to interpret as we investigate the role of proteins that appear to be involved throughout exocytosis, e.g., Synaptotagmin. The question is whether super-resolution microscopy can help in this quest by providing a link between morphological (EM) and functional data (membrane capacitance recording, carbon fiber amperometry or TIRFM).

SUPER-RESOLUTION MICROSCOPY

The aim of super-resolution microscopy is to provide similar resolution as EM but with light microscopy. In light microscopy the wave-like nature of light limits spatial resolution to half the wavelength of the observed light. This so called diffraction barrier was established by Ernst Abbé 140 years ago and is expressed by the formula:

$$d = \frac{\lambda}{2(n \sin\theta)}$$

(with d the diameter of the spot generated by light of the wavelength λ that travels in a medium with refractive index n and converges with an angle θ).

All microscopy technologies developed at the end of the twentieth century, such as confocal microscopy or TIRFM, improve the signal-to-noise ratio and thus produced highly contrasted and crisp images that showed a wealth of unprecedented details, but the resolution was still diffraction limited. An early approach was to use deconvolution algorithms to subtract the predicted point spread function (PSF) of individual fluorophores from the image and thus to reduce the contribution of diffracted light. This technique produces images with even better signal-to-noise ratio, but the resolution improvement is modest. Furthermore, due to the use of flawed PSFs, this technique is prone to generate artifacts like non existing signal patterns. The new super-resolution microscopy methods have addressed most of these problems and can achieve a resolution down to 10 nm (Hell, 2009; Dani and Huang, 2010; Tonnesen and Nagerl, 2013a).

STRUCTURED ILLUMINATION MICROSCOPY (SIM)

SIM achieves super-resolution by extracting fine structural details from the interference of a structure with predetermined illumination patterns. When a periodic illumination pattern, such as stripes, is applied to a fluorescent sample, an interference pattern is generated. The diffraction-limited fringes of this interference pattern, called moiré fringes, contain information about underlying structural pattern of the sample that cannot be observed with conventional light microscopy. By shifting and rotating the illumination pattern, sub-diffraction-limited structural information of the sample can be extracted from Fourier transformations of the resulting interference pattern (Gustafsson, 2000; Heintzmann et al., 2002) (**Figure 2A**). This produces a doubling of both lateral and axial resolution reaching 100 and 300 nm, respectively. The resolution of the calculated image depends on the number of unique raw images acquired with different diffraction patterns/orientations. In order to generate a single plane highly resolved image a minimum of 15 different illumination patterns have to be applied. Currently, the minimum time required for this acquisition is about 300 ms for a single plane and about 8 s for 7 μm thick chromaffin cells (Shao et al., 2011). This time frame is incompatible for life imaging of fast moving structures like LDCVs. However, it can easily be used to visualize 3D distribution of LDCVs in fixed cells without the need of lengthy procedures used in EM. Furthermore, it allows performing precise colocalization studies (Fiolka et al., 2012) in immune cells (Brown et al., 2011; Pattu et al., 2011; Matti et al., 2013) and neurons (Pielage et al., 2008; Sheets et al., 2012; Khuong et al., 2013) that might help to uncover interactions between proteins.

PHOTOACTIVATED LOCALIZATION MICROSCOPY (PALM) AND STOCHASTIC OPTICAL RECONSTRUCTION MICROSCOPY (STORM)

In PALM or STORM the resolution has been improved to much greater extent since they provide a lateral resolution of 10–30 nm and about 50 nm axial resolution (Betzig et al., 2006; Hess et al., 2006; Rust et al., 2006; Huang et al., 2008; Tatavarty et al., 2009; Shim et al., 2012). Both PALM and STORM rely on the property of certain fluorophores that can be photoactivated and switched on and off alternately (Folling et al., 2008; Shim et al., 2012). PALM relies on photoactivated fluorescent proteins (Betzig et al., 2006; Hess et al., 2006) while STORM, also called direct STORM (dSTORM), was developed using cyanide dyes (Bates et al., 2005; Rust et al., 2006; Heilemann et al., 2008). To generate super-resolved images, the fluorescence of the sample is first entirely quenched with the normal excitation wavelength of the fluorophore, converting it from a ground state to a metastable dark state. Then fluorescence is slowly reactivated, either by itself or by a mild illumination with light at 405 nm (**Figure 2B**).

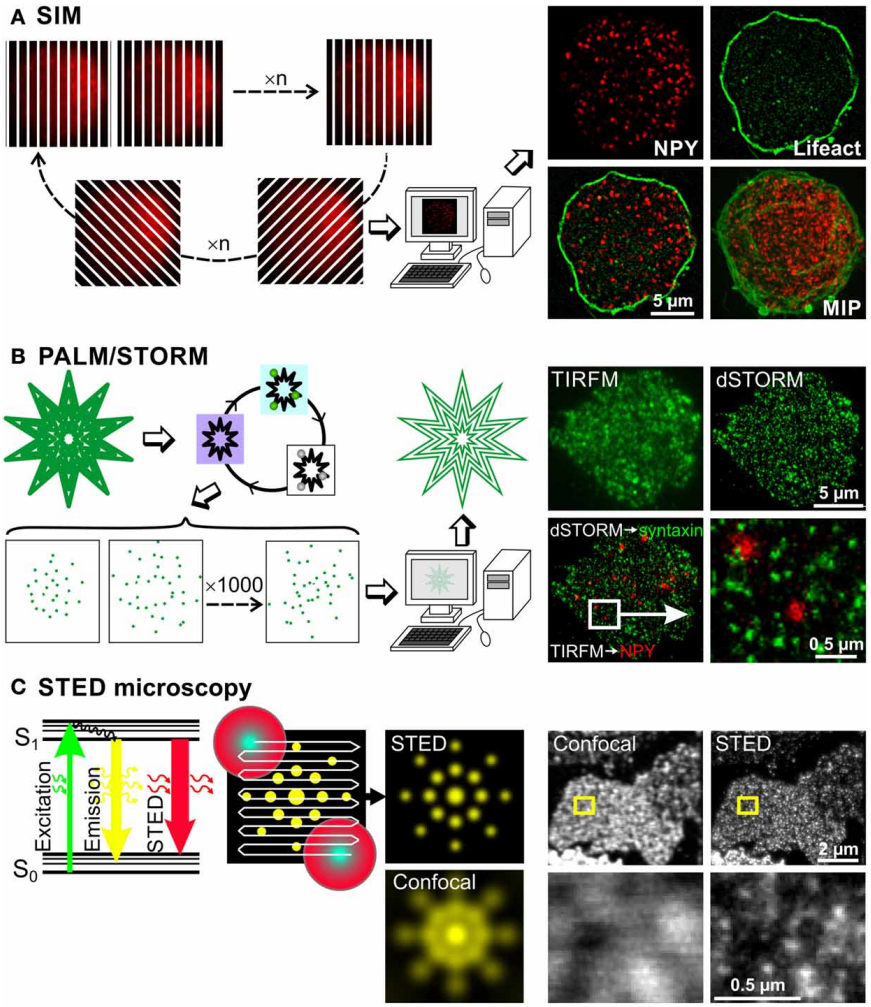

FIGURE 2 | Super-resolution microscopy methods to investigate chromaffin cell function. Basic principles of three super-resolution microscopy methods are depicted on the left, while some exemplary images using the respective technique are shown on the right. **(A)** In SIM microscopy a stripe pattern of light, which is shifted and rotated, is applied to the cell, so that the entire cell is illuminated within several images. These images contain sub-diffraction-limited structural information, which is extracted via computer processing using Fourier transformations. Resulting images have a lateral and axial resolution of 100 and 300 nm, respectively. This can be appreciated on images of a bovine chromaffin cell, expressing NPY-mCherry and Lifeact-GFP labeling LDCVs and the F-actin, respectively. MIP: maximum intensity projection. **(B)** The principle of PALM and STORM exploit the properties of certain fluorophores that can be switched on and off. At first, all the fluorophores are pushed in a metastable dark state by illuminating them with their specific excitation light. Then, few molecules are brought back to the ground state using a mild illumination at usually 405 nm and visualized using their excitation light, which switches them off again. These cycles are repeated up to 10,000 times generating a movie of blinking fluorophores. The labeled structure is then reconstituted by plotting their exact calculated position. This method generates images with lateral resolution of 10 to 30 nm. This is shown on pictures of a bovine chromaffin cell. The LDCVs were marked by NPY-mCherry overexpression via Semliki Forest virus (shown in red) and the native syntaxin1 (shown in green) was labeled via monoclonal antibody (Synaptic Systems GmbH) and Alexa 647 anti-mouse secondary antibody (Invitrogen). The gain of resolution can clearly be appreciated by comparing the pictures of syntaxin1 acquired with TIRFM and the picture of the same cell acquired with dSTORM. Due to dSTORM resolution, we observed that LDCVs were usually not located on syntaxin1 clusters. **(C)** As can be seen on the Jablonski diagram, the energy of an excited fluorescent molecule can be completely depleted by a photon that matches the energy difference between its excited (S1) and the ground electronic state (S0) before spontaneous fluorescence emission occurs. This process effectively depletes the S1 state of a fluorescent molecule by using a depleting laser that has high photon density, and a higher wavelength than the emission wavelength of the fluorophore. In this example a fluorescent protein such as YFP is excited at 514 nm and releases its fluorescent light at around 520 nm. The stimulated emitted photons are not visible for the light detector (photomultiplier tube, avalanche photodiode) as they travel in the same direction as the stimulating laser beam but good emission filters are needed to block scattered light. Using this technique a STED beam consisting of a beam at the excitation wavelength surrounded by a donut shaped red light beam is applied to the probe. Normal emission occurs only from the central spot thus defining the size of the measured voxel. The STED beam scans the entire probe and the super resolved image is generated online. The lateral resolution is generally 20–50 nm. This very high resolution can be appreciated on the images taken from Sieber et al. (2006) in which syntaxin1 was visualized using antibody labeling on membrane sheets generated from syntaxin1 overexpressing PC12 cells. Images in the lower row correspond to a magnification of the small yellow square drawn on the images in the upper row.

Importantly, not all the fluorescence is reactivated simultaneously, instead individual fluorophores are activated stochastically over time. They are visualized by the normal excitation light, which also brings them back in the dark state. A movie of blinking fluorescent molecules is then acquired over several minutes. Their position can be precisely determined using a simple Gaussian fit algorithm, as long as their fluorescent signals do not overlap. The quality of the position determination and thus of the final image resolution depends on the signal-to-noise ratio of the original image, on the internal jittering of the microscope and on the labeling density of the marked structure. The super-resolution image is then reconstructed by plotting the peak position of all blinking molecules. Depending on the sample size and the staining quality, 100 to 10,000 images have to be acquired to reconstruct one single image. Due to the large number of images that need to be recorded and their lengthy processing, this technique is not applicable to life cell imaging. However, PALM was recently used to follow single fluorescent proteins over time in living cells (Tatavarty et al., 2009; Izeddin et al., 2011; Sochacki et al., 2012). When comparing PALM to STORM, both produce images with similar resolution although STORM relies on antibody labeling which increases the length between the protein of interest and the fluorescent label (but see Ries et al., 2012). Furthermore, in STORM a toxic reducing buffer is used to reactivate the cyanide fluorophore (but see Klein et al., 2011). On the other hand, PALM relies on the overexpression of proteins tagged to individual fluorescent proteins, thus overexpression artifacts can occur. In brief, despite their respective weakness, PALM and STORM clearly close the gap between EM and light microscopy. They allow very precise localization of proteins in the cell without the need of complex immunogold techniques (Mennella et al., 2012; Macgillavry et al., 2013).

STIMULATED EMISSION DEPLETION (STED) MICROSCOPY

In contrast to the aforementioned super-resolution microscopy techniques, STED microscopy does not rely on post processing of blurry raw images but rather uses a specific illumination method and photo-physics to generate directly highly resolved images. In STED microscopy the excited fluorescent dye molecules return to the ground state (S0, **Figure 2C**) via the process of stimulated emission, which is induced by a STED laser beam. The wavelength of the STED beam is at the tail end of the emission spectrum of the dye, where it does not excite the dye and where it can be spectrally separated from the spontaneous fluorescence. The fluorescence quenching scales with the intensity of the STED laser beam. The trick is to focus a depletion laser into a donut shape and superimpose this onto the focused laser excitation spot (**Figure 2C** middle). The spot in the middle of the donut, from which the normal emission occurs, can be made as small as 5.8 nm in diameter (Rittweger et al., 2009) but is usually 20 to 50 nm large. The emission depletion light beam can also be formed in an elongated spherical shape to limit the emission to a volume of 45 nm lateral and 108 nm axial resolution (Wildanger et al., 2009). The generation of an image is similar to classical confocal microscopy but due to the very small voxel size, the scanning speed is relatively slow. Improved hardware allowed the reduction of the excitation beam power and the implementation of live imaging. In 2008, Westphal et al. (2008) visualized moving recycling synaptic vesicles labeled with antibody and in the same year the technique was further adapted to visualize fluorescent proteins in living cells (Hein et al., 2008; Nagerl et al., 2008). Other developments made dual color imaging possible enabling colocalization studies (Donnert et al., 2007; Pellett et al., 2011; Tonnesen et al., 2011). STED provides a resolution that is comparable to EM to identify fine structures, such as Bruchpilot, at the active zone of the drosophila neuromuscular junction (Kittel et al., 2006) or dynamic changes of dendritic spines (Nagerl and Bonhoeffer, 2010; Blom et al., 2011; Urban et al., 2011; Tonnesen and Nagerl, 2013b).

SUPER-RESOLUTION MICROSCOPY TO STUDY CHROMAFFIN CELLS: PRESENT AND FUTURE

The impact of super-resolution microscopy in the field of neuroendocrinology is just about to spark. STED microscopy has been used to verify that the size of LDCVs was unaltered upon overexpression of a mutated Munc18-1 in neuroendocrine cells (Jorgacevski et al., 2011). SIM was applied to show that a mutated form of synaptobrevin was correctly sorted to LDCVs upon overexpression in mouse chromaffin cells (Borisovska et al., 2012). Furthermore, SIM was used to reveal that the cellular distribution of NPY-mCherry labeled LDCVs was normal and that it was not affected by t-SNARE and Munc18-2 overexpression (Hugo et al., 2013). PALM was used to uncover the size and the shape of clathrin coated pits in PC12 cells during reuptake of vesicular acetylcholine transporters (Sochacki et al., 2012). However, super-resolution microscopy has primarily been used to examine clustering of syntaxin1 and SNAP 25 in the PM. The morphology and the dynamics of syntaxin1 clusters were studied in cracked open PC12 cells using STED (Sieber et al., 2007). In contrast to what was shown using confocal microscopy, Lopez et al. (2009) and Bar-On et al. (2012) used PALM to demonstrate that syntaxin1 and SNAP-25 clusters have a different morphology and that their colocalization is weak in PC12 cells. Additionally, PALM helped to establish that clustered SNARE proteins are not involved in LDCV docking or fusion (Yang et al., 2012). Using a very elegant combination of STED microscopy and Förster resonance energy transfer (FRET) Rickman et al. (2010) showed that overlapping t-SNARE clusters can contain fully assembled t-SNARE acceptor complexes. Finally, PIP2 and PIP3 clustering, that are believed to play a role in the t-SNARE organization, have been investigated using STORM (Wang and Richards, 2012).

Super-resolution microscopy will help us to understand the detailed molecular interactions in chromaffin cells function. As discussed in the introduction, one crucial issue is to clearly demonstrate the correlation between the functional and the morphological data on docking. Another important aspect in chromaffin cell research is to uncover at which time point during the exocytotic process, docking and priming factors bind to the release machinery of LDCVs. FRET is the tool of choice to demonstrate protein interactions in living cells. However, with the remarkable exceptions of Lam et al. (2010) and Zhao et al. (2013), several relatively inconclusive trials using FRET were made to study the interaction of the SNAREs during exocytosis. Thus, it is unlikely that FRET can be used to study the interaction of

priming or docking factors with either the LDCVs or the SNARE core complex. One solution to address these problems might be to use a combination of super-resolution microscopy and EM, doing correlative light-electron microscopy (Sjollema et al., 2012). This technique will help us to uncover a relationship between the distance of LDCVs to the plasma membrane and their association with any of these proteins. Finally, aspects of LDCV biogenesis or protein recycling might be better understood using methods such as SIM in combination with molecular manipulations such as gene deletion or protein overexpression.

ACKNOWLEDGMENTS

Research in our lab has been funded by grants from the Deutsche Forschungsgemeinschaft (SFB 530 and SFB 894) and by competitive, local funding of the Saarland University.

REFERENCES

Ashery, U., Varoqueaux, F., Voets, T., Betz, A., Thakur, P., Koch, H., et al. (2000). Munc13-1 acts as a priming factor for large dense-core vesicles in bovine chromaffin cells. *EMBO J.* 19, 3586–3596. doi: 10.1093/emboj/19.14.3586

Axelrod, D. (1981). Cell-substrate contacts illuminated by total internal reflection fluorescence. *J. Cell Biol.* 89, 141–145. doi: 10.1083/jcb.89.1.141

Bar-On, D., Wolter, S., van de Linde, S., Heilemann, M., Nudelman, G., Nachliel, E., et al. (2012). Super-resolution imaging reveals the internal architecture of nano-sized syntaxin clusters. *J. Biol. Chem.* 287, 27158–27167. doi: 10.1074/jbc.M112.353250

Bates, M., Blosser, T. R., and Zhuang, X. (2005). Short-range spectroscopic ruler based on a single-molecule optical switch. *Phys. Rev. Lett.* 94, 108101. doi: 10.1103/PhysRevLett.94.108101

Becherer, U., Medart, M. R., Schirra, C., Krause, E., Stevens, D., and Rettig, J. (2012). Regulated exocytosis in chromaffin cells and cytotoxic T lymphocytes: how similar are they? *Cell Calcium* 52, 303–312. doi: 10.1016/j.ceca.2012.04.002

Becherer, U., and Rettig, J. (2006). Vesicle pools, docking, priming, and release. *Cell Tissue Res.* 326, 393–407. doi: 10.1007/s00441-006-0243-z

Betzig, E., Patterson, G. H., Sougrat, R., Lindwasser, O. W., Olenych, S., Bonifacino, J. S., et al. (2006). Imaging intracellular fluorescent proteins at nanometer resolution. *Science* 313, 1642–1645. doi: 10.1126/science.1127344

Blom, H., Ronnlund, D., Scott, L., Spicarova, Z., Widengren, J., Bondar, A., et al. (2011). Spatial distribution of Na+-K+-ATPase in dendritic spines dissected by nanoscale superresolution STED microscopy. *BMC Neurosci.* 12:16. doi: 10.1186/1471-2202-12-16

Borges, R., Camacho, M., and Gillis, K. D. (2008). Measuring secretion in chromaffin cells using electrophysiological and electrochemical methods. *Acta Physiol. (Oxf.)* 192, 173–184. doi: 10.1111/j.1748-1716.2007.01814.x

Borisovska, M., Schwarz, Y. N., Dhara, M., Yarzagaray, A., Hugo, S., Narzi, D., et al. (2012). Membrane-proximal tryptophans of synaptobrevin II stabilize priming of secretory vesicles. *J. Neurosci.* 32, 15983–15997. doi: 10.1523/JNEUROSCI.6282-11.2012

Borisovska, M., Zhao, Y., Tsytsyura, Y., Glyvuk, N., Takamori, S., Matti, U., et al. (2005). v-SNAREs control exocytosis of vesicles from priming to fusion. *EMBO J.* 24, 2114–2126. doi: 10.1038/sj.emboj.7600696

Brown, A. C. N., Oddos, S., Dobbie, I. M., Alakoskela, J., Parton, R. M., Eissmann, P., et al. (2011). Remodelling of Cortical Actin Where Lytic Granules Dock at Natural Killer Cell Immune Synapses Revealed by Super-Resolution Microscopy. *PLoS Biol.* 9:e1001152. doi: 10.1371/journal.pbio.1001152

Bruns, D., and Jahn, R. (2002). Molecular determinants of exocytosis. *Pflugers Arch.* 443, 333–338. doi: 10.1007/s00424-001-0742-4

Dani, A., and Huang, B. (2010). New resolving power for light microscopy: applications to neurobiology. *Curr. Opin. Neurobiol.* 20, 648–652. doi: 10.1016/j.conb.2010.07.006

de Wit, H. (2010). Morphological docking of secretory vesicles. *Histochem. Cell Biol.* 134, 103–113. doi: 10.1007/s00418-010-0719-5

de Wit, H., Walter, A. M., Milosevic, I., Gulyas-Kovacs, A., Riedel, D., Sorensen, J. B., et al. (2009). Synaptotagmin-1 docks secretory vesicles to syntaxin-1/SNAP-25 acceptor complexes. *Cell* 138, 935–946. doi: 10.1016/j.cell.2009.07.027

Donnert, G., Keller, J., Wurm, C. A., Rizzoli, S. O., Westphal, V., Schonle, A., et al. (2007). Two-color far-field fluorescence nanoscopy. *Biophys. J.* 92, L67–L69. doi: 10.1529/biophysj.107.104497

Fiolka, R., Shao, L., Rego, E. H., Davidson, M. W., and Gustafsson, M. G. L. (2012). Time-lapse two-color 3D imaging of live cells with doubled resolution using structured illumination. *Proc. Natl. Acad. Sci. U.S.A.* 109, 5311–5315. doi: 10.1073/pnas.1119262109

Folling, J., Bossi, M., Bock, H., Medda, R., Wurm, C. A., Hein, B., et al. (2008). Fluorescence nanoscopy by ground-state depletion and single-molecule return. *Nat. Methods* 5, 943–945. doi: 10.1038/nmeth.1257

Gillis, K. D., Mossner, R., and Neher, E. (1996). Protein kinase C enhances exocytosis from chromaffin cells by increasing the size of the readily releasable pool of secretory granules. *Neuron* 16, 1209–1220. doi: 10.1016/S0896-6273(00)80147-6

Gustafsson, M. G. (2000). Surpassing the lateral resolution limit by a factor of two using structured illumination microscopy. *J. Microsc.* 198, 82–87. doi: 10.1046/j.1365-2818.2000.00710.x

Heilemann, M., van de Linde, S., Schüttpelz, M., Kasper, R., Seefeldt, B., Mukherjee, A., et al. (2008). Subdiffraction-resolution fluorescence imaging with conventional fluorescent probes. *Angew. Chem. Int. Ed. Engl.* 47, 6172–6176. doi: 10.1002/anie.200802376

Hein, B., Willig, K. I., and Hell, S. W. (2008). Stimulated emission depletion (STED) nanoscopy of a fluorescent protein-labeled organelle inside a living cell. *Proc. Natl. Acad. Sci. U.S.A.* 105, 14271–14276. doi: 10.1073/pnas.0807705105

Heintzmann, R., Jovin, T. M., and Cremer, C. (2002). Saturated patterned excitation microscopy–a concept for optical resolution improvement. *J. Opt. Soc. Am. A Opt. Image Sci. Vis.* 19, 1599–1609. doi: 10.1364/JOSAA.19.001599

Hell, S. W. (2009). Microscopy and its focal switch. *Nat. Methods* 6, 24–32. doi: 10.1038/nmeth.1291

Hess, S. T., Girirajan, T. P., and Mason, M. D. (2006). Ultra-high resolution imaging by fluorescence photoactivation localization microscopy. *Biophys. J.* 91, 4258–4272. doi: 10.1529/biophysj.106.091116

Huang, B., Wang, W., Bates, M., and Zhuang, X. (2008). Three-dimensional super-resolution imaging by stochastic optical reconstruction microscopy. *Science* 319, 810–813. doi: 10.1126/science.1153529

Hugo, S., Dembla, E., Halimani, M., Matti, U., Rettig, J., and Becherer, U. (2013). Deciphering dead-end docking of large dense core vesicles in bovine chromaffin cells. *J. Neurosci.* 33, 17123–17137. doi: 10.1523/JNEUROSCI.1589-13.2013

Izeddin, I., Specht, C. G., Lelek, M., Darzacq, X., Triller, A., Zimmer, C., et al. (2011). Super-resolution dynamic imaging of dendritic spines using a low-affinity photoconvertible actin probe. *PLoS ONE* 6:e15611. doi: 10.1371/journal.pone.0015611

Jahn, R., and Fasshauer, D. (2012). Molecular machines governing exocytosis of synaptic vesicles. *Nature* 490, 201–207. doi: 10.1038/nature11320

Johns, L. M., Levitan, E. S., Shelden, E. A., Holz, R. W., and Axelrod, D. (2001). Restriction of secretory granule motion near the plasma membrane of chromaffin cells. *J. Cell Biol.* 153, 177–190. doi: 10.1083/jcb.153.1.177

Jorgacevski, J., Potokar, M., Grilc, S., Kreft, M., Liu, W., Barclay, J. W., et al. (2011). Munc18-1 tuning of vesicle merger and fusion pore properties. *J. Neurosci.* 31, 9055–9066. doi: 10.1523/JNEUROSCI.0185-11.2011

Kaplan, J. H., and Ellis-Davies, G. C. (1988). Photolabile chelators for the rapid photorelease of divalent cations. *Proc. Natl. Acad. Sci. U.S.A.* 85, 6571–6575. doi: 10.1073/pnas.85.17.6571

Kasai, H., Takahashi, N., and Tokumaru, H. (2012). Distinct initial SNARE configurations underlying the diversity of exocytosis. *Physiol. Rev.* 92, 1915–1964. doi: 10.1152/physrev.00007.2012

Khuong, T. M., Habets, R. L., Kuenen, S., Witkowska, A., Kasprowicz, J., Swerts, J., et al. (2013). Synaptic PI(3, 4, 5)P3 is required for Syntaxin1A clustering and neurotransmitter release. *Neuron* 77, 1097–1108. doi: 10.1016/j.neuron.2013.01.025

Kittel, R. J., Wichmann, C., Rasse, T. M., Fouquet, W., Schmidt, M., Schmid, A., et al. (2006). Bruchpilot promotes active zone assembly, Ca^{2+} channel clustering, and vesicle release. *Science* 312, 1051–1054. doi: 10.1126/science.1126308

Klein, T., Löschberger, A., Proppert, S., Wolter, S., van de Linde, S., and Sauer, M. (2011). Live-cell dSTORM with SNAP-tag fusion proteins. *Nat. Methods* 8, 7–9. doi: 10.1038/nmeth0111-7b

Lam, A. D., Ismail, S., Wu, R., Yizhar, O., Passmore, D. R., Ernst, S. A., et al. (2010). Mapping dynamic protein interactions to insulin secretory granule behavior with TIRF-FRET. *Biophys. J.* 99, 1311–1320. doi: 10.1016/j.bpj.2010.06.014

Lopez, I., Ortiz, J. A., Villanueva, J., Torres, V., Torregrosa-Hetland, C. J., del Mar Frances, M., et al. (2009). Vesicle Motion and Fusion are Altered in Chromaffin Cells with Increased SNARE Cluster Dynamics. *Traffic* 10, 172–185. doi: 10.1111/j.1600-0854.2008.00861.x

Macgillavry, H. D., Song, Y., Raghavachari, S., and Blanpied, T. A. (2013). Nanoscale Scaffolding Domains within the Postsynaptic Density Concentrate Synaptic AMPA Receptors. *Neuron* 78, 615–622. doi: 10.1016/j.neuron.2013.03.009

Matti, U., Pattu, V., Halimani, M., Schirra, C., Krause, E., Liu, Y., et al. (2013). Synaptobrevin2 is the v-SNARE required for cytotoxic T-lymphocyte lytic granule fusion. *Nat. Commun.* 4:1439. doi: 10.1038/ncomms2467

Mennella, V., Keszthelyi, B., McDonald, K. L., Chhun, B., Kan, F., Rogers, G. C., et al. (2012). Subdiffraction-resolution fluorescence microscopy reveals a domain of the centrosome critical for pericentriolar material organization. *Nat. Cell Biol.* 14, 1159–1168. doi: 10.1038/ncb2597

Nagerl, U. V., and Bonhoeffer, T. (2010). Imaging living synapses at the nanoscale by STED microscopy. *J. Neurosci.* 30, 9341–9346. doi: 10.1523/JNEUROSCI.0990-10.2010

Nagerl, U. V., Willig, K. I., Hein, B., Hell, S. W., and Bonhoeffer, T. (2008). Live-cell imaging of dendritic spines by STED microscopy. *Proc. Natl. Acad. Sci. U.S.A.* 105, 18982–18987. doi: 10.1073/pnas.0810028105

Neher, E., and Marty, A. (1982). Discrete changes of cell membrane capacitance observed under conditions of enhanced secretion in bovine adrenal chromaffin cells. *Proc. Natl. Acad. Sci. U.S.A.* 79, 6712–6716. doi: 10.1073/pnas.79.21.6712

Neher, E., and Zucker, R. S. (1993). Multiple calcium-dependent processes related to secretion in bovine chromaffin cells. *Neuron* 10, 21–30. doi: 10.1016/0896-6273(93)90238-M

Nofal, S., Becherer, U., Hof, D., Matti, U., and Rettig, J. (2007). Primed vesicles can be distinguished from docked vesicles by analyzing their mobility. *J. Neurosci.* 27, 1386–1395. doi: 10.1523/JNEUROSCI.4714-06.2007

Oheim, M., Loerke, D., Stuhmer, W., and Chow, R. H. (1998). The last few milliseconds in the life of a secretory granule. Docking, dynamics and fusion visualized by total internal reflection fluorescence microscopy (TIRFM). *Eur. Biophys. J.* 27, 83–98. doi: 10.1007/s002490050114

Oheim, M., and Stuhmer, W. (2000). Tracking chromaffin granules on their way through the actin cortex. *Eur. Biophys. J.* 29, 67–89. doi: 10.1007/s002490050253

Pasche, M., Matti, U., Hof, D., Rettig, J., and Becherer, U. (2012). Docking of LDCVs is modulated by lower intracellular $[Ca^{2+}]$ than priming. *PLoS ONE* 7:e36416. doi: 10.1371/journal.pone.0036416

Pattu, V., Qu, B., Marshall, M., Becherer, U., Junker, C., Matti, U., et al. (2011). Syntaxin7 Is Required for Lytic Granule Release from Cytotoxic T Lymphocytes. *Traffic* 12, 890–901. doi: 10.1111/j.1600-0854.2011.01193.x

Pellett, P. A., Sun, X., Gould, T. J., Rothman, J. E., Xu, M. Q., Correa, I. R. Jr, et al. (2011). Two-color STED microscopy in living cells. *Biomed. Opt. Express* 2, 2364–2371. doi: 10.1364/BOE.2.002364

Pielage, J., Cheng, L., Fetter, R. D., Carlton, P. M., Sedat, J. W., and Davis, G. W. (2008). A presynaptic giant ankyrin stabilizes the NMJ through regulation of presynaptic microtubules and transsynaptic cell adhesion. *Neuron* 58, 195–209. doi: 10.1016/j.neuron.2008.02.017

Pollard, H. B., Creutz, C. E., Fowler, V., Scott, J., and Pazoles, C. J. (1982). Calcium-dependent regulation of chromaffin granule movement, membrane contact, and fusion during exocytosis. *Cold Spring Harb. Symp. Quant. Biol.* 46(Pt 2), 819–834. doi: 10.1101/SQB.1982.046.01.077

Rickman, C., Medine, C. N., Dun, A. R., Moulton, D. J., Mandula, O., Halemani, N. D., et al. (2010). t-SNARE Protein Conformations Patterned by the Lipid Microenvironment. *J. Biol. Chem.* 285, 13535–13541. doi: 10.1074/jbc.M109.091058

Ries, J., Kaplan, C., Platonova, E., Eghlidi, H., and Ewers, H. (2012). A simple, versatile method for GFP-based super-resolution microscopy via nanobodies. *Nat. Methods* 9, 582–584. doi: 10.1038/nmeth.1991

Rittweger, E., Wildanger, D., and Hell, S. W. (2009). Far-field fluorescence nanoscopy of diamond color centers by ground state depletion. *Epl* 84, 14001. doi: 10.1209/0295-5075/86/14001

Rizo, J., and Sudhof, T. C. (2012). The membrane fusion enigma: SNAREs, Sec1/Munc18 proteins, and their accomplices–guilty as charged. *Annu. Rev. Cell Dev. Biol.* 28, 279–308. doi: 10.1146/annurev-cellbio-101011-155818

Rust, M. J., Bates, M., and Zhuang, X. (2006). Sub-diffraction-limit imaging by stochastic optical reconstruction microscopy (STORM). *Nat. Methods* 3, 793–795. doi: 10.1038/nmeth929

Schneider, F. H., Smith, A. D., and Winkler, H. (1967). Secretion from the adrenal medulla: biochemical evidence for exocytosis. *Br. J. Pharmacol. Chemother.* 31, 94–104. doi: 10.1111/j.1476-5381.1967.tb01980.x

Shao, L., Kner, P., Rego, E. H., and Gustafsson, M. G. (2011). Super-resolution 3D microscopy of live whole cells using structured illumination. *Nat. Methods* 8, 1044–1046. doi: 10.1038/nmeth.1734

Sheets, L., Kindt, K. S., and Nicolson, T. (2012). Presynaptic CaV1.3 channels regulate synaptic ribbon size and are required for synaptic maintenance in sensory hair cells. *J. Neurosci.* 32, 17273–17286. doi: 10.1523/JNEUROSCI.3005-12.2012

Shim, S. H., Xia, C., Zhong, G., Babcock, H. P., Vaughan, J. C., Huang, B., et al. (2012). Super-resolution fluorescence imaging of organelles in live cells with photoswitchable membrane probes. *Proc. Natl. Acad. Sci. U.S.A.* 109, 13978–13983. doi: 10.1073/pnas.1201882109

Sieber, J. J., Willig, K. I., Heintzmann, R., Hell, S. W., and Lang, T. (2006). The SNARE motif is essential for the formation of syntaxin clusters in the plasma membrane. *Biophys. J.* 90, 2843–2851. doi: 10.1529/biophysj.105.079574

Sieber, J. J., Willig, K. I., Kutzner, C., Gerding-Reimers, C., Harke, B., Donnert, G., et al. (2007). Anatomy and dynamics of a supramolecular membrane protein cluster. *Science* 317, 1072–1076. doi: 10.1126/science.1141727

Sjollema, K. A., Schnell, U., Kuipers, J., Kalicharan, R., and Giepmans, B. N. (2012). Correlated light microscopy and electron microscopy. *Methods Cell Biol.* 111, 157–173. doi: 10.1016/B978-0-12-416026-2.00009-1

Sochacki, K. A., Larson, B. T., Sengupta, D. C., Daniels, M. P., Shtengel, G., Hess, H. F., et al. (2012). Imaging the post-fusion release and capture of a vesicle membrane protein. *Nat. Commun.* 3:1154. doi: 10.1038/ncomms2158

Sorensen, J. B. (2004). Formation, stabilisation and fusion of the readily releasable pool of secretory vesicles. *Pflugers Arch.* 448, 347–362. doi: 10.1007/s00424-004-1247-8

Speidel, D., Bruederle, C. E., Enk, C., Voets, T., Varoqueaux, F., Reim, K., et al. (2005). CAPS1 regulates catecholamine loading of large dense-core vesicles. *Neuron* 46, 75–88. doi: 10.1016/j.neuron.2005.02.019

Stevens, D. R., Schirra, C., Becherer, U., and Rettig, J. (2011). Vesicle pools: lessons from adrenal chromaffin cells. *Front. Synaptic Neurosci.* 3:2. doi: 10.3389/fnsyn.2011.00002

Steyer, J. A., Horstmann, H., and Almers, W. (1997). Transport, docking and exocytosis of single secretory granules in live chromaffin cells. *Nature* 388, 474–478.

Studer, D., Graber, W., Al-Amoudi, A., and Eggli, P. (2001). A new approach for cryofixation by high-pressure freezing. *J. Microsc.* 203, 285–294. doi: 10.1046/j.1365-2818.2001.00919.x

Sudhof, T. C. (2012). Calcium control of neurotransmitter release. *Cold Spring Harb Perspect. Biol.* 4:a011353. doi: 10.1101/cshperspect.a011353

Tatavarty, V., Kim, E. J., Rodionov, V., and Yu, J. (2009). Investigating subspine actin dynamics in rat hippocampal neurons with super-resolution optical imaging. *PLoS ONE* 4:e7724. doi: 10.1371/journal.pone.0007724

Tonnesen, J., Nadrigny, F., Willig, K. I., Wedlich-Soldner, R., and Nagerl, U. V. (2011). Two-color STED microscopy of living synapses using a single laser-beam pair. *Biophys. J.* 101, 2545–2552. doi: 10.1016/j.bpj.2011.10.011

Tonnesen, J., and Nagerl, U. V. (2013a). Superresolution imaging for neuroscience. *Exp. Neurol.* 242, 33–40. doi: 10.1016/j.expneurol.2012.10.004

Tonnesen, J., and Nagerl, U. V. (2013b). Two-color STED imaging of synapses in living brain slices. *Methods Mol. Biol.* 950, 65–80. doi: 10.1007/978-1-62703-137-0-5

Toonen, R. F., Wierda, K., Sons, M. S., de Wit, H., Cornelisse, L. N., Brussaard, A., et al. (2006). Munc18-1 expression levels control synapse recovery by regulating readily releasable pool size. *Proc. Natl. Acad. Sci. U.S.A.* 103, 18332–18337. doi: 10.1073/pnas.0608507103

Urban, N. T., Willig, K. I., Hell, S. W., and Nagerl, U. V. (2011). STED nanoscopy of actin dynamics in synapses deep inside living brain slices. *Biophys. J.* 101, 1277–1284. doi: 10.1016/j.bpj.2011.07.027

Vanhecke, D., Graber, W., and Studer, D. (2008). Close-to-native ultrastructural preservation by high pressure freezing. *Methods Cell Biol.* 88, 151–164. doi: 10.1016/S0091-679X(08)00409-3

Verhage, M., and Sorensen, J. B. (2008). Vesicle docking in regulated exocytosis. *Traffic* 9, 1414–1424. doi: 10.1111/j.1600-0854.2008.00759.x

Villanueva, J., Torregrosa-Hetland, C. J., Garcia-Martinez, V., del Mar Frances, M., Viniegra, S., and Gutierrez, L. M. (2012). The F-actin cortex in chromaffin granule dynamics and fusion: a minireview. *J. Mol. Neurosci.* 48, 323–327. doi: 10.1007/s12031-012-9718-4

Voets, T., Neher, E., and Moser, T. (1999). Mechanisms underlying phasic and sustained secretion in chromaffin cells from mouse adrenal slices. *Neuron* 23, 607–615. doi: 10.1016/S0896-6273(00)80812-0

Wang, J., and Richards, D. A. (2012). Segregation of PIP2 and PIP3 into distinct nanoscale regions within the plasma membrane. *Biol. Open* 1, 857–862. doi: 10.1242/bio.20122071

Westphal, V., Rizzoli, S. O., Lauterbach, M. A., Kamin, D., Jahn, R., and Hell, S. W. (2008). Video-rate far-field optical nanoscopy dissects synaptic vesicle movement. *Science* 320, 246–249. doi: 10.1126/science.1154228

Wightman, R. M., Jankowski, J. A., Kennedy, R. T., Kawagoe, K. T., Schroeder, T. J., Leszczyszyn, D. J., et al. (1991). Temporally resolved catecholamine spikes correspond to single vesicle release from individual chromaffin cells. *Proc. Natl. Acad. Sci. U.S.A.* 88, 10754–10758. doi: 10.1073/pnas.88.23.10754

Wildanger, D., Medda, R., Kastrup, L., and Hell, S. W. (2009). A compact STED microscope providing 3D nanoscale resolution. *J. Microsc.* 236, 35–43. doi: 10.1111/j.1365-2818.2009.03188.x

Yang, L., Dun, A. R., Martin, K. J., Qiu, Z., Dunn, A., Lord, G. J., et al. (2012). Secretory vesicles are preferentially targeted to areas of low molecular SNARE density. *PLoS ONE* 7:e49514. doi: 10.1371/journal.pone.0049514

Yizhar, O., and Ashery, U. (2008). Modulating vesicle priming reveals that vesicle immobilization is necessary but not sufficient for fusion-competence. *PLoS ONE* 3:e2694. doi: 10.1371/journal.pone.0002694

Yizhar, O., Matti, U., Melamed, R., Hagalili, Y., Bruns, D., Rettig, J., et al. (2004). Tomosyn inhibits priming of large dense-core vesicles in a calcium-dependent manner. *Proc. Natl. Acad. Sci. U.S.A.* 101, 2578–2583. doi: 10.1073/pnas.0308700100

Zhao, Y., Fang, Q., Herbst, A. D., Berberian, K. N., Almers, W., and Lindau, M. (2013). Rapid structural change in synaptosomal-associated protein 25 (SNAP25) precedes the fusion of single vesicles with the plasma membrane in live chromaffin cells. *Proc. Natl. Acad. Sci. U.S.A.* 110, 14249–14254. doi: 10.1073/pnas.1306699110

Conflict of Interest Statement: The authors declare that the research was conducted in the absence of any commercial or financial relationships that could be construed as a potential conflict of interest.

Received: 10 June 2013; accepted: 04 November 2013; published online: 25 November 2013.

Citation: Bost A, Pasche M, Schirra C and Becherer U (2013) Super-resolution microscopy in studying neuroendocrine cell function. Front. Neurosci. 7:222. doi: 10.3389/fnins.2013.00222

This article was submitted to Neuroendocrine Science, a section of the journal Frontiers in Neuroscience.

frontiers in
ENDOCRINOLOGY

MINI REVIEW ARTICLE
published: 17 October 2013
doi: 10.3389/fendo.2013.00147

Exocytosis through the lens

Alicja Graczyk and Colin Rickman*

Institute of Biological Chemistry, Biophysics and Bioengineering, School of Engineering and Physical Sciences, Heriot-Watt University, Edinburgh, UK

Edited by:
Stephane Gasman, Centre National de la Recherche Scientifique, France

Reviewed by:
Luke Chamberlain, University of Strathclyde, UK
Derek Toomre, Yale University, USA

****Correspondence:***
Colin Rickman, Institute of Biological Chemistry, Biophysics and Bioengineering, School of Engineering and Physical Sciences, Heriot-Watt University, Edinburgh EH14 4AS, UK
e-mail: c.rickman@hw.ac.uk

Exocytosis, the process in which material is transported from the cell interior to the extracellular space, proceeds through a complex mechanism. Defects in this process are linked to a number of serious illnesses including diabetes, cancer, and a range of neuropathologies. In neuroendocrine cells, exocytosis involves the fusion of secretory vesicles, carrying signaling molecules, with the plasma membrane through the coordinated interplay of proteins, lipids, and small molecules. This process is highly regulated and occurs in a complex three-dimensional environment within the cell precisely coupled to the stimulus. The study of exocytosis poses significant challenges, involving rapidly changing, nano-scale, protein–protein, and protein–lipid interactions, at specialized sites in the cell. Over the last decade our understanding of neuroendocrine exocytosis has been greatly enhanced by developments in fluorescence microscopy. Modern microscopy encompasses a toolbox of advanced techniques, pushing the limits of sensitivity and resolution, to probe different properties of exocytosis. In more recent years, the development of super-resolution microscopy techniques, side-stepping the limits of optical resolution imposed by the physical properties of light, have started to provide an unparalleled view of exocytosis. In this review we will discuss how advances in fluorescence microscopy are shedding light on the spatial and temporal organization of the exocytotic machinery.

Keywords: exocytosis, super-resolution microscopy, palmitic acids, STED, storm, SNARE proteins, membrane fusion

INTRODUCTION

Regulated exocytosis is a fundamental process of multicellular life, permitting cells with diverse functions, and properties to act in a coordinated manner. In vertebrates, this cell–cell communication occurs over short distances and between small numbers of cells, for example in neurons, or over longer ranges encompassing many cell types and organs in the case of neuroendocrine signaling (1). In all examples of regulated exocytosis, the final stages of membrane fusion, lipid mixing, and content release are catalyzed by the coordinated action of the SNARE (soluble NSF attachment protein receptor) proteins (2–4). In neurons and neuroendocrine cells three SNARE proteins act synergistically to drive membrane fusion; syntaxin and SNAP-25 on the plasma membrane, and synaptobrevin in secretory vesicles (4–6). Together, these three proteins form a four helical complex, which drives the merger of the plasma and vesicular membranes (7–9). *In vitro* biochemical studies have described many of the individual stages of SNARE protein action; through the formation of a stable binary intermediate, the zippering of the SNARE complex, the formation of cis and trans complexes, and established the SNAREs as the minimal machinery required for exocytosis (6, 8–13). In parallel, *in vivo* studies have demonstrated the importance of the SNARE proteins in the physiological development and functioning of secretory cells and organs (14–16).

This complex cascade of protein–protein interactions provides challenges and opportunities to investigation through the use of optical microscopy (**Figure 1**). Optical microscopy inherently provides spatial information, and with improvements in detection technologies, enhanced sensitivity, and speed. By sampling specific wavelengths of visible light, in fluorescence microscopy, it is possible to discriminate multiple labels within a sample (17). This has been used extensively to study exocytotic events in a large number of secretory cell types from dissociated single cells up to intra-vital imaging in whole organisms. The use of fluorescence microscopy provides a huge improvement over electron microscopy, which is incompatible with live cell imaging and often suffers from an inability to discriminate between objects in the resulting image. However, fluorescence microscopy achieves this at a cost; significantly lower resolution. While electron microscopy is ultimately able to resolve objects to the sub-nanometer range, permitting the generation of protein structures with atomic resolution, fluorescence microscopy is typically limited in resolving power to hundreds of nanometers. The resolution on an optical microscope is limited by two factors, aberration and diffraction, which both serve to blur the image and limit the ability to distinguish two adjacent points (17). Aberration can be corrected through the expensive optics found on modern microscopes, but diffraction is ultimately governed by the wavelength of light and the aperture of the objective according to the Abbe formula and Rayleigh criterion (17, 18). Most fluorophores used in cellular imaging emit light in the wavelength range of 400–700 nm which results in a lateral limit of resolution for standard diffraction-limited microscopes of between 170 and 300 nm respectively (**Figure 2**). Now, new technological breakthroughs are pushing the limits in resolution in the spatial and temporal domains revising our understanding of the process of neuroendocrine exocytosis. This short review will cover some of the highlights of how microscopy has advanced our understanding of neuroendocrine secretion.

TEMPORAL INVESTIGATION OF THE PROCESS OF EXOCYTOSIS

A key characteristic of all regulated exocytosis, regardless of the type of specialized cell studied is that it is a rapid process. Globally, for all secretory vesicles in a cell the rate of cargo release may be slow and multiphasic, but at the single vesicle level the process of bilayer merger and cargo release occurs over a very fast timescale (19, 20). To examine a dynamic process using fluorescence microscopy requires a high temporal resolution. This is difficult to achieve using confocal laser scanning microscopy, due to the requirement for scanning (**Figure 2**). Widefield techniques, which provide spatial information through sensitive cameras can achieve high temporal sampling frequencies at the expense of axial resolution (17). A major advance was achieved through the invention of the total internal reflection fluorescence microscope (TIRFM), which uses total internal reflection to establish an evanescent wave at the coverslip (21). This permits the high temporal resolution of widefield camera-based microscopy but in a thin axial section at the plasma membrane. One of the first applications of this technique was to observe the fusion of secretory vesicles with the plasma membrane (19, 22, 23). Initial experiments examining the fusion process utilized acidic dyes, such as Acridine orange, but these were soon superseded by fluorescently labeled cargo molecules (24, 25). In these early studies it was clear that, at rest, the secretory vesicles are highly dynamic in the cell interior while vesicles at the plasma membrane were largely immobile (22, 26, 27). This supported the hypothesis from electrophysiological data that different pools of secretory vesicles exist with different release properties (20). Secretory vesicles at the plasma membrane do not exhibit free diffusion but instead demonstrate a caged, or tethered behavior, termed morphological docking. Upon stimulation a proportion of these morphologically docked vesicles fuse with the plasma membrane releasing their cargo (28). Using high speed imaging under TIRFM illumination, Degtyar and colleagues demonstrated that immediately prior to fusion, secretory vesicles undergo a rapid lateral movement (29). The mechanisms behind this are unclear but it may serve to sample a larger area of the plasma membrane, enhancing the probability of SNARE interactions, or be a direct result of the formation of the SNARE complexes themselves. While TIRFM provides high temporal resolution of exocytotic events at the plasma membrane, it cannot observe events over the entire cell surface or at depth, in clusters of cells (17). Spinning disk confocal microscopy has been employed to study vesicle fusion throughout cells clusters and in polarized pancreatic acini (30, 31). These studies are beginning to move the temporal study of vesicle dynamics and fusion from single cells toward whole organs and beyond.

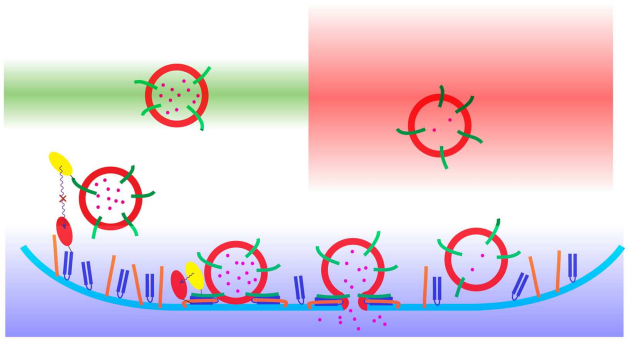

FIGURE 1 | A schematic representation of the process of neuroendocrine exocytosis as observed using diffraction-limited fluorescence microscopy. The synaptic vesicles (red) with the cargo (pink) undergo fusion with the plasma membrane (blue). The color gradients show the areas of the sample acquisition: CLSM (green), WF (red), and TIRFM (blue). The principle of Förster resonance energy transfer (FRET) microscopy is presented with the use of yellow ovals [located on synaptobrevin (green)] and red ovals [located on SNAP-25 (navy blue)]. The Förster resonance energy transfer occurs only when the distance between the donor (yellow) and the acceptor (red) fluorophores are in the range of 1–10 nm. The third SNARE protein, syntaxin, is denoted in orange.

		CLSM	STED	CW-STED	3D-SIM	TIRFM	PALM/STORM
$\sim\lambda_{em}$/nm		460-670	600-700	500-600	460-670	460-670	500-670
Resolution (*localisation precision)	$\sim D_{x,y}$/nm	180-250	60	70	100-130	180-250	*30
	$\sim D_z$/nm	500-700	700	560	250-340	100-400	100-400
	time	ms-s	s	s	s	ms	ms-min
Depth range		100 µm	100 µm	100 µm	50 µm	400 nm	400 nm

FIGURE 2 | Summary of diffraction-limited and super-resolution microscopy approaches. Seven microscopy techniques are detailed: confocal laser scanning microscopy (CLSM), stimulated emission depletion microscopy (STED), continuous wave STED (CW-STED), structured illumination microscopy (3D-SIM), total internal reflection fluorescence microscopy (TIRF), photoactivation localization microscopy (PALM), and stochastic optical reconstruction microscopy (STORM). The table shows the typical operational emission wavelengths, lateral and axial resolutions, the temporal resolution of data acquisition, and the sampling depth range. For PALM and STORM microscopy the typical lateral localization precision is stated. For further information regarding the referenced techniques (63).

While secretory vesicles provide an ideal object to image, being larger and more sparsely distributed than the limits imposed by diffraction, they are only one part of the story of exocytosis. Imaging of proteins is confounded by limited resolution, however, this has not prevented the development of innovative solutions to probe SNARE protein function with high temporal resolution. Fluorescence recovery after photobleaching (FRAP) has been widely used to examine the molecular motion of SNARE proteins on the plasma membrane (32). By selectively bleaching fluorescently labeled SNAREs in a sub region of the plasma membrane the recovery of fluorescence in this region through diffusion can be monitored. Sieber and co-workers used FRAP to measure the diffusion of syntaxin molecules on the plasma membrane to derive a dynamic model of SNARE organization (33). In a subsequent study by the same group FRAP was used to probe the intermolecular interactions of SNAP-25 and syntaxin (34), supporting *in vitro* observations of a 1:1 binary intermediate (11, 13). FRAP provides a global average for the diffusion rate of the population of molecules being studied. Due to the high density of the molecules, their individual motion cannot be resolved using diffraction-limited microscopy. However, using an adaptation of a scanning confocal microscope in which the laser beam is parked to a single point in space, diffusion of molecules through the beam can be monitored. This approach called fluorescence correlation spectroscopy (FCS) has been used extensively in *in vitro* reconstituted studies of SNARE protein organization (35–37). FCS studies showed that synaptobrevin and syntaxin both preferentially sequester in the liquid-disordered phase of giant unilamellar vesicles (35). This argues against a classical raft hypothesis for SNARE protein organization, however, the situation in cellular membranes may be more complicated due to the diversity of lipid species present.

RESOLVING THE MOLECULAR ORGANIZATION AND INTERACTIONS UNDERLYING EXOCYTOSIS

The proteins responsible for driving the process of exocytosis are un-resolvable due to their size and high density in neuroendocrine cells using diffraction-limited microscopes. In the last 5 years there has been a revolution in cell imaging with the introduction of super-resolution microscope techniques, which have pushed the ability to resolve objects through supramolecular imaging down to single molecule detection (38) (**Figure 2**). These techniques can be broadly divided into two classes; hardware approaches and localization approaches. Stimulated emission depletion microscopy (STED) and structured illumination microscopy (SIM) achieve the enhancement in resolution through alterations in the illumination of the sample (39–41). This achieves a two to sixfold enhancement in the optical resolution of the microscope over the theoretical limit imposed by the diffraction of light. STED can be implemented using either pulsed lasers or constant wave lasers (CW-STED) (42); the former providing enhanced lateral resolution while the latter provides simpler implementation. The second class of super-resolution techniques utilize localization of emission to achieve single molecule imaging (43). These single molecule localization microscopy (SMLM) techniques include photoactivation localization microscopy (PALM), ground state depletion with individual molecule return (GSDIM), and stochastic optical reconstruction microscopy (STORM and dSTORM) (44–47). All of these SMLM approaches take advantage of the ability to switch molecules between light and dark states to decrease the number of fluorescent molecules observed at one time. By repeated recording it is then possible to observe many tens of thousands of individual, fluorescently labeled, proteins and compute their position with a precision of 5–20 nm.

These super-resolution techniques have been utilized to investigate the organization of the plasma membrane secretory machinery. Over the last decade it has become clear that the plasma membrane SNAREs, syntaxin, and SNAP-25 are not uniformly distributed over the plasma membrane, but instead are observed to exists in a clustered morphology (13, 48–53). These studies used diffraction-limited techniques and largely agreed that clusters were of the order of 200 nm in diameter. It is important to note that using these microscopes, as a result of diffraction of the light through the optics, any object of approximately 200 nm or less would appear this size. Regardless, a number of important observations were made with relation to the dependency of the integrity of these clusters on cholesterol and their partial colocalization with secretory vesicles (48–50). In 2007 a major advance was reported using STED microscopy, which showed that syntaxin forms clusters of approximately 50 nm in size. Based on computer modeling this supramolecular assembly was hypothesized to contain around 70 molecules of syntaxin and required functional SNARE domains of syntaxin (33). In a subsequent study STED was used to probe the involvement of phosphatidylinositol (4,5) bisphosphate (PIP2) in syntaxin clustering. This study concluded that cluster formation required the combined clustering of PIP2 and syntaxin acting synergistically together (54). Importantly, the measured size of the clusters falls at the limit of accuracy of the STED microscope used and so this can only act as an upper limit to the size of a cluster. More recently, SMLM has been employed to investigate SNARE organization on the plasma membrane (55, 56). This goes beyond the observation of multi-protein structures to localize the individual molecular components. dSTORM imaging demonstrated a clustered morphology for both syntaxin and SNAP-25 (55, 56). This non-homogeneous distribution was also observed using PALM and recapitulated in live cells using single particle tracking PALM (sptPALM) (56). This latter technique also observed that syntaxin and SNAP-25 molecules cannot freely diffuse on the plasma membrane, but instead are restricted to as yet undefined microdomains. Interestingly using these super-resolution molecular techniques, the secretory vesicles were not localized to the higher density plasma membrane SNARE clusters (56). This appears at odds with the previous observation of partial colocalization with SNARE clusters using diffraction-limited techniques (48–50). However, this apparent discrepancy is most likely due to the level of "detail" resolved using the respective technique.

Although super-resolution techniques provide unparalleled resolution they are limited to describing the position of protein molecules with no information on interaction status. However, it is possible to probe interactions of molecules over distances below 10 nm using Förster resonance energy transfer (FRET) microscopy

(57). This has been employed to study protein–protein interactions between the SNAREs, providing key insights into how these molecules interact in a cellular environment and how this is regulated (54, 58–60). There are two main approaches for the determination of FRET; intensity based techniques including sensitized emission and acceptor photobleaching, and fluorescence lifetime imaging (FLIM) (17). All of these techniques measure the effect of non-radioactive energy transfer between the donor and acceptor molecules. In terms of SNARE clustering, FRET has successfully been used to examine protein clustering in artificial liposomes, observing clustering through exclusion from high cholesterol regions as well as probing the intra-cluster interactions of syntaxin and SNAP-25 (52, 61, 62).

CONCLUSION

The development of new microscopy techniques with ever higher temporal and spatial resolution has mirrored the requirements and advancements of the field of neuroendocrine secretion. This biological system serves as an excellent test bed for many of the new emerging technology as a result of our already considerable understanding and also the specific problems and opportunities offered. The next big step is to combine super-resolution, high speed, and functional imaging into single experiments. The iterative process of technological advancement and new biological findings will continue until the ultimate experiment of being able to watch a complete single fusion event with sub-molecular resolution of multiple protein components is achieved.

REFERENCES

1. Bellen H. *Neurotransmitter Release, Frontiers in Molecular Biology*. Oxford: Oxford University Press (1999).
2. Jahn R, Scheller RH. SNAREs – engines for membrane fusion. *Nat Rev Mol Cell Biol* (2006) **7**:631–43. doi:10.1038/nrm2002
3. Martens S, McMahon HT. Mechanisms of membrane fusion: disparate players and common principles. *Nat Rev Mol Cell Biol* (2008) **9**:543–56. doi:10.1038/nrm2417
4. Sollner T, Whiteheart SW, Brunner M, Erdjument-Bromage H, Geromanos S, Tempst P, et al. SNAP receptors implicated in vesicle targeting and fusion. *Nature* (1993) **362**:318–24. doi:10.1038/362318a0
5. Lin RC, Scheller RH. Structural organization of the synaptic exocytosis core complex. *Neuron* (1997) **19**:1087–94. doi:10.1016/S0896-6273(00)80399-2
6. Weber T, Zemelman BV, McNew JA, Westermann B, Gmachl M, Parlati F, et al. SNAREpins: minimal machinery for membrane fusion. *Cell* (1998) **92**:759–72. doi:10.1016/S0092-8674(00)81404-X
7. Otto H, Hanson PI, Jahn R. Assembly and disassembly of a ternary complex of synaptobrevin, syntaxin, and SNAP-25 in the membrane of synaptic vesicles. *Proc Natl Acad Sci U S A* (1997) **94**:6197–201. doi:10.1073/pnas.94.12.6197
8. Stein A, Weber G, Wahl MC, Jahn R. Helical extension of the neuronal SNARE complex into the membrane. *Nature* (2009) **460**:525–8. doi:10.1038/nature08156
9. Sutton RB, Fasshauer D, Jahn R, Brunger AT. Crystal structure of a SNARE complex involved in synaptic exocytosis at 2.4 A resolution. *Nature* (1998) **395**:347–53. doi:10.1038/26412
10. Bowen ME, Weninger K, Brunger AT, Chu S. Single molecule observation of liposome-bilayer fusion thermally induced by soluble N-ethyl maleimide sensitive-factor attachment protein receptors (SNAREs). *Biophys J* (2004) **87**:3569–84. doi:10.1529/biophysj.104.048637
11. Fasshauer D, Margittai M. A transient interaction of SNAP-25 and syntaxin nucleates SNARE assembly. *J Biol Chem* (2004) **279**:7613–21. doi:10.1074/jbc.M312064200
12. Fasshauer D, Antonin W, Subramaniam V, Jahn R. SNARE assembly and disassembly exhibit a pronounced hysteresis. *Nat Struct Biol* (2002) **9**:144–51. doi:10.1038/nsb750
13. Rickman C, Meunier FA, Binz T, Davletov B. High affinity interaction of syntaxin and SNAP-25 on the plasma membrane is abolished by botulinum toxin E. *J Biol Chem* (2004) **279**:644–51. doi:10.1074/jbc.M310879200
14. Gerber SH, Rah JC, Min SW, Liu X, De Wit H, Dulubova I, et al. Conformational switch of syntaxin-1 controls synaptic vesicle fusion. *Science* (2008) **321**:1507–10. doi:10.1126/science.1163174
15. Schoch S, Deák F, Königstorfer A, Mozhayeva M, Sara Y, Südhof TC, et al. SNARE function analyzed in synaptobrevin/VAMP knockout mice. *Science* (2001) **294**:1117–22. doi:10.1126/science.1064335
16. Washbourne P, Thompson PM, Carta M, Costa ET, Mathews JR, Lopez-Benditó G, et al. Genetic ablation of the t-SNARE SNAP-25 distinguishes mechanisms of neuroexocytosis. *Nat Neurosci* (2002) **5**:19–26. doi:10.1038/nn783
17. Lakowicz JR. *Principles of Fluorescence Spectroscopy*. Third ed. New York: Springer (2006).
18. Abbe E. Beiträge zur Theorie des Mikroskops und der mikroskopischen Wahrnehmung. *Arch Mikrosk Anat* (1873) **9**:413–68. doi:10.1007/BF02956173
19. Oheim M, Loerke D, Stühmer W, Chow RH. The last few milliseconds in the life of a secretory granule. *Eur Biophys J* (1998) **27**:83–98. doi:10.1007/s002490050114
20. Voets T, Neher E, Moser T. Mechanisms underlying phasic and sustained secretion in chromaffin cells from mouse adrenal slices. *Neuron* (1999) **23**:607–15. doi:10.1016/S0896-6273(00)80812-0
21. Axelrod D. Cell-substrate contacts illuminated by total internal reflection fluorescence. *J Cell Biol* (1981) **89**:141–5. doi:10.1083/jcb.89.1.141
22. Steyer JA, Almers W. Tracking single secretory granules in live chromaffin cells by evanescent-field fluorescence microscopy. *Biophys J* (1999) **76**:2262–71. doi:10.1016/S0006-3495(99)77382-0
23. Steyer JA, Horstmann H, Almers W. Transport, docking and exocytosis of single secretory granules in live chromaffin cells. *Nature* (1997) **388**:474–8. doi:10.1038/41329
24. Greaves J, Duncan RR, Tapechum S, Apps DK, Shipston MJ, Chow RH. Use of ANF-EGFP for the visualization of secretory vesicles in bovine adrenal chromaffin cells. *Ann N Y Acad Sci* (2002) **971**:275–6. doi:10.1111/j.1749-6632.2002.tb04477.x
25. Han W, Ng YK, Axelrod D, Levitan ES. Neuropeptide release by efficient recruitment of diffusing cytoplasmic secretory vesicles. *Proc Natl Acad Sci USA* (1999) **96**:14577–82. doi:10.1073/pnas.96.25.14577
26. Stevens DR, Schirra C, Becherer U, Rettig J. Vesicle pools: lessons from adrenal chromaffin cells. *Front Synaptic Neurosci* (2011) **3**:2. doi:10.3389/fnsyn.2011.00002
27. Zenisek D, Steyer JA, Almers W. Transport, capture and exocytosis of single synaptic vesicles at active zones. *Nature* (2000) **406**:849–54. doi:10.1038/35022500
28. Steyer JA, Almers W. A real-time view of life within 100 nm of the plasma membrane. *Nat Rev Mol Cell Biol* (2001) **2**:268–75. doi:10.1038/35067069
29. Degtyar VE, Allersma MW, Axelrod D, Holz RW. Increased motion and travel, rather than stable docking, characterize the last moments before secretory granule fusion. *Proc Natl Acad Sci U S A* (2007) **104**:15929–34. doi:10.1073/pnas.0705406104
30. Fernandez NA, Liang T, Gaisano HY. Live pancreatic acinar imaging of exocytosis using syncollin-pHluorin. *Am J Physiol Cell Physiol* (2011) **300**:C1513–23. doi:10.1152/ajpcell.00433.2010
31. Rutter GA, Loder MK, Ravier MA. Rapid three-dimensional imaging of individual insulin release events by Nipkow disc confocal microscopy. *Biochem Soc Trans* (2006) **34**:675–8. doi:10.1042/BST0340675
32. Axelrod D, Koppel DE, Schlessinger J, Elson E, Webb WW. Mobility measurement by analysis of fluorescence photobleaching recovery kinetics. *Biophys J* (1976) **16**:1055–69. doi:10.1016/S0006-3495(76)85755-4
33. Sieber JJ, Willig KI, Kutzner C, Gerding-Reimers C, Harke B, Donnert G, et al. Anatomy and dynamics of a supramolecular membrane protein cluster. *Science* (2007) **317**:1072–6. doi:10.1126/science.1141727
34. Halemani ND, Bethani I, Rizzoli SO, Lang T. Structure and dynamics of a two-helix SNARE complex in live cells. *Traffic* (2010) **11**:394–404. doi:10.1111/j.1600-0854.2009.01020.x
35. Bacia K, Schuette CG, Kahya N, Jahn R, Schwille P. SNAREs prefer liquid-disordered over "raft" (liquid-ordered) domains when reconstituted into giant unilamellar vesicles. *J Biol Chem* (2004) **279**:37951–5. doi:10.1074/jbc.M407020200

36. Cypionka A, Stein A, Hernandez JM, Hippchen H, Jahn R, Walla PJ. Discrimination between docking and fusion of liposomes reconstituted with neuronal SNARE-proteins using FCS. *Proc Natl Acad Sci USA* (2009) **106**:18575–80. doi:10.1073/pnas.0906677106
37. Qian H, Elson EL. Distribution of molecular aggregation by analysis of fluctuation moments. *Proc Natl Acad Sci U S A* (1990) **87**:5479–83. doi:10.1073/pnas.87.14.5479
38. Huang B, Bates M, Zhuang X. Super-resolution fluorescence microscopy. *Annu Rev Biochem* (2009) **78**:993–1016. doi:10.1146/annurev.biochem.77.061906.092014
39. Gustafsson MG. Surpassing the lateral resolution limit by a factor of two using structured illumination microscopy. *J Microsc* (2000) **198**:82–7. doi:10.1046/j.1365-2818.2000.00710.x
40. Hein B, Willig KI, Hell SW. Stimulated emission depletion (STED) nanoscopy of a fluorescent protein-labeled organelle inside a living cell. *Proc Natl Acad Sci U S A* (2008) **105**:14271–6. doi:10.1073/pnas.0807705105
41. Hell SW. Far-field optical nanoscopy. *Science* (2007) **316**:1153–8. doi:10.1126/science.1137395
42. Moneron G, Medda R, Hein B, Giske A, Westphal V, Hell SW. Fast STED microscopy with continuous wave fiber lasers. *Opt Express* (2010) **18**:1302–9. doi:10.1364/OE.18.001302
43. McEvoy AL, Greenfield D, Bates M, Liphardt J. Q&A: single-molecule localization microscopy for biological imaging. *BMC Biol* (2010) **8**:106. doi:10.1186/1741-7007-8-106
44. Betzig E, Patterson GH, Sougrat R, Lindwasser OW, Olenych S, Bonifacino JS, et al. Imaging intracellular fluorescent proteins at nanometer resolution. *Science* (2006) **313**:1642–5. doi:10.1126/science.1127344
45. Hess ST, Girirajan TPK, Mason MD. Ultra-high resolution imaging by fluorescence photoactivation localization microscopy. *Biophys J* (2006) **91**:4258–72. doi:10.1529/biophysj.106.091116
46. Rust M, Bates M, Zhuang X. Sub-diffraction-limit imaging by stochastic optical reconstruction microscopy (STORM). *Nat Methods* (2006) **3**:793–5. doi:10.1038/nmeth929
47. van de Linde S, Löschberger A, Klein T, Heidbreder M, Wolter S, Heilemann M, et al. Direct stochastic optical reconstruction microscopy with standard fluorescent probes. *Nat Protoc* (2011) **6**:991–1009. doi:10.1038/nprot.2011.336
48. Barg S, Knowles MK, Chen X, Midorikawa M, Almers W. Syntaxin clusters assemble reversibly at sites of secretory granules in live cells. *Proc Natl Acad Sci U S A* (2010) **107**:20804–9. doi:10.1073/pnas.1014823107
49. Knowles MK, Barg S, Wan L, Midorikawa M, Chen X, Almers W. Single secretory granules of live cells recruit syntaxin-1 and synaptosomal associated protein 25 (SNAP-25) in large copy numbers. *Proc Natl Acad Sci U S A* (2010) **107**:20810–5. doi:10.1073/pnas.1014840107
50. Lang T, Bruns D, Wenzel D, Riedel D, Holroyd P, Thiele C, et al. SNAREs are concentrated in cholesterol-dependent clusters that define docking and fusion sites for exocytosis. *EMBO J* (2001) **20**:2202–13. doi:10.1093/emboj/20.9.2202
51. Lang T. SNARE proteins and "membrane rafts". *J Physiol* (2007) **585**:693–8. doi:10.1113/jphysiol.2007.134346
52. Rickman C, Medine CN, Dun AR, Moulton DJ, Mandula O, Halemani ND, et al. t-SNARE protein conformations patterned by the lipid micro-environment. *J Biol Chem* (2010) **285**:13535–41. doi:10.1074/jbc.M109.091058
53. Zilly FE, Halemani ND, Walrafen D, Spitta L, Schreiber A, Jahn R, et al. Ca2+ induces clustering of membrane proteins in the plasma membrane via electrostatic interactions. *EMBO J* (2011) **30**:1209–20. doi:10.1038/emboj.2011.53
54. van den Bogaart G, Meyenberg K, Risselada HJ, Amin H, Willig KI, et al. Membrane protein sequestering by ionic protein–lipid interactions. *Nature* (2011) **479**:552–5. doi:10.1038/nature10545
55. Bar-On D, Wolter S, van de Linde S, Heilemann M, Nudelman G, Nachliel E, et al. Super-resolution imaging reveals the internal architecture of nano-sized syntaxin clusters. *J Biol Chem* (2012) **287**:27158–67. doi:10.1074/jbc.M112.353250
56. Yang L, Dun AR, Martin KJ, Qiu Z, Dunn A, Lord GJ, et al. Secretory vesicles are preferentially targeted to areas of low molecular SNARE density. *PLoS ONE* (2012) **7**:e49514. doi:10.1371/journal.pone.0049514
57. Xia Z, Liu Y. Reliable and global measurement of fluorescence resonance energy transfer using fluorescence microscopes. *Biophys J* (2001) **81**:2395–402. doi:10.1016/S0006-3495(01)75886-9
58. An SJ, Almers W. Tracking SNARE complex formation in live endocrine cells. *Science* (2004) **306**:1042–6. doi:10.1126/science.1102559
59. Degtyar V, Hafez IM, Bray C, Zucker RS. Dance of the SNAREs: assembly and rearrangements detected with FRET at neuronal synapses. *J Neurosci* (2013) **33**:5507–23. doi:10.1523/JNEUROSCI.2337-12.2013
60. Rickman C, Medine CN, Bergmann A, Duncan RR. Functionally and spatially distinct modes of munc18-syntaxin 1 interaction. *J Biol Chem* (2007) **282**:12097–103. doi:10.1074/jbc.M700227200
61. Murray D, Tamm L. Molecular mechanism of cholesterol- and polyphosphoinositide-mediated syntaxin clustering. *Biochemistry* (2011) **50**:9014–22. doi:10.1021/bi201307u
62. Murray DH, Tamm LK. Clustering of syntaxin-1A in model membranes is modulated by phosphatidylinositol 4,5-bisphosphate and cholesterol. *Biochemistry* (2009) **48**:4617–25. doi:10.1021/bi9003217
63. Schermelleh L, Heintzmann R, Leonhardt H. A guide to super-resolution fluorescence microscopy. *J Cell Biol* (2010) **190**:165–75. doi:10.1083/jcb.201002018

Conflict of Interest Statement: The authors declare that the research was conducted in the absence of any commercial or financial relationships that could be construed as a potential conflict of interest.

Received: 07 June 2013; accepted: 02 October 2013; published online: 17 October 2013.

*Citation: Graczyk A and Rickman C (2013) Exocytosis through the lens. Front. Endocrinol. **4**:147. doi: 10.3389/fendo.2013.00147*

This article was submitted to Neuroendocrine Science, a section of the journal Frontiers in Endocrinology.

frontiers in
ENDOCRINOLOGY

REVIEW ARTICLE
published: 04 September 2013
doi: 10.3389/fendo.2013.00114

Imaging large cohorts of single ion channels and their activity

Katia Hiersemenzel, Euan R. Brown and Rory R. Duncan*

Edinburgh Super-Resolution Imaging Consortium (ESRIC), Institute of Biological Chemistry, Biophysics and Bioengineering, School of Engineering and Physical Sciences, Heriot-Watt University, Edinburgh, UK

Edited by:
Stephane Gasman, Centre National de la Recherche Scientifique, France

Reviewed by:
Silvio O. Rizzoli, Göttingen Graduate School for Neurosciences, Germany
Ludovic Richert, Centre National de la Recherche Scientifique, France

***Correspondence:**
Rory R. Duncan, Edinburgh Super-Resolution Imaging Consortium (ESRIC), Institute of Biological Chemistry, Biophysics and Bioengineering, School of Engineering and Physical Sciences, Heriot-Watt University, Edinburgh EH14 4AS, UK
e-mail: r.r.duncan@hw.ac.uk

As calcium is the most important signaling molecule in neurons and secretory cells, amongst many other cell types, it follows that an understanding of calcium channels and their regulation of exocytosis is of vital importance. Calcium imaging using calcium dyes such as Fluo3, or FRET-based dyes that have been used widely has provided invaluable information, which combined with modeling has estimated the subtypes of channels responsible for triggering the exocytotic machinery as well as inferences about the relative distances away from vesicle fusion sites these molecules adopt. Importantly, new super-resolution microscopy techniques, combined with novel Ca^{2+} indicators and imaginative imaging approaches can now define directly the nano-scale locations of very large cohorts of single channel molecules in relation to single vesicles. With combinations of these techniques the activity of individual channels can be visualized and quantified using novel Ca^{2+} indicators. Fluorescently labeled specific channel toxins can also be used to localize endogenous assembled channel tetramers. Fluorescence lifetime imaging microscopy and other single-photon-resolution spectroscopic approaches offer the possibility to quantify protein–protein interactions between populations of channels and the SNARE protein machinery for the first time. Together with simultaneous electrophysiology, this battery of quantitative imaging techniques has the potential to provide unprecedented detail describing the locations, dynamic behaviors, interactions, and conductance activities of many thousands of channel molecules and vesicles in living cells.

Keywords: PALM, storm, STED, super-resolution, TIRFM, imaging, microscopy, ion channel

EXOCYTOSIS

Ion channel biology is central to all physiology and regulated exocytosis, the process of secretion in specialized cells such as neurons and neuroendocrine cells, underlies physiological cell-to-cell signaling (1). Mis-regulation of exocytosis leads variously to a number of different conditions, including diabetes (2), neurological disorders (3), growth and sleep disorders (4), and asthma (5). Regulated exocytosis does not proceed spontaneously, but requires an influx of calcium ions through voltage-gated calcium channels (VGCCs), with the final fusion event at the plasma membrane driven by synaptotagmin-dependent mechanotransduction (6, 7) to the core SNARE complex comprising syntaxins, SNAP-25/23/29 (both target, or t-SNAREs) and synaptobrevins (a vesicular, or v-SNARE) (8–10) as well as SM proteins, such as munc18 (11–14). In both neurons and endocrine cells the voltage-dependent calcium influx is typically shaped by a classical negative feedback role for large-conductance calcium- and voltage-activated potassium (BK) channels (15–17). Thus disruption of either VGCC and/or BK channel function also leads to defects in physiology (18–20) [for example, chronic inflammatory pain is associated (21) with exon-18 splice variants (22) that lack the putative motif ("synprint") (23) in N-type VGCCs that is thought to interact directly with the secretory machinery]. Central to all these models is the requirement for secretory vesicles to be appropriately localized with the secretory machinery and VGCC and BK channels. Our understanding of ion channel biology has been defined largely by electrophysiological approaches, due to their high temporal resolution and single molecule sensitivity. Recent, rapid advancements in super-resolution imaging now offer the opportunity to test directly long-standing hypotheses regarding ion channel locations, interactions, dynamics, and compositions in living cells.

VOLTAGE-GATED CALCIUM CHANNELS AND EXOCYTOSIS

Voltage-gated calcium channels are the voltage sensors that convert cell depolarization into a cytoplasmic calcium signal, which subsequently triggers regulated exocytosis. A multiplicity of calcium channel subtypes is expressed in excitable cells (including neurons, chromaffin, and pancreatic beta cells as excitable secretory cell types) (24–26). Seven genes encode high voltage-activated channels (HVA) L (Ca_v 1.1–1.4), P/Q (Ca_v 2.1), N (Ca_v 2.2), and R (Ca_v 2.3) type. Three genes encode low voltage-activated channels (LVA, Ca_v 3.1–3, known as T-type channels). In neurons and endocrine cells VGCCs regulate a variety of other fundamental cellular processes in addition to controlling vesicle fusion; decades of research have defined electrophysiologically the relative contribution of each subtype to secretion (19, 25). For example, in mouse adrenal chromaffin cells, responsible for catecholamine (e.g., adrenaline) secretion, and in pancreatic beta cells, which release insulin in response to elevated blood glucose, N- and L-type calcium channels play a major role in both exocytosis and

in other cellular signaling such as shaping the action potential and pacemaker currents in chromaffin cells but N-, P/Q-, and R VGCCs are also present. Importantly, our understanding of the spatial organization of the different VGCC subtypes is immature (**Table 1**) and in this respect their interactions and spatio-temporal patterning in the functional- and molecular-vicinity of the fusion complex is of particular interest.

LARGE-CONDUCTANCE CALCIUM ACTIVATED POTASSIUM CHANNELS AND EXOCYTOSIS

As BK channels, encoded by a single gene, have a key role in modulating the calcium signal that leads to vesicle fusion (18–20) there has been considerable effort in trying to estimate the distances between Ca^{2+} and K^+ channels, their inter-channel interactions (physical and functional) (16, 30, 63), VGCC and BK interactions with the exocytotic machinery itself, particularly with syntaxin1 (21, 31–33), and in the distances between these channels and large dense-cored vesicles (64). Mathematical modeling of calcium concentration nano-domains near the intracellular mouth of channels, combined with the determination of the Ca^{2+} sensitivity of the secretory machinery (i.e., synaptotagmin) have led to the concept that secretory vesicles reside very close to VGCCs in the membrane, and slightly further away from BK channels (34–37, 64). Determining the precise concentration of Ca^{2+} required to elicit exocytosis is confounded by spatial heterogeneity in the cell that to date has been impossible to measure accurately; however, it is likely that fusion competent vesicles in secretory cells are targeted somehow to the sites at the membrane experiencing high Ca^{2+} concentrations – i.e., very close to the mouth of a calcium channel (34).

FUNCTIONAL COUPLING OF ION CHANNELS WITH EXOCYTOSIS

Our understanding of the functional coupling of ion channels with the secretory apparatus comes from diffraction-limited microscopy, binary biochemical binding determined *in vitro*, and electrophysiology. The first can only resolve, at the very best, clusters of ion channels and approximate distances in images in the order of 250 nm. *In vitro* biochemistry, whilst invaluable, cannot deliver the "where's and when's" of interactions in cells and so overlooks the key elements of spatio-temporal regulation. Electrophysiology can resolve single ion channel activities, or entire cell cohorts of activity, but with limited spatial resolution. It thus remains unknown how: (i) membrane cohorts of single ion channels are spatially distributed, (ii) the proportion of *active* ion channels compared to the total pool (Ca^{2+} and K^+) reside within functionally meaningful distances of fusion competent- and/or incompetent-vesicles, (iii) how the dynamics of channel activity may correlate with their spatial pattern *and/or* interactions with the SNARE molecular machinery in intact cells, and (iv) whether every channel at the membrane is functional. It is clear that new tools are required to address these questions.

SUPER-RESOLUTION IMAGING AND EXOCYTOSIS

The membrane-trafficking field has a strong history of using cutting-edge techniques and imaging is no exception. Super-resolution microscopy is an emerging powerful tool to further research on ion channels and calcium signaling involved in exocytosis, and have already been applied in studies of the exocytotic machinery (12, 38–41). Our own recent work revealed that the majority of vesicles do not access the necessary compliment of SNARE molecular machinery at the membrane required for fusion (12, 40, 42). Furthermore, vesicle dynamics are also segregated, not only spatially at the membrane but also by vesicle age as we showed that vesicles are prioritized for release according to the time since their assembly (43). This mini-review summarizes the main super-resolution imaging modalities and illustrates their potential uses in quantifying ion channel molecular biology in relation to exocytosis. **Table 2** summarizes the super-resolution imaging modalities described and their (potential) uses in examining ion channel biology.

TOTAL INTERNAL REFLECTION FLUORESCENCE MICROSCOPY

Total internal reflection fluorescence microscopy (TIRFM) is an optical technique that allows the evanescent illumination of a thin optical section (~100 nm) near the base of a cell (44). For TIRFM the use of the high NA objective becomes relevant in combination with the low refractive index of aqueous cell media. When the illumination laser encounters the interface between these refractive indices at a shallower angle than the so-called critical angle, then total internal reflection occurs, creating an evanescent wave at the interface. This extends and illuminates with an exponential decay only about 100 nm into the specimen before it becomes too

Table 1 | Voltage-gated calcium channel cohort activities that have been imaged.

Channel type	System	Optical calcium events term	Imaging technique	Conditions	Reference
L-type	Rat myocytes	Sparkletts	Confocal	Enhanced extracellular Ca^{2+} (20 mM) required for imaging	(27, 28)
	Rat myocytes	Sparkletts	TIFRM using Fluo-f5	Calcium channels in clusters	
T-type	nd	nd	nd	Nd	nd
N-type	*Xenopus* oocytes	Single channel calcium fluorescence transients (SCCaFTs)	TIFRM using fluorescent calcium indicator (Fluo-4)	Heterologously expressed channels	(29)
P/Q type	nd	nd	nd	Nd	nd

nd= not done.

Table 2 | Summary of available super-resolution microscopy and spectroscopic approaches and their potential for ion channel imaging.

Imaging modality	Description and potential for ion channel imaging	Reference
STED	Genuine sub-diffraction-limit imaging using a "depletion" laser to reduce the size of the point-spread-function. Resolution to ∼50 nm, potential for resolving small channel clusters at the plasma membrane	(49–53)
TIRFM	Limits the excitation in a sample to a thin (100 s of nanometers) optical section primarily at the base of a cell adhered to a glass cover-glass. The high contrast and rapid imaging data delivered makes this approach ideal for examining ion channel distributions, trafficking, and movements at the cell surface, with diffraction-limited resolution. Used for optical patching to localize ion channel activity	(13, 41–43)
SIM	Illumination of the sample with a known pattern allows the mathematical reconstruction of images from moiré fringes, thus revealing high-frequency, sub-diffraction structures. Potential for visualizing ion channel clusters (resolution ∼85 nm) or intracellular trafficking	(58, 59)
PALM	Localization microscopy that determines the location of single molecule fluorescent signals. Separates signals in time by photo-activating subsets of fluorescent proteins repetitively. Ideal for quantifying the spatial arrangements of cohorts of single channel subunits	(44, 45)
STORM/GSDIM/ DSTORM	Localization microscopies that determine single molecule locations. Separates signals in time by photo-switching subsets of fluorescent molecules from bright to dark, or spectral forms. May be used with immunodetection to localize cohorts of endogenous channel subunits with 5–20 nm certainty	(42, 46)
sptPALM	Single-particle-tracking PALM, localizes photo-activated fluorescent proteins in living cells over time to allow the tracking of single molecules. Ideal for quantifying the movements of cohorts of single ion channels at the cell surface with 20–50 nm certainty	(12, 36, 48)
Fluorescence lifetime imaging microscopy (FLIM)	Quantifies the fluorescence lifetime of a fluorophore to aid with either contrast (by measuring an additional parameter in an image dataset) or in particular, to quantify FRET. Ideal for quantifying ion channel molecular interactions anywhere in 3-D in a cell	(20, 21, 42–47)
Fluorescence correlation spectroscopy (FCS)	Quantifies the diffusion of single fluorescent molecules through small excitation volumes in 3-D. Delivers directly molecular number, concentration, diffusion rates, and potentially interactions from living samples or using purified samples *in vitro*. Ideal for quantifying dynamic ion channel molecular behaviors	(56–59)

weak to excite fluorophores. This creates a high-contrast image of the plasma membrane and adjacent structures with little background fluorescence from the intracellular compartments of the cell. This allows the imaging of ion channels, vesicles, and exocytotic proteins in living samples with high temporal resolution (13, 42, 45, 46). TIRFM is the foundation for a number of super-resolution approaches that take advantage of the thin optical section generated in order to reduce out-of-focus signal.

SINGLE MOLECULE LOCALIZATION MICROSCOPIES

An impressive pallet of fluorescent proteins (FP) has been created, each with different excitation and emission wavelengths. Not only has the color range been refined, but also the use: through modification of the molecular structure, photo-activatable (PA) FPs have been developed, permitting applications in advanced microscopy such as photoactivation localization microscopy (PALM) (47, 48). Techniques such as PALM, ground-state depletion with immediate molecular return (GSDIM) (49), and stochastic optical switching microscopy (STORM) (50) have circumvented the diffraction-limit of resolution to permit the localization of single molecule point-spread-function (PSF) signals that are separated in time. STORM and GSDIM detect PSF-signals from single organic dye molecules; a potentially high density of molecules (e.g., fluorescent-conjugated antibody-detected epitopes) in the sample is driven into a long-lived, optically inactive "dark state" using a combination of high illumination power and specialized, highly reducing buffers. Single fluorescent molecules then spontaneously and randomly re-emerge to emit photons during subsequent imaging (**Figure 1**). This permits the acquisition of single PSF-signals that are sparsely distributed in a time-resolved dataset. PALM employs PA encodable FP (47, 48). These molecules are inherently non-fluorescent but can be altered conformationally, using short-wavelength illumination in order to render them fluorescent. By determining empirically the dose of activation energy required in order to activate a sparse fraction of all PA-molecules, again, single PSF-signals can be acquired. Rapid imaging trains capture the fluorescent data, before single molecules are irreversibly photo-destroyed by bleaching and other processes. Cycles of activation, followed by imaging and photo-destruction are repeated over and over again acquiring 1000 s of images in total. PALM is already starting to be used to define ion channel molecule localization, recently employed to image single aquaporin molecules (51).

Single molecule signals can be identified by their shape, size, expected fluorescent intensity (i.e., they are PSFs) as well as by their quantal "on–off" behavior. Mathematical fitting, localizing the centroid of these PSFs defines the precise *xy* coordinates from

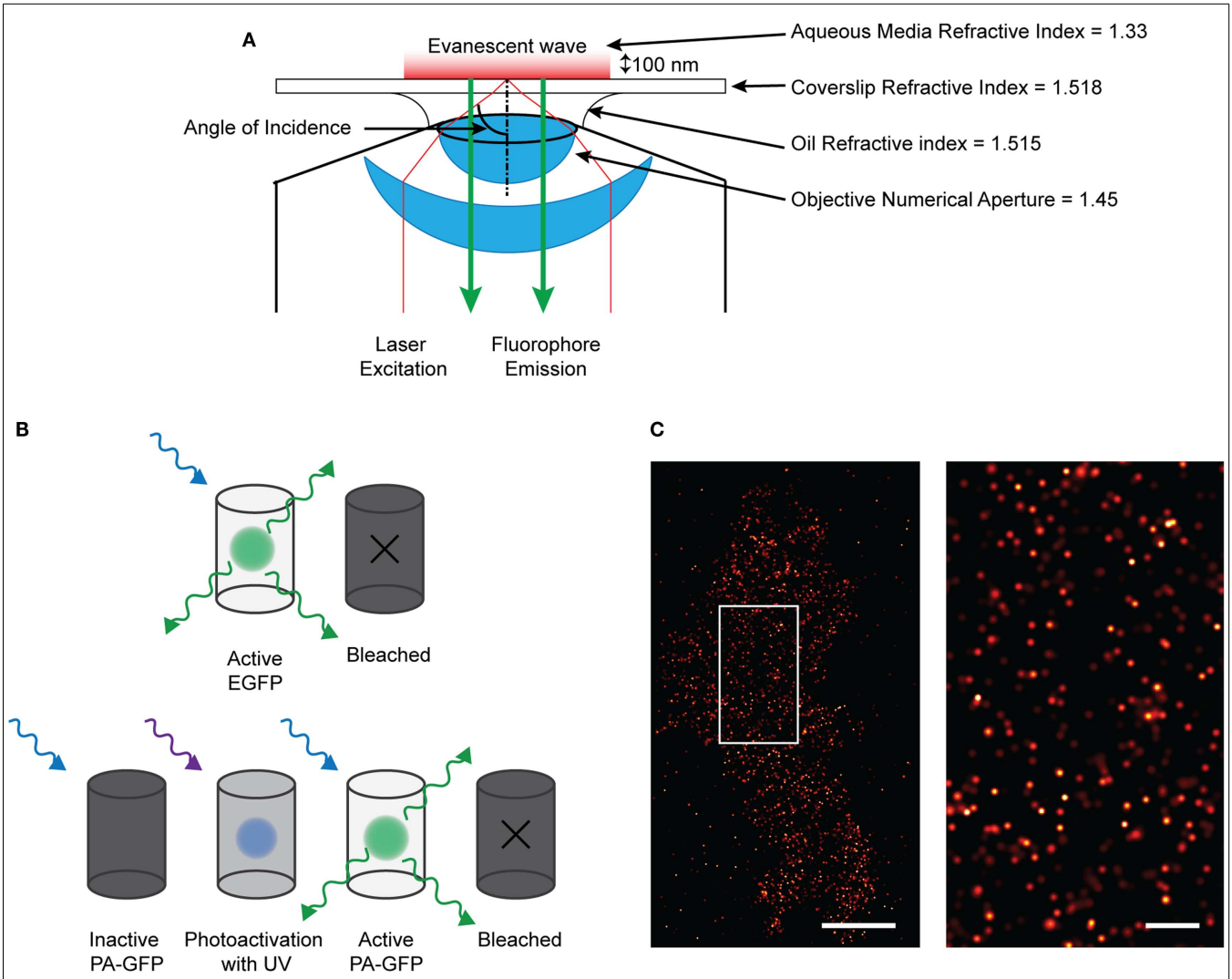

FIGURE 1 | Single molecule imaging using PALM technique. (A) Diagram of the TIRF microscopy setup. By angling the excitation light beam though a combination of the refractive indices of the lense, oil, coverslip, and aqueous media, the beam is reflected at the glass/media interface and is directed back into the objective. This creates an evanescent wave at the interface which effectively excites fluorophores only about 100 nm into the sample. Therefore only those fluorescent proteins or dyes within that region will be excited and emit fluorescence which can be detected. **(B)** Demonstrating the difference between EGFP and PA-GFP. EGFP will absorb and emit light without prior activation before bleaching off. PA-GFP needs to be activated by short-wavelength light before it is confirmationally able to absorb excitation and emit light. **(C)** (left) Localized and rendered PALM image of BK channels on the plasma membrane of a HEK293 cell (scale bar: 5 μm) with a region of interest (right) showing the localization of molecules in detail (scale bar: 1 μm).

where the signals arose; the certainty of localization is affected by brightness, noise, and pixel size. By rendering coordinates, a virtual image is created which shows the coordinate positions of all the molecules on the plasma membrane that have emitted. A variation of PALM combines single-particle tracking, so termed sptPALM (52), allowing the high-precision tracking of many 1000 s of single molecule signals with high temporal resolution.

SIMULATED EMISSION DEPLETION MICROSCOPY

The underlying limitation with microscopy is the diffraction-limited width of the PSF. Single molecule localization microscopies (SMLMs) circumvent this by determining the centroids derived from single molecule PSFs, and though these are excellent techniques, they are not imaging directly sub-diffraction structures. Simulated emission depletion microscopy (STED) presents a fundamentally different approach, directly manipulating the PSF through the use of stimulated emission to deplete fluorophores before they fluoresce (53). On a conventional scanning microscope, the sample is raster scanned with an excitation beam, which increases the energy of the fluorophores from the ground state S_0 to the exited singlet state S_1. The fluorophores spontaneously relax, emitting photons as they return to the ground state, which is detected as fluorescence. This process typically occurs on a nanosecond timescale. In STED microscopy a second depletion laser, is used immediately after the excitation beam (**Figure 2**). The depletion laser forces the excited fluorophores back

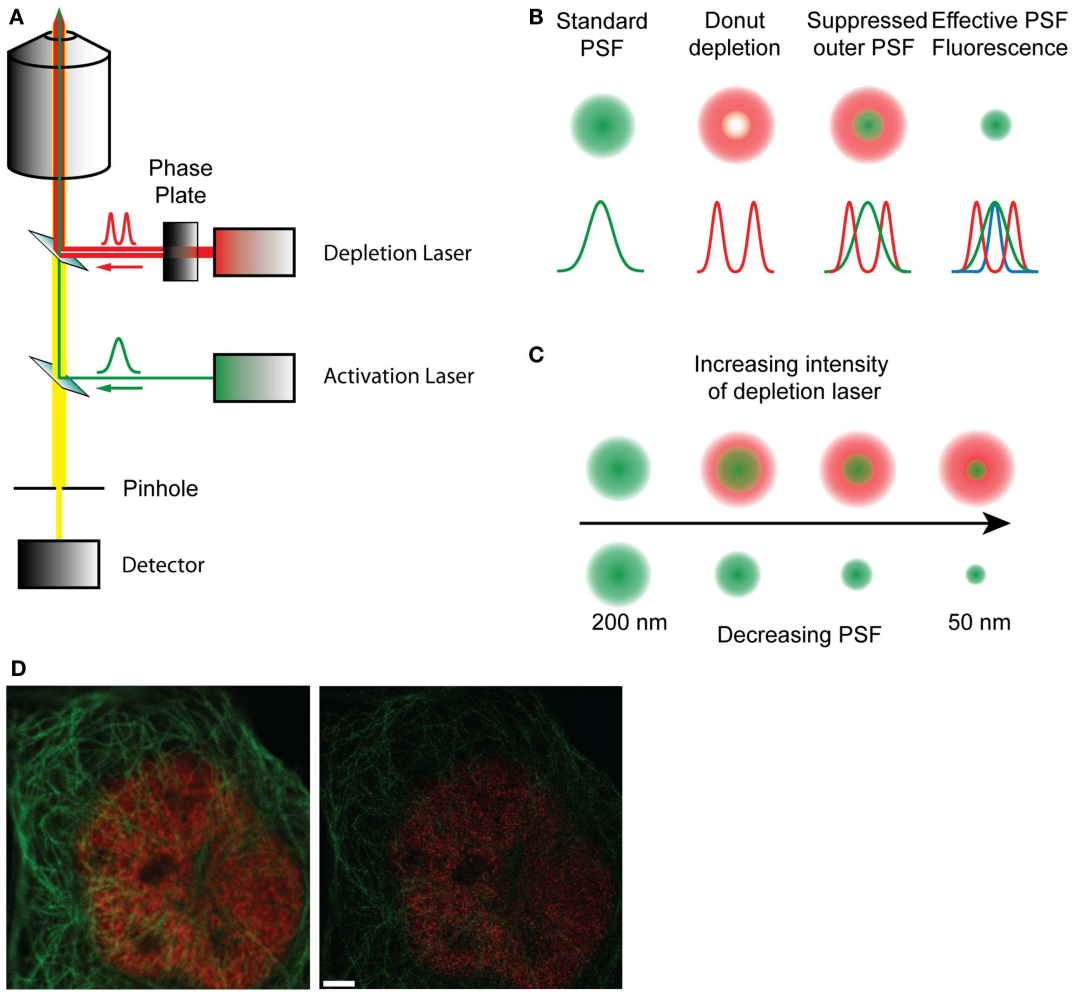

FIGURE 2 | (A) Schematic diagram of a STED microscope setup. The activation laser is overlaid with the depletion laser that passes through a phase plate, and focused to a focal point in the sample. The fluorescence emitted by the sample passes through a pinhole and is collected in the detector. **(B)** Representation of how the effective point spread function is formed by the overlap of the standard PSF and the depletion PSF. **(C)** With increasing intensity of the depletion laser the shape of the donut changes, decreasing the size of the inner ring and therefore reducing the effective PSF of the fluorophore from 200 nm to about 50 nm, effectively increasing resolution. **(D)** A raw confocal (left) and STED image (right) showing the improvement in detail and resolution. Red stain – nuclear pores, green stain – microtubules. Scale bar, 500 nm.

to the ground state via stimulated emission, a process that typically occurs on a picosecond timescale. This effectively forces depleted fluorophores into a dark state before traditional spontaneous fluorescence can occur. By using a phase mask profile with a donut-shaped depletion pattern, that perfectly overlaps the initial excitation beam, the effective PSF becomes defined by the geometry of the donut inner ring and the depletion laser power. The optical resolution can be considerably improved, to around 70 nm, to give a higher resolution data compared to standard diffraction-limited image. Gated-STED (gSTED) (54) combines this with time-correlated detection and pulsed excitation to further increase resolution, reduce noise, and improve utility with living samples enormously by reducing illumination energies (54–56). STED has been used to examine Ca^{2+} channel clustering induced by the exocytotic machinery (57) as well as probing the nano-scale structure of the synapse (38, 39, 58). The advent of less cytotoxic gSTED technologies will increase the utility of this approach in cell biology.

STRUCTURED ILLUMINATION MICROSCOPY

Structured illumination microscopy (SIM) illuminates samples with a grid pattern and a sinusoidal excitation, providing a known high-frequency structured pattern (59, 60). Mathematical approaches are then applied to reconstruct a real image from the emission data, with the ability to resolve structures at around half the diffraction-limit (i.e., around 85 nm resolution in general). Importantly, SIM also improves the axial resolution in images and can be used anywhere in 3-D, albeit in around 300 nm z-volumes, in multiple spectral colors. SIM has not yet been used to examine ion channel biology, to our knowledge, but clear opportunities exist, perhaps for studying intracellular channels beyond the reach of TIRF-limited approaches.

QUANTIFYING PROTEIN–PROTEIN INTERACTIONS IN CELLS

Förster resonance energy transfer (FRET) is a physical effect where energy can be transferred in a non-radiative way between a high-energy fluorescent donor molecule and a lower energy proximal acceptor, if the absorption and emission spectra of each, respectively, overlap. As FRET is strongly dependent on the inter-fluorophore distance and falls off with the sixth-power of distance, it occurs only on the nanometer scale. For this reason, FRET between two fluorescent molecules is commonly interpreted as indicating a direct interaction (61). Quantifying FRET is notoriously unreliable however, especially when using fluorescence intensity as a read-out. When FRET occurs, the energy transfer from the donor to an acceptor provides a rapid route to relaxation for the excited donor molecule, resulting in a significantly shortened fluorescence lifetime. Measuring the excited-state fluorescence lifetime of the donor molecule in each pixel of an image, known as fluorescence lifetime imaging microscopy (FLIM), therefore provides a direct and quantitative approach to this problem. FLIM has been widely used to quantify FRET between the SNAREs and binding partners inside intact cells (20, 21, 42–46, 48) and could be applied similarly to the study of ion channels; for example, it has been long-thought that VGCCs containing the so-called "synprint" (31) site interact directly with syntaxin and synaptotagmin but this has never been measured directly in intact cells.

FLUORESCENCE CORRELATION SPECTROSCOPY

Although powerful, FLIM suffers from slow temporal resolution, as commonly 10,000–100,000 s of photons must be acquired from each pixel in the image in order to build a large enough sample of time-tagged photons to permit accurate data fitting (62). In addition, in FRET experiments, the absence of a detected FRET signal does not necessarily mean that no interaction has occurred, leading to potential false-negative conclusions. Fluorescence Correlation Spectroscopy (FCS) acquires intensity fluctuations caused by fluorescence emission as molecules diffuse across a tiny excitation volume held stationary in a living sample (63–65). This approach thus calculates the diffusion rates, concentrations, and molecular numbers of molecules under scrutiny. As diffusion depends directly upon mass, a simultaneous decrease in diffusion rate and cross-correlation of signals between two different fluorescent molecules in the excitation volume provides unequivocal evidence of an interaction, on the millisecond timescale.

SUPER-RESOLUTION IMAGING OF ION CHANNELS

Single molecule localization microscopy can be applied to ion channels (51), to define the precise locations of large cohorts of single molecules. Furthermore, it is possible to combines SMLMs with diffraction-limited imaging, in order to capture data describing the locations of single channels and single vesicles, for example. This approach would allow appraisals such as "nearest-neighbor" analyses, to determine the distances between vesicle centers and their adjacent ion channel molecules. These approaches were used recently, finding that in contrast to previous understanding, the majority of the secretory machinery is segregated spatially from secretory vesicles, with protein molecules moving between membrane "hotspots" distinct from vesicle docking sites (12, 40).

IMAGING ION CHANNEL ACTIVITY – "OPTICAL PATCHING"

Patch-clamp electrophysiology is the ideal technique to determine the functionality of single ion channel molecules. Combined with fluorescent Ca^{2+} indicators, voltage-clamping can be used to deliver a train of tiny depolarizations, designed to open and close ion channels very rapidly. Image processing approaches may then be used, similarly to SMLM approaches, to localize the centroid position of the fluorescent signal reporting the ion channel location in a technique called optical patching (66–68). This approach has been used to great effect to report the locations of large-conductance, long open-dwell time IP3 receptors in cells (66); with the advent of image data "de-noising" strategies (40, 69) and faster camera detectors, optical patching promises to be useful for localizing single VGCCs in living cell membranes, combined with TIRFM.

IMAGING ION CHANNEL TETRAMERS

Active VGCCs and K channel alpha subunits are known to be tetramers; it difficult, however, to determine whether the channels detected on the cell surface using any of the approaches described above, are assembled alpha subunits. The study of ion channel function has been aided greatly over the years by the discovery that several potent natural toxins bind to specific ion channel targets with exquisite sensitivity and affinity. Recent work has taken advantage of this, using fluorescent-conjugates of these toxins to localize ion channels in intact cells. For example, ω-conotoxin is a peptidyl toxin originally isolated from the fish-hunting cone snail *Conus magnus* (70, 71) and is a specific N-type calcium channel blocker. This toxin has been used in the past to label neurons and neuromuscular junctions, revealing ion channel localization in diffraction-limited images (72). These approaches can now be combined with SMLM, as recently described using a Na^{+}-channel toxin in order to define the nano-scale locations of single assembled tetrameric alpha subunits (73). Combined with patch-clamp electrophysiology, these approaches offer the promise of manipulating channel behavior and localizing large cohorts of single molecules, simultaneously.

In summary, ion channel biology is uniquely placed in having diverse single molecule-resolution biophysical approaches available; electrophysiology and the newly emerging super-resolution imaging and spectroscopic approaches. Together, these promise to further our understanding not only of ion channel behavior, but also of channel location, function, and relationship with vesicles and the exocytotic molecular machinery.

REFERENCES

1. Sudhof TC. The synaptic vesicle cycle – a cascade of protein-protein interactions. *Nature* (1995) **375**:645–53. doi:10.1038/375645a0
2. Wheeler MB, Sheu L, Ghai M, Bouquillon A, Grondin G, Weller U, et al. Characterization of SNARE protein expression in beta cell lines and pancreatic islets. *Endocrinology* (1996) **137**:1340–8. doi:10.1210/en.137.4.1340
3. Bommert K, Charlton MP, DeBello WM, Chin GJ, Betz H, Augustine GJ. Inhibition of neurotransmitter release by C2-domain peptides implicates synaptotagmin in exocytosis. *Nature* (1993) **363**:163–5. doi:10.1038/363163a0

4. Klingseisen A, Jackson AP. Mechanisms and pathways of growth failure in primordial dwarfism. *Genes Dev* (2011) **25**:2011–24. doi:10.1101/gad.169037
5. Evans C, Kheradmand F, Corry D, Tuvim M, Densmore C, Waldrep C, et al. Gene therapy of mucus hypersecretion in experimental asthma. *Chest* (2002) **121**:90S–1. doi:10.1378/chest.121.3_suppl.90S-a
6. Fernández-Chacón R, Königstorfer A, Gerber SH, García J, Matos MF, Stevens CF, et al. Synaptotagmin I functions as a calcium regulator of release probability. *Nature* (2001) **410**:41–9. doi:10.1038/35065004
7. Brose N, Petrenko AG, Sudhof TC, Jahn R. Synaptotagmin: a calcium sensor on the synaptic vesicle surface. *Science* (1992) **256**:1021–5. doi:10.1126/science.1589771
8. Chapman ER, An S, Barton N, Jahn R. SNAP-25, a t-SNARE which binds to both syntaxin and synaptobrevin via domains that may form coiled coils. *J Biol Chem* (1994) **269**:27427–32.
9. Rizo J, Sudhof TC. Snares and Munc18 in synaptic vesicle fusion. *Nat Rev Neurosci* (2002) **3**:641–53.
10. Sutton RB, Fasshauer D, Jahn R, Brunger AT. Crystal structure of a SNARE complex involved in synaptic exocytosis at 2.4 A resolution. *Nature* (1998) **395**:347–53. doi:10.1038/26412
11. Medine CN, Rickman C, Chamberlain LH, Duncan RR. Munc18-1 prevents the formation of ectopic SNARE complexes in living cells. *J Cell Sci* (2007) **120**:4407–15. doi:10.1242/jcs.020230
12. Smyth AM, Yang L, Martin KJ, Hamilton C, Lu W, Cousin MA, et al. Munc18-1 protein molecules move between membrane molecular depots distinct from vesicle docking sites. *J Biol Chem* (2013) **288**:5102–13. doi:10.1074/jbc.M112.407585
13. Rickman C, Duncan RR. Munc18/Syntaxin interaction kinetics control secretory vesicle dynamics. *J Biol Chem* (2010) **285**:3965–72. doi:10.1074/jbc.M109.040402
14. Rickman C, Medine CN, Bergmann A, Duncan RR. Functionally and spatially distinct modes of munc18-syntaxin 1 interaction. *J Biol Chem* (2007) **282**:12097–103. doi:10.1074/jbc.M700227200
15. Berkefeld H, Sailer CA, Bildl W, Rohde V, Thumfart JO, Eble S, et al. BKCa-Cav channel complexes mediate rapid and localized Ca2+-activated K+ signaling. *Science* (2006) **314**:615–20. doi:10.1126/science.1132915
16. Berkefeld H, Fakler B. Repolarizing responses of BKCa-Cav complexes are distinctly shaped by their Cav subunits. *J Neurosci.* (2008) **28**:8238–45. doi:10.1523/JNEUROSCI.2274-08.2008
17. Fakler B, Adelman JP. Control of K(Ca) channels by calcium nano/microdomains. *Neuron* (2008) **59**:873–81. doi:10.1016/j.neuron.2008.09.001
18. Purcell EK, Liu L, Thomas PV, Duncan RK. Cholesterol influences voltage-gated calcium channels and BK-type potassium channels in auditory hair cells. *PLoS ONE* (2011) **6**:e26289. doi:10.1371/journal.pone.0026289
19. Braun M, Ramracheya R, Bengtsson M, Zhang Q, Karanauskaite J, Partridge C, et al. Voltage-gated ion channels in human pancreatic beta-cells: electrophysiological characterization and role in insulin secretion. *Diabetes* (2008) **57**:1618–28. doi:10.2337/db07-0991
20. Düfer M, Neye Y, Hörth K, Krippeit-Drews P, Hennige A, Widmer H, et al. BK channels affect glucose homeostasis and cell viability of murine pancreatic beta cells. *Diabetologia* (2011) **54**:423–32. doi:10.1007/s00125-010-1936-0
21. Asadi S, Javan M, Ahmadiani A, Sanati MH. Alternative splicing in the synaptic protein interaction site of rat Ca(v)2.2 (alpha (1B)) calcium channels: changes induced by chronic inflammatory pain. *J Mol Neurosci* (2009) **39**:40–8. doi:10.1007/s12031-008-9159-2
22. Rajapaksha WR, Wang D, Davies JN, Chen L, Zamponi GW, Fisher TE. Novel splice variants of rat CaV2.1 that lack much of the synaptic protein interaction site are expressed in neuroendocrine cells. *J Biol Chem* (2008) **283**:15997–6003. doi:10.1074/jbc.M710544200
23. Rettig J, Sheng ZH, Kim DK, Hodson CD, Snutch TP, Catterall WA. Isoform-specific interaction of the alpha1A subunits of brain Ca2+ channels with the presynaptic proteins syntaxin and SNAP-25. *Proc Natl Acad Sci U S A* (1996) **93**:7363–8. doi:10.1073/pnas.93.14.7363
24. Yang S-N, Berggren P-O. The role of voltage-gated calcium channels in pancreatic beta-cell physiology and pathophysiology. *Endocr Rev* (2006) **27**:621–76. doi:10.1210/er.2005-0888
25. Mahapatra S, Calorio C, Vandael DH, Marcantoni A, Carabelli V, Carbone E. Calcium channel types contributing to chromaffin cell excitability, exocytosis and endocytosis. *Cell Calcium* (2012) **51**:321–30. doi:10.1016/j.ceca.2012.01.005
26. Liu L, Rittenhouse AR. Effects of arachidonic acid on unitary calcium currents in rat sympathetic neurons. *J Physiol* (2000) **525**(Pt 2):391–404. doi:10.1111/j.1469-7793.2000.00391.x
27. Wang SQ, Song LS, Lakatta EG, Cheng H. Ca2+ signalling between single L-type Ca2+ channels and ryanodine receptors in heart cells. *Nature* (2001) **410**:592–6. doi:10.1038/35066597
28. Navedo MF, Amberg GC, Votaw VS, Santana LF. Constitutively active L-type Ca2+ channels. *Proc Natl Acad Sci U S A* (2005) **102**:11112–7. doi:10.1073/pnas.0500360102
29. Demuro A, Parker I. Imaging the activity and localization of single voltage-gated Ca(2+) channels by total internal reflection fluorescence microscopy. *Biophys J* (2004) **86**:3250–9. doi:10.1016/S0006-3495(04)74373-8
30. Berkefeld H, Fakler B, Schulte U. Ca2+ activated K+ channels: from protein complexes to function. *Physiol Rev.* (2010) **90**:1437–59. doi:10.1152/physrev.00049.2009
31. Sheng ZH, Yokoyama CT, Catterall WA. Interaction of the synprint site of N-type Ca2+ channels with the C2B domain of synaptotagmin I. *Proc Natl Acad Sci U S A* (1997) **94**:5405–10. doi:10.1073/pnas.94.10.5405
32. Davies JN, Jarvis SE, Zamponi GW. Bipartite syntaxin 1A interactions mediate CaV2.2 calcium channel regulation. *Biochem Biophys Res Commun* (2011) **411**:562–8. doi:10.1016/j.bbrc.2011.06.185
33. Zamponi GW. Regulation of presynaptic calcium channels by synaptic proteins. *J Pharmacol Sci* (2003) **92**:79–83. doi:10.1254/jphs.92.79
34. Becherer U, Moser T, Stühmer W, Oheim M. Calcium regulates exocytosis at the level of single vesicles. *Nat Neurosci* (2003) **6**:846–53. doi:10.1038/nn1087
35. Dodge FA Jr, Rahamimoff R. Co-operative action a calcium ions in transmitter release at the neuromuscular junction. *J Physiol* (1967) **193**:419–32.
36. Coorssen JR, Blank PS, Albertorio F, Bezrukov L, Kolosova I, Chen X, et al. Regulated secretion: SNARE density, vesicle fusion and calcium dependence. *J Cell Sci* (2003) **116**:2087–97. doi:10.1242/jcs.00374
37. Zucker RS, Fogelson AL. Relationship between transmitter release and presynaptic calcium influx when calcium enters through discrete channels. *Proc Natl Acad Sci U S A* (1986) **83**:3032–6. doi:10.1073/pnas.83.9.3032
38. Willig KI, Rizzoli SO, Westphal V, Jahn R, Hell SW. STED microscopy reveals that synaptotagmin remains clustered after synaptic vesicle exocytosis. *Nature* (2006) **440**:935–9. doi:10.1038/nature04592
39. Westphal V, Rizzoli SO, Lauterbach MA, Kamin D, Jahn R, Hell SW. Video-rate far-field optical nanoscopy dissects synaptic vesicle movement. *Science* (2008) **320**:246–9. doi:10.1126/science.1154228
40. Yang L, Dun AR, Martin KJ, Qiu Z, Dunn A, Lord GJ, et al. Secretory vesicles are preferentially targeted to areas of low molecular SNARE density. *PLoS ONE* (2012) **7**:e49514. doi:10.1371/journal.pone.0049514
41. Bar-On D, Wolter S, van de Linde S, Heilemann M, Nudelman G, Nachliel E, et al. Super-resolution imaging reveals the internal architecture of nano-sized syntaxin clusters. *J Biol Chem* (2012). doi:10.1074/jbc.M112.353250 Available from: http://www.ncbi.nlm.nih.gov/pubmed/22700970
42. Rickman C, Medine CN, Dun AR, Moulton DJ, Mandula O, Halemani ND, et al. t-SNARE protein conformations patterned by the lipid microenvironment. *J Biol Chem* (2010) **285**:13535–41. doi:10.1074/jbc.M109.091058
43. Duncan RR, Greaves J, Wiegand UK, Matskevich I, Bodammer G, Apps DK, et al. Functional and spatial segregation of secretory vesicle pools according to vesicle age. *Nature* (2003) **422**:176–80. doi:10.1038/nature01389
44. Axelrod D. Cell-substrate contacts illuminated by total internal reflection fluorescence. *J Cell Biol* (1981) **89**:141–5. doi:10.1083/jcb.89.1.141
45. Degtyar VE, Allersma MW, Axelrod D, Holz RW. Increased motion and travel, rather than stable docking, characterize the last moments before secretory granule fusion. *Proc Natl Acad Sci U S A* (2007) **104**:15929–34. doi:10.1073/pnas.0705406104
46. Steyer JA, Horstmann H, Almers W. Transport, docking and exocytosis of single secretory granules in live chromaffin cells. *Nature* (1997) **388**:474–8. doi:10.1038/41329
47. Betzig E, Patterson GH, Sougrat R, Lindwasser OW, Olenych S,

Bonifacino JS, et al. Imaging intracellular fluorescent proteins at nanometer resolution. *Science* (2006) **313**:1642–5. doi:10.1126/science.1127344
48. Hess ST, Girirajan TPK, Mason MD. Ultra-high resolution imaging by fluorescence photoactivation localization microscopy. *Biophys J* (2006) **91**:4258–72. doi:10.1529/biophysj.106.091116
49. Fölling J, Bossi M, Bock H, Medda R, Wurm CA, Hein B, et al. Fluorescence nanoscopy by ground-state depletion and single-molecule return. *Nat Methods* (2008) **5**:943–5. doi:10.1038/nmeth.1257
50. Rust MJ, Bates M, Zhuang X. Sub-diffraction-limit imaging by stochastic optical reconstruction microscopy (STORM). *Nat Methods* (2006) **3**:793–5. doi:10.1038/nmeth929
51. Rossi A, Moritz TJ, Ratelade J, Verkman AS. Super-resolution imaging of aquaporin-4 orthogonal arrays of particles in cell membranes. *J Cell Sci* (2012) **125**:4405–12. doi:10.1242/jcs.109603
52. Manley S, Gillette JM, Patterson GH, Shroff H, Hess HF, Betzig E, et al. High-density mapping of single-molecule trajectories with photoactivated localization microscopy. *Nat Methods* (2008) **5**:155–7. doi:10.1038/nmeth.1176
53. Hell SW, Wichmann J. Breaking the diffraction resolution limit by stimulated emission: stimulated-emission-depletion fluorescence microscopy. *Opt Lett* (1994) **19**:780–2. doi:10.1364/OL.19.000780
54. Vicidomini G, Moneron G, Han KY, Westphal V, Ta H, Reuss M, et al. Sharper low-power STED nanoscopy by time gating. *Nat Methods* (2011) **8**:571–3. doi:10.1038/nmeth.1624
55. Moffitt JR, Osseforth C, Michaelis J. Time-gating improves the spatial resolution of STED microscopy. *Opt Express* (2011) **19**:4242–54. doi:10.1364/OE.19.004242
56. Berning S, Willig KI, Steffens H, Dibaj P, Hell SW. Nanoscopy in a living mouse brain. *Science* (2012) **335**:551. doi:10.1126/science.1215369
57. Kittel RJ, Wichmann C, Rasse TM, Fouquet W, Schmidt M, Schmid A, et al. Bruchpilot promotes active zone assembly, Ca2+ channel clustering, and vesicle release. *Science* (2006) **312**:1051–4. doi:10.1126/science.1126308
58. Opazo F, Punge A, Bückers J, Hoopmann P, Kastrup L, Hell SW, et al. Limited intermixing of synaptic vesicle components upon vesicle recycling. *Traffic* (2010) **11**:800–12. doi:10.1111/j.1600-0854.2010.01058.x
59. Gustafsson MG. Surpassing the lateral resolution limit by a factor of two using structured illumination microscopy. *J Microsc* (2000) **198**:82–7. doi:10.1046/j.1365-2818.2000.00710.x
60. Bailey B, Farkas DL, Taylor DL, Lanni F. Enhancement of axial resolution in fluorescence microscopy by standing-wave excitation. *Nature* (1993) **366**:44–8. doi:10.1038/366044a0
61. Duncan RR, Bergmann A, Cousin MA, Apps DK, Shipston MJ. Multi-dimensional time-correlated single photon counting (TCSPC) fluorescence lifetime imaging microscopy (FLIM) to detect FRET in cells. *J Microsc* (2004) **215**:1–12. doi:10.1111/j.0022-2720.2004.01343.x
62. Medine CN, McDonald A, Bergmann A, Duncan RR. Time-correlated single photon counting FLIM: some considerations for physiologists. *Microsc Res Tech* (2007) **70**:420–5. doi:10.1002/jemt.20425
63. Kim SA, Heinze KG, Schwille P. Fluorescence correlation spectroscopy in living cells. *Nat Methods* (2007) **4**:963–73. doi:10.1038/nmeth1104
64. Kim SA, Sanabria H, Digman MA, Gratton E, Schwille P, Zipfel WR, et al. Quantifying translational mobility in neurons: comparison between current optical techniques. *J Neurosci* (2010) **30**:16409–16. doi:10.1523/JNEUROSCI.3063-10.2010
65. Elson EL, Webb WW. Concentration correlation spectroscopy: a new biophysical probe based on occupation number fluctuations. *Annu Rev Biophys Bioeng* (1975) **4**:311–34. doi:10.1146/annurev.bb.04.060175.001523
66. Parker I, Smith IF. Recording single-channel activity of inositol trisphosphate receptors in intact cells with a microscope, not a patch clamp. *J Gen Physiol* (2010) **136**:119–27. doi:10.1085/jgp.200910390
67. Smith IF, Wiltgen SM, Shuai J, Parker I. Ca(2+) puffs originate from pre-established stable clusters of inositol trisphosphate receptors. *Sci Signal* (2009) **2**:ra77. doi:10.1126/scisignal.2000466
68. Shuai J, Parker I. Optical single-channel recording by imaging Ca2+ flux through individual ion channels: theoretical considerations and limits to resolution. *Cell Calcium* (2005) **37**:283–99. doi:10.1016/j.ceca.2004.10.008
69. Parton RM, Hamilton RS, Ball G, Yang L, Cullen CF, Lu W, et al. A PAR-1-dependent orientation gradient of dynamic microtubules directs posterior cargo transport in the Drosophila oocyte. *J Cell Biol* (2011) **194**:121–35. doi:10.1083/jcb.201103160
70. Nielsen KJ, Schroeder T, Lewis R. Structure – activity relationships of v-conotoxins at N-type voltage-sensitive calcium channels. *J Mol Recognit* (2000) **13**:55–70. doi:10.1002/(SICI)1099-1352(200003/04)13:2<55::AID-JMR488>3.0.CO;2-O
71. Olivera BM, Gray WR, Zeikus R, McIntosh JM, Varga J, Rivier J, et al. Peptide neurotoxins from fish-hunting cone snails. *Science* (1985) **230**:1338–43. doi:10.1126/science.4071055
72. Jones OT, Kunze DL, Angelides KJ. Localization and mobility of omega-conotoxin-sensitive Ca2+ channels in hippocampal CA1 neurons. *Science* (1989) **244**:1189–93. doi:10.1126/science.2543080
73. Ondrus AE, Lee HL, Iwanaga S, Parsons WH, Andresen BM, Moerner WE, et al. Fluorescent saxitoxins for live cell imaging of single voltage-gated sodium ion channels beyond the optical diffraction limit. *Chem Biol* (2012) **19**(7):902–12. doi:10.1016/j.chembiol.2012.05.021

Conflict of Interest Statement: The authors declare that the research was conducted in the absence of any commercial or financial relationships that could be construed as a potential conflict of interest.

Received: 30 May 2013; accepted: 16 August 2013; published online: 04 September 2013.
*Citation: Hiersemenzel K, Brown ER and Duncan RR (2013) Imaging large cohorts of single ion channels and their activity. Front. Endocrinol. **4**:114. doi: 10.3389/fendo.2013.00114*
This article was submitted to Neuroendocrine Science, a section of the journal Frontiers in Endocrinology.